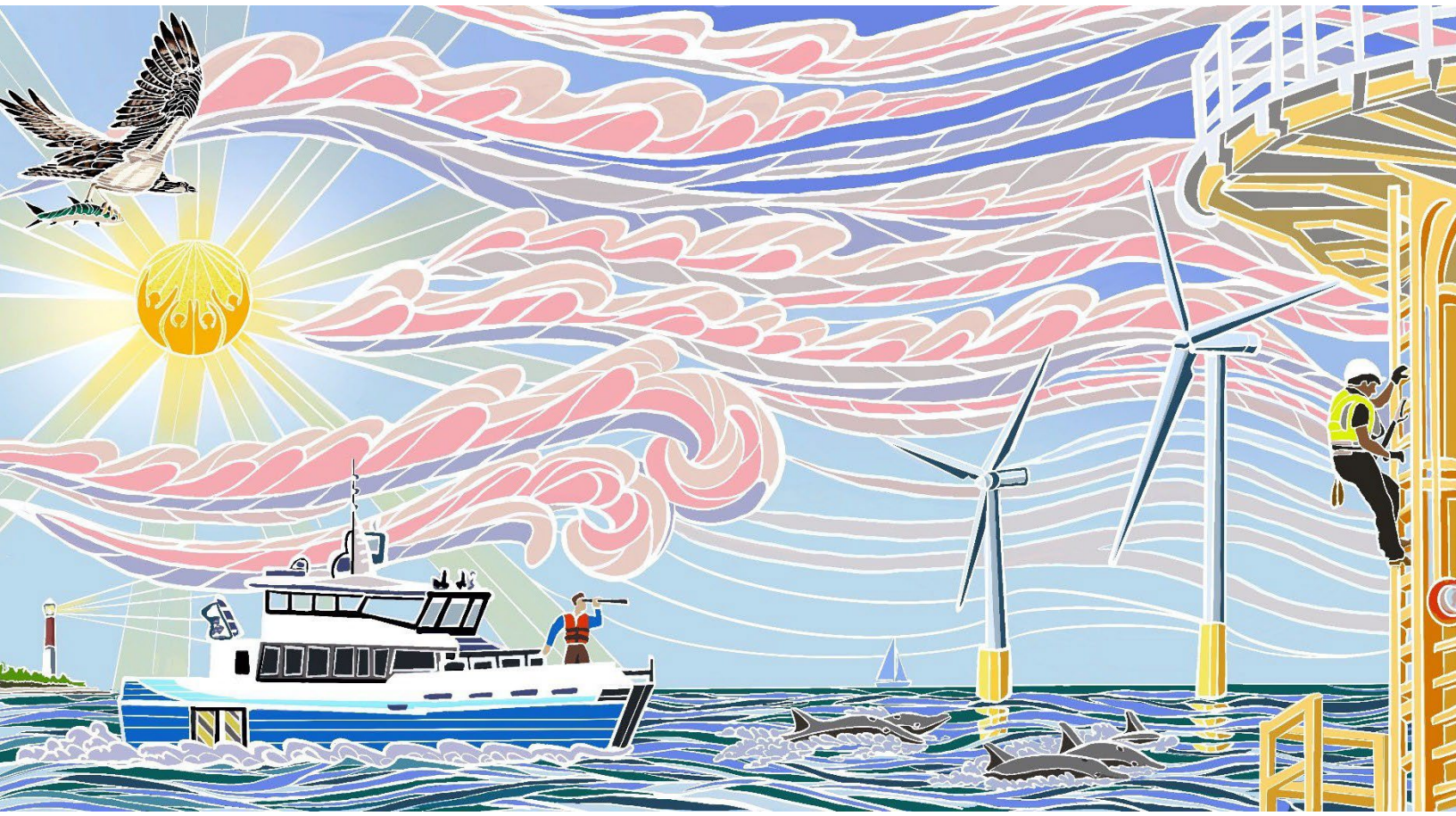

Appendix II-F2

Avian Appendix

March 2024

Note: At the time of the initial development of this report, development of a substation and/or converter station at the Brook Road Site in Howell Township, New Jersey was considered. The Brook Road site is now expected to be prepared and developed as part of the State of New Jersey Board of Public Utility (BPU) State Agreement Approach 1.0 (SAA)1 to support the delivery of offshore wind energy onshore. In collaboration with the regional gird operator PJM Interconnection (PJM) NJBPU conducted a study that examined whether an integrated suite of open access transmission facilities designated to support the delivery of offshore wind energy onshore could best facilitate meeting New Jersey's expanded offshore wind goals. Under the SAA 1.0 Award all permitting for site preparation activities, including construction activities to provide a "fit for purpose" site, for an associated substation and/or converter station will be the responsibility of the BPU's SAA-awardee at the Brook Road Site. Therefore, impacts associated with site preparation have not been considered as part of the Project Design Envelope (PDE) of the Project. Discussion of the site has been retained as part of the study area in this report to demonstrate the completeness of Atlantic Shores' multi-year development efforts.

[1] New Jersey Board of Public Utilities Selects Offshore Wind Transmission Project Proposed by Mid-Atlantic Offshore Development and Jersey Central Power & Light Company in First in Nation State Agreement Approach Solicitation

Appendix II-F2

Supporting Material for Avian Assessment: Data Sources, Methods, and Results

September 2023

Prepared by:

Biodiversity Research Institute

276 Canco Road

Portland, ME 04103

Table of Contents

1. Summary 1

2. Introduction 3

2.1. Project Description 3

2.2. Methods Overview 10

3. Birds – Onshore Methods and Results 12

3.1. Onshore Overview 12

3.2. Methods and Data Sources 16

3.3. Results 17

4. Birds – Offshore: Methods 39

4.1. Exposure Framework 39

5. Birds – Offshore: Results 75

5.1. Coastal birds 75

5.2. Marine birds 94

6. References 137

7. Applying a Community Distance Model to Correct Density Estimates of Seabirds in New Jersey Waters 145

7.1. Background 145

7.2. Methods 145

7.3. Results and Discussion 147

7.4. Conclusions 152

8. Birds – Offshore: Seasonal Maps 153

List of Figures

FIGURE 2-1: OVERVIEW OF ONSHORE AND OFFSHORE PROJECT COMPONENTS. 5

FIGURE 2-2: ESTIMATED TOTAL BIRD ABUNDANCE FROM THE MDAT MODELS. THE MODELS HIGHLIGHT THAT OVERALL ABUNDANCE IS LOWER IN THE LEASE AREA THAN ADJACENT NEARSHORE WATERS. INFORMATION PROVIDED BY NOAA AND USED WITH PERMISSION. 6

FIGURE 3-1: NEW JERSEY ONSHORE PROJECT AREAS AND ONSHORE INTERCONNECTION CABLE ROUTE OPTIONS FOR THE EXISTING ATLANTIC SUBSTATION AND LARRABEE SUBSTATION. 14

FIGURE 3-2: NEW YORK ONSHORE PROJECT AREAS AND ONSHORE INTERCONNECTION CABLE ROUTE OPTIONS FOR THE EXISTING FRESH KILLS SUBSTATION, GOETHALS SUBSTATION, AND GOWANUS SUBSTATION 15

FIGURE 3-3: 10-YEAR MONTHLY TOTAL NUMBER OF UNIQUE ENCOUNTERS (TOTAL DETECTIONS) BY EBIRD LIST (DUPLICATE LIST POSTINGS REMOVED) OF ROSEATE TERNS IN COASTAL NEW YORK (UPPER PANEL) AND NEW JERSEY (LOWER PANEL), DERIVED FROM THE EBIRD DATABASE. 30

FIGURE 3-4: 10-YEAR MONTHLY TOTAL NUMBER OF UNIQUE ENCOUNTERS (TOTAL DETECTIONS) BY EBIRD LIST (DUPLICATE LIST POSTINGS REMOVED) OF RED KNOTS IN COASTAL NEW YORK (UPPER PANEL) AND NEW JERSEY (LOWER PANEL), DERIVED FROM THE EBIRD DATABASE. 32

FIGURE 3-5: USFWS PROPOSED RED KNOT CRITICAL HABITAT (AS OF SEPTEMBER 2021) IN RELATION TO ONSHORE AND OFFSHORE PROJECT AREAS. 33

FIGURE 3-6: 10-YEAR MONTHLY TOTAL NUMBER OF UNIQUE ENCOUNTERS (TOTAL DETECTIONS) BY EBIRD LIST (DUPLICATE LIST POSTINGS REMOVED) OF PIPING PLOVERS IN COASTAL NEW YORK (UPPER PANEL) AND NEW JERSEY (LOWER PANEL), DERIVED FROM THE EBIRD DATABASE. 35

FIGURE 3-7: APPROXIMATE PIPING PLOVER NESTING AREAS (2021) IN RELATION TO THE NEW JERSEY PROJECT LANDFALL AREAS 36

FIGURE 3-8: APPROXIMATE PIPING PLOVER NESTING AREAS (2018) IN NEW YORK (NYDEC 2018) 37

FIGURE 3-9: 10-YEAR MONTHLY TOTAL NUMBER OF UNIQUE ENCOUNTERS (TOTAL DETECTIONS) BY EBIRD LIST (DUPLICATE LIST POSTINGS REMOVED) OF SALTMARSH SPARROWS IN COASTAL NEW YORK (UPPER PANEL) AND NEW JERSEY (LOWER PANEL), DERIVED FROM THE EBIRD DATABASE. 38

FIGURE 4-1: MAP OF DIGITAL AERIAL SURVEY TRANSECTS ACROSS THE LEASE AREA 41

FIGURE 4-2: SEASONAL SURVEY EFFORT OF ATLANTIC SHORES APEM DIGITAL AERIAL SURVEYS. SURVEY EFFORT TOTALED WITHIN EACH FULL OR PARTIAL LEASE BLOCK 42

FIGURE 4-3: MAP OF NJDEP BASELINE STUDIES SURVEY TRANSECTS AND THE ATLANTIC SHORES LEASE AREAS. 44

FIGURE 4-4: NJDEP BASELINE STUDIES SURVEY EFFORT BY SEASON. WHILE EFFORT VARIED BY OCS LEASE BLOCK AND SEASON, THE ENTIRE NJDEP BASELINE STUDIES AREA, INCLUDING THE LEASE AREA, WAS THOROUGHLY SURVEYED EACH SEASON. 45

FIGURE 4-5: EXAMPLE MDAT ABUNDANCE MODEL FOR THE NORTHERN GANNET (*MORUS BASSANUS*) IN FALL. 47

Figure 4-6: Constrained refined Delaunay triangulation spatial mesh. 55

Figure 4-7: Example of the (a.) non-standardized mean density/km^2 estimates from the INLA models with the raw observations (black points) overlaid and the (b.) standardized density proportions (of total density) visualized as percentiles. 56

Figure 4-8: Example map of relative density proportions locally and regionally for the Northern Gannet in fall. 58

Figure 5-1: Shorebirds observed in the NJDEP boat-based surveys, by season. 76

Figure 5-2: Modeled flight paths of migratory shorebirds equipped with nanotags (Loring et al. 2020). ... 79

Figure 5-3: Modeled flight paths of migratory Piping Plovers equipped with nanotags (Loring et al. 2019).80

Figure 5-4: Modeled flight paths of migratory Red Knots equipped with nanotags (Loring et al. 2020). 81

Figure 5-5: Movements of 11 Red Knots tagged at Brigantine, New Jersey, in 2020, as they depart on migration. Straight-line flight paths of two birds (204370 and 204375, overlapping in map) crossed OCS-A 0549. 82

Figure 5-6: Movements of 29 Red Knots tagged in coastal New Jersey, in 2021, as they depart on migration. Straight-line flight paths of three birds (224083, 224097, and 224099) crossed OCS-A 0549. 83

Figure 5-7: Movements of 1 Red Knots tagged in coastal New Jersey, in 2022, as they depart on migration. Straight-line flight paths of one bird (233781) crossed OCS-A 0549. 84

Figure 5-8: Coastal dabbling ducks, geese, and swans observed in the NJDEP boat-based surveys, by season.85

Figure 5-9: Coastal diving ducks observed in the NJDEP boat-based surveys, by season. 86

Figure 5-10: Grebes observed in the NJDEP boat-based surveys, by season. 87

Figure 5-11: Herons and egrets observed in the NJDEP boat-based surveys, by season. 88

Figure 5-12: Track lines of Great Blue Herons captured in Maine and equipped with satellite transmitters provided by Maine Department of Inland Fisheries and Wildlife. 89

Figure 5-13: Flight heights (m) of Great Blue Herons satellite-tagged in Maine, flying over the Atlantic OCS, in relation to the upper and lower limits of the RSZ (23.78 to 319.68 m [78.02 to 1,048.82 ft]). 90

Figure 5-14: Location estimates from satellite transmitters on Peregrine Falcons and Merlins tracked from three raptor research stations along the Atlantic coast, 2010–2018 (DeSorbo, Persico, et al. 2018).91

Figure 5-15: Dynamic Brownian bridge movement models for osprey (n = 127) that were tracked with satellite transmitters. 92

Figure 5-16: Songbirds (Passerines) observed in the NJDEP boat-based surveys, by season. 93

Figure 5-17: Seasonal distributions of all species observed across the Lease Area, modeled from monthly digital aerial surveys carried out in the area from October 2020–May 2021. 95

FIGURE 5-18: SEASONAL DISTRIBUTIONS OF LOONS ACROSS THE LEASE AREA, MODELED FROM MONTHLY DIGITAL AERIAL SURVEYS CARRIED OUT IN THE AREA FROM OCTOBER 2020–MAY 2021. 103

FIGURE 5-19: DYNAMIC BROWNIAN BRIDGE MOVEMENT MODELS FOR RED-THROATED LOONS..... 104

FIGURE 5-20: FLIGHT HEIGHTS (M) OF LOONS DERIVED FROM THE NORTHWEST ATLANTIC SEABIRD CATALOG. 105

FIGURE 5-21: SEASONAL DISTRIBUTIONS OF SCOTERS ACROSS THE LEASE AREA, MODELED FROM MONTHLY DIGITAL AERIAL SURVEYS CARRIED OUT IN THE AREA FROM OCTOBER 2020–MAY 2021. 107

FIGURE 5-22: DYNAMIC BROWNIAN BRIDGE MOVEMENT MODELS FOR SURF SCOTER. 108

FIGURE 5-23: DYNAMIC BROWNIAN BRIDGE MOVEMENT MODELS FOR BLACK SCOTER..... 109

FIGURE 5-24: DYNAMIC BROWNIAN BRIDGE MOVEMENT MODELS FOR WHITE-WINGED SCOTER. 110

FIGURE 5-25: DYNAMIC BROWNIAN BRIDGE MOVEMENT MODELS FOR LONG-TAILED DUCK..... 111

FIGURE 5-26: FLIGHT HEIGHTS (M) OF SEA DUCKS DERIVED FROM THE NORTHWEST ATLANTIC SEABIRD CATALOG. 112

FIGURE 5-27: FLIGHT HEIGHTS (M) OF SHEARWATERS, PETRELS, AND STORM-PETRELS DERIVED FROM THE NORTHWEST ATLANTIC SEABIRD CATALOG..... 114

FIGURE 5-28: TRACK LINES OF 10 BLACK-CAPPED PETRELS TAGGED WITH SOLAR SATELLITE TRANSMITTERS OFF OF CAPE HATTERAS, NORTH CAROLINA (ATLANTIC SEABIRDS 2020). 115

FIGURE 5-29: BLACK-CAPPED PETREL OBSERVATIONS FROM THE NORTHWEST ATLANTIC SEABIRD CATALOG. DATA PROVIDED BY NOAA AND USED WITH PERMISSION. 116

FIGURE 5-30: DYNAMIC BROWNIAN BRIDGE MOVEMENT MODELS FOR NORTHERN GANNETS..... 117

FIGURE 5-31: FLIGHT HEIGHTS (M) OF NORTHERN GANNET DERIVED FROM THE NORTHWEST ATLANTIC SEABIRD CATALOG. 118

FIGURE 5-32: FLIGHT HEIGHTS (M) OF CORMORANTS AND PELICANS DERIVED FROM THE NORTHWEST ATLANTIC SEABIRD CATALOG..... 120

FIGURE 5-33: SEASONAL DISTRIBUTIONS OF SMALL GULLS ACROSS THE LEASE AREA, MODELED FROM MONTHLY DIGITAL AERIAL SURVEYS CARRIED OUT IN THE AREA FROM OCTOBER 2020–MAY 2021. 123

FIGURE 5-34: SEASONAL DISTRIBUTIONS OF MEDIUM GULLS ACROSS THE LEASE AREA, MODELED FROM MONTHLY DIGITAL AERIAL SURVEYS CARRIED OUT IN THE AREA FROM OCTOBER 2020–MAY 2021. 124

FIGURE 5-35: SEASONAL DISTRIBUTIONS OF LARGE GULLS ACROSS THE LEASE AREA, MODELED FROM MONTHLY DIGITAL AERIAL SURVEYS CARRIED OUT IN THE AREA FROM OCTOBER 2020–MAY 2021. 125

FIGURE 5-36: FLIGHT HEIGHTS (M) OF JAEGERS AND GULLS DERIVED FROM THE NORTHWEST ATLANTIC SEABIRD CATALOG. 126

FIGURE 5-37: MODELED FLIGHT PATHS OF MIGRATORY COMMON TERNS EQUIPPED WITH NANOTAGS (LORING ET AL. 2019)..... 128

FIGURE 5-38: FLIGHT HEIGHTS (M) OF TERNS DERIVED FROM THE NORTHWEST ATLANTIC SEABIRD CATALOG. 129

FIGURE 5-39: ROSEATE TERN OBSERVATIONS FROM THE NORTHWEST ATLANTIC SEABIRD CATALOG. DATA PROVIDED BY NOAA AND USED WITH PERMISSION....130

FIGURE 5-40: MODELED FLIGHT PATHS OF MIGRATORY ROSEATE TERNS EQUIPPED WITH NANOTAGS (LORING ET AL. 2019).131

FIGURE 5-41: MODEL-ESTIMATED FLIGHT ALTITUDE RANGES (M) OF ROSEATE TERNS. 132

FIGURE 5-42: SEASONAL DISTRIBUTIONS OF AUKS ACROSS THE LEASE AREA, MODELED FROM MONTHLY DIGITAL AERIAL SURVEYS CARRIED OUT IN THE AREA FROM OCTOBER 2020–MAY 2021. 134

FIGURE 5-43: SEASONAL DISTRIBUTIONS OF MURRES ACROSS THE LEASE AREA, MODELED FROM MONTHLY DIGITAL AERIAL SURVEYS CARRIED OUT IN THE AREA FROM OCTOBER 2020–MAY 2021. 135

FIGURE 5-44: FLIGHT HEIGHTS (M) OF AUKS DERIVED FROM THE NORTHWEST ATLANTIC SEABIRD CATALOG. 136

FIGURE 7-1: DETECTION CURVE ESTIMATED USING A HAZARD FUNCTION FROM A COMMUNITY DISTANCE SAMPLING MODEL (TOP) AND A HISTOGRAM OF DETECTION DISTANCES (BOTTOM) FOR ALL TERN SPECIES.....148

FIGURE 7-2: DETECTION CURVE ESTIMATED USING A HAZARD FUNCTION FROM A COMMUNITY DISTANCE SAMPLING MODEL (TOP) AND A HISTOGRAM OF DETECTION DISTANCES (BOTTOM) FOR NORTHERN GANNETS. 149

FIGURE 7-3: DETECTION CURVE ESTIMATED USING A HAZARD FUNCTION FROM A COMMUNITY DISTANCE SAMPLING MODEL (TOP) AND A HISTOGRAM OF DETECTION DISTANCES (BOTTOM) FOR THE TWO LOON SPECIES.....150

List of Tables

Table 2-1: List of species detected or predicted within the Lease Area based on various sources (NJDEP, MDAT, APEM, IPaC), plus federally listed species that may occur in the area, and their conservation status. 7

Table 3-1: Road and transmission line co-occurrence with onshore interconnection cable route options. 17

Table 3-2: Habitat associations of onshore interconnection cable options. 17

Table 3-3: List of species observed by eBird users in the general Onshore Project Area, their primary and general breeding habitats, and presence at each site. Species that were observed less than 30 days per year are not included in this list. A/L = Atlantic and/or Larrabee, A = Atlantic, L = Larrabee, FG/GO = Fresh Kills/Goethals and/or Gowanus, FG = Fresh Kills and/or Goethals, GO = Gowanus. 18

Table 3-4: Complete list of species observed by eBird users in the general Onshore Project Area, their federal and state conservation statuses, and presence indicated in the IPaC database (https://ipac.ecosphere.fws.gov/). Note: BCC = Bird of Conservation Concern, PS = Potentially susceptible to development. 21

Table 4-1: Digital aerial survey dates 40

Table 4-2: Avian species identified in the digital aerial survey imagery. 54

Table 4-3: Species and categories included in each taxonomic group. 54

Table 4-4: Definitions of exposure levels developed for the avian assessment for each species and season. 62

Table 4-5: Assessment criteria used for assigning species to final exposure levels. 63

Table 4-6: Examples of scientific literature used in the vulnerability analysis for each taxa group. 65

Table 4-7: Assessment criteria used for assigning species to each behavioral vulnerability level. 65

Table 4-8: Data sources and scoring of factors used in the vulnerability assessment. 68

Table 4-9: WTG specifications used in the vulnerability analysis; mean lower low water (MLLW) is the average height of the lowest tide recorded at a tide station each day during the recording period. 71

Table 4-10: Vulnerability uncertainty adapted from Wade et al. (2016) to include only species occurring in North America. 74

Table 5-1: Mean annual naive densities (uncorrected count/km2 of survey transect) within the Lease Area and the NJDEP boat-based survey area of the Atlantic Outer Continental Shelf. 96

Table 5-2: Seasonal species naive densities (uncorrected count/km2 of survey transect) in the Atlantic Shores Lease Area OCS-A 0549 and the NJDEP boat-based survey area of the Atlantic Outer Continental Shelf. 98

TABLE 5-3: VULNERABILITY ASSESSMENT RANKINGS BY SPECIES WITHIN EACH BROAD TAXONOMIC GROUPING. 101

TABLE 5-4: SEASONAL EXPOSURE RANKINGS FOR THE LOON GROUP. 103

TABLE 5-5: VULNERABILITY ASSESSMENT RANKINGS BY SPECIES FOR THE LOON GROUP. NOTE: IN THE COP, "MINIMAL" IS ADDED TO THE COLLISION VULNERABILITY SCORE BECAUSE THERE IS LITTLE EVIDENCE IN THE LITERATURE THAT LOONS ARE VULNERABLE TO COLLISION BECAUSE THEY HAVE SUCH A STRONG AVOIDANCE RESPONSE. 105

TABLE 5-6: SEASONAL EXPOSURE RANKINGS FOR THE SEA DUCK GROUP.....106

TABLE 5-7: VULNERABILITY ASSESSMENT RANKINGS BY SPECIES FOR THE SEA DUCK GROUP. 112

TABLE 5-8: SEASONAL EXPOSURE RANKINGS FOR THE SHEARWATER AND PETREL GROUP. 113

TABLE 5-9: VULNERABILITY ASSESSMENT RANKINGS BY SPECIES FOR THE SHEARWATER AND PETREL GROUP. 114

TABLE 5-10: SEASONAL EXPOSURE RANKINGS FOR THE NORTHERN GANNET. 117

TABLE 5-11: VULNERABILITY ASSESSMENT RANKINGS BY SPECIES FOR THE GANNET GROUP. 118

TABLE 5-12: SEASONAL EXPOSURE RANKINGS FOR THE CORMORANT AND PELICAN GROUP. 119

TABLE 5-13: VULNERABILITY ASSESSMENT RANKINGS BY SPECIES FOR THE CORMORANT AND PELICAN GROUP.....120

TABLE 5-14: SEASONAL EXPOSURE RANKINGS FOR THE GULL GROUP. 121

TABLE 5-15: VULNERABILITY ASSESSMENT RANKINGS BY SPECIES FOR THE GULL GROUP.....126

TABLE 5-16: SEASONAL EXPOSURE RANKINGS FOR THE TERN GROUP. 127

TABLE 5-17: VULNERABILITY ASSESSMENT RANKINGS BY SPECIES FOR THE TERN GROUP.....129

TABLE 5-18: SEASONAL EXPOSURE RANKINGS FOR THE AUK GROUP. 133

TABLE 5-19: VULNERABILITY ASSESSMENT RANKINGS BY SPECIES FOR THE AUK GROUP. 136

TABLE 7-1: ESTIMATES OF DETECTION PROBABILITY FOR EACH TAXONOMIC GROUP TESTED USING A HAZARD DETECTION FUNCTION FROM A COMMUNITY DISTANCE SAMPLING MODEL.....151

List of Acronyms and Abbreviations

BOEM	Bureau of Ocean Energy Management
COP	Construction and Operations Plan
dBBMM	dynamic Brownian bridge movement model
ESA	Endangered Species Act
GF	Gaussian field
GSD	ground sampling distance
INLA	integrated nested Laplace approximation
IPaC	Information for Planning and Consultation
m	meter
MDAT	Marine-life Data and Analysis Team
mi	mile
MLLW	mean lower low water
MW	megawatt
NJDEP	New Jersey Department of Environmental Protection
NOAA	National Oceanic and Atmospheric Administration
OCS	Outer Continental Shelf
OSS	offshore substation
PiF	Partners in Flight
POI	point of interconnection
PTT	Argos platform terminal transmitter
RSZ	rotor swept zone
SDJV	Sea Duck Joint Venture
UD	utilization distribution
USFWS	United States Fish and Wildlife Service
WEA	wind energy area
WTG	wind turbine generator

1. Summary

Atlantic Shores Offshore Wind, LLC (Atlantic Shores) is submitting a Construction and Operations Plan (COP) to the Bureau of Ocean Energy Management (BOEM) for the development of an offshore wind energy generation project (Project) within Lease Area OCS-A 0549 (Lease Area). Lease Area OCS-A 0549 is located north of and directly abuts Lease Area OCS-A 0499.

The Lease Area is approximately 81,129 acres (328.3 square kilometers [km^2]) in size and is located on the Atlantic Outer Continental Shelf (OCS) within the New Jersey Wind Energy Area. At its closest point, the Lease Area is approximately 8.4 miles (mi; 13.5 kilometers [km]) from the New Jersey coast, and approximately 60 mi (96.6 km) from the New York State coast. Water depths in the Lease Area range from 66 to 98 feet (ft; 20 to 30 meters [m]).

Atlantic Shores proposes to construct, install, operate, and decommission up to three offshore Export Cable Corridors (ECCs) within federal, New Jersey, and New York State waters; landfall sites; onshore interconnection cable routes; and onshore substations and/or converter stations. Existing facilities will be used to support operations and maintenance.

The COP has been developed in accordance with 30 CFR Part 585, as well as stipulations in Atlantic Shores' Lease Agreement OCS-A 0549. Section 4.3 Birds of the COP Volume II describes the presence of birds and suitable bird habitat in the Offshore Project Area and the Onshore Project Area. Potential Project-related effects on birds and suitable bird habitat are also discussed. This Appendix to the COP provides detailed supporting information for both the offshore and onshore components of the Project.

Offshore, there are taxonomic sections on avian exposure (likelihood of occurrence) and vulnerability. Exposure to the Lease Area is assessed using Project-specific digital aerial surveys, New Jersey boat-based surveys, regional models, and tracking data.

Aerial surveys: A series of eight digital aerial surveys were flown across the Lease Area, from October 2020 to May 2021. Spatially explicit models were fit to the year-round and seasonal survey data by species and taxa group using integrated nested Laplace approximation (INLA), to model the observation density and account for the spatial dependence among observations. The surveys provide density estimates for three seasons to support understanding individual-level exposure, and the spatial models provide information on how birds are distributed across the Lease Area.

Boat-based surveys: The New Jersey Department of Environmental Protection (NJDEP) Ocean/Wind Power Ecological Baseline Studies (NJDEP Baseline Studies) included monthly boat-based avian surveys conducted offshore of New Jersey between January 2008 and December 2009. An effort was made to distance-correct the data using community distance models and standard distance correction methods, but the models had a poor fit and correction was not applied. The naive density estimates were used in the exposure assessment to determine how the density of birds in the Lease Area compares to surveys in other areas during the NJDEP Baseline Studies.

MDAT models: Seasonal predictions of bird density were developed by the National Oceanic and Atmospheric Administration (NOAA) to support Atlantic marine renewable energy planning, which describe regional-scale patterns of abundance. The models were used in the exposure assessment to determine how the density of birds in the Lease Area compares to other areas along the Atlantic OCS. These models, along with the boat-based surveys and modeled digital surveys, are presented for each species and season at the end of the Appendix.

Tracking data: Numerous tracking studies are available along the Atlantic OCS to improve the understanding of bird exposure to the Lease Area. Atlantic Shores conducted a GPS tracking study of Red Knots (*Calidris canutus rufa*) in coastal New Jersey; the United States Fish and Wildlife Service (USFWS) tracked shorebirds (Red Knot, Piping Plover [*Charadrius melodus*], Roseate Tern [*Sterna dougallii*]) with nanotags; BOEM supported satellite tracking of diving birds (Red-throated Loon [*Gavia stellata*, Northern Gannet [*Morus bassanus*], and Surf Scoter [*Melanitta perspicillata*]); and other researchers have tracked sea ducks, herons, falcons, and Osprey (*Pandion haliaetus*). Collectively, these data provide information on the potential exposure of these species to the Lease Area.

Vulnerability: For the birds exposed to the Lease Area, vulnerability to collision and displacement was then assessed using a scoring process for marine birds, and the literature for nonmarine birds as discussed in Section 4.3 Birds of the COP Volume II. This assessment of vulnerability focused on documented avoidance behaviors, estimated flight heights, and other factors. Flight heights used in the assessment were gathered from the datasets in the Northwest Atlantic Seabird Catalog.

The onshore section includes maps of the cable landfall areas, interconnection cable routes, substation and/or converter station locations, and points of interconnection (POIs). Tables detail the habitat types associated with each of the onshore Project components and the degree that they are co-located with existing development. A list of birds that may occur is presented based on eBird records within 9.3 mi (15 km) of onshore components, as well as monthly eBird records of Red Knot and Piping Plover detections. Maps and tables provide estimates on the distance of known Piping Plover nesting locations in relation to cable landfall sites, as well as areas being considered for Red Knot critical habitat. Overall, these robust datasets provide support for the offshore and onshore risk assessment detailed in the COP.

2. Introduction

This Appendix provides support for the detailed avian assessment provided in Section 4.3 Birds of the COP Volume II. Section 3 of this Appendix focuses on the birds in the onshore environment; Section 4 provides specific details on the methods used for the offshore assessment; Section 5 focuses on birds in the offshore environment and includes details on seasonal densities of birds exposed to Lease Area OCS-A 0549; Section 6 lists the literature cited; Section 7 describes the methods for applying a community distance model to correct density estimates of birds in New Jersey waters; and Section 8 provides seasonal exposure maps for marine birds.

2.1. Project Description

Atlantic Shores proposes to construct, operate, and decommission an offshore renewable wind energy project in the Lease Area, along with associated offshore and onshore cables, and onshore substations and/or converter stations. The Lease Area is within the New Jersey Wind Energy Area and may include an array of up to 157 wind turbine generators (WTGs); multiple offshore substations (OSSs); and a meteorological (met) tower and/or meteorological and oceanographic (metocean) buoys. The WTGs and OSSs will be connected by a system of high-voltage inter-array cables.

The WTGs and OSSs will be aligned in a uniform grid with multiple lines of orientation allowing straight transit through the Lease Area. The WTG grid and OSS positions associated with the Project are a continuation of the grid within the adjacent Lease Area OCS-A 0499 and are designed to maximize offshore renewable wind energy production while minimizing effects on existing marine uses in the Offshore Project Area.

Due to its location in the Mid-Atlantic Bight, which overlaps with northern and southern species assemblages, the Lease Area may be used by a diverse array of marine birds. Taxa groups including terns, phalaropes, and shearwaters may forage on surface prey in offshore waters such as the Lease Area, yet it is difficult to obtain information on prey availability at such a small spatial scale (Gulka et al. 2023). Furthermore, the MDAT marine bird relative density and distribution models, which integrate oceanographic features such as sea surface temperature that are linked with foraging behaviors (e.g., Jakubas et al. 2020), estimate that avian abundance within the Wind Farm Area will be relatively lower than closer to the New Jersey shore (Figure 2-2; Winship et al. 2018).

Offshore export cables will transmit electricity from the Lease Area to onshore transmission systems via landfall sites in one or more of the following locations: southern Monmouth County, New Jersey; the vicinity of Asbury Park in northern Monmouth County, New Jersey; southwest Staten Island, New York; northeast Staten Island, New York; and Brooklyn, New York (Figure 2-1). At landfall, horizontal directional drilling will be employed to support each export cables' offshore-to-onshore transition. From each landfall site, interconnection cables will travel underground primarily along existing roadways and/or utility rights-of-way to new onshore substation and/or converter station sites. Eight onshore substation and/or converter station sites are currently being considered, with three in New York and five in New Jersey. The final locations and footprint extent of each substation/converter station site is currently being finalized and will be provided when available. Onshore interconnection cable routes will lead to an electric

transmission substation POI. The POIs currently under consideration are the existing Larrabee and Atlantic Substations in Monmouth County, New Jersey; and the existing Fresh Kills, Goethals and Gowanus substations in Richmond and Kings Counties, respectively, in New York (Figure 2-1).

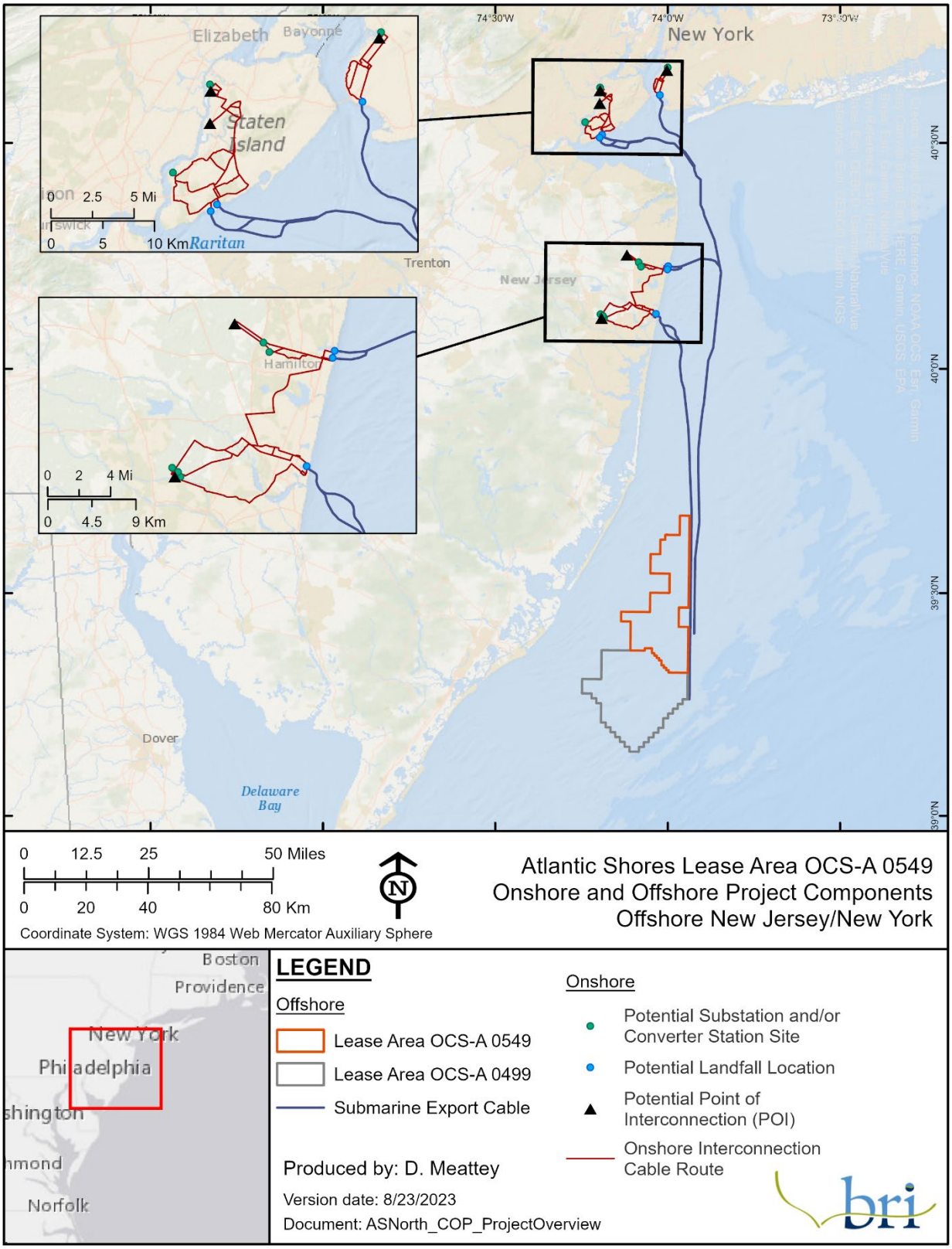

Figure 2-1: Overview of onshore and offshore Project components.

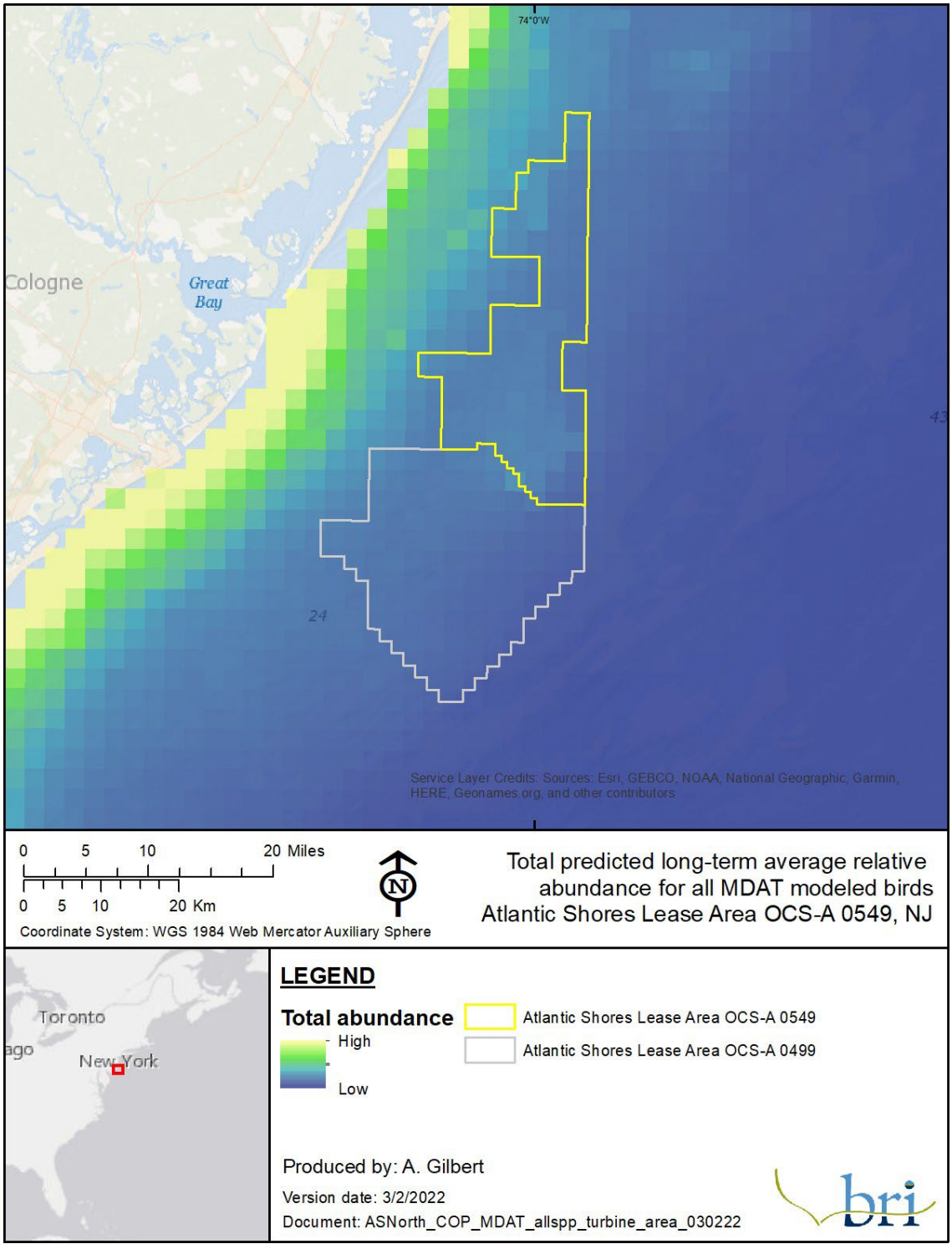

Figure 2-2: Estimated total bird abundance from the MDAT models. The models highlight that overall abundance is lower in the Lease Area than adjacent nearshore waters. Information provided by NOAA and used with permission.

Table 2-1: **List of species detected or predicted within the Lease Area based on various sources (NJDEP, MDAT, APEM, IPaC), plus federally listed species that may occur in the area, and their conservation status.**

Common Name	Latin Name	Source				Conservation Status[1]	
		NJDEP	MDAT	APEM	IPaC	Federal	NJ State
Ducks, geese, and swans							
Northern Pintail	*Anas acuta*	•					
American Black Duck	*Anas rubripes*	•					
Gadwall	*Mareca strepera*	•					
Sea ducks							
Long-tailed Duck	*Clangula hyemalis*	•	•				
Black Scoter	*Melanitta americana*	•	•				
White-winged Scoter	*Melanitta fusca*	•	•	•			
Surf Scoter	*Melanitta perspicillata*	•	•	•			
Common Eider	*Somateria mollissima*	•	•				
Loons							
Common Loon	*Gavia immer*	•	•	•	•		
Red-throated Loon	*Gavia stellata*	•	•	•	•		
Shearwaters and petrels							
Great Shearwater	*Ardenna gravis*	•	•				
Cory's Shearwater	*Calonectris diomedea*	•	•			BCC	
Wilson's Storm-Petrel	*Oceanites oceanicus*	•	•		•		
Gannets							
Northern Gannet	*Morus bassanus*	•	•	•			
Cormorants and pelicans							
Brown Pelican	*Pelecanus occidentalis*	•	•				
Double-crested Cormorant	*Phalacrocorax auritus*	•	•				
Jaegers and gulls							
Bonaparte's Gull	*Chroicocephalus philadelphia*	•	•	•			
Herring Gull	*Larus argentatus*	•	•	•			
Ring-billed Gull	*Larus delawarensis*	•	•	•			
Lesser Black-backed Gull	*Larus fuscus*	•					
Great Black-backed Gull	*Larus marinus*	•	•	•			
Laughing Gull	*Leucophaeus atricilla*	•	•	•			
Black-legged Kittiwake	*Rissa tridactyla*	•	•	•			
Parasitic Jaeger	*Stercorarius parasiticus*	•	•				

Common Name	Latin Name	Source				Conservation Status[1]	
		NJDEP	MDAT	APEM	IPaC	Federal	NJ State
Sabine's Gull	*Xema sabini*	•					
Terns							
Black Tern	*Chlidonias niger*	•					
Forster's Tern	*Sterna forsteri*	•					
Common Tern	*Sterna hirundo*	•	•				SC
Royal Tern	*Thalasseus maximus*	•	•		•		
Roseate Tern	*Sterna dougallii*				•	E	E
Auks							
Razorbill	*Alca torda*	•	•	•	•		
Dovekie	*Alle alle*	•	•		•		
Common Murre	*Uria aalge*	•	•		•		
Atlantic Puffin	*Fratercula arctica*				•		
Shorebirds							
Pectoral Sandpiper	*Calidris melanotos*	•					
American Woodcock	*Scolopax minor*	•					
Red Knot	*Calidris canutus rufa*				•	T	E
Piping Plover	*Charadrius melodus*				•	T	E
Passerines							
Northern Flicker	*Colaptes auratus*	•					
Gray Catbird	*Dumetella carolinensis*	•					
Barn Swallow	*Hirundo rustica*	•					
Orchard Oriole	*Icterus spurius*	•					
Dark-eyed Junco	*Junco hyemalis*	•					
Song Sparrow	*Melospiza melodia*	•					
Brown-headed Cowbird	*Molothrus ater*	•					
Purple Martin	*Progne subis*	•					
Bank Swallow	*Riparia riparia*	•					
Ovenbird	*Seiurus aurocapilla*	•					
Northern Parula	*Setophaga americana*	•					SC
Yellow Warbler	*Setophaga petechia*	•					
Grebes							
Horned Grebe	*Podiceps auritus*	•	•				

Common Name	Latin Name	Source				Conservation Status[1]	
		NJDEP	MDAT	APEM	IPaC	Federal	NJ State
Raptors							
Peregrine Falcon	*Falco peregrinus*	•					
Osprey	*Pandion haliaetus*	•					

[1] E = Endangered, T = Threatened, SC = Special Concern, BCC = Birds of Conservation Concern

2.2. Methods Overview

2.2.1. Offshore

For each subject group addressed under this assessment, species occurrence and area use were identified and evaluated using multiple information sources, including (but not limited to): Lease Area- specific digital aerial surveys conducted by APEM Ltd., an aerial wildlife surveying company; NJDEP Baseline Studies boat-based surveys; National Oceanic and Atmospheric Administration (NOAA) Marine-Life Data and Analysis Team (MDAT) bird distribution models; Northwest Atlantic Seabird Catalog; eBird and other occurrence and phenology data; individual tracking studies; relevant current literature; and published species accounts.

Most species were assessed within general taxonomic groups (e.g., wading birds), however species with federal listing status, or candidate species, were individually assessed, namely the Piping Plover (*Charadrius melodus*), Red Knot (*Calidris canutus rufa*), Roseate Tern (*Sterna dougallii*), and Black-capped Petrel (*Pterodroma hasitata*).

The results sections of this Appendix address exposure and vulnerability of coastal birds and marine birds separately, and includes maps, tables, and figures for each major taxonomic group. Exposure assessment maps, tables, and figures are presented for both coastal and marine birds based on the aforementioned data sources.

For the offshore assessment, a semi-quantitative approach was taken that first describes the species that would potentially be exposed to the Lease Area, and the vulnerability of the species exposed. The assessment process was as follows:

- *Exposure* – The first step in the process was to assess exposure for each species and each taxonomic group, where 'exposure' is defined as the extent of overlap between a species' seasonal or annual distribution and the Lease Area. For species where site-specific data was available, a semi-quantitative exposure assessment was conducted. This exposure assessment was focused exclusively on the horizontal, or two-dimensional, likelihood that a bird would use the Lease Area.
- *Relative Vulnerability* – Vulnerability was then assessed for marine birds using a scoring process. For the purposes of this analysis, vulnerability is defined as the degree to which a species is expected to be affected by WTGs in the Lease Area, based on known behavioral responses to similar offshore developments. This assessment of vulnerability focused on documented avoidance behaviors, estimated flight heights, and other factors. The results provide a relative categorical vulnerability score among the species exposed to the Project—e.g., the species that are least likely to collide with turbines receive a minimal collision score—and is not intended provide an absolute likelihood of collision or displacement. Flight heights used in the assessment were gathered from the NJDEP Baseline Studies (local) and non-digital aerial survey datasets in the Northwest Atlantic Seabird Catalog (regional). Vulnerability of non-marine migratory birds is discussed in Section 4.3 Birds of the COP Volume II.

2.2.2. Onshore

The Onshore Methods and Results section of this Appendix includes maps of the proposed landfall sites, interconnection cable routes, substation/converter station sites, and POIs. A tables details the habitat types associated with the onshore interconnection cable routes, and the degree that they are co-located with existing development. A list of birds that may occur is presented based on eBird records within 9.3 mi (15 km) of onshore components, as well as monthly eBird records of Red Knot and Piping Plover detections. Because eBird effort is inconsistent, the 9.3-mi (15-km) buffer was used to include more sites where birds were observed, to ensure most species using the general area were recorded. Maps and tables provide estimates on the distance of known Piping Plover nesting locations in relation to cable landfall sites, as well as areas being considered for Red Knot critical habitat.

3. Birds – Onshore Methods and Results

This section provides tables, maps, and figures to support the discussion in Section 4.3 Birds of the COP Volume II about the birds that may be affected by construction and operation of the onshore Project components. These components include landfall sites, onshore interconnection cables, onshore substations and/or converter stations, and POIs. The habitat that would be modified by onshore project components is described and the birds likely to occur in the habitat are provided. Additional information is provided on federally listed species.

3.1. Onshore Overview

The Project includes landfall sites and associated onshore interconnection cable routes and substations and/or converter stations. Energy from the OSSs will be delivered to landfall sites in New Jersey and/or New York via 230 kV to 275 kV HVAC and/or 320 kV to 525 kV high voltage direct current (HVDC) export cables (Figure 3-1 and Figure 3-2). Energy delivery would be made to New Jersey using HVAC and/or HVDC export cables while delivery to New York would be made via HVDC export cables only. Atlantic Shores has identified potential landfall sites in southern Monmouth County, New Jersey; in the vicinity of Asbury Park in northern Monmouth County, New Jersey; on southwest Staten Island, New York; on northeast Staten Island and in Brooklyn, New York (see Section 4.7 Landfall Sites of the COP Volume II for details on the landfall sites).

Three ECCs have been identified:

- The Monmouth ECC extends from the Lease Area to the potential landfall locations in southern Monmouth County, New Jersey. The total length of the Monmouth ECC associated with the Project is approximately 59.2 mi (95.3 km) from the Lease Area to the farthest landfall site in New Jersey. The Monmouth ECC is also included in the COP for Lease Area OCS-A 0499.[1]
- The Northern ECC extends north from the Lease Area to the New York State waters boundary to reach several potential landfall sites on Staten Island and in Brooklyn, New York. The total length of the Northern ECC associated with the Project is approximately 65.2 mi (104.9 km) from the Lease Area to the potential landfall sites in Brooklyn.

At the landfall sites in both New Jersey and New York, horizontal directional drilling (HDD) will be used for the export cables' offshore-to-onshore transition. The HDD landfall technique has been selected both to ensure stable cable burial along the coast and to avoid nearshore and shoreline impacts. From each landfall site, new 230 kV to 275 kV HVAC and/or 320 kV to 525 kV HVDC onshore interconnection cables will travel underground primarily along existing roadways, and/or utility rights-of-way to new onshore substation and/or converter station sites. Eight

[1] As described in the COP for Lease Area OCS-A 0499, the Monmouth ECC extends from the southern portion of the lease area north and west to landfall locations in southern Monmouth County, New Jersey. Export cables associated with Lease Area OCS-A 0549 may be co-located within the Monmouth ECC but will be separate and distinct from the export cables associated with Lease Area OCS-A 0499.

onshore substation and/or converter station sites are being considered, with three in New York and five in New Jersey. Potential impacts at these sites may include tree clearing and temporary and/or permanent impacts to wildlife and/or wetlands based on final layouts. At the onshore substations and/or converter stations, HVDC will be converted to HVAC (if required) and the transmission voltage will be stepped up or stepped down in preparation for interconnection with the electrical grid at one of the identified POIs.

Atlantic Shores has identified potential POIs in both New Jersey and New York. These POIs are typically existing electric transmission substations with direct connectivity into the electric grid. The POIs currently under consideration are the existing Larrabee and Atlantic Substations in Monmouth County, New Jersey and the existing Fresh Kills, Goethals and Gowanus substations in Richmond and Kings Counties, respectively, in New York (Figure 3-1 and Figure 3-2). The Project requires the ability to interconnect at multiple POIs to accommodate the maximum amount of electricity that could be generated by the Project. Atlantic Shores has formally filed for queue positions at each of the POIs in New Jersey through PJM Interconnection, which is a regional transmission organization that coordinates the movement of wholesale electricity and at each of the POIs in in New Jersey, and in New York through the New York Independent System Operator (NYISO).

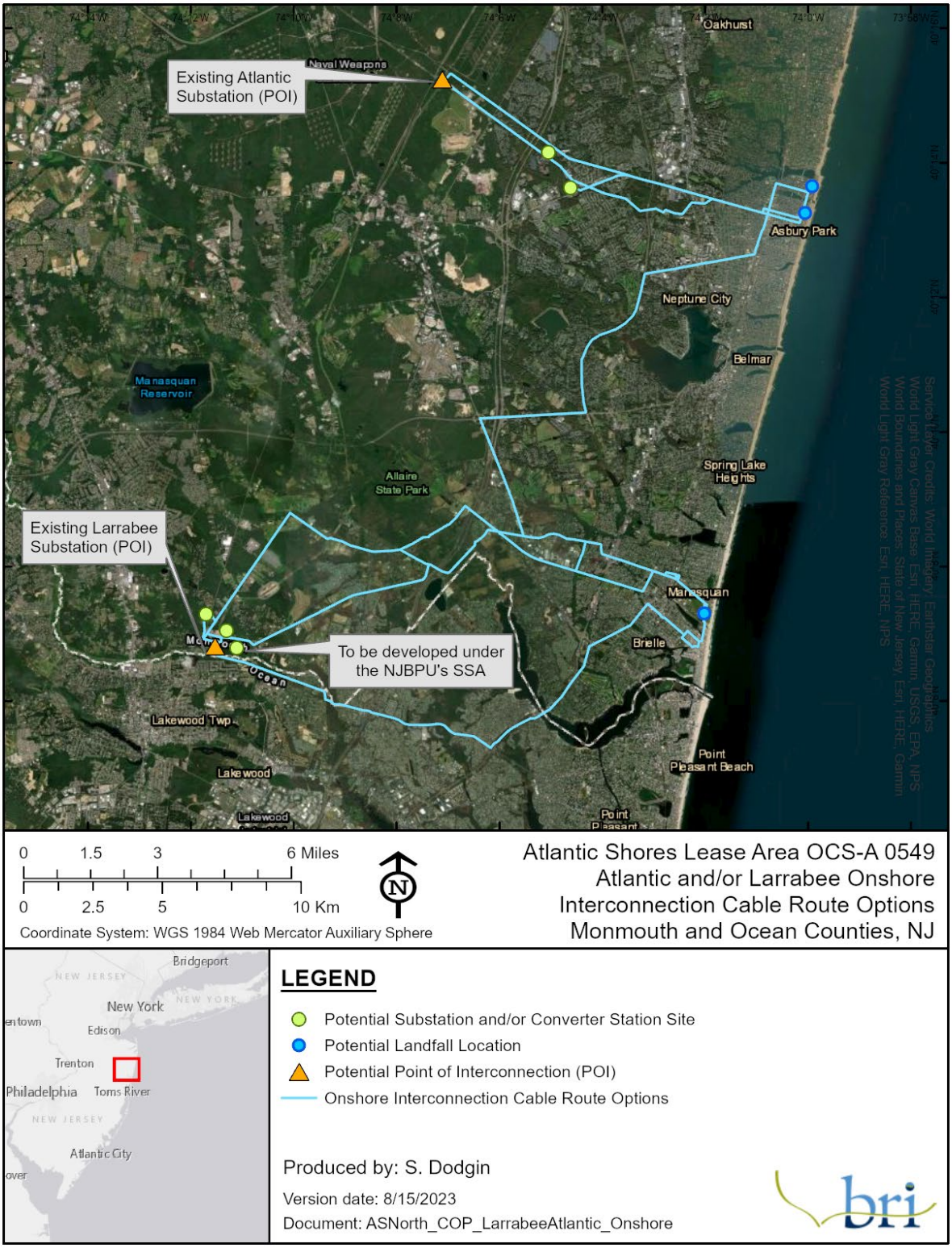

Figure 3-1: New Jersey Onshore Project Areas and onshore interconnection cable route options for the existing Atlantic Substation and Larrabee Substation.

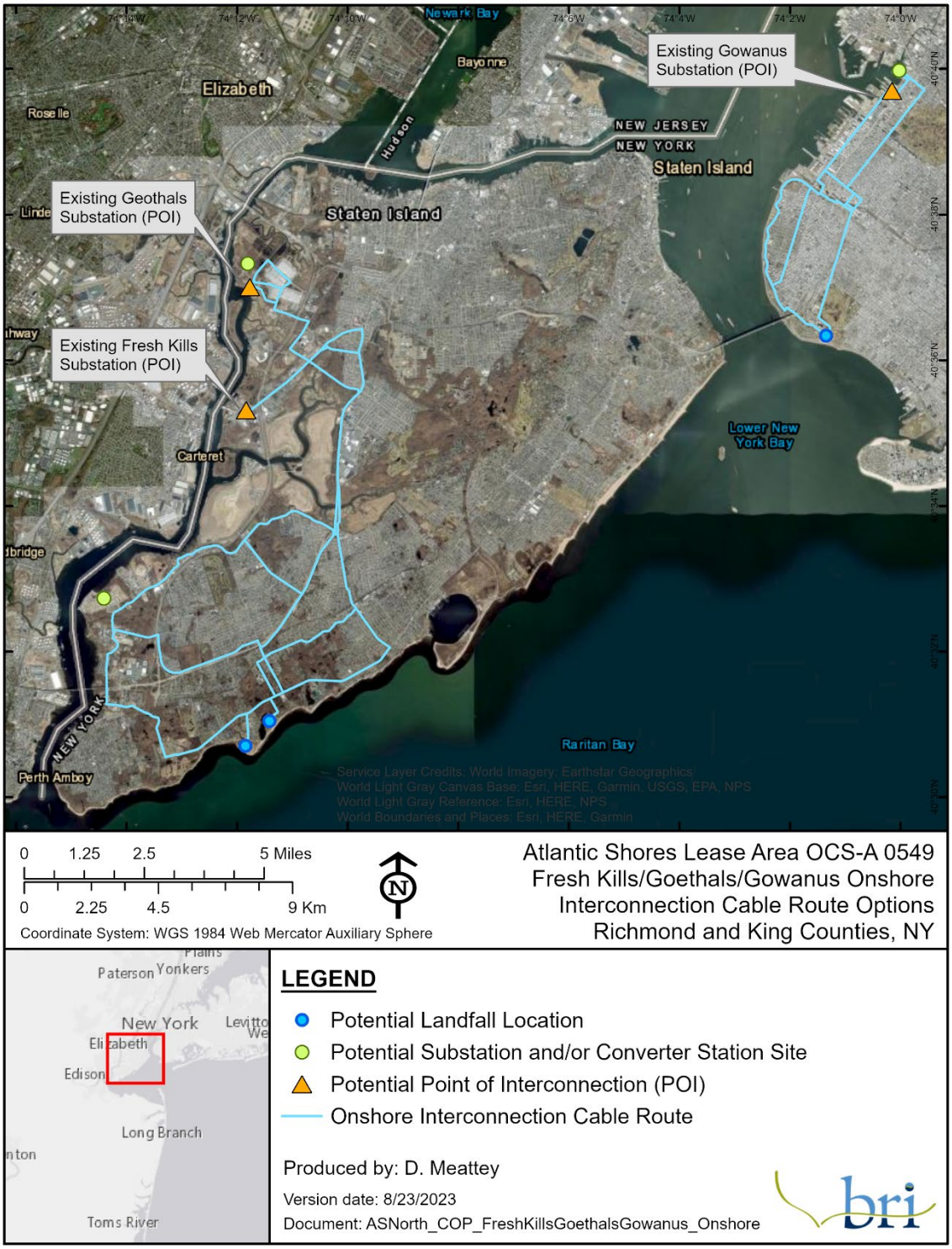

Figure 3-2: New York Onshore Project Areas and onshore interconnection cable route options for the existing Fresh Kills Substation, Goethals Substation, and Gowanus Substation.

3.2. Methods and Data Sources

3.2.1. Onshore Interconnection Cable Route Habitat Assessment

The habitat potentially to be disturbed by the onshore interconnection cable routes was assessed by calculating the overlap of the routes with local habitat types; and then by calculating the percentage each route was co-located with existing development as well as overlapping other landcover (habitat) types. The habitat types were determined for each cable route using the National Land Cover Database (NLCD).[2] A 50m buffer was applied to either side of each proposed cable route. This buffer width was expected to account for potential disturbance across the construction right-of-way. The area of each landscape type within each buffered cable route was calculated by first intersecting the NLCD raster with buffered cable route using the crop function from package "Raster" (Hijmans 2022) in R version 4.1.1 (R Core Team 2021) and then summarizing the area covered by each landcover type in each route.

Co-occurrence of the interconnection cable route options with existing linear infrastructure was also assessed in ArcGIS (ESRI v10.8.1). Road centerlines for the State of New Jersey were downloaded from the New Jersey Geographic Information Network and New York State road centerlines were downloaded from the New York State GIS Clearinghouse. The centerlines were then clipped to the buffered cable route layers. All road features that ran parallel to the cable route were manually selected and summed for total road length and percentage of total route length. These same methods were used to assess total, and percentage co-occurrence with existing transmission line corridors using the Electrical Power Transmission Lines layer developed for the Homeland Infrastructure Foundation-Level Data.[3]

3.2.2. Avian Data Sources and Methods

Data on possible bird species present, including Red Knot and Piping Plover, were primarily compiled from eBird citizen science data (Sullivan et al. 2009) from within a 9.3-mi (15-km) buffer of the centroid of the onshore sites, and were temporally constrained to the prior 10 years of data (2012-2022). In addition, the USFWS IPaC database (USFWS 2020) was queried using a polygon encompassing the entire Onshore Project Area. Piping Plover nesting sites in coastal New Jersey were mapped based on sites identified in Heiser and Davis (2021).

[2] https://www.mrlc.gov/data/nlcd-2016-land-cover-conus

[3] https://gii.dhs.gov/HIFLD

3.3. Results

3.3.1. Co-occurrence with existing development and habitat

Table 3-1: Road and transmission line co-occurrence with onshore interconnection cable route options.

Onshore Route Options	Co occurrence with Existing Roads and Transmission Lines		
	Total Length (ft)	Co located (ft)	% of Total Length
Atlantic and/or Larrabee	15,798	15,798	100
Atlantic	67,393	67,393	100
Larrabee	229,624	226,202	98.5
Fresh Kills and/or Goethals	192,148	192,148	100
Gowanus	77,921	76,889	98.7

Table 3-2: Habitat associations of onshore interconnection cable options.

Onshore Route Options	Total Area (km^2)	Habitat Type (% of Total Area)							
		Barren	Developed	Forested	Herbaceous	Planted/ Cultivated	Shrubland	Water	Wetlands
Atlantic and/or Larrabee	0.5	0.0	99.8	0.0	0.2	0.0	0.0	0.0	0.0
Atlantic	2.0	1.7	68.6	14.1	0.2	0.3	0.3	0.0	15.0
Larrabee	6.8	0.6	75.8	13.1	0.3	2.1	0.8	0.1	7.3
Fresh Kills and/or Goethals	5.7	0.0	80.7	7.5	0.4	0.1	0.1	0.4	10.8
Gowanus	2.3	1.1	94.2	0.9	2.5	0.5	0.9	0.0	0.0

[1] Barren Land includes classifications of Dry Salt Flats, Beaches, Sandy Areas other than Beaches, Bare Exposed Rock, Strip Mines, Quarries, Gravel Pits, Transitional Areas, and Mixed Barren Land.

3.3.2. Species Potentially Present within the Onshore Facilities Area

Due to the mobility of birds, a variety of species have the potential to pass through the habitats within or adjacent to the Onshore Project Area. Table 3-3 lists species of greatest conservation need (SGCN) identified by the State of New Jersey for their State Wildlife Action Plan (SWAP)[4] in 2018 and by the State of New York Wildlife Action Plan[5] in 2015 for species detected at least 30 days over the last ten years within 9.3 mi (15 km) of the centroid of the onshore sites in the eBird database. State listed species for New York were obtained online and for New Jersey from the 2018 SWAP. The Federal and IPaC of each species is included. There are 3 federally listed and 79 New Jersey and 8 New York state-listed species that may occur in the vicinity of the Onshore Facilities. Additionally, we provide species habitat associations obtained from species fact sheets from the BirdLife International Data Zone.[6] Table 3-4 lists all species detected at least 30 days over the last ten years (2012-2022) within 9.3 mi (15 km) of the centroid of the onshore sites in the eBird database.

[4] https://www.nj.gov/dep/fgw/ensp/waphome.htm;
[5] https://www.dec.ny.gov/animals/7179.html
[7] http://seamap.env.duke.edu/models/mdat

Table 3-3: List of species observed by eBird users in the general Onshore Project Area, their primary and general breeding habitats, and presence at each site. Species that were observed less than 30 days per year are not included in this list. A/L = Atlantic and/or Larrabee, A = Atlantic, L = Larrabee, FG/GO = Fresh Kills/Goethals and/or Gowanus, FG = Fresh Kills and/or Goethals, GO = Gowanus.

Common Name	*Latin Name*	Primary Habitat	General Breeding Habitat	New Jersey			New York		
				A/L	A	L	FG/GO	FG	GO
Brant	*Branta bernicla*	Coastal	Grassland	•	•	•	•	•	•
American Black Duck	*Anas rubripes*	Freshwater	Wetland	•	•	•	•	•	•
Northern Pintail	*Anas acuta*	Freshwater, Marine	Wetland, Coastal	•	•	•	•	•	•
Common Eider	*Somateria mollissima*	Marine	Coastal, Intertidal	•	•	•	•		
Hooded Merganser	*Lophodytes cucullatus*	Freshwater	Forest, Wetland	•	•	•	•	•	•
Pied-billed Grebe	*Podilymbus podiceps*	Coastal	Wetland	•	•	•	•	•	•
Black-billed Cuckoo	*Coccyzus erythropthalmus*	Terrestrial	Forest, Shrubland	•	•	•			
Common Nighthawk	*Chordeiles minor*	Terrestrial, Aquatic	Grassland, Forest, Wetland	•	•	•	•	•	•
Chimney Swift	*Chaetura pelagica*	Terrestrial	Forest	•	•	•	•	•	•
King Rail	*Rallus elegans*	Freshwater	Wetland				•	•	•
Clapper Rail	*Rallus crepitans*	Freshwater	Marine Intertidal, Forest, Wetland	•	•	•	•	•	•
Virginia Rail	*Rallus limicola*	Freshwater	Wetland					•	
Common Gallinule	*Gallinula galeata*	Freshwater, Marine	Coastal/Supratidal, Wetland	•	•				
American Oystercatcher	*Haematopus palliatus*	Marine	Marine Intertidal	•	•	•	•	•	•
Piping Plover	*Charadrius melodus*	Marine	Coastal/Supratidal, Wetland	•	•	•	•		
Whimbrel	*Numenius phaeopus*	Terrestrial	Forest, Grassland, Shrubland	•	•	•	•		
Ruddy Turnstone	*Arenaria interpres*	Freshwater	Grassland, Wetland	•	•	•	•	•	•
Red Knot	*Calidris canutus*	Marine	Grassland, Wetland				•		
Sanderling	*Calidris alba*	Marine	Grassland	•	•	•	•	•	
Purple Sandpiper	*Calidris maritima*	Freshwater, Marine	Grassland, Intertidal, Wetland	•	•	•			
Semipalmated Sandpiper	*Calidris pusilla*	Freshwater, Marine	Grassland, Wetland	•	•	•	•	•	•
American Woodcock	*Scolopax minor*	Terrestrial	Forest	•	•	•	•	•	•
Spotted Sandpiper	*Actitis macularius*	Freshwater	Wetland	•	•	•	•	•	•
Willet	*Tringa semipalmata*	Marine	Intertidal, Wetland)	•	•	•	•	•	
Least Tern	*Sternula antillarum*	Marine	Coastal, Intertidal	•	•	•	•	•	•
Caspian Tern	*Hydroprogne caspia*	Freshwater, Marine	Wetland, Coastal, Intertidal	•	•	•	•	•	•
Black Tern	*Chlidonias niger*	Freshwater, Marine	Marine, Wetland				•		
Roseate Tern	*Sterna dougallii*	Marine	Coastal, Marine	•		•			
Common Tern	*Sterna hirundo*	Freshwater, Marine	Coastal/Supratidal, Wetland	•	•	•	•	•	•
Forster's Tern	*Sterna forsteri*	Marine	Marine, Wetland	•	•	•	•	•	•
Black Skimmer	*Rynchops niger*	Marine	Intertidal, Wetland	•	•	•	•	•	•
Common Loon	*Gavia immer*	Aquatic	Wetland, Marine	•	•	•	•	•	•
American Bittern	*Botaurus lentiginosus*	Freshwater	Wetland				•	•	
Great Blue Heron	*Ardea herodias*	Terrestrial, Aquatic	Forest, Intertidal, Wetland	•	•	•	•	•	•

Common Name	*Latin Name*	Primary Habitat	General Breeding Habitat	New Jersey			New York		
				A/L	A	L	FG/GO	FG	GO
Snowy Egret	*Egretta thula*	Terrestrial, Aquatic	Forest, Intertidal, Wetland	•	•	•	•	•	•
Little Blue Heron	*Egretta caerulea*	Terrestrial, Aquatic	Forest, Intertidal, Wetland	•	•	•	•	•	•
Tricolored Heron	*Egretta tricolor*	Terrestrial, Aquatic	Forest, Intertidal, Wetland			•			
Black-crowned Night-Heron	*Nycticorax nycticorax*	Terrestrial, Aquatic	Forest, Intertidal, Wetland	•	•	•	•	•	•
Yellow-crowned Night-Heron	*Nyctanassa violacea*	Terrestrial, Aquatic	Forest, Intertidal, Wetland	•	•	•	•	•	•
Glossy Ibis	*Plegadis falcinellus*	Terrestrial, Aquatic	Wetland, Coastal	•	•	•	•	•	•
Osprey	*Pandion haliaetus*	Terrestrial, Aquatic	Forest, Coastal, Wetland	•	•	•	•	•	•
Northern Harrier	*Circus hudsonius*	Terrestrial, Aquatic	Forest, Grassland, Shrubland, Wetland	•	•	•	•	•	•
Sharp-shinned Hawk	*Accipiter striatus*	Terrestrial	Forest, Savanna, Shrubland	•	•	•	•	•	•
Cooper's Hawk	*Accipiter cooperii*	Terrestrial	Forest	•	•	•	•	•	•
Bald Eagle	*Haliaeetus leucocephalus*	Terrestrial, Aquatic	Wetland, Forest, Intertidal	•	•	•	•	•	•
Red-shouldered Hawk	*Buteo lineatus*	Terrestrial	Forest	•	•	•	•	•	•
Broad-winged Hawk	*Buteo platypterus*	Terrestrial	Forest	•	•	•	•	•	
Barred Owl	*Strix varia*	Terrestrial	Forest, Wetland	•	•	•			
Short-eared Owl	*Asio flammeus*	Terrestrial	Grassland				•		•
Red-headed Woodpecker	*Melanerpes erythrocephalus*	Terrestrial	Forest, Grassland				•	•	
American Kestrel	*Falco sparverius*	Terrestrial, Aquatic	Forest, Grassland, Shrubland, Wetland	•	•	•	•	•	•
Peregrine Falcon	*Falco peregrinus*	Terrestrial, Aquatic	Non-breeder	•	•	•	•	•	•
Acadian Flycatcher	*Empidonax virescens*	Terrestrial	Forest, Wetland	•	•	•			
Willow Flycatcher	*Empidonax traillii*	Terrestrial	Shrubland, Wetland	•	•	•	•	•	•
Least Flycatcher	*Empidonax minimus*	Terrestrial	Forest, Shrubland	•	•	•	•	•	•
Yellow-throated Vireo	*Vireo flavifrons*	Terrestrial	Forest	•	•	•	•	•	
Blue-headed Vireo	*Vireo solitarius*	Terrestrial	Forest	•	•	•	•	•	•
Horned Lark	*Eremophila alpestris*	Terrestrial	Grassland, Shrubland, Coastal	•	•	•	•	•	•
Bank Swallow	*Riparia riparia*	Terrestrial, Aquatic	Grassland, Wetland	•	•	•	•	•	•
Cliff Swallow	*Petrochelidon pyrrhonota*	Terrestrial, Aquatic	Forest, Grassland, Wetlands	•	•	•			
Winter Wren	*Troglodytes hiemalis*	Terrestrial	Forest, Shrubland	•	•	•	•	•	•
Marsh Wren	*Cistothorus palustris*	Terrestrial, Aquatic	Wetland, Intertidal, Wetland	•	•	•	•	•	•
Brown Thrasher	*Toxostoma rufum*	Terrestrial	Shrubland, Forest	•	•	•	•	•	•
Veery	*Catharus fuscescens*	Terrestrial	Forest	•	•	•	•	•	•
Gray-cheeked Thrush	*Catharus minimus*	Terrestrial	Shrubland, Forest, Grassland				•	•	•
Wood Thrush	*Hylocichla mustelina*	Terrestrial	Forest	•	•	•	•	•	•
Grasshopper Sparrow	*Ammodramus savannarum*	Terrestrial	Grassland, Shrubland	•	•	•			
Field Sparrow	*Spizella pusilla*	Terrestrial	Forest, Grassland, Shrubland	•	•	•	•	•	•
Vesper Sparrow	*Pooecetes gramineus*	Terrestrial	Grassland, Shrubland						•
Seaside Sparrow	*Ammospiza maritima*	Coastal	Intertidal			•	•	•	
Saltmarsh Sparrow	*Ammospiza caudacuta*	Terrestrial, Aquatic	Marine Intertidal			•	•	•	•
Savannah Sparrow	*Passerculus sandwichensis*	Terrestrial, Aquatic	Coastal, Grassland, Shrubland, Wetland	•	•	•	•	•	•

Common Name	*Latin Name*	Primary Habitat	General Breeding Habitat	New Jersey			New York		
				A/L	A	L	FG/GO	FG	GO
Eastern Towhee	*Pipilo erythrophthalmus*	Terrestrial	Forest, Shrubland	•	•	•	•	•	•
Bobolink	*Dolichonyx oryzivorus*	Terrestrial	Grassland	•	•		•	•	•
Eastern Meadowlark	*Sturnella magna*	Terrestrial	Grassland, Shrubland	•	•	•			
Rusty Blackbird	*Euphagus carolinus*	Terrestrial, Aquatic	Wetland	•	•	•	•	•	
Worm-eating Warbler	*Helmitheros vermivorum*	Terrestrial	Forest	•	•	•			
Louisiana Waterthrush	*Parkesia motacilla*	Terrestrial, Aquatic	Forest, Wetland, Shrubland	•	•	•		•	
Blue-winged Warbler	*Vermivora cyanoptera*	Terrestrial	Grassland, Shrubland	•	•	•	•	•	•
Black-and-white Warbler	*Mniotilta varia*	Terrestrial	Forest	•	•	•	•	•	•
Prothonotary Warbler	*Protonotaria citrea*	Terrestrial	Forest		•	•			
Nashville Warbler	*Leiothlypis ruficapilla*	Terrestrial	Forest	•	•	•	•	•	•
Hooded Warbler	*Setophaga citrina*	Terrestrial	Forest	•	•	•	•	•	
Cape May Warbler	*Setophaga tigrina*	Terrestrial	Forest	•	•	•	•	•	•
Northern Parula	*Setophaga americana*	Terrestrial	Forest	•	•	•	•	•	•
Bay-breasted Warbler	*Setophaga castanea*	Terrestrial	Forest	•	•	•	•	•	•
Blackburnian Warbler	*Setophaga fusca*	Terrestrial	Forest	•	•	•	•	•	•
Black-throated Blue Warbler	*Setophaga caerulescens*	Terrestrial	Forest	•	•	•	•	•	•
Prairie Warbler	*Setophaga discolor*	Terrestrial	Shrubland, Forest	•	•	•	•	•	•
Black-throated Green Warbler	*Setophaga virens*	Terrestrial	Forest, Wetland	•	•	•	•	•	•
Canada Warbler	*Cardellina canadensis*	Terrestrial	Forest	•	•	•	•	•	•
Scarlet Tanager	*Piranga olivacea*	Terrestrial	Forest	•	•	•	•	•	•
Dickcissel	*Spiza americana*	Terrestrial	Grassland				•	•	•

Table 3-4: Complete list of species observed by eBird users in the general Onshore Project Area, their federal and state conservation statuses, and presence indicated in the IPaC database (https://ipac.ecosphere.fws.gov/). Note: BCC = Bird of Conservation Concern, PS = Potentially susceptible to development.

Common Name	Scientific Name	Federally Listed	New Jersey			New York			IPaC
			State Listed	SGCN	Focal Species	State Listed	SGCN	High Priority	
Snow Goose	*Anser caerulescens*								
Greater White-fronted Goose	*Anser albifrons*								
Pink-footed Goose	*Anser brachyrhynchus*								
Brant	*Branta bernicla*			•					
Cackling Goose	*Branta hutchinsii*								
Canada Goose	*Branta canadensis*								
Mute Swan	*Cygnus olor*								
Wood Duck	*Aix sponsa*								
Blue-winged Teal	*Spatula discors*								
Northern Shoveler	*Spatula clypeata*								
Gadwall	*Mareca strepera*								
Eurasian Wigeon	*Mareca penelope*								
American Wigeon	*Mareca americana*								
Mallard	*Anas platyrhynchos*								
American Black Duck	*Anas rubripes*			•			•	•	
Northern Pintail	*Anas acuta*			•			•		
Green-winged Teal	*Anas crecca*								
Canvasback	*Aythya valisineria*								
Redhead	*Aythya americana*								
Ring-necked Duck	*Aythya collaris*								
Greater Scaup	*Aythya marila*						•		
Lesser Scaup	*Aythya affinis*						•		
King Eider	*Somateria spectabilis*								
Common Eider	*Somateria mollissima*			•			•		PS
Harlequin Duck	*Histrionicus histrionicus*						•		
Surf Scoter	*Melanitta perspicillata*						•		PS
White-winged Scoter	*Melanitta deglandi*								PS
Black Scoter	*Melanitta americana*						•		PS
Long-tailed Duck	*Clangula hyemalis*						•		PS
Bufflehead	*Bucephala albeola*								
Common Goldeneye	*Bucephala clangula*						•		
Hooded Merganser	*Lophodytes cucullatus*		•						
Common Merganser	*Mergus merganser*								
Red-breasted Merganser	*Mergus serrator*								PS

Common Name	Scientific Name	Federally Listed	New Jersey			New York			IPaC
			State Listed	SGCN	Focal Species	State Listed	SGCN	High Priority	
Ruddy Duck	*Oxyura jamaicensis*						•		
Northern Bobwhite	*Colinus virginianus*			•	•		•	•	
Wild Turkey	*Meleagris gallopavo*								
Ruffed Grouse	*Bonasa umbellus*			•			•		
Pied-billed Grebe	*Podilymbus podiceps*		•	•	•		•		
Horned Grebe	*Podiceps auritus*						•		
Red-necked Grebe	*Podiceps grisegena*								
Western Grebe	*Aechmophorus occidentalis*								
Rock Pigeon	*Columba livia*								
Mourning Dove	*Zenaida macroura*								
Yellow-billed Cuckoo	*Coccyzus americanus*								
Black-billed Cuckoo	*Coccyzus erythropthalmus*		•	•			•		BCC
Common Nighthawk	*Chordeiles minor*		•	•			•	•	
Chuck-will's-widow	*Antrostomus carolinensis*			•					
Eastern Whip-poor-will	*Antrostomus vociferus*		•						BCC
Chimney Swift	*Chaetura pelagica*			•					BCC
Ruby-throated Hummingbird	*Archilochus colubris*								
Calliope Hummingbird	*Selasphorus calliope*								
King Rail	*Rallus elegans*		•	•			•	•	BCC
Clapper Rail	*Rallus crepitans*			•					
Virginia Rail	*Rallus limicola*		•						
Sora	*Porzana carolina*		•	•					
Common Gallinule	*Gallinula galeata*		•						
American Coot	*Fulica americana*								
Black Rail	*Laterallus jamaicensis*		•	•	•	•	•	•	
American Oystercatcher	*Haematopus palliatus*		•	•	•				BCC
Black-bellied Plover	*Pluvialis squatarola*						•		
American Golden-Plover	*Pluvialis dominica*								
Semipalmated Plover	*Charadrius semipalmatus*								
Piping Plover	*Charadrius melodus*	T	•	•	•	•	•	•	
Killdeer	*Charadrius vociferus*								
Upland Sandpiper	*Bartramia longicauda*		•	•			•	•	
Whimbrel	*Numenius phaeopus*		•	•			•	•	
Marbled Godwit	*Limosa fedoa*			•					
Ruddy Turnstone	*Arenaria interpres*			•	•		•		BCC
Red Knot	*Calidris canutus*	T	•	•	•		•	•	
Sanderling	*Calidris alba*		•	•					

Common Name	Scientific Name	Federally Listed	New Jersey			New York			IPaC
			State Listed	SGCN	Focal Species	State Listed	SGCN	High Priority	
Dunlin	*Calidris alpina*								
Purple Sandpiper	*Calidris maritima*			•			•		BCC
Baird's Sandpiper	*Calidris bairdii*								
Least Sandpiper	*Calidris minutilla*								
White-rumped Sandpiper	*Calidris fuscicollis*								
Pectoral Sandpiper	*Calidris melanotos*								
Semipalmated Sandpiper	*Calidris pusilla*		•	•			•	•	
Western Sandpiper	*Calidris mauri*								
Short-billed Dowitcher	*Limnodromus griseus*						•	•	BCC
American Woodcock	*Scolopax minor*			•	•		•		
Wilson's Snipe	*Gallinago delicata*								
Wilson's Phalarope	*Phalaropus tricolor*			•					
Spotted Sandpiper	*Actitis macularius*		•						
Solitary Sandpiper	*Tringa solitaria*								
Greater Yellowlegs	*Tringa melanoleuca*						•		
Willet	*Tringa semipalmata*			•			•		BCC
Lesser Yellowlegs	*Tringa flavipes*								BCC
Dovekie	*Alle alle*								
Razorbill	*Alca torda*						•		PS
Bonaparte's Gull	*Chroicocephalus philadelphia*						•		
Black-headed Gull	*Chroicocephalus ridibundus*								
Little Gull	*Hydrocoloeus minutus*						•	•	
Laughing Gull	*Leucophaeus atricilla*						•		
Ring-billed Gull	*Larus delawarensis*								PS
Herring Gull	*Larus argentatus*								
Iceland Gull	*Larus glaucoides*								
Lesser Black-backed Gull	*Larus fuscus*								
Glaucous Gull	*Larus hyperboreus*								
Great Black-backed Gull	*Larus marinus*								
Least Tern	*Sternula antillarum*		•	•	•		•		
Gull-billed Tern	*Gelochelidon nilotica*		•	•			•		BCC
Caspian Tern	*Hydroprogne caspia*		•				•		
Black Tern	*Chlidonias niger*			•		•	•	•	
Roseate Tern	*Sterna dougallii*	E	•	•		•	•	•	PS
Common Tern	*Sterna hirundo*		•	•	•		•		
Forster's Tern	*Sterna forsteri*			•	•		•		
Royal Tern	*Thalasseus maximus*								PS

Common Name	Scientific Name	Federally Listed	New Jersey			New York			IPaC
			State Listed	SGCN	Focal Species	State Listed	SGCN	High Priority	
Black Skimmer	*Rynchops niger*		•	•	•		•	•	BCC
Red-throated Loon	*Gavia stellata*								PS
Pacific Loon	*Gavia pacifica*								
Common Loon	*Gavia immer*			•			•		PS
Wilson's Storm-Petrel	*Oceanites oceanicus*								
Brown Booby	*Sula leucogaster*								
Northern Gannet	*Morus bassanus*								
Great Cormorant	*Phalacrocorax carbo*								
Double-crested Cormorant	*Nannopterum auritum*								PS
Brown Pelican	*Pelecanus occidentalis*								PS
American Bittern	*Botaurus lentiginosus*		•	•			•		
Least Bittern	*Ixobrychus exilis*		•	•			•		
Great Blue Heron	*Ardea herodias*		•						
Great Egret	*Ardea alba*						•		
Snowy Egret	*Egretta thula*		•	•	•		•		
Little Blue Heron	*Egretta caerulea*		•	•	•		•		
Tricolored Heron	*Egretta tricolor*		•	•	•		•		
Cattle Egret	*Bubulcus ibis*		•	•			•	•	
Green Heron	*Butorides virescens*								
Black-crowned Night-Heron	*Nycticorax nycticorax*		•	•			•		
Yellow-crowned Night-Heron	*Nyctanassa violacea*		•	•			•		
Glossy Ibis	*Plegadis falcinellus*		•				•		
Black Vulture	*Coragyps atratus*								
Turkey Vulture	*Cathartes aura*								
Osprey	*Pandion haliaetus*		•	•					
Golden Eagle	*Aquila chrysaetos*			•		•	•		Eagle Act
Northern Harrier	*Circus hudsonius*		•	•	•				
Sharp-shinned Hawk	*Accipiter striatus*		•						
Cooper's Hawk	*Accipiter cooperii*		•						
Northern Goshawk	*Accipiter gentilis*		•	•			•		
Bald Eagle	*Haliaeetus leucocephalus*		•	•			•		Eagle Act
Red-shouldered Hawk	*Buteo lineatus*		•	•			•		
Broad-winged Hawk	*Buteo platypterus*		•	•					
Red-tailed Hawk	*Buteo jamaicensis*								
Barn Owl	*Tyto alba*		•	•			•	•	
Eastern Screech-Owl	*Megascops asio*								
Great Horned Owl	*Bubo virginianus*								

Common Name	Scientific Name	Federally Listed	New Jersey			New York			IPaC
			State Listed	SGCN	Focal Species	State Listed	SGCN	High Priority	
Snowy Owl	*Bubo scandiacus*								
Barred Owl	*Strix varia*		•	•					
Long-eared Owl	*Asio otus*		•	•			•		BCC
Short-eared Owl	*Asio flammeus*		•	•		•	•	•	
Belted Kingfisher	*Megaceryle alcyon*								
Yellow-bellied Sapsucker	*Sphyrapicus varius*								
Red-headed Woodpecker	*Melanerpes erythrocephalus*		•	•	•		•	•	BCC
Red-bellied Woodpecker	*Melanerpes carolinus*								
Downy Woodpecker	*Dryobates pubescens*								
Hairy Woodpecker	*Dryobates villosus*								
Pileated Woodpecker	*Dryocopus pileatus*								
Northern Flicker	*Colaptes auratus*								
American Kestrel	*Falco sparverius*		•	•			•		
Merlin	*Falco columbarius*								
Peregrine Falcon	*Falco peregrinus*		•	•	•	•	•		
Monk Parakeet	*Myiopsitta monachus*								
Olive-sided Flycatcher	*Contopus cooperi*			•					
Eastern Wood-Pewee	*Contopus virens*								
Acadian Flycatcher	*Empidonax virescens*			•					
Willow Flycatcher	*Empidonax traillii*			•					
Least Flycatcher	*Empidonax minimus*		•						
Eastern Phoebe	*Sayornis phoebe*								
Great Crested Flycatcher	*Myiarchus crinitus*								
Eastern Kingbird	*Tyrannus tyrannus*								
White-eyed Vireo	*Vireo griseus*								
Yellow-throated Vireo	*Vireo flavifrons*			•					
Blue-headed Vireo	*Vireo solitarius*		•						
Warbling Vireo	*Vireo gilvus*								
Red-eyed Vireo	*Vireo olivaceus*								
Loggerhead Shrike	*Lanius ludovicianus*		•	•		•	•	•	
Blue Jay	*Cyanocitta cristata*								
American Crow	*Corvus brachyrhynchos*								
Fish Crow	*Corvus ossifragus*								
Common Raven	*Corvus corax*								
Carolina Chickadee	*Poecile carolinensis*								
Black-capped Chickadee	*Poecile atricapillus*								
Tufted Titmouse	*Baeolophus bicolor*								

Common Name	Scientific Name	Federally Listed	New Jersey			New York			IPaC
			State Listed	SGCN	Focal Species	State Listed	SGCN	High Priority	
Horned Lark	*Eremophila alpestris*		•	•			•	•	
Northern Rough-winged Swallow	*Stelgidopteryx serripennis*								
Purple Martin	*Progne subis*								
Tree Swallow	*Tachycineta bicolor*								
Bank Swallow	*Riparia riparia*			•					
Barn Swallow	*Hirundo rustica*								
Cliff Swallow	*Petrochelidon pyrrhonota*		•						
Ruby-crowned Kinglet	*Corthylio calendula*								
Golden-crowned Kinglet	*Regulus satrapa*								
Red-breasted Nuthatch	*Sitta canadensis*								
White-breasted Nuthatch	*Sitta carolinensis*								
Brown Creeper	*Certhia americana*								
Blue-gray Gnatcatcher	*Polioptila caerulea*								
House Wren	*Troglodytes aedon*								
Winter Wren	*Troglodytes hiemalis*		•						
Sedge Wren	*Cistothorus stellaris*		•	•					
Marsh Wren	*Cistothorus palustris*			•					
Carolina Wren	*Thryothorus ludovicianus*								
European Starling	*Sturnus vulgaris*								
Gray Catbird	*Dumetella carolinensis*								
Brown Thrasher	*Toxostoma rufum*		•	•			•	•	
Northern Mockingbird	*Mimus polyglottos*								
Eastern Bluebird	*Sialia sialis*								
Veery	*Catharus fuscescens*		•	•					
Gray-cheeked Thrush	*Catharus minimus*		•						
Bicknell's Thrush	*Catharus bicknelli*			•			•	•	
Swainson's Thrush	*Catharus ustulatus*								
Hermit Thrush	*Catharus guttatus*								
Wood Thrush	*Hylocichla mustelina*		•	•	•		•		BCC
American Robin	*Turdus migratorius*								
Cedar Waxwing	*Bombycilla cedrorum*								
House Sparrow	*Passer domesticus*								
American Pipit	*Anthus rubescens*								
House Finch	*Haemorhous mexicanus*								
Purple Finch	*Haemorhous purpureus*								
Common Redpoll	*Acanthis flammea*								
Red Crossbill	*Loxia curvirostra*								

Common Name	Scientific Name	Federally Listed	New Jersey			New York			IPaC
			State Listed	SGCN	Focal Species	State Listed	SGCN	High Priority	
Pine Siskin	*Spinus pinus*								
American Goldfinch	*Spinus tristis*								
Snow Bunting	*Plectrophenax nivalis*								
Grasshopper Sparrow	*Ammodramus savannarum*		•	•	•		•	•	
Chipping Sparrow	*Spizella passerina*								
Field Sparrow	*Spizella pusilla*			•					
American Tree Sparrow	*Spizelloides arborea*								
Fox Sparrow	*Passerella iliaca*								
Dark-eyed Junco	*Junco hyemalis*								
White-crowned Sparrow	*Zonotrichia leucophrys*								
White-throated Sparrow	*Zonotrichia albicollis*								
Vesper Sparrow	*Pooecetes gramineus*		•	•	•		•	•	
Seaside Sparrow	*Ammospiza maritima*			•					
Nelson's Sparrow	*Ammospiza nelsoni*								
Saltmarsh Sparrow	*Ammospiza caudacuta*		•	•					
Savannah Sparrow	*Passerculus sandwichensis*		•	•					
Henslow's Sparrow	*Centronyx henslowii*		•	•					
Song Sparrow	*Melospiza melodia*								
Lincoln's Sparrow	*Melospiza lincolnii*								
Swamp Sparrow	*Melospiza georgiana*								
Eastern Towhee	*Pipilo erythrophthalmus*			•					
Yellow-breasted Chat	*Icteria virens*		•	•			•	•	
Bobolink	*Dolichonyx oryzivorus*		•	•	•		•	•	BCC
Eastern Meadowlark	*Sturnella magna*		•	•	•		•	•	
Orchard Oriole	*Icterus spurius*								
Baltimore Oriole	*Icterus galbula*								
Red-winged Blackbird	*Agelaius phoeniceus*								
Brown-headed Cowbird	*Molothrus ater*								
Rusty Blackbird	*Euphagus carolinus*			•			•	•	
Common Grackle	*Quiscalus quiscula*								
Boat-tailed Grackle	*Quiscalus major*								
Ovenbird	*Seiurus aurocapilla*								
Worm-eating Warbler	*Helmitheros vermivorum*		•	•			•		
Louisiana Waterthrush	*Parkesia motacilla*			•			•		
Northern Waterthrush	*Parkesia noveboracensis*								
Golden-winged Warbler	*Vermivora chrysoptera*		•	•	•		•	•	
Blue-winged Warbler	*Vermivora cyanoptera*			•	•		•		BCC

Common Name	Scientific Name	Federally Listed	New Jersey			New York			IPaC
			State Listed	SGCN	Focal Species	State Listed	SGCN	High Priority	
Black-and-white Warbler	*Mniotilta varia*			•					
Prothonotary Warbler	*Protonotaria citrea*			•	•		•	•	BCC
Swainson's Warbler	*Limnothlypis swainsonii*			•					
Tennessee Warbler	*Leiothlypis peregrina*								
Orange-crowned Warbler	*Leiothlypis celata*								
Nashville Warbler	*Leiothlypis ruficapilla*		•						
Kentucky Warbler	*Geothlypis formosa*		•	•	•				BCC
Common Yellowthroat	*Geothlypis trichas*								
Hooded Warbler	*Setophaga citrina*		•	•					
American Redstart	*Setophaga ruticilla*								
Cape May Warbler	*Setophaga tigrina*			•					
Cerulean Warbler	*Setophaga cerulea*		•	•	•		•		BCC
Northern Parula	*Setophaga americana*		•	•					
Magnolia Warbler	*Setophaga magnolia*								
Bay-breasted Warbler	*Setophaga castanea*			•			•	•	
Blackburnian Warbler	*Setophaga fusca*		•	•					
Yellow Warbler	*Setophaga petechia*								
Chestnut-sided Warbler	*Setophaga pensylvanica*								
Blackpoll Warbler	*Setophaga striata*								
Black-throated Blue Warbler	*Setophaga caerulescens*		•	•			•		
Palm Warbler	*Setophaga palmarum*								
Pine Warbler	*Setophaga pinus*								
Yellow-rumped Warbler	*Setophaga coronata*								
Prairie Warbler	*Setophaga discolor*			•			•		BCC
Black-throated Green Warbler	*Setophaga virens*		•	•					
Canada Warbler	*Cardellina canadensis*		•	•			•	•	BCC
Wilson's Warbler	*Cardellina pusilla*								
Summer Tanager	*Piranga rubra*			•					
Scarlet Tanager	*Piranga olivacea*			•	•		•		
Northern Cardinal	*Cardinalis cardinalis*								
Rose-breasted Grosbeak	*Pheucticus ludovicianus*								
Blue Grosbeak	*Passerina caerulea*								
Indigo Bunting	*Passerina cyanea*								
Dickcissel	*Spiza americana*			•					

3.3.3. Endangered and Threatened Species

3.3.3.1. Roseate Tern

In 1987, the U.S. Fish and Wildlife Service listed the northeastern breeding population of Roseate Tern as Endangered due to population declines related to hunting in the early 20th century, habitat loss, and gull encroachment (Nisbet and Spendelow 1999). Most of the northeastern breeding Roseate Tern population nest on islands off the coast of Buzzards Bay, Massachusetts and Long Island, New York. Individuals are expected to be present near the Onshore and Offshore Facilities areas during the breeding season and spring and fall migration. The New York and New Jersey eBird databases respectively contain 2,483 and 637 Roseate Tern detections from 2012 to 2022 with nearly all observation occurring between May and October (Figure 3-3). However, only 68 detections were made within the Onshore Facilities area during this period.

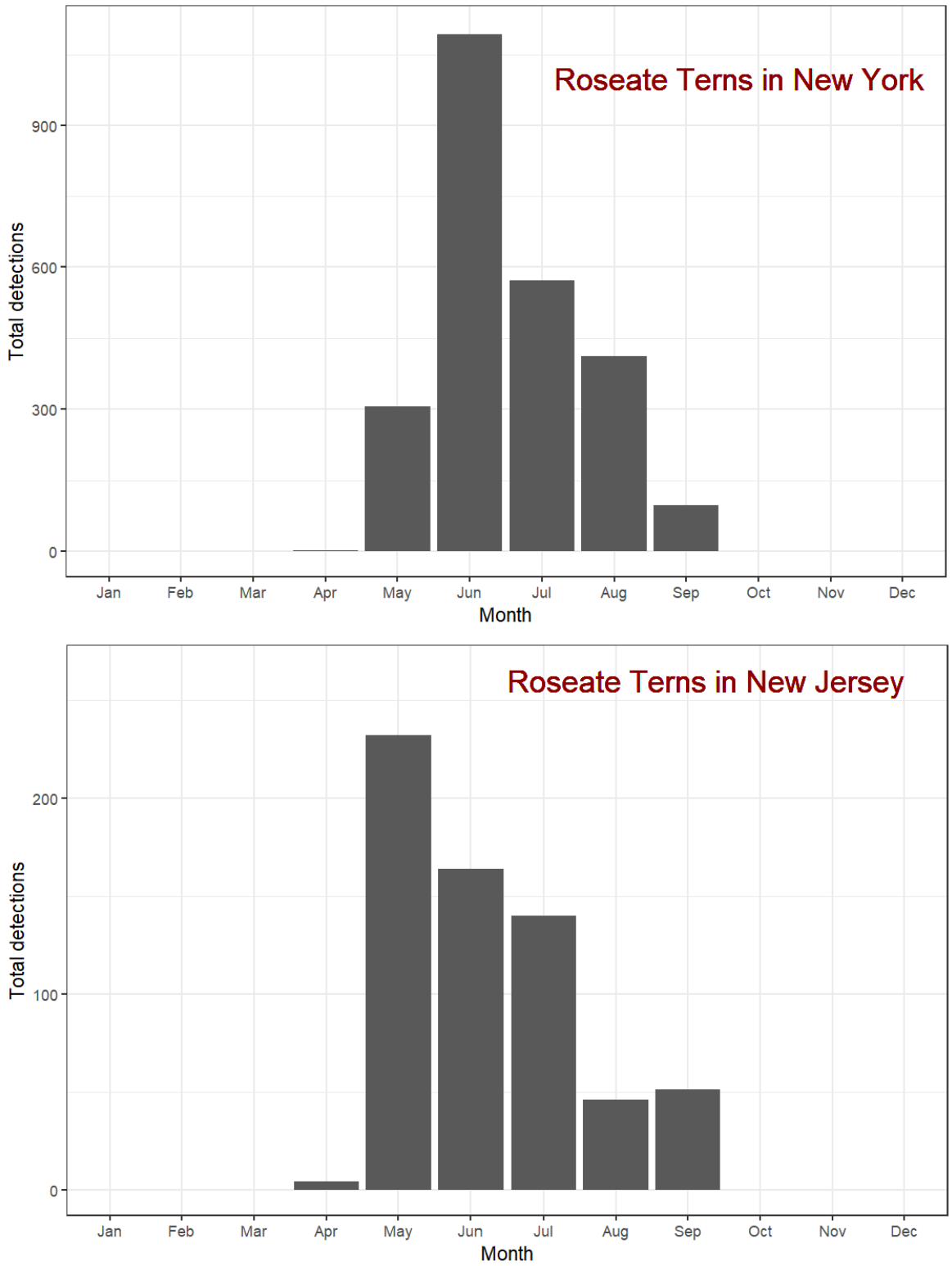

Figure 3-3: 10-year monthly total number of unique encounters (total detections) by eBird list (duplicate list postings removed) of Roseate Terns in coastal New York (upper panel) and New Jersey (lower panel), derived from the eBird database.

3.3.3.2. Red Knot

In 2014, USFWS listed the North Atlantic subspecies of Red Knot (*Calidris canutus rufa*) as Threatened under the Endangered Species Act of 1973 (USFWS 2015). In New York, Red Knot is listed as Threatened, and in New Jersey it is listed as Endangered. Located approximately 100 miles south of the Onshore Facilities area, the Delaware Bay is the most important spring stopover site for a select species of shorebirds, including Red Knot. The *rufa* subspecies breeds in the central and eastern Canadian Arctic and winters at sites as far south as Tierra del Fuego, Argentina. During both migrations, Red Knots use key staging and stopover areas to rest and feed where they utilize habitats including sandy coastal beaches, at or near tidal inlets, or the mouths of bays and estuaries, salt marshes, tidal mudflats, and sandy/gravel beaches where they feed on clams, crustaceans, and invertebrates. The eBird database indicates that 44 total Red Knot detections were made within the Onshore Facilities areas between 2012 and 2022 and that most Red Knots arrive in New York and New Jersey in May and leave by November (Figure 3-4). No part of the Onshore Facilities is near Red Knot critical habitat areas proposed by the USFWS (Figure 3-5).

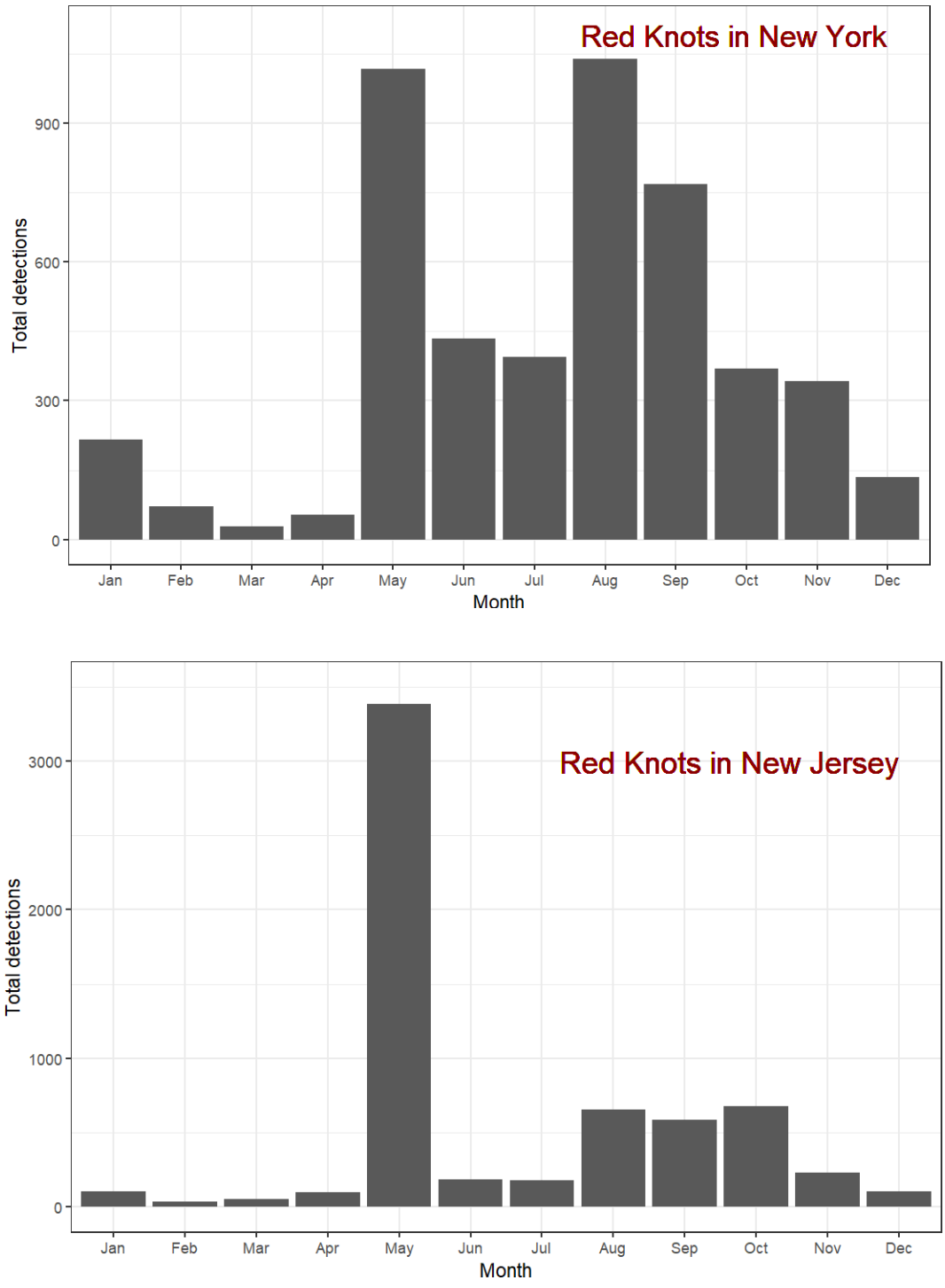

Figure 3-4: 10-year monthly total number of unique encounters (total detections) by eBird list (duplicate list postings removed) of Red Knots in coastal New York (upper panel) and New Jersey (lower panel), derived from the eBird database.

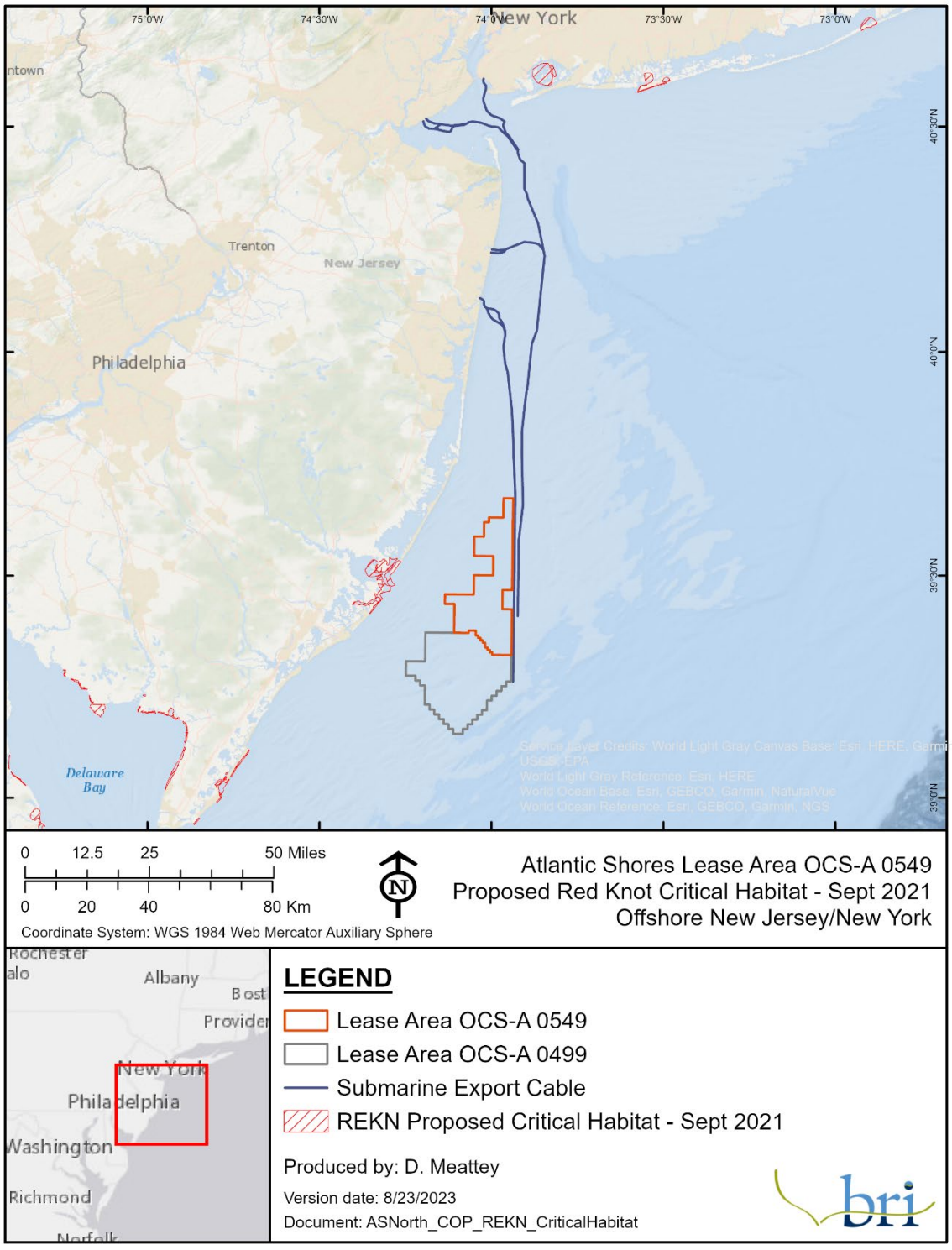

Figure 3-5: USFWS proposed Red Knot critical habitat (as of September 2021) in relation to Onshore and Offshore Project Areas.

3.3.3.3. Piping Plover

The Atlantic Coast population of the Piping Plover was federally listed as Threatened in 1986 and is also listed by the State of New Jersey and New York. Piping Plovers nest on coastal beaches, sandflats at the ends of sand spits and barrier islands, gently sloped foredunes, sparsely vegetated dunes, and washover areas cut into or between dunes. Breeding Piping Plovers feed on exposed wet sand in wash zones; intertidal ocean beach; wrack lines; washover passes; mud, sand, and algal flats; and shorelines of streams, ephemeral ponds, lagoons, and salt marshes by probing for invertebrates at or just below the surface. They use beaches adjacent to foraging areas for roosting and preening. Small sand dunes, debris, and sparse vegetation within adjacent beaches provides shelter from wind and extreme temperatures. The eBird database contains 795 Piping Plover detections at the potential cable landfall areas between 2012 and 2022. Piping Plovers arrive in New York and New Jersey in March, nest along the coasts, and leave by October Figure 3-6 - Figure 3-8). Nests were observed in Sea Girt (one at National Guard Training Center and one at Wreck Pond) near the Atlantic and/or Larrabee Onshore Interconnection Cable Route (Heiser and Davis 2021); recent nesting data was not available for New York. Active Piping Plover nests closest to the New York Onshore Facilities area were recorded at Breezy Point and Fort Tilden in the Rockaways in 2018 (Figure 3-8). All nesting beaches are more than six miles away from the nearest landfall; thus, no impacts are expected.

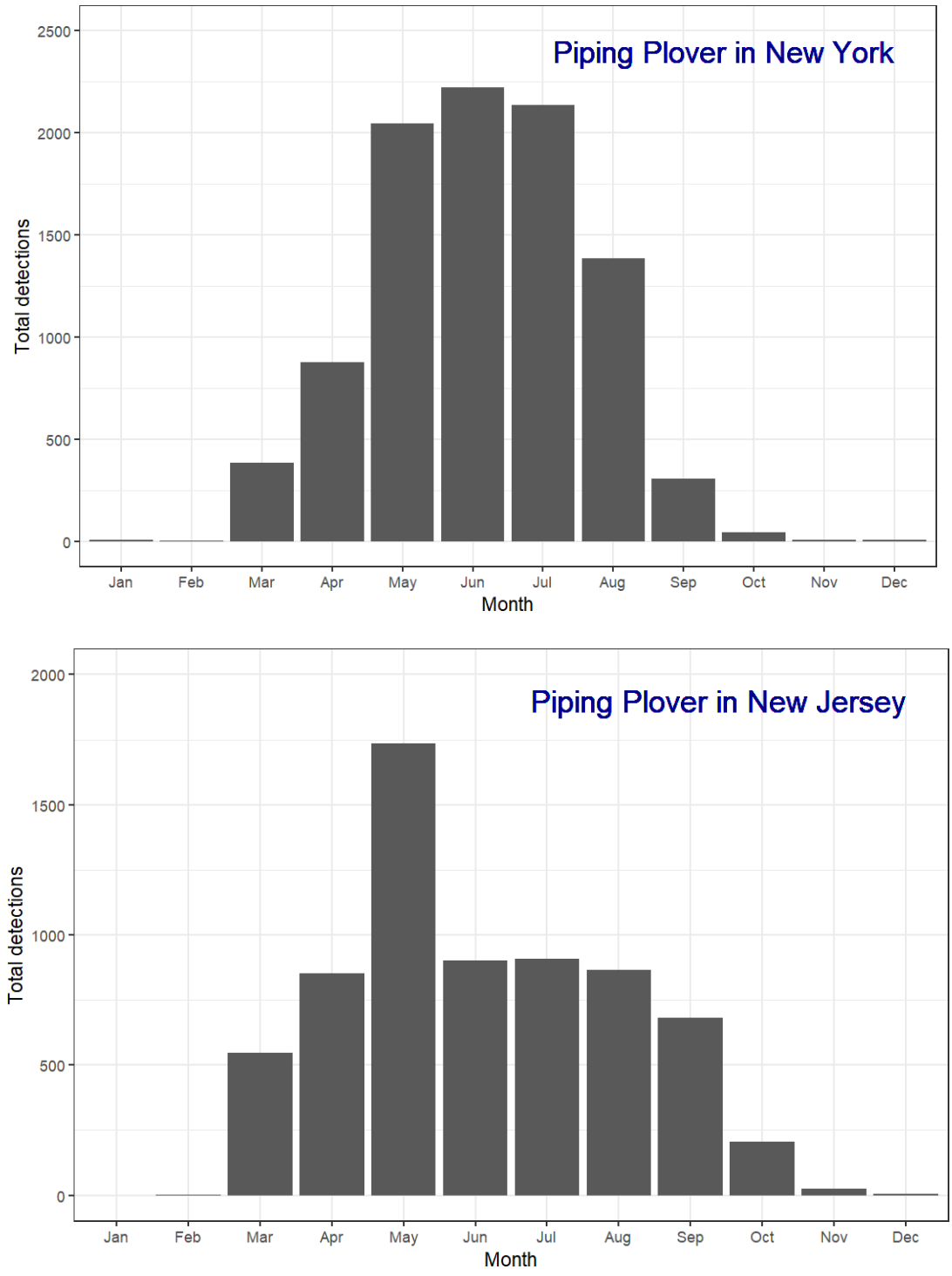

Figure 3-6: 10-year monthly total number of unique encounters (total detections) by eBird list (duplicate list postings removed) of Piping Plovers in coastal New York (upper panel) and New Jersey (lower panel), derived from the eBird database.

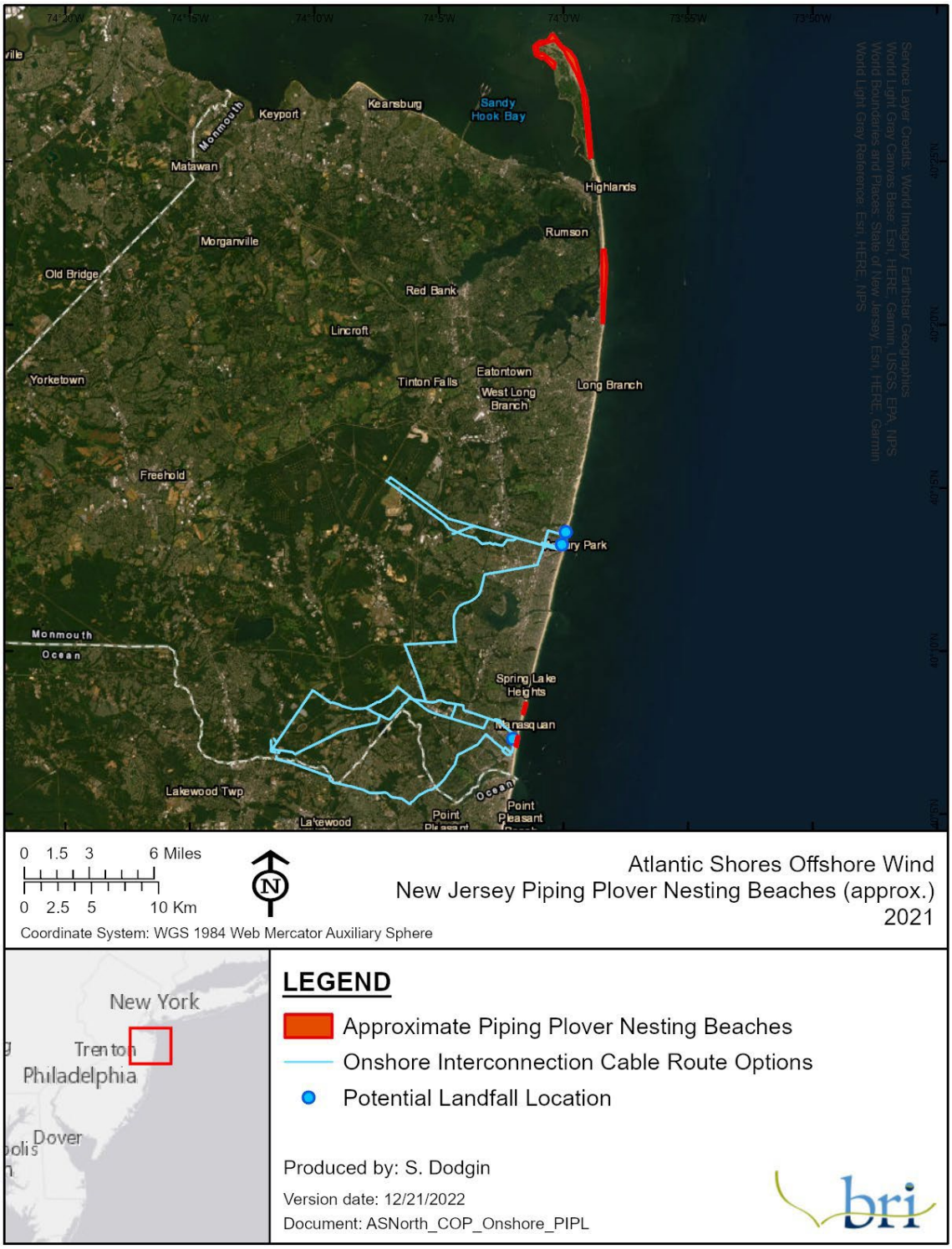

NOTE: Nest site locations are approximations based on site names provided in reports. Nesting reports were unavailable for New York. The absence of noted sites does not mean that they do not exist.

Figure 3-7: Approximate Piping Plover nesting areas (2021) in relation to the New Jersey Project Landfall Areas.

Figure 3-8: Approximate Piping Plover nesting areas (2018) in New York (NYDEC 2018)

3.3.3.4. Saltmarsh Sparrow

The eBird database contains 373 Saltmarsh Sparrow detections at the potential cable landfall areas between 2012 and 2022. Most Saltmarsh Sparrows arrive in New York and New Jersey in May and leave by November; however, a small portion appear to be present year-round (Figure 3-9). Saltmarsh Sparrows are habitat specialists and have an extremely narrow suitability range. Suitable habitat consists of high marsh vegetation with dense layers of thatch for nest construction and protection from tides (Hartley and Weldon 2020). Consensus on the Saltmarsh Sparrow's conservation classification has not been reached by the USFWS (Clark 2020), however it is listed as a species of greatest conservation need in New Jersey. State and federal agencies recognize the species population is in decline and have formed a partnership with the Atlantic Coast Joint Venture to conserve Saltmarsh Sparrows and coastal marshes (Atlantic Coast Joint Venture 2022). The potential Project landfalls are located in highly developed areas, consisting primarily of impervious surfaces. Although suitable habitat appears to exist within the area of potential landfall development, no disturbance to Saltmarsh Sparrow is anticipated because all routes and landfalls are co-located with existing development. Furthermore, saltmarsh sparrows do not utilize beaches or dunes for foraging or breeding and thus would not be impacted by disturbance related to connecting the offshore export cable routes to the landfalls.

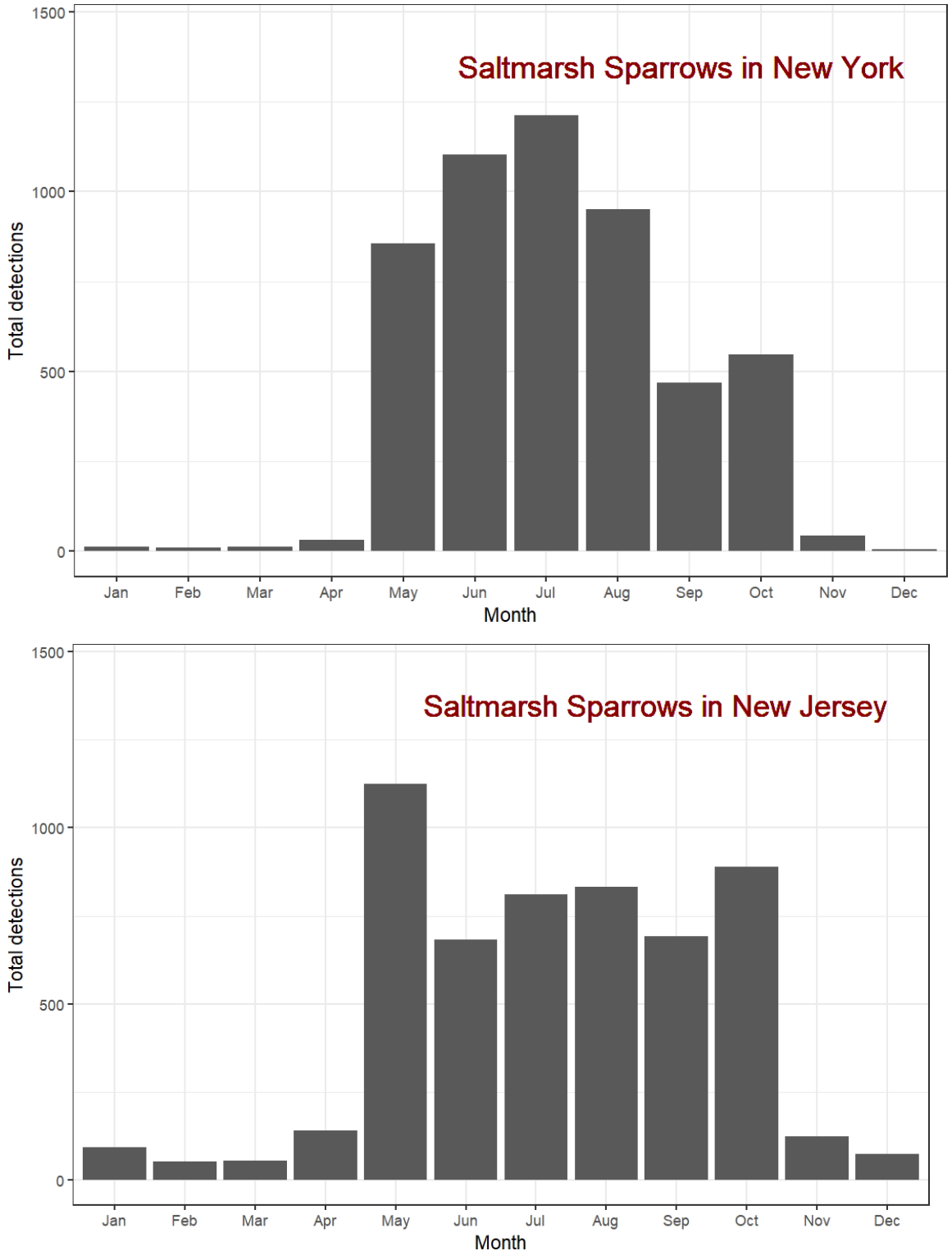

Figure 3-9: 10-year monthly total number of unique encounters (total detections) by eBird list (duplicate list postings removed) of Saltmarsh Sparrows in coastal New York (upper panel) and New Jersey (lower panel), derived from the eBird database.

3.3.3.5. Eastern Black Rail

No Eastern Black Rail detections were reported in the vicinity of the Onshore Facilities areas in the eBird database between 2012 and 2022. Eastern Black Rails are habitat specialists and have an extremely narrow suitability range. Suitable habitat consists of coastal wetlands characterized by shallow fresh to brackish water and dense emergent vegetation (USFWS 2020). While suitable habitat within the area of potential landfall development may exist, disturbance to the Eastern Black Rail is not anticipated. Although this species is notoriously secretive (Atlantic Coast Joint Venture 2020) and could explain why no detections were recorded over the past 10 years in eBird, the landfalls and cable routes are co-located with existing infrastructure. Additionally, Eastern Black Rails reside exclusively in marshlands which are not expected to be impacted by Onshore Facilities Construction. For the reasons stated above, and due to the lack of evidence of presence within the area of interest since 2012, disturbance to Eastern Black Rails is not anticipated.

4. Birds – Offshore: Methods

This section provides a detailed overview of the data sources and methods used in the exposure and vulnerability assessments. Exposure was assessed for each species and taxonomic group, where 'exposure' is defined as the extent of overlap between a species' seasonal or annual distribution and the Lease Area. Vulnerability was then assessed for marine birds using a scoring process focused on documented avoidance behaviors, estimated flight heights, and other factors.

4.1. Exposure Framework

Exposure has both a horizontal and vertical component. The exposure assessment focused exclusively on the horizontal exposure of birds. Vertical exposure (i.e., flight height) was considered within the assessment of vulnerability. The exposure assessment was quantitative where site-specific survey data were available. For birds with no available site-specific data, species accounts and literature were used to conduct a qualitative assessment in the body of the COP. For all marine birds, exposure was considered both in the context of the proportion of the population predicted to be exposed to the Lease Area as well as absolute numbers of individuals. The following sections introduce the data sources used in the analysis, the methods used to map species exposure, methods used to assign an exposure metric, methods to aggregate scores to year and taxonomic group, and interpretation of exposure scores.

4.1.1. Exposure Assessment Data Sources and Coverage

To assess the proportion of marine bird populations exposed to the Lease Area, three primary information sources were used to evaluate local and regional marine bird use: (1) digital aerial surveys, conducted by APEM, (2) the NJDEP Baseline Studies conducted by Geo-Marine, Inc. (2010), and (3) Version 2 of the MDAT marine bird relative density and distribution models (Curtice et al. 2019). The APEM surveys provide the most current local coverage across the Lease Area plus buffer and the NJDEP Baseline Studies provide an important local context. The MDAT models are modeled abundance data providing a large regional context for the Lease Area but are built from offshore survey data collected from 1978–2016. Each of these primary sources is described in more detail below, along with additional data sources that inform the avian impact assessment. Data

collected during these surveys are in general agreement with BOEM guidelines and the goals detailed above and described below.

4.1.1.1. APEM Digital Aerial Surveys

A series of eight digital aerial surveys were flown across the Lease Area, from October 2020 to May 2021 (Table 4-1, Figure 4-1). Note: no surveys were flown in summer months (see Figure 4-2 for seasonal effort). Approximately 40% of the Lease Area plus a 2.5-nautical mile (4-km) buffer was surveyed; but only a quarter of the resulting images (representing ~10% of the Lease Area) were analyzed. These surveys were flown at an altitude of 1,360 ft (415 m) and collected photographic imagery at a resolution of 0.6 in (1.5 cm) ground sampling distance (GSD). Using APEM's Shearwater III camera system, each image footprint was approximately 17.28 acres (0.070 km^2). Surveys were conducted in weather conditions that did not limit the ability to identify marine fauna at or near the water surface – cloud base >1,400 ft (427 m), visibility >3 mi (5 km), wind speed <30 knots (35 mph), and a Beaufort Scale sea state of 3 (small waves with few whitecaps) or less, ideally 2 (small waves with no whitecaps) or less to maximize accuracy of identifications. On days with little cloud cover, surveys avoided the middle of the day to minimize glint (strong reflected light off the sea) that makes finding and subsequently identifying the marine fauna recorded in the images more difficult. The onboard camera technician continuously monitored the images collected and, if they ceased to be of sufficient quality, surveys were ceased until suitable conditions returned.

On completion of each survey flight, all images were saved and backed up locally. Management of the data was overseen in the United States with a secondary data manager in the United Kingdom. Once the images had been processed and screened for potential targets, data was examined by taxonomic experts for completion of species identifications and associated QA/QC.

Table 4-1: Digital aerial survey dates

Survey	Year	Date	Season
1	2020	15 October	fall
2		07 November	
3		03 December	winter
4	2021	06 January	
5		06 March	spring
6		20 March	
7		20 April	
8		07 May	

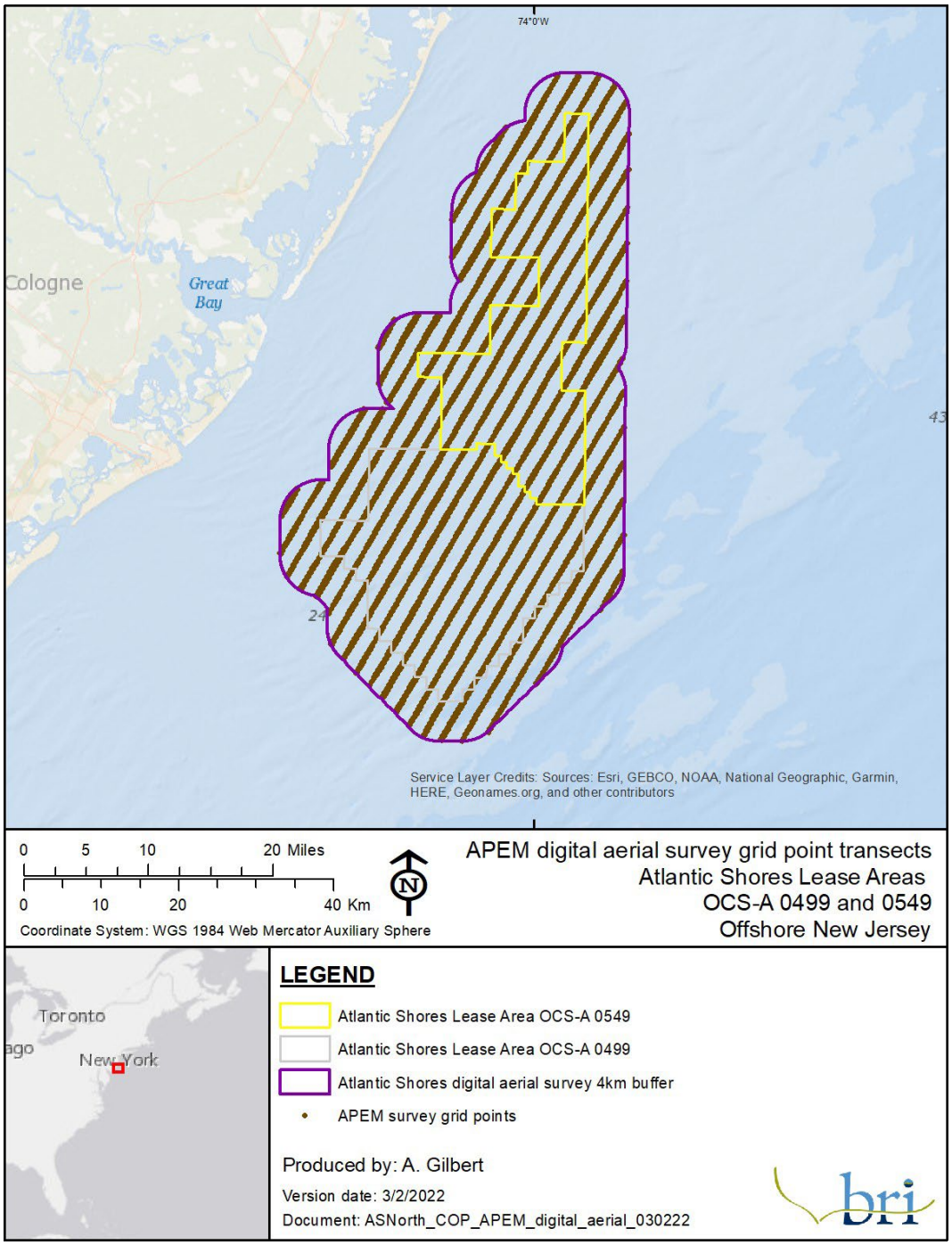

Figure 4-1: Map of digital aerial survey transects across the Lease Area.

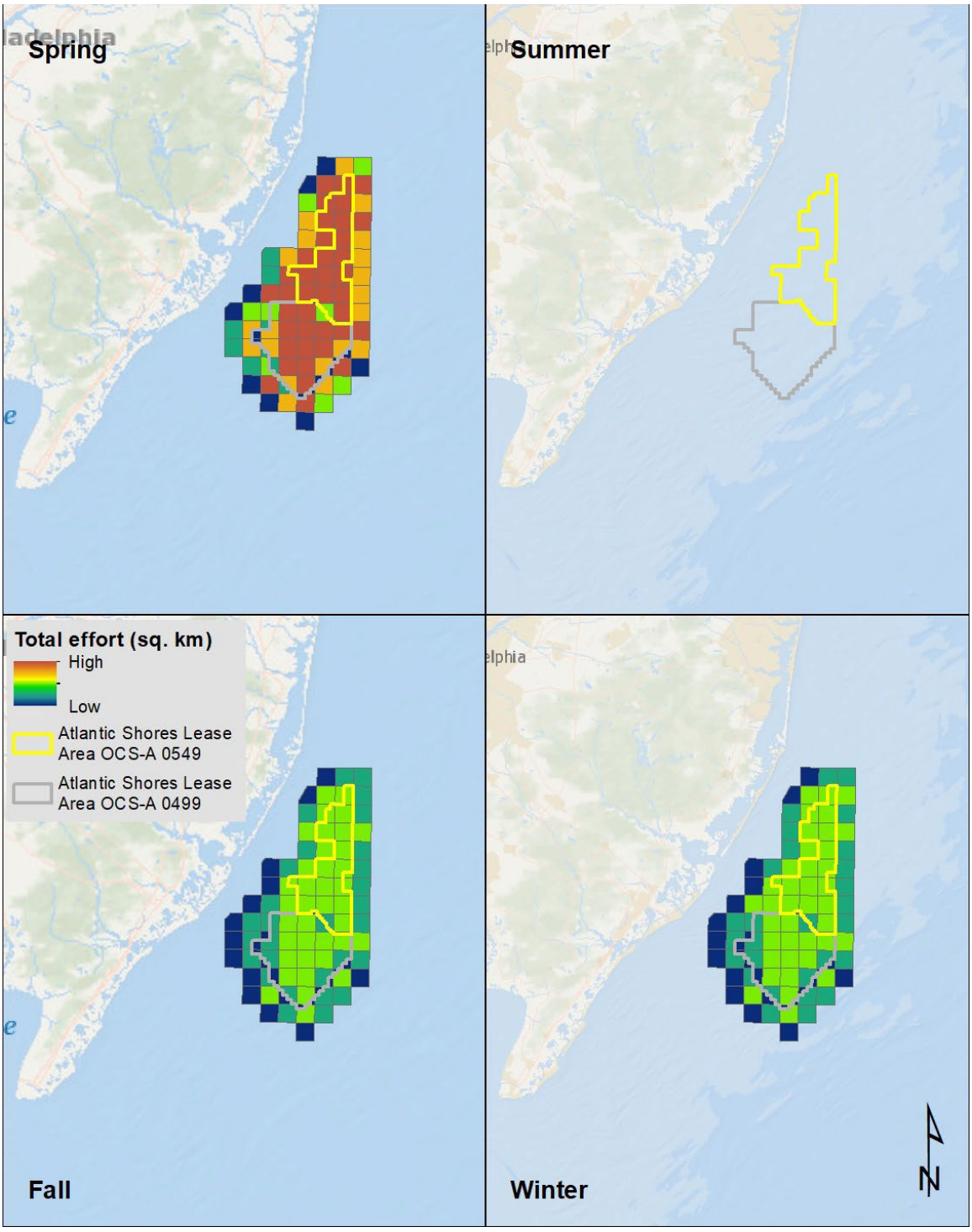

NOTE: The seasonal effort is the total number of km^2 of effort flown in each lease block in each season. Since there was unbalanced effort seasonally, there is greater effort in spring and none in summer. The season definitions and effort are detailed in Table 4-1.

Figure 4-2: Seasonal survey effort of Atlantic Shores APEM digital aerial surveys. Survey effort totaled within each full or partial lease block.

4.1.1.2. NJDEP Baseline Studies

The NJDEP Baseline Studies included monthly boat-based avian surveys conducted coastally and further offshore of New Jersey (Geo-Marine 2010). The offshore study area covered from approximately the 32-ft (10-m) isobath to an outer boundary at 20 nautical miles (37 km) from shore, and extended from Hereford Inlet, just north of Cape May, north to the Route 37 bridge at Seaside Heights (Figure 4-3). Shipboard surveys were conducted between January of 2008 and December of 2009. Due to weather, February 2008 and December 2009 survey effort was less than typical, but all other surveys were conducted in a double saw-tooth design covering the entire NJDEP Baseline Studies study area. In addition, supplemental offshore saw-tooth surveys were conducted between August and December 2009, and six days of offshore surveys were conducted in concert with sea watches (land-based seaward counts) at Barnegat Light and north end of Avalon. The supplemental surveys were meant to determine if increased survey effort influenced abundance estimates.

Offshore and coastal surveys were conducted using a hybrid distance sampling/strip transect method, while the boat was traveling at 10 knots during daylight hours, and visibility was at least 4.3 mi (7 km). Observers recorded distance and angle to all animals, including birds both flying and sitting on the water, focusing effort within 300 m (984 ft) ahead and to the side of the survey vessel. Observers viewed within a 90-degree bow- to-beam arc off either side of the vessel. During offshore saw-tooth surveys, a closing method for marine mammals was used where, when marine mammals were sighted, the vessel went off transect to identify the species present and estimate the group size (if more than one was present). During these off-transect periods, observations were designated as "off" until they returned to the original transect line, when they were designated as "on". This approach increases the chances of double-counting but should improve estimates of marine mammal
group size and identification rates. Estimated flight heights were recorded during surveys (as 1 ft [0.3 m], 25 ft [7.6 m], 50 ft [15.2 m], 100 ft [30.5 m], 200 ft [70 m], 300 ft [91 m], 500 ft [152 m], and 1,000+ ft [305+ m] above sea level) and basic behavioral states were noted.

During both coastal and boat-based surveys, a total of 176,217 birds was recorded, consisting of 153 species, including many migrant land birds. The addition of non-target taxa (e.g., bats, butterflies, marine mammals) resulted in a total of 201 identification codes, some of which were not identified to species (e.g., unknown small tern). The overall patterns indicate higher species densities closer to shore, although spring and summer appear to show higher relative densities offshore. No federally listed bird species were detected during these surveys. As discussed below, the NJDEP Baseline Studies boat-based survey data are displayed as proportions of total effort-corrected counts and displayed as quantiles.

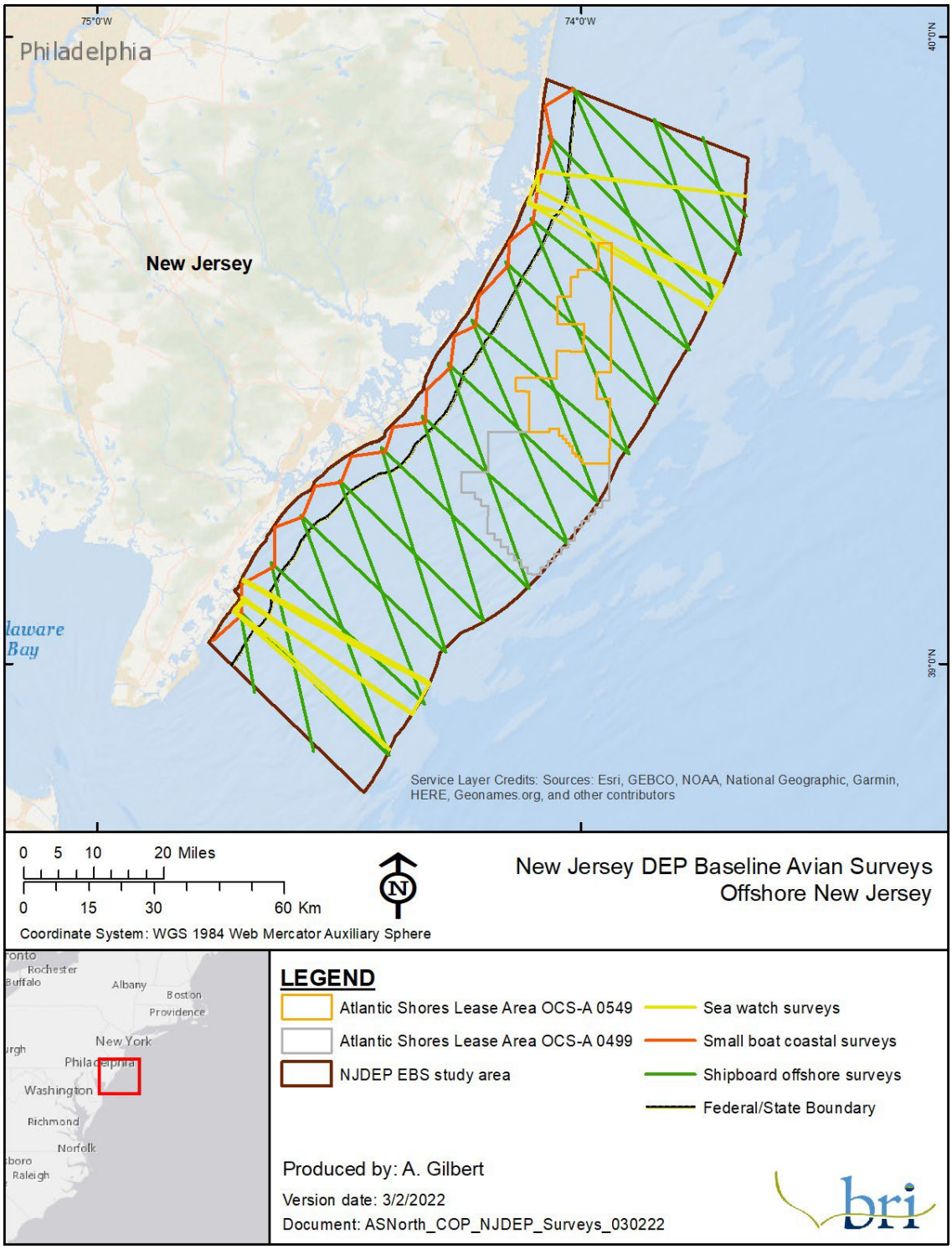

Figure 4-3: Map of NJDEP Baseline Studies survey transects and the Atlantic Shores Lease Areas.

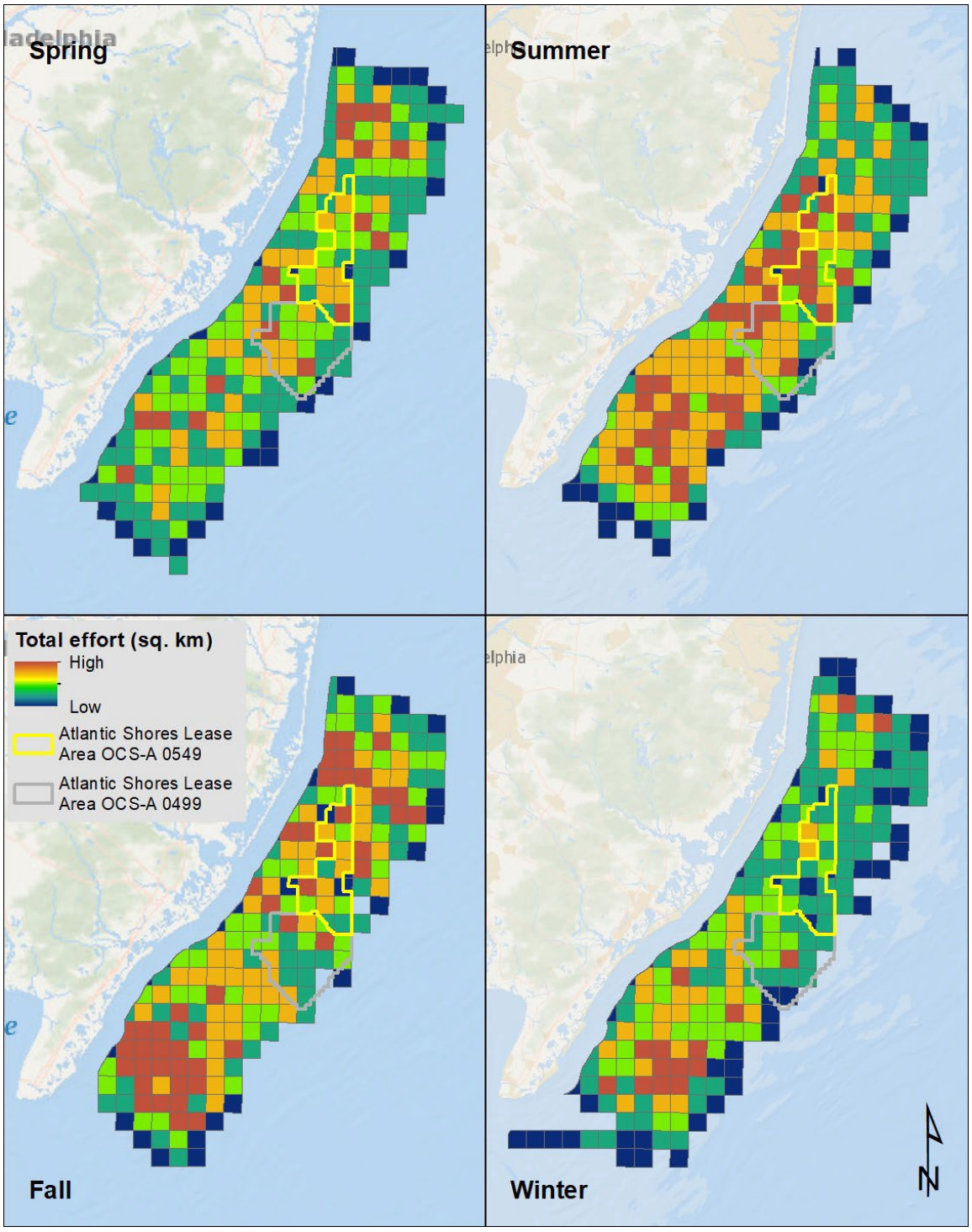

NOTE: Relative effort (in km^2) is shown across the study area by season. Red is higher effort (more km^2 covered); blue is lower effort.

Figure 4-4: NJDEP Baseline Studies survey effort by season. While effort varied by OCS lease block and season, the entire NJDEP Baseline Studies area, including the Lease Area, was thoroughly surveyed each season.

4.1.1.3. Marine Bird Abundance and Occurrence Models (Version 2)

Seasonal predictions of density were developed to support Atlantic marine renewable energy planning. Distributed as MDAT bird models (Winship et al. 2018; Curtice et al. 2019), they describe regional-scale patterns of abundance. Updates to these models (Version 2) are available directly from Duke University's Marine Geospatial Ecology Lab MDAT model web page.[7] The MDAT analysis integrated survey data (1978–2016) from the Atlantic Offshore Seabird Dataset Catalog[8] with a range of environmental predictor variables to produce long-term average annual and seasonal models (Figure 4-5). These models were developed to support marine spatial planning in the Atlantic. In Version 2, relative abundance and distribution models were produced for 47 avian species using Atlantic waters in the U.S. from Florida to Maine; this resource provides an excellent regional context to local relative densities estimated from boat-based surveys.

The digital aerial surveys, NJDEP Baseline Studies, and MDAT models each have strengths and weaknesses. The data from the digital aerial surveys and NJDEP Baseline Studies were collected in a standardized, comprehensive way, and are relatively recent, so they describe recent distribution patterns in the Lease Area and surrounding areas. However, these surveys covered a fairly small area relative to the Northwest Atlantic distribution of most marine bird species, and the limited number of surveys conducted in each season means that individual observations (or lack of observations, for rare species) may in some cases carry substantial weight in determining seasonal exposure.

The MDAT models, in contrast to the baseline surveys, include data collected at much larger geographic and temporal scales, and use a range of survey methods. The larger geographic scale is helpful for determining the importance of the Lease Area to marine birds, relative to other available locations in the Northwest Atlantic, and is thus essential for determining overall exposure. However, these models are based on data from decades of surveys and long-term climatological averages of dynamic covariates; given changing climate conditions, these models may no longer accurately reflect current distribution patterns. Model outputs that incorporate environmental covariates to predict distributions across a broad spatial scale may also vary in the accuracy of those predictions at a local scale.

[7] http://seamap.env.duke.edu/models/mdat

[8] https://coast.noaa.gov/digitalcoast/data/atloffshoreseabird.html

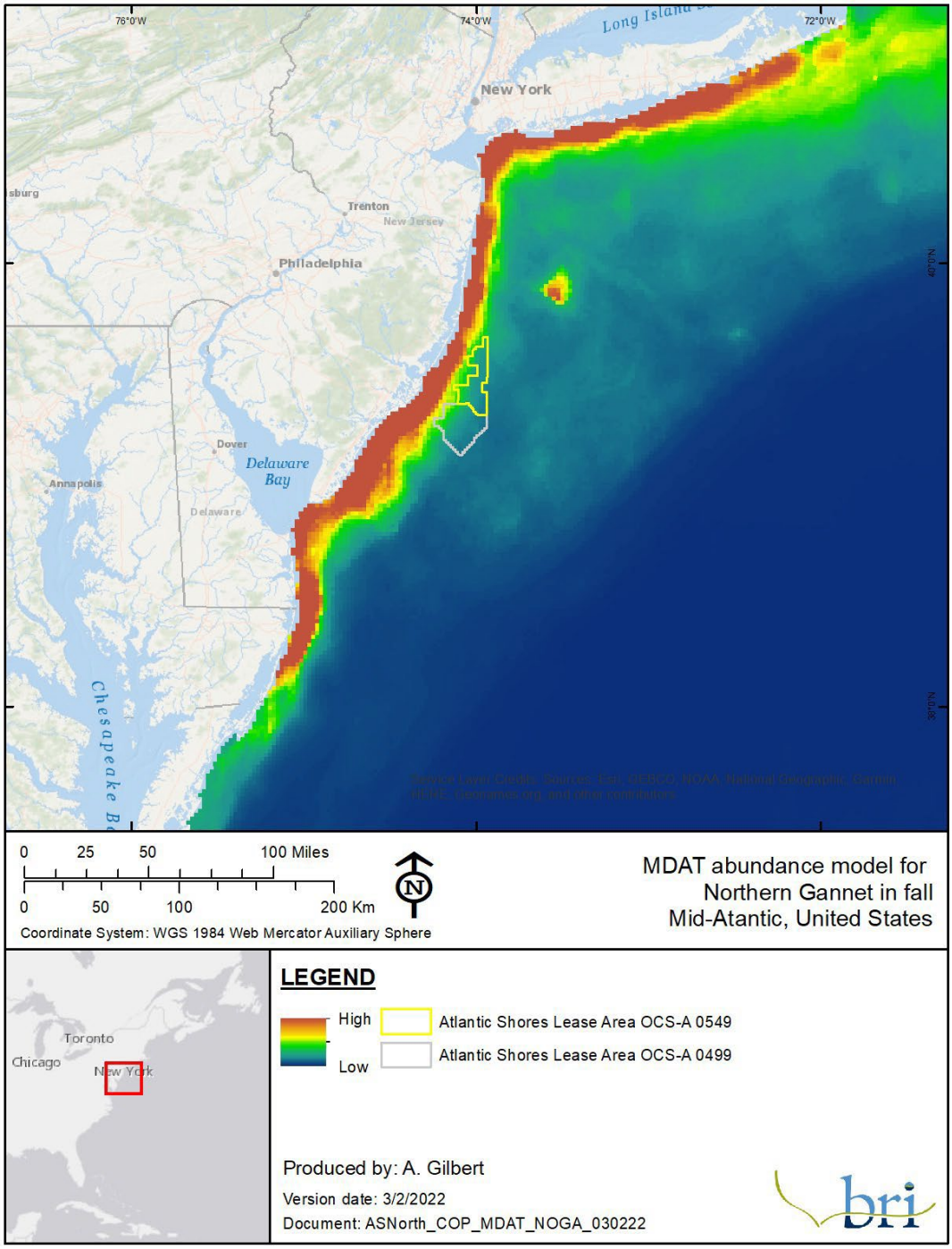

Figure 4-5: Example MDAT abundance model for the Northern Gannet (*Morus bassanus*) in fall.

4.1.2. Secondary Sources

4.1.2.1. Northwest Atlantic Seabird Catalog

The Northwest Atlantic Seabird Catalog is the comprehensive database for offshore and coastal seabird surveys conducted in U.S. Atlantic waters from Maine to Florida. The database contains records from 1938–2019, having more than 200 datasets and approximately 750,000 observation records along with associated effort information (Arliss Winship, pers. comm., 17 Nov 2021). The database is currently being managed by NOAAs National Center for Coastal Ocean Science. With BOEM's approval, NOAA provided the Catalog database to BRI to make queries for this assessment. All relevant data from the Catalog were mapped to determine the occurrence of rare species within the Lease Area.

4.1.2.2. Mid-Atlantic Diving Bird Tracking Study

A satellite telemetry tracking study in the Mid-Atlantic was developed and supported by BOEM and the USFWS with objectives aimed at determining fine scale use and movement patterns of three species of marine diving birds during migration and winter (Spiegel et al. 2017; Stenhouse et al. 2020). These species – the Red-throated Loon, Surf Scoter, and Northern Gannet– are all considered species of conservation concern and exhibit various traits that make them vulnerable to offshore wind development. Nearly 400 individuals were tracked using satellite transmitters, Argos platform terminal transmitters (PTTs), over the course of five years (2012–2016), including some Surf Scoters tagged as part of the Atlantic and Great Lakes Sea Duck Migration Study by the Sea Duck Joint Venture (SDJV).[9] Results provide a better understanding of how these diving birds use offshore areas of the Mid-Atlantic OCS and beyond.

Utilization distributions (UDs) were determined for each species by calculating individual level dynamic Brownian bridge movement model (dBBMM) surfaces (Kranstauber et al. 2012) using package Move for R (Kranstauber and Smolla 2016). Separate dBBMM surfaces were calculated for each of two winters with at least five days of data and combined into a weighted mean surface for each animal (as a percentage of the total number of days represented in the surface) with a minimum 30 total combined days of data. This method of combining multiple seasons was used for the migration periods as well, but with relaxed requirements for days of data, requiring only five days per year and seven total days per period since migration duration often occurred over a much shorter time period. Utilization contour levels of 50%, 75%, and 95% were calculated for the mean UD surface. The final UD was cropped to the 95% contour for mapping and further analyses (Spiegel et al. 2017).

4.1.2.3. Migrant Raptor Studies Falcons

To facilitate research efforts on migrant raptors (e.g., migration routes, stopover sites, space use relative to Atlantic OCS wintering/summer range, origins, contaminant exposure), BRI has deployed satellite transmitters on fall migrating raptors at three different raptor migration research stations along the north Atlantic coast (DeSorbo et al. 2012; DeSorbo, Gilpatrick, et al.

[9] https://seaduckjv.org/science-resources/atlantic-and-great-lakes-sea-duck-migration-study

2018; DeSorbo, Persico, et al. 2018). Research stations include Block Island in Rhode Island, Monhegan Island in Maine, and Cutler in Maine.

Data from satellite-tagged Peregrine Falcons (*Falco prergrinus*) and Merlins (*Falco columbarius*) identifies fall migration routes along the Atlantic Flyway. Positional data was filtered to remove poor-quality locations using the Douglas Argos Filtering tool (Douglas et al. 2012) available online on the Movebank data repository,[10] where these data are stored and processed. A request for data use was made to Chris DeSorbo, Raptor Program Director at BRI, who provided permission to use the results of the migrant raptor studies.

Osprey

Between 2000 and 2019, 106 tracking devices were fitted to Ospreys (*Pandion haliaetus*) predominantly at Chesapeake Bay and in northern New Hampshire (www.ospreytrax.com). This data set includes both adults and juvenile Ospreys but represents the first dedicated study of dispersal and migration in juveniles. Satellite transmitters were used in early years, but beginning in 2012, higher-resolution cellular GPS transmitters were deployed on adult males to better document their migration (Horton et al. 2014).

Separately, Argos satellite transmitters were deployed on Ospreys in the U.S. and Canada between 1995 and 2001 (Martell et al. 2001; Martell and Douglas 2019). Tagging locations included areas in Oregon, Washington, Minnesota, New York, and New Jersey. Birds tagged in eastern states generally migrated along the Atlantic coast.

To characterize potential utilization of the offshore environment by Ospreys, UDs were generated for individual animals using a dBBMM (Kranstauber et al. 2012). Both Argos satellite data and GPS-derived positional data were used from the two different telemetry datasets from Movebank. Both datasets were compiled and a max speed filter by animal was applied, which excluded locations with instantaneous speeds greater than 62 mph (100 kmph) and also filtered points outside of an extent including the eastern U.S. and Atlantic Canada (including all offshore points for this region). Individual dBBMMs were generated for the last 365 consecutive days of available data per tag (or less if the tags provide less than 365 consecutive days), thus representing an annual cycle within the U.S. Models were composited into a weighted UD for the sampled population, weighting each animal's UD by the number of days data were available of the total number of days of all animals providing models.

4.1.2.4. Tracking movements of vulnerable terns and shorebirds in the Northwest Atlantic using nanotags

Since 2013, BOEM and the USFWS have supported a study using nanotags (coded VHF tags) and an array of automated very high frequency (VHF) radio telemetry stations to track the movements of vulnerable terns and shorebirds. The study was designed to assess the degree to which these species use offshore Federal waters during breeding, pre-migratory staging periods, and on their migrations. In a pilot study in 2013, researchers attached nanotags to Common Terns (*Sterna hirundo*) and American Oystercatchers (*Haematopus palliatus*) and set up eight automated sentry stations (Loring et al. 2017). Having proved the methods successful, the study

[10] https://www.movebank.org

was expanded to 16 automated stations in 2014, and from 2015–2017, tagging efforts included Endangered Species Act-listed (ESA-listed) species, Piping Plovers and Roseate Terns. This study provided new information on the offshore movements and flight altitudes for these species gathered from a total of 33 automated telemetry stations deployed across Atlantic coastal states, including areas of Massachusetts, New York, New Jersey, Delaware, and Virginia (Loring et al. 2019).

4.1.2.5. Tracking movements of Red Knots in U.S. Atlantic Outer Continental Shelf Waters

Building from a previous tracking study, Red Knots of the *rufa* subspecies were fitted with digital VHF transmitters during their 2016 southbound migration at stopover locations and along the Atlantic coast in both Canada and the U.S. Individuals were tracked using radio telemetry stations within the study area that extended from Cape Cod, Massachusetts to Back Bay, Virginia. Modeling techniques were developed to describe the frequency and offshore movements over Federal waters and specific wind energy areas (WEAs) within the study area. The primary study objectives were to: develop models related to offshore movements for Red Knots; assess the exposure to each WEA during southbound migration; and examine WEA exposure and migratory departure movements in relation to meteorological conditions (Loring et al. 2018).

4.1.2.6. Atlantic Shores Red Knot tracking study

Atlantic Shores is currently funding a multi-year study using Argos satellite tags with GPS sensors deployed on southbound birds staging in New Jersey that have the potential to fly through the Lease Area. The project was initiated in 2020, in collaboration with Wildlife Restoration Partnerships (WRP), the U.S. Fish and Wildlife Service (USFWS) and Normandeau Associates and continued in 2021 and 2022 with WRP, USFWS, NJ Audubon, and BRI. To date, a total of 62 tags have been deployed on Red Knots (29 in 2020, 31 in 2021, 2 in 2022).

4.1.2.7. Sea Duck Tracking Studies

The Atlantic and Great Lakes Sea Duck Migration Study, a multi-partner collaboration, was initiated by the SDJV in 2009 with the goals of: (1) fully describing full annual cycle migration patterns for four species of sea ducks (Surf Scoter, Black Scoter [*Melanitta americana*], White-winged Scoter [*Melanitta deglandi*], and Long-tailed Duck [*Clangula hyemalis*]), (2) mapping local movements and estimating length-of-stay during winter for individual radio-marked ducks in areas proposed for placement of WTGs, (3) identifying nearshore and offshore habitats of high significance to sea ducks to help inform habitat conservation efforts, and (4) estimating rates of annual site fidelity to wintering areas, breeding areas, and molting areas for all four focal species in the Atlantic flyway. To date, over 500 transmitters have been deployed in the U.S. and Canada by a broad range of project partners. These collective studies have led to increased understanding of annual cycle dynamics of sea ducks, as well as potential interactions with and impacts from offshore wind energy development (Loring et al. 2014; SDJV 2015; Meattey et al. 2018; Meattey et al. 2019).

As part of a satellite telemetry tracking study in the Mid-Atlantic, BOEM and the USFWS also partnered with the SDJV during 2012–2016 to deploy transmitters in Surf Scoters, with the aim of determining fine scale use and movement patterns of three species of marine diving birds during migration and winter (Spiegel et al. 2017).

UDs were determined for each species by calculating individual level dBBMM surfaces (Kranstauber et al. 2012) using package Move for R (Kranstauber and Smolla 2016). Separate dBBMM surfaces were calculate for each of two winters with at least five days of data and combined into a weighted mean surface for each animal (as a percentage of the total number of days represented in the surface) with a minimum 30 total combined days of data. This method of combining multiple seasons was used for the migration periods as well, but with relaxed requirements for days of data, requiring only five days per year and seven total days per period since migration duration often occurred over a much shorter time period. Utilization contour levels of 50%, 75%, and 95% were calculated for the mean UD surface. The final UD was cropped to the 95% contour for mapping and further analyses (Spiegel et al. 2017).

4.1.3. Spatial Density Modeling Using Digital Aerial Survey Data

4.1.3.1. Data Compilation

Bird observations were collected from eight digital aerial surveys conducted approximately monthly from October 2020 to May 2021, covering fall, winter, and spring seasons. These aerial surveys were conducted using the standard APEM protocol (4.1.1.1). Bird observations were identified from digital images using a combination of automated (artificial intelligence) and manual (seabird experts) methods. Birds were identified to species level when possible and were otherwise assigned to the lowest possible taxonomic group (e.g., "Auk - species unknown" or "Murre - species unknown"). Taxa groups were created to include species-unknown observations with taxonomically similar species (e.g., All identified scoter species plus unknown scoter category). In sum, the observation data included 17 species (Table 4-2) and eight taxonomic groups (Table 4-3). Along with the full year-round data set, each species/group was subset into three seasonal data sets for density modeling. Only species/groups with greater than 10 observations in the given season were used to build spatial models.

4.1.3.2. Data Analysis

To model the observation density and account for the spatial dependence among observations, we fit spatially-explicit log Gaussian Cox Poisson process models to the year-round and seasonal survey data by species and taxa group using integrated nested Laplace approximation (Rue et al. 2009) for approximate Bayesian inference. The spatial dependence in the data is accounted for by incorporating a Gaussian Markov random field into the models. Briefly, Log Gaussian Cox Poisson models estimate the point density using a log link function such that the log of the spatial inhomogeneous intensity function (λ) at any point is assumed to be normally distributed (Gaussian Markov random field; Møller and Waagepetersen 2007). We implemented the stochastic partial differential equations approach (Lindgren et al. 2011) to incorporate the spatial random effect as a latent Gaussian field (GF) with a Matérn covariance structure to account for the spatial dependence in the data. Put another way, densities are more likely to be similar in

adjacent spatial units than remote units, and these models estimate these spatial correlations to estimate changes in density over space.

To approximate the continuous space of the data, we constructed a constrained refined Delaunay triangulation spatial mesh covering the entire survey area (Figure 4-6). An area of coarser density mesh (10% of the survey area diameter) was added beyond that to remove boundary effects that cause increased variance at the borders (Lindgren et al. 2011). We built the mesh using all bird observation points as the initial triangulation nodes, with a maximum triangle edge of 700 m (2,297 ft) for the inner mesh (i.e., survey area) and 7 km (4.3 mi) for the outer mesh. To avoid very small triangles, we also set a cutoff of 1 km (0.6 mi), such that points at a closer distance than this are replaced by a single vertex prior to mesh creation. We estimated smooth density surfaces by modeling the intensity (λ) at each spatial location (s) as a function of the spatial random effect (*u*).

$$\lambda(s) = \exp(\beta_0 + A u(s))$$

where β_0 is an intercept term that we set to zero and **u** is the GF representing the spatial random effect. The spatial effect **u** can be approximated at any point within the triangulated domain, using the projector matrix **A** to link the spatial GF (defined by the mesh vertices or nodes) to the locations of the observed data, s (Krainski et al. 2018). The Matérn covariance matrix for the spatial effect was parameterized using penalized complexity priors (Fuglstad et al. 2018), where the hyperparameters of range (*r*) and the marginalized standard deviation of the field (σ) define the spatial random effect so that $P(r > r_0) = p$ and $P(\sigma > \sigma_0) = p$. For these models, we used uninformed priors, so the prior probability of the spatial range being less than 9,000 was 0.001 and the probability of spatial variance being less than 900 was 0.001.

Species/group density predictions were made to the BOEM ~1,200-m (3,937-ft) resolution aliquot grid encompassing the Atlantic Shores Lease Area with a 4km (2.5-mi) buffer. Density predictions of all species/groups were converted into density proportions by dividing the expected density at each prediction point by the sum of that group's expected density across the prediction grid. All models were fit in R version 4.0.2, (R Core Team 2020), using the R-INLA (version 21.02.23, https://www.r-inla.org, Lindgren and Rue 2015) and inlabru (version 2.3.1, Bachl et al. 2019) packages.

Table 4-2: Avian species identified in the digital aerial survey imagery.

Common Name	Scientific Name	Total Observations
Atlantic Puffin	*Fratercula arctica*	2
Black-legged Kittiwake	*Rissa tridactyla*	24
Black Scoter	*Melanitta americana*	44
Bonaparte's Gull	*Chroicocephalus philadelphia*	1,218
Common Loon	*Gavia immer*	1,241
Gadwall	*Mareca strepera*	1
Great Black-backed Gull	*Larus marinus*	181
Herring Gull	*Larus argentatus*	138
Laughing Gull	*Leucophaeus atricilla*	452
Manx Shearwater	*Puffinus puffinus*	1
Northern Gannet	*Morus bassanus*	934
Razorbill	*Alca torda*	9
Red-throated Loon	*Gavia stellata*	129
Red Phalarope	*Phalaropus fulicarius*	41
Ring-billed Gull	*Larus delawarensis*	2
Surf Scoter	*Melanitta perspicillata*	1
White-winged Scoter	*Melanitta deglandi*	505

Table 4-3: Species and categories included in each taxonomic group.

Group	Categories in Group	Total Observations
Terns	Common Tern, Forster's Tern	5
Murres	Common Murre, Thick-billed Murre	26
Auks	Atlantic Puffin, Auk-species unknown, Common Murre, Thick-billed Murre, Murre/Razorbill, Razorbill	116
Gulls, small	Bonaparte's Gull, Gull-species unknown–Small	1,537
Gulls, medium	Black-legged Kittiwake, Laughing Gull, Ring-billed Gull	478
Gulls, large	Great Black-backed Gull, Herring Gull, Gull-species unknown–Large	340
Loons	Common Loon, Loon-species unknown, Red-throated Loon	1,418
Scoters	Black Scoter, Scoter unid., Surf Scoter, White-winged Scoter	1,912

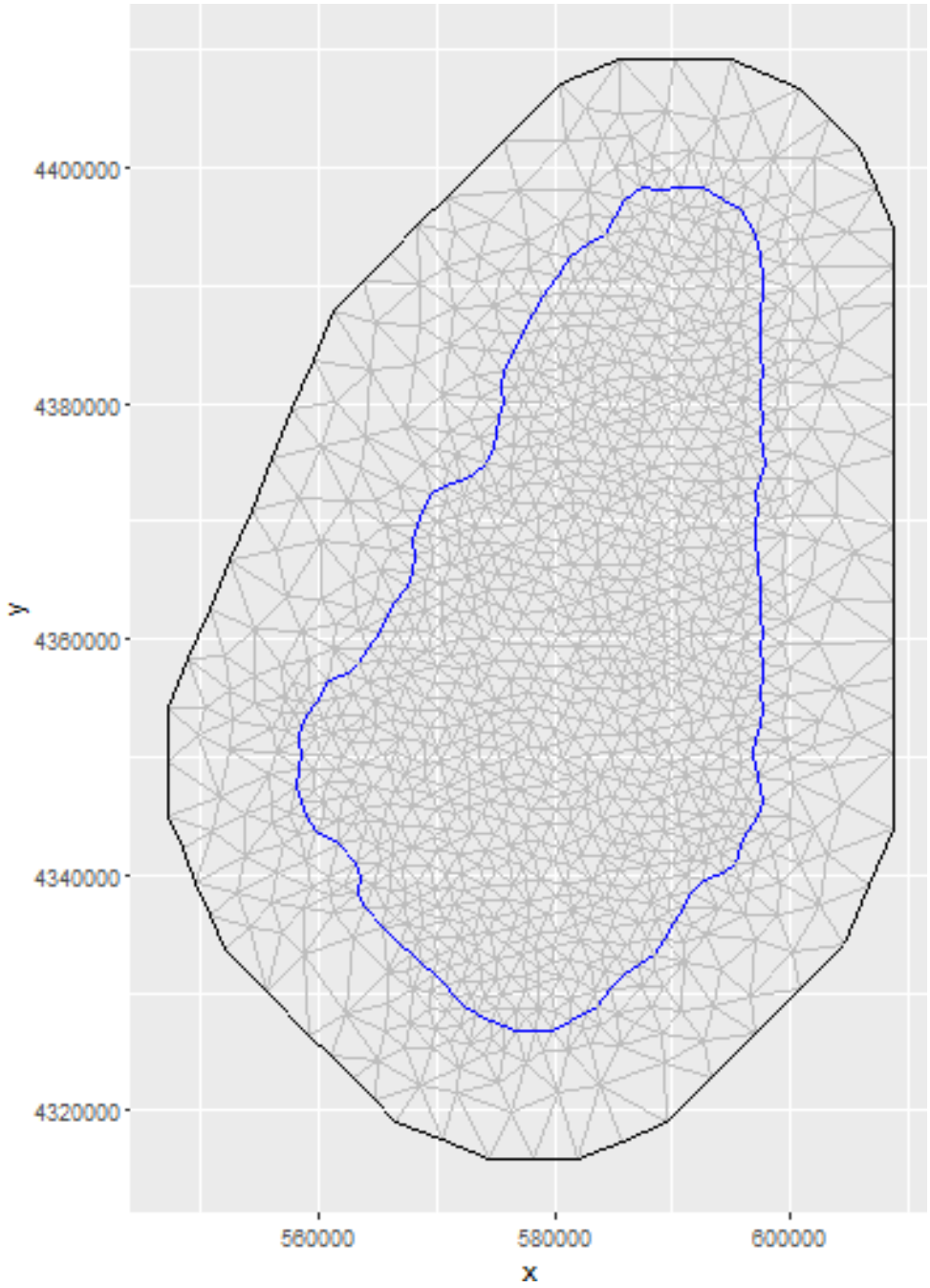

Figure 4-6: Constrained refined Delaunay triangulation spatial mesh.

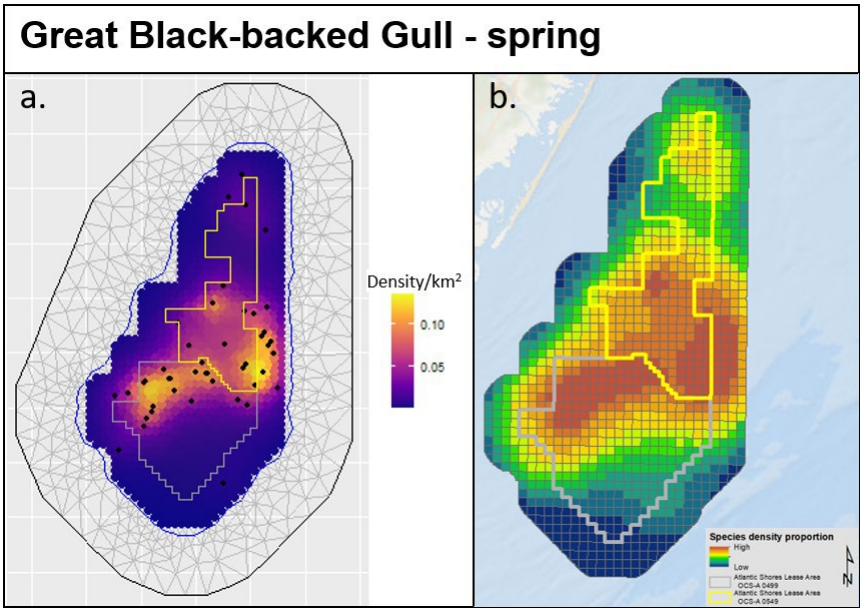

NOTE: The density estimates from the models were converted to density quantiles by dividing the density at each prediction point by the sum of that species/group's density across the prediction grid. These standardized density quantiles were then categorized into 10 percentile groups for visualization purposes, ranging from low to high standardized density proportion. The raw model output (a.) shows the triangulation mesh used for the INLA model estimation, the inner mesh boundary (blue outline), the inner mesh prediction area (red outline), the Atlantic Shores Lease Area OCS-A 0549 prediction grid (yellow outline), and the Atlantic Shores Lease Area OCS-A 0499 (gray outline). Prediction points in a. are sized to present a continuous density surface.

Figure 4-7: Example of the (a.) non-standardized mean density/km^2 estimates from the INLA models with the raw observations (black points) overlaid and the (b.) standardized density proportions (of total density) visualized as percentiles.

4.1.4. Community Distance Modeling Using NJDEP Baseline Studies Boat Survey Data

Boat-based surveys are a standardized methodology to describe patterns of distribution and abundance in the marine environment. A known bias in this method is that individuals farther from the transect line are more difficult to detect than those closer to the center (Buckland et al. 2001). This bias causes surveyors to underestimate the total number of animals in the survey area (Camphuysen et al. 2004). Estimating detection probability for rare species can also be difficult due to a lack of observations, so researchers have developed new methods for estimating detection probabilities of communities to address this issue (Sollmann et al. 2016). These community-based methods can be beneficial for surveys of wind energy projects as they can help account for problems relating to surveys of relatively small areas or including data from rare species.

We attempted to distance correct the NJDEP boat-based survey data using community distance models. However, while model convergence was adequate, and this modeling approach often fitted reasonable detection curves for some species groups, there were several indications that the models did not reliably correct density estimates across all species groups. Thus, we chose not to use the modeled values and instead relied on naive density estimates in the exposure assessment (see Section 6 for further details).

Given that the exposure assessment examines the relative differences in densities across the survey area on a species/season basis across the survey area, we expect the detection bias inherent in the boat-based data should have no effect on the exposure results because of any correction for differences in detectability would scale all density results equally for any season/species combination. However, because the detection probability of the APEM digital aerial surveys is expected to be near 100%, we recommend that the digital aerial surveys be considered to have the most current and accurate density estimates for the Lease Area for those species in which data are available.

4.1.5. Exposure Mapping

Maps were developed to display local and regional context for exposure assessments. A three-panel map was created for each species-season (winter: December–February; spring: March–May; summer: June–August; and fall: September–November) combination that includes MDAT models, regional NJDEP baselines survey data, and spatial models of local APEM digital aerial data. Any species-season combination which did not at least have modeled APEM digital aerial data, MDAT model, or NJDEP survey data (i.e., blank maps) were left out of the final map set. An example map for Northern Gannet in fall is provided in Figure 4-8, while the complete set of species-season maps can be found in Section 8.

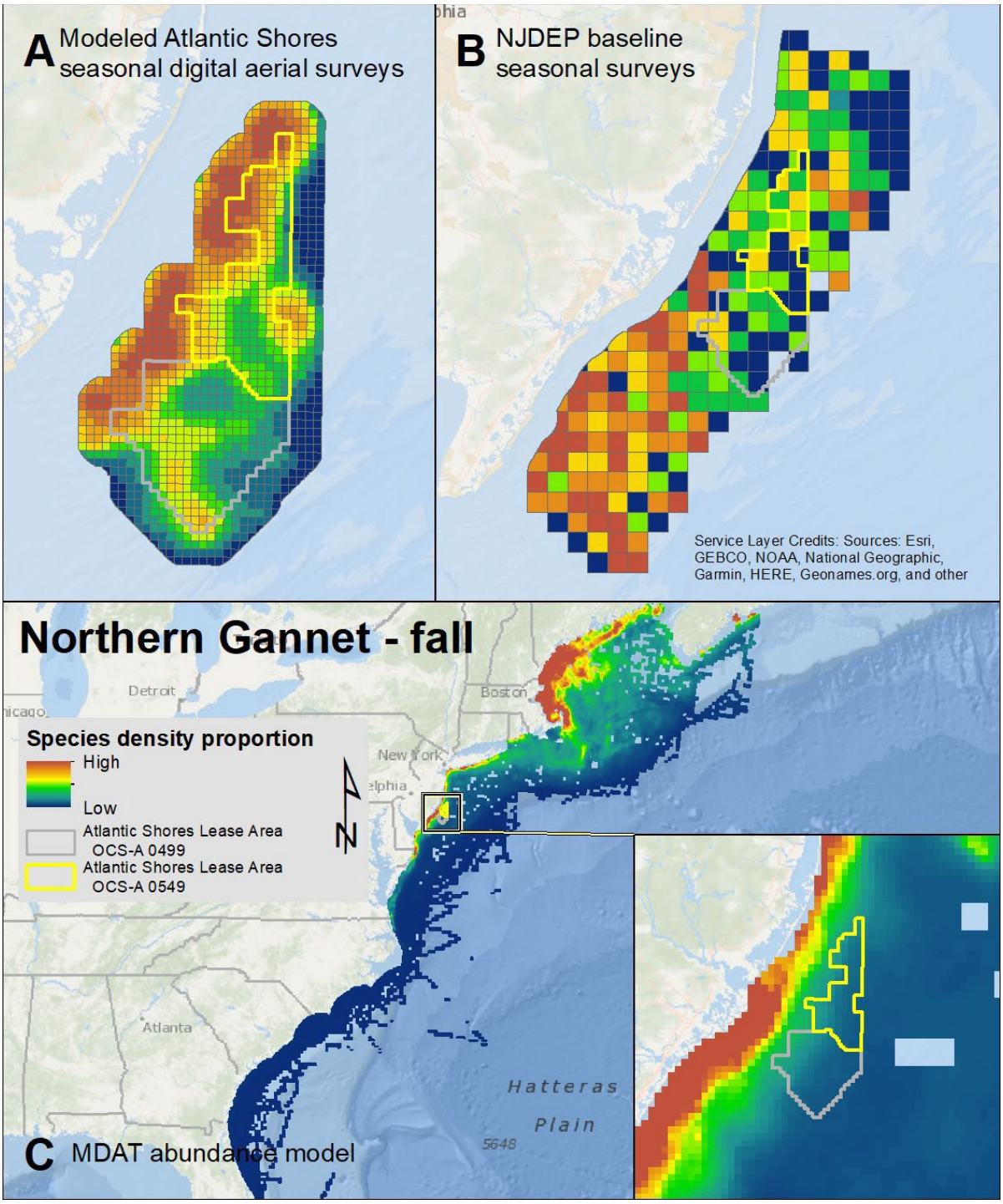

Figure 4-8: Example map of relative density proportions locally and regionally for the Northern Gannet in fall.

Panel A presents the standardized digital aerial survey data visualized as percentiles derived standardized density proportions (of total density). Standardized density proportions were calculated from modeled mean density/km^2 estimates from the INLA models as described above in 4.1.1.2. The density estimates from the models were converted to density quantiles by dividing the density at each prediction point by the sum of that species/group's density across the prediction grid. These standardized density quantiles were then categorized into 10 percentile groups for visualization purposes, ranging from low to high standardized density proportion.

Panel B presents the NJDEP Baseline Studies boat-based survey data as proportions of total effort-corrected counts and displayed as quantiles. The proportion of the total effort-corrected counts (total counts per km^2 of survey area) was calculated for each BOEM designated OCS[11] Lease Block,[12] across all surveys in each season. This method was useful as it scaled all effort-corrected count data from 0–1 to standardize data visualizations among species. Standardized effort-corrected count data were categorized into six quantiles for all non-zero data plus a zero category since data were often highly skewed towards zero.

Panel C includes density estimates from MDAT models presented at two different scales – the density models over the U.S. Atlantic coast, and, in an inset map, a zoom in on the modeled densities similar to the map display in panel B. Density data are scaled in a similar way to the baseline survey data, so that the low–high designation for density is similar across species and datasets. However, there are no true zeroes in the MDAT model outputs, and thus no special category for them in the MDAT maps. All MDAT models were masked to remove areas of zero effort within a season. These zero-effort areas do have density estimates, but generally are of low confidence, so they were excluded from mapping and analysis to reduce anomalies in predicted species densities and to strengthen the analysis. While the color scale for the MDAT density estimates is approximately matched to that used for the baseline survey data, the values that underlie them are different (the MDAT estimates are symbolized using an ArcMap default color scale, which uses standard deviations from the mean to determine the color scale rather than quantiles).

Overall, these maps should be viewed in a broadly relative way between local, regional, and coast-wide assessments, and even across species.

---

[11] The OCS is defined by the U.S. Department of the Interior (www.bsee.gov/newsroom/library/glossary) as:

> *All submerged lands seaward and outside the area of lands beneath navigable waters. Lands beneath navigable waters are interpreted as extending from the coastline 3 nautical miles into the Atlantic Ocean, the Pacific Ocean, the Arctic Ocean, and the Gulf of Mexico excluding the coastal waters off Texas and western Florida. Lands beneath navigable waters are interpreted as extending from the coastline 3 marine leagues into the Gulf of Mexico off Texas and western Florida.*

[12] OCS Lease Blocks are defined (https://catalog.data.gov/dataset/outer-continental-shelf-lease-blocks-atlantic-region-nad83) as:

> *small geographic areas within an Official Protraction Diagram (OPD) for leasing and administrative purposes. These blocks have been clipped along the Submerged Lands Act (SLA) boundary and along the Continental Shelf Boundaries. Additional details are available from: https://www.boem.gov/BOEM- Newsroom/Library/Publications/1999/99-0006-pdf.aspx.*

4.1.5.1. Exposure Assessment Metrics

Avian exposure to the Lease Area was assessed for each species by calculating effort-corrected counts for the NJDEP boat-based surveys on a local level and using the MDAT models on a regional level. The exposure scores were developed from the NJDEP boat-based surveys and MDAT models by comparing bird densities in the Lease Area with all other possible Lease Area-sized areas within the survey area for each dataset. For each species the mean densities were compiled for each Lease Area-sized area, quantiles calculated for the set of all Lease Area-sized areas, and a categorical score was assigned to each quantile. If the Lease Area was in the top quartile, a bird would get a high exposure score; if it was in the bottom, a minimal score. The analysis was done in the following two steps:

Step 1, assess regional exposure using MDAT models: Using the MDAT outputs, masked to remove zero-effort predicted cells, the predicted seasonal density surface for a given species was aggregated into a series of rectangles that were approximately the same size as the Lease Area, and the mean density estimate of each rectangle was calculated. This process compiled a dataset of density estimates for all species surveyed, for areas the same size as the Lease Area. The 25th, 50th, and 75th weighted quantiles of this dataset were calculated, and the quantile into which the density estimate for the Lease Area fell for a given species and season combination was identified. Quantiles were weighted by using the proportion of the total density across the entire modeled area that each sample represented. Thus, quantile breaks represent proportions of the total seabird density rather than proportions of the raw data. A categorical score was assigned to the Lease Area for each season-species: 0 (Minimal) was assigned when the density estimate for the Lease Area was in the bottom 25%; 1 (Low) when it was between 25% and 50%; 2 (Medium) when it was between 50% and 75%; and 3 (High) when it was in the top quartile (greater than 75%). While a "high" score does suggest importance within a regional scale, these scores need to be considered in context of scores at each spatial scale when assessing overall importance to the species in a season.

Step 2, assess local exposure using the NJDEP boat-based survey: A similar process was used to categorize each species-season combination using the baseline survey data. To compare the Lease Area to other locations within the survey region, the nearest 26 OCS full or partial Lease Blocks to each OCS Lease Block surveyed in the NJDEP boat-based survey area in each season (winter, n = 239; spring, n = 254; summer, n = 239; and fall, n = 235) were identified and the relative density of each OCS Lease Block group was calculated. Thus, a dataset of relative densities for all possible Lease Area-sized OCS Lease Block groups was generated within the survey region using the baseline survey data. This data set was used to assign scores to all species-season combinations, based on the same quartile categories described for the MDAT models above. If a score for a species-season combination was not available using the baseline survey data (local assessment), and because the avian surveys made every effort to survey all species, then the local assessment score was assigned a zero because no animals were sighted for that species-season combination.

4.1.5.2. Species Exposure Scoring

To determine the relative exposure for a given species and season in the Lease Area compared to all other areas, the MDAT quartile score and baseline survey data quartile score were added together to create a final exposure metric that ranged from 0 to 6. The density information at both spatial scales were equally weighted, and thus represent both the local and regional importance of the Lease Area to a given species during a given season. However, if a species-season combination was not available for the MDAT regional assessment, then the score from the local assessment (baseline survey data) was accepted as the best available information for that species-season, and it was scaled to range from 0 to 6 (e.g., essentially doubled to match the final combined score).

The exposure score was categorized as Minimum (a combined score of 0), Low (combined score of 1–2), Medium (combined score of 3–4), or High (combined score of 5–6; Table 4-4). In general terms, species-season combinations labeled as 'Minimum' had low densities at both the local and regional spatial scales. 'Low' exposure was assessed for species with below-average densities at both spatial scales, or above-average density at one of the two spatial scales and low density at the other scale. 'Medium' exposure describes several different combinations of densities; one or both spatial scales must be at least above-average density, but this category can also include species-season combinations where density was high for one spatial scale and low for another. 'High' exposure is when density is high at both spatial scales, or one is high and the other is above average. Both local and regional exposure scores were viewed as equal in importance in the assessment of exposure. All exposure determinations are highlighted in bold throughout the text.

Table 4-4: Definitions of exposure levels developed for the avian assessment for each species and season.

NOTE: The listed scores represent the exposure scores from the local NJDEP boat-based survey data and the regional MDAT models on the left and right, respectively.

Exposure Level	Definition	Scores
Minimal	Densities at both local and regional scales are below the 25th percentile.	0, 0
Low	Local and/or regional density is between the 25th and 50th percentiles. **OR** Local density is between the 50th and 75th percentiles and regional density is below the 25th percentile, or vice versa.	1, 1 2, 0
Medium	Local or regional density is between the 50th and 75th percentiles. **OR** Local density is between the 50th and 75th percentiles and regional density between the 25th and 50th percentiles, or vice versa. **OR** Local density is greater than the 75th percentile and regional density is below the 25th percentile, or vice versa. **OR** Local density is greater than the 75th percentile of all densities and regional density is between the 25th and 50th percentiles of all densities (or vice versa).	2, 2 2, 1 3, 0 3, 1
High	Densities at both local and regional scales are above the 75th percentile. **OR** Local densities are greater than the 75th percentile and regional densities are between the 50th and 75th percentiles, or vice versa.	3, 3 3, 2

4.1.5.3. Aggregated Annual Exposure Scores

To understand the total exposure across the annual cycle for each species, seasonal scores were summed to obtain an annual score that ranged from 0–12. These annual scores were then mapped to exposure categories of Minimal (0–2), Low (3–5), Medium (6–8), and High (9–12). The annual exposure category for a species represents the seasonally integrated risk across the annual cycle.

Finally, because these scores are relative to seasonal distribution, estimates of count density were provided within the Lease Area and over the entire survey area for each species from the baseline survey data. Uncommon species with few detections in the Lease Area may be somewhat over-rated for exposure using this method, while common species with relatively few

detections in the Lease Area may be effectively under-rated in terms of total exposure to the Lease Area. Density estimates (count per km^2) are presented to provide context for the exposure scores.

4.1.5.4. Interpreting Exposure Scores

The final exposure scores for each species and season, as well as the aggregated annual scores, should be interpreted as a measure of the relative importance of the Lease Area for a species, as compared to other surveyed areas in the region and in the Northwest Atlantic. It does not indicate the absolute number of individuals likely to be exposed. Rather, the exposure score attempts to provide regional and population-level context for each species.

A High exposure score indicates that the observed and predicted densities of the species in the Lease Area were high relative to densities of that species in other surveyed areas. Conversely, a Low or Minimal exposure score means that the species was predicted to occur at lower densities in the Lease Area than in other locations. A Minimal exposure score should not be interpreted to mean there are no individuals of that species in the Lease Area. In fact, common species may receive a Minimal exposure score even if there are substantial numbers of individuals in the Lease Area, so long as their predicted densities *outside* the Lease Area are comparatively higher. The quantitative annual exposure score was then considered with additional species-specific information, along with expert opinion, to place each species within a final exposure category (described below in Section 4.1.5.5

4.1.5.5. Exposure Categories

The quantitative assessment of exposure (described above), other locally available data, existing literature, and species accounts were utilized to develop a final qualitative exposure determination. Final exposure level categories used in this assessment are described in Table 4-5 below.

Table 4-5: Assessment criteria used for assigning species to final exposure levels.

Final Exposure Level	Definition
Minimal	Minimal seasonal exposure scores in all seasons or Minimal score in all but one season. **OR** Based on the literature—and, if available, other locally available tracking or survey data—little to no evidence of use of the Lease Area or offshore environment for breeding, wintering, or staging, and low predicted use during migration.
Low	Low exposure scores in two or more seasons, or Medium exposure score in one season. **OR** Based on the literature—and, if available, other locally available tracking or survey data—low evidence of use of the Lease Area or offshore environment during any season.

Final Exposure Level	Definition
Medium	Medium exposure scores in two or more seasons, or High exposure score in one season. **OR** Based on the literature—and, if available, other locally available tracking or survey data—moderate evidence of the Lease Area or use of the offshore environment during any season.
High	High exposure scores in two or more seasons. **OR** Based on the literature—and, if available, other locally available tracking or survey data—high evidence of use of the Lease Area or offshore environment, and the offshore environment is primary habitat during any season.

4.1.6. Vulnerability Framework

Researchers in Europe and the U.S. have assessed the vulnerability of birds to offshore wind farms and general disturbance by combining ordinal scores across a range of key variables (Furness et al. 2013; Willmott et al. 2013; Wade et al. 2016; Kelsey et al. 2018; Fliessbach et al. 2019). The purpose of these indices was to prioritize species in environmental assessments (Desholm 2009) and provide a relative rank of vulnerability (Willmott et al. 2013). Importantly, past assessments and the one conducted here are intended to support decision-making by ranking the relative likelihood that a species will be sensitive to offshore wind farms but should not be interpreted as an absolute determination that there will or will not be collision mortality or habitat loss. Therefore, the results should be interpreted as a guide to species that have a higher likelihood of vulnerability.

The existing vulnerability methods assess individual-level vulnerability to collision and displacement independently and then incorporate population-level vulnerability to develop a final *species-specific* vulnerability score. These past efforts provide useful rankings across a region but are not designed to assess the vulnerability of birds to a particular wind farm or certain WTG designs. Collision risk models (e.g., Band 2012) do estimate site-specific mortality, but are substantially influenced by assumptions about avoidance rates (Chamberlain et al. 2006). Furthermore, collision risk models do not explicitly assess vulnerability to displacement (i.e., macro avoidance behaviors, leading to temporary or permanent displacement from a wind farm area, which can cause effective habitat loss). Thus, there is a need to develop a *project- specific* vulnerability score for each species that is inclusive of both collision and displacement and has fewer assumptions.

The scoring process in this assessment builds from the existing methods, incorporates the specifications of the WTGs being considered by Atlantic Shores, utilizes local bird conservation status, and limits the vulnerability score to the species observed in the local surveys. The results from this scoring method may differ for some species from the qualitative determinations made in other Construction and Operations Plan assessments because the input parameters use specific categorical definitions that in some cases are conservative (e.g., > 40% macro-avoidance

receives the highest score; see below and Table 4-8). The literature is also used to interpret scoring results (see Table 4-6 for examples), and, if empirical studies indicate a lower or higher vulnerability, a range is added to the final score (see uncertainty discussion below). For species or species groups for which inputs are lacking, the literature is used to qualitatively determine a vulnerability ranking using the criteria in Table 4-7. Below is a description of the scoring approach.

Table 4-6: Examples of scientific literature used in the vulnerability analysis for each taxa group.

Taxa Group	Examples of Literature Referenced
Non marine Birds	
Shorebirds	Howell et al. 2019; Loring et al. 2020; Shwemmer et al. 2023
Wading birds	Mateos- Rodríguez and Liechti 2012; Willmott et al. 2013; Dolinski 2019
Raptors	Hill et al. 2014; Skov et al. 2016; Jacobsen et al. 2019
Songbirds	Petersen et al. 2006; Hüppop et al. 2006; Erickson et al. 2014
Marine Birds	
Sea Ducks	Delsholm and Kahlert 2005; Langston 2013; Fox and Petersen 2019
Auks	Cook et al. 2012; Wade et al. 2016; Welcker and Nehls 2016
Jaegers & Gulls	Krijgsveld et al. 2011; Johnston et al. 2014; Vanermen et al. 2015
Terns	Burger et al. 2011; Willmott et al. 2013; Loring et al. 2019
Loons	Garthe and Hüppop 2004; Lindeboom et al. 2011; Furness et al. 2013
Shearwaters, Petrels & Storm-Petrels	Montevecchi 2006; Rodríguez et al. 2017; Wade et al. 2016
Gannets, Cormorants, & Pelicans	Lindeboom et al. 2011; Vanermen et al. 2015; Skov et al. 2018

Table 4-7: Assessment criteria used for assigning species to each behavioral vulnerability level.

Behavioral Vulnerability Level	Definition
Minimal	0–0.25 ranking for collision or displacement risk in vulnerability scoring. **OR** No evidence of collisions or displacement in the literature. Unlikely to fly within the rotor-swept zone (RSZ).

Low	0.26–0.5 ranking for collision or displacement risk in vulnerability scoring. **OR** Little evidence of collisions or displacement in the literature. Rarely flies within the RSZ.
Medium	0.51–0.75 ranking for collision or displacement risk in vulnerability scoring. **OR** Evidence of collisions or displacement in the literature. Occasionally flies within the RSZ.
High	0.76–1.0 ranking for collision or displacement risk in vulnerability scoring. **OR** Significant evidence of collisions or displacement in the literature. Regularly flies within the RSZ.

4.1.6.1. Population Vulnerability

Many factors contribute to how sensitive a population is to mortality or habitat loss related to the presence of a wind farm, including vital rates, existing population trends, and relative abundance of birds (Goodale and Stenhouse 2016). In this avian risk assessment, the relative abundance of birds is accounted for by the exposure analysis described above. The vulnerability assessment creates a population vulnerability (PV) score by using Partners in Flight (PiF) "continental combined score" (CCSmax), a local "state status" (SSmax), and adult survival score (AS); (Equation 1 below). Survival is included as an independent variable that is not accounted for in the CCSmax. This approach is based upon methods used by Kelsey et al. (2018) and Fliessbach et al. (2019).

Each factor included in this assessment (CCSmax, SSmax, and AS) is weighted equally and receives a categorical score of 1–5 (Table 4-8). The final population level vulnerability scores are rescaled to a 0–1 scale, divided into quartiles, and are then translated into four final vulnerability categories (Table 4-7). As using quartiles creates hard cut-off points and there is uncertainty present in all inputs (see discussion on uncertainty below), using scores alone can potentially misrepresent vulnerability (e.g., a 0.545 PV score leading to a *minimal* category). To account for this, the scores are considered along with information in existing literature. If there is evidence in the literature that conflicts with the vulnerability score, then the score will be appropriately adjusted (up or down) according to documented empirical evidence. For example, if a PV score was assessed as *low*, but a paper indicated an increasing population, the score would be adjusted up to include a range of *minimal–low*.

$$PPPP = CCCCCCCCCCC + CCCCCCCCCC + AACC \qquad \textit{Equation 1}$$

Specifics for each factor in PV are as follows:

- *CCSmax* is included in scoring because it integrates various factors PiF used to indicate global population health. It represents the maximum value for breeding and non-breeding birds developed by PiF, and combines the scores for population size, distribution, global threat status, and population trend (Panjabi et al. 2019). The CCSmax score from PiF was rescaled to a 1–5 scale to achieve consistent scoring among factors.
- *SSmax* is included in scoring to account for local conservation status, which is not included in the CCSmax. Local conservation status is generally determined independently by states and accounts for the local population size, population trends, and stressors on a species within a particular state. It was developed following methods by (Adams et al. 2016) in which the State conservation status for the relevant adjacent states is placed within five categories (1 = no ranking to 5 = endangered), and then, for each species, the maximum State ranking is selected.
- *AS* is included in the scoring because species with higher adult survival rates are more sensitive to increases in adult mortality because they tend to be species that are also long-lived and have low annual reproductive success (e.g., K strategists) (Desholm 2009;

Adams et al. 2016). The five categories are based upon those used in several vulnerability assessments (Willmott et al. 2013; Kelsey et al. 2018; Fliessbach et al. 2019), and the species-specific values were used from (Willmott et al. 2013).

Table 4-8: Data sources and scoring of factors used in the vulnerability assessment.

Vulnerability Component	Factor	Definition and Source	Scoring
Population Vulnerability (PV)	continental combined score *(CCSmax)*	CCSmax is Partners in Flight continental combined score: pif.birdconservancy.org/ACAD/Database.aspx.	1 = Minor population sensitivity 2 = Low population sensitivity 3 = Medium population sensitivity 4 = High population sensitivity 5 = Very-High population sensitivity
	state status *(SSmax)*	SSmax from New Jersey from Adams et al. (2016).	1 = No Ranking[1] 2 = State/Federal Special Concern 3 = State/Federal Threatened 4 = State/Federal Endangered 5 = State & Federal End and/or Thr
	adult survival (AS)	AS score: scores and categories taken from Willmott et al. (2013).	1 = <0.75 2 = 0.75 to 0.80 3 = >0.80 to 0.85 4 = >0.85 to 0.90 5 = >0.90
Collision Vulnerability (CV)	*rotor swept zone (RSZt)*	WTG specific percentage of flight heights in RSZ. Flight heights modeled from Northwest Atlantic Seabird Catalog. Categories from Kelsey et al. (2018).	1 = < 5% in RSZ 3 = 5–20% in RSZ 5 = > 20% in RSZ
	macro-avoidance (MAc)	Avoidance rates and scoring categories from Willmott et al. (2013) and Kelsey et al. (2018).	1 = >40% avoidance 2 = 30 to 40% avoidance 3 = 18 to 29% avoidance 4 = 6 to 17% avoidance 5 = 0 to 5% avoidance

Vulnerability Component	Factor	Definition and Source	Scoring
	Nocturnal Flight Activity (NFA); Diurnal Flight Activity (DFA).	NFA scores were taken from Willmot et al. (2013); DFA was calculated using NJDEP boat-based survey data that records behavior including if birds are sitting or flying.	1 = 0–20% 2 = 21–40% 3 = 41–60% 4 = 61–80% 5 = 81–100%
Displacement Vulnerability (DV)	*MAd*	Macro-avoidance rates (MAd) that would decrease collision risk from Willmott et al. (2013) and Kelsey et al. (2018).	1 = 0–5% avoidance 2 = 6–17% avoidance 3 = 18–29% avoidance 4 = 30–40% avoidance 5 = > 40% avoidance
	Habitat flexibility (HF)	The degree to which a species is considered a habitat generalist (i.e., can forage in a variety of habitats) or a specialist (i.e., requires specific habitat and prey type). HF score and categories taken from Willmott et al. (2013).	0 = species does not forage in the Atlantic Outer Continental Shelf 1 = species uses a wide range of habitats over a large area and usually has a wide range of prey available to them 2 to 4 = grades of behavior between scores 1 and 5 5 = species with habitat- and prey-specific requirements that do not have much flexibility in diving-depth or choice of prey species

[1] Actual definitions for State conservation ranking may be adjusted to follow individual State language.

4.1.6.2. Collision Vulnerability

Collision vulnerability (CV) assessments can include a variety of factors including nocturnal flight activity, diurnal flight activity, avoidance, proportion of time within the rotor swept zone (RSZ), maneuverability in flight, and percentage of time flying (Furness et al. 2013; Willmott et al. 2013; Kelsey et al. 2018). The assessment process conducted here follows Kelsey et al. (2018) and includes proportion of time within the RSZ (RSZt), a measure of avoidance (MAc), and flight activity (NFA and DFA; Equation 2 below). Each factor was weighted equally and given a categorical score of 1–5 (Table 4-8). The final collision vulnerability scores were rescaled to a 0–1 scale, divided into quartiles, and then translated into four final vulnerability categories (Table 4-7). As described in the PV section, the score is then considered along with information available in existing literature; if there is sufficient evidence to deviate from the quantitative score, a CV categorical range is assigned for each species.

$$CCPP = RRCCRRRR + MMAAWW + (NNNNAA + DDNNAA)/2 \qquad \textit{Equation 2}$$

Specifics for each factor in CV are as follows:

- RSZt is included in the score to account for the probability that a bird may fly through the RSZ. Flight height data was selected from the Northwest Atlantic Seabird Catalog and included NJDEP boat-based surveys. Flight heights calculated from digital aerial survey methods were excluded because the methods have not been validated (Thaxter et al. 2015) and the standard flight height data used in European collision assessments (Masden 2019) is modeled primarily from boat-based survey (Johnston et al. 2014). Three additional boat-based datasets were excluded because there was low confidence in the data (collected by citizen science efforts, less standardized, and of lower quality) or estimated flight heights only included part of the air space below 300 m (984 ft).

Many of the boat-based datasets provided flight heights as categorical ranges for which the mid-value of the range in meters were determined, as well as the lower and upper bounds of the category. Upper bounds that were given as greater than X m were capped at 500 m (1,640 ft) to estimate upper bounds. A few datasets provided exact flight height estimates which resulted in upper and lower ranges being the same as the mid-value. A total of 100 randomized datasets were generated per species using the uniform distribution to select possible flight height values between lower and upper flight height bounds. Similar to methods from Johnston et al. (2014), flight heights were modeled using a smooth spline of the square root of the binned counts in 10-m (32-ft) bins. The integration of the smooth spline model count within each 1 m (3 ft) increment was calculated and the mean and standard deviation of all 100 models were calculated across all 1-m (3-ft) increments. The proportion of animals within each RSZ was estimated by summing the 1 m (3 ft) count integrations and dividing by the total estimate count of animals across all RSZ zones, then values were converted to a 1–5 scale based upon the categories used by Kelsey et al. (2018; see Table 4-8). The RSZ was defined by minimum and maximum WTG options being considered for the Lease Area (two different power unit ranges at

two different tower heights; Table 4-9). The analysis was conducted in R Version 4.1.1.[13] Of note, there are several important uncertainties in flight height estimates: flight heights from boats can be skewed low; flight heights are generally recorded during daylight and in fair weather; and flight heights may change when WTGs are present.

Table 4-9: WTG specifications used in the vulnerability analysis; mean lower low water (MLLW) is the average height of the lowest tide recorded at a tide station each day during the recording period.

WTG Parameter	Measurement
Maximum tip height (MLLW)	319.68 m (1,048.82 ft)
Minimum tip clearance/air gap (MLLW)	23.78 m (78.02 ft)

- MAc is included in the score to account for macro-avoidance rates that would decrease collision risk. Macro-avoidance is defined as a bird's ability to change course to avoid the entire wind farm area (Kelsey et al. 2018), versus meso-avoidance (avoiding individual WTGs), and micro-avoidance (avoiding WTG blades; Skov et al. 2018). The scores used in the assessment were based on Willmott et al. (2013), who conducted a literature review to determine known macro-avoidance rates and then converted them to a 1–5 score based upon the categories in Table 4-8. The MAc indicates that this factor is used in the CV versus the MAd, which was used in the displacement vulnerability (DV) score (described below). For the assessment conducted here, Willmott et al. (2013) avoidance rates were updated to reflect the most recent empirical studies (Krijgsveld et al. 2011; Cook et al. 2012; Vanermen et al. 2015; Cook et al. 2018), and indexes (Garthe and Hüppop 2004; Furness et al. 2013; Bradbury et al. 2014; Adams et al. 2016; Wade et al. 2016; Kelsey et al. 2018). For the empirical studies, the average avoidance was used when a range was provided in a paper. For the indices, the scores were converted to a continuous value using the median of a scores range; only one value was entered for related indices (e.g., Adams et al. 2016 and Kelsey et al. 2018). When multiple values were available for a species, the mean value was calculated. For some species, averaging the avoidance rates across both the empirical studies and indices led to some studies being counted multiple times. Indices were included to capture how the authors interpreted the avoidance studies and determined avoidance rates for species where data was not available. There are several important uncertainties in determining avoidances rates: the studies were all conducted in Europe; the studies were conducted at wind farms with WTGs smaller than are proposed for the Lease Area; the methods used to record avoidance rates varied and included surveys, radar, and observers; the analytical methods used to estimate avoidance rates also varied significantly between studies; and the avoidance rate for species where empirical data is not available were assumed to be similar to closely-related species.

[13] R Core Team (2021). R: A language and environment for statistical computing. R Foundation for Statistical Computing, Vienna, Austria. URL https://www.R-project.org

- NFA and DFA include scores of estimate percentage of time spent flying at night and during the day based upon the assumption that more time spent flying would increase collision risk. The NFA scores were taken directly from the scores, based upon literature review, from Willmott et al. (2013). The DFA score was calculated from the baseline survey data that categorized if a bird was sitting or flying for each bird observation. Per Kelsey et al. (2018), the NFA and DFA scores were equally weighted and averaged.

4.1.6.3. Displacement Vulnerability

Rankings of DV account for two factors: (1) disturbance from ship/helicopter traffic and the wind farm structures (MAd), and (2) habitat flexibility (HF; Furness et al. 2013; Kelsey et al. 2018). This assessment combines these two factors, weights them equally, and categorizes them from 1–5 (Equation 3 below; Table 4-7). It is worth noting that while Furness et al. (2013) down-weighted the DV score by dividing by 10 (they assumed displacement would have lower impacts on the population), the assessment conducted here maintains the two scores on the same scale.

Empirical studies indicate that for some species, particularly sea ducks, avoidance behavior may change over time and that several years after projects have been built some individuals may forage within the wind farm. The taxonomic specific text indicates whether there is evidence that displacement may be partially temporary. The final displacement vulnerability scores are rescaled to a 0–1 scale, divided into quartiles, and translated into four final vulnerability categories (Table 4-8). As described in the PV section, the score is then considered along with the literature; if there is sufficient evidence to deviate from the quantitative score, a DV categorical range is assigned for each species.

$$DDPP = MMAAMM + HHNN \qquad \textit{Equation 3}$$

Specifics for each factor in DV are as follows:

- *MAd* is included to account for behavioral responses from birds that lead to macro-avoidance of wind farms, and that have the potential to cause effective habitat loss if the birds are permanently displaced (Fox et al. 2006). The MAd scores used in the assessment were based on Willmott et al. (2013) but updated to reflect the most recent empirical studies (Krijgsveld et al. 2011; Cook et al. 2012; Vanermen et al. 2015; Cook et al. 2018; Skov et al. 2018), and indexes (Garthe and Hüppop 2004; Furness et al. 2013; Bradbury et al. 2014; Adams et al. 2016; Wade et al. 2016; Kelsey et al. 2018). See MAc above for further details. The scores are the same as the MAc scores described above, but, following methods from Kelsey et al. (2018), are inverted so that a high avoidance rate (greater than 40%) is scored as a 5. Since the greater than 40% cutoff is a low threshold, many species can receive a high 5 score; there is a large range within this high category that includes species documented to have moderate avoidance rates (e.g., terns) and species with near complete avoidance (e.g., loons).
- *HF* accounts for the degree to which a species is considered a habitat generalist (i.e., can forage in a variety of habitats) or a specialist (i.e., requires specific habitat and prey type). The assumption is that generalists are less likely to be affected by displacement, whereas

specialists are more likely to be affected (Kelsey et al. 2018). The values for HF used in this assessment were taken from Willmott et al. (2013). Note that Willmott et al. (2013) used a 1–5 scale plus a "0" to indicate that a species does not forage in the OCS.

4.1.6.4. Uncertainty

Uncertainty is recognized in this assessment for both exposure and vulnerability. Given the natural variability of ecosystems and recognized knowledge gaps, assessing how anthropogenic actions will affect the environment inherently involves a degree of uncertainty (Walker et al. 2003). Broadly defined, uncertainty is incomplete information about a subject (Masden et al. 2015) or a deviation from absolute determinism (Walker et al. 2003). In the risk assessment conducted here, uncertainty is broadly recognized as a factor in the process, and is accounted for by including, based upon the best available data, a range for the exposure, vulnerability, and population scores when appropriate.

For offshore wind avian assessments, uncertainty primarily arises from two sources: predictions of bird use of a project area and region (i.e., exposure); and our understanding of how birds interact with WTGs (i.e., vulnerability). While uncertainty will always be present in any assessment of offshore wind and acquiring data on bird movements during hours of darkness and in poor weather is difficult, overall knowledge on bird use of the marine environment has improved substantially in recent years through local survey efforts, revised regional modeling efforts, and individual tracking studies. For many species, multiple data sources may be available to make an exposure assessment, such as survey and individual tracking data. If the data sources show differing patterns in use of the wind farm area, then a range of exposure is provided (e.g., minimal–low) to account for all available data and to capture knowledge gaps and general uncertainty about bird movements.

Similarly, knowledge has been increasing on the vulnerability of birds to offshore wind facilities in Europe (e.g., Skov et al. 2018). Vulnerability assessments have either incorporated uncertainty into the scoring process to calculate a range of ranks (Willmott et al. 2013; Kelsey et al. 2018) or have developed separate standalone tables (Wade et al. 2016). In order to keep the scoring process as simple as possible, this assessment does not directly include uncertainty in the scoring, rather it uses the uncertainty assessment conducted by Wade et al. (2016) as a reference (Table 4-10). Scientific literature that provides additional insights to the vulnerability of marine and non-marine birds to offshore wind facilities is listed in Table 4-6. Like exposure, if there is evidence in the literature, or from other data sources, that conflicts with the vulnerability score, the score will be adjusted up or down, as appropriate, to include a range that extends into the next category. This approach accounts for knowledge gaps and general uncertainty about vulnerability.

Table 4-10: Vulnerability uncertainty adapted from Wade et al. (2016) to include only species occurring in North America.

Species	Scientific Name	Uncertainty Level: % of time at altitudes overlapping with turbine blades	Uncertainty Score	Uncertainty Level: Displacement caused by structures	Uncertainty Score	Uncertainty Level: Displacement casued by vessels and/or helicopters	Uncertainty Score	Uncertainty Level: Use of tidal races	Uncertainty Score	Overall Uncertainty Score (max 20)
European Storm-Petrel	*Hydrobates pelagicus*	Very high	1	Very high	1	High	2	Very high	1	5
Leach's Storm-Petrel	*Hydrobates leucorhous*	Very high	1	Very high	1	High	2	Very high	1	5
Sooty Shearwater	*Ardenna grisea*	Very high	1	Very high	1	High	2	Very high	1	5
Parasitic Jaeger	*Stercorarius parasiticus*	Moderate	3	Very high	1	Very high	1	Very high	1	6
Common Goldeneye	*Bucephala clangula*	Very high	1	Very high	1	High	2	High	2	6
Greater Scaup	*Aythya marila*	Very high	1	Very high	1	High	2	High	2	6
Manx Shearwater	*Puffinus puffinus*	High	2	Very high	1	High	2	Very high	1	6
Horned Grebe	*Podiceps auritus*	Very high	1	High	2	High	2	Very high	1	6
Long-tailed Duck	*Clangula hyemalis*	Very high	1	High	2	High	2	High	2	7
Roseate Tern	*Sterna dougallii*	Very high	1	High	2	High	2	High	2	7
Great Skua	*Stercorarius skua*	Moderate	3	High	2	High	2	Very high	1	8
Little Tern	*Sterna albifrons*	Very high	1	Moderate	3	Very High	1	Moderate	3	8
Black-headed Gull	*Chroicocephalus redibundus*	Moderate	3	Moderate	3	High	2	Very high	1	9
Northern Fulmar	*Fulmarus glacialis*	Low	4	High	2	High	2	Very high	1	9
Artic Tern	*Sterna paradisaea*	Moderate	3	Moderate	3	High	2	High	2	10
Common Loon	*Gavia immer*	High	2	High	2	Very high	1	Very low	5	10
Dovekie	*Alle alle*	Very high	1	Low	4	Low	4	Very high	1	10
Arctic Loon	*Gavia arctica*	High	2	Moderate	3	High	2	Low	4	11
Common Gull	*Larus canus*	Low	4	Low	4	High	2	Very high	1	11
Common Eider	*Somateria mollissima*	Moderate	3	Moderate	3	Moderate	3	Moderate	3	12
Sandwich Tern	*Thalasseus sandvicensis*	Low	4	Low	4	High	2	High	2	12
Black Guillemot	*Cepphus grylle*	Very high	1	High	2	Very low	5	Very low	5	13
Great black-backed Gull	*Larus marinus*	Low	4	Very low	5	Moderate	3	Very high	1	13
Great Cormorant	*Phalacrocorax carbo*	Moderate	3	Very low	5	High	2	Moderate	3	13
Black-legged Kittiwake	*Rissa tridactyla*	Very low	5	Very low	5	High	2	High	2	14
Common Tern	*Sterna hirundo*	Very low	5	Low	4	High	2	Moderate	3	14
Herring Gull	*Larus argentatus*	Very low	5	Very low	5	Moderate	3	Very high	1	14
Lesser black-backed Gull	*Larus fuscus*	Very low	5	Very low	5	Moderate	3	Very high	1	14
Northern Gannet	*Morus bassanus*	Very low	5	Very low	5	High	2	High	2	14
Red-throated Loon	*Gavia stellata*	Low	4	Low	4	High	2	Low	4	14
Black Scoter	*Melanitta americana*	Low	4	Very low	5	Low	4	High	2	15
Atlantic Puffin	*Fratercula arctica*	Moderate	3	Moderate	3	Very low	5	Very low	5	16
Razorbill	*Alca torda*	Low	4	Very low	5	Very low	5	Low	4	18
Common Murre	*Uria aalge*	Low	4	Very low	5	Very low	5	Very low	5	19

5. Birds – Offshore: Results

Interpretation of the results are presented in Section 4.3 Birds of the COP Volume II. The results provided below are organized by sections addressing exposure and vulnerability of coastal birds and marine birds separately and include maps, tables, and figures for each species or species group. ESA-listed and candidate species are assessed individually.

5.1. Coastal birds

The following section presents the results of the coastal bird exposure assessment. Exposure assessment maps, tables, and figures are presented based on numerous references and data sets, including, but not limited to, the APEM digital aerial surveys, NJDEP boat-based surveys, Northwest Atlantic Seabird Catalog data, occurrence data, individual tracking data, relevant literature, and species accounts. Since there is a diversity of data sources, a variety of data analysis methods are used that all support exposure and vulnerability assessments. For coastal birds, the relative behavioral vulnerability assessment is discussed in Section 4.3 Birds of the COP Volume II and is primarily based upon the literature and expert opinion.

5.1.1. Shorebirds

5.1.1.1. Maps

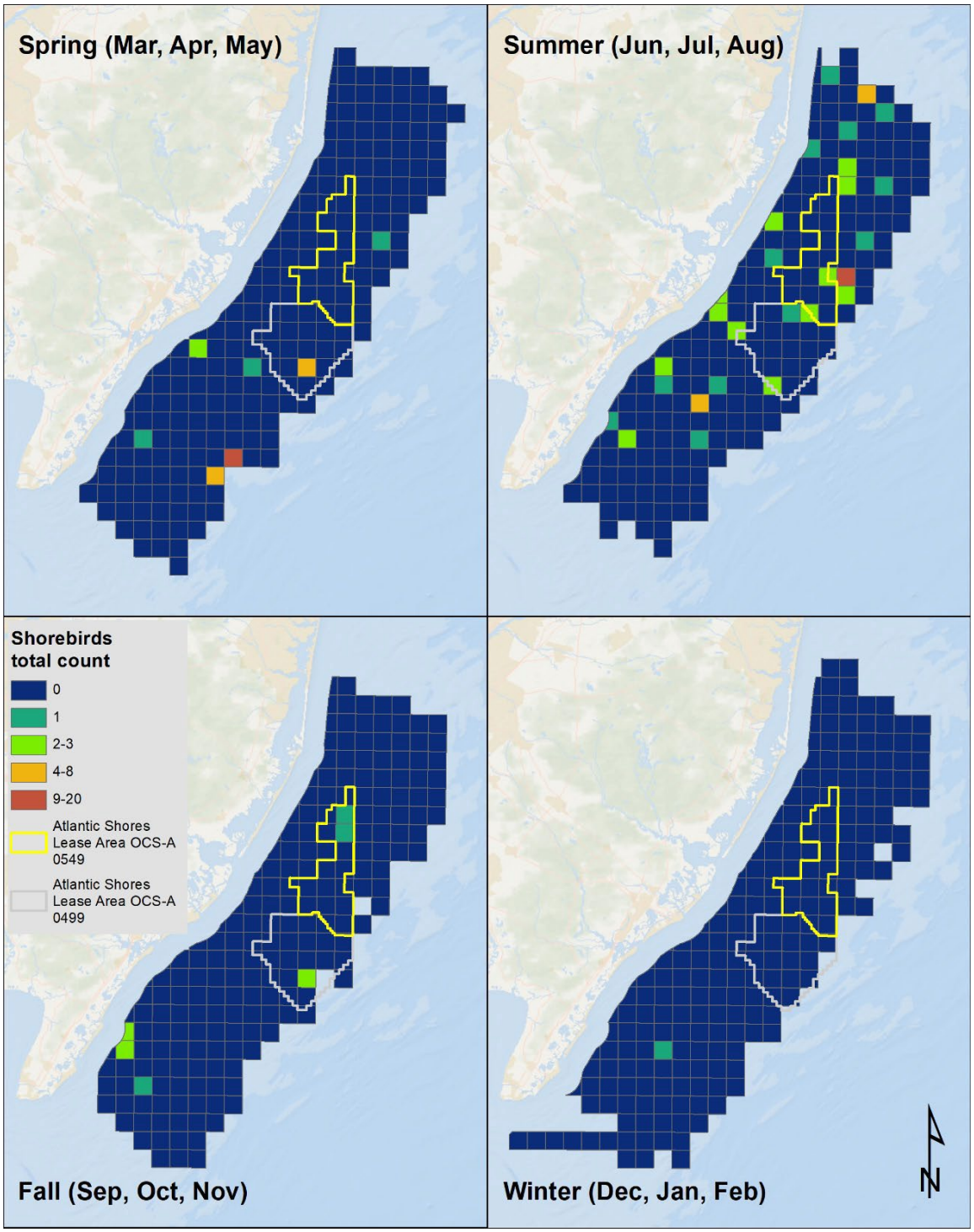

Figure 5-1: Shorebirds observed in the NJDEP boat-based surveys, by season.

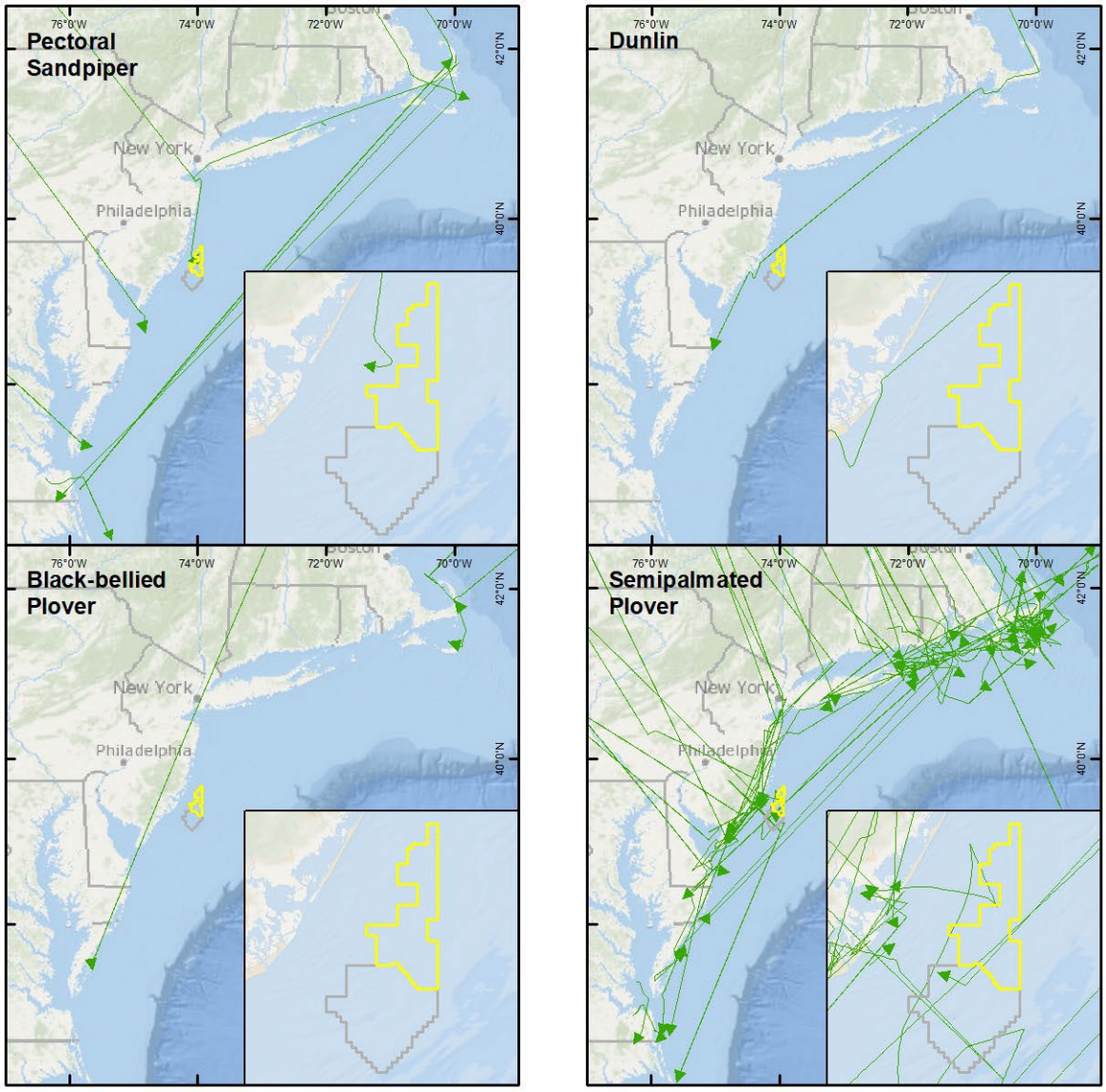
Pectoral Sandpiper
Dunlin
Black-bellied Plover
Semipalmated Plover
New York
Philadelphia
76°0'W
74°0'W
72°0'W
70°0'W
42°0'N
40°0'N
0 75 150 300 Miles
0 125 250 500 Km
CS: WGS 1984 Web Mercator Auxiliary Sphere
Atlantic Shores Lease Area OCS-A 0549
Atlantic Shores Lease Area OCS-A 0499
Fall flight paths
Produced by: A. Gilbert
Version date: 3/2/2022
Document: ASNorth_COP_LoringMotus_PESA_DUNL_BBPL_SEPL_030222

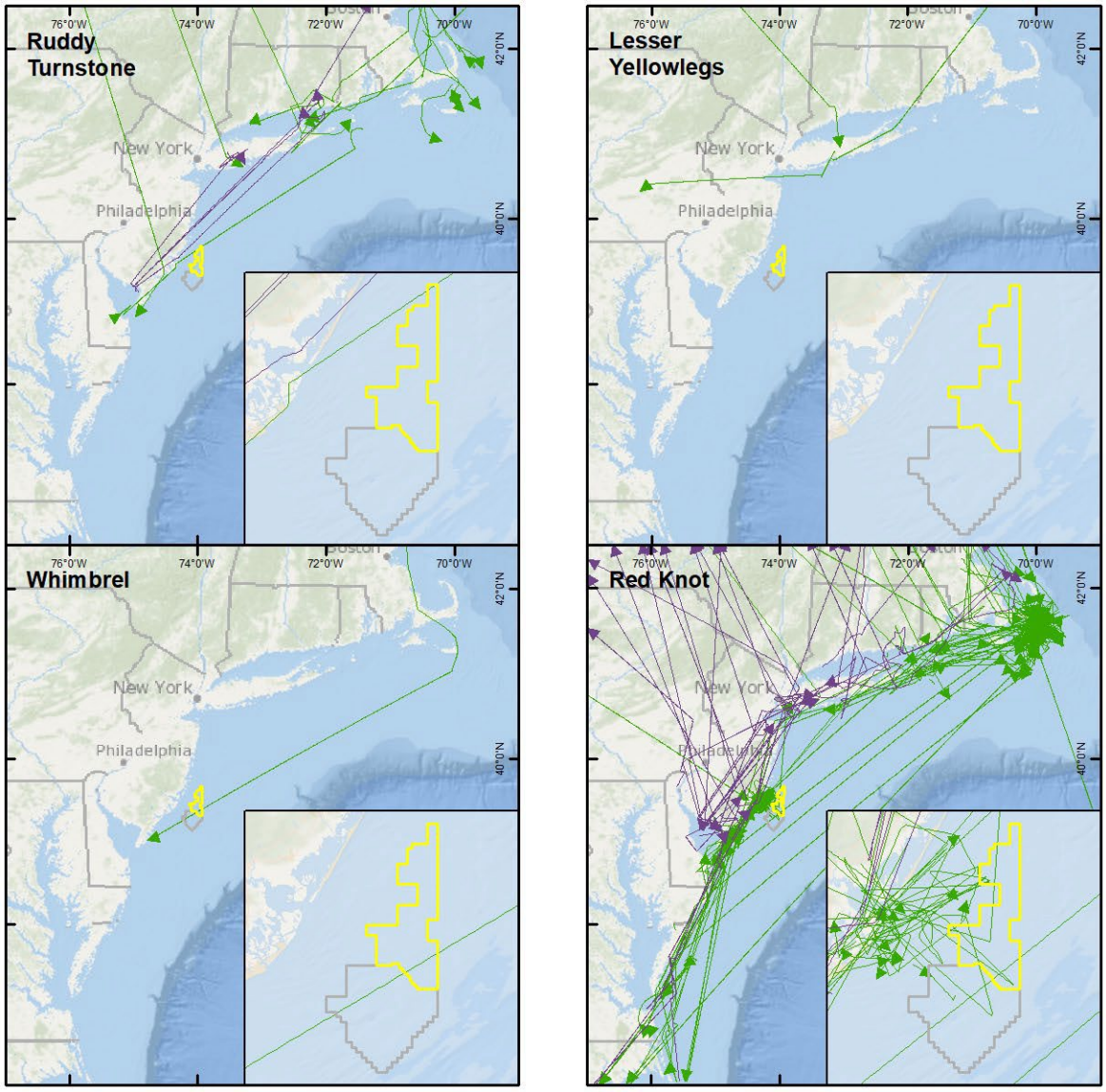
Ruddy Turnstone
Lesser Yellowlegs
Whimbrel
Red Knot
New York
Philadelphia
76°0'W
74°0'W
72°0'W
70°0'W
42°0'N
40°0'N
bri
Produced by: A. Gilbert
Version date: 3/2/2022
Document: ASNorth_COP_LoringMotus_RUTU_LEYE_WHIM_REKN_030222
0 75 150 300 Miles
0 125 250 500 Km
CS: WGS 1984 Web Mercator Auxiliary Sphere
N
Atlantic Shores Lease Area OCS-A 0549
Atlantic Shores Lease Area OCS-A 0499
Spring flight paths
Fall flight paths

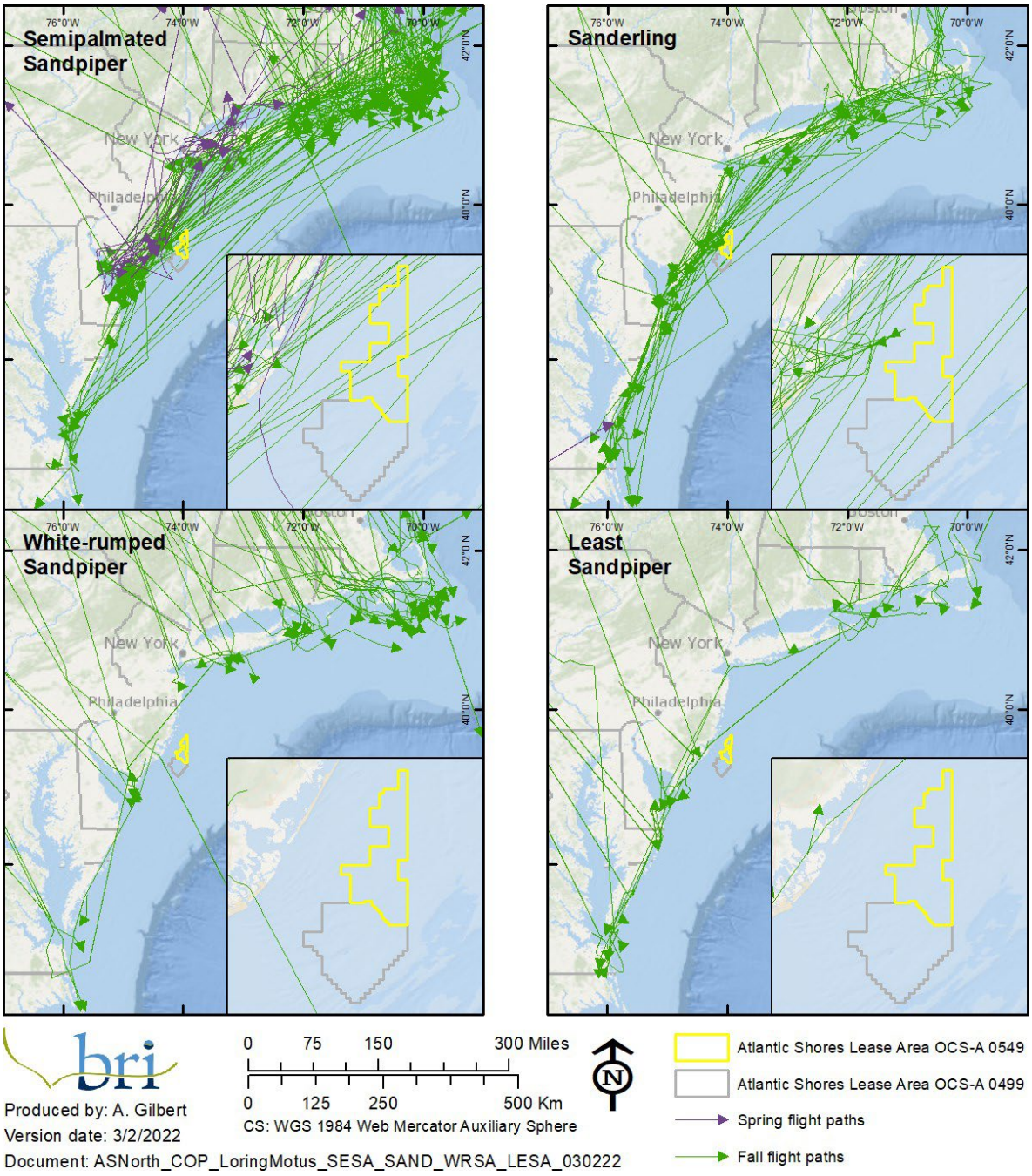

NOTE: Tracks are not actual flight paths but interpolated (model-generated) flight paths. Flight paths were modeled by detections of movements between land-based towers. Towers had a typical detection range <9.3 mi (<15 km), so birds were only detected when flying within approximately 9.3 mi (15 km) of one of the towers. (See Fig. 5 [tower locations] in Loring et al. [2019] and Appendix K [detection probability] for details. Appendices are found at: https://espis.boem.gov/final%20reports/BOEM_2019-017a.pdf.) Data provided by USFWS and used with permission.

Figure 5-2: **Modeled flight paths of migratory shorebirds equipped with nanotags (Loring et al. 2020).**

5.1.2. Endangered Shorebird Species

5.1.2.1. Piping Plover

5.1.2.1.1. Maps

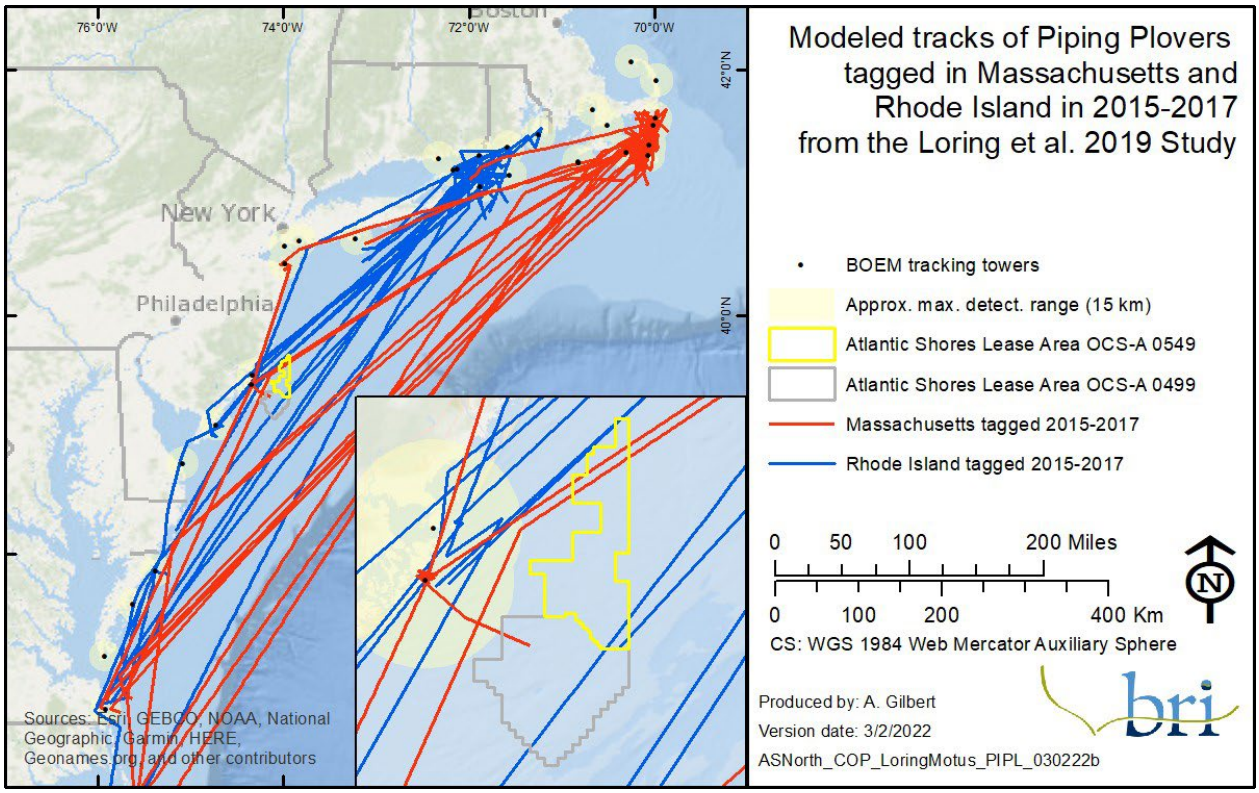

NOTE: Tracks are not actual flight paths but interpolated (model-generated) flight paths. Flight paths were modeled by detections of movements between land-based towers. Towers had a typical detection range <9.3 mi (<15 km), so birds were only detected when flying within approximately 9.3 mi (15 km) of one of the towers. (See Fig. 5 [tower locations] in Loring et al. [2019] and Appendix K [detection probability] for details. Appendices are found at: https://espis.boem.gov/final%20reports/BOEM_2019-017a.pdf.) Data provided by USFWS and used with permission.

Figure 5-3: Modeled flight paths of migratory Piping Plovers equipped with nanotags (Loring et al. 2019).

5.1.2.2. Red Knot

5.1.2.2.1. Maps

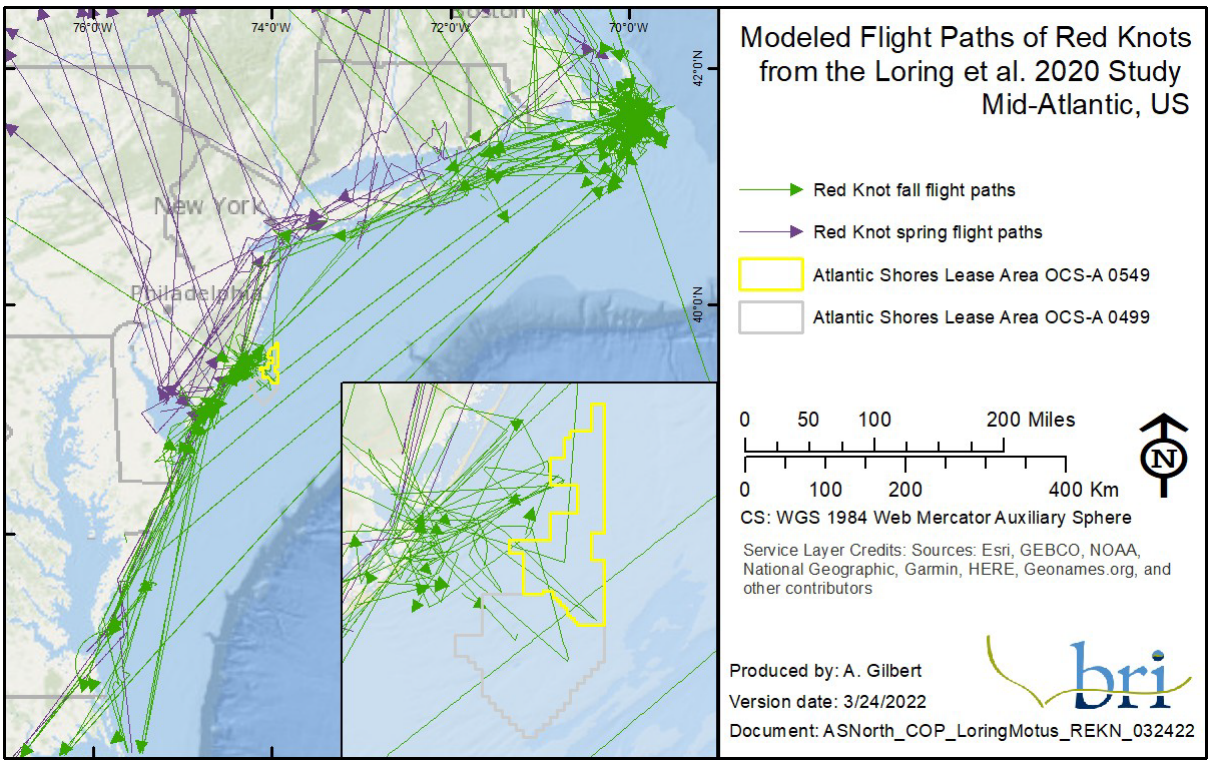

NOTE: Tracks are not actual flight paths but interpolated (model generated) flight paths. Flight paths were modeled by detections of movements between land-based towers. Towers had a typical detection range <9.3 mi (<15 km), so birds were only detected when flying within approximately 9.3 mi (15 km) of one of the towers. (See Fig. 5 [tower locations] in Loring et al. [2019] and Appendix K [detection probability] for details). Appendices are found at: https://espis.boem.gov/final%20reports/BOEM_2019-017a.pdf. Data provided by USFWS and used with permission.

Figure 5-4: Modeled flight paths of migratory Red Knots equipped with nanotags (Loring et al. 2020).

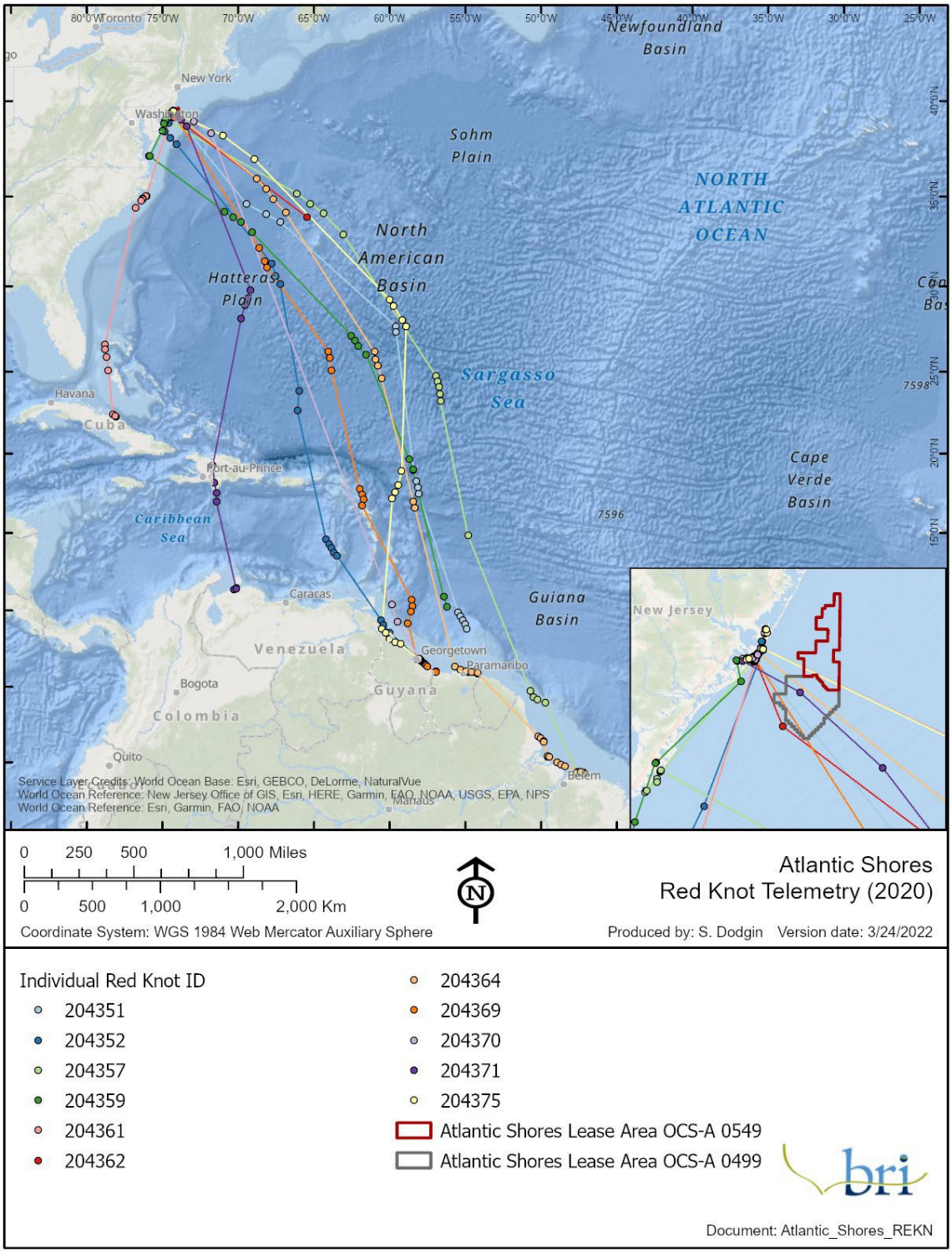

Figure 5-5: Movements of 11 Red Knots tagged at Brigantine, New Jersey, in 2020, as they depart on migration. Straight-line flight paths of two birds (204370 and 204375, overlapping in map) crossed OCS-A 0549.

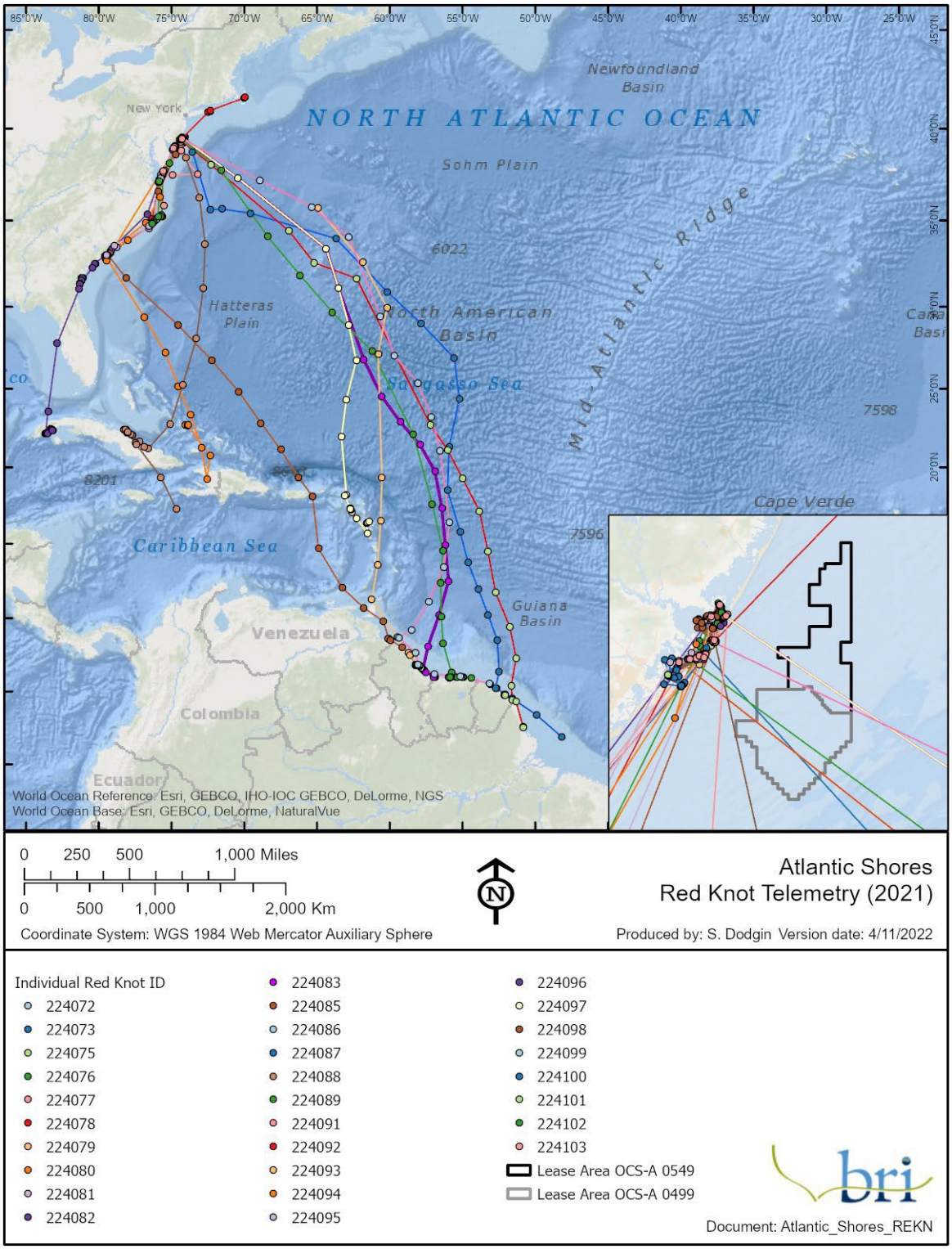

Figure 5-6: Movements of 29 Red Knots tagged in coastal New Jersey, in 2021, as they depart on migration. Straight-line flight paths of three birds (224083, 224097, and 224099) crossed OCS-A 0549.

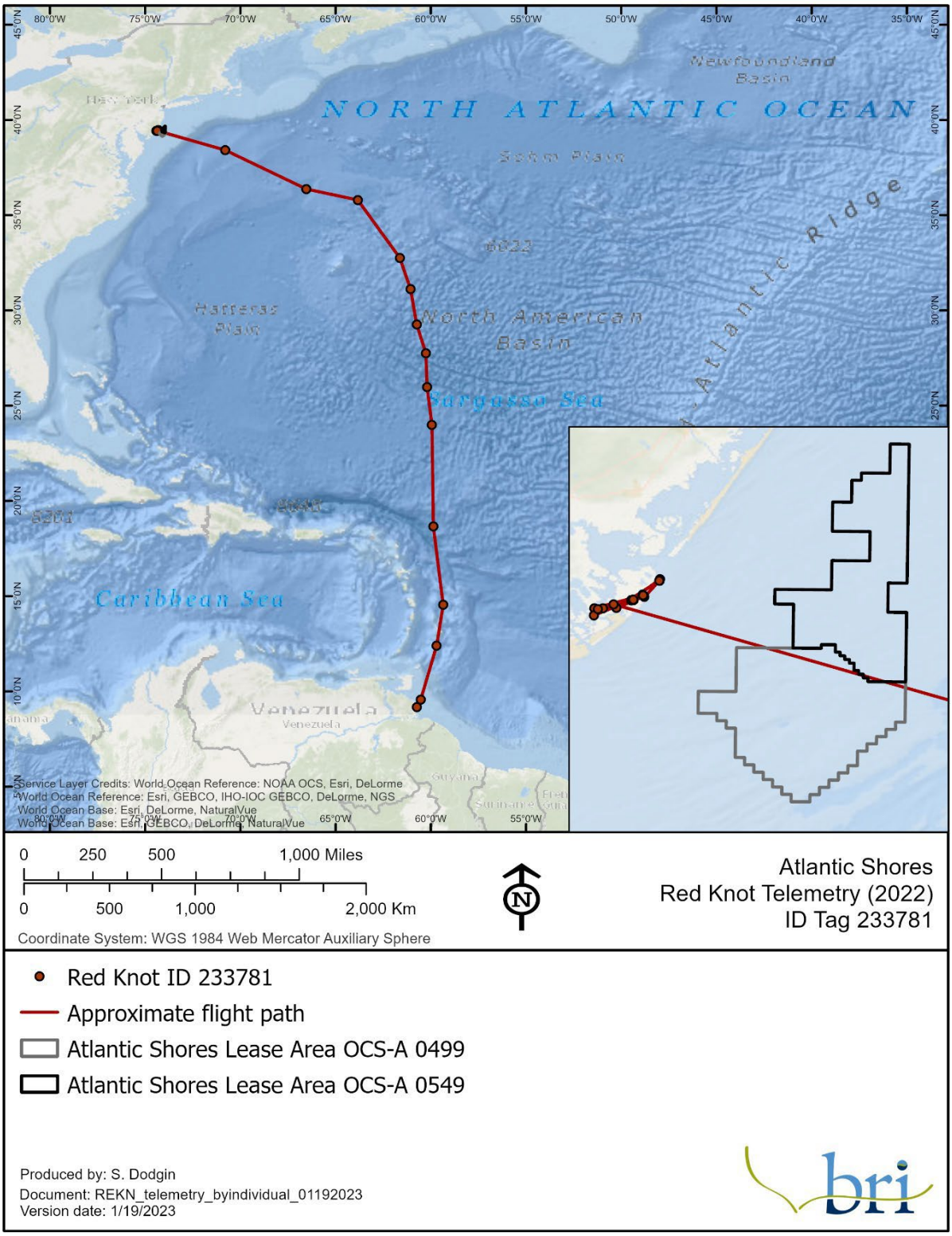

Figure 5-7: Movements of 1 Red Knots tagged in coastal New Jersey, in 2022, as they depart on migration. Straight-line flight paths of one bird (233781) crossed OCS-A 0549.

Coastal Waterbirds (waterfowl)

5.1.1.1 Maps

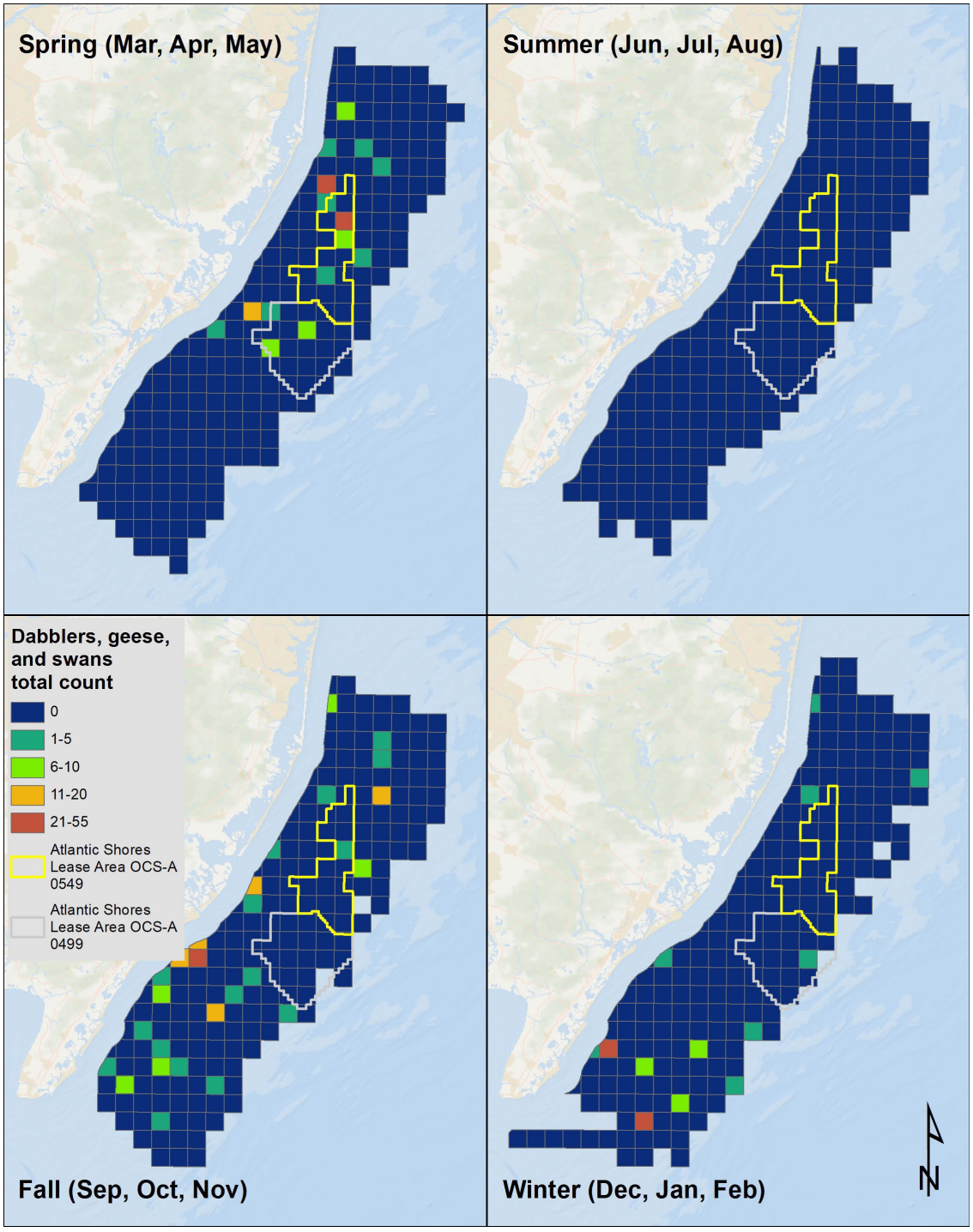

Figure 5-8: Coastal dabbling ducks, geese, and swans observed in the NJDEP boat-based surveys, by season.

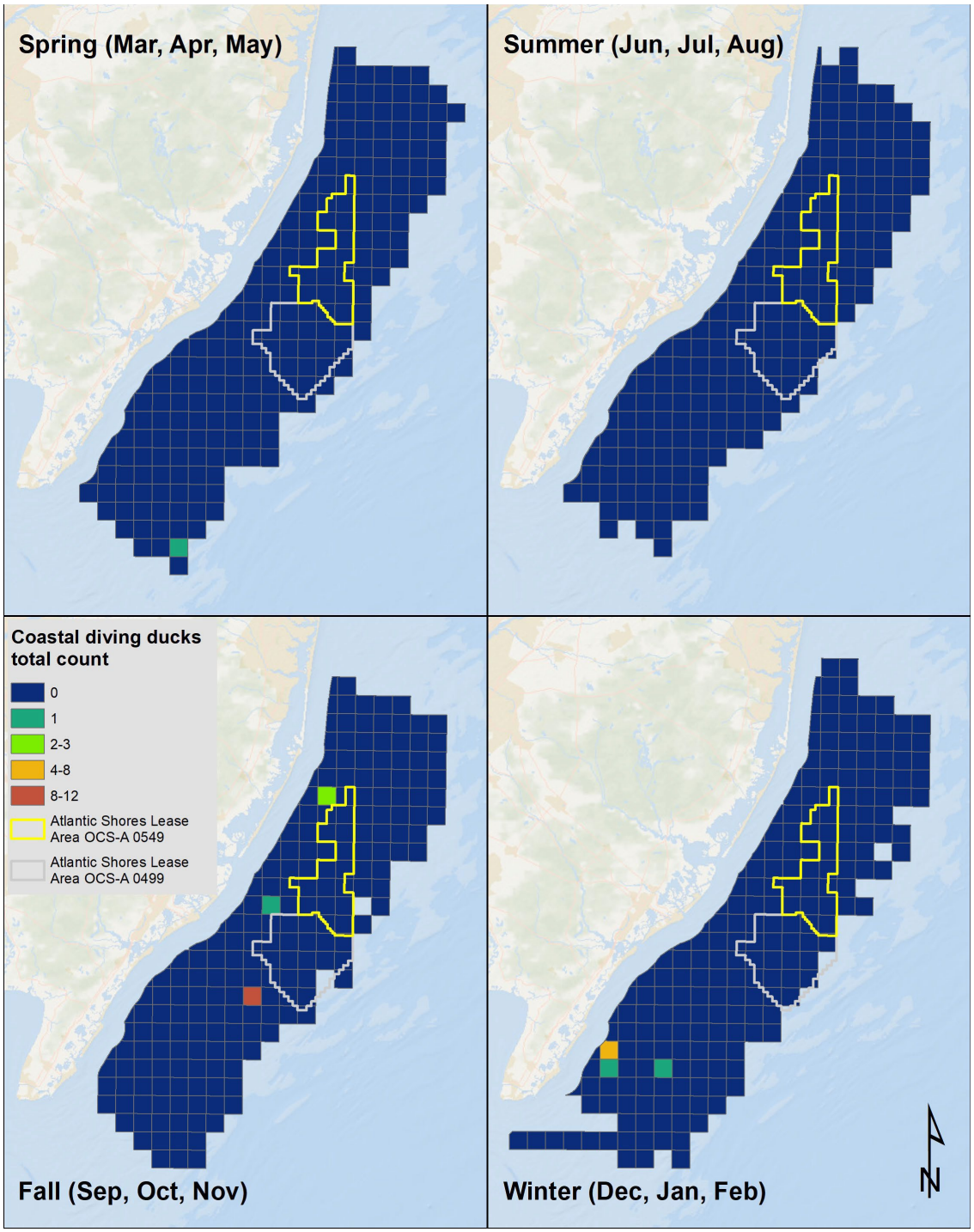

Figure 5-9: Coastal diving ducks observed in the NJDEP boat-based surveys, by season.

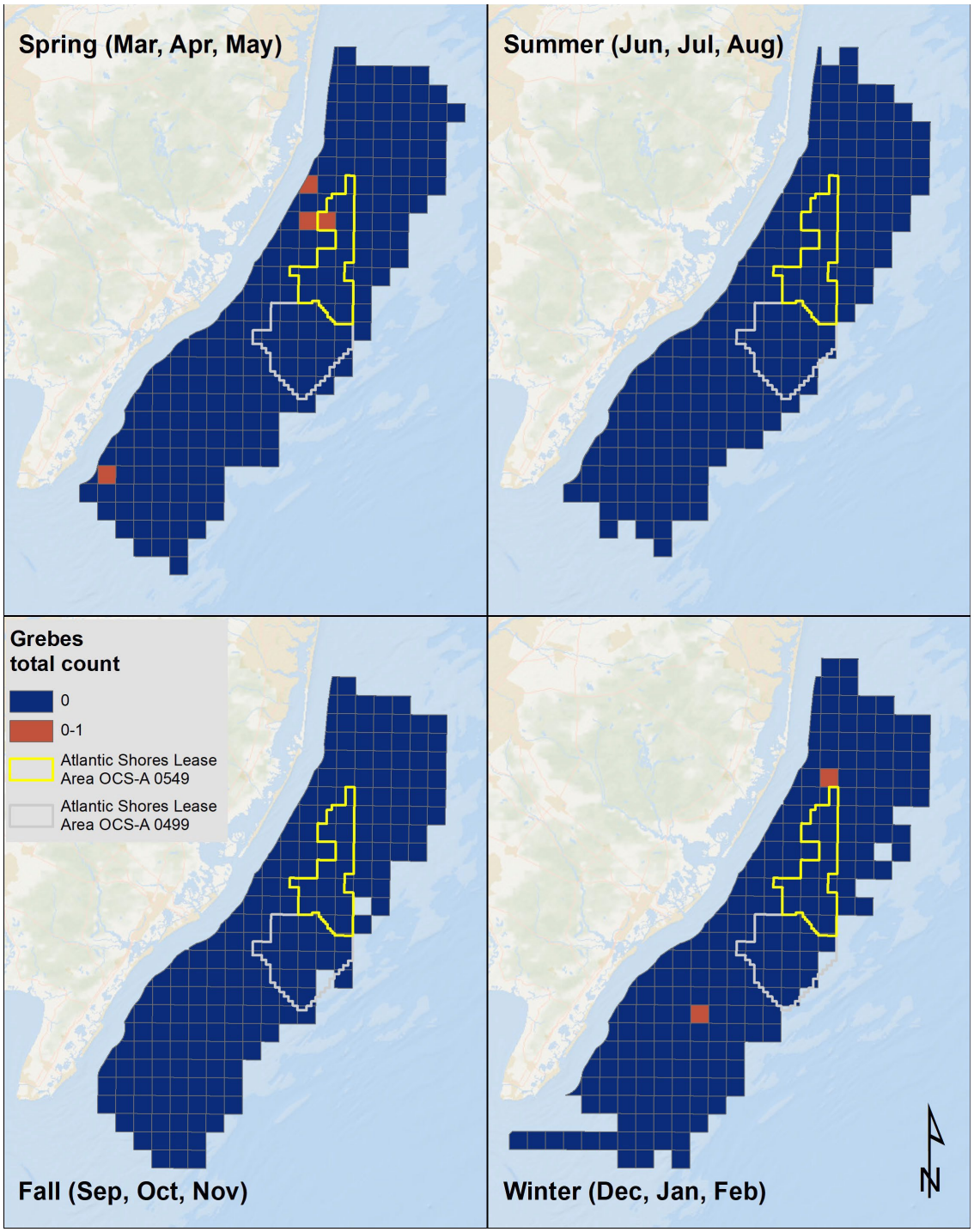

Figure 5-10: Grebes observed in the NJDEP boat-based surveys, by season.

5.1.3. Wading Birds

5.1.3.1. Maps and Figures

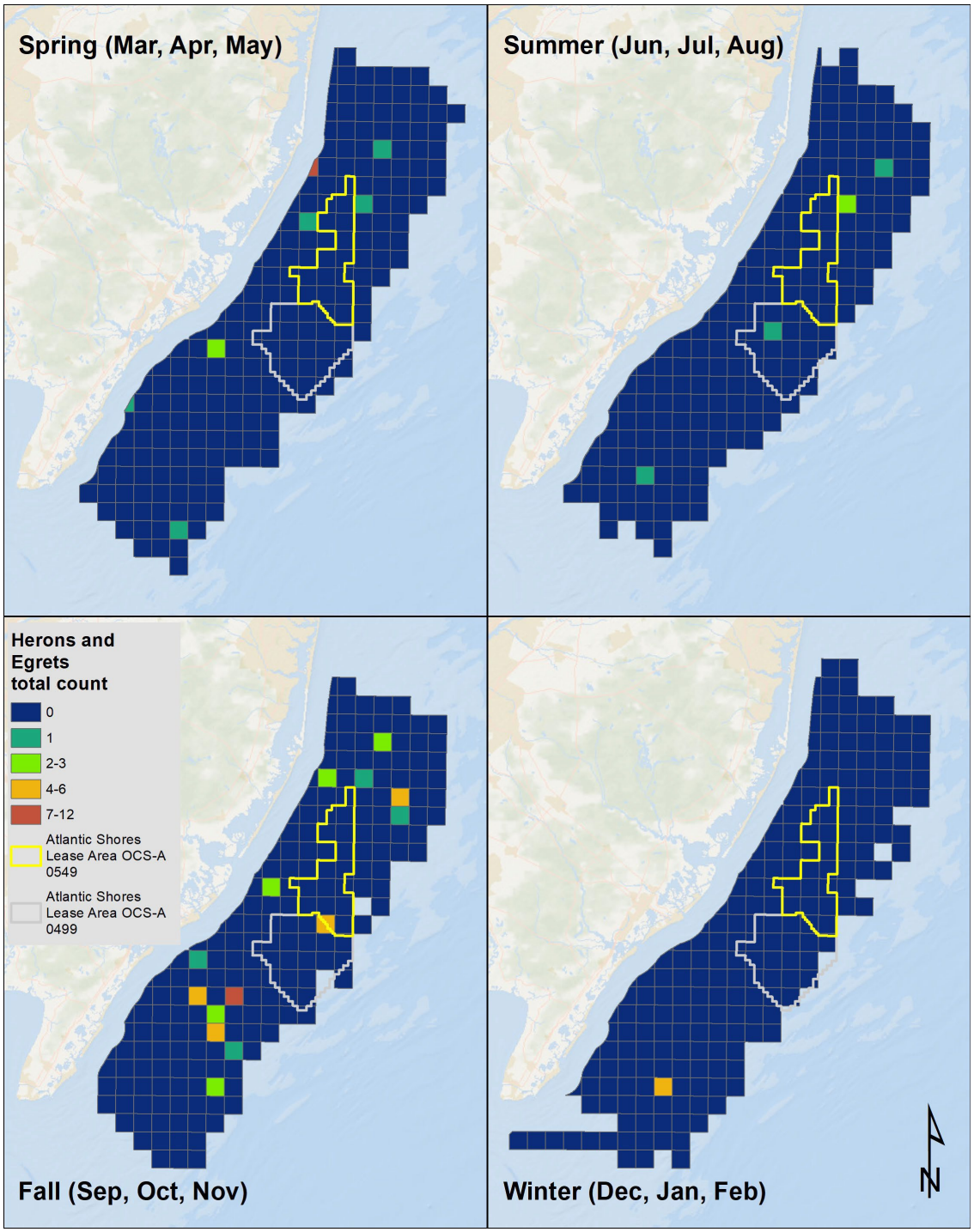

Figure 5-11: Herons and egrets observed in the NJDEP boat-based surveys, by season.

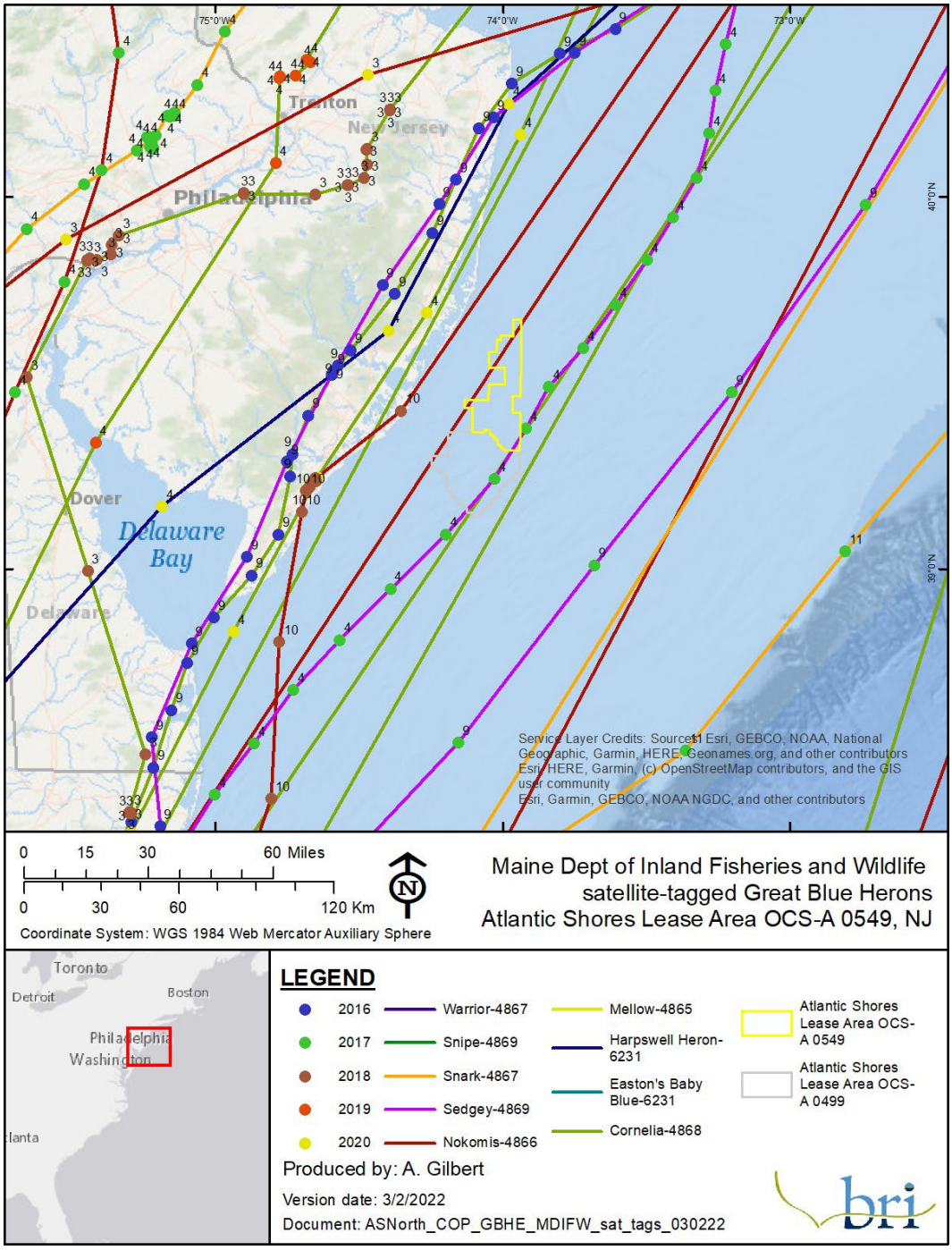

Figure 5-12: Track lines of Great Blue Herons captured in Maine and equipped with satellite transmitters provided by Maine Department of Inland Fisheries and Wildlife.

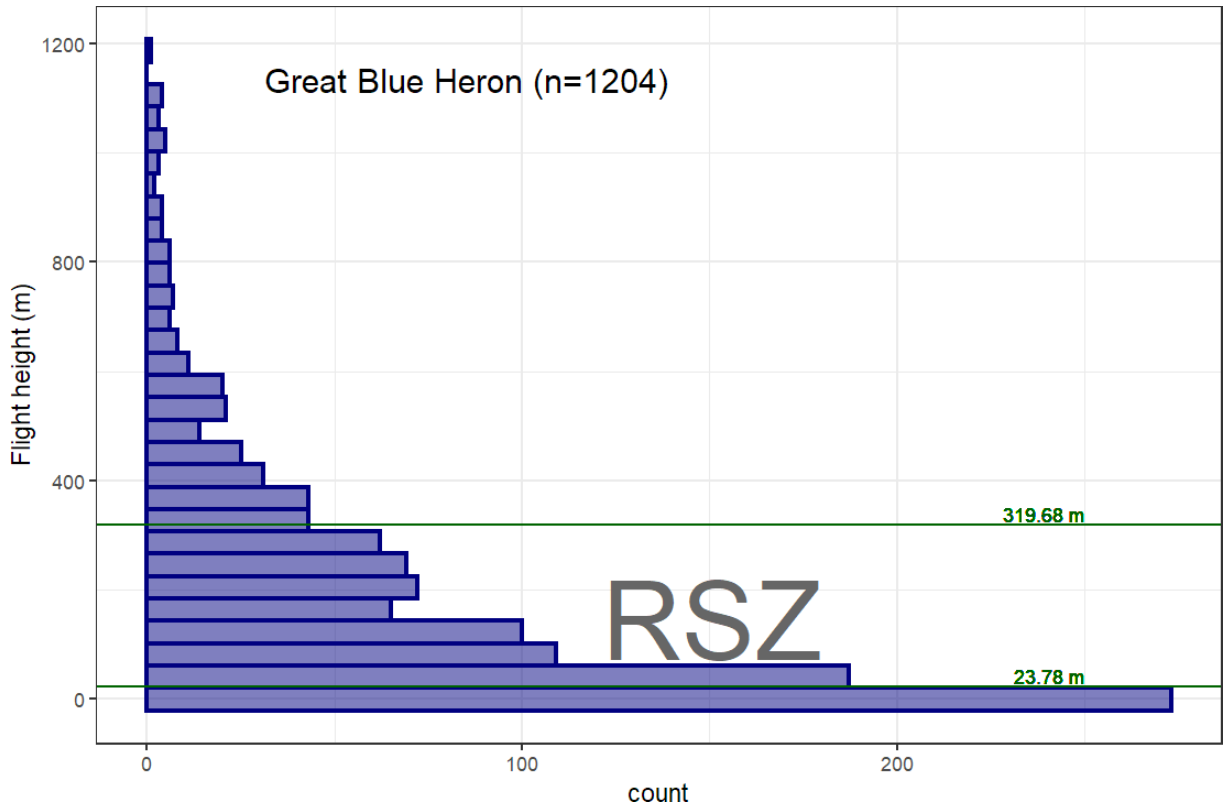

Figure 5-13: Flight heights (m) of Great Blue Herons satellite-tagged in Maine, flying over the Atlantic OCS, in relation to the upper and lower limits of the RSZ (23.78 to 319.68 m [78.02 to 1,048.82 ft]).

5.1.4. Raptors

5.1.4.1. Maps

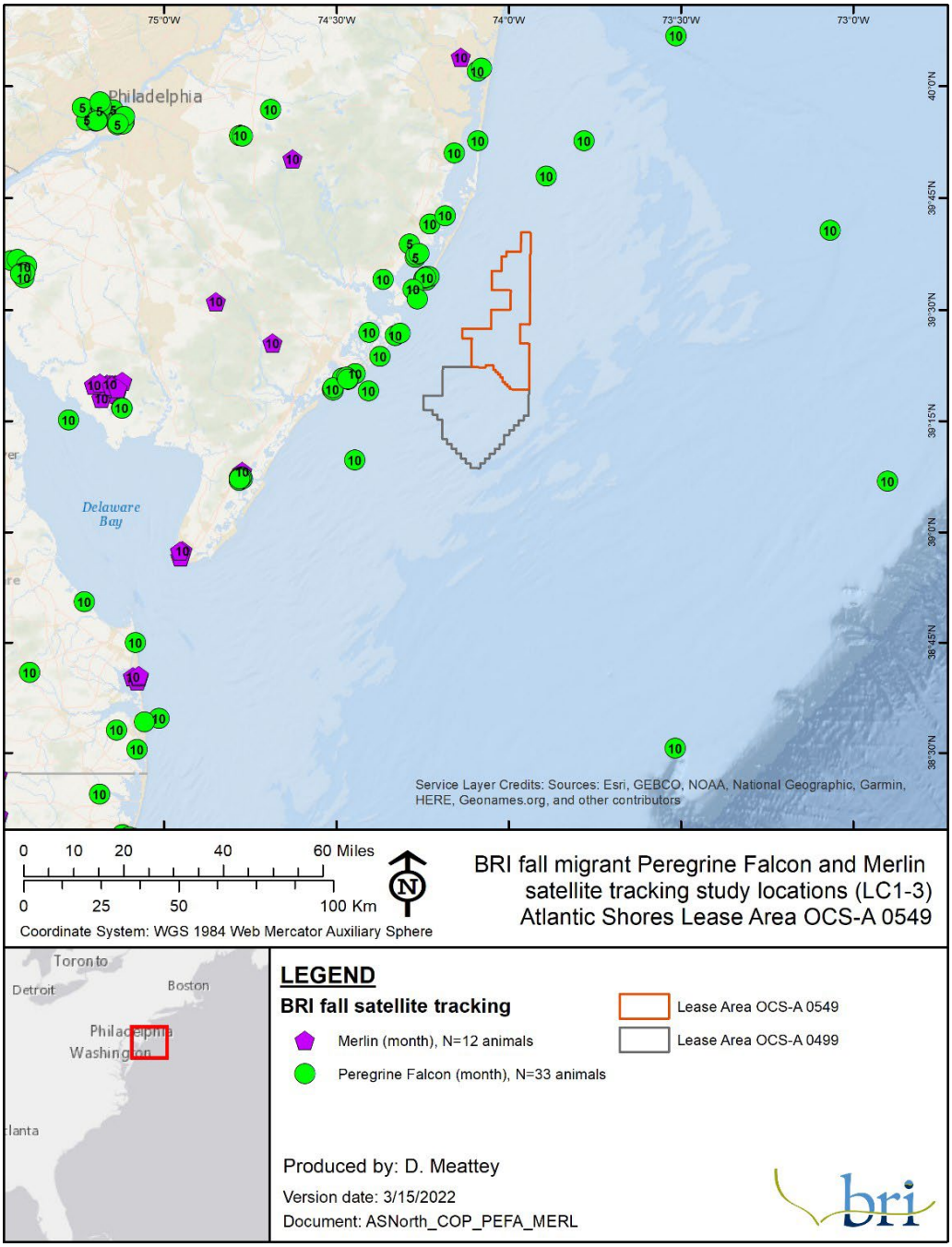

Figure 5-14: Location estimates from satellite transmitters on Peregrine Falcons and Merlins tracked from three raptor research stations along the Atlantic coast, 2010–2018 (DeSorbo, Persico, et al. 2018).

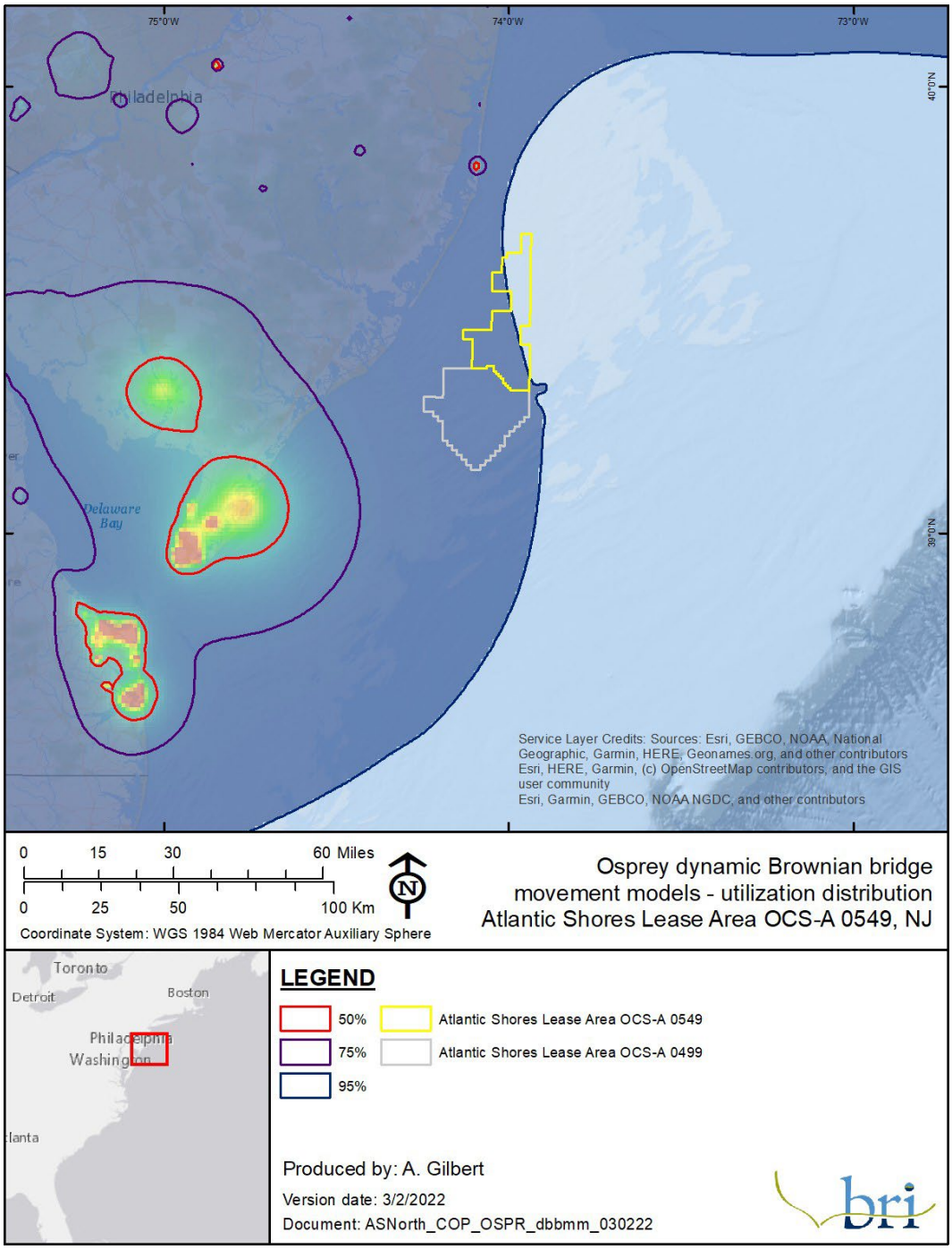

NOTE: The contours represent the percentage of the use area across the UD surface and represent various levels of use from 50% (core use) to 95% (home range).

Figure 5-15: Dynamic Brownian bridge movement models for osprey (n = 127) that were tracked with satellite transmitters.

5.1.5. Songbirds

5.1.5.1. Maps

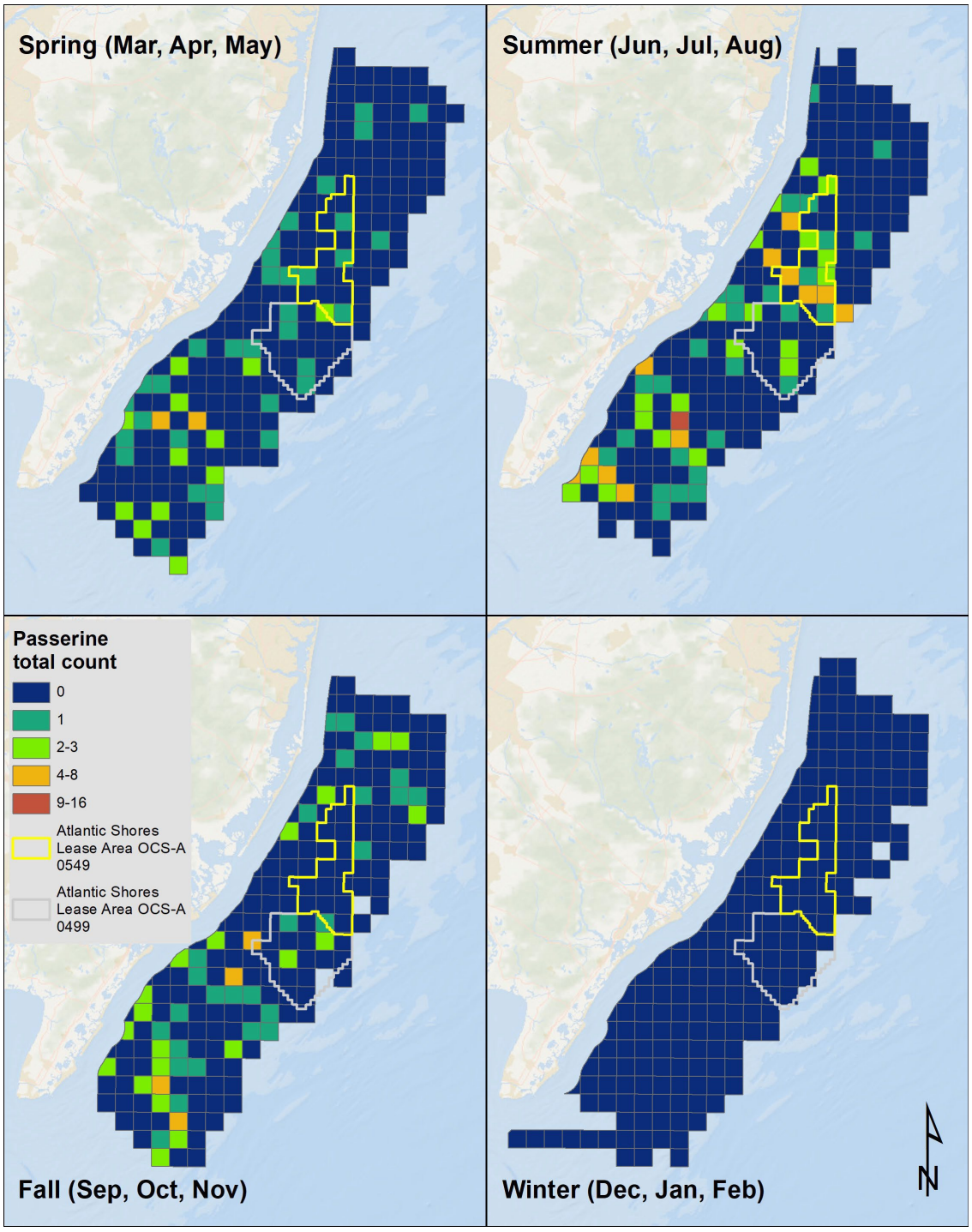

Figure 5-16: Songbirds (Passerines) observed in the NJDEP boat-based surveys, by season.

5.2. Marine birds

The following section presents results of marine bird exposure and vulnerability assessments. Marine birds were assessed by species within each major taxonomic group, which included loons, sea ducks, petrels and allies, gannets and allies, gulls and allies, terns, and auks. Exposure assessment maps, tables, and figures are presented based on numerous references and information sources including, but not limited to, the APEM digital aerial surveys, NJDEP boat-based surveys, NOAA MDAT models, occurrence data, individual tracking data, relevant literature, and species accounts.

There are noticeable differences in the mean densities of animals detected within the Lease Area when comparing values from NJDEP boat-based surveys to the modeled APEM digital aerial surveys. A number of factors come into play that each contribute to these observed differences: temporal variation, platform (boat vs. aerial), and analysis. Species-specific density estimates are affected differently by each of these factors.

Temporal variability (seasonal and annual differences) in species density are prevalent, which is why surveys are ideally conducted for multiple seasons and over several years (Camphuysen et al. 2004). The NJDEP boat-based surveys were conducted in 2008–2009 (more than two years), while digital aerial surveys were conducted in 2020–2021 (one year). Temporal differences can be explained by variation in tides, weather patterns, prey distribution, population differences, timing of survey (e.g., when during the day or even month), and other factors (Camphuysen et al. 2004; Bolduc and Fifield 2017). These factors do not affect species the same, thus, temporal differences may be important (to a greater or lesser degree) in explaining differences between the two surveys, depending on the species.

In the sections below, a relative behavioral vulnerability assessment, including flight height data relative to proposed WTG parameters, is presented for each species. Flight heights are presented at the taxonomic level for brevity, though species-specific flight heights are accounted for in each vulnerability assessment. Flight heights used in the assessment were gathered from datasets in the Northwest Atlantic Seabird Catalog including the NJDEP boat-based surveys.

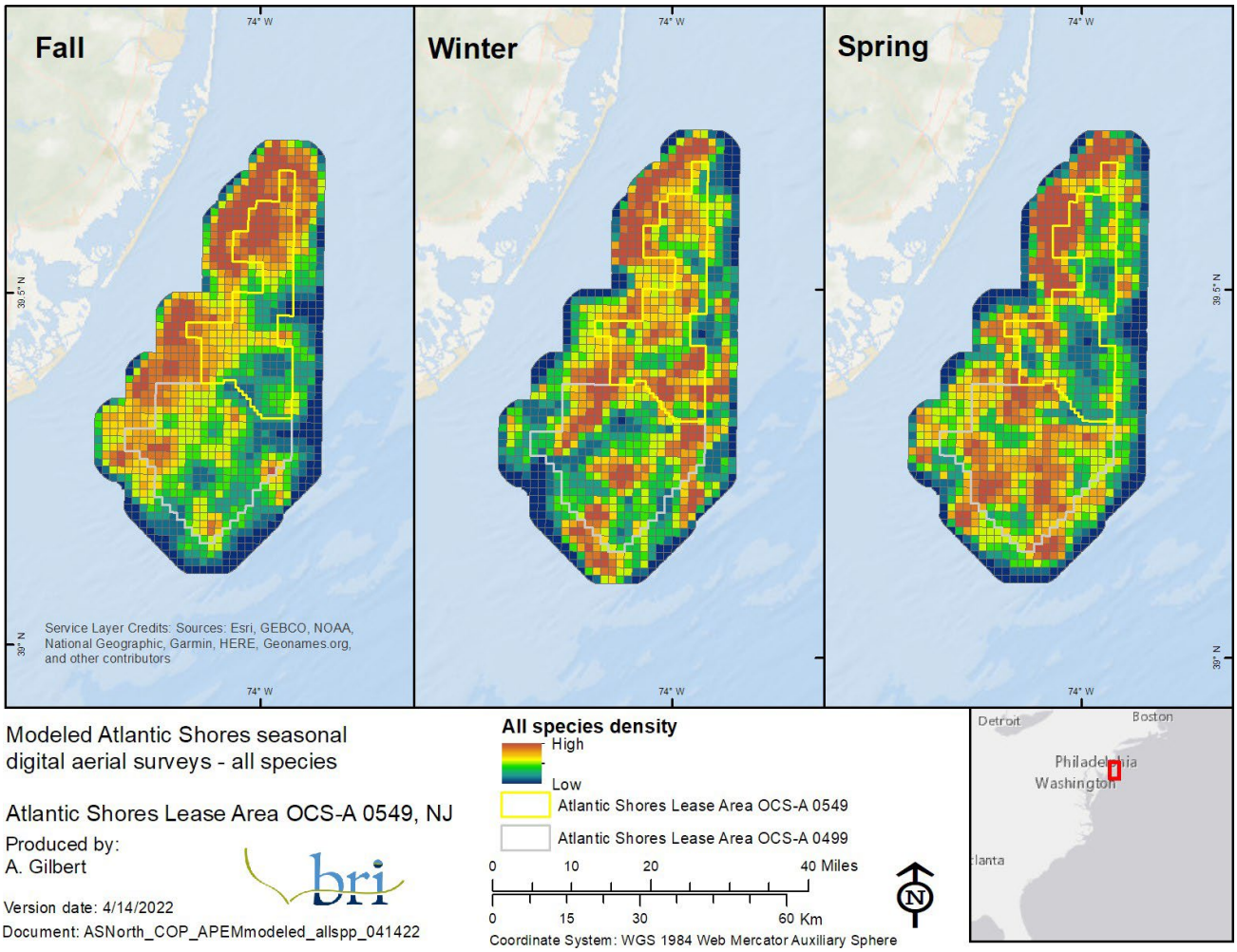

Figure 5-17: Seasonal distributions of all species observed across the Lease Area, modeled from monthly digital aerial surveys carried out in the area from October 2020–May 2021.

Table 5-1: Mean annual naive densities (uncorrected count/km^2 of survey transect) within the Lease Area and the NJDEP boat-based survey area of the Atlantic Outer Continental Shelf.

Species	Mean relative density (total count/km^2) in Atlantic Shores Lease Area OCS A 0549	Mean relative density (total count/km^2) in NJDEP survey area
Sea Ducks		
Common Eider	0.002	0.001
Surf Scoter	0.317	0.467
White-winged Scoter	0.003	0.037
Black Scoter	0.03	0.264
Long-tailed Duck	0.008	0.08
Red-breasted Merganser	0	0.004
Unidentified Scoter	0.021	0.083
Unidentified Diving/Sea Duck	0	0
Loons		
Red-throated Loon	0.128	0.221
Common Loon	0.282	0.465
Unidentified Loon	0.002	0.002
Shearwaters and Petrels		
Wilson's Storm-Petrel	0.214	0.466
Leach's Storm-Petrel	0	0.001
Northern Fulmar	0	0
Cory's Shearwater	0.033	0.046
Sooty Shearwater	0	0.001
Great Shearwater	0.005	0.005
Manx Shearwater	0	0.001
Audubon's Shearwater	0	0
Unidentified Shearwater	0	0
Unidentified Storm-petrel	0.002	0.001
Gannet		
Northern Gannet	0.297	1.522
Cormorants and Pelicans		
Double-crested Cormorant	0.012	0.183
Great Cormorant	0	0.001
Brown Pelican	0	0.001
Unidentified Cormorant	0	0
Gulls and Jaegers		
Pomarine Jaeger	0	0
Parasitic Jaeger	0.009	0.004
Black-legged Kittiwake	0.004	0.026
Sabine's Gull	0.002	0.001
Bonaparte's Gull	0.076	0.116
Little Gull	0	0
Laughing Gull	0.29	0.547

Species	Mean relative density (total count/km^2) in Atlantic Shores Lease Area OCS A 0549	Mean relative density (total count/km^2) in NJDEP survey area
Ring-billed Gull	0.002	0.014
Herring Gull	0.307	0.532
Iceland Gull	0	0
Lesser Black-backed Gull	0.004	0.001
Great Black-backed Gull	0.16	0.278
Unidentified small gull	0	0.002
Unidentified Jaeger	0	0
Unidentified Large Gull	0.006	0.02
Terns		
Least Tern	0	0.002
Caspian Tern	0	0
Black Tern	0.001	0.001
Common Tern	0.323	0.265
Forster's Tern	0.015	0.07
Royal Tern	0.004	0.019
Unidentified Small Gull/Tern	0	0
Unidentified large Tern	0	0
Unidentified small Tern	0.004	0.021
Auks		
Dovekie	0.006	0.017
Common Murre	0.005	0.005
Thick-billed Murre	0	0.002
Razorbill	0.261	0.111
Black Guillemot	0	0
Atlantic Puffin	0	0
Unidentified Alcid	0.019	0.011

Table 5-2: Seasonal species naive densities (uncorrected count/km^2 of survey transect) in the Atlantic Shores Lease Area OCS-A 0549 and the NJDEP boat-based survey area of the Atlantic Outer Continental Shelf.

NOTE: Table displays densities within Lease Area OCS-A 0549 and the NJDEP boat-based survey area of the Atlantic Outer Continental Shelf; and modeled densities from the APEM digital aerial surveys within the Lease Area and within the entire APEM digital aerial survey area.

	Mean naive density (uncorrected count/km^2)											Modeled density (animals/km^2)					
	Lease Area OCS A 0549					NJDEP survey area						Lease Area OCS A 0549			APEM survey area		
Species	annual	winter	spring	summer	fall	annual	winter	spring	summer	fall	Total count	winter	spring	fall	winter	spring	fall
Sea ducks																	
Common Eider	0.002	0	0	0	0.006	<0.001	0	0	0	0.004	6	·	·	·	·	·	·
Surf Scoter	0.317	0	1.445	0	0	0.467	0.098	0.654	0	0.966	2574	·	·	·	·	·	·
White-winged Scoter	0.003	0	0.005	0	0.005	0.037	0.113	0.058	0	0.005	238	0.047	0.206	·	0.098	0.122	·
Black Scoter	0.029	0.066	0.072	0	0	0.264	0.208	0.416	0	0.450	1530	·	·	<0.001	·	·	0.002
Long-tailed Duck	0.008	0	0.040	0	0	0.080	0.261	0.151	0	0	393	·	·	·	·	·	·
Red-breasted Merganser	0	0	0	0	0	0.004	0.009	0.004	0	0.003	18	·	·	·	·	·	·
Unidentified Scoter	0.021	0	0.114	0	0	0.083	0.042	0.208	0	0.172	532	·	·	·	·	·	·
Mean Scoter Group	·	·	·	·	·	·	·	·	·	·	·	0.137	0.69	0.003	0.220	0.372	0.064
Loons																	
Red-throated Loon	0.128	0.041	0.448	0	0.004	0.221	0.351	0.464	0	0.067	929	0.026	0.048	·	0.016	0.050	·
Common Loon	0.282	0.330	0.747	0.008	0.171	0.465	0.596	0.817	0.038	0.387	2221	0.406	0.225	0.182	0.339	0.236	0.130
Unidentified Loon	0.002	0	0	0	0.005	0.002	0.005	0.002	0	<0.001	9	·	·	·	·	·	·
Mean Loon Group	·	·	·	·	·	·	·	·	·	·	·	0.457	0.286	0.195	0.364	0.301	0.138
Shearwaters and Petrels																	
Wilson's Storm-Petrel	0.214	0	0	0.578	0.094	0.466	0	0	2.355	0.140	2566	·	·	·	·	·	·
Leach's Storm-Petrel	0	0	0	0	0	<0.001	0	0	0.001	0	2	·	·	·	·	·	·
Northern Fulmar	0	0	0	0	0	<0.001	0.001	0	0	<0.001	3	·	·	·	·	·	·
Cory's Shearwater	0.033	0	0	0.084	0.043	0.046	0	0	0.144	0.032	220	·	·	·	·	·	·
Sooty Shearwater	0	0	0	0	0	0.001	0	0	0.006	0	8	·	·	·	·	·	·
Great Shearwater	0.005	0	0	0.012	0.008	0.005	0	0	0.006	0.015	33	·	·	·	·	·	·
Manx Shearwater	0	0	0	0	0	<0.001	<0.001	0.004	<0.001	0	6	·	·	·	·	·	·
Audubon's Shearwater	0	0	0	0	0	<0.001	0	0	0	0.001	1	·	·	·	·	·	·
Unidentified Shearwater	0	0	0	0	0	<0.001	0	0	0	0.001	1	·	·	·	·	·	·

Species	Mean naive density (uncorrected count/km^2)											Modeled density (animals/km^2)					
	Lease Area OCS A 0549					NJDEP survey area						Lease Area OCS A 0549			APEM survey area		
	annual	winter	spring	summer	fall	annual	winter	spring	summer	fall	Total count	winter	spring	fall	winter	spring	fall
Unidentified Storm-petrel	0.002	0	0	0.005	0	<0.001	0	0	0.001	0.001	4	·	·	·	·	·	·
Gannet																	
Northern Gannet	0.297	0.633	0.549	0.136	0.208	1.522	1.671	1.853	0.258	1.710	7478	0.262	0.152	0.089	0.173	0.264	0.089
Cormorants and Pelicans																	
Double-crested Cormorant	0.012	0	0	0.038	0	0.183	0.016	0.038	0.010	0.760	1348	·	·	·	·	·	·
Great Cormorant	0	0	0	0	0	<0.001	0	0	0	0.002	3	·	·	·	·	·	·
Brown Pelican	0	0	0	0	0	0.001	0	0	0.004	<0.001	8	·	·	·	·	·	·
Gulls and Jaegers																	
Pomarine Jaeger	0	0	0	0	0	<0.001	0	0	0	0.001	2	·	·	·	·	·	·
Parasitic Jaeger	0.009	0	0	0	0.041	0.004	0	<0.001	0.002	0.014	24	·	·	·	·	·	·
Black-legged Kittiwake	0.004	0.011	0	0	0.004	0.026	0.036	0	0	0.150	146	0.017	·	·	0.012	·	·
Sabine's Gull	0.002	0	0	0	0.005	0.001	0	0	0.008	<0.001	2	·	·	·	·	·	·
Bonaparte's Gull	0.076	0.024	0.209	0	0.092	0.116	0.175	0.166	0	0.125	554	0.414	·	0.176	0.307	·	0.104
Little Gull	0	0	0	0	0	<0.001	0	<0.001	0	<0.001	2	·	·	·	·	·	·
Laughing Gull	0.290	0	0.093	0.445	0.541	0.547	0.006	0.159	0.854	1.208	3279	0.376	·	·	0.194	·	·
Ring-billed Gull	0.002	0	0	0	0.005	0.014	0.017	0.002	0	0.062	59	·	·	·	·	·	·
Herring Gull	0.307	0.522	0.631	0.120	0.238	0.532	0.536	0.956	0.087	0.457	2605	0.061	0.049	0.003	0.033	0.032	0.004
Iceland Gull	0	0	0	0	0	<0.001	0.001	0	0	0	1	·	·	·	·	·	·
Lesser Black-backed Gull	0.004	0	0	0	0.013	0.001	0	0.002	<0.001	0.002	8	·	·	·	·	·	·
Great Black-backed Gull	0.160	0.025	0.219	0.166	0.292	0.278	0.205	0.286	0.144	0.422	1259	0.076	0.046	0.016	0.061	0.028	0.010
Unidentified small gull	0	0	0	0	0	0.002	0.003	0	0	0	3	·	·	·	·	·	·
Unidentified Jaeger	0	0	0	0	0	<0.001	0	0	<0.001	0	1	·	·	·	·	·	·
Unidentified Large Gull	0.006	0.015	0.011	0	0.006	0.020	0.038	0.016	<0.001	0.016	105	·	·	·	·	·	·
Mean Gull Group	·	·	·	·	·	·	·	·	·	·	·	0.348	0.103	0.169	0.234	0.070	0.097
Terns																	
Least Tern	0	0	0	0	0	0.002	0	0.001	0.004	0	2	·	·	·	·	·	·
Caspian Tern	0	0	0	0	0	<0.001	0	<0.001	0	<0.001	2	·	·	·	·	·	·
Black Tern	0.001	0	0	0	0.006	0.001	0	0	0.004	<0.001	9	·	·	·	·	·	·
Common Tern	0.323	0	0.054	0.819	0.111	0.265	0	0.153	0.753	0.100	1484	·	·	·	·	·	·

Species	Mean naive density (uncorrected count/km^2)											Modeled density (animals/km^2)					
	Lease Area OCS A 0549					NJDEP survey area						Lease Area OCS A 0549			APEM survey area		
	annual	winter	spring	summer	fall	annual	winter	spring	summer	fall	Total count	winter	spring	fall	winter	spring	fall
Forster's Tern	0.015	0	0.022	0	0.034	0.070	0	0.042	0.017	0.323	431	·	·	·	·	·	·
Royal Tern	0.004	0	0	0	0.013	0.019	0	<0.001	0.049	0.028	79	·	·	·	·	·	·
Unidentified small Tern	0.004	0	0	0.013	0	0.021	0	0.040	0.030	0.030	136	·	·	·	·	·	·
Auks																	
Dovekie	0.006	0.026	0	0	0	0.017	0.062	0.007	0	0	95	·	·	·	·	·	·
Common Murre	0.005	0.015	0.014	0	0	0.005	0.017	0.008	0	0	22	·	·	·	·	·	·
Thick-billed Murre	0	0	0	0	0	0.002	0.005	0.004	0	0	8	·	·	·	·	·	·
Razorbill	0.261	0.065	1.084	0	0	0.111	0.138	0.425	0	0	677	·	·	·	·	·	·
Black Guillemot	0	0	0	0	0	<0.001	0	<0.001	0	0	1	·	·	·	·	·	·
Atlantic Puffin	0	0	0	0	0	<0.001	0.001	0	0	0	1	·	·	·	·	·	·
Unidentified Alcid	0.019	0.007	0.052	0	0	0.011	0.015	0.016	0	0	36	·	·	·	·	·	·
Mean Auk Group	·	·	·	·	·	·	·	·	·	·	·	0.012	0.059	·	0.015	0.035	·

Table 5-3: Vulnerability assessment rankings by species within each broad taxonomic grouping.

Species	Collision Vulnerability	Displacement Vulnerability	Population Vulnerability
Sea Ducks			
Black Scoter	low (0.37)	high (0.9)	low (0.4)
Common Eider	low (0.3)	high (0.9)	low (0.47)
Long-tailed Duck	low (0.33)	high (0.9)	low (0.27)
Red-breasted Merganser	low (0.4)	medium (0.5)	low (0.27)
Surf Scoter	low (0.33)	high (0.9)	medium (0.53)
White-winged Scoter	low (0.37)	high (0.8)	medium (0.53)
Auks			
Atlantic Puffin	minimal (0.2)	high (0.8)	medium (0.53)
Black Guillemot	low (0.33)	high (0.9)	low (0.4)
Common Murre	low (0.27)	high (0.8)	low (0.4)
Dovekie	low (0.27)	medium (0.7)	low (0.4)
Razorbill	minimal (0.23)	high (0.8)	medium (0.6)
Gulls			
Black-legged Kittiwake	medium (0.57)	medium (0.6)	low (0.33)
Bonaparte's Gull	low (0.43)	medium (0.5)	low (0.33)
Great Black-backed Gull	medium (0.6)	medium (0.7)	minimal (0.2)
Herring Gull	medium (0.67)	medium (0.5)	medium (0.53)
Laughing Gull	medium (0.53)	medium (0.5)	low (0.4)
Parasitic Jaeger	medium (0.57)	low (0.3)	low (0.4)
Pomarine Jaeger	medium (0.67)	low (0.3)	low (0.4)
Ring-billed Gull	medium (0.6)	low (0.4)	low (0.33)
Terns			
Common Tern	low (0.33)	high (0.8)	medium (0.6)
Forster's Tern	medium (0.6)	medium (0.5)	low (0.4)
Roseate Tern	low (0.3)	high (0.8)	high (0.87)
Royal Tern	medium (0.57)	medium (0.5)	medium (0.53)
Loons			
Common Loon	low (0.33)	high (0.8)	medium (0.53)
Red-throated Loon	low (0.43)	high (0.9)	low (0.47)
Shearwaters and Petrels			
Audubon's Shearwater	low (0.4)	medium (0.6)	medium (0.73)
Cory's Shearwater	low (0.4)	medium (0.6)	medium (0.6)
Great Shearwater	low (0.37)	medium (0.6)	medium (0.67)
Leach's Storm-Petrel	low (0.43)	medium (0.6)	low (0.47)
Manx Shearwater	low (0.4)	medium (0.6)	medium (0.53)
Northern Fulmar	low (0.4)	medium (0.6)	low (0.47)
Sooty Shearwater	low (0.37)	medium (0.6)	medium (0.53)
Wilson's Storm-Petrel	low (0.43)	medium (0.6)	low (0.4)
Gannet			
Northern Gannet	medium (0.6)	medium (0.6)	low (0.47)
Cormorants and Pelicans			

Species	Collision Vulnerability	Displacement Vulnerability	Population Vulnerability
Brown Pelican	medium (0.5)	medium (0.5)	low (0.4)
Double-crested Cormorant	medium (0.73)	low (0.4)	minimal (0.13)

5.2.1. Loons

5.2.1.1. Exposure Tables, Maps, and Figures

Table 5-4: Seasonal exposure rankings for the loon group.

Species	Season	Local Rank	Regional Rank	Total Rank	Exposure Score
Red-throated Loon	Winter	0	1	1	low
	Spring	1	2	3	medium
	Summer	0	·	0	minimal
	Fall	0	2	2	low
Common Loon	Winter	0	2	2	low
	Spring	1	3	4	medium
	Summer	0	1	1	low
	Fall	0	2	2	low

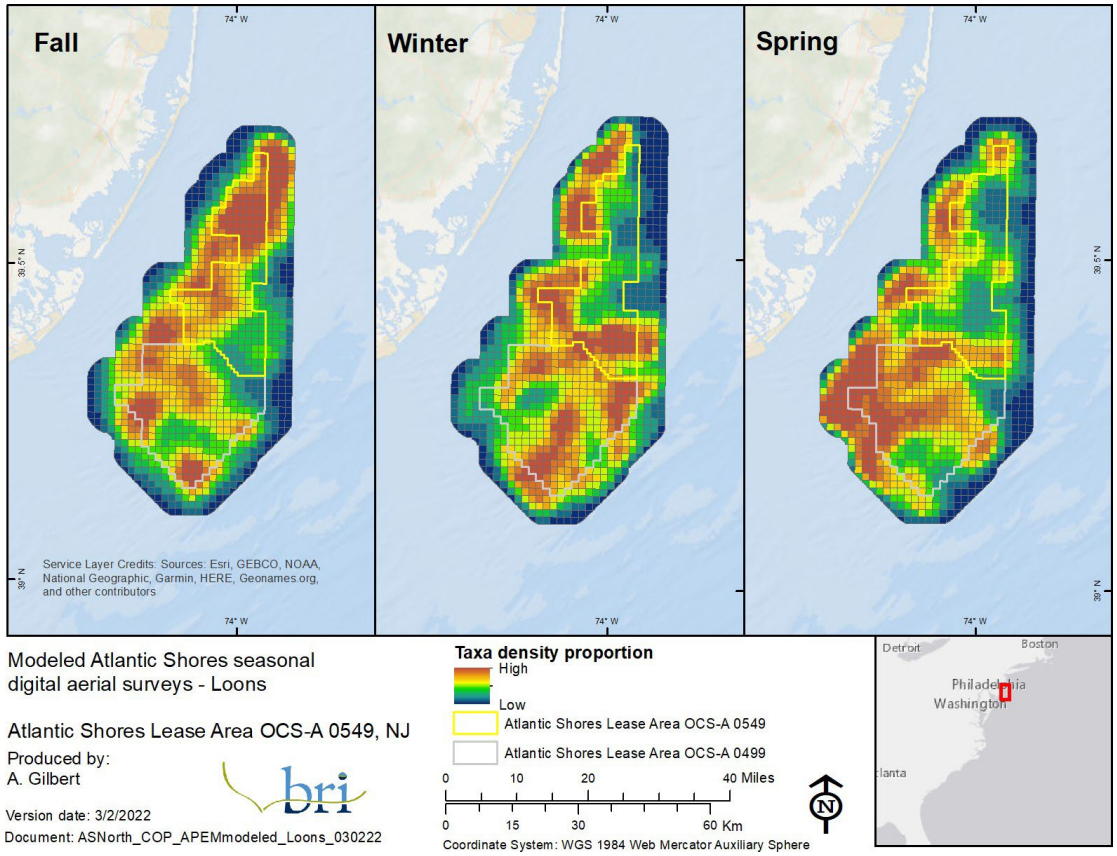

Figure 5-18: Seasonal distributions of loons across the Lease Area, modeled from monthly digital aerial surveys carried out in the area from October 2020–May 2021.

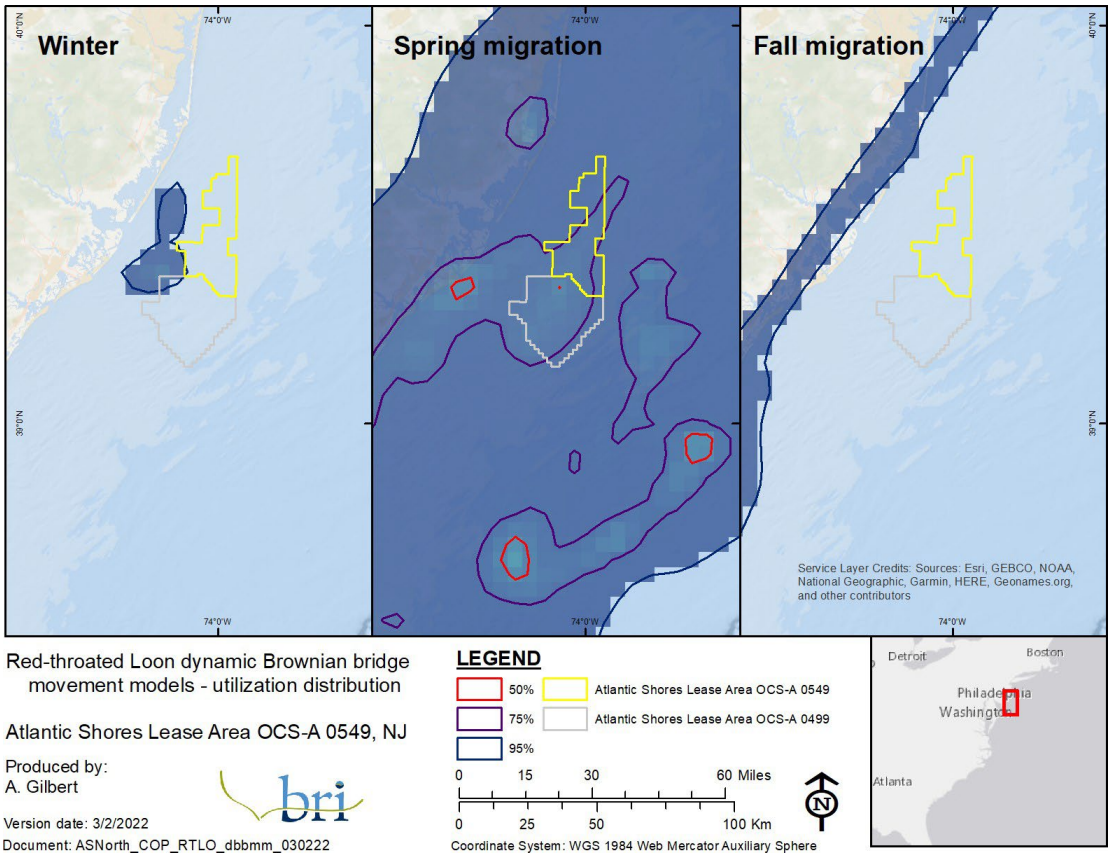

NOTE: (n = 46, 46, 31 [winter, spring, fall]) that were tracked with satellite transmitters; the contours represent the percentage of the use area across the UD surface and represent various levels of use from 50% (core use) to 95% (home range). Data provided by BOEM and used with permission.

Figure 5-19: Dynamic Brownian bridge movement models for Red-throated Loons.

5.2.1.2. Relative Behavioral Vulnerability Figures and Tables

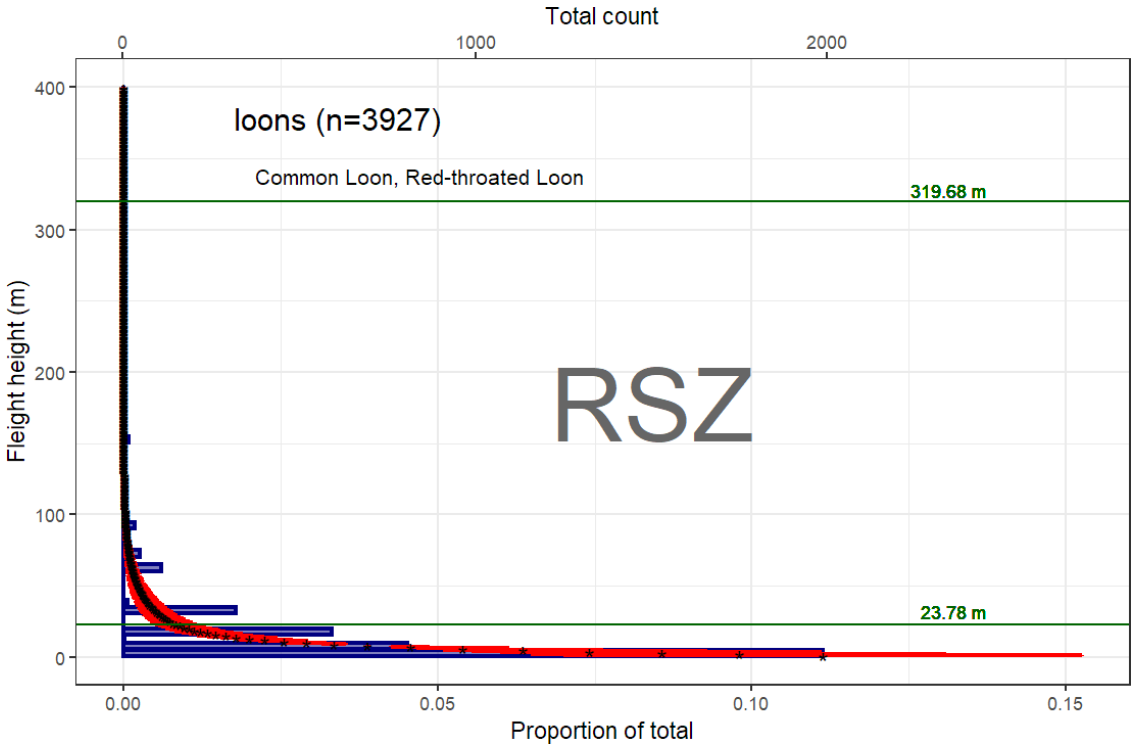

NOTE: Figure shows the actual number of birds in 5-m (16-ft) intervals (blue bars), the modeled average flight height in 1-m (3-ft) intervals (black asterisks), and the standard deviation (red lines), in relation to the upper and lower limits of the RSZ (23.78 m to 319.68 m [78.02 ft to 1,048.82 ft]).

Figure 5-20: Flight heights (m) of loons derived from the Northwest Atlantic Seabird Catalog.

Table 5-5: Vulnerability assessment rankings by species for the loon group. NOTE: In the COP, "minimal" is added to the Collision Vulnerability score because there is little evidence in the literature that loons are vulnerable to collision because they have such a strong avoidance response.

Species	Collision Vulnerability	Displacement Vulnerability	Population Vulnerability
Common Loon	low (0.33)	high (0.8)	medium (0.53)
Red-throated Loon	low (0.43)	high (0.9)	low (0.47)

5.2.2. Sea Ducks

5.2.2.1. Exposure Tables, Maps, and Figures

Table 5-6: Seasonal exposure rankings for the sea duck group.

Species	Season	Local Rank	Regional Rank	Total Rank	Exposure Score
Common Eider	Winter	0	0	0	minimal
	Spring	0	0	0	minimal
	Summer	0	0	0	minimal
	Fall	0	2	2	low
Surf Scoter	Winter	0	1	1	low
	Spring	1	1	2	low
	Summer	0	·	0	minimal
	Fall	0	1	1	low
White-winged Scoter	Winter	0	1	1	low
	Spring	0	2	2	low
	Summer	0	·	0	minimal
	Fall	0	0	0	minimal
Black Scoter	Winter	0	0	0	minimal
	Spring	0	0	0	minimal
	Summer	0	·	0	minimal
	Fall	0	1	1	low
Long-tailed Duck	Winter	0	0	0	minimal
	Spring	0	0	0	minimal
	Summer	0	·	0	minimal
	Fall	0	1	1	low
Red-breasted Merganser	Winter	0	1	1	low
	Spring	0	0	0	minimal
	Summer	0	·	0	minimal
	Fall	0	·	0	minimal

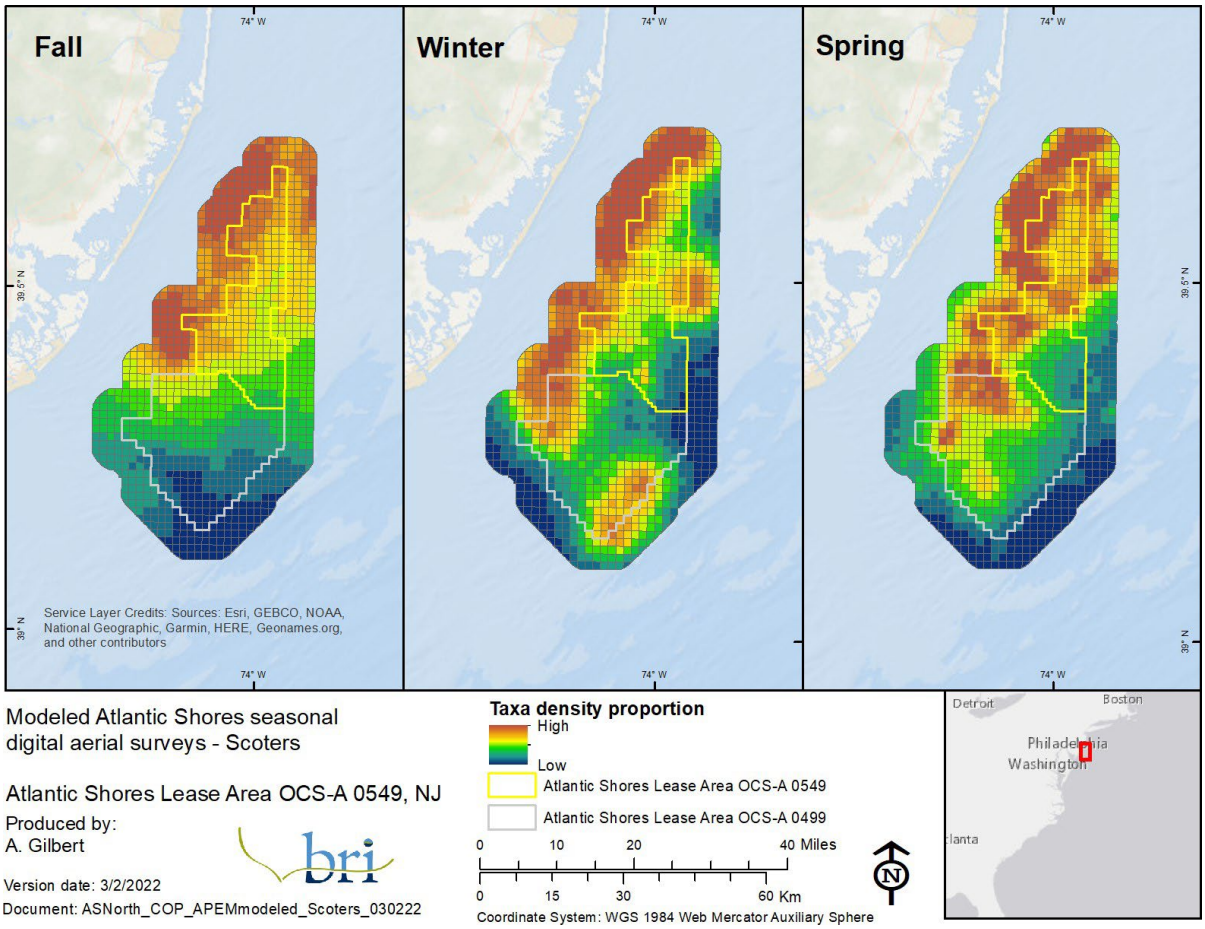

Figure 5-21: Seasonal distributions of scoters across the Lease Area, modeled from monthly digital aerial surveys carried out in the area from October 2020–May 2021.

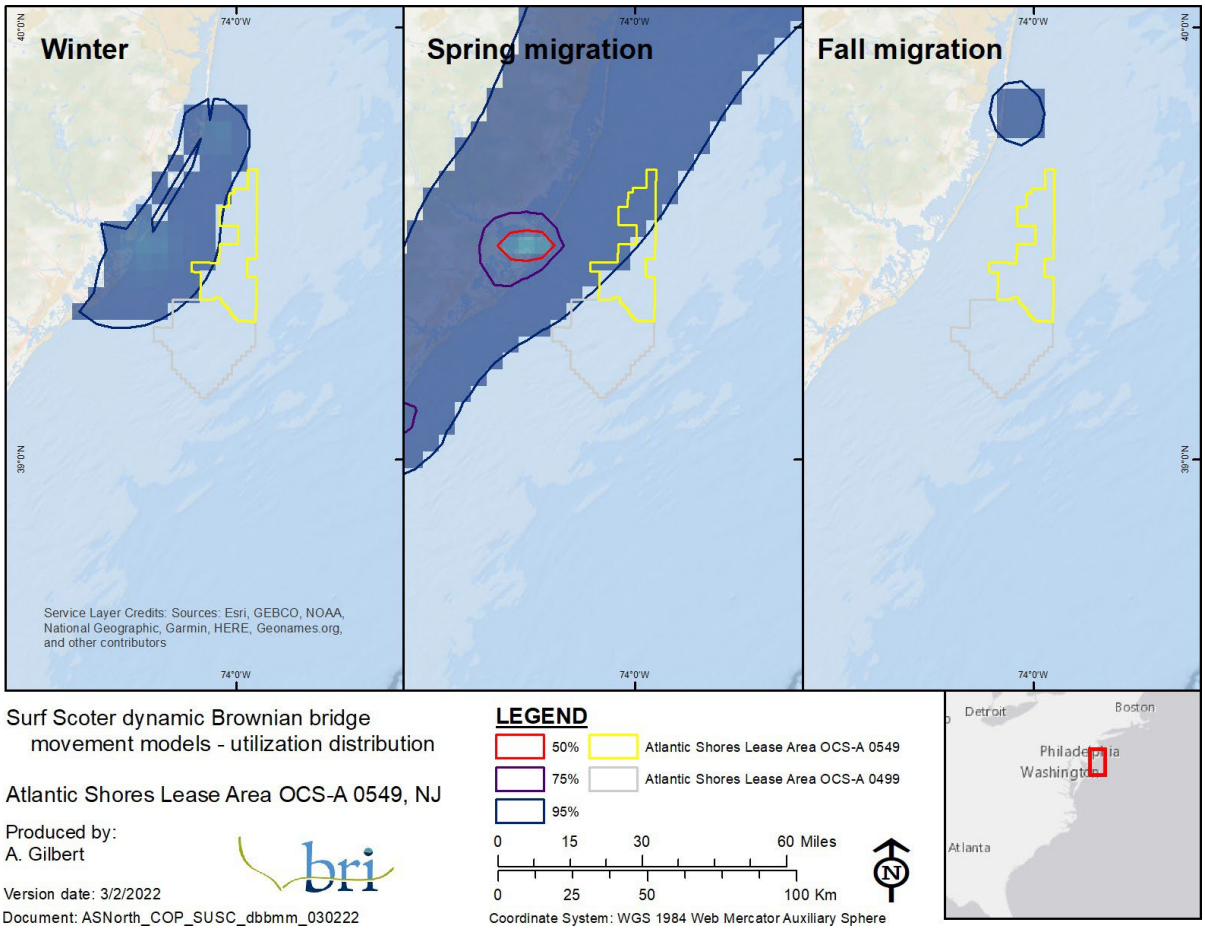

NOTE: (n = 78, 87, 83 [winter, spring, fall]) that were tracked with satellite transmitters; the contours represent the percentage of the use area across the UD surface and represent various levels of use from 50% (core use) to 95% (home range). Data provided by multiple sea duck researchers and used with permission.

Figure 5-22: Dynamic Brownian bridge movement models for Surf Scoter.

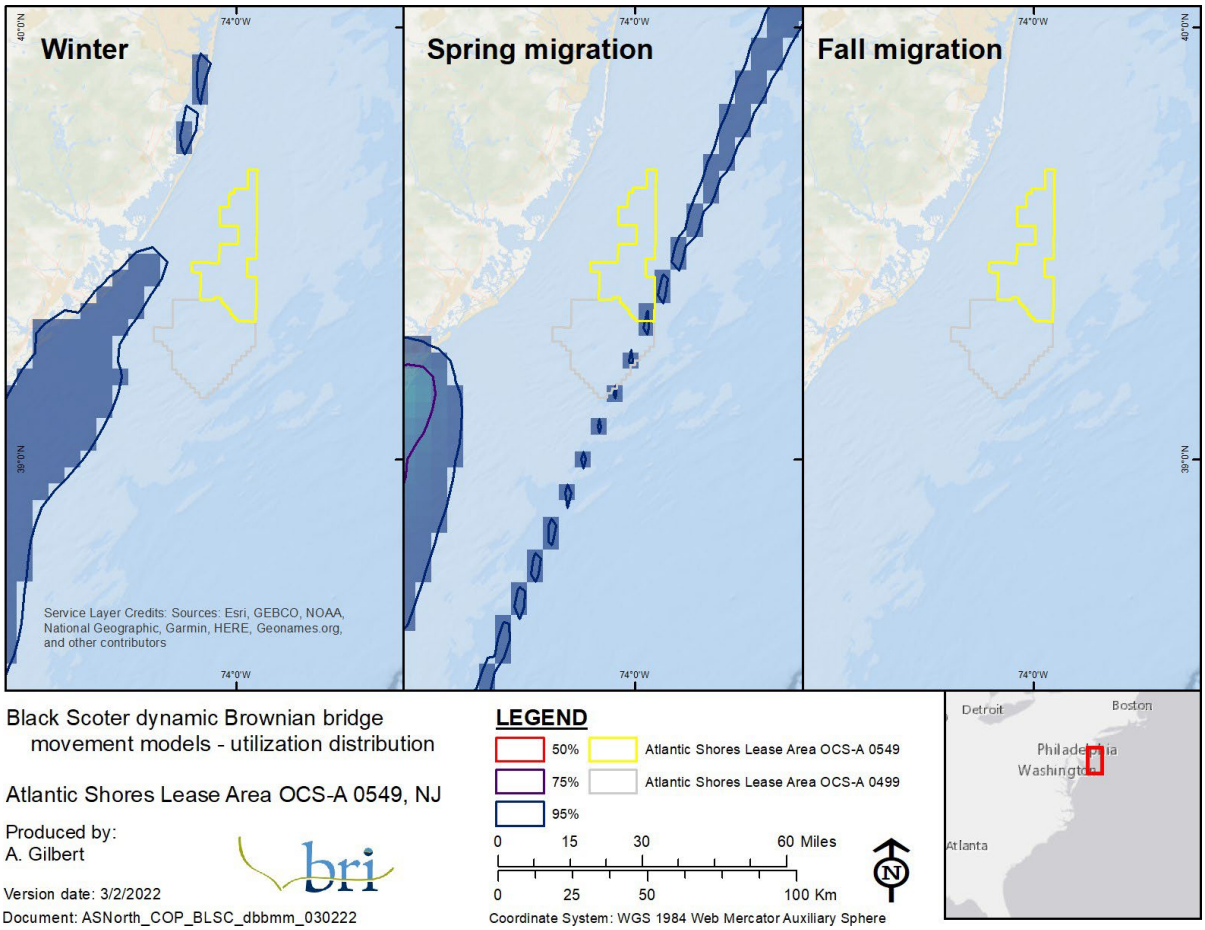

NOTE: (n = 61, 76, 80 [winter, spring, fall]) that were tracked with satellite transmitters; the contours represent the percentage of the use area across the UD surface and represent various levels of use from 50% (core use) to 95% (home range). Data provided by multiple sea duck researchers and used with permission.

Figure 5-23: Dynamic Brownian bridge movement models for Black Scoter.

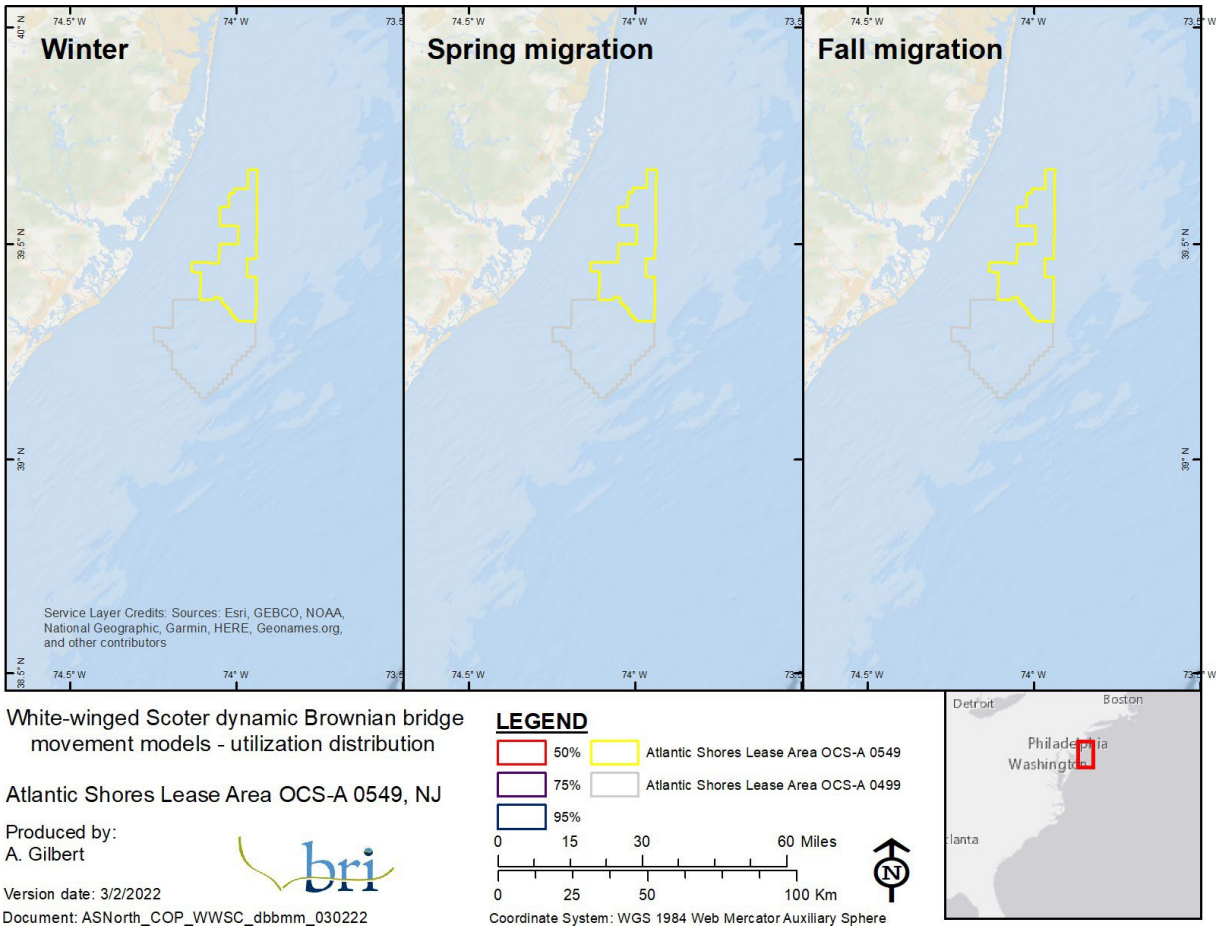

NOTE: (n = 66, 45, 62 [winter, spring, fall]) that were tracked with satellite transmitters: the contours represent the percentage of the use area across the UD surface and represent various levels of use from 50% (core use) to 95% (home range). Data provided by multiple sea duck researchers and used with permission.

Figure 5-24: Dynamic Brownian bridge movement models for White-winged Scoter.

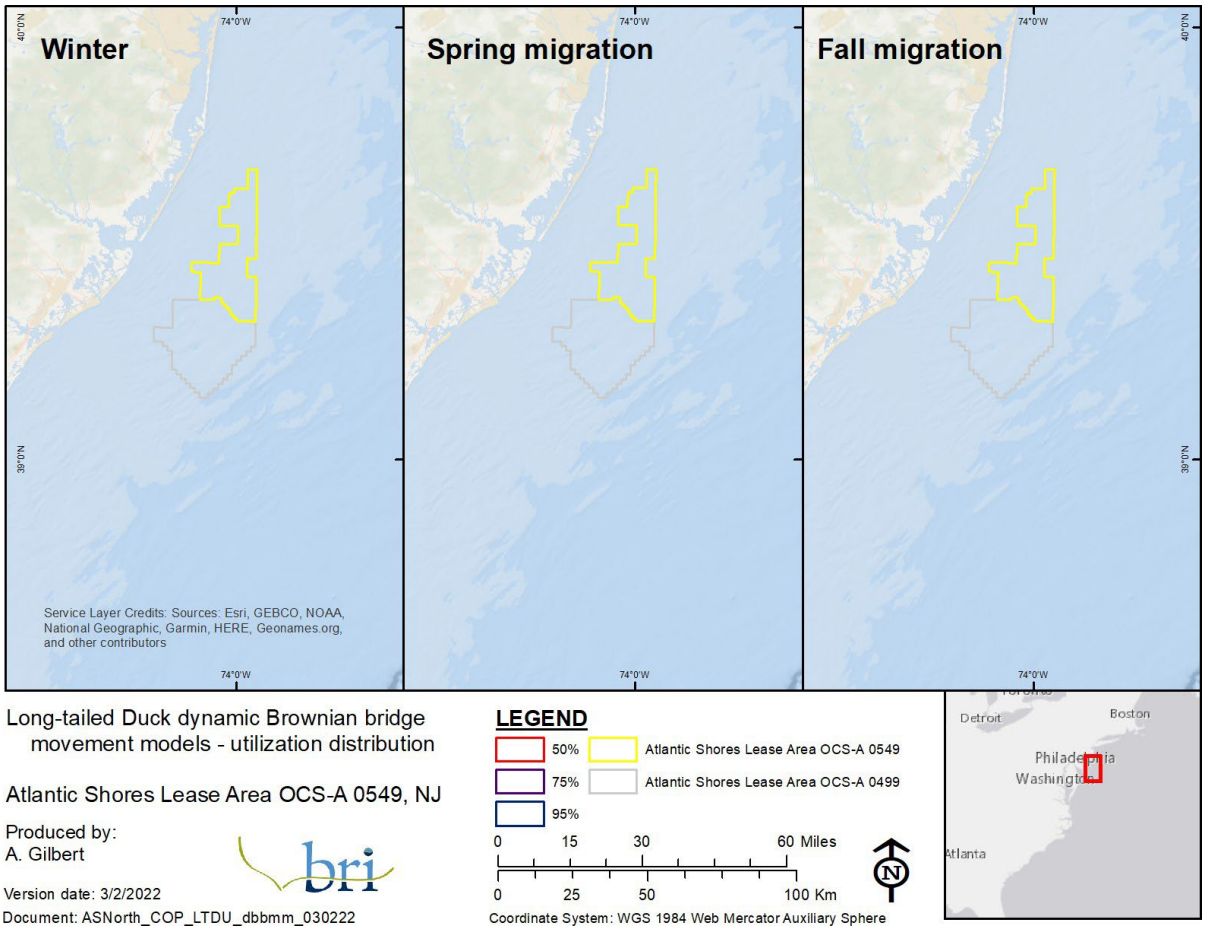

NOTE: (n = 49, 60, 37 [winter, spring, fall]) that were tracked with satellite transmitters; the contours represent the percentage of the use area across the UD surface and represent various levels of use from 50% (core use) to 95% (home range). Data provided by multiple sea duck researchers and used with permission.

Figure 5-25: Dynamic Brownian bridge movement models for Long-tailed Duck.

5.2.2.2. Relative Behavioral Vulnerability Figures and Tables

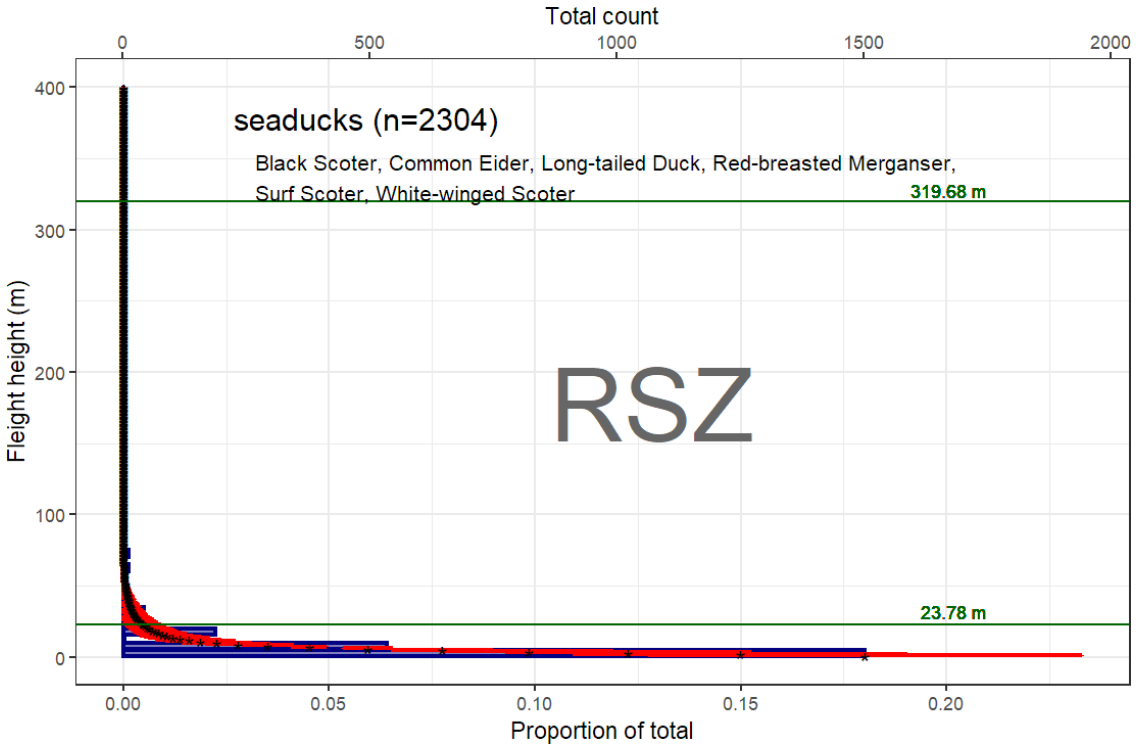

NOTE: Figure shows the actual number of birds in 5-m (16-ft) intervals (blue bars), the modeled average flight height in 1-m (3-ft) intervals (black asterisks), and the standard deviation (red lines), in relation to the upper and lower limits of the RSZ (23.78 m to 319.68 m [78.02 ft to 1,048.82 ft]).

Figure 5-26: Flight heights (m) of sea ducks derived from the Northwest Atlantic Seabird Catalog.

Table 5-7: Vulnerability assessment rankings by species for the sea duck group.

NOTE: In the COP, "medium" is added to the Displacement Vulnerability score because there is evidence in the literature that some sea ducks will return to offshore wind farms several years after operation.

Species	Collision Vulnerability	Displacement Vulnerability	Population Vulnerability
Black Scoter	low (0.37)	high (0.9)	low (0.4)
Common Eider	low (0.3)	high (0.9)	low (0.47)
Long-tailed Duck	low (0.33)	high (0.9)	low (0.27)
Red-breasted Merganser	low (0.4)	medium (0.5)	low (0.27)
Surf Scoter	low (0.33)	high (0.9)	medium (0.53)
White-winged Scoter	low (0.37)	high (0.8)	medium (0.53)

5.2.3. Shearwaters and Petrels

5.2.3.1. Exposure Tables, Maps, and Figures

Table 5-8: Seasonal exposure rankings for the shearwater and petrel group.

Species	Season	Local Rank	Regional Rank	Total Rank	Exposure Score
Northern Fulmar	Winter	0	0	0	minimal
	Spring	0	0	0	minimal
	Summer	0	0	0	minimal
	Fall	0	0	0	minimal
Cory's Shearwater	Winter	0	·	0	minimal
	Spring	0	0	0	minimal
	Summer	0	0	0	minimal
	Fall	1	0	1	low
Sooty Shearwater	Winter	0	·	0	minimal
	Spring	0	0	0	minimal
	Summer	0	0	0	minimal
	Fall	0	0	0	minimal
Great Shearwater	Winter	0	0	0	minimal
	Spring	0	0	0	minimal
	Summer	3	0	3	medium
	Fall	0	0	0	minimal
Manx Shearwater	Winter	0	·	0	minimal
	Spring	0	0	0	minimal
	Summer	0	0	0	minimal
	Fall	0	0	0	minimal
Audubon's Shearwater	Winter	0	0	0	minimal
	Spring	0	0	0	minimal
	Summer	0	0	0	minimal
	Fall	0	0	0	minimal
Wilson's Storm-Petrel	Winter	0	·	0	minimal
	Spring	0	0	0	minimal
	Summer	0	0	0	minimal
	Fall	0	0	0	minimal
Leach's Storm-Petrel	Winter	0	·	0	minimal
	Spring	0	0	0	minimal
	Summer	0	0	0	minimal
	Fall	0	0	0	minimal

5.2.3.2. Relative Behavioral Vulnerability Figures and Tables

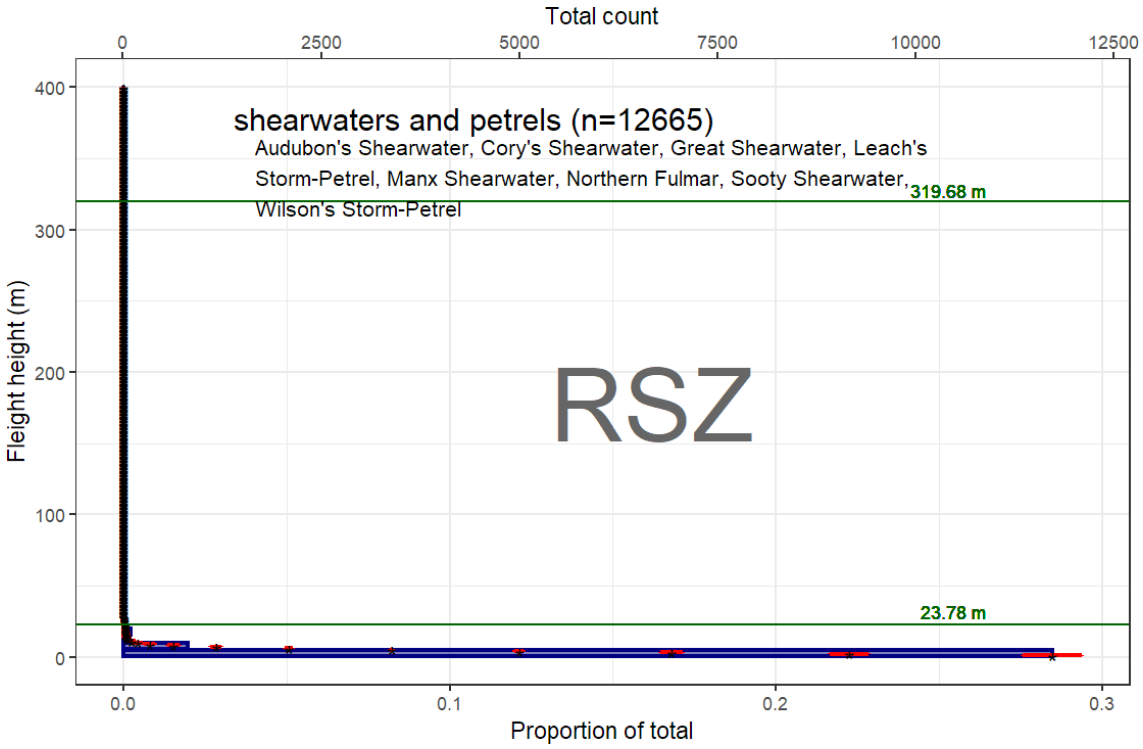

NOTE: Figure shows the actual number of birds in 5-m (16-ft) intervals (blue bars), the modeled average flight height in 1-m (3-ft) intervals (black asterisks), and the standard deviation (red lines), in relation to the upper and lower limits of the RSZ (23.78 m to 319.68 m [78.02 ft to 1,048.82 ft]).

Figure 5-27: Flight heights (m) of shearwaters, petrels, and storm-petrels derived from the Northwest Atlantic Seabird Catalog.

Table 5-9: Vulnerability assessment rankings by species for the shearwater and petrel group.

Species	Collision Vulnerability	Displacement Vulnerability	Population Vulnerability
Audubon's Shearwater	low (0.4)	medium (0.6)	medium (0.73)
Cory's Shearwater	low (0.4)	medium (0.6)	medium (0.6)
Great Shearwater	low (0.37)	medium (0.6)	medium (0.67)
Leach's Storm-Petrel	low (0.43)	medium (0.6)	low (0.47)
Manx Shearwater	low (0.4)	medium (0.6)	medium (0.53)
Northern Fulmar	low (0.4)	medium (0.6)	low (0.47)
Sooty Shearwater	low (0.37)	medium (0.6)	medium (0.53)
Wilson's Storm-Petrel	low (0.43)	medium (0.6)	low (0.4)

5.2.4. Candidate Petrel Species

5.2.4.1. Black-capped Petrel

5.2.4.1.1. Maps

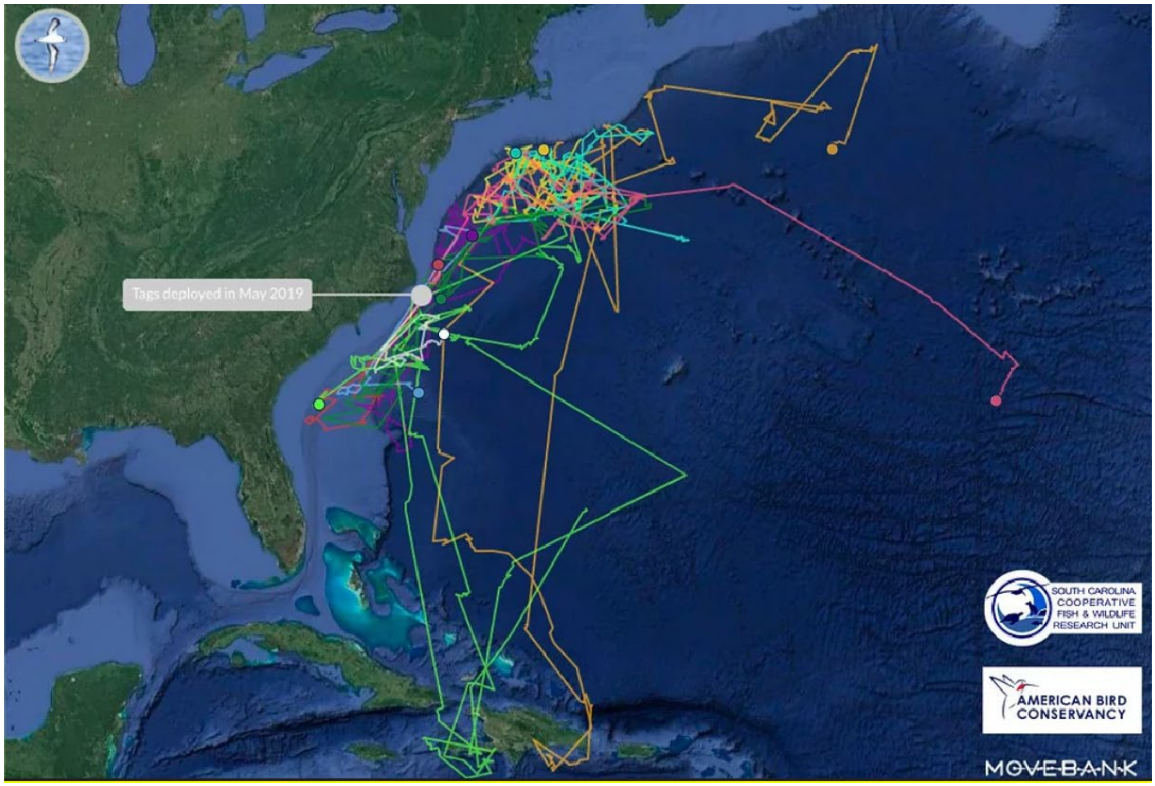

Figure 5-28: Track lines of 10 Black-capped Petrels tagged with solar satellite transmitters off of Cape Hatteras, North Carolina (Atlantic Seabirds 2020).

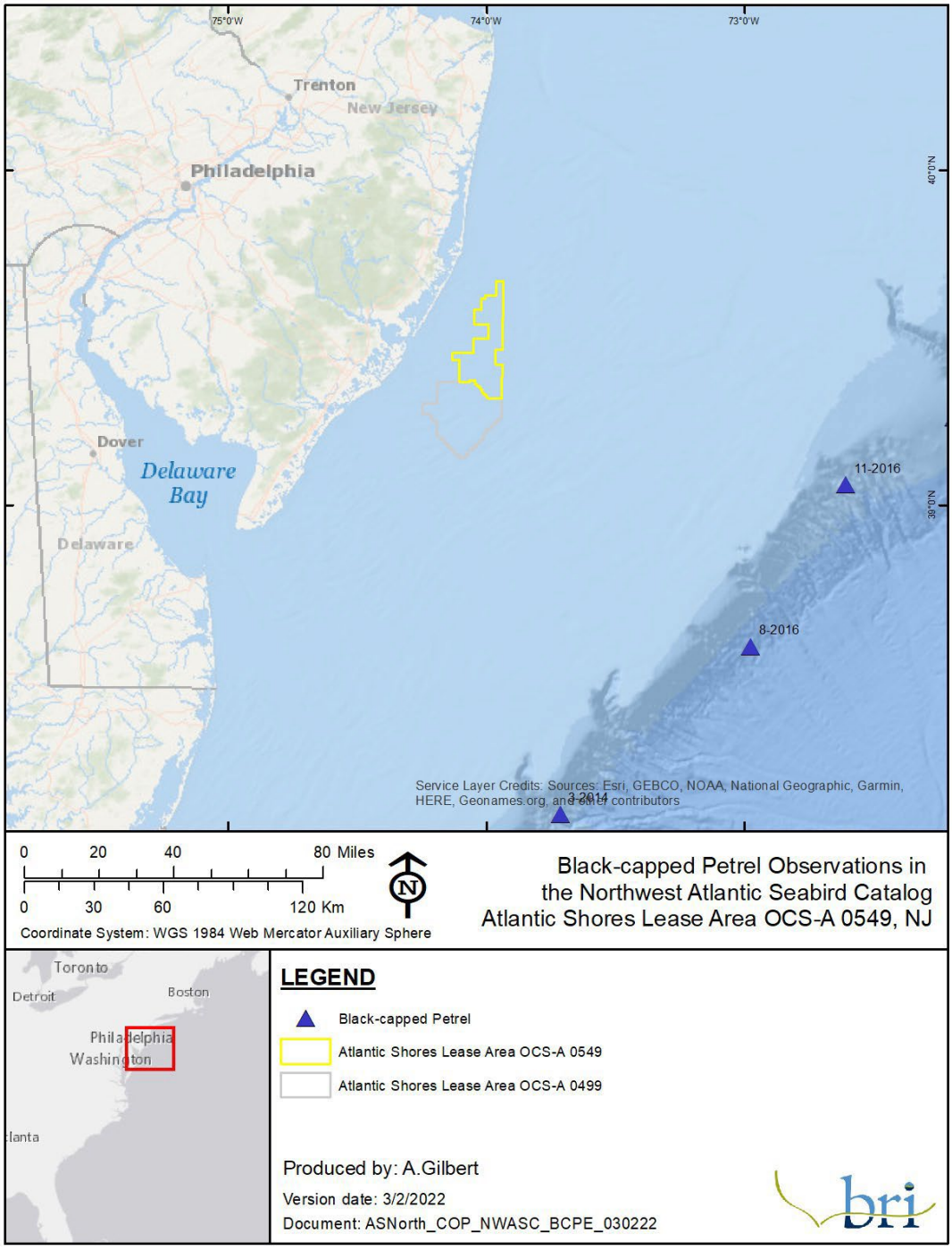

Figure 5-29: Black-capped Petrel observations from the Northwest Atlantic Seabird Catalog. Data provided by NOAA and used with permission.

5.2.5. Gannets, Cormorants, and Pelicans

5.2.5.1. Gannets

5.2.5.1.1. Exposure Tables, Maps, and Figures

Table 5-10: Seasonal exposure rankings for the Northern Gannet.

Species	Season	Local Rank	Regional Rank	Total Rank	Exposure Score
Northern Gannet	Winter	0	0	0	minimal
	Spring	0	1	1	low
	Summer	0	0	0	minimal
	Fall	0	0	0	minimal

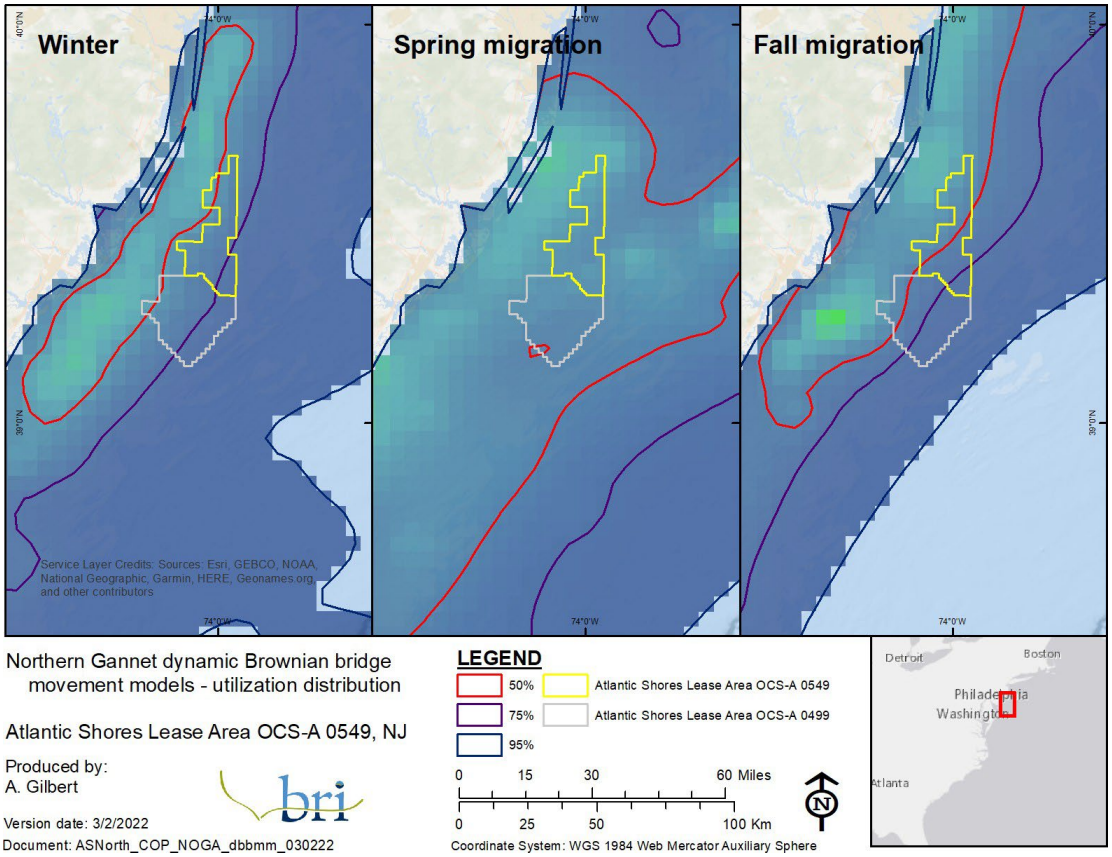

NOTE: (n = 34, 35, 36 [winter, spring, fall]) that were tracked with satellite transmitters; the contours represent the percentage of the use area across the UD surface and represent various levels of use from 50% (core use) to 95% (home range). Data provided by BOEM and used with permission.

Figure 5-30: Dynamic Brownian bridge movement models for Northern Gannets.

5.2.5.1.2. Relative Behavioral Vulnerability Figures and Tables

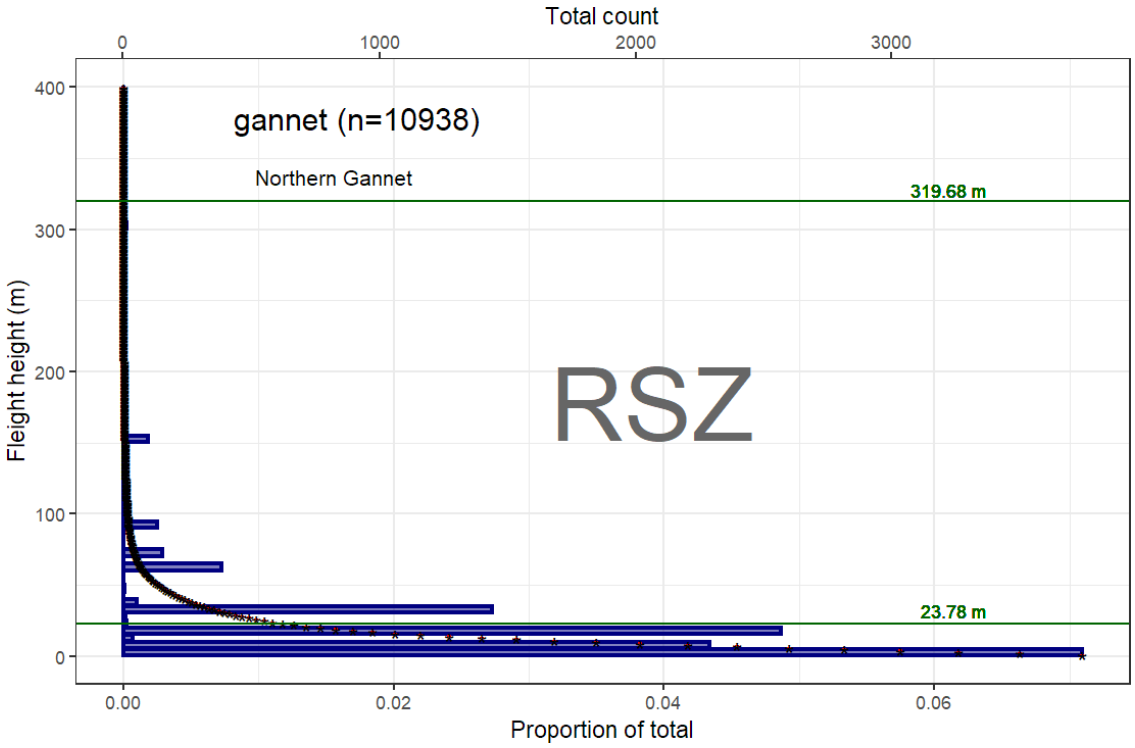

NOTE: Figure shows the actual number of birds in 5-m (16-ft) intervals (blue bars), the modeled average flight height in 1-m (3-ft) intervals (black asterisks), and the standard deviation (red lines), in relation to the upper and lower limits of the RSZ (23.78 m to 319.68 m [78.02 ft to 1,048.82 ft]).

Figure 5-31: Flight heights (m) of Northern Gannet derived from the Northwest Atlantic Seabird Catalog.

Table 5-11: Vulnerability assessment rankings by species for the gannet group.

Species	Collision Vulnerability	Displacement Vulnerability	Population Vulnerability
Northern Gannet	medium (0.6)	medium (0.6)	low (0.47)

5.2.5.2. Cormorants and Pelicans

5.2.5.2.1. Exposure Tables, Maps, and Figures

Table 5-12: Seasonal exposure rankings for the cormorant and pelican group.

Species	Season	Local Rank	Regional Rank	Total Rank	Exposure Score
Double-crested Cormorant	Winter	0	1	1	low
	Spring	0	0	0	minimal
	Summer	3	1	4	medium
	Fall	0	1	1	low
Great Cormorant	Winter	0	·	0	minimal
	Spring	0	·	0	minimal
	Summer	0	·	0	minimal
	Fall	0	·	0	minimal
Brown Pelican	Winter	0	0	0	minimal
	Spring	0	0	0	minimal
	Summer	0	0	0	minimal
	Fall	0	0	0	minimal

5.2.1.1.1 Relative Behavioral Vulnerability Figures and Tables

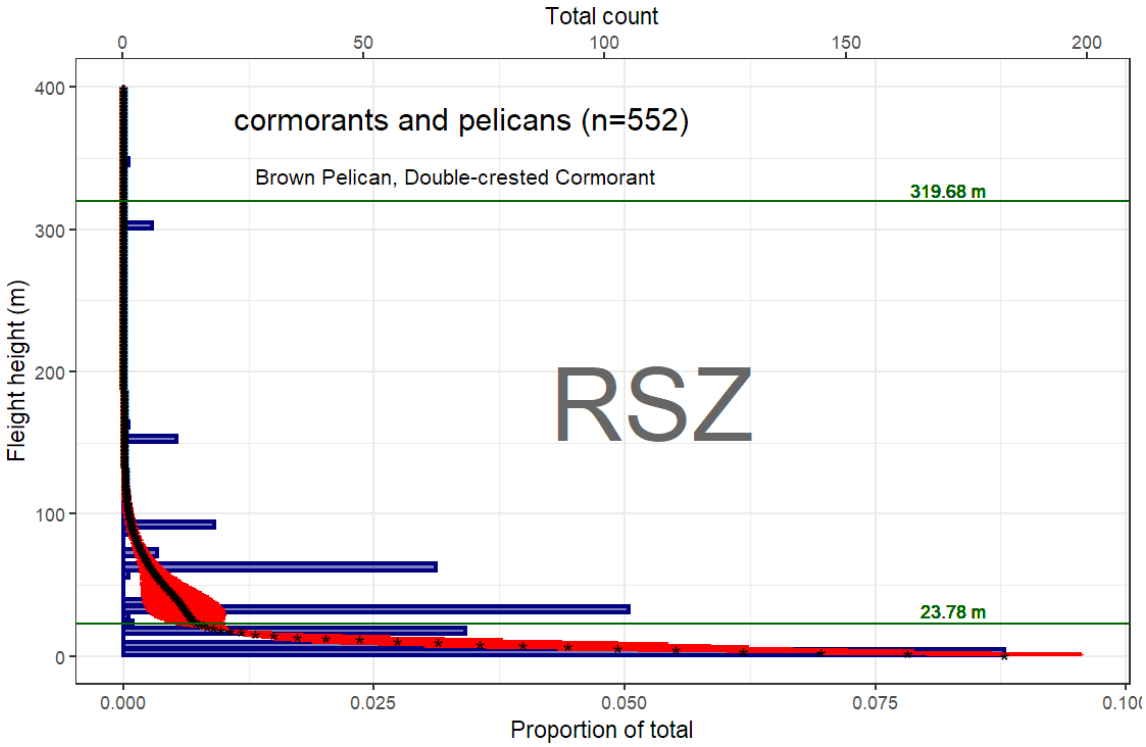

NOTE: Figure shows the actual number of birds in 5-m (16-ft) intervals (blue bars), the modeled average flight height in 1-m (3-ft) intervals (black asterisks), and the standard deviation (red lines), in relation to the upper and lower limits of the RSZ (23.78 m to 319.68 m [78.02 ft to 1,048.82 ft]).

Figure 5-32: Flight heights (m) of cormorants and pelicans derived from the Northwest Atlantic Seabird Catalog.

Table 5-13: Vulnerability assessment rankings by species for the cormorant and pelican group.

Species	Collision Vulnerability	Displacement Vulnerability	Population Vulnerability
Brown Pelican	medium (0.5)	medium (0.5)	low (0.4)
Double-crested Cormorant	medium (0.73)	low (0.4)	minimal (0.13)

5.2.6. Gulls and Jaegers

5.2.6.1. Exposure Tables, Maps, and Figures

Table 5-14: Seasonal exposure rankings for the gull group.

Species	Season	Local Rank	Regional Rank	Total Rank	Exposure Score*
Pomarine Jaeger	Winter	0	·	0	minimal
	Spring	0	0	0	minimal
	Summer	0	0	0	minimal
	Fall	0	0	0	minimal
Parasitic Jaeger	Winter	0	·	0	minimal
	Spring	0	1	1	low
	Summer	0	0	0	minimal
	Fall	3	0	3	medium
Black-legged Kittiwake	Winter	0	0	0	minimal
	Spring	0	0	0	minimal
	Summer	0	·	0	minimal
	Fall	0	0	0	minimal
Sabine's Gull	Winter	0	·	0	minimal
	Spring	0	·	0	minimal
	Summer	0	·	0	minimal
	Fall	3	·	6	high
Bonaparte's Gull	Winter	0	0	0	minimal
	Spring	1	2	3	medium
	Summer	0	·	0	minimal
	Fall	0	1	1	low
Little Gull	Winter	0	·	0	minimal
	Spring	0	·	0	minimal
	Summer	0	·	0	minimal
	Fall	0	·	0	minimal
Laughing Gull	Winter	0	0	0	minimal
	Spring	0	0	0	minimal
	Summer	0	2	2	low
	Fall	0	0	0	minimal
Ring-billed Gull	Winter	0	1	1	low
	Spring	0	0	0	minimal
	Summer	0	2	2	low
	Fall	0	1	1	low
Herring Gull	Winter	1	1	2	low
	Spring	0	2	2	low
	Summer	1	0	1	low
	Fall	0	0	0	minimal
Iceland Gull	Winter	0	·	0	minimal
	Spring	0	·	0	minimal

Species	Season	Local Rank	Regional Rank	Total Rank	Exposure Score*
	Summer	0	·	0	minimal
	Fall	0	·	0	minimal
Lesser Black-backed Gull	Winter	0	·	0	minimal
	Spring	0	·	0	minimal
	Summer	0	·	0	minimal
	Fall	3	·	6	high
Great Black-backed Gull	Winter	0	0	0	minimal
	Spring	1	0	1	low
	Summer	1	0	1	low
	Fall	1	0	1	low

*Note: The high fall ranking of Sabine's Gull and Lesser Black-backed Gull was the result of only a few observations of the gulls in the fall, which were located within the Lease Area. This does not represent actual high exposure. See Map 95 and 120 in Section 8.

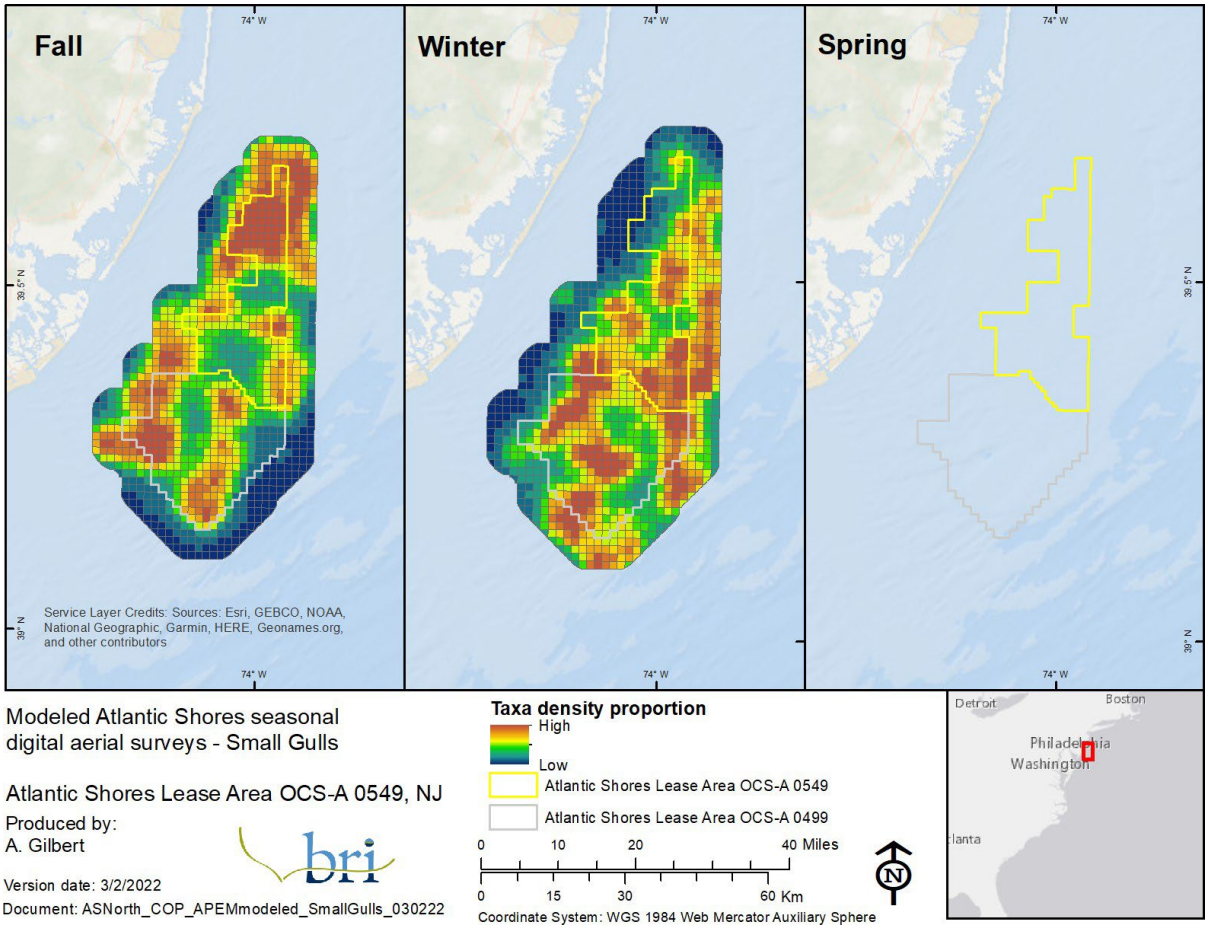

Figure 5-33: Seasonal distributions of small gulls across the Lease Area, modeled from monthly digital aerial surveys carried out in the area from October 2020–May 2021.

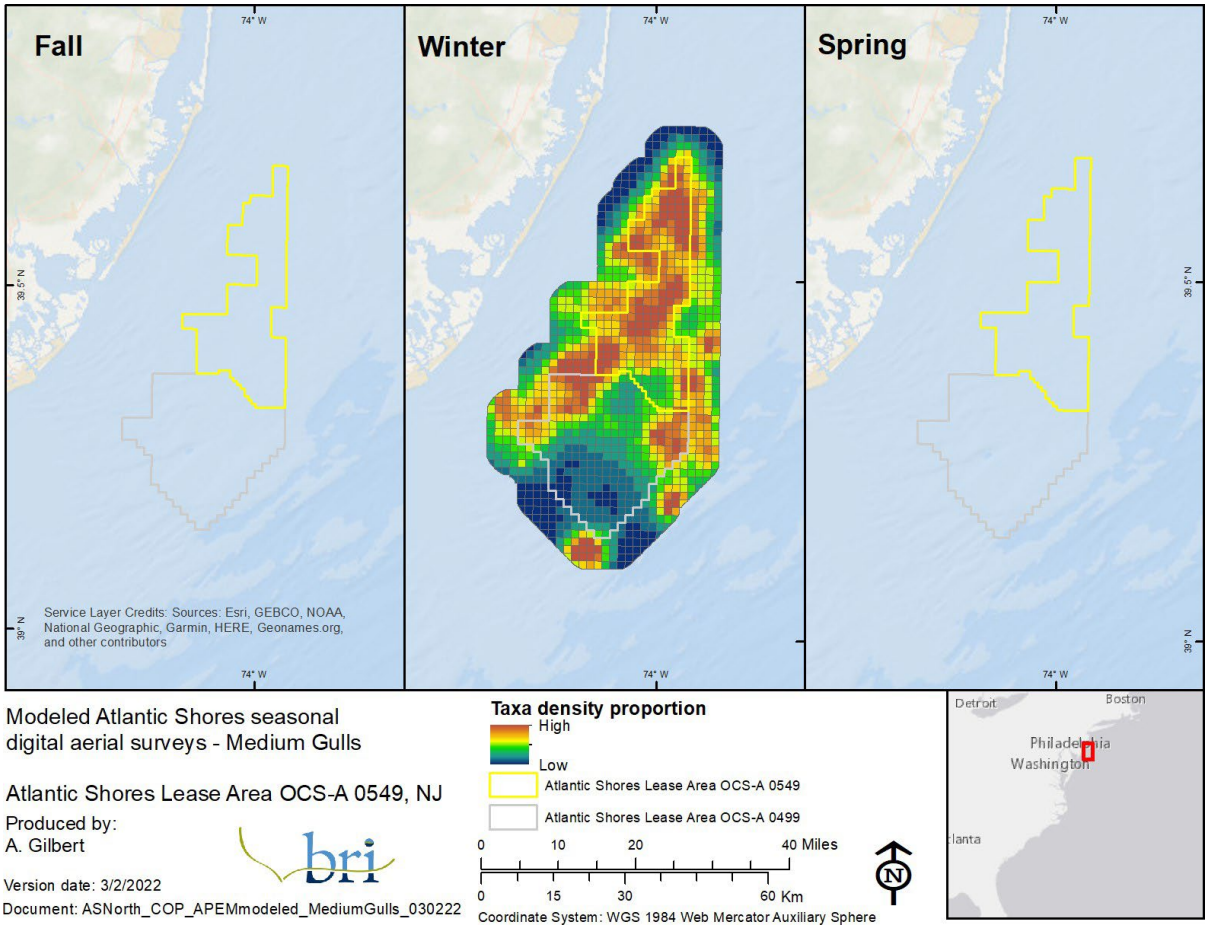

Figure 5-34: Seasonal distributions of medium gulls across the Lease Area, modeled from monthly digital aerial surveys carried out in the area from October 2020–May 2021.

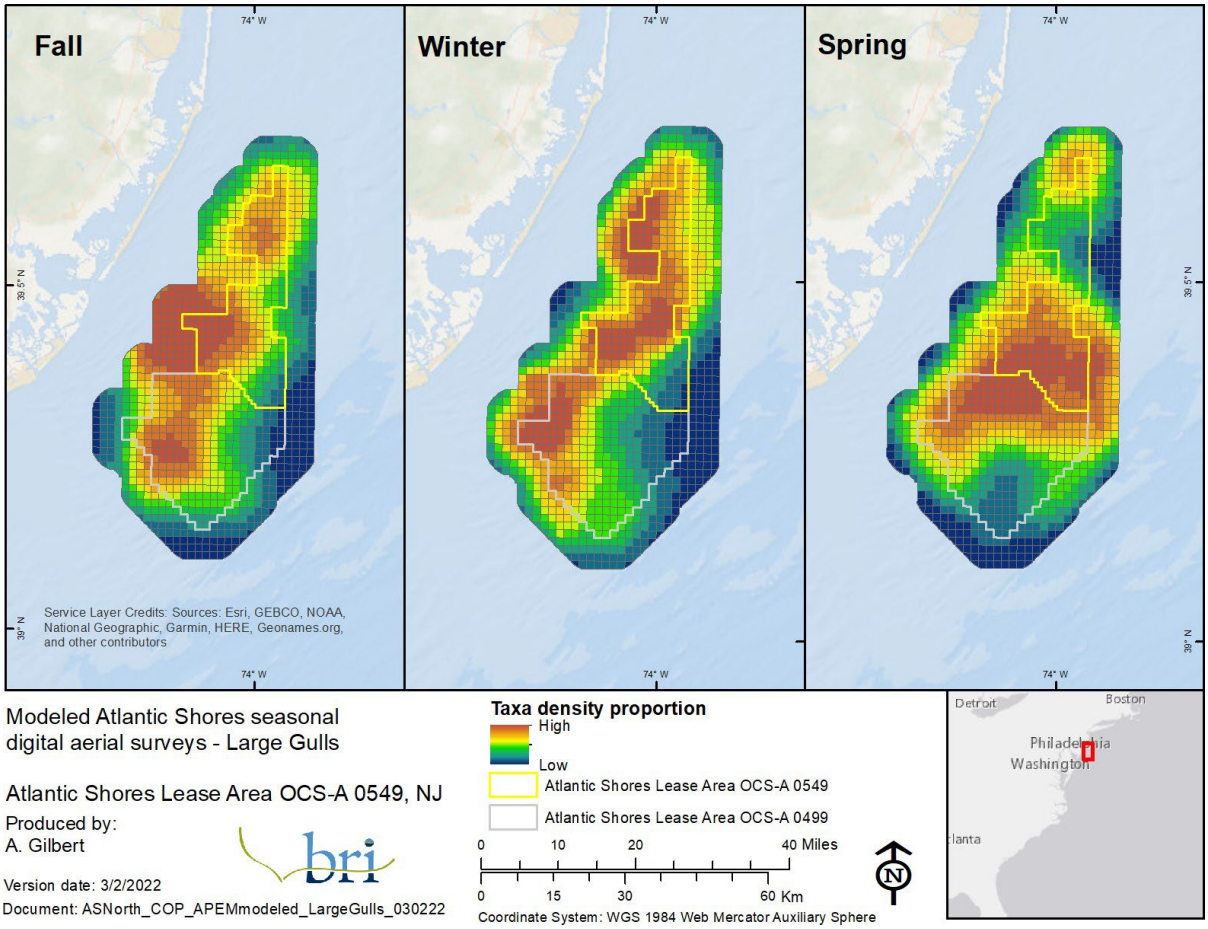

Figure 5-35: Seasonal distributions of large gulls across the Lease Area, modeled from monthly digital aerial surveys carried out in the area from October 2020–May 2021.

5.2.6.2. Relative Behavioral Vulnerability Figures and Tables

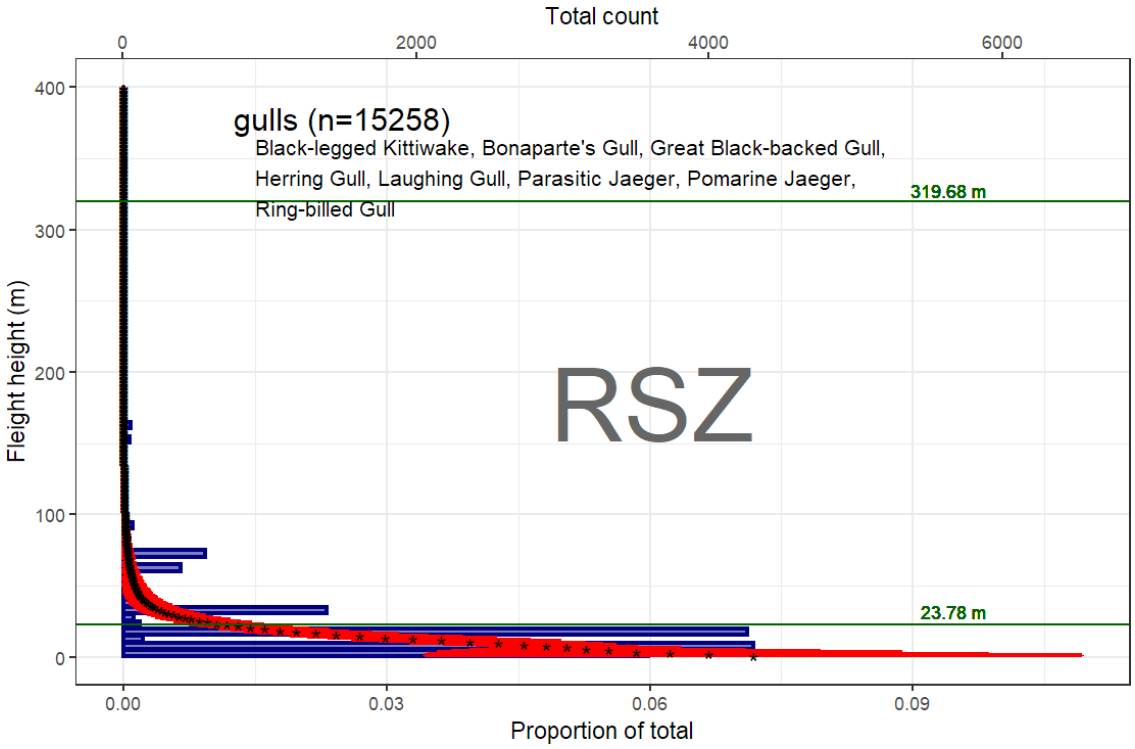

NOTE: Figure shows the actual number of birds in 5-m (16-ft) intervals (blue bars), the modeled average flight height in 1-m (3-ft) intervals (black asterisks), and the standard deviation (red lines), in relation to the upper and lower limits of the RSZ (23.78 m to 319.68 m [78.02 ft to 1,048.82 ft]).

Figure 5-36: Flight heights (m) of jaegers and gulls derived from the Northwest Atlantic Seabird Catalog.

Table 5-15: Vulnerability assessment rankings by species for the gull group.

Species	Collision Vulnerability	Displacement Vulnerability	Population Vulnerability
Black-legged Kittiwake	medium (0.57)	medium (0.6)	low (0.33)
Bonaparte's Gull	low (0.43)	medium (0.5)	low (0.33)
Great Black-backed Gull	medium (0.6)	medium (0.7)	minimal (0.2)
Herring Gull	medium (0.67)	medium (0.5)	medium (0.53)
Laughing Gull	medium (0.53)	medium (0.5)	low (0.4)
Parasitic Jaeger	medium (0.57)	low (0.3)	low (0.4)
Pomarine Jaeger	medium (0.67)	low (0.3)	low (0.4)
Ring-billed Gull	medium (0.6)	low (0.4)	low (0.33)

5.2.7. Terns

5.2.7.1. Exposure Tables, Maps, and Figures

Table 5-16: Seasonal exposure rankings for the tern group.

Species	Season	Local Rank	Regional Rank	Total Rank	Exposure Score*
Least Tern	Winter	0	·	0	minimal
	Spring	0	·	0	minimal
	Summer	0	0	0	minimal
	Fall	0	0	0	minimal
Caspian Tern	Winter	0	·	0	minimal
	Spring	0	·	0	minimal
	Summer	0	·	0	minimal
	Fall	0	·	0	minimal
Black Tern	Winter	0	·	0	minimal
	Spring	0	·	0	minimal
	Summer	0	·	0	minimal
	Fall	3	·	6	high
Common Tern	Winter	0	·	0	minimal
	Spring	0	3	3	medium
	Summer	1	3	4	medium
	Fall	1	2	3	medium
Forster's Tern	Winter	0	·	0	minimal
	Spring	0	·	0	minimal
	Summer	0	·	0	minimal
	Fall	0	·	0	minimal
Royal Tern	Winter	0	·	0	minimal
	Spring	0	0	0	minimal
	Summer	0	0	0	minimal
	Fall	0	0	0	minimal

*Note: The high fall ranking of Black Tern was the result of only one observation of a Black Tern in the fall, which was located within the Lease Area. This does not represent actual high exposure. See Map 135 in Section 8.

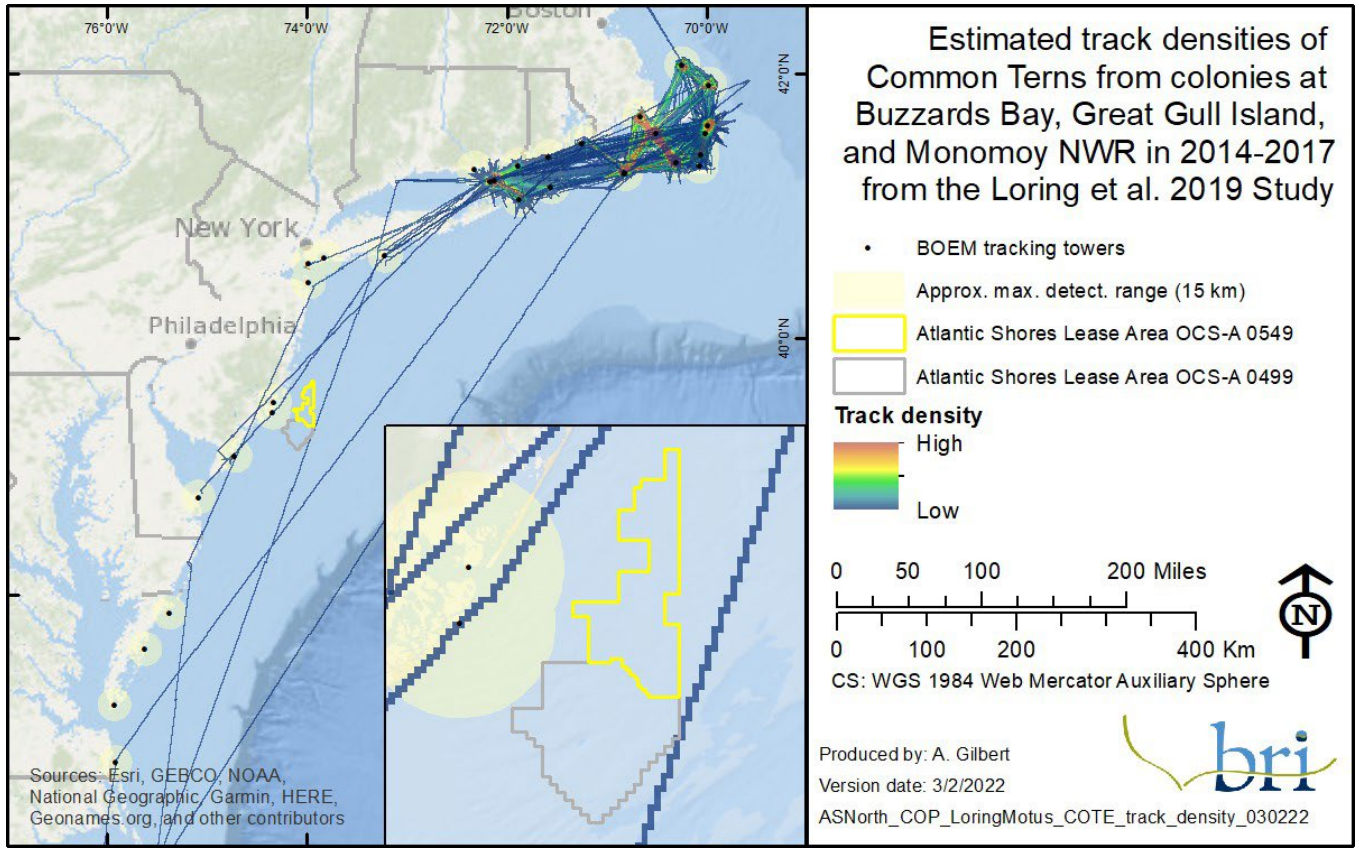

NOTE: Tracks are not actual flight paths but interpolated (model-generated) flight paths. Flight paths were modeled by detections of movements between land-based towers. Towers had a typical detection range <9.3 mi (<15 km), so birds were only detected when flying within approximately9.3 mi (15 km) of one of the towers. (See Fig. 5 [tower locations] in Loring et al. [2019] and Appendix K [detection probability] for details. Appendices are found at: https://espis.boem.gov/final%20reports/BOEM_2019-017a.pdf.) Data provided by USFWS and used with permission.

Figure 5-37: Modeled flight paths of migratory Common Terns equipped with nanotags (Loring et al. 2019).

5.2.7.2. Behavioral Vulnerability Figures and Tables

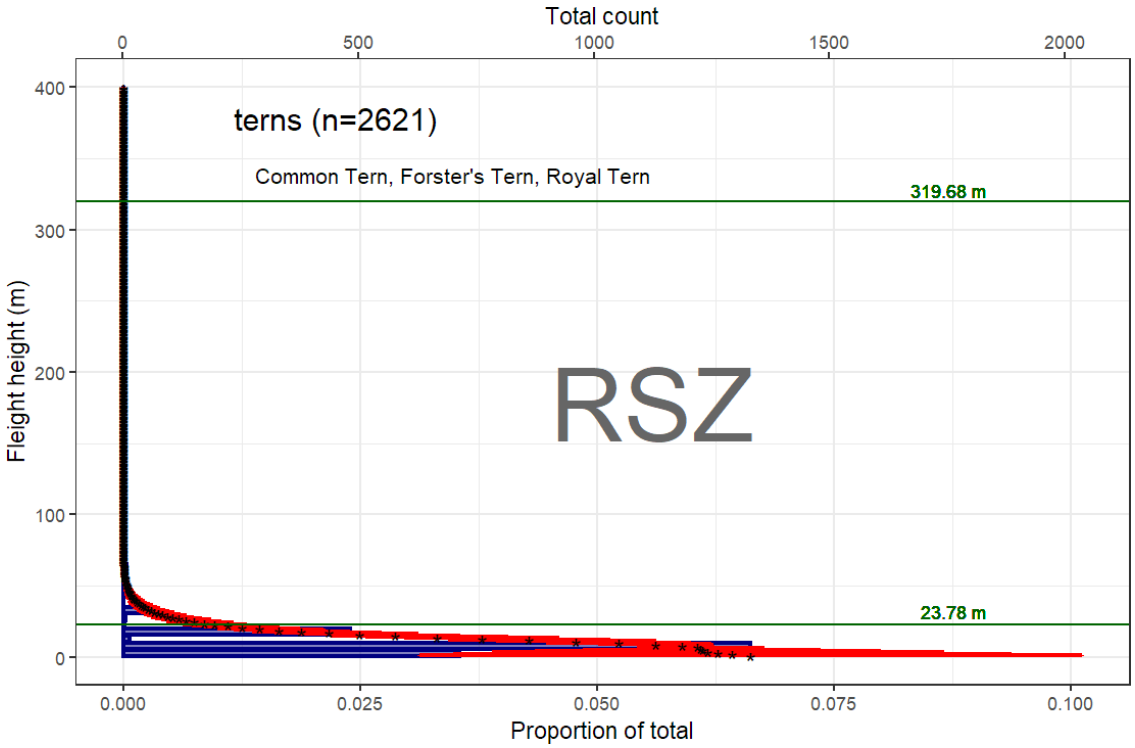

NOTE: Figure shows the actual number of birds in 5-m (16-ft) intervals (blue bars), the modeled average flight height in 1-m (3-ft) intervals (black asterisks), and the standard deviation (red lines), in relation to the upper and lower limits of the RSZ (23.78 m to 319.68 m [78.02 ft to 1,048.82 ft]).

Figure 5-38: Flight heights (m) of terns derived from the Northwest Atlantic Seabird Catalog.

Table 5-17: Vulnerability assessment rankings by species for the tern group.

NOTE: in the COP, "low" is added to the Displacement Vulnerability score because terns receive a low disturbance score in Wade et al. (2016); terns were determined to have a 30% macro avoidance of turbines at Egmond aan Zee (Cook et al. 2012); and displacement in terns has not been well studied.

Species	Collision Vulnerability	Displacement Vulnerability	Population Vulnerability
Common Tern	low (0.33)	high (0.8)	medium (0.6)
Forster's Tern	medium (0.6)	medium (0.5)	low (0.4)
Roseate Tern	low (0.3)	high (0.8)	high (0.87)
Royal Tern	medium (0.57)	medium (0.5)	medium (0.53)

5.2.8. Federally Endangered Tern Species

5.2.8.1. Roseate Tern

5.2.8.1.1. Exposure Tables, Maps, and Figures

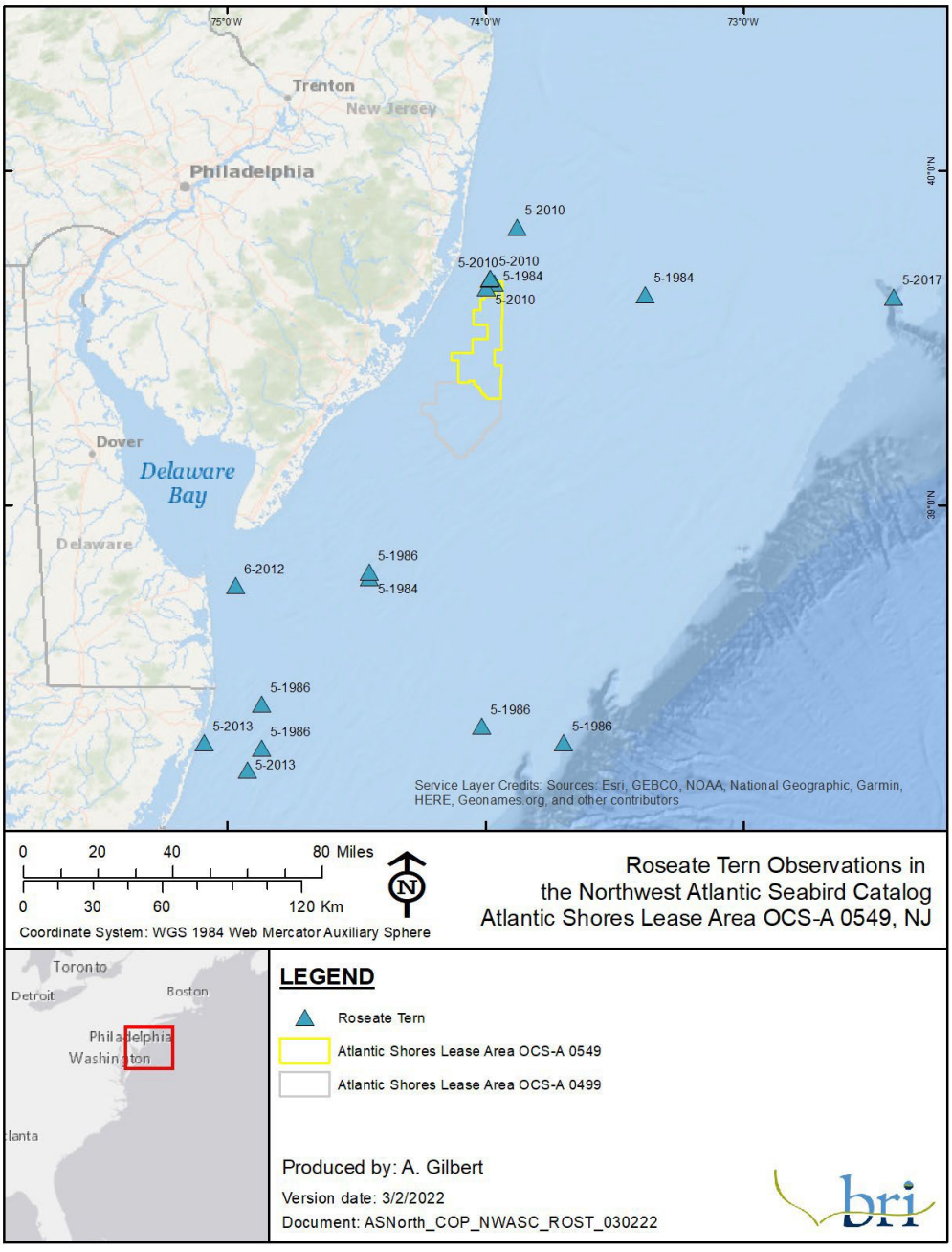

Figure 5-39: Roseate Tern observations from the Northwest Atlantic Seabird Catalog. Data provided by NOAA and used with permission.

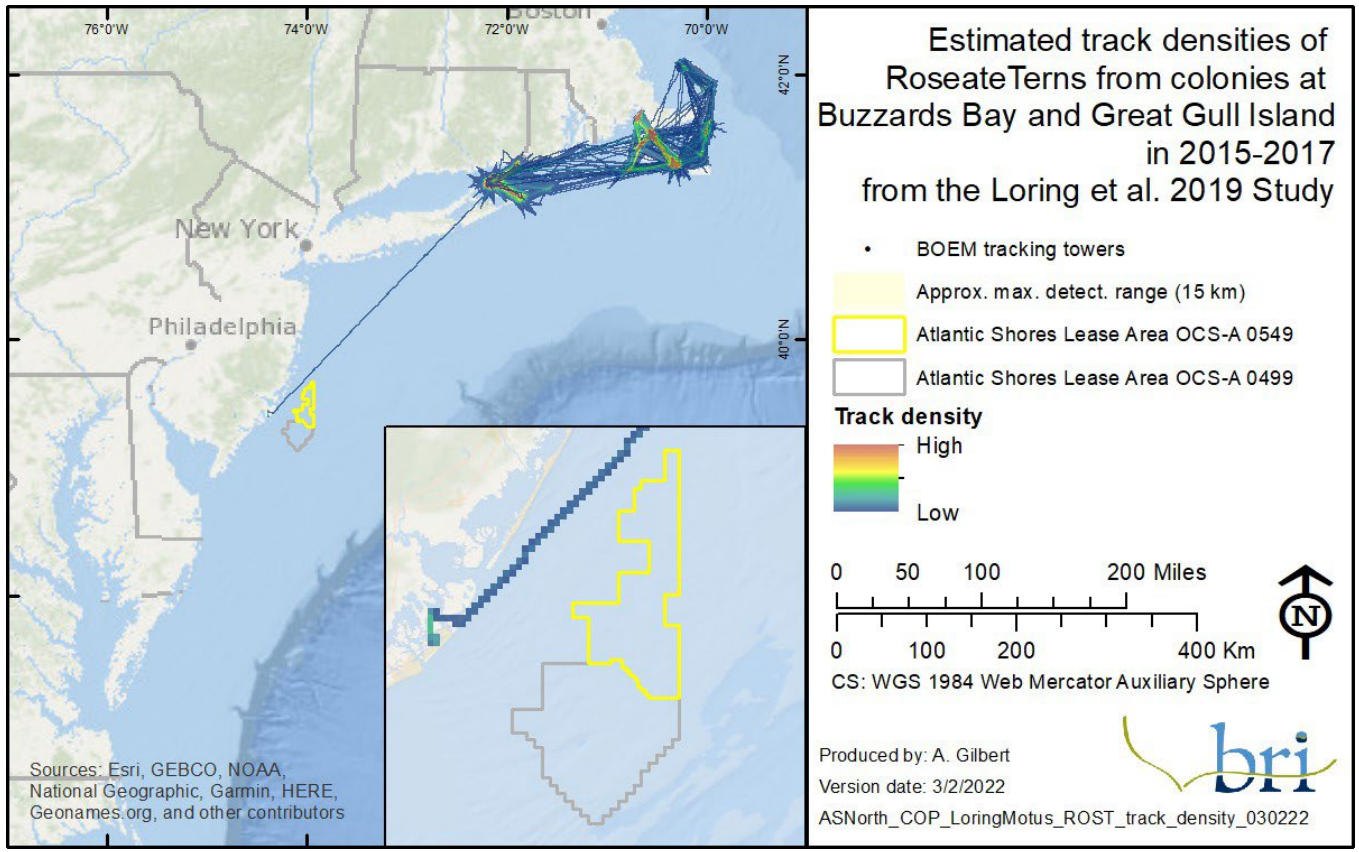

NOTE: Tracks are not actual flight paths but interpolated (model-generated) flight paths. Flight paths were modeled by detections of movements between land-based towers. Towers had a typical detection range <9.3 mi (<15 km), so birds were only detected when flying within approximately 9.3 mi (15 km) of one of the towers. (See Fig. 5 [tower locations] in Loring et al. [2019] and Appendix K [detection probability] for details. Appendices are found at: https://espis.boem.gov/final%20reports/BOEM_2019-017a.pdf.) Data provided by USFWS and used with permission.

Figure 5-40: Modeled flight paths of migratory Roseate Terns equipped with nanotags (Loring et al. 2019).

5.2.8.1.2. Relative Behavioral Vulnerability Figures and Tables

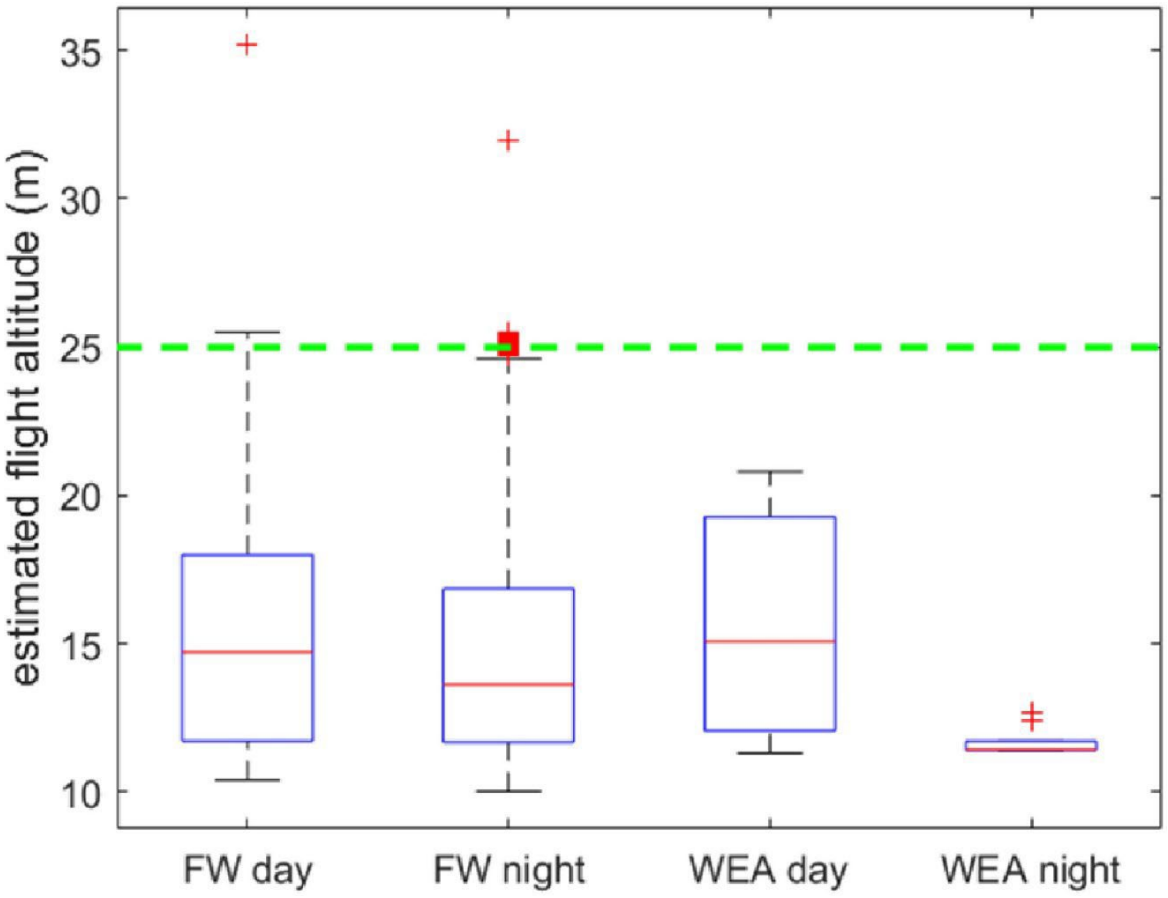

NOTE: During exposure to Federal waters and Atlantic OCS WEAs during day and night. The green-dashed line represents the lower limit of an idealized RSZ used in the study (25 m [82 ft]; from Loring et al. [2019]).

Figure 5-41: Model-estimated flight altitude ranges (m) of Roseate Terns.

5.2.9. Auks

5.2.9.1. Exposure Tables, Maps, and Figures

Table 5-18: Seasonal exposure rankings for the auk group.

Species	Season	Local Rank	Regional Rank	Total Rank	Exposure Score
Dovekie	Winter	0	0	0	minimal
	Spring	0	0	0	minimal
	Summer	0	0	0	minimal
	Fall	0	0	0	minimal
Common Murre	Winter	0	0	0	minimal
	Spring	0	0	0	minimal
	Summer	0	·	0	minimal
	Fall	0	·	0	minimal
Thick-billed Murre	Winter	0	0	0	minimal
	Spring	0	0	0	minimal
	Summer	0	·	0	minimal
	Fall	0	·	0	minimal
Razorbill	Winter	0	1	1	low
	Spring	1	2	3	medium
	Summer	0	0	0	minimal
	Fall	0	0	0	minimal
Black Guillemot	Winter	0	·	0	minimal
	Spring	0	·	0	minimal
	Summer	0	0	0	minimal
	Fall	0	·	0	minimal
Atlantic Puffin	Winter	0	0	0	minimal
	Spring	0	0	0	minimal
	Summer	0	0	0	minimal
	Fall	0	0	0	minimal

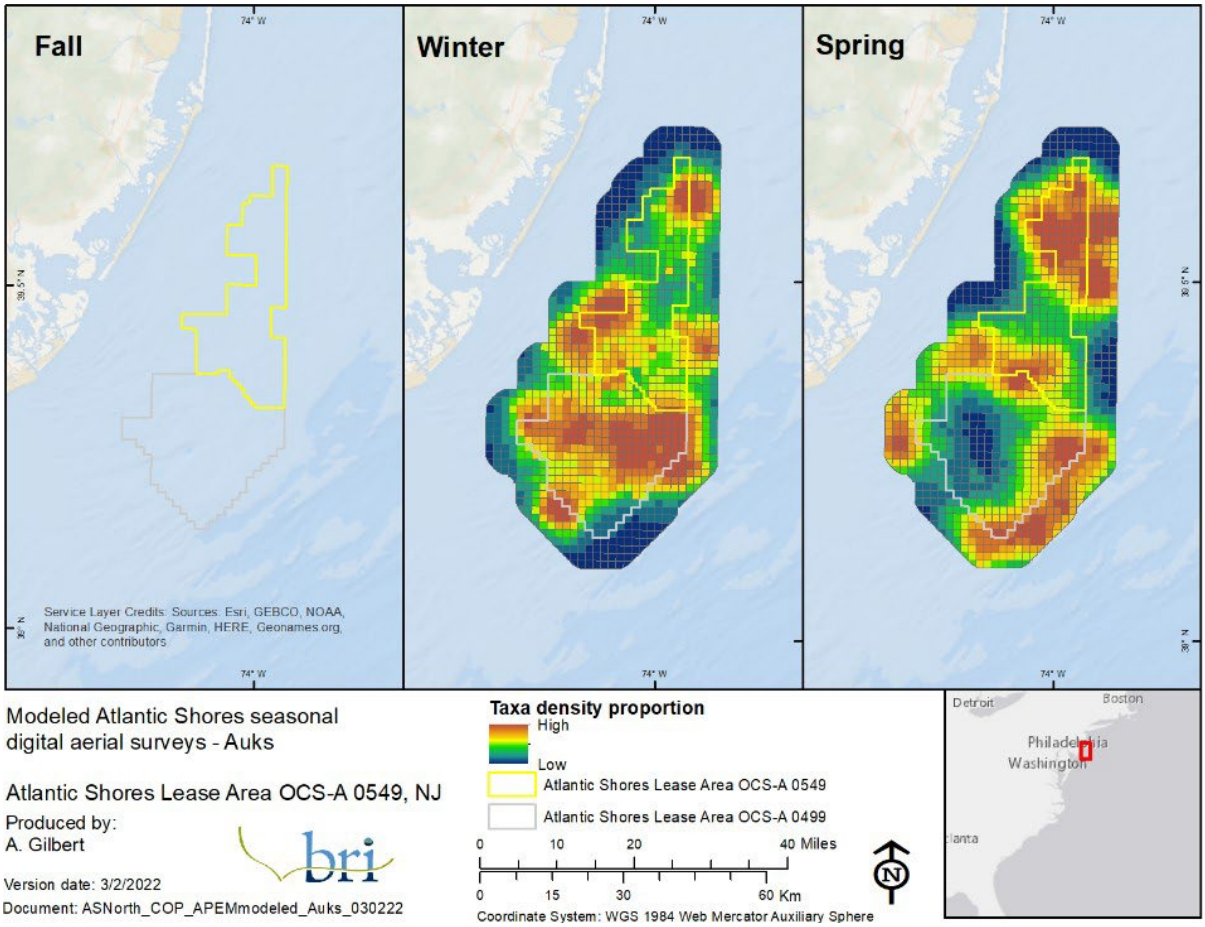

Figure 5-42: Seasonal distributions of auks across the Lease Area, modeled from monthly digital aerial surveys carried out in the area from October 2020–May 2021.

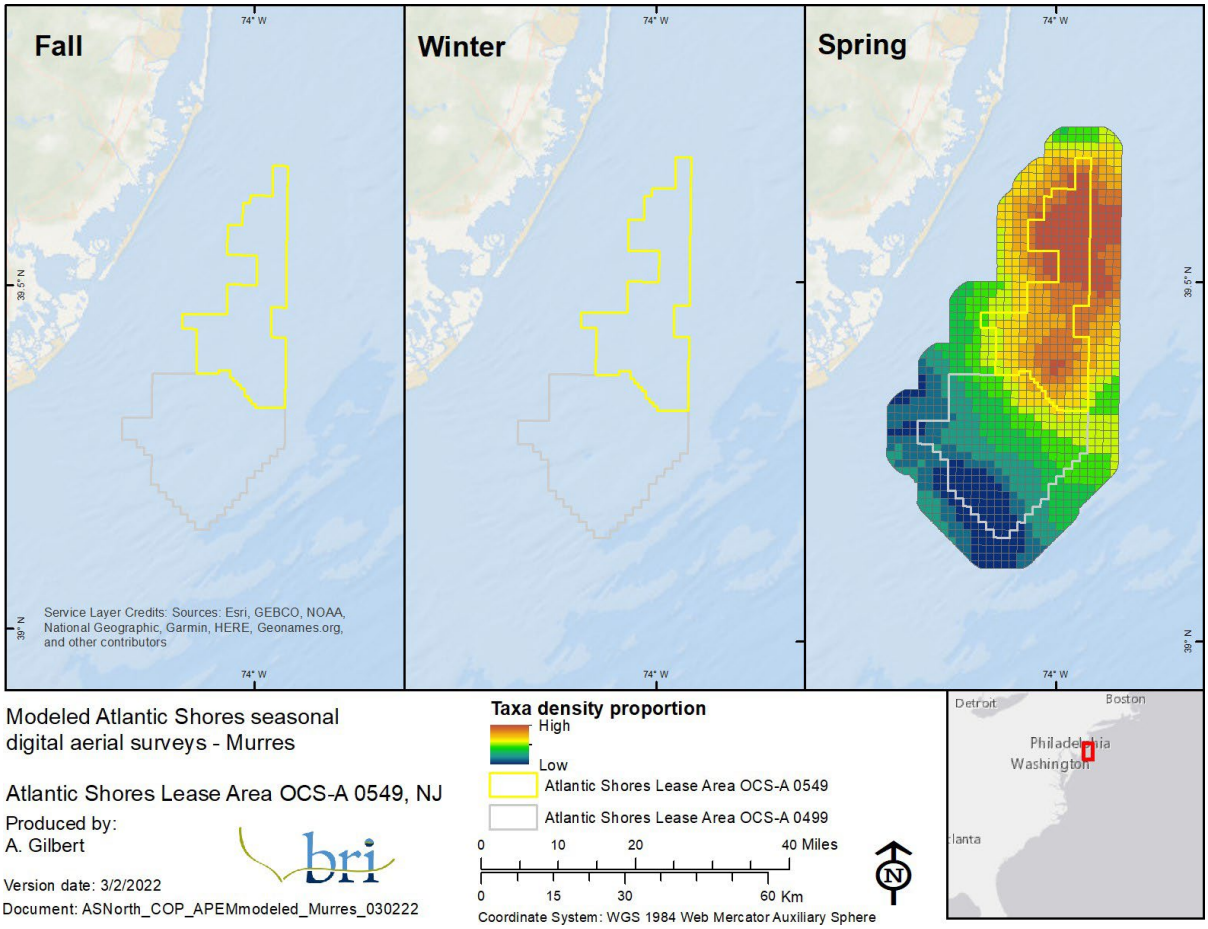

Figure 5-43: Seasonal distributions of murres across the Lease Area, modeled from monthly digital aerial surveys carried out in the area from October 2020–May 2021.

5.2.9.2. Relative Behavioral Vulnerability Figures and Tables

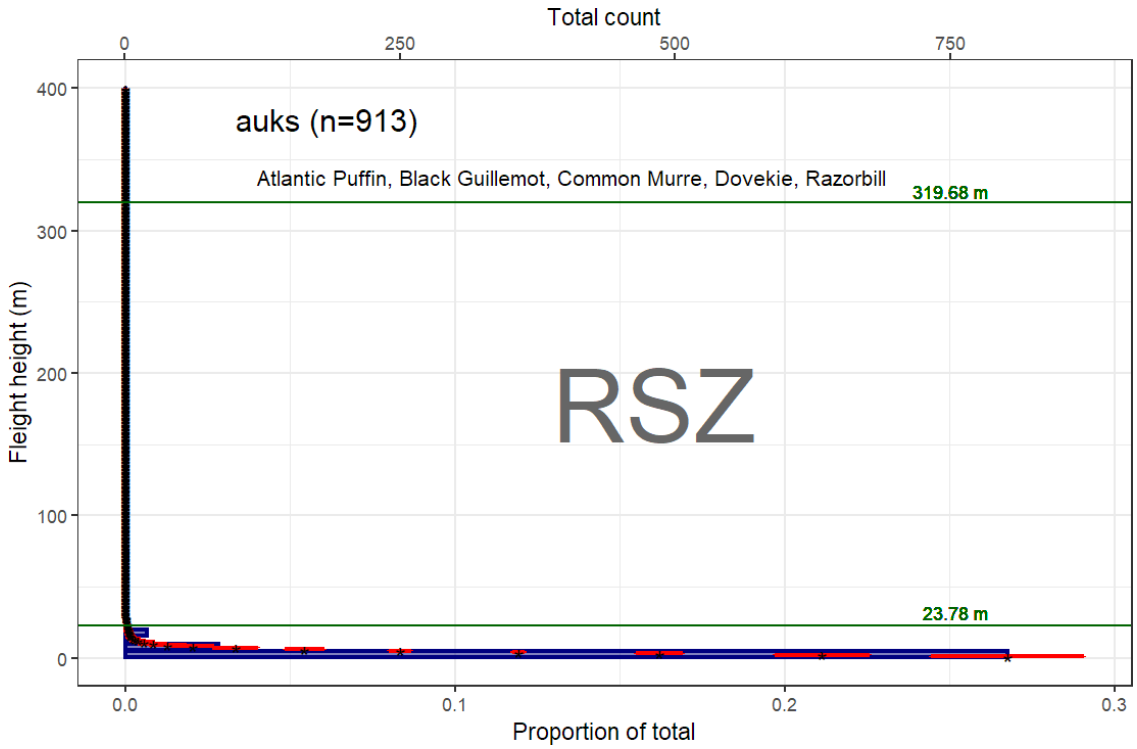

NOTE: Figure shows the actual number of birds in 5-m (16-ft) intervals (blue bars), the modeled average flight height in 1-m (3-ft) intervals (black asterisks), and the standard deviation (red lines), in relation to the upper and lower limits of the RSZ (23.78 m to 319.68 m [78.02 ft to 1,048.82 ft]).

Figure 5-44: Flight heights (m) of auks derived from the Northwest Atlantic Seabird Catalog.

Table 5-19: Vulnerability assessment rankings by species for the auk group.

Species	Collision Vulnerability	Displacement Vulnerability	Population Vulnerability
Atlantic Puffin	minimal (0.2)	high (0.8)	medium (0.53)
Black Guillemot	low (0.33)	high (0.9)	low (0.4)
Common Murre	low (0.27)	high (0.8)	low (0.4)
Dovekie	low (0.27)	medium (0.7)	low (0.4)
Razorbill	minimal (0.23)	high (0.8)	medium (0.6)

6. References

Adams J, Kelsey EC, Felis J, Pereksta DM. 2016. Collision and displacement vulnerability among marine birds of the California Current System associated with offshore wind energy infrastructure. U.S. Geological Survey Open-File Report 2016-1154.

Anderson JR. 1976. A Land Use and Land Cover Classification System For Use WIth Remote Sensor Data. Vol. 964. US Government Printing Office.

Bachl FE, Lindgren F, Borchers DL, Illian JB. 2019. inlabru: an R package for Bayesian spatial modelling from ecological survey data. Methods Ecol Evol. 10(6):760–766. doi:10.1111/2041-210X.13168. [accessed 2021 Nov 22]. https://onlinelibrary.wiley.com/doi/full/10.1111/2041-210X.13168.

Band W. 2012. Using a collision risk model to assess bird collision risk for offshore windfarms. Report commissioned by The Crown Estate, through the British Trust for Ornithology, via its Strategic Ornithological Support Services, Project SOSS-02. http://www.bto.org/sites/default/files/u28/downloads/Projects/Final_Report_SOSS02_Band1ModelGuidance.pdf.

Bolduc F, Fifield DA. 2017. Seabirds at-sea surveys: The line-transect method outperforms the point-transect alternative. Open Ornithol J. 10(1):42–52. doi:10.2174/1874453201710010042.

Bradbury G, Trinder M, Furness B, Banks AN, Caldow RWG, Hume D. 2014. Mapping seabird sensitivity to offshore wind farms. PLoS One. 9(9):e106366. doi:10.1371/journal.pone.0106366.

Buckland ST, Anderson DR, Burnham KP, Laake JL, Borchers DL, Thomas L. 2001. Introduction to distance sampling: estimating abundance of biological populations. Oxford, U.K.: Oxford University Press.

Camphuysen KCJ, Fox TAD, Mardik LMF, Petersen IK. 2004. Toward standardised seabirds at sea census techniques in connection with environmental impact assessments for offshore wind farms in the U.K. COWRIE BAM 02-2002. Report by Royal Netherlands Institute for Sea Research and the Danish National Environmental Research Institute to Crown Estate Commissioners, London, U.K. 38 pp. http://www.thecrownestate.co.uk/1352_bird_survey_phase1_final_04_05_06.pdf.

Chamberlain DE, Rehfisch MR, Fox AD, Desholm M, Anthony SJ. 2006. The effect of avoidance rates on bird mortality predictions made by wind turbine collision risk models. Ibis (Lond 1859). 148:198–202. doi:10.1111/j.1474-919X.2006.00507.x.

Cook ASCP, Humphreys EM, Bennet F, Masden EA, Burton NHK. 2018. Quantifying avian avoidance of offshore wind turbines: Current evidence and key knowledge gaps. Mar Environ Res. 140:278–288. doi:https://doi.org/10.1016/j.marenvres.2018.06.017.

http://www.sciencedirect.com/science/article/pii/S014111361830179X.

Cook ASCP, Johnston A, Wright LJ, Burton NHK. 2012. A Review of Flight Heights and Avoidance Rates of Birds in Relation to Offshore Wind Farms. BTO Research Report Number 618. British Trust for Ornithology, Thetford, U.K. 61 pp. http://www.bto.org/sites/default/files/u28/downloads/Projects/Final_Report_SOSS02_BTOReview.pdf.

Curtice C, Cleary J, Scumchenia E, Halpin PN. 2019. Marine-life Data and Analysis Team (MDAT) technical report on the methods and development of marine-life data to support regional ocean planning and management. Prepared on behalf of the Marine-life Data and Analysis Team (MDAT).

Desholm M. 2009. Avian sensitivity to mortality: Prioritising migratory bird species for assessment at proposed wind farms. J Environ Manage. 90(8):2672–2679.

DeSorbo CR, Gilpatrick L, Persico C, Hanson W. 2018. Pilot Study: Establishing a Migrant Raptor Research Station at the Naval and Telecommunications Area Master Station Atlantic Detachment Cutler, Cutler Maine. Biodiversity Research Institute, Portland, Maine. 6 pp.

DeSorbo CR, Persico C, Gilpatrick L. 2018. Studying migrant raptors using the Atlantic Flyway. Block Island Raptor Research Station, Block Island, RI: 2017 season. BRI Report # 2018-12 submitted to The Nature Conservancy, Block Island, Rhode Island, and The Bailey Wildlife Foundation, Cambridge, Massachusetts. Biodiversity Research Institute, Portland, Maine. 35 pp.

DeSorbo CR, Wright KG, Gray R. 2012. Bird Migration Stopover Sites: Ecology of Nocturnal and Diurnal Raptors at Monhegan Island. Report BRI 2012-09 submitted to the Maine Outdoor Heritage Fund, Pittston, Maine, and the Davis Conservation Foundation, Yarmouth, Maine. Biodiversity Research Institute, Gorham, Maine. 43 pp. http://www.briloon.org/raptors/monhegan.

Douglas DC, Weinzierl R, Davidson SC, Kays R, Wikelski M, Bohrer G. 2012. Moderating Argos location errors in animal tracking data. Methods Ecol Evol. 3(6):999–1007. doi:10.1111/j.2041-210X.2012.00245.x.

Fliessbach KL, Borkenhagen K, Guse N, Markones N, Schwemmer P, Garthe S. 2019. A ship traffic disturbance vulnerability index for Northwest European seabirds as a tool for marine spatial planning. Front Mar Sci. 6:192.

Fox AD, Desholm M, Kahlert J, Christensen TK, Petersen IK. 2006. Information needs to support environmental impact assessment of the effects of European marine offshore wind farms on birds. Ibis (Lond 1859). 148:129–144. doi:10.1111/j.1474-919X.2006.00510.x.

Fuglstad GA, Simpson D, Lindgren F, Rue H. 2018. Constructing Priors that Penalize the Complexity of Gaussian Random Fields. https://doi.org/101080/0162145920171415907. 114(525):445–452. doi:10.1080/01621459.2017.1415907. [accessed 2021 Nov 22]. https://www.tandfonline.com/doi/abs/10.1080/01621459.2017.1415907.

Furness RW, Wade HM, Masden EA. 2013. Assessing vulnerability of marine bird populations to offshore wind farms. J Environ Manage. 119:56–66. doi:10.1016/j.jenvman.2013.01.025. http://dx.doi.org/10.1016/j.jenvman.2013.01.025.

Garthe S, Hüppop O. 2004. Scaling possible adverse effects of marine wind farms on seabirds: developing and applying a vulnerability index. J Appl Ecol. 41(4):724–734. doi:10.1111/j.0021-8901.2004.00918.x.

Geo-Marine. 2010. Ocean/Wind Power Ecological Baseline Studies, January 2008 - December 2009 - Final Report. Volume II: Avian Studies. Geo-Marine, Inc., Plano, TX. 2109 pp.

Goodale MW, Stenhouse IJ. 2016. A conceptual model to determine vulnerability of wildlife populations to offshore wind energy development. Human-Wildlife Interact. 10(1):53–61. doi:10.26077/1d31-m472.

Gulka J, Berlin AM, Friedland KD, Gilbert AT, Goetsch C, Montevecchi WA, Perry M, Stenhouse IJ, Williams KA, Adams EM. 2023. Assessing individual movement, habitat use, and behavior of non-breeding marine birds in relation to prey availability in the US Atlantic. Mar Ecol Prog Ser. 711: 77-99. https://doi.org/10.3354/meps14316

Heiser E, Davis C. 2021. Piping Plover Nesting Results in New Jersey: 2020. Conserve Wildlife Foundation of New Jersey & New Jersey Division of Fish and Wildlife Endangered and Nongame Species Program.

Hijmans RJ. 2022. raster: Geographic Data Analysis and Modeling. R package version 3.5-15. https://CRAN.R-project.org/package=raster

Horton TW, Bierregaard RO, Zawar-Reza P, Holdaway RN, Sagar P. 2014. Juvenile Osprey navigation during trans-oceanic migration. PLoS One. 9(12). doi:10.1371/journal.pone.0114557.

Jakubas D, Wojczulanis-Jakubas K, Iliszko LM, Kidawa D, Boehnke R, Błachowiak-Samołyk K, Stempniewicz L. 2020. Flexibility of little auks foraging in various oceanographic features in a changing Arctic. Sci Rep 10: 8283 https://doi.org/10.1038/s41598-020-65210-x

Johnston A, Cook ASCP, Wright LJ, Humphreys EM, Burton NHK. 2014. Modelling flight heights of marine birds to more accurately assess collision risk with offshore wind turbines. J Appl Ecol. 51(1):31–41. doi:10.1111/1365-2664.12191.

Kelsey EC, Felis JJ, Czapanskiy M, Pereksta DM, Adams J. 2018. Collision and displacement vulnerability to offshore wind energy infrastructure among marine birds of the Pacific Outer Continental Shelf. J Environ Manage. 227:229–247. doi:10.1016/j.jenvman.2018.08.051.

Krainski E, Gómez-Rubio V, Bakka H, Lenzi A, Castro-Camilo D, Simpson D, Lindgren F, Rue H. 2018 Dec 7. Advanced Spatial Modeling with Stochastic Partial Differential Equations Using R and INLA. Adv Spat Model with Stoch Partial Differ Equations Using R INLA. doi:10.1201/9780429031892. [accessed 2021 Nov 22]. https://www.taylorfrancis.com/books/mono/10.1201/9780429031892/advanced-spatial-

modeling-stochastic-partial-differential-equations-using-inla-elias-krainski-virgilio-gómez-rubio-haakon-bakka-amanda-lenzi-daniela-castro-camilo-daniel-simpson-finn-lindgren-.

Kranstauber B, Kays R, Lapoint SD, Wikelski M, Safi K. 2012. A dynamic Brownian bridge movement model to estimate utilization distributions for heterogeneous animal movement. J Anim Ecol. 81(4):738–46. doi:10.1111/j.1365-2656.2012.01955.x.

Kranstauber B, Smolla M. 2016. Move: Visualizing and Analyzing Animal Track Data. R package

version 2.1.0. https://cran.r-project.org/package=move.

Krijgsveld KL, Fljn RC, Japink M, van Horssen PW, Heunks C, Collier MP, Poot MJM, Beuker D, Birksen S. 2011. Effect Studies Offshore Wind Farm Egmond aan Zee: Final Report on Fluxes, Flight Altitudes and Behaviour of Flying Birds. Bureau Waardenburg report no. 10-219. Institute for Marine Resources & Ecosystem Studies, Wageningen UR, Netherlands.

Lindgren F, Rue H. 2015. Bayesian Spatial Modelling with R - INLA . J Stat Softw. 63(19). doi:10.18637/jss.v063.i19.

Lindgren F, Rue H, Lindstrom J. 2011. An explicit link between gaussian fields and gaussian Markov random fields: the stochastic partial differential equation approach (with discussion). J R Stat Soc B. 73(4):423–498. doi:10.1111/j.1467-9868.2011.00777.x.

Loring PH, Paton PWC, Osenkowski JE, Gilliland SG, Savard J-PL, Mcwilliams SR. 2014. Habitat use and selection of black scoters in southern New England and siting of offshore wind energy facilities. J Wildl Manage. 78(4):645–656. doi:10.1002/jwmg.696.

Loring P, Goyert H, Griffin C, Sievert P, Paton P. 2017. Tracking Movements of Common Terns, Endangered Roseate Terns, and Threatened Piping Plovers in the Northwest Atlantic. 2017 Annual Report to the Bureau of Ocean Energy Management. US Fish and Wildlife Service, Hadley, MA. 134 pp.

Loring PH, McLaren JD, Smith PA, Niles LJ, Koch SL, Goyert HF, Bai H. 2018. Tracking Movements of Threatened Migratory rufa Red Knots in U.S. Atlantic Outer Continental Shelf Waters. OCS Study BOEM 2018-046. U.S. Department of the Interior, Bureau of Ocean Energy Management, Sterling, VA. 145 pp.

Loring PH, Paton PWC, McLaren JD, Bai H, Janaswamy R, Goyert HF, Griffin CR, Sievert PR. 2019. Tracking offshore occurrence of Common Terns, endangered Roseate Terns, and threatened Piping Plovers with VHF arrays. OCS Study BOEM 2019-017. US Department of the Interior, Bureau of Ocean Energy Management, Sterling, VA. 140 pp. https://espis.boem.gov/final reports/BOEM_2019-017.pdf.

Loring, P., A. Lenske, J. McLaren, M. Aikens, A. Anderson, Y. Aubrey, E. Dalton, A. Dey, C. Friis, D. Hamilton, B. Holberton, D. Kriensky, D. Mizrahi, L. Niles, K. L. Parkins, J. Paquet, F. Sanders, A. Smith, Y. Turcotte, A. Vitz, & P. Smith. 2020. Tracking Movements of Migratory Shorebirds in the US Atlantic Outer Continental Shelf Region. Sterling (VA): US Department of the Interior, Bureau of Ocean Energy Management. OCS Study BOEM 2021-008. 104 p.

Martell MS, Douglas D. 2019. Data from: Fall migration routes, timing, and wintering sites of North American Ospreys as determined by satellite telemetry. Movebank Data Repos. doi:doi:10.5441/001/1.sv6335t3.

Martell MS, Henny CJ, Nye PE, Solensky MJ. 2001. Fall migration routes, timing, and wintering sites of North American Ospreys as determined by satellite telemetry. Condor. 103(4):715–724.

doi:doi:10.1650/0010-5422(2001)103[0715:FMRTAW]2.0.CO;2
url:https://sora.unm.edu/node/54078.

Masden EA. 2019. Avian Stochastic CRM v2.3.1.

Masden EA, McCluskie A, Owen E, Langston RHW. 2015. Renewable energy developments in an uncertain world: The case of offshore wind and birds in the UK. Mar Policy. 51:169–172. doi:https://doi.org/10.1016/j.marpol.2014.08.006.

Meattey DE, Mcwilliams SR, Paton PWC, Lepage C, Gilliland SG, Savoy L, Olsen GH, Osenkowski JE. 2019. Resource selection and wintering phenology of White-winged Scoters in southern New England : Implications for offshore wind energy development. 121:1–18. doi:10.1093/condor/duy014.

Meattey DE, McWilliams SR, Paton PWC, Lepage C, Gilliland SG, Savoy L, Olsen GH, Osenkowski JE. 2018. Annual cycle of White-winged Scoters (*Melanitta fusca*) in eastern North America: migratory phenology, population delineation, and connectivity. Can J Zool. 96:1353–1365.

Møller J, Waagepetersen RP. 2007. Modern Statistics for Spatial Point Processes*. Scand J Stat. 34(4):643–684. doi:10.1111/J.1467-9469.2007.00569.X. [accessed 2021 Nov 22]. https://onlinelibrary.wiley.com/doi/full/10.1111/j.1467-9469.2007.00569.x.

New York Department of Environmental Conservation. 2018. 2018 Long Island Colonial Waterbird & Piping Plover Update Harbor Herons & Other Waterbirds of the Greater NY/NJ Harbor Working Group. Available at https://www.hudsonriver.org/wp-content/uploads/2017/11/Jennings_NYSDEC-Region1_LI-Update_2018.pdf.

Panjabi AO, Easton WE, Blancher PJ, Shaw AE, Andres BA, Beardmore CJ, Camfield AF, Demarest DW, Dettmers R, Keller RH, et al. 2019. Avian Conservation Assessment Database Handbook, Version 2019. Partners in Flight Technical Series No. 8. Available from pif.birdconservancy.org/acad_handbook.pdf.

R Core Team. 2021. R: A language and environment for statistical computing. R Foundation for Statistical Computing, Vienna, Austria. URL https://www.R-project.org/.

Rue H, Martino S, Chopin N. 2009. Approximate Bayesian inference for latent Gaussian models using integrated nested Laplace approximations (with discussion). J R Stat Soc B. 71:319–392. doi:10.1111/j.1467-9868.2008.00700.x.

SDJV. 2015. Atlantic and Great Lakes Sea Duck Migration Study: progress report June 2015.

Skov H, Heinanen S, Norman T, Ward RM, Mendez-Roldan S, Ellis I. 2018. ORJIP Bird Collision and Avoidance Study. Final Report - April 2018. Report by NIRAS and DHI to The Cabon Trust, U.K. 247 pp.

Sollmann R, Gardner B, Williams KA, Gilbert AT, Veit RR. 2016. A hierarchical distance sampling

model to estimate abundance and covariate associations of species and communities. Methods Ecol Evol. 7(5):529–537.

Spiegel CS, Berlin AM, Gilbert AT, Gray CO, Montevecchi WA, Stenhouse IJ, Ford SL, Olsen GH, Fiely JL, Savoy L, et al. 2017. Determining fine-scale use and movement patterns of diving bird species in Federal waters of the Mid-Atlantic United States using satellite telemetry. OCS Study BOEM 2017-069. Department of the Interior, Bureau of Ocean Energy Management, Sterling, VA. 293 pp. https://www.boem.gov/espis/5/5635.pdf.

Stenhouse IJ, Berlin AM, Gilbert AT, Goodale MW, Gray CE, Montevecchi WA, Savoy L, Spiegel CS. 2020. Assessing the exposure of three diving bird species to offshore wind areas on the U.S. Atlantic Outer Continental Shelf using satellite telemetry. Divers Distrib. n/a(n/a). doi:10.1111/ddi.13168. https://doi.org/10.1111/ddi.13168.

Sullivan BL, Wood CL, Iliff MJ, Bonney RE, Fink D, Kelling S. 2009. eBird: A citizen-based bird observation network in the biological sciences. Biol Conserv. 142(10):2282–2292. doi:10.1016/j.biocon.2009.05.006. http://dx.doi.org/10.1016/j.biocon.2009.05.006.

Thaxter CB, Ross-Smith VH, Bouten W. 2015. Seabird – wind farm interactions during the breeding season vary within and between years: A case study of lesser black-backed gull *Larus fuscus* in the UK. Biol Conserv. 186:347–358. doi:10.1016/j.biocon.2015.03.027.

U.S. Fish and Wildlife Service. 2015. Status of the Species - Red Knot.

U.S. Fish and Wildlife Service. 2020. Information for Planning and Consultation (IPaC). Retrieved from: https://ecos.fws.gov/ipac/user/login.

Vanermen N, Onkelinx T, Courtens W, Van de walle M, Verstraete H, Stienen EWM. 2015. Seabird avoidance and attraction at an offshore wind farm in the Belgian part of the North Sea. Hydrobiologia. 756(1):51–61. doi:10.1007/s10750-014-2088-x.

Wade HM, Masden EA, Jackson AC, Furness RW. 2016. Incorporating data uncertainty when estimating potential vulnerability of Scottish seabirds to marine renewable energy developments. Mar Policy. 70:108–113. doi:10.1016/j.marpol.2016.04.045.

Walker WE, Harremoes P, Rotmans J, Van Der Sluijs JP, Van Asselt MBA, Janssen P, Krayer Von Krauss MP. 2003. Defining Uncertainty. Integr Assess. https://www.narcis.nl/publication/RecordID/oai:tudelft.nl:uuid:fdc0105c-e601-402a-8f16-ca97e9963592.

Willmott JR, Forcey G, Kent A. 2013. The Relative Vulnerability of Migratory Bird Species to Offshore Wind Energy Projects on the Atlantic Outer Continental Shelf: An Assessment Method and Database. OCS Study BOEM 2013-207. Final Report to the U.S. Department of the Interior, Bureau of Ocean Energy Management, Herndon, VA. 275 pp.

Winship AJ, Kinlan BP, White TP, Leirness JB, Christensen J. 2018. Modeling At-Sea Density of

Marine Birds to Support Atlantic Marine Renewable Energy Planning: Final Report. OCS Study BOEM 2018-010. U.S. Department of the Interior, Bureau of Ocean Energy Management, Office of Renewable Energy Programs, Sterling, VA. 67 pp.

7. Applying a Community Distance Model to Correct Density Estimates of Seabirds in New Jersey Waters

7.1. Background

Boat-based surveys are a standardized methodology to describe patterns of distribution and abundance in the marine environment. A known bias in this method is that individuals further from the transect line are more difficult to detect than those closer to the center (Buckland et al. 2001). This bias causes surveyors to underestimate the total number of animals in the survey area. Importantly, this bias can be variable by species and survey conditions, where it can be challenging to compare detection-naïve density estimates among species or surveys (Camphuysen et al. 2004). Estimating detection probability for rare species can be difficult due to a lack of observations, so researchers have developed new methods for estimating detection probabilities of communities have to address this issue (Sollmann et al. 2016). These community-based methods can be beneficial for surveys of wind energy projects as they can help account for problems relating to surveys of relatively small areas or including data from rare species.

Objectives

This analysis aims to correct the density estimates for all bird species detected in boat surveys in and around the Project Area. We used a community distance modeling approach to obtain estimates of detection probability for species groups found in the surveys. After we evaluate the efficacy of the modeling technique, we can then use these estimates to correct the estimates of total population size (or density) in the region to account for this source of bias. These estimates can then inform collision risk models or other conservation or management applications.

7.2. Methods

Boat-based survey data from New Jersey were collected as part of the New Jersey Offshore Wind Power Ecological Baseline Study (New Jersey Department of Environmental Protection) in 2008-2009. Surveys from the 'Offshore' and 'Sawtooth' protocols were selected to avoid issues in data collection that came from other survey types in the Project (e.g., coastal seawatch surveys). A distance survey protocol was implemented in these surveys (Buckland et al. 2001), where the distance from the transect line to the animal was estimated for all detected animals. A 300-m (984-ft) strip transect was surveyed off the boat, but animals outside the strip were also included if detected and time allowed for observation outside this primary observation area (the 300-m [984-ft] strip). Species were assigned a taxonomic group that ranged from multi-species 'sea ducks' to single species 'gannets.' Detections could be of individual animals or groups, and the group size was estimated for most detections.

To estimate detection probabilities for each taxonomic group, thus estimating the total population size of the group using the study area, a community distance model was parameterized in nimble (www.r-nimble.org) within R (R Core Team 2020). The observed data were parsed into transects, truncated to those less than 400 m (1,312 ft) from the transect line, then placed in eight 50-m (164-ft) distance bins to parameterize the

model. The core of the model is a distance detection model (Buckland et al. 2001) that uses a key function to describe the change in detection probability with distance from the transect line. The community distance model generalizes this detection function across multiple species and assumes that each species has a similar functional relationship with detection probability (Sollmann et al. 2016). While Sollmann et al. (2016) uses a half-normal detection function, here we expanded their approach to also include a hazard rate function:

$$pp_{iiiiii} = 1 - \exp\left(-\left(\frac{MM_{ii}^{2}}{\overline{\sigma\sigma_{iiii}}}\right)^{-\theta\theta_{jj}}\right)$$

Where, pp_{iiiiii} is the detection probability of a given distance band for survey transect *i*, species *j*, and distance band *b*; pp_{iiiiii} is the mean distance to the transect line, MM_{ii} is the distance from the middle of the distance band to the transect centerline, while $\sigma\sigma$ and $\theta\theta$ are the shape and scale parameters that vary by species and transect. These probabilities are then summed across all distance bands to determine the detection probability for a given species and transect. The general form of the community distance sampling model shares information across species using a random effects approach. This process works similarly across both half-normal and hazard detection functions, here we use a shrinkage model to share information across the hazard model shape parameter:

$$\log(\sigma\sigma_{iii}) = \alpha\alpha_{iiii} + \boldsymbol{\beta\beta}_{iiii}\boldsymbol{XX}$$

$$\alpha\alpha_{iiii} \sim NNNNrrCCCCNN(\mu\mu_{\alpha\alpha}, \sigma\sigma_{\alpha\alpha})$$

$$\boldsymbol{\beta\beta}_{iiii} \sim NNNNrrCCCCNN(\boldsymbol{\mu\mu}_{\boldsymbol{\beta\beta}}, \boldsymbol{\sigma\sigma}_{\boldsymbol{\beta\beta}})$$

Where $\alpha\alpha_{ii}$ is the species j intercept for the hazard rate function and $\boldsymbol{\beta\beta}_{\boldsymbol{iiii}}$ is a vector of parameters that describe relationships to a vector of covariates (**X**). Information can be shared among taxonomic groups can be shared in both the intercept and slope parameter estimates and facilitates estimation of detection probabilities even in species with small sample sizes. These data are used to calculate the detection probability for each distance band, which are then summed to estimate the detection probability for the entire survey. In this case, we do not use additional covariates to explain detection probability, and the description is present to describe future possibilities.

Finally, group size estimates are also known to be influenced by detection probability. Groups farther away from the boat tend to be underestimated, particularly if the species spends time underwater. To estimate this effect, we use a linear model:

$$\log(MM_i) = \beta\beta_0 + \beta\beta_{ppppppppp}pp_{ii}$$

Where $MM_{\bar{ii}}$ is the average detection-corrected group size for transect i and the $\beta\beta$ parameters are either the intercept or the slope of the linear equation. However, like the detection functions, we use a shrinkage effect to share data among taxa groups:

$$\log(\text{MM}_{ii}) = \beta\beta_{0ii} + \beta\beta_{\text{ppppppppp},ii}\text{pp}_{ii}$$

$$\beta\beta_{0ii} \sim NNNNrrCCCC\mathbb{N}(\mu\mu_{gggg0}, \sigma\sigma_{gggg0})$$

$$\beta\beta_{\text{ppppppppp},ii} \sim NNNNrrCCCC\mathbb{N}(\mu\mu_{gggg1}, \sigma\sigma_{gggg1})$$

We are now sharing information on the intercept and slope parameters across j species using the two $\mu\mu$ and $\sigma\sigma$ parameters. The mean group size when detection probability is one is estimated by adding $\beta\beta_0$ and $\beta\beta_{\text{ppppppppp}}$ for each species.

Once the survey specific detection probability is estimated for each taxonomic group, then a Horvitz-Thompson estimator is used to calculate the total population size for each species on each survey:

$$= \quad \quad$$

Where, pp_{kkii} is the estimated total population size for survey *k* and species *j*, pp_{kkii} is the detection probability, and $MM_{\bar{kk}\,ii}$ is the average detection-corrected group size for survey *k* and species *j*. The ratio the total study area (A) over the surveyed area (a) scales the estimate to the total study area. Note that if no individuals are found on the survey, then this estimator cannot provide non-zero estimates of $pp?_{kkii}$. Density estimates were obtained by dividing pp?_{kkii} by the study area (km^2).

Both half-normal and hazard detection functions were tested on the survey data. Additionally, observation data were filtered based on flight height. Initial model criticism suggested that flying birds were frequently detected 0 m (0 ft) from the transect line, which indicated that assumptions of distance sampling were violated (i.e., that animals were observed when first detected and randomly within the survey area). Therefore, we decided to analyze data from animals 25 m (82 ft) above sea level or lower to limit the issues associated with large numbers of birds detected on the transect line. Model fit was assessed using visual comparison of the detection curve and empirical data.

7.3. Results and Discussion

Model fit was variable across species using a hazard detection function. Some species showed reasonable fit (terns or gannets; Figure 7-1 and Figure 7-2), while others did not (loons; Figure 7-3). The group size model did not indicate that group size was strongly influenced by detection probability for any species.

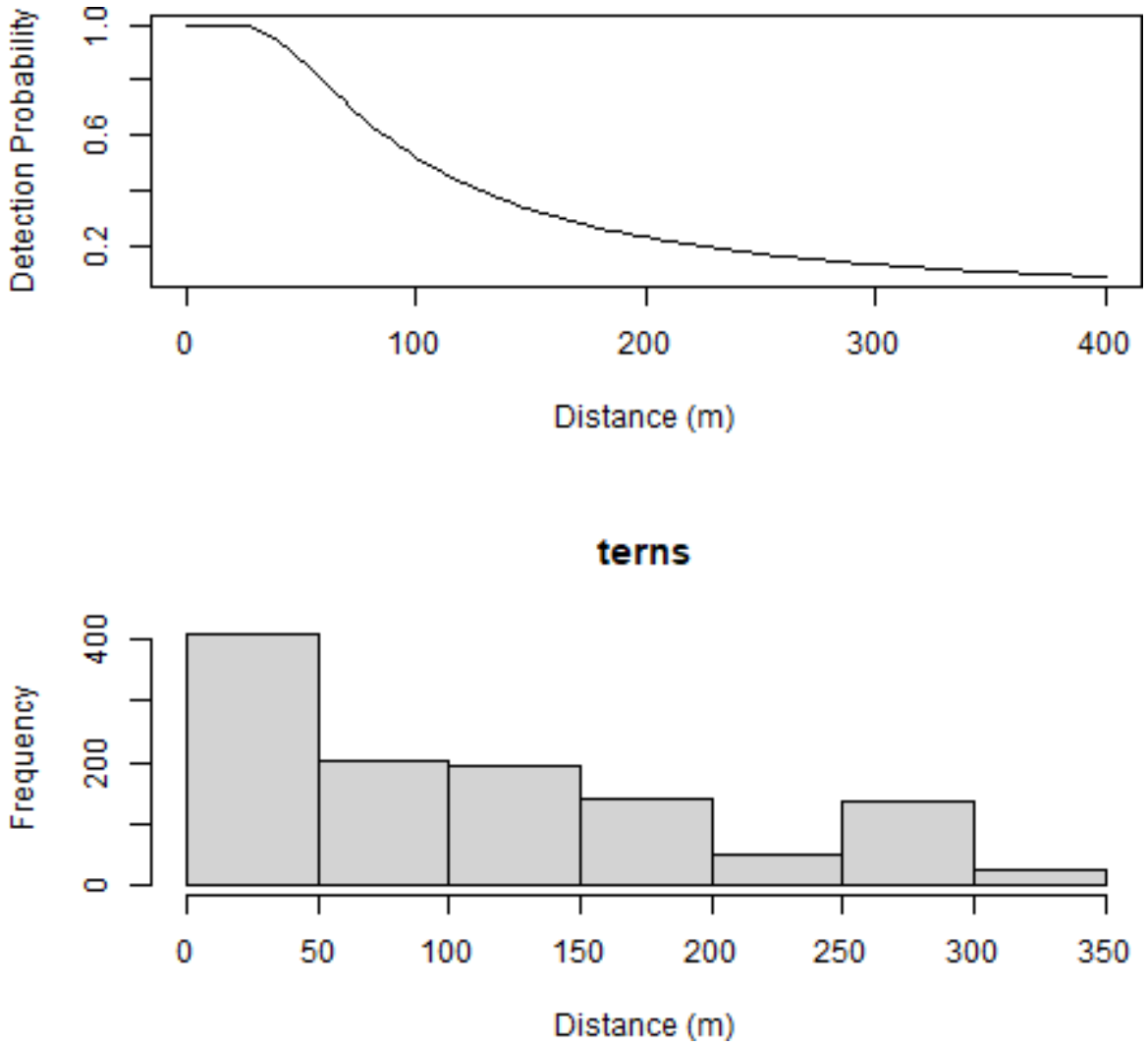

NOTE: Only birds 25 m (82 ft) or less from the ocean's surface were used in this analysis.

Figure 7-1: Detection curve estimated using a hazard function from a community distance sampling model (top) and a histogram of detection distances (bottom) for all tern species.

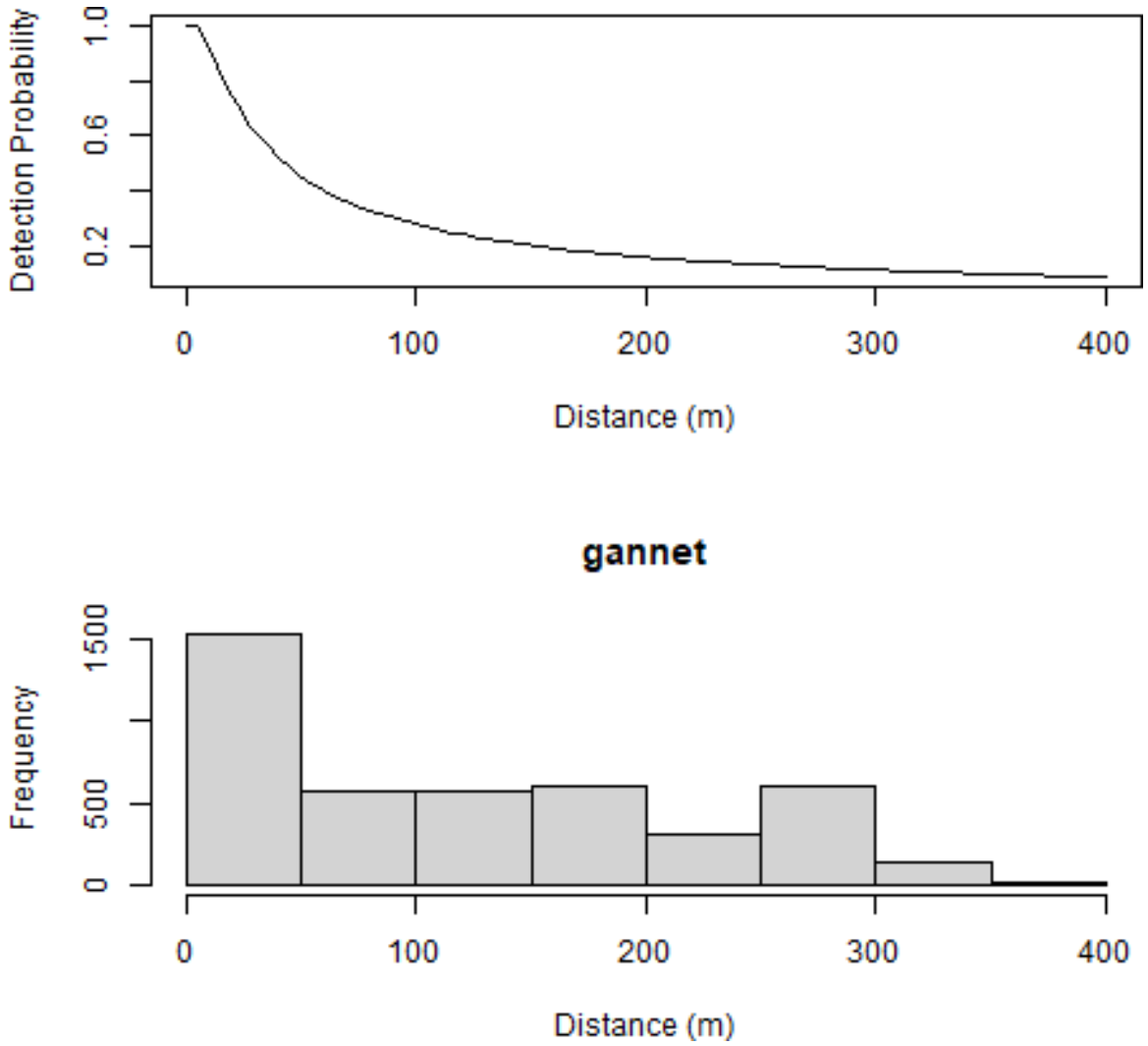

NOTE: Only birds 25 m (82 ft) or less from the ocean's surface were used in this analysis.

Figure 7-2: Detection curve estimated using a hazard function from a community distance sampling model (top) and a histogram of detection distances (bottom) for northern gannets.

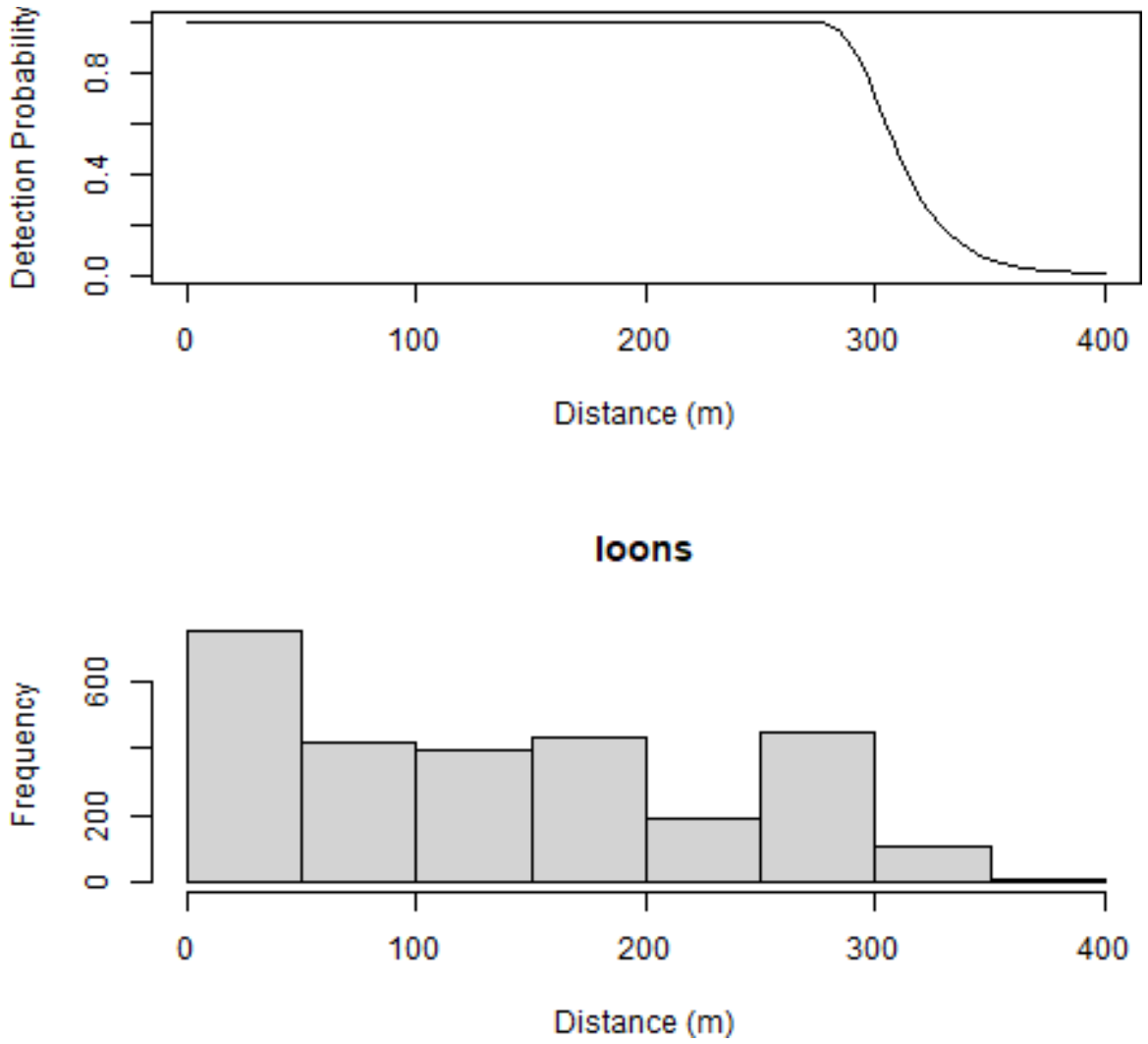

NOTE: Only birds 25 m (82 ft) or less from the ocean's surface were used in this analysis.

Figure 7-3: Detection curve estimated using a hazard function from a community distance sampling model (top) and a histogram of detection distances (bottom) for the two loon species.

Note with these examples the significant drop in detections between the 0-50-m (0-164-ft) range and the 50-100-m (164-328-ft) range. Many species showed evidence of a large number of detections on the transect line. Additionally, there is often a spike in detections from 250-300 m (820-984 ft), which could indicate observers were underestimating the distance of the first detection to include the species in the survey area (0–300 m [0–984 ft]).

The half-normal model did not appear to fit these data well, as most species show rapid detection declines at some point in the detection curve. As such, we are not describing those results here. But the issues with this endeavor do not lie with model fit specifically, the model results also appeared to suggest that there are issues with these data. We found that detection probabilities varied significantly by species and that species that often are easy to detect (e.g., northern gannets) were challenging in this survey (Table 7-1). They were the second most difficult to detect taxonomic group, even more than smaller birds like terns, gulls, and sea ducks. Outside of gannets, the loon model also appeared to produce nonsensical results, with nearly 100% of loons detected within the 300-m (984-ft) survey strip. This outcome is extremely unlikely and these results do not make sense given what we know about these species in this region.

Table 7-1: Estimates of detection probability for each taxonomic group tested using a hazard detection function from a community distance sampling model.

NOTE: Detection probability is estimated over a 300-m (984-ft) strip transect.

Taxonomic Group	Detection Probability
Shearwaters and petrels	0.62
Gulls	0.47
Northern Gannet	0.29
Terns	0.45
Loons	0.99
Sea ducks	0.35
Dabblers, geese, and swans	0.23
Shorebirds	0.20
Cormorants and pelicans	0.62
Auks	0.28

Taken together, these results indicate that there is an issue with the distance sampling protocols employed. It is likely that animals are not detected immediately upon entry into the study area, or there is bias in the observers' distance estimates. Further, it seems likely that some animals are attracted to the boat and likely biasing the distance estimates low. In sum, we suspect there are some significant issues with these data that make distance sampling models challenging to fit and the values that come from them possibly spurious. As such, we chose not to use these estimates of detection probability to correct the densities of seabirds in the study area.

7.4. Conclusions

While model convergence was adequate, and this modeling approach often fitted reasonable detection curves for these species groups, there are several reasons why we do not think that these results are useful for correcting density estimates. Our past experience with boat surveys suggests that Northern Gannets are one of the easiest to detect species in the region. Their large white bodies are notable in the air and on the water from a significant distance. Moreover, other issues with the data lead to equally unlikely models where detection probability was nearly perfect for 300 m (984 ft) for loons. Our experience with these types of data suggests that both of these outcomes are extremely unlikely. With additional time, some of these issues might be addressed to correct some of these issues, but the current state of the analysis is concerning enough for us to avoid using them at the moment.

These issues in data collection, paired with the knowledge that these data are almost 15 years out of date, we think that results from this model are not worth inclusion in the risk analysis. While there are also issues with using uncorrected density estimates from boat surveys with known distance biases, the most parsimonious solution is to use the uncorrected density estimates as this action involves the fewest number of assumptions. Future work should consider collecting more survey data from this area to update our understanding of regional seabird density patterns.

8. Birds – Offshore: Seasonal Maps

Table of Maps

Map 1. NJDEP baseline seasonal survey effort. Survey effort totaled within each full or partial lease block inside and outside the Atlantic Shores Lease Area OCS-A 0549. 18
Map 2. Atlantic Shores digital aerial seasonal survey effort. Survey effort totaled within each full or partial lease block inside and outside the Atlantic Shores Lease Area OCS-A 0549. 19
Map 3. Spring Common Eider modeled density proportions in the Atlantic Shores seasonal digital aerial surveys (A), density proportions in the NJDEP baseline survey data (B), and the MDAT model outputs at local and regional scales (C). The scale for all maps is representative of relative spatial variation in the sites within the season for each information source. 20
Map 4. Summer Common Eider modeled density proportions in the Atlantic Shores seasonal digital aerial surveys (A), density proportions in the NJDEP baseline survey data (B), and the MDAT model outputs at local and regional scales (C). The scale for all maps is representative of relative spatial variation in the sites within the season for each information source. 21
Map 5. Fall Common Eider modeled density proportions in the Atlantic Shores seasonal digital aerial surveys (A), density proportions in the NJDEP baseline survey data (B), and the MDAT model outputs at local and regional scales (C). The scale for all maps is representative of relative spatial variation in the sites within the season for each information source. 22
Map 6. Winter Common Eider modeled density proportions in the Atlantic Shores seasonal digital aerial surveys (A), density proportions in the NJDEP baseline survey data (B), and the MDAT model outputs at local and regional scales (C). The scale for all maps is representative of relative spatial variation in the sites within the season for each information source. 23
Map 7. Spring Surf Scoter modeled density proportions in the Atlantic Shores seasonal digital aerial surveys (A), density proportions in the NJDEP baseline survey data (B), and the MDAT model outputs at local and regional scales (C). The scale for all maps is representative of relative spatial variation in the sites within the season for each information source. 24
Map 8. Fall Surf Scoter modeled density proportions in the Atlantic Shores seasonal digital aerial surveys (A), density proportions in the NJDEP baseline survey data (B), and the MDAT model outputs at local and regional scales (C). The scale for all maps is representative of relative spatial variation in the sites within the season for each information source. 25
Map 9. Winter Surf Scoter modeled density proportions in the Atlantic Shores seasonal digital aerial surveys (A), density proportions in the NJDEP baseline survey data (B), and the MDAT model outputs at local and regional scales (C). The scale for all maps is representative of relative spatial variation in the sites within the season for each information source. 26
Map 10. Spring White-winged Scoter modeled density proportions in the Atlantic Shores seasonal digital aerial surveys (A), density proportions in the NJDEP baseline survey data (B), and the MDAT model outputs at local and regional scales (C). The scale for all maps is representative of relative spatial variation in the sites within the season for each information source. 27
Map 11. Fall White-winged Scoter modeled density proportions in the Atlantic Shores seasonal digital aerial surveys (A), density proportions in the NJDEP baseline survey data (B), and the MDAT model outputs at local and regional scales (C). The scale for all maps is representative of relative spatial variation in the sites within the season for each information source. 28

Map 12. Winter White-winged Scoter modeled density proportions in the Atlantic Shores seasonal digital aerial surveys (A), density proportions in the NJDEP baseline survey data (B), and the MDAT model outputs at local and regional scales (C). The scale for all maps is representative of relative spatial variation in the sites within the season for each information source. 29
Map 13. Spring Black Scoter modeled density proportions in the Atlantic Shores seasonal digital aerial surveys (A), density proportions in the NJDEP baseline survey data (B), and the MDAT model outputs at local and regional scales (C). The scale for all maps is representative of relative spatial variation in the sites within the season for each information source. 30
Map 14. Fall Black Scoter modeled density proportions in the Atlantic Shores seasonal digital aerial surveys (A), density proportions in the NJDEP baseline survey data (B), and the MDAT model outputs at local and regional scales (C). The scale for all maps is representative of relative spatial variation in the sites within the season for each information source. 31
Map 15. Winter Black Scoter modeled density proportions in the Atlantic Shores seasonal digital aerial surveys (A), density proportions in the NJDEP baseline survey data (B), and the MDAT model outputs at local and regional scales (C). The scale for all maps is representative of relative spatial variation in the sites within the season for each information source. 32
Map 16. Spring Long-tailed Duck modeled density proportions in the Atlantic Shores seasonal digital aerial surveys (A), density proportions in the NJDEP baseline survey data (B), and the MDAT model outputs at local and regional scales (C). The scale for all maps is representative of relative spatial variation in the sites within the season for each information source. 33
Map 17. Fall Long-tailed Duck modeled density proportions in the Atlantic Shores seasonal digital aerial surveys (A), density proportions in the NJDEP baseline survey data (B), and the MDAT model outputs at local and regional scales (C). The scale for all maps is representative of relative spatial variation in the sites within the season for each information source. 34
Map 18. Winter Long-tailed Duck modeled density proportions in the Atlantic Shores seasonal digital aerial surveys (A), density proportions in the NJDEP baseline survey data (B), and the MDAT model outputs at local and regional scales (C). The scale for all maps is representative of relative spatial variation in the sites within the season for each information source. 35
Map 19. Spring Red-breasted Merganser modeled density proportions in the Atlantic Shores seasonal digital aerial surveys (A), density proportions in the NJDEP baseline survey data (B), and the MDAT model outputs at local and regional scales (C). The scale for all maps is representative of relative spatial variation in the sites within the season for each information source. 36
Map 20. Fall Red-breasted Merganser modeled density proportions in the Atlantic Shores seasonal digital aerial surveys (A), density proportions in the NJDEP baseline survey data (B), and the MDAT model outputs at local and regional scales (C). The scale for all maps is representative of relative spatial variation in the sites within the season for each information source. 37
Map 21. Winter Red-breasted Merganser modeled density proportions in the Atlantic Shores seasonal digital aerial surveys (A), density proportions in the NJDEP baseline survey data (B), and the MDAT model outputs at local and regional scales (C). The scale for all maps is representative of relative spatial variation in the sites within the season for each information source. 38
Map 22. Spring Red-throated Loon modeled density proportions in the Atlantic Shores seasonal digital aerial surveys (A), density proportions in the NJDEP baseline survey data (B), and the MDAT model

outputs at local and regional scales (C). The scale for all maps is representative of relative spatial variation in the sites within the season for each information source. 39
Map 23. Fall Red-throated Loon modeled density proportions in the Atlantic Shores seasonal digital aerial surveys (A), density proportions in the NJDEP baseline survey data (B), and the MDAT model outputs at local and regional scales (C). The scale for all maps is representative of relative spatial variation in the sites within the season for each information source. 40
Map 24. Winter Red-throated Loon modeled density proportions in the Atlantic Shores seasonal digital aerial surveys (A), density proportions in the NJDEP baseline survey data (B), and the MDAT model outputs at local and regional scales (C). The scale for all maps is representative of relative spatial variation in the sites within the season for each information source. 41
Map 25. Spring Common Loon modeled density proportions in the Atlantic Shores seasonal digital aerial surveys (A), density proportions in the NJDEP baseline survey data (B), and the MDAT model outputs at local and regional scales (C). The scale for all maps is representative of relative spatial variation in the sites within the season for each information source. 42
Map 26. Summer Common Loon modeled density proportions in the Atlantic Shores seasonal digital aerial surveys (A), density proportions in the NJDEP baseline survey data (B), and the MDAT model outputs at local and regional scales (C). The scale for all maps is representative of relative spatial variation in the sites within the season for each information source. 43
Map 27. Fall Common Loon modeled density proportions in the Atlantic Shores seasonal digital aerial surveys (A), density proportions in the NJDEP baseline survey data (B), and the MDAT model outputs at local and regional scales (C). The scale for all maps is representative of relative spatial variation in the sites within the season for each information source. 44
Map 28. Winter Common Loon modeled density proportions in the Atlantic Shores seasonal digital aerial surveys (A), density proportions in the NJDEP baseline survey data (B), and the MDAT model outputs at local and regional scales (C). The scale for all maps is representative of relative spatial variation in the sites within the season for each information source. 45
Map 29. Spring Horned Grebe modeled density proportions in the Atlantic Shores seasonal digital aerial surveys (A), density proportions in the NJDEP baseline survey data (B), and the MDAT model outputs at local and regional scales (C). The scale for all maps is representative of relative spatial variation in the sites within the season for each information source. 46
Map 30. Fall Horned Grebe modeled density proportions in the Atlantic Shores seasonal digital aerial surveys (A), density proportions in the NJDEP baseline survey data (B), and the MDAT model outputs at local and regional scales (C). The scale for all maps is representative of relative spatial variation in the sites within the season for each information source. 47
Map 31. Winter Horned Grebe modeled density proportions in the Atlantic Shores seasonal digital aerial surveys (A), density proportions in the NJDEP baseline survey data (B), and the MDAT model outputs at local and regional scales (C). The scale for all maps is representative of relative spatial variation in the sites within the season for each information source. 48
Map 32. Spring Red-necked Grebe modeled density proportions in the Atlantic Shores seasonal digital aerial surveys (A), density proportions in the NJDEP baseline survey data (B), and the MDAT model outputs at local and regional scales (C). The scale for all maps is representative of relative spatial variation in the sites within the season for each information source. 49

Map 33. Fall Red-necked Grebe modeled density proportions in the Atlantic Shores seasonal digital aerial surveys (A), density proportions in the NJDEP baseline survey data (B), and the MDAT model outputs at local and regional scales (C). The scale for all maps is representative of relative spatial variation in the sites within the season for each information source. 50
Map 34. Winter Red-necked Grebe modeled density proportions in the Atlantic Shores seasonal digital aerial surveys (A), density proportions in the NJDEP baseline survey data (B), and the MDAT model outputs at local and regional scales (C). The scale for all maps is representative of relative spatial variation in the sites within the season for each information source. 51
Map 35. Spring Wilson's Storm-Petrel modeled density proportions in the Atlantic Shores seasonal digital aerial surveys (A), density proportions in the NJDEP baseline survey data (B), and the MDAT model outputs at local and regional scales (C). The scale for all maps is representative of relative spatial variation in the sites within the season for each information source. 52
Map 36. Summer Wilson's Storm-Petrel modeled density proportions in the Atlantic Shores seasonal digital aerial surveys (A), density proportions in the NJDEP baseline survey data (B), and the MDAT model outputs at local and regional scales (C). The scale for all maps is representative of relative spatial variation in the sites within the season for each information source. 53
Map 37. Fall Wilson's Storm-Petrel modeled density proportions in the Atlantic Shores seasonal digital aerial surveys (A), density proportions in the NJDEP baseline survey data (B), and the MDAT model outputs at local and regional scales (C). The scale for all maps is representative of relative spatial variation in the sites within the season for each information source. 54
Map 38. Winter Wilson's Storm-Petrel modeled density proportions in the Atlantic Shores seasonal digital aerial surveys (A), density proportions in the NJDEP baseline survey data (B), and the MDAT model outputs at local and regional scales (C). The scale for all maps is representative of relative spatial variation in the sites within the season for each information source. 55
Map 39. Spring Leach's Storm-Petrel modeled density proportions in the Atlantic Shores seasonal digital aerial surveys (A), density proportions in the NJDEP baseline survey data (B), and the MDAT model outputs at local and regional scales (C). The scale for all maps is representative of relative spatial variation in the sites within the season for each information source. 56
Map 40. Summer Leach's Storm-Petrel modeled density proportions in the Atlantic Shores seasonal digital aerial surveys (A), density proportions in the NJDEP baseline survey data (B), and the MDAT model outputs at local and regional scales (C). The scale for all maps is representative of relative spatial variation in the sites within the season for each information source. 57
Map 41. Fall Leach's Storm-Petrel modeled density proportions in the Atlantic Shores seasonal digital aerial surveys (A), density proportions in the NJDEP baseline survey data (B), and the MDAT model outputs at local and regional scales (C). The scale for all maps is representative of relative spatial variation in the sites within the season for each information source. 58
Map 42. Winter Leach's Storm-Petrel modeled density proportions in the Atlantic Shores seasonal digital aerial surveys (A), density proportions in the NJDEP baseline survey data (B), and the MDAT model outputs at local and regional scales (C). The scale for all maps is representative of relative spatial variation in the sites within the season for each information source. 59
Map 43. Spring Northern Fulmar modeled density proportions in the Atlantic Shores seasonal digital aerial surveys (A), density proportions in the NJDEP baseline survey data (B), and the MDAT model

outputs at local and regional scales (C). The scale for all maps is representative of relative spatial variation in the sites within the season for each information source. 60
Map 44. Summer Northern Fulmar modeled density proportions in the Atlantic Shores seasonal digital aerial surveys (A), density proportions in the NJDEP baseline survey data (B), and the MDAT model outputs at local and regional scales (C). The scale for all maps is representative of relative spatial variation in the sites within the season for each information source. 61
Map 45. Fall Northern Fulmar modeled density proportions in the Atlantic Shores seasonal digital aerial surveys (A), density proportions in the NJDEP baseline survey data (B), and the MDAT model outputs at local and regional scales (C). The scale for all maps is representative of relative spatial variation in the sites within the season for each information source. 62
Map 46. Winter Northern Fulmar modeled density proportions in the Atlantic Shores seasonal digital aerial surveys (A), density proportions in the NJDEP baseline survey data (B), and the MDAT model outputs at local and regional scales (C). The scale for all maps is representative of relative spatial variation in the sites within the season for each information source. 63
Map 47. Spring Cory's Shearwater modeled density proportions in the Atlantic Shores seasonal digital aerial surveys (A), density proportions in the NJDEP baseline survey data (B), and the MDAT model outputs at local and regional scales (C). The scale for all maps is representative of relative spatial variation in the sites within the season for each information source. 64
Map 48. Summer Cory's Shearwater modeled density proportions in the Atlantic Shores seasonal digital aerial surveys (A), density proportions in the NJDEP baseline survey data (B), and the MDAT model outputs at local and regional scales (C). The scale for all maps is representative of relative spatial variation in the sites within the season for each information source. 65
Map 49. Fall Cory's Shearwater modeled density proportions in the Atlantic Shores seasonal digital aerial surveys (A), density proportions in the NJDEP baseline survey data (B), and the MDAT model outputs at local and regional scales (C). The scale for all maps is representative of relative spatial variation in the sites within the season for each information source. 66
Map 50. Winter Cory's Shearwater modeled density proportions in the Atlantic Shores seasonal digital aerial surveys (A), density proportions in the NJDEP baseline survey data (B), and the MDAT model outputs at local and regional scales (C). The scale for all maps is representative of relative spatial variation in the sites within the season for each information source. 67
Map 51. Spring Sooty Shearwater modeled density proportions in the Atlantic Shores seasonal digital aerial surveys (A), density proportions in the NJDEP baseline survey data (B), and the MDAT model outputs at local and regional scales (C). The scale for all maps is representative of relative spatial variation in the sites within the season for each information source. 68
Map 52. Summer Sooty Shearwater modeled density proportions in the Atlantic Shores seasonal digital aerial surveys (A), density proportions in the NJDEP baseline survey data (B), and the MDAT model outputs at local and regional scales (C). The scale for all maps is representative of relative spatial variation in the sites within the season for each information source. 69
Map 53. Fall Sooty Shearwater modeled density proportions in the Atlantic Shores seasonal digital aerial surveys (A), density proportions in the NJDEP baseline survey data (B), and the MDAT model outputs at local and regional scales (C). The scale for all maps is representative of relative spatial variation in the sites within the season for each information source. 70

Map 54. Winter Sooty Shearwater modeled density proportions in the Atlantic Shores seasonal digital aerial surveys (A), density proportions in the NJDEP baseline survey data (B), and the MDAT model outputs at local and regional scales (C). The scale for all maps is representative of relative spatial variation in the sites within the season for each information source. 71
Map 55. Spring Great Shearwater modeled density proportions in the Atlantic Shores seasonal digital aerial surveys (A), density proportions in the NJDEP baseline survey data (B), and the MDAT model outputs at local and regional scales (C). The scale for all maps is representative of relative spatial variation in the sites within the season for each information source. 72
Map 56. Summer Great Shearwater modeled density proportions in the Atlantic Shores seasonal digital aerial surveys (A), density proportions in the NJDEP baseline survey data (B), and the MDAT model outputs at local and regional scales (C). The scale for all maps is representative of relative spatial variation in the sites within the season for each information source. 73
Map 57. Fall Great Shearwater modeled density proportions in the Atlantic Shores seasonal digital aerial surveys (A), density proportions in the NJDEP baseline survey data (B), and the MDAT model outputs at local and regional scales (C). The scale for all maps is representative of relative spatial variation in the sites within the season for each information source. 74
Map 58. Winter Great Shearwater modeled density proportions in the Atlantic Shores seasonal digital aerial surveys (A), density proportions in the NJDEP baseline survey data (B), and the MDAT model outputs at local and regional scales (C). The scale for all maps is representative of relative spatial variation in the sites within the season for each information source. 75
Map 59. Spring Manx Shearwater modeled density proportions in the Atlantic Shores seasonal digital aerial surveys (A), density proportions in the NJDEP baseline survey data (B), and the MDAT model outputs at local and regional scales (C). The scale for all maps is representative of relative spatial variation in the sites within the season for each information source. 76
Map 60. Summer Manx Shearwater modeled density proportions in the Atlantic Shores seasonal digital aerial surveys (A), density proportions in the NJDEP baseline survey data (B), and the MDAT model outputs at local and regional scales (C). The scale for all maps is representative of relative spatial variation in the sites within the season for each information source. 77
Map 61. Fall Manx Shearwater modeled density proportions in the Atlantic Shores seasonal digital aerial surveys (A), density proportions in the NJDEP baseline survey data (B), and the MDAT model outputs at local and regional scales (C). The scale for all maps is representative of relative spatial variation in the sites within the season for each information source. 78
Map 62. Winter Manx Shearwater modeled density proportions in the Atlantic Shores seasonal digital aerial surveys (A), density proportions in the NJDEP baseline survey data (B), and the MDAT model outputs at local and regional scales (C). The scale for all maps is representative of relative spatial variation in the sites within the season for each information source. 79
Map 63. Spring Audubon's Shearwater modeled density proportions in the Atlantic Shores seasonal digital aerial surveys (A), density proportions in the NJDEP baseline survey data (B), and the MDAT model outputs at local and regional scales (C). The scale for all maps is representative of relative spatial variation in the sites within the season for each information source. 80
Map 64. Summer Audubon's Shearwater modeled density proportions in the Atlantic Shores seasonal digital aerial surveys (A), density proportions in the NJDEP baseline survey data (B), and the MDAT

model outputs at local and regional scales (C). The scale for all maps is representative of relative spatial variation in the sites within the season for each information source. 81
Map 65. Fall Audubon's Shearwater modeled density proportions in the Atlantic Shores seasonal digital aerial surveys (A), density proportions in the NJDEP baseline survey data (B), and the MDAT model outputs at local and regional scales (C). The scale for all maps is representative of relative spatial variation in the sites within the season for each information source. 82
Map 66. Winter Audubon's Shearwater modeled density proportions in the Atlantic Shores seasonal digital aerial surveys (A), density proportions in the NJDEP baseline survey data (B), and the MDAT model outputs at local and regional scales (C). The scale for all maps is representative of relative spatial variation in the sites within the season for each information source. 83
Map 67. Spring Northern Gannet modeled density proportions in the Atlantic Shores seasonal digital aerial surveys (A), density proportions in the NJDEP baseline survey data (B), and the MDAT model outputs at local and regional scales (C). The scale for all maps is representative of relative spatial variation in the sites within the season for each information source. 84
Map 68. Summer Northern Gannet modeled density proportions in the Atlantic Shores seasonal digital aerial surveys (A), density proportions in the NJDEP baseline survey data (B), and the MDAT model outputs at local and regional scales (C). The scale for all maps is representative of relative spatial variation in the sites within the season for each information source. 85
Map 69. Fall Northern Gannet modeled density proportions in the Atlantic Shores seasonal digital aerial surveys (A), density proportions in the NJDEP baseline survey data (B), and the MDAT model outputs at local and regional scales (C). The scale for all maps is representative of relative spatial variation in the sites within the season for each information source. 86
Map 70. Winter Northern Gannet modeled density proportions in the Atlantic Shores seasonal digital aerial surveys (A), density proportions in the NJDEP baseline survey data (B), and the MDAT model outputs at local and regional scales (C). The scale for all maps is representative of relative spatial variation in the sites within the season for each information source. 87
Map 71. Spring Double-crested Cormorant modeled density proportions in the Atlantic Shores seasonal digital aerial surveys (A), density proportions in the NJDEP baseline survey data (B), and the MDAT model outputs at local and regional scales (C). The scale for all maps is representative of relative spatial variation in the sites within the season for each information source. 88
Map 72. Summer Double-crested Cormorant modeled density proportions in the Atlantic Shores seasonal digital aerial surveys (A), density proportions in the NJDEP baseline survey data (B), and the MDAT model outputs at local and regional scales (C). The scale for all maps is representative of relative spatial variation in the sites within the season for each information source. 89
Map 73. Fall Double-crested Cormorant modeled density proportions in the Atlantic Shores seasonal digital aerial surveys (A), density proportions in the NJDEP baseline survey data (B), and the MDAT model outputs at local and regional scales (C). The scale for all maps is representative of relative spatial variation in the sites within the season for each information source. 90
Map 74. Winter Double-crested Cormorant modeled density proportions in the Atlantic Shores seasonal digital aerial surveys (A), density proportions in the NJDEP baseline survey data (B), and the MDAT model outputs at local and regional scales (C). The scale for all maps is representative of relative spatial variation in the sites within the season for each information source. 91

Map 75. Spring Great Cormorant modeled density proportions in the Atlantic Shores seasonal digital aerial surveys (A), density proportions in the NJDEP baseline survey data (B), and the MDAT model outputs at local and regional scales (C). The scale for all maps is representative of relative spatial variation in the sites within the season for each information source. 92
Map 76. Fall Great Cormorant modeled density proportions in the Atlantic Shores seasonal digital aerial surveys (A), density proportions in the NJDEP baseline survey data (B), and the MDAT model outputs at local and regional scales (C). The scale for all maps is representative of relative spatial variation in the sites within the season for each information source. 93
Map 77. Winter Great Cormorant modeled density proportions in the Atlantic Shores seasonal digital aerial surveys (A), density proportions in the NJDEP baseline survey data (B), and the MDAT model outputs at local and regional scales (C). The scale for all maps is representative of relative spatial variation in the sites within the season for each information source. 94
Map 78. Spring Brown Pelican modeled density proportions in the Atlantic Shores seasonal digital aerial surveys (A), density proportions in the NJDEP baseline survey data (B), and the MDAT model outputs at local and regional scales (C). The scale for all maps is representative of relative spatial variation in the sites within the season for each information source. 95
Map 79. Summer Brown Pelican modeled density proportions in the Atlantic Shores seasonal digital aerial surveys (A), density proportions in the NJDEP baseline survey data (B), and the MDAT model outputs at local and regional scales (C). The scale for all maps is representative of relative spatial variation in the sites within the season for each information source. 96
Map 80. Fall Brown Pelican modeled density proportions in the Atlantic Shores seasonal digital aerial surveys (A), density proportions in the NJDEP baseline survey data (B), and the MDAT model outputs at local and regional scales (C). The scale for all maps is representative of relative spatial variation in the sites within the season for each information source. 97
Map 81. Winter Brown Pelican modeled density proportions in the Atlantic Shores seasonal digital aerial surveys (A), density proportions in the NJDEP baseline survey data (B), and the MDAT model outputs at local and regional scales (C). The scale for all maps is representative of relative spatial variation in the sites within the season for each information source. 98
Map 82. Spring Pomarine Jaeger modeled density proportions in the Atlantic Shores seasonal digital aerial surveys (A), density proportions in the NJDEP baseline survey data (B), and the MDAT model outputs at local and regional scales (C). The scale for all maps is representative of relative spatial variation in the sites within the season for each information source. 99
Map 83. Summer Pomarine Jaeger modeled density proportions in the Atlantic Shores seasonal digital aerial surveys (A), density proportions in the NJDEP baseline survey data (B), and the MDAT model outputs at local and regional scales (C). The scale for all maps is representative of relative spatial variation in the sites within the season for each information source. 100
Map 84. Fall Pomarine Jaeger modeled density proportions in the Atlantic Shores seasonal digital aerial surveys (A), density proportions in the NJDEP baseline survey data (B), and the MDAT model outputs at local and regional scales (C). The scale for all maps is representative of relative spatial variation in the sites within the season for each information source. 101
Map 85. Winter Pomarine Jaeger modeled density proportions in the Atlantic Shores seasonal digital aerial surveys (A), density proportions in the NJDEP baseline survey data (B), and the MDAT model

outputs at local and regional scales (C). The scale for all maps is representative of relative spatial variation in the sites within the season for each information source. 102
Map 86. Spring Parasitic Jaeger modeled density proportions in the Atlantic Shores seasonal digital aerial surveys (A), density proportions in the NJDEP baseline survey data (B), and the MDAT model outputs at local and regional scales (C). The scale for all maps is representative of relative spatial variation in the sites within the season for each information source. 103
Map 87. Summer Parasitic Jaeger modeled density proportions in the Atlantic Shores seasonal digital aerial surveys (A), density proportions in the NJDEP baseline survey data (B), and the MDAT model outputs at local and regional scales (C). The scale for all maps is representative of relative spatial variation in the sites within the season for each information source. 104
Map 88. Fall Parasitic Jaeger modeled density proportions in the Atlantic Shores seasonal digital aerial surveys (A), density proportions in the NJDEP baseline survey data (B), and the MDAT model outputs at local and regional scales (C). The scale for all maps is representative of relative spatial variation in the sites within the season for each information source. 105
Map 89. Winter Parasitic Jaeger modeled density proportions in the Atlantic Shores seasonal digital aerial surveys (A), density proportions in the NJDEP baseline survey data (B), and the MDAT model outputs at local and regional scales (C). The scale for all maps is representative of relative spatial variation in the sites within the season for each information source. 106
Map 90. Spring Black-legged Kittiwake modeled density proportions in the Atlantic Shores seasonal digital aerial surveys (A), density proportions in the NJDEP baseline survey data (B), and the MDAT model outputs at local and regional scales (C). The scale for all maps is representative of relative spatial variation in the sites within the season for each information source. 107
Map 91. Fall Black-legged Kittiwake modeled density proportions in the Atlantic Shores seasonal digital aerial surveys (A), density proportions in the NJDEP baseline survey data (B), and the MDAT model outputs at local and regional scales (C). The scale for all maps is representative of relative spatial variation in the sites within the season for each information source. 108
Map 92. Winter Black-legged Kittiwake modeled density proportions in the Atlantic Shores seasonal digital aerial surveys (A), density proportions in the NJDEP baseline survey data (B), and the MDAT model outputs at local and regional scales (C). The scale for all maps is representative of relative spatial variation in the sites within the season for each information source. 109
Map 93. Spring Sabine's Gull modeled density proportions in the Atlantic Shores seasonal digital aerial surveys (A), density proportions in the NJDEP baseline survey data (B), and the MDAT model outputs at local and regional scales (C). The scale for all maps is representative of relative spatial variation in the sites within the season for each information source. 110
Map 94. Summer Sabine's Gull modeled density proportions in the Atlantic Shores seasonal digital aerial surveys (A), density proportions in the NJDEP baseline survey data (B), and the MDAT model outputs at local and regional scales (C). The scale for all maps is representative of relative spatial variation in the sites within the season for each information source. 111
Map 95. Fall Sabine's Gull modeled density proportions in the Atlantic Shores seasonal digital aerial surveys (A), density proportions in the NJDEP baseline survey data (B), and the MDAT model outputs at local and regional scales (C). The scale for all maps is representative of relative spatial variation in the sites within the season for each information source. 112

Map 96. Winter Sabine's Gull modeled density proportions in the Atlantic Shores seasonal digital aerial surveys (A), density proportions in the NJDEP baseline survey data (B), and the MDAT model outputs at local and regional scales (C). The scale for all maps is representative of relative spatial variation in the sites within the season for each information source. 113
Map 97. Spring Bonaparte's Gull modeled density proportions in the Atlantic Shores seasonal digital aerial surveys (A), density proportions in the NJDEP baseline survey data (B), and the MDAT model outputs at local and regional scales (C). The scale for all maps is representative of relative spatial variation in the sites within the season for each information source. 114
Map 98. Fall Bonaparte's Gull modeled density proportions in the Atlantic Shores seasonal digital aerial surveys (A), density proportions in the NJDEP baseline survey data (B), and the MDAT model outputs at local and regional scales (C). The scale for all maps is representative of relative spatial variation in the sites within the season for each information source. 115
Map 99. Winter Bonaparte's Gull modeled density proportions in the Atlantic Shores seasonal digital aerial surveys (A), density proportions in the NJDEP baseline survey data (B), and the MDAT model outputs at local and regional scales (C). The scale for all maps is representative of relative spatial variation in the sites within the season for each information source. 116
Map 100. Spring Little Gull modeled density proportions in the Atlantic Shores seasonal digital aerial surveys (A), density proportions in the NJDEP baseline survey data (B), and the MDAT model outputs at local and regional scales (C). The scale for all maps is representative of relative spatial variation in the sites within the season for each information source. 117
Map 101. Fall Little Gull modeled density proportions in the Atlantic Shores seasonal digital aerial surveys (A), density proportions in the NJDEP baseline survey data (B), and the MDAT model outputs at local and regional scales (C). The scale for all maps is representative of relative spatial variation in the sites within the season for each information source. 118
Map 102. Winter Little Gull modeled density proportions in the Atlantic Shores seasonal digital aerial surveys (A), density proportions in the NJDEP baseline survey data (B), and the MDAT model outputs at local and regional scales (C). The scale for all maps is representative of relative spatial variation in the sites within the season for each information source. 119
Map 103. Spring Laughing Gull modeled density proportions in the Atlantic Shores seasonal digital aerial surveys (A), density proportions in the NJDEP baseline survey data (B), and the MDAT model outputs at local and regional scales (C). The scale for all maps is representative of relative spatial variation in the sites within the season for each information source. 120
Map 104. Summer Laughing Gull modeled density proportions in the Atlantic Shores seasonal digital aerial surveys (A), density proportions in the NJDEP baseline survey data (B), and the MDAT model outputs at local and regional scales (C). The scale for all maps is representative of relative spatial variation in the sites within the season for each information source. 121
Map 105. Fall Laughing Gull modeled density proportions in the Atlantic Shores seasonal digital aerial surveys (A), density proportions in the NJDEP baseline survey data (B), and the MDAT model outputs at local and regional scales (C). The scale for all maps is representative of relative spatial variation in the sites within the season for each information source. 122
Map 106. Winter Laughing Gull modeled density proportions in the Atlantic Shores seasonal digital aerial surveys (A), density proportions in the NJDEP baseline survey data (B), and the MDAT model outputs at

local and regional scales (C). The scale for all maps is representative of relative spatial variation in the sites within the season for each information source. 123
Map 107. Spring Ring-billed Gull modeled density proportions in the Atlantic Shores seasonal digital aerial surveys (A), density proportions in the NJDEP baseline survey data (B), and the MDAT model outputs at local and regional scales (C). The scale for all maps is representative of relative spatial variation in the sites within the season for each information source. 124
Map 108. Summer Ring-billed Gull modeled density proportions in the Atlantic Shores seasonal digital aerial surveys (A), density proportions in the NJDEP baseline survey data (B), and the MDAT model outputs at local and regional scales (C). The scale for all maps is representative of relative spatial variation in the sites within the season for each information source. 125
Map 109. Fall Ring-billed Gull modeled density proportions in the Atlantic Shores seasonal digital aerial surveys (A), density proportions in the NJDEP baseline survey data (B), and the MDAT model outputs at local and regional scales (C). The scale for all maps is representative of relative spatial variation in the sites within the season for each information source. 126
Map 110. Winter Ring-billed Gull modeled density proportions in the Atlantic Shores seasonal digital aerial surveys (A), density proportions in the NJDEP baseline survey data (B), and the MDAT model outputs at local and regional scales (C). The scale for all maps is representative of relative spatial variation in the sites within the season for each information source. 127
Map 111. Spring Herring Gull modeled density proportions in the Atlantic Shores seasonal digital aerial surveys (A), density proportions in the NJDEP baseline survey data (B), and the MDAT model outputs at local and regional scales (C). The scale for all maps is representative of relative spatial variation in the sites within the season for each information source. 128
Map 112. Summer Herring Gull modeled density proportions in the Atlantic Shores seasonal digital aerial surveys (A), density proportions in the NJDEP baseline survey data (B), and the MDAT model outputs at local and regional scales (C). The scale for all maps is representative of relative spatial variation in the sites within the season for each information source. 129
Map 113. Fall Herring Gull modeled density proportions in the Atlantic Shores seasonal digital aerial surveys (A), density proportions in the NJDEP baseline survey data (B), and the MDAT model outputs at local and regional scales (C). The scale for all maps is representative of relative spatial variation in the sites within the season for each information source. 130
Map 114. Winter Herring Gull modeled density proportions in the Atlantic Shores seasonal digital aerial surveys (A), density proportions in the NJDEP baseline survey data (B), and the MDAT model outputs at local and regional scales (C). The scale for all maps is representative of relative spatial variation in the sites within the season for each information source. 131
Map 115. Spring Iceland Gull modeled density proportions in the Atlantic Shores seasonal digital aerial surveys (A), density proportions in the NJDEP baseline survey data (B), and the MDAT model outputs at local and regional scales (C). The scale for all maps is representative of relative spatial variation in the sites within the season for each information source. 132
Map 116. Fall Iceland Gull modeled density proportions in the Atlantic Shores seasonal digital aerial surveys (A), density proportions in the NJDEP baseline survey data (B), and the MDAT model outputs at local and regional scales (C). The scale for all maps is representative of relative spatial variation in the sites within the season for each information source. 133

Map 117. Winter Iceland Gull modeled density proportions in the Atlantic Shores seasonal digital aerial surveys (A), density proportions in the NJDEP baseline survey data (B), and the MDAT model outputs at local and regional scales (C). The scale for all maps is representative of relative spatial variation in the sites within the season for each information source. 134
Map 118. Spring Lesser Black-backed Gull modeled density proportions in the Atlantic Shores seasonal digital aerial surveys (A), density proportions in the NJDEP baseline survey data (B), and the MDAT model outputs at local and regional scales (C). The scale for all maps is representative of relative spatial variation in the sites within the season for each information source. 135
Map 119. Summer Lesser Black-backed Gull modeled density proportions in the Atlantic Shores seasonal digital aerial surveys (A), density proportions in the NJDEP baseline survey data (B), and the MDAT model outputs at local and regional scales (C). The scale for all maps is representative of relative spatial variation in the sites within the season for each information source. 136
Map 120. Fall Lesser Black-backed Gull modeled density proportions in the Atlantic Shores seasonal digital aerial surveys (A), density proportions in the NJDEP baseline survey data (B), and the MDAT model outputs at local and regional scales (C). The scale for all maps is representative of relative spatial variation in the sites within the season for each information source. 137
Map 121. Winter Lesser Black-backed Gull modeled density proportions in the Atlantic Shores seasonal digital aerial surveys (A), density proportions in the NJDEP baseline survey data (B), and the MDAT model outputs at local and regional scales (C). The scale for all maps is representative of relative spatial variation in the sites within the season for each information source. 138
Map 122. Spring Great Black-backed Gull modeled density proportions in the Atlantic Shores seasonal digital aerial surveys (A), density proportions in the NJDEP baseline survey data (B), and the MDAT model outputs at local and regional scales (C). The scale for all maps is representative of relative spatial variation in the sites within the season for each information source. 139
Map 123. Summer Great Black-backed Gull modeled density proportions in the Atlantic Shores seasonal digital aerial surveys (A), density proportions in the NJDEP baseline survey data (B), and the MDAT model outputs at local and regional scales (C). The scale for all maps is representative of relative spatial variation in the sites within the season for each information source. 140
Map 124. Fall Great Black-backed Gull modeled density proportions in the Atlantic Shores seasonal digital aerial surveys (A), density proportions in the NJDEP baseline survey data (B), and the MDAT model outputs at local and regional scales (C). The scale for all maps is representative of relative spatial variation in the sites within the season for each information source. 141
Map 125. Winter Great Black-backed Gull modeled density proportions in the Atlantic Shores seasonal digital aerial surveys (A), density proportions in the NJDEP baseline survey data (B), and the MDAT model outputs at local and regional scales (C). The scale for all maps is representative of relative spatial variation in the sites within the season for each information source. 142
Map 126. Spring Least Tern modeled density proportions in the Atlantic Shores seasonal digital aerial surveys (A), density proportions in the NJDEP baseline survey data (B), and the MDAT model outputs at local and regional scales (C). The scale for all maps is representative of relative spatial variation in the sites within the season for each information source. 143
Map 127. Summer Least Tern modeled density proportions in the Atlantic Shores seasonal digital aerial surveys (A), density proportions in the NJDEP baseline survey data (B), and the MDAT model outputs at

local and regional scales (C). The scale for all maps is representative of relative spatial variation in the sites within the season for each information source. 144
Map 128. Fall Least Tern modeled density proportions in the Atlantic Shores seasonal digital aerial surveys (A), density proportions in the NJDEP baseline survey data (B), and the MDAT model outputs at local and regional scales (C). The scale for all maps is representative of relative spatial variation in the sites within the season for each information source. 145
Map 129. Winter Least Tern modeled density proportions in the Atlantic Shores seasonal digital aerial surveys (A), density proportions in the NJDEP baseline survey data (B), and the MDAT model outputs at local and regional scales (C). The scale for all maps is representative of relative spatial variation in the sites within the season for each information source. 146
Map 130. Spring Caspian Tern modeled density proportions in the Atlantic Shores seasonal digital aerial surveys (A), density proportions in the NJDEP baseline survey data (B), and the MDAT model outputs at local and regional scales (C). The scale for all maps is representative of relative spatial variation in the sites within the season for each information source. 147
Map 131. Fall Caspian Tern modeled density proportions in the Atlantic Shores seasonal digital aerial surveys (A), density proportions in the NJDEP baseline survey data (B), and the MDAT model outputs at local and regional scales (C). The scale for all maps is representative of relative spatial variation in the sites within the season for each information source. 148
Map 132. Winter Caspian Tern modeled density proportions in the Atlantic Shores seasonal digital aerial surveys (A), density proportions in the NJDEP baseline survey data (B), and the MDAT model outputs at local and regional scales (C). The scale for all maps is representative of relative spatial variation in the sites within the season for each information source. 149
Map 133. Spring Black Tern modeled density proportions in the Atlantic Shores seasonal digital aerial surveys (A), density proportions in the NJDEP baseline survey data (B), and the MDAT model outputs at local and regional scales (C). The scale for all maps is representative of relative spatial variation in the sites within the season for each information source. 150
Map 134. Summer Black Tern modeled density proportions in the Atlantic Shores seasonal digital aerial surveys (A), density proportions in the NJDEP baseline survey data (B), and the MDAT model outputs at local and regional scales (C). The scale for all maps is representative of relative spatial variation in the sites within the season for each information source. 151
Map 135. Fall Black Tern modeled density proportions in the Atlantic Shores seasonal digital aerial surveys (A), density proportions in the NJDEP baseline survey data (B), and the MDAT model outputs at local and regional scales (C). The scale for all maps is representative of relative spatial variation in the sites within the season for each information source. 152
Map 136. Winter Black Tern modeled density proportions in the Atlantic Shores seasonal digital aerial surveys (A), density proportions in the NJDEP baseline survey data (B), and the MDAT model outputs at local and regional scales (C). The scale for all maps is representative of relative spatial variation in the sites within the season for each information source. 153
Map 137. Spring Common Tern modeled density proportions in the Atlantic Shores seasonal digital aerial surveys (A), density proportions in the NJDEP baseline survey data (B), and the MDAT model outputs at local and regional scales (C). The scale for all maps is representative of relative spatial variation in the sites within the season for each information source. 154

Map 138. Summer Common Tern modeled density proportions in the Atlantic Shores seasonal digital aerial surveys (A), density proportions in the NJDEP baseline survey data (B), and the MDAT model outputs at local and regional scales (C). The scale for all maps is representative of relative spatial variation in the sites within the season for each information source. 155
Map 139. Fall Common Tern modeled density proportions in the Atlantic Shores seasonal digital aerial surveys (A), density proportions in the NJDEP baseline survey data (B), and the MDAT model outputs at local and regional scales (C). The scale for all maps is representative of relative spatial variation in the sites within the season for each information source. 156
Map 140. Winter Common Tern modeled density proportions in the Atlantic Shores seasonal digital aerial surveys (A), density proportions in the NJDEP baseline survey data (B), and the MDAT model outputs at local and regional scales (C). The scale for all maps is representative of relative spatial variation in the sites within the season for each information source. 157
Map 141. Spring Forster's Tern modeled density proportions in the Atlantic Shores seasonal digital aerial surveys (A), density proportions in the NJDEP baseline survey data (B), and the MDAT model outputs at local and regional scales (C). The scale for all maps is representative of relative spatial variation in the sites within the season for each information source. 158
Map 142. Summer Forster's Tern modeled density proportions in the Atlantic Shores seasonal digital aerial surveys (A), density proportions in the NJDEP baseline survey data (B), and the MDAT model outputs at local and regional scales (C). The scale for all maps is representative of relative spatial variation in the sites within the season for each information source. 159
Map 143. Fall Forster's Tern modeled density proportions in the Atlantic Shores seasonal digital aerial surveys (A), density proportions in the NJDEP baseline survey data (B), and the MDAT model outputs at local and regional scales (C). The scale for all maps is representative of relative spatial variation in the sites within the season for each information source. 160
Map 144. Winter Forster's Tern modeled density proportions in the Atlantic Shores seasonal digital aerial surveys (A), density proportions in the NJDEP baseline survey data (B), and the MDAT model outputs at local and regional scales (C). The scale for all maps is representative of relative spatial variation in the sites within the season for each information source. 161
Map 145. Spring Royal Tern modeled density proportions in the Atlantic Shores seasonal digital aerial surveys (A), density proportions in the NJDEP baseline survey data (B), and the MDAT model outputs at local and regional scales (C). The scale for all maps is representative of relative spatial variation in the sites within the season for each information source. 162
Map 146. Summer Royal Tern modeled density proportions in the Atlantic Shores seasonal digital aerial surveys (A), density proportions in the NJDEP baseline survey data (B), and the MDAT model outputs at local and regional scales (C). The scale for all maps is representative of relative spatial variation in the sites within the season for each information source. 163
Map 147. Fall Royal Tern modeled density proportions in the Atlantic Shores seasonal digital aerial surveys (A), density proportions in the NJDEP baseline survey data (B), and the MDAT model outputs at local and regional scales (C). The scale for all maps is representative of relative spatial variation in the sites within the season for each information source. 164
Map 148. Winter Royal Tern modeled density proportions in the Atlantic Shores seasonal digital aerial surveys (A), density proportions in the NJDEP baseline survey data (B), and the MDAT model outputs at

local and regional scales (C). The scale for all maps is representative of relative spatial variation in the sites within the season for each information source. 165
Map 149. Spring Dovekie modeled density proportions in the Atlantic Shores seasonal digital aerial surveys (A), density proportions in the NJDEP baseline survey data (B), and the MDAT model outputs at local and regional scales (C). The scale for all maps is representative of relative spatial variation in the sites within the season for each information source. 166
Map 150. Summer Dovekie modeled density proportions in the Atlantic Shores seasonal digital aerial surveys (A), density proportions in the NJDEP baseline survey data (B), and the MDAT model outputs at local and regional scales (C). The scale for all maps is representative of relative spatial variation in the sites within the season for each information source. 167
Map 151. Fall Dovekie modeled density proportions in the Atlantic Shores seasonal digital aerial surveys (A), density proportions in the NJDEP baseline survey data (B), and the MDAT model outputs at local and regional scales (C). The scale for all maps is representative of relative spatial variation in the sites within the season for each information source. 168
Map 152. Winter Dovekie modeled density proportions in the Atlantic Shores seasonal digital aerial surveys (A), density proportions in the NJDEP baseline survey data (B), and the MDAT model outputs at local and regional scales (C). The scale for all maps is representative of relative spatial variation in the sites within the season for each information source. 169
Map 153. Spring Common Murre modeled density proportions in the Atlantic Shores seasonal digital aerial surveys (A), density proportions in the NJDEP baseline survey data (B), and the MDAT model outputs at local and regional scales (C). The scale for all maps is representative of relative spatial variation in the sites within the season for each information source. 170
Map 154. Fall Common Murre modeled density proportions in the Atlantic Shores seasonal digital aerial surveys (A), density proportions in the NJDEP baseline survey data (B), and the MDAT model outputs at local and regional scales (C). The scale for all maps is representative of relative spatial variation in the sites within the season for each information source. 171
Map 155. Winter Common Murre modeled density proportions in the Atlantic Shores seasonal digital aerial surveys (A), density proportions in the NJDEP baseline survey data (B), and the MDAT model outputs at local and regional scales (C). The scale for all maps is representative of relative spatial variation in the sites within the season for each information source. 172
Map 156. Spring Thick-billed Murre modeled density proportions in the Atlantic Shores seasonal digital aerial surveys (A), density proportions in the NJDEP baseline survey data (B), and the MDAT model outputs at local and regional scales (C). The scale for all maps is representative of relative spatial variation in the sites within the season for each information source. 173
Map 157. Fall Thick-billed Murre modeled density proportions in the Atlantic Shores seasonal digital aerial surveys (A), density proportions in the NJDEP baseline survey data (B), and the MDAT model outputs at local and regional scales (C). The scale for all maps is representative of relative spatial variation in the sites within the season for each information source. 174
Map 158. Winter Thick-billed Murre modeled density proportions in the Atlantic Shores seasonal digital aerial surveys (A), density proportions in the NJDEP baseline survey data (B), and the MDAT model outputs at local and regional scales (C). The scale for all maps is representative of relative spatial variation in the sites within the season for each information source. 175

Map 159. Spring Razorbill modeled density proportions in the Atlantic Shores seasonal digital aerial surveys (A), density proportions in the NJDEP baseline survey data (B), and the MDAT model outputs at local and regional scales (C). The scale for all maps is representative of relative spatial variation in the sites within the season for each information source. 176
Map 160. Summer Razorbill modeled density proportions in the Atlantic Shores seasonal digital aerial surveys (A), density proportions in the NJDEP baseline survey data (B), and the MDAT model outputs at local and regional scales (C). The scale for all maps is representative of relative spatial variation in the sites within the season for each information source. 177
Map 161. Fall Razorbill modeled density proportions in the Atlantic Shores seasonal digital aerial surveys (A), density proportions in the NJDEP baseline survey data (B), and the MDAT model outputs at local and regional scales (C). The scale for all maps is representative of relative spatial variation in the sites within the season for each information source. 178
Map 162. Winter Razorbill modeled density proportions in the Atlantic Shores seasonal digital aerial surveys (A), density proportions in the NJDEP baseline survey data (B), and the MDAT model outputs at local and regional scales (C). The scale for all maps is representative of relative spatial variation in the sites within the season for each information source. 179
Map 163. Spring Black Guillemot modeled density proportions in the Atlantic Shores seasonal digital aerial surveys (A), density proportions in the NJDEP baseline survey data (B), and the MDAT model outputs at local and regional scales (C). The scale for all maps is representative of relative spatial variation in the sites within the season for each information source. 180
Map 164. Summer Black Guillemot modeled density proportions in the Atlantic Shores seasonal digital aerial surveys (A), density proportions in the NJDEP baseline survey data (B), and the MDAT model outputs at local and regional scales (C). The scale for all maps is representative of relative spatial variation in the sites within the season for each information source. 181
Map 165. Fall Black Guillemot modeled density proportions in the Atlantic Shores seasonal digital aerial surveys (A), density proportions in the NJDEP baseline survey data (B), and the MDAT model outputs at local and regional scales (C). The scale for all maps is representative of relative spatial variation in the sites within the season for each information source. 182
Map 166. Winter Black Guillemot modeled density proportions in the Atlantic Shores seasonal digital aerial surveys (A), density proportions in the NJDEP baseline survey data (B), and the MDAT model outputs at local and regional scales (C). The scale for all maps is representative of relative spatial variation in the sites within the season for each information source. 183
Map 167. Spring Atlantic Puffin modeled density proportions in the Atlantic Shores seasonal digital aerial surveys (A), density proportions in the NJDEP baseline survey data (B), and the MDAT model outputs at local and regional scales (C). The scale for all maps is representative of relative spatial variation in the sites within the season for each information source. 184
Map 168. Summer Atlantic Puffin modeled density proportions in the Atlantic Shores seasonal digital aerial surveys (A), density proportions in the NJDEP baseline survey data (B), and the MDAT model outputs at local and regional scales (C). The scale for all maps is representative of relative spatial variation in the sites within the season for each information source. 185
Map 169. Fall Atlantic Puffin modeled density proportions in the Atlantic Shores seasonal digital aerial surveys (A), density proportions in the NJDEP baseline survey data (B), and the MDAT model outputs at

local and regional scales (C). The scale for all maps is representative of relative spatial variation in the sites within the season for each information source. 186
Map 170. Winter Atlantic Puffin modeled density proportions in the Atlantic Shores seasonal digital aerial surveys (A), density proportions in the NJDEP baseline survey data (B), and the MDAT model outputs at local and regional scales (C). The scale for all maps is representative of relative spatial variation in the sites within the season for each information source. 187
Map 171. Spring Red-necked Phalarope modeled density proportions in the Atlantic Shores seasonal digital aerial surveys (A), density proportions in the NJDEP baseline survey data (B), and the MDAT model outputs at local and regional scales (C). The scale for all maps is representative of relative spatial variation in the sites within the season for each information source. 188
Map 172. Summer Red-necked Phalarope modeled density proportions in the Atlantic Shores seasonal digital aerial surveys (A), density proportions in the NJDEP baseline survey data (B), and the MDAT model outputs at local and regional scales (C). The scale for all maps is representative of relative spatial variation in the sites within the season for each information source. 189
Map 173. Fall Red-necked Phalarope modeled density proportions in the Atlantic Shores seasonal digital aerial surveys (A), density proportions in the NJDEP baseline survey data (B), and the MDAT model outputs at local and regional scales (C). The scale for all maps is representative of relative spatial variation in the sites within the season for each information source. 190
Map 174. Winter Red-necked Phalarope modeled density proportions in the Atlantic Shores seasonal digital aerial surveys (A), density proportions in the NJDEP baseline survey data (B), and the MDAT model outputs at local and regional scales (C). The scale for all maps is representative of relative spatial variation in the sites within the season for each information source. 191
Map 175. Spring Red Phalarope modeled density proportions in the Atlantic Shores seasonal digital aerial surveys (A), density proportions in the NJDEP baseline survey data (B), and the MDAT model outputs at local and regional scales (C). The scale for all maps is representative of relative spatial variation in the sites within the season for each information source. 192
Map 176. Summer Red Phalarope modeled density proportions in the Atlantic Shores seasonal digital aerial surveys (A), density proportions in the NJDEP baseline survey data (B), and the MDAT model outputs at local and regional scales (C). The scale for all maps is representative of relative spatial variation in the sites within the season for each information source. 193
Map 177. Fall Red Phalarope modeled density proportions in the Atlantic Shores seasonal digital aerial surveys (A), density proportions in the NJDEP baseline survey data (B), and the MDAT model outputs at local and regional scales (C). The scale for all maps is representative of relative spatial variation in the sites within the season for each information source. 194
Map 178. Winter Red Phalarope modeled density proportions in the Atlantic Shores seasonal digital aerial surveys (A), density proportions in the NJDEP baseline survey data (B), and the MDAT model outputs at local and regional scales (C). The scale for all maps is representative of relative spatial variation in the sites within the season for each information source. 195

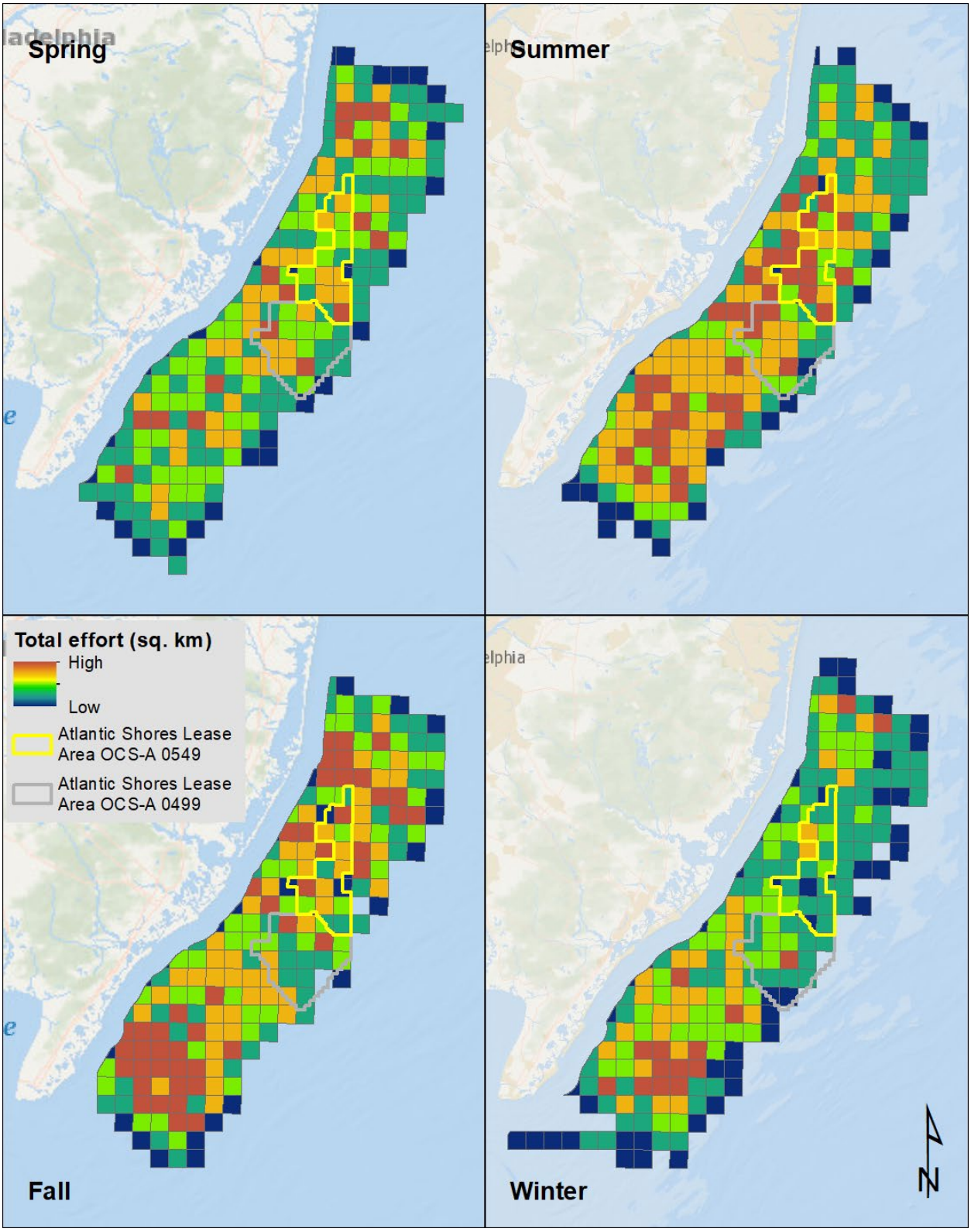

Map 1. NJDEP baseline seasonal survey effort. Survey effort totaled within each full or partial lease block inside and outside the Atlantic Shores Lease Area OCS-A 0549.

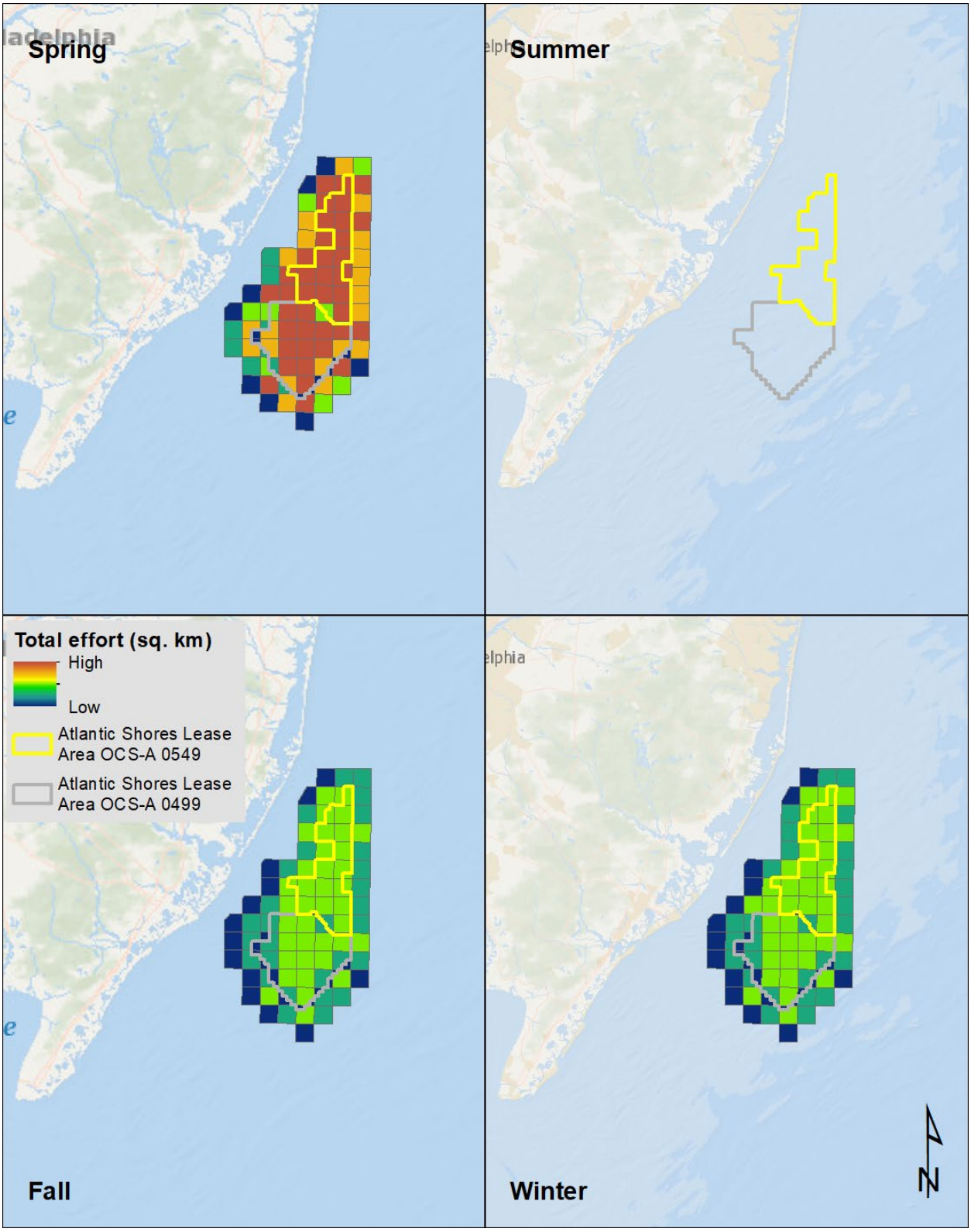

Map 2. Atlantic Shores digital aerial seasonal survey effort. Survey effort totaled within each full or partial lease block inside and outside the Atlantic Shores Lease Area OCS-A 0549.

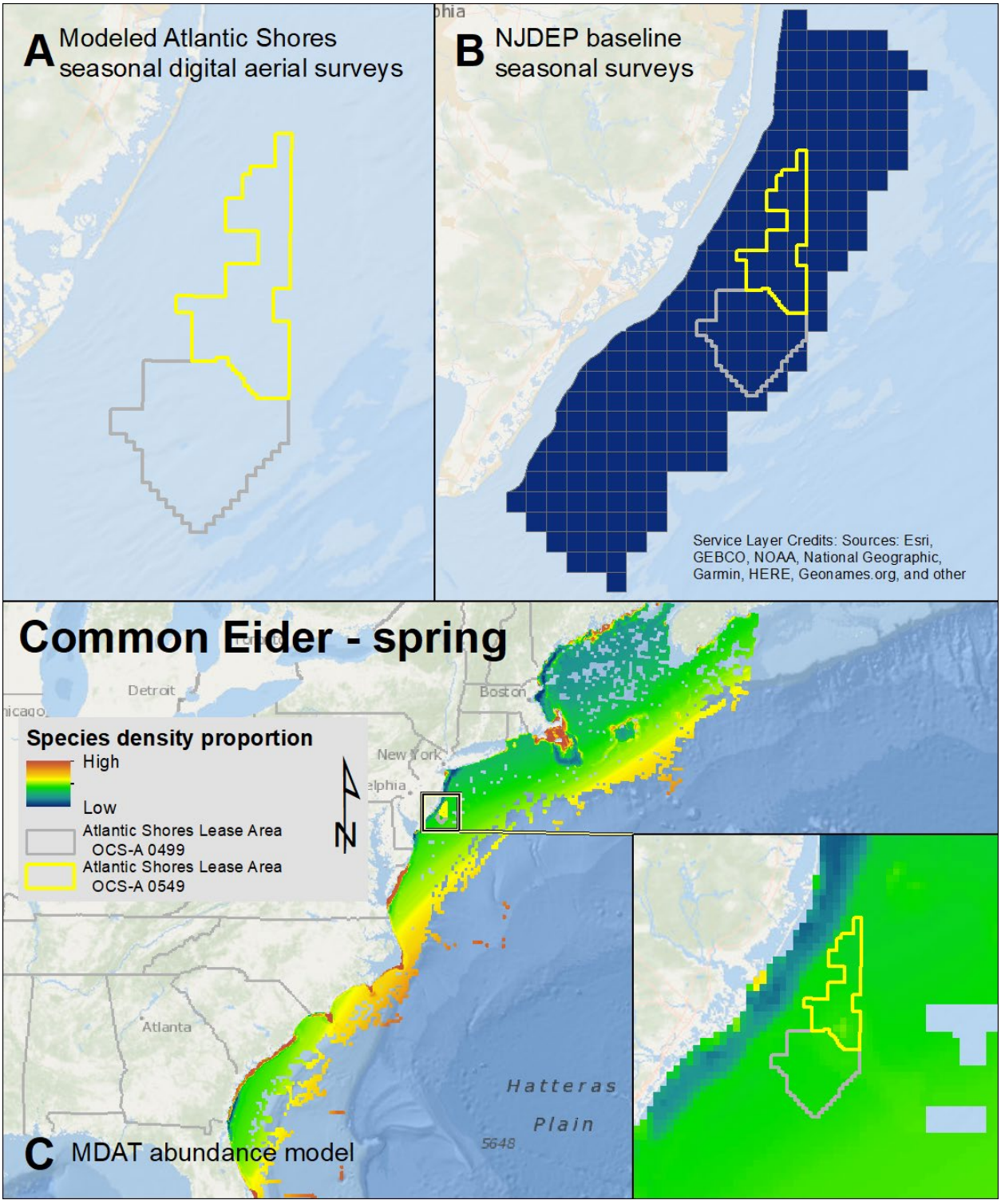

Map 3. Spring Common Eider modeled density proportions in the Atlantic Shores seasonal digital aerial surveys (A), density proportions in the NJDEP baseline survey data (B), and the MDAT model outputs at local and regional scales (C). The scale for all maps is representative of relative spatial variation in the sites within the season for each information source.

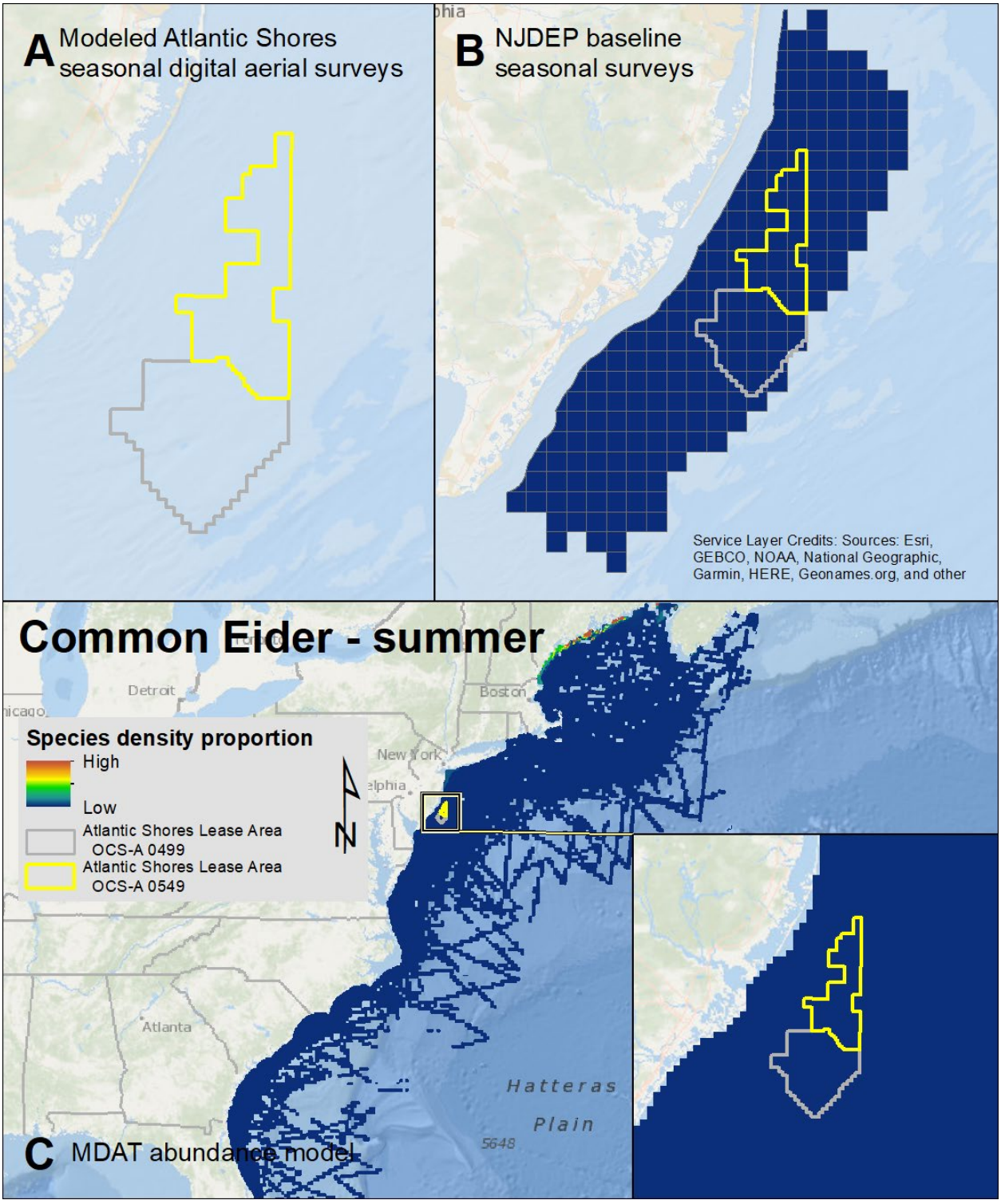

Map 4. Summer Common Eider modeled density proportions in the Atlantic Shores seasonal digital aerial surveys (A), density proportions in the NJDEP baseline survey data (B), and the MDAT model outputs at local and regional scales (C). The scale for all maps is representative of relative spatial variation in the sites within the season for each information source.

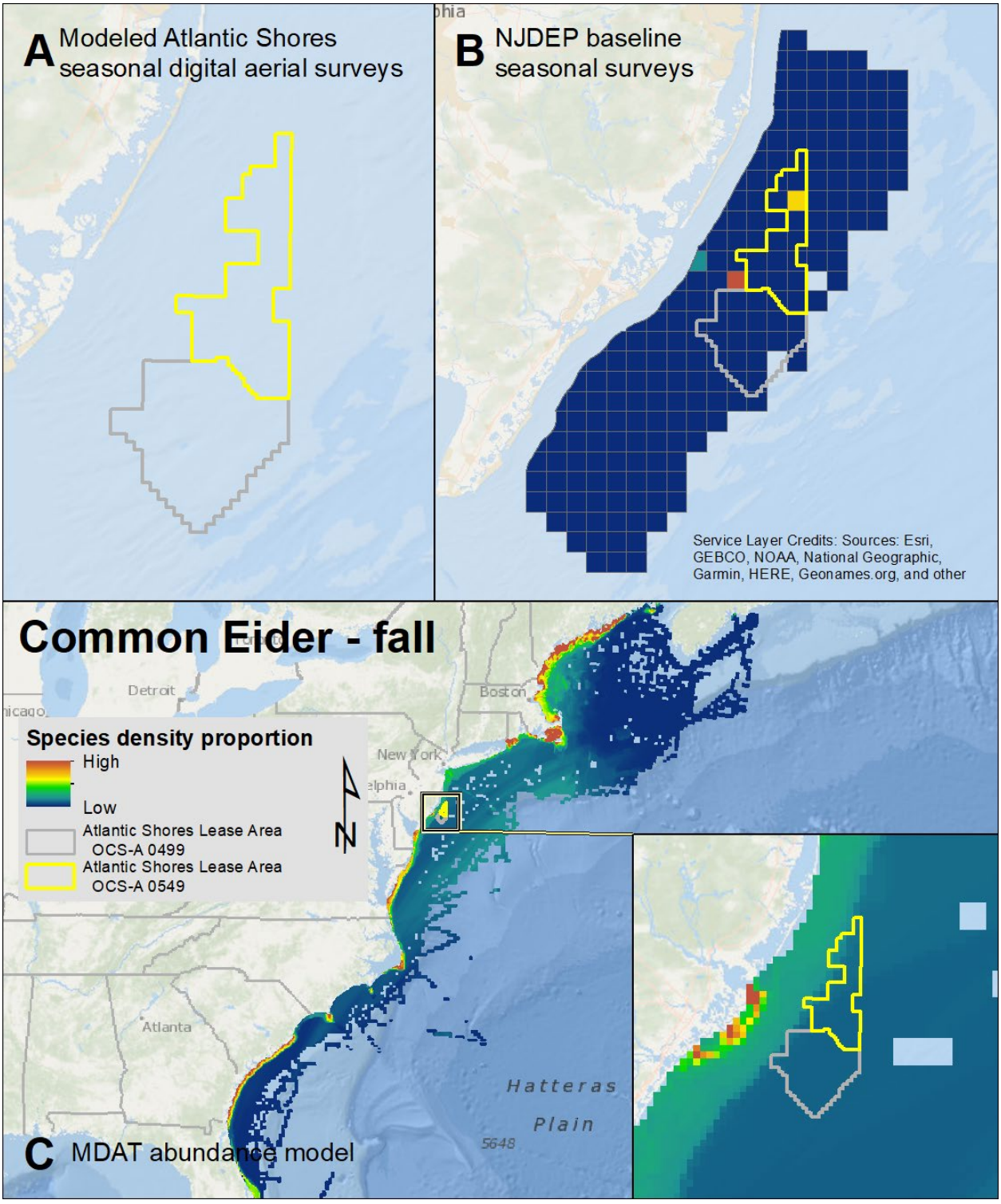

Map 5. Fall Common Eider modeled density proportions in the Atlantic Shores seasonal digital aerial surveys (A), density proportions in the NJDEP baseline survey data (B), and the MDAT model outputs at local and regional scales (C). The scale for all maps is representative of relative spatial variation in the sites within the season for each information source.

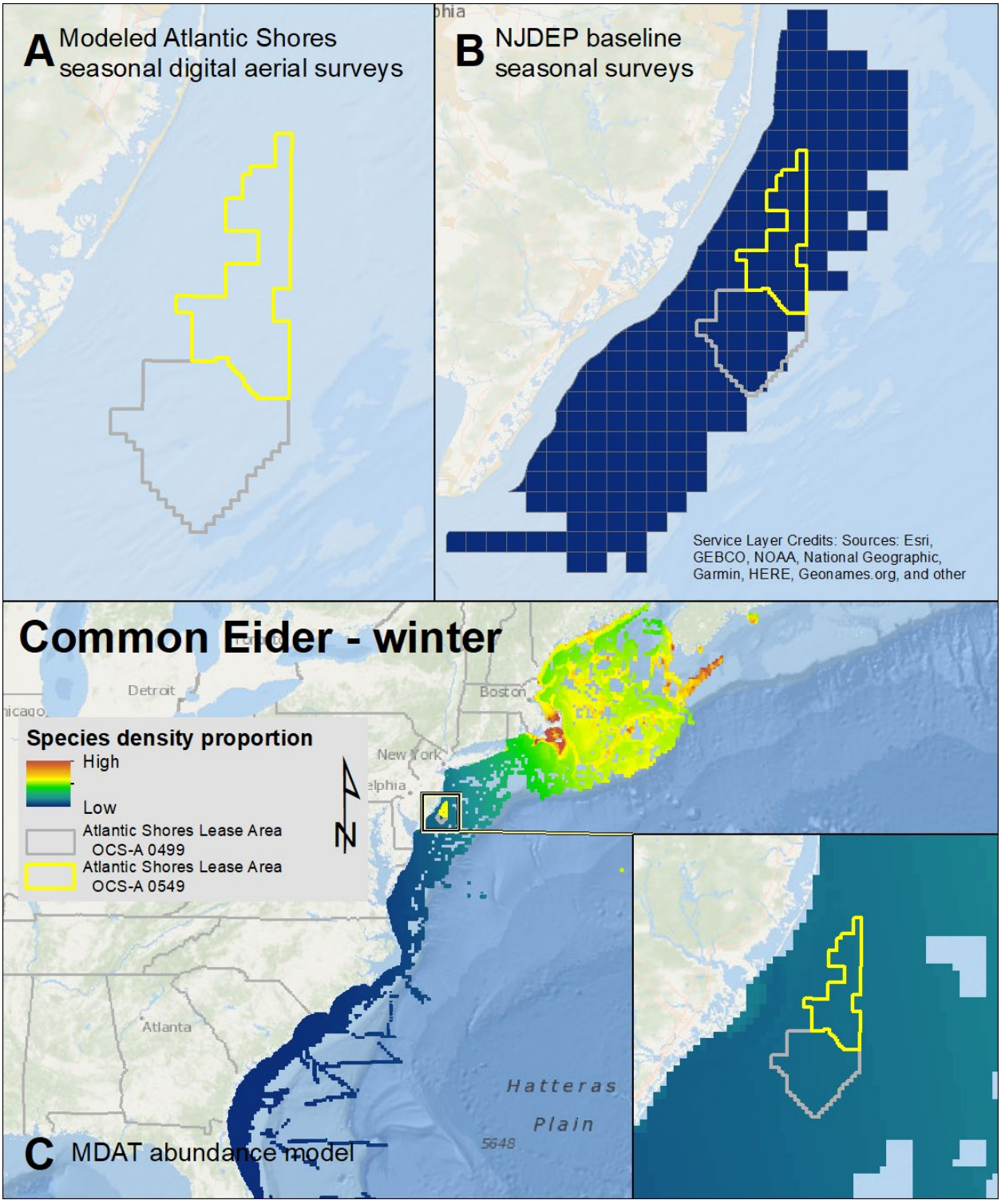

Map 6. Winter Common Eider modeled density proportions in the Atlantic Shores seasonal digital aerial surveys (A), density proportions in the NJDEP baseline survey data (B), and the MDAT model outputs at local and regional scales (C). The scale for all maps is representative of relative spatial variation in the sites within the season for each information source.

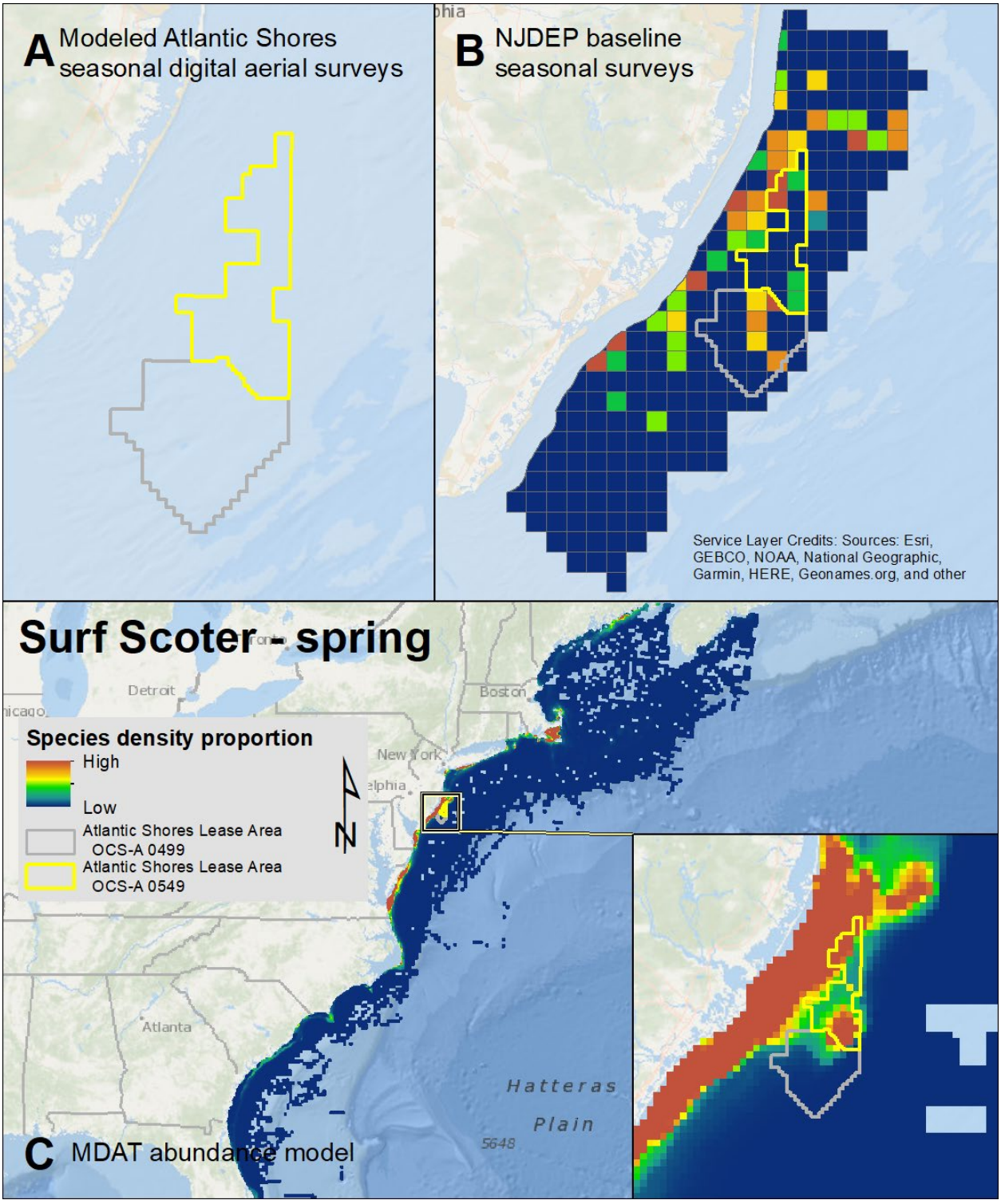

Map 7. Spring Surf Scoter modeled density proportions in the Atlantic Shores seasonal digital aerial surveys (A), density proportions in the NJDEP baseline survey data (B), and the MDAT model outputs at local and regional scales (C). The scale for all maps is representative of relative spatial variation in the sites within the season for each information source.

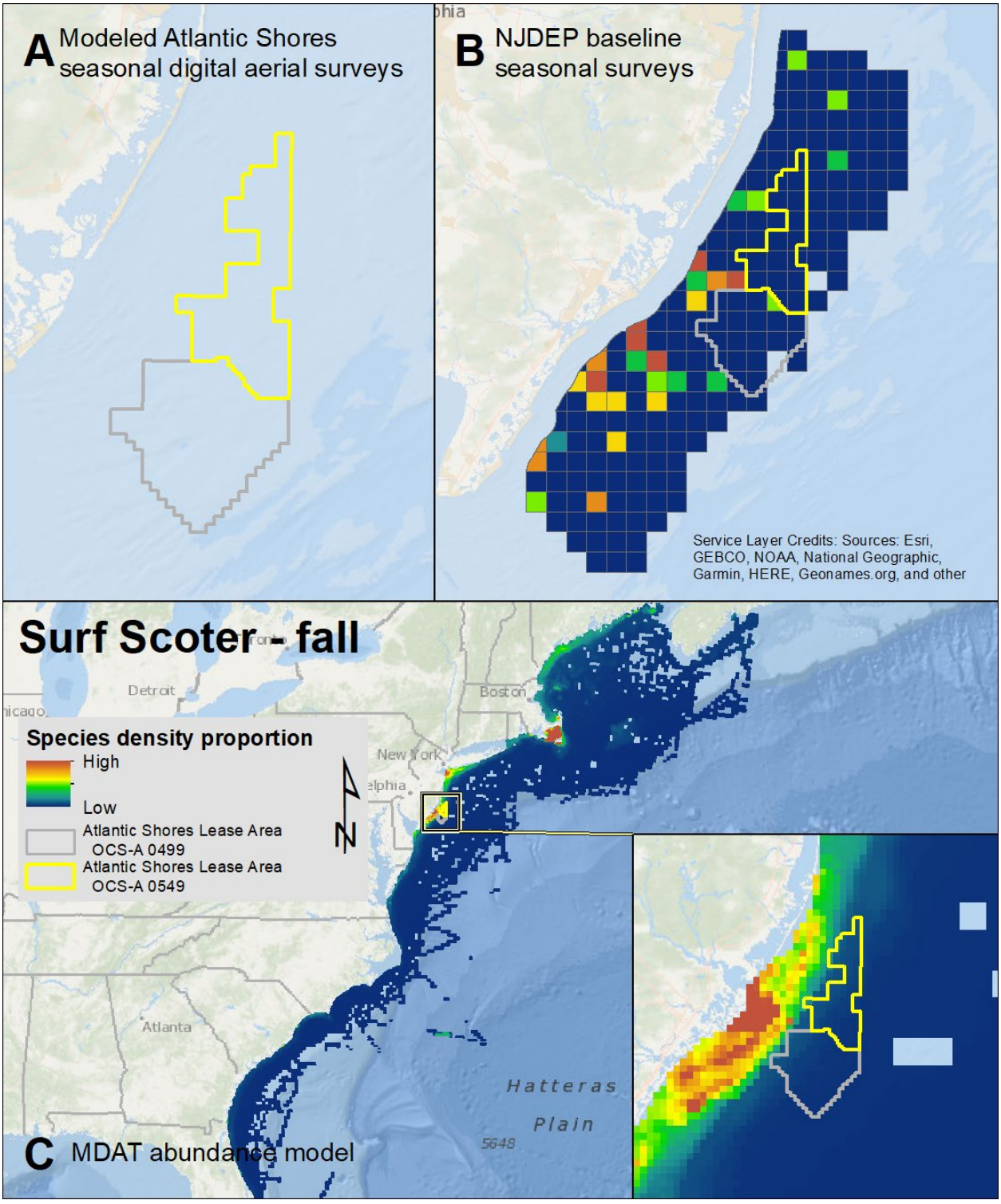

Map 8. Fall Surf Scoter modeled density proportions in the Atlantic Shores seasonal digital aerial surveys (A), density proportions in the NJDEP baseline survey data (B), and the MDAT model outputs at local and regional scales (C). The scale for all maps is representative of relative spatial variation in the sites within the season for each information source.

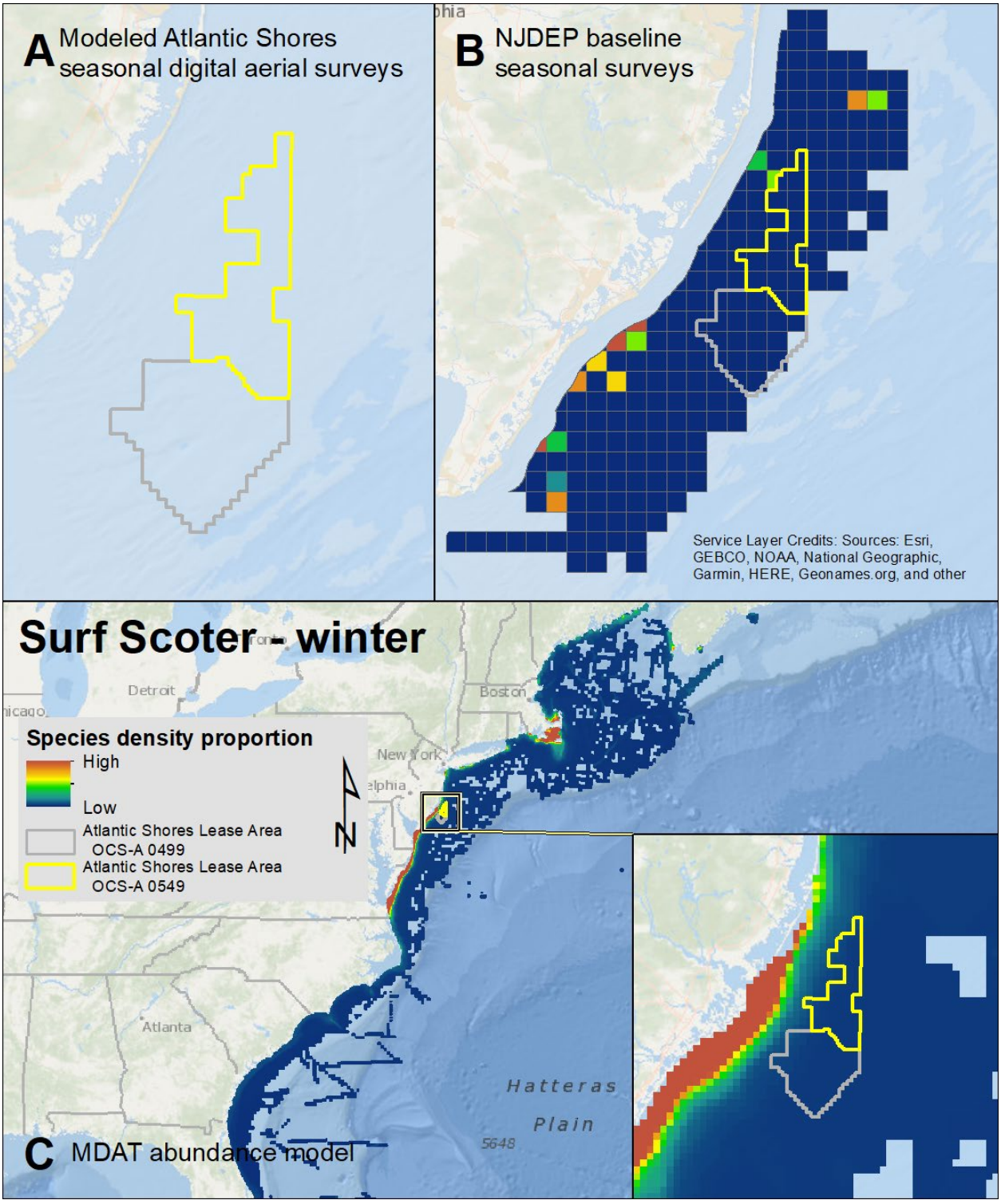

Map 9. Winter Surf Scoter modeled density proportions in the Atlantic Shores seasonal digital aerial surveys (A), density proportions in the NJDEP baseline survey data (B), and the MDAT model outputs at local and regional scales (C). The scale for all maps is representative of relative spatial variation in the sites within the season for each information source.

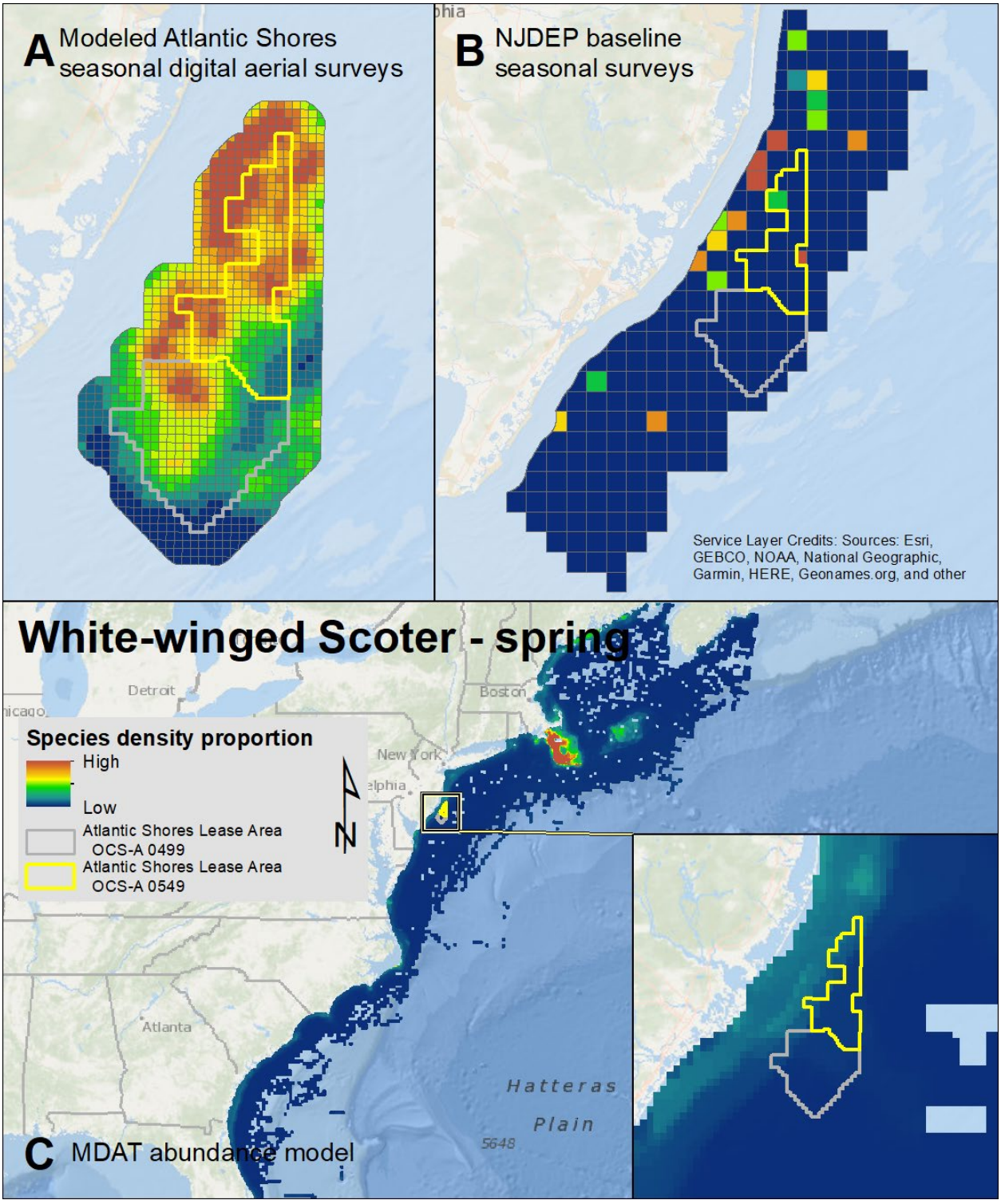

Map 10. Spring White-winged Scoter modeled density proportions in the Atlantic Shores seasonal digital aerial surveys (A), density proportions in the NJDEP baseline survey data (B), and the MDAT model outputs at local and regional scales (C). The scale for all maps is representative of relative spatial variation in the sites within the season for each information source.

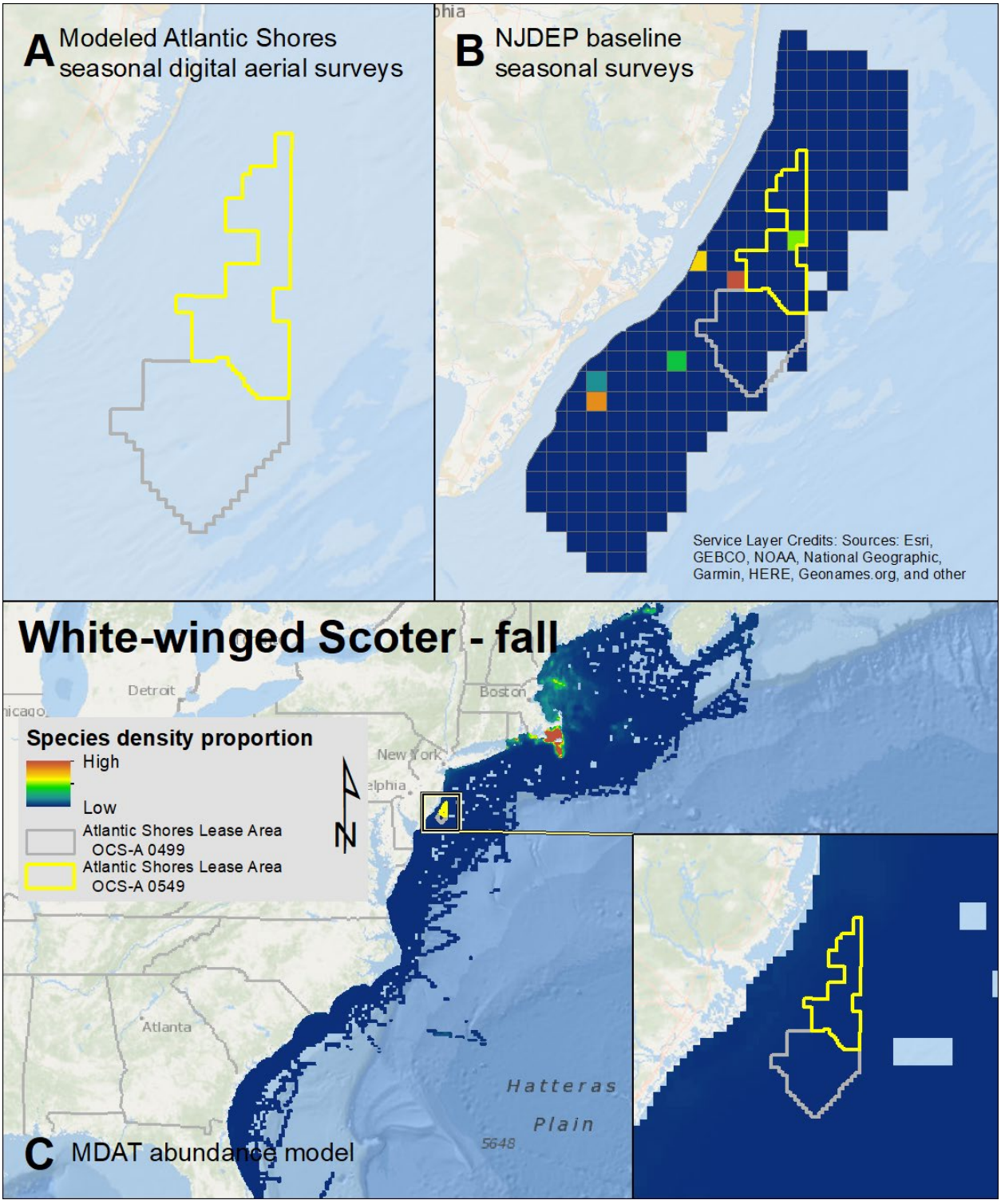

Map 11. Fall White-winged Scoter modeled density proportions in the Atlantic Shores seasonal digital aerial surveys (A), density proportions in the NJDEP baseline survey data (B), and the MDAT model outputs at local and regional scales (C). The scale for all maps is representative of relative spatial variation in the sites within the season for each information source.

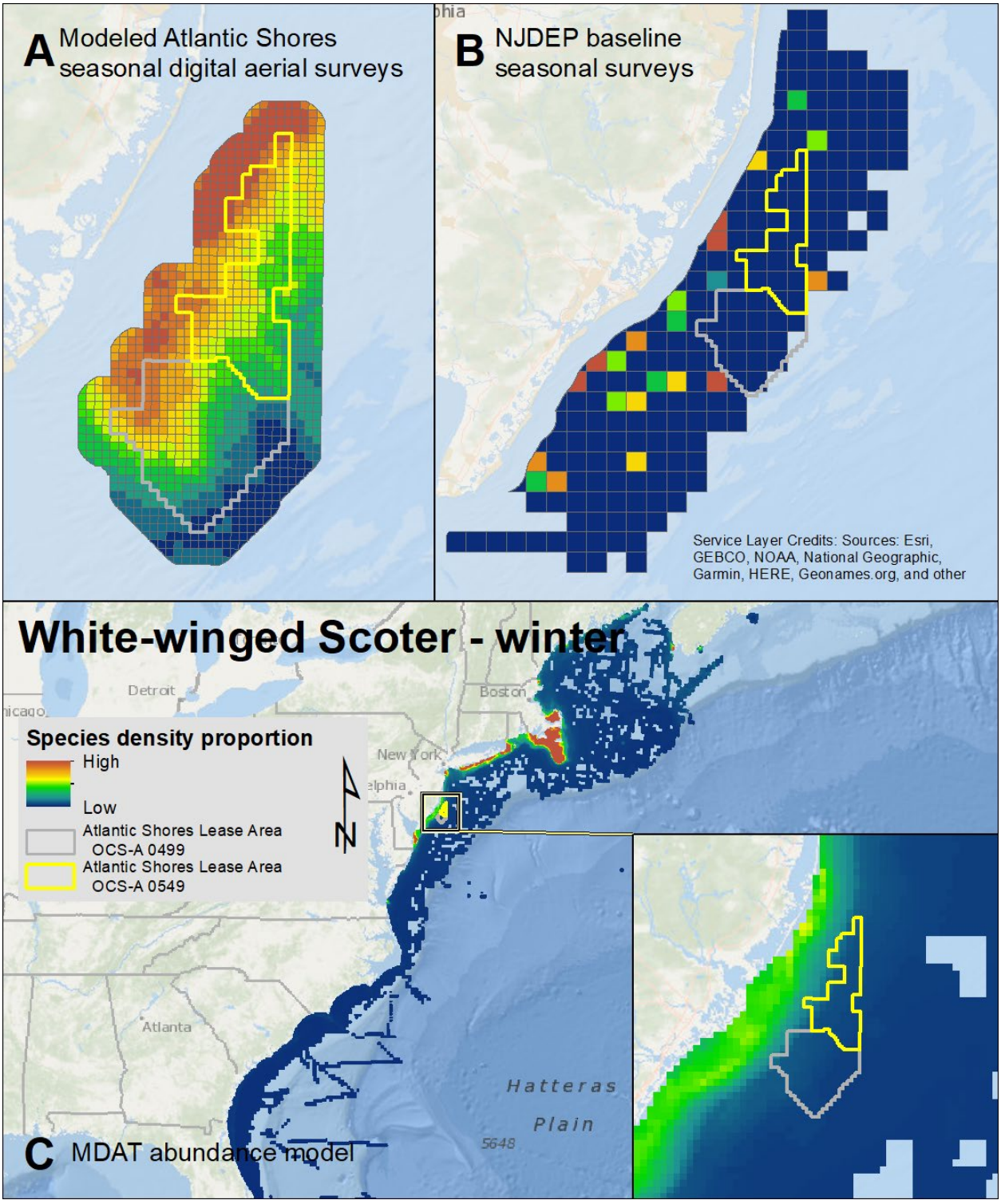

Map 12. Winter White-winged Scoter modeled density proportions in the Atlantic Shores seasonal digital aerial surveys (A), density proportions in the NJDEP baseline survey data (B), and the MDAT model outputs at local and regional scales (C). The scale for all maps is representative of relative spatial variation in the sites within the season for each information source.

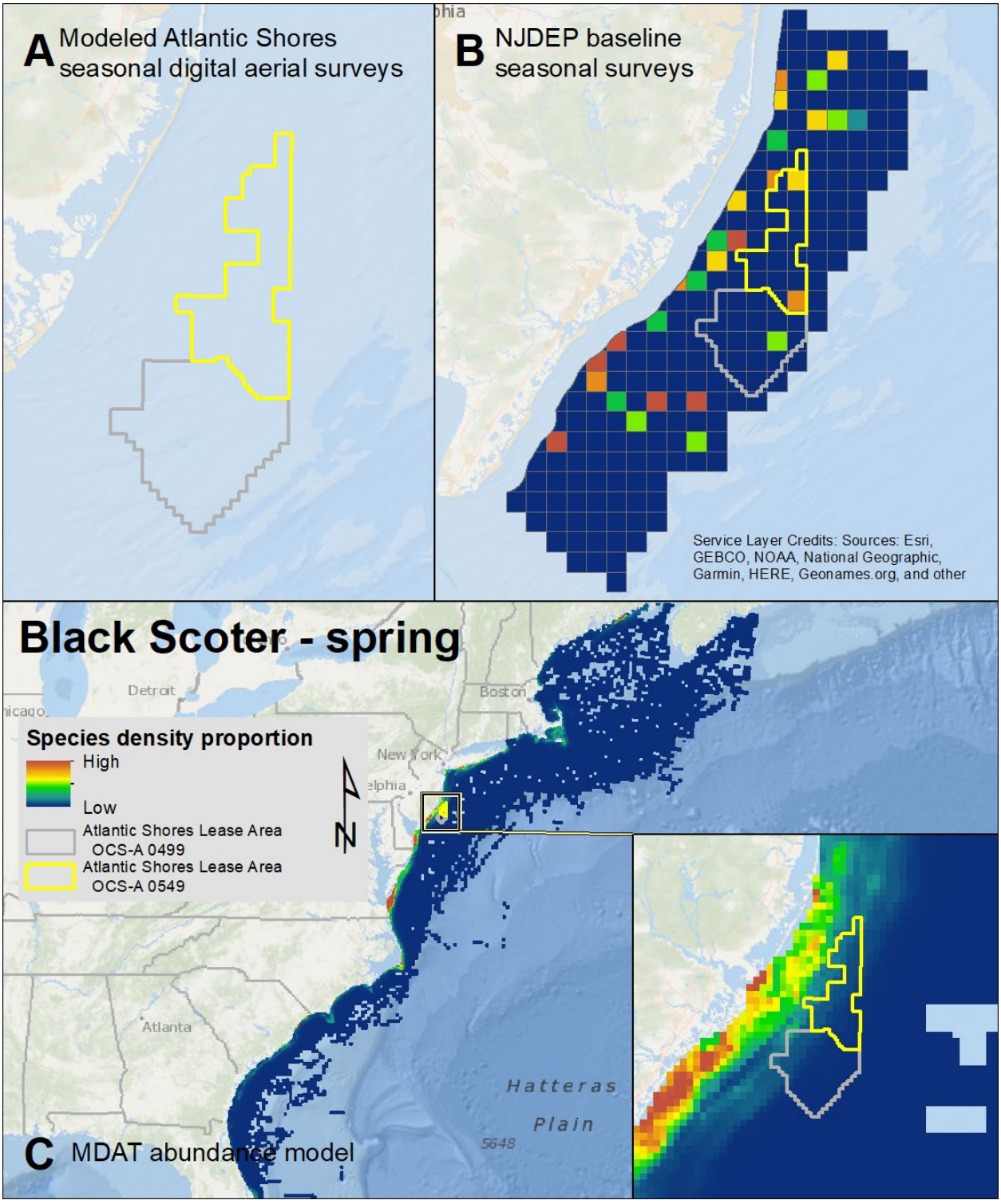

Map 13. Spring Black Scoter modeled density proportions in the Atlantic Shores seasonal digital aerial surveys (A), density proportions in the NJDEP baseline survey data (B), and the MDAT model outputs at local and regional scales (C). The scale for all maps is representative of relative spatial variation in the sites within the season for each information source.

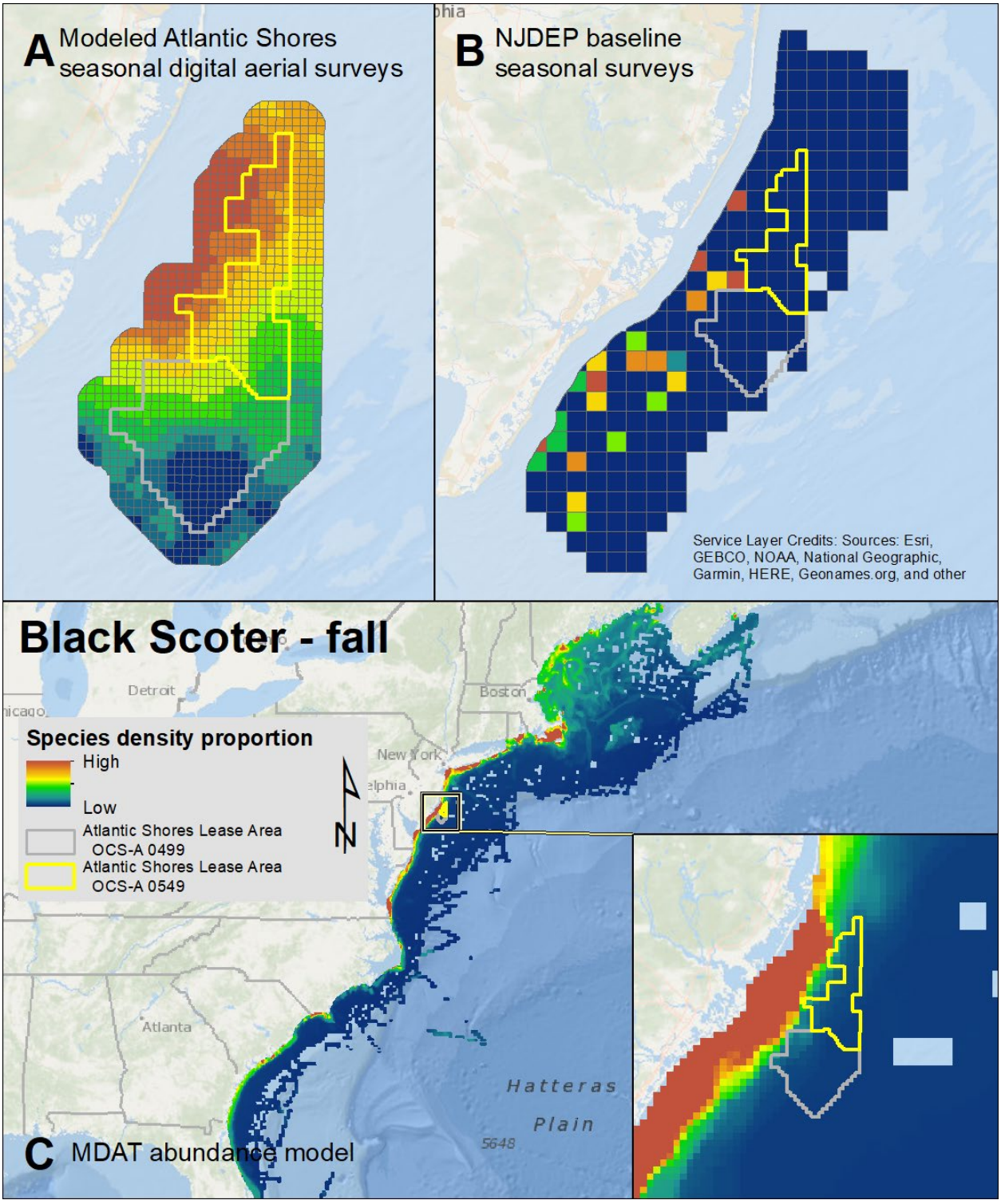

Map 14. Fall Black Scoter modeled density proportions in the Atlantic Shores seasonal digital aerial surveys (A), density proportions in the NJDEP baseline survey data (B), and the MDAT model outputs at local and regional scales (C). The scale for all maps is representative of relative spatial variation in the sites within the season for each information source.

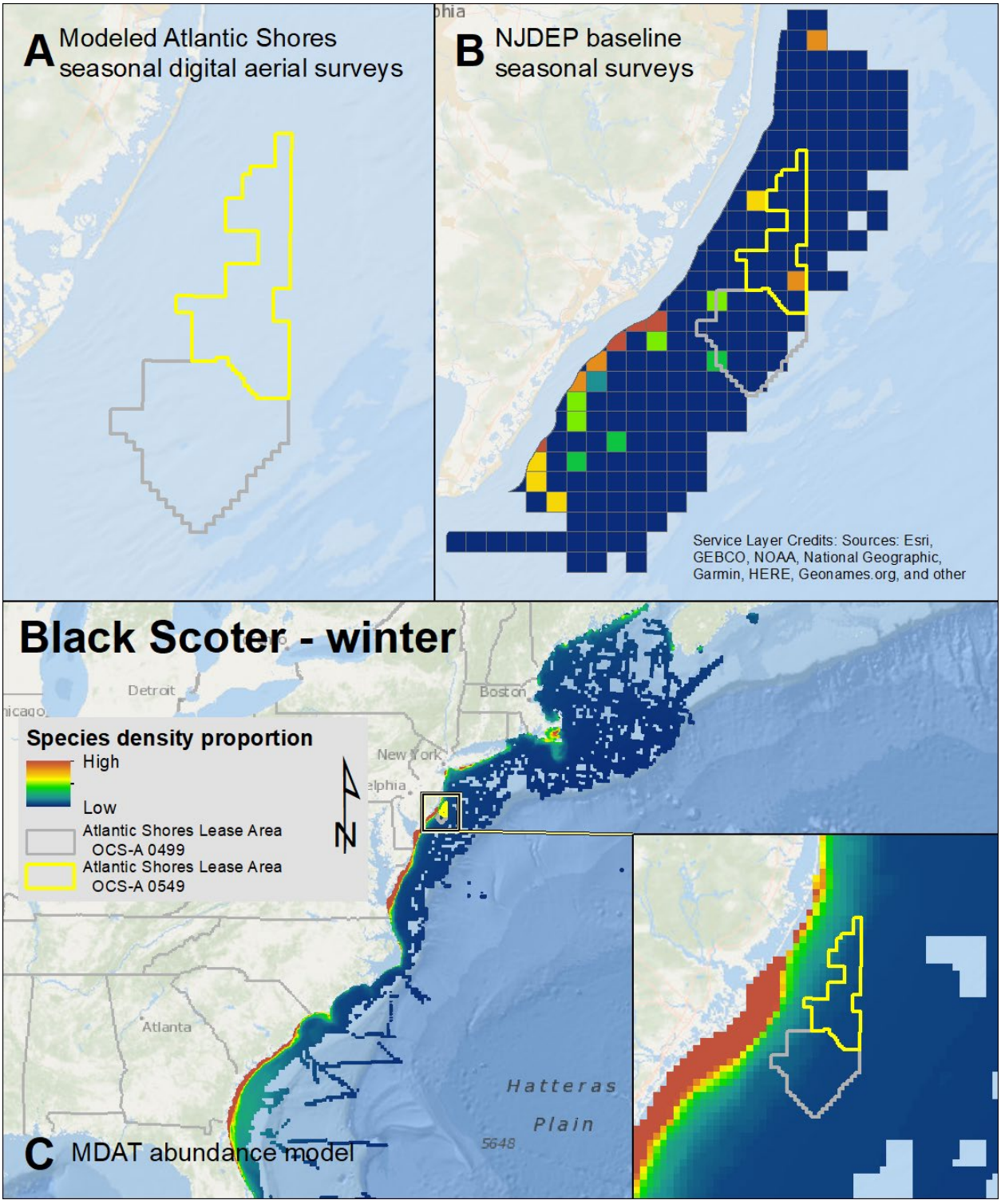

Map 15. Winter Black Scoter modeled density proportions in the Atlantic Shores seasonal digital aerial surveys (A), density proportions in the NJDEP baseline survey data (B), and the MDAT model outputs at local and regional scales (C). The scale for all maps is representative of relative spatial variation in the sites within the season for each information source.

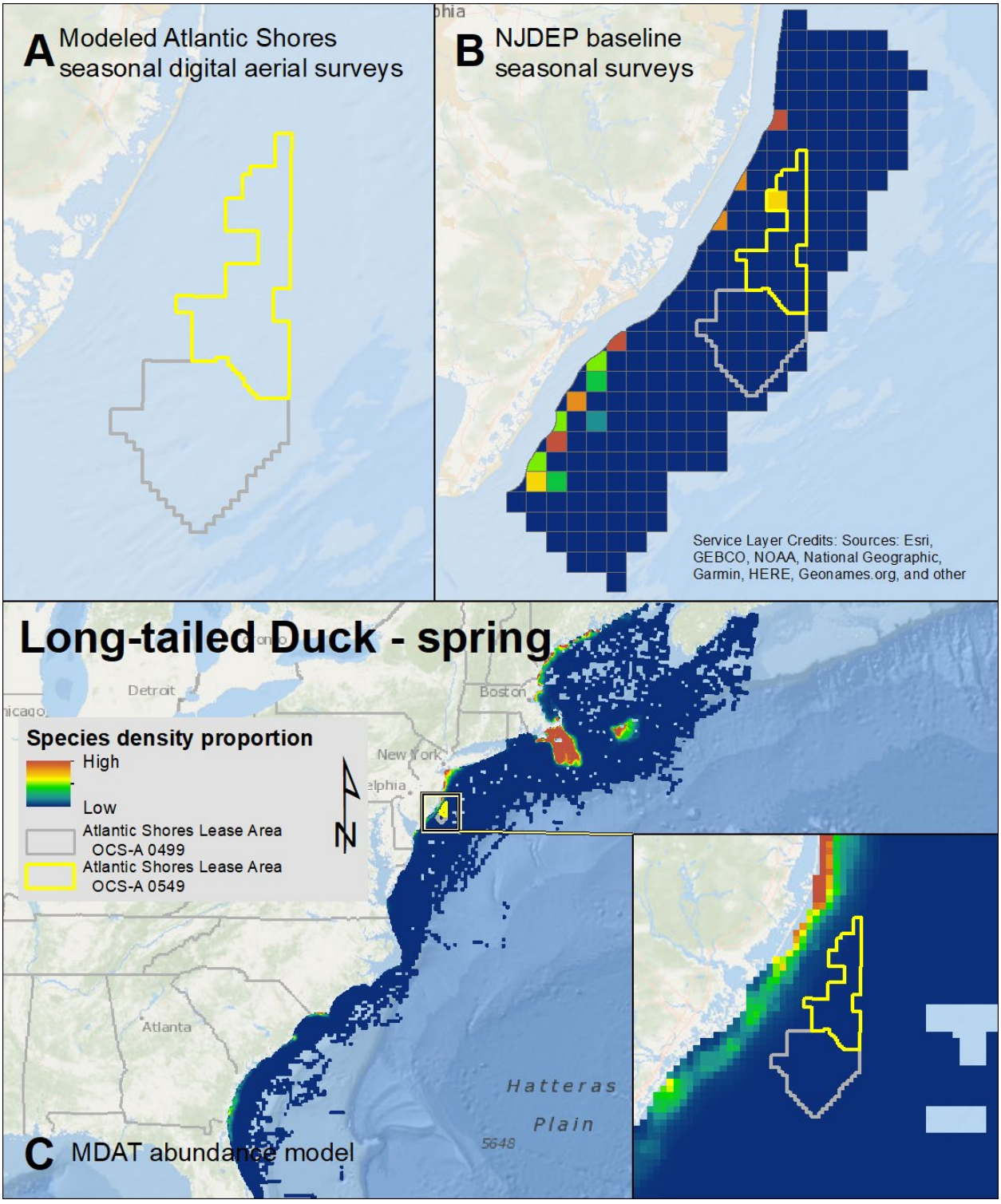

Map 16. Spring Long-tailed Duck modeled density proportions in the Atlantic Shores seasonal digital aerial surveys (A), density proportions in the NJDEP baseline survey data (B), and the MDAT model outputs at local and regional scales (C). The scale for all maps is representative of relative spatial variation in the sites within the season for each information source.

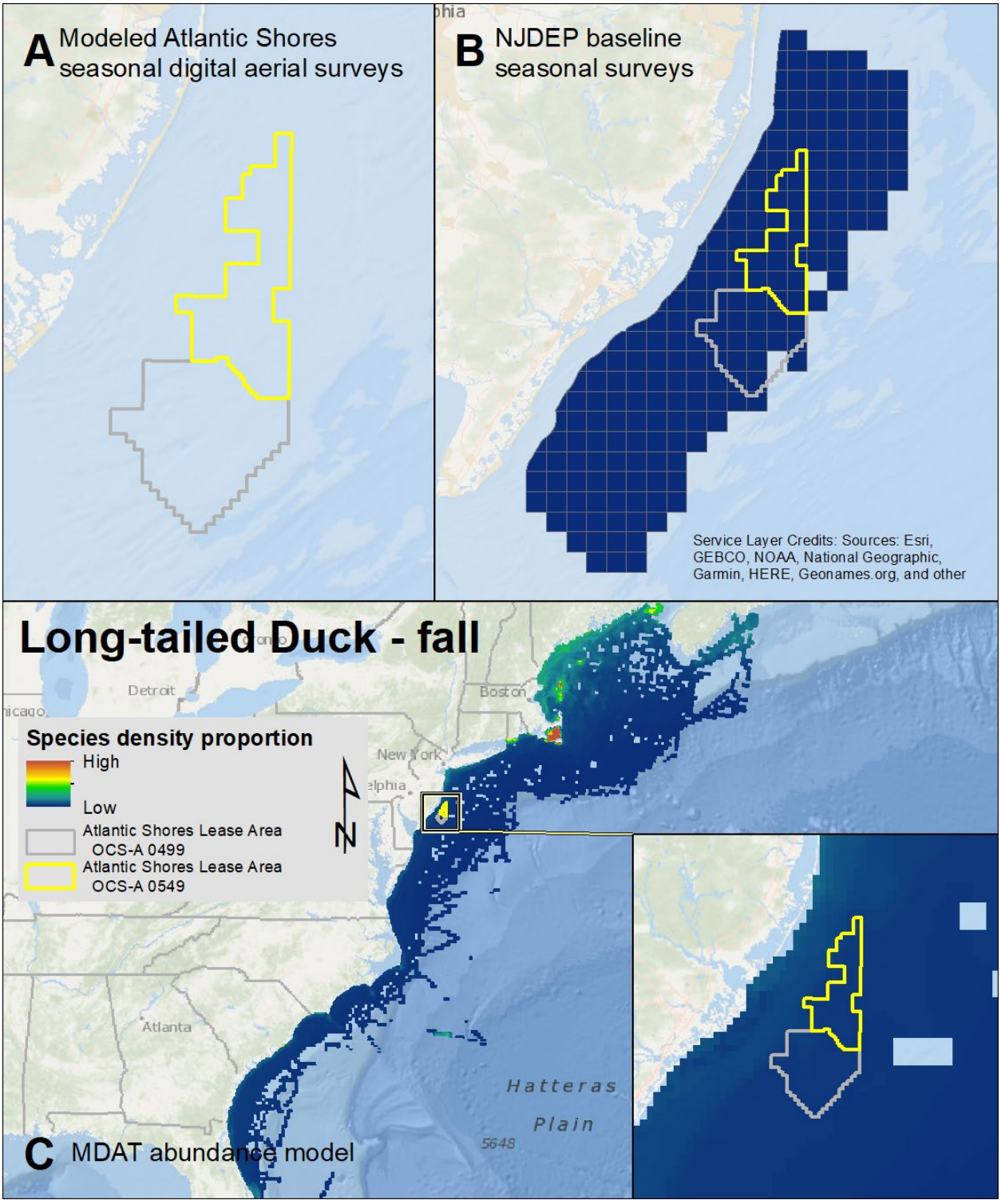

Map 17. Fall Long-tailed Duck modeled density proportions in the Atlantic Shores seasonal digital aerial surveys (A), density proportions in the NJDEP baseline survey data (B), and the MDAT model outputs at local and regional scales (C). The scale for all maps is representative of relative spatial variation in the sites within the season for each information source.

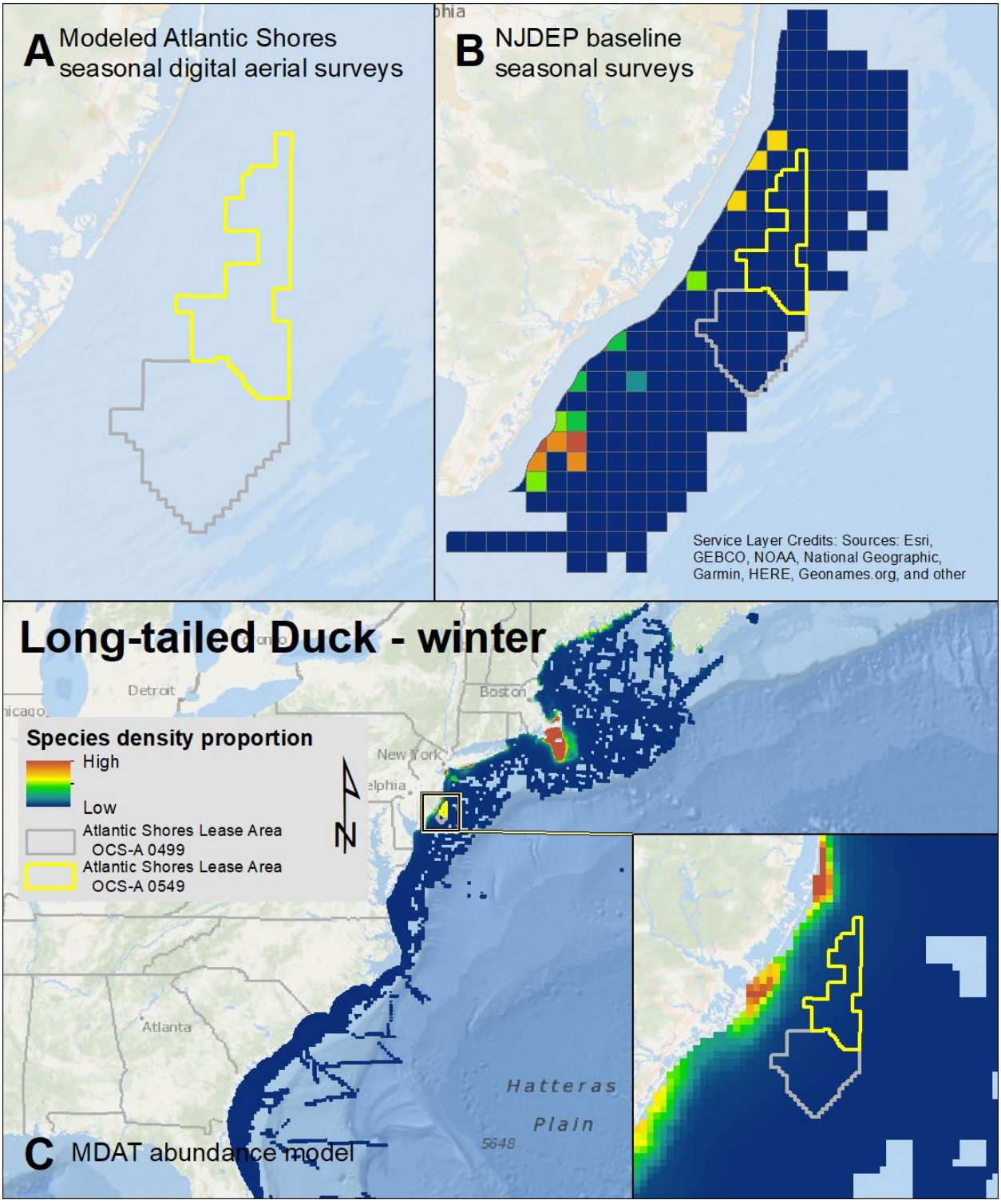

Map 18. Winter Long-tailed Duck modeled density proportions in the Atlantic Shores seasonal digital aerial surveys (A), density proportions in the NJDEP baseline survey data (B), and the MDAT model outputs at local and regional scales (C). The scale for all maps is representative of relative spatial variation in the sites within the season for each information source.

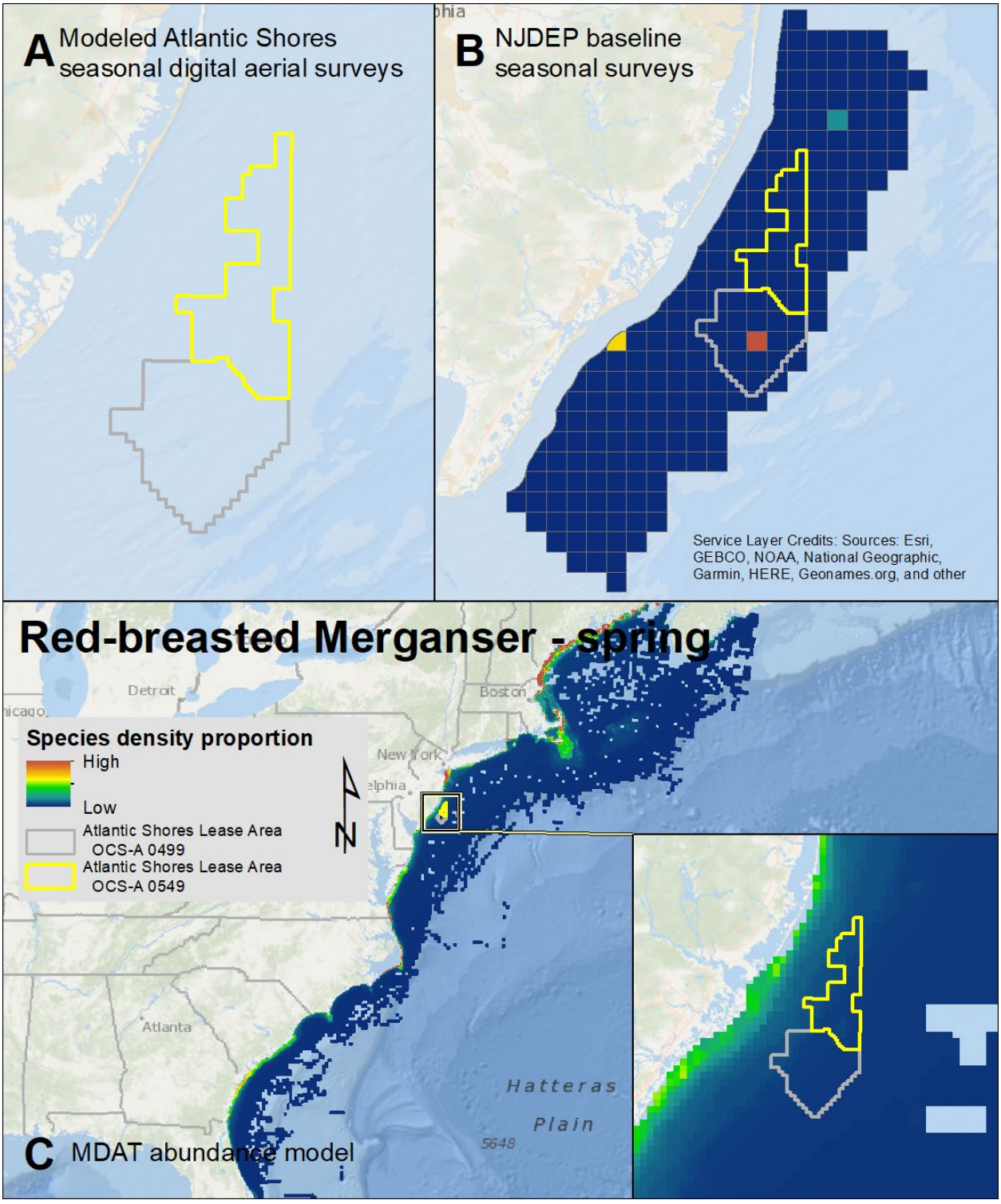

Map 19. Spring Red-breasted Merganser modeled density proportions in the Atlantic Shores seasonal digital aerial surveys (A), density proportions in the NJDEP baseline survey data (B), and the MDAT model outputs at local and regional scales (C). The scale for all maps is representative of relative spatial variation in the sites within the season for each information source.

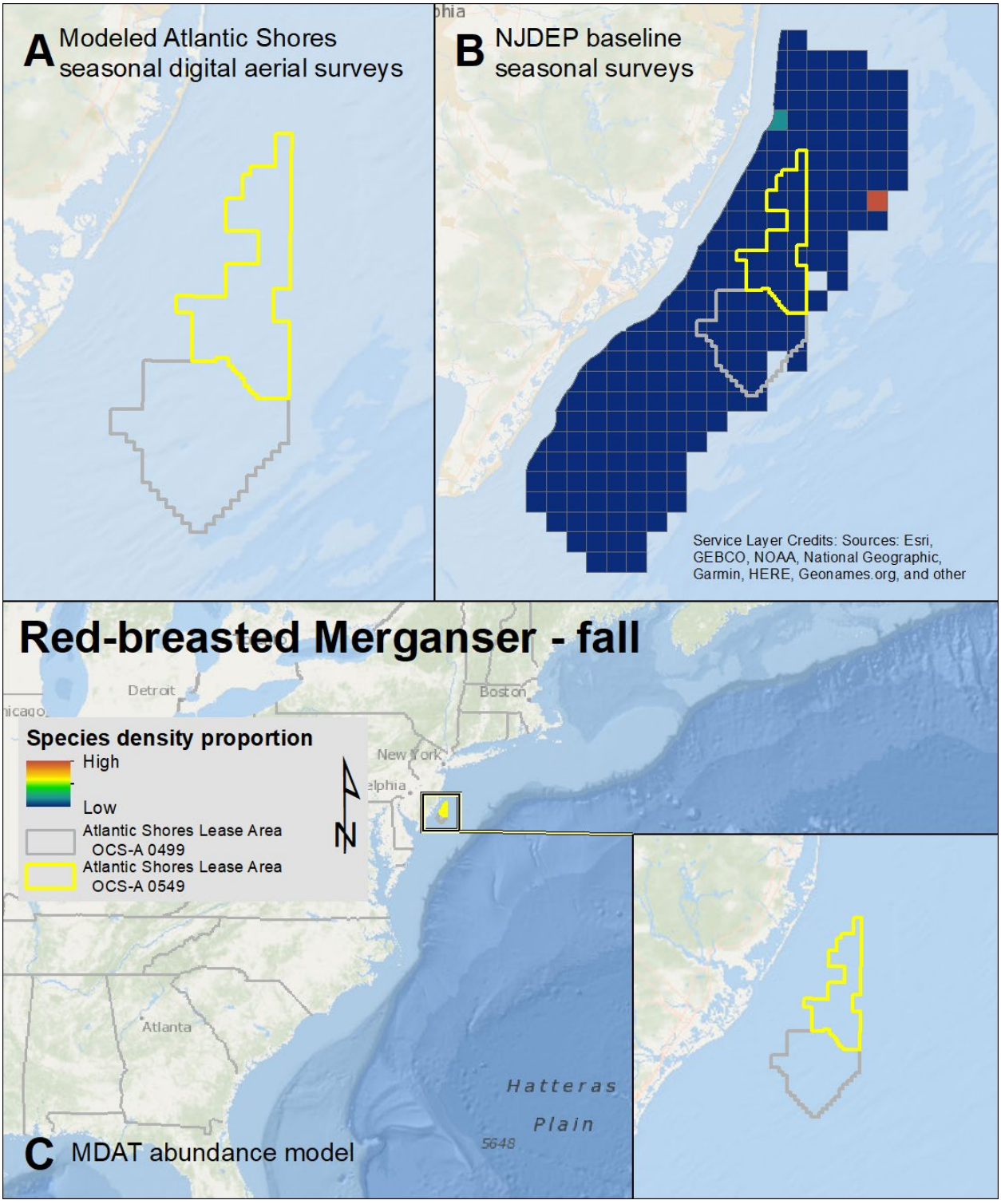

Map 20. Fall Red-breasted Merganser modeled density proportions in the Atlantic Shores seasonal digital aerial surveys (A), density proportions in the NJDEP baseline survey data (B), and the MDAT model outputs at local and regional scales (C). The scale for all maps is representative of relative spatial variation in the sites within the season for each information source.

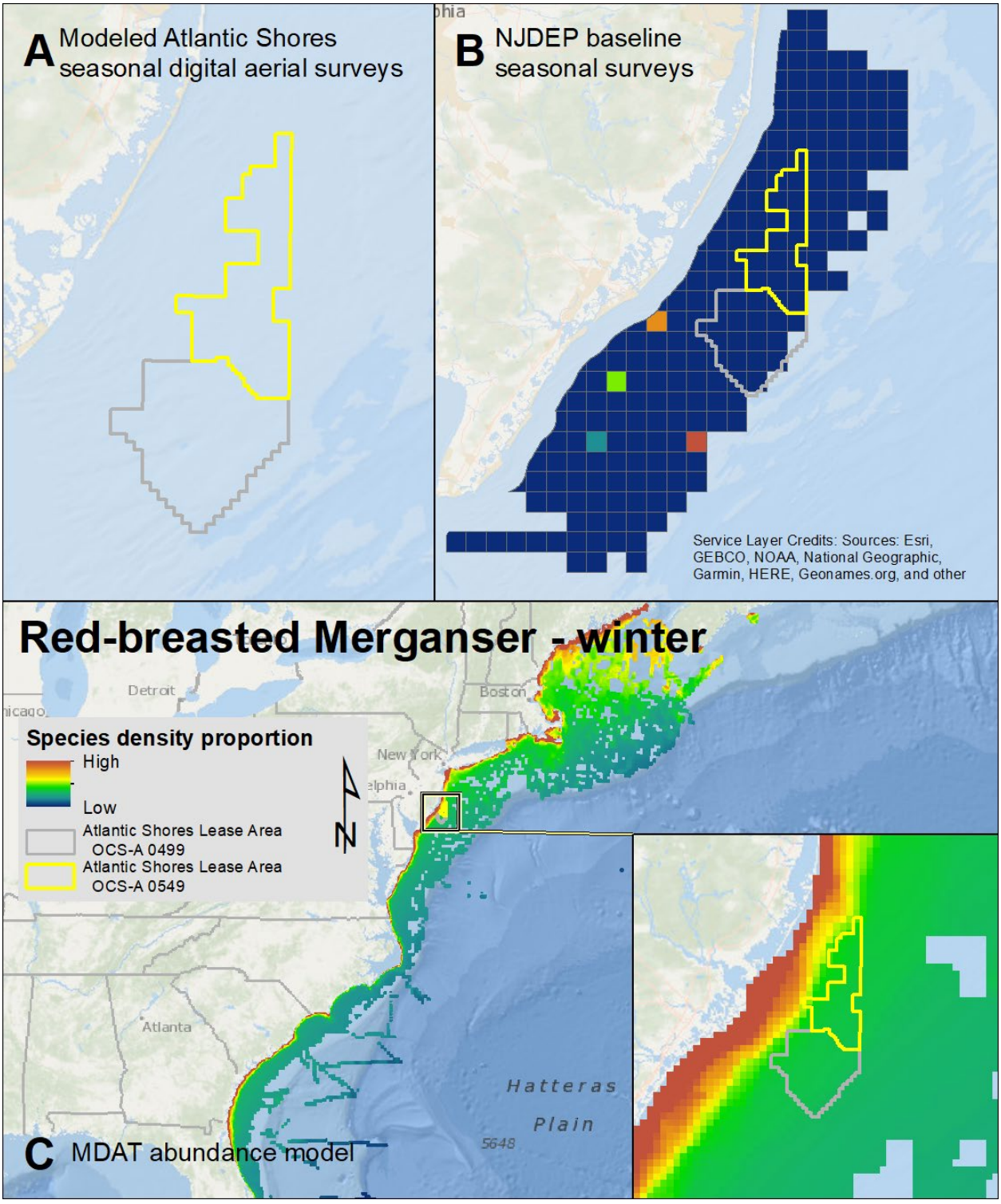

Map 21. Winter Red-breasted Merganser modeled density proportions in the Atlantic Shores seasonal digital aerial surveys (A), density proportions in the NJDEP baseline survey data (B), and the MDAT model outputs at local and regional scales (C). The scale for all maps is representative of relative spatial variation in the sites within the season for each information source.

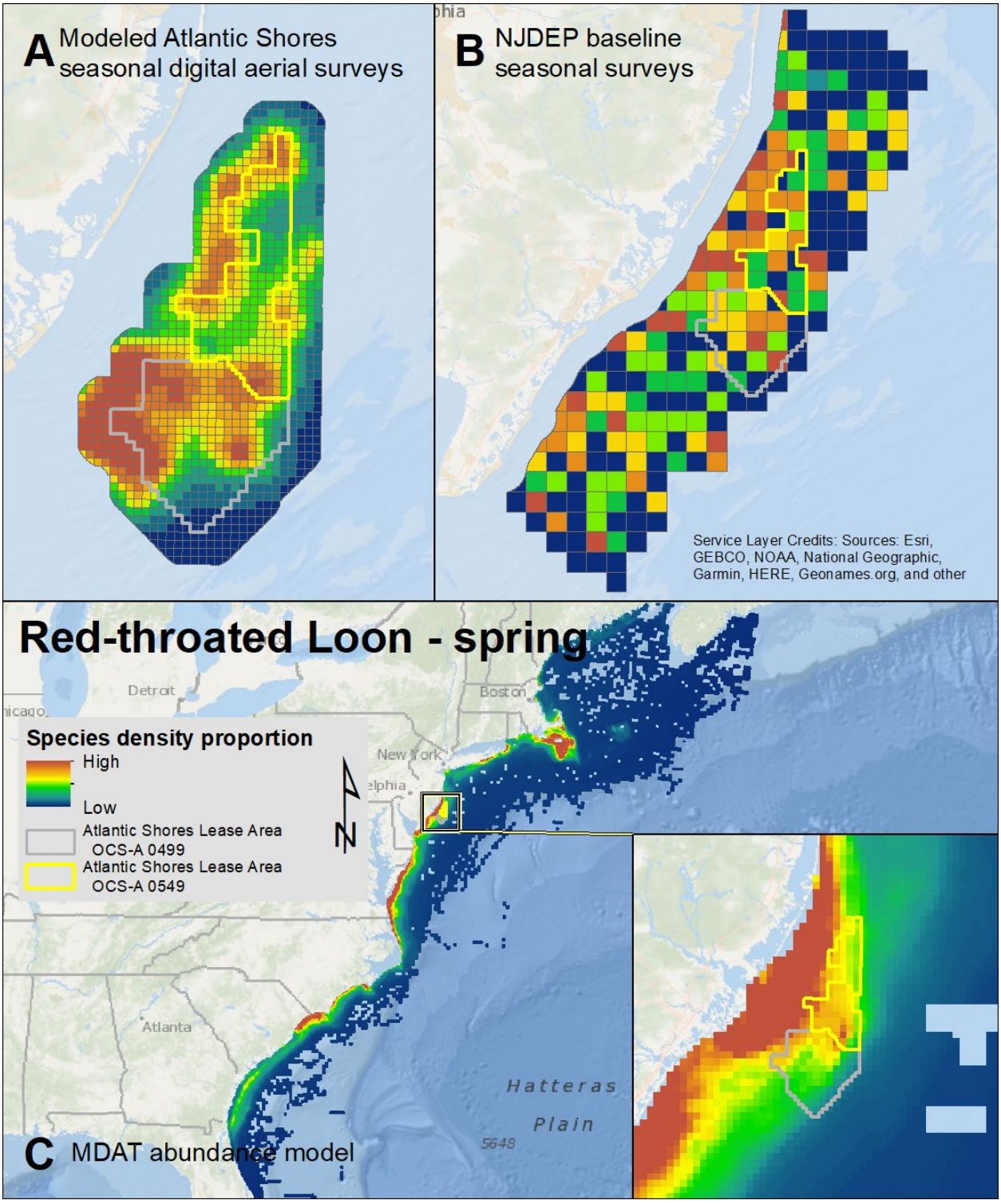

Map 22. Spring Red-throated Loon modeled density proportions in the Atlantic Shores seasonal digital aerial surveys (A), density proportions in the NJDEP baseline survey data (B), and the MDAT model outputs at local and regional scales (C). The scale for all maps is representative of relative spatial variation in the sites within the season for each information source.

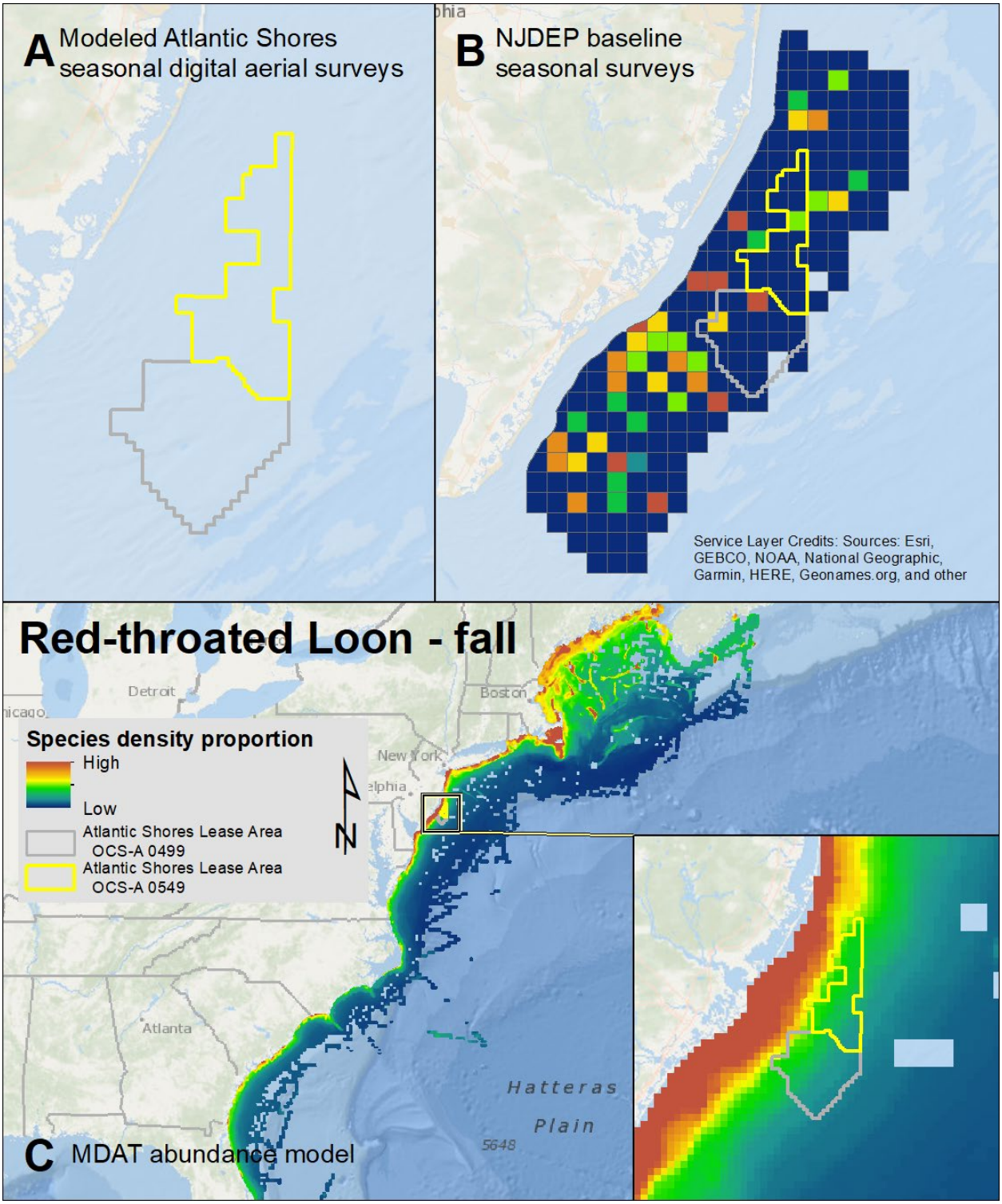

Map 23. Fall Red-throated Loon modeled density proportions in the Atlantic Shores seasonal digital aerial surveys (A), density proportions in the NJDEP baseline survey data (B), and the MDAT model outputs at local and regional scales (C). The scale for all maps is representative of relative spatial variation in the sites within the season for each information source.

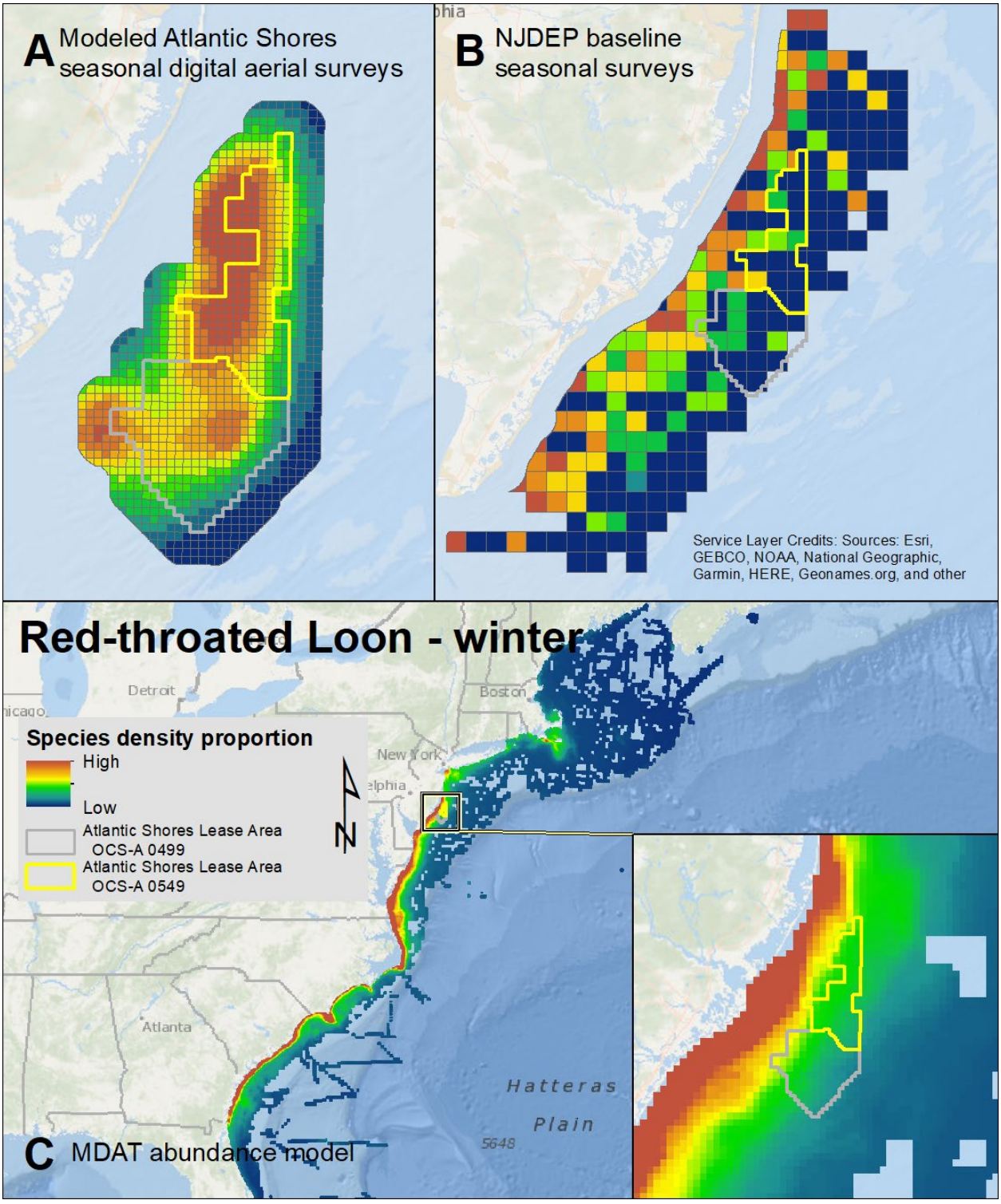

Map 24. Winter Red-throated Loon modeled density proportions in the Atlantic Shores seasonal digital aerial surveys (A), density proportions in the NJDEP baseline survey data (B), and the MDAT model outputs at local and regional scales (C). The scale for all maps is representative of relative spatial variation in the sites within the season for each information source.

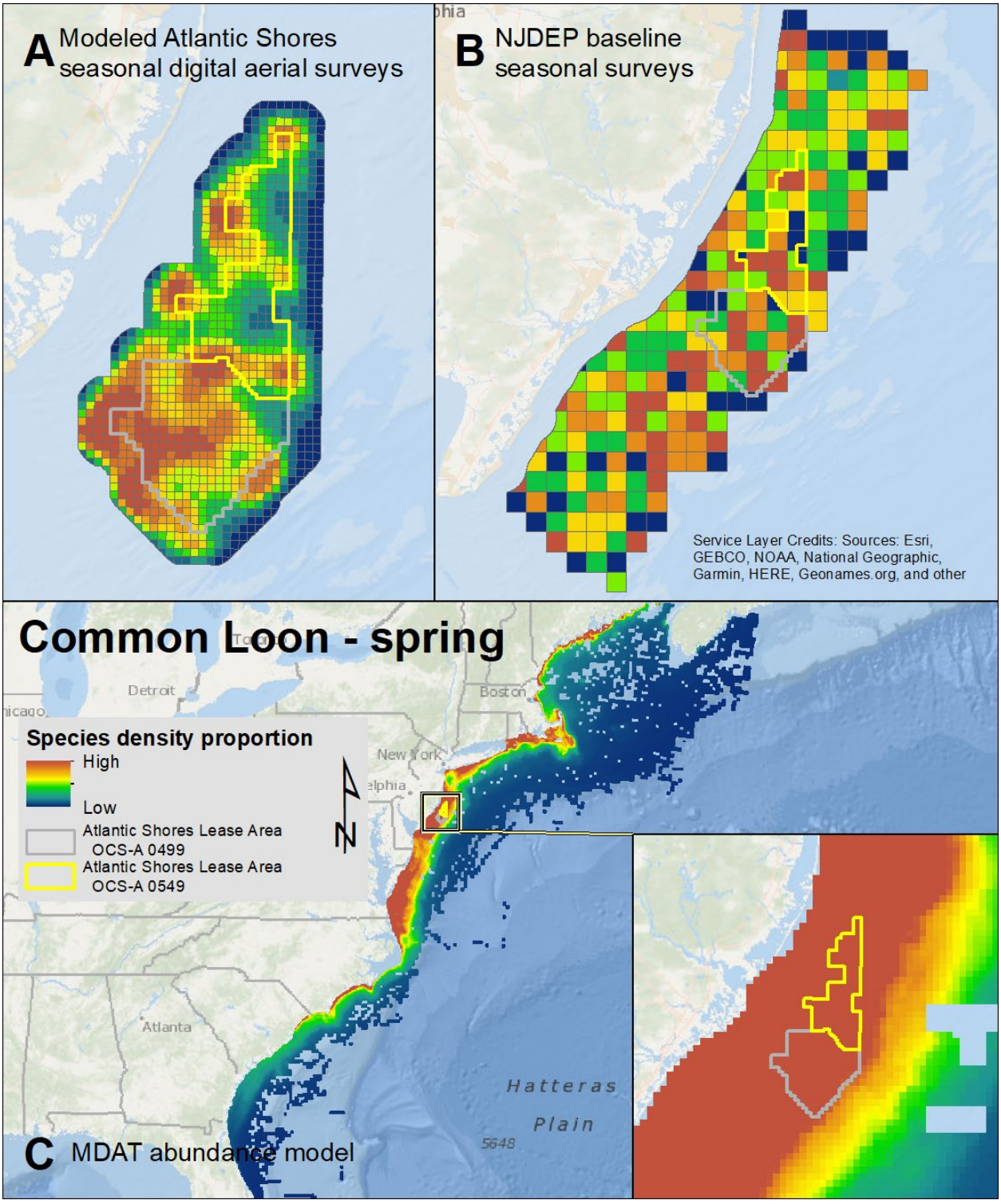

Map 25. Spring Common Loon modeled density proportions in the Atlantic Shores seasonal digital aerial surveys (A), density proportions in the NJDEP baseline survey data (B), and the MDAT model outputs at local and regional scales (C). The scale for all maps is representative of relative spatial variation in the sites within the season for each information source.

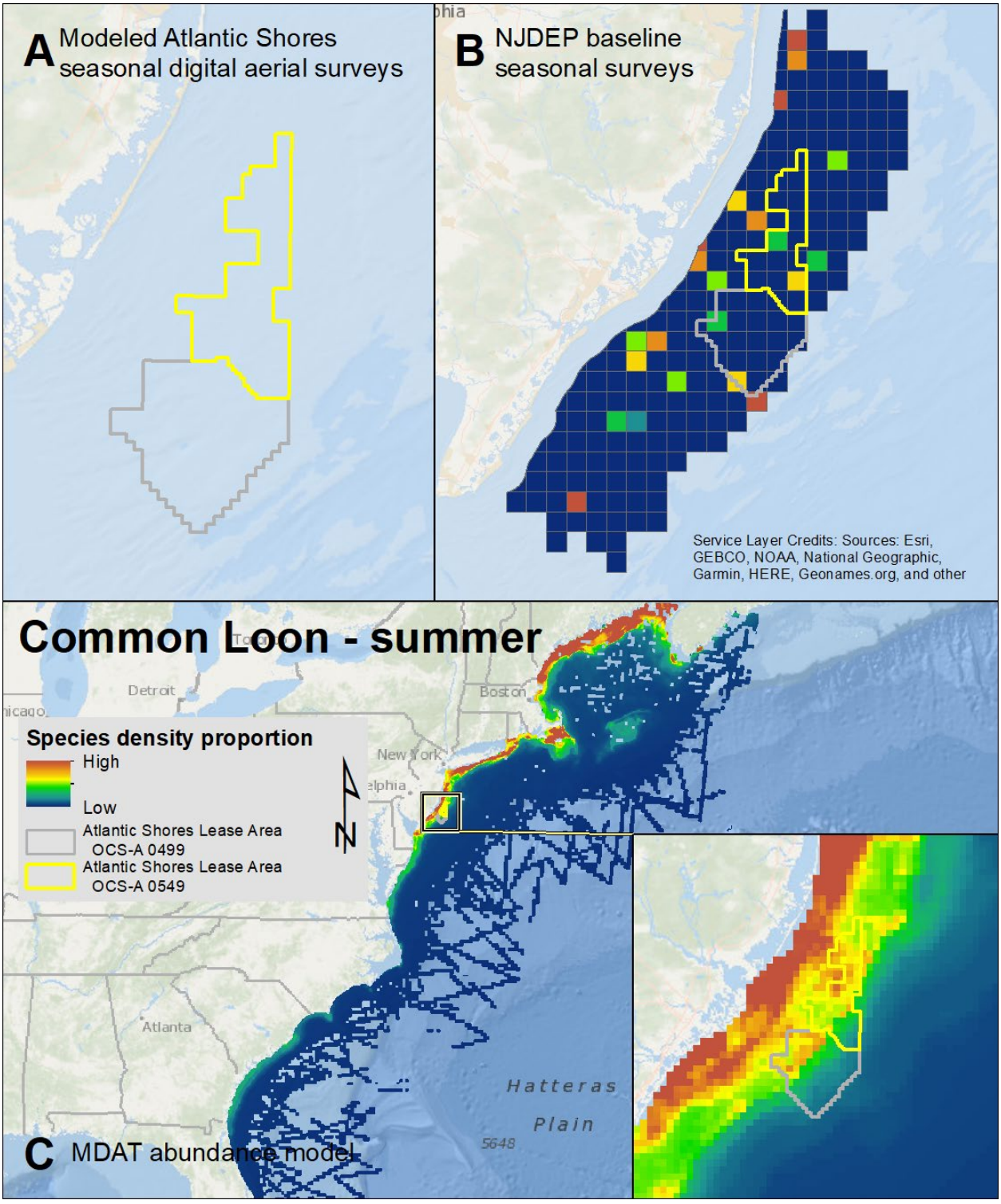

Map 26. Summer Common Loon modeled density proportions in the Atlantic Shores seasonal digital aerial surveys (A), density proportions in the NJDEP baseline survey data (B), and the MDAT model outputs at local and regional scales (C). The scale for all maps is representative of relative spatial variation in the sites within the season for each information source.

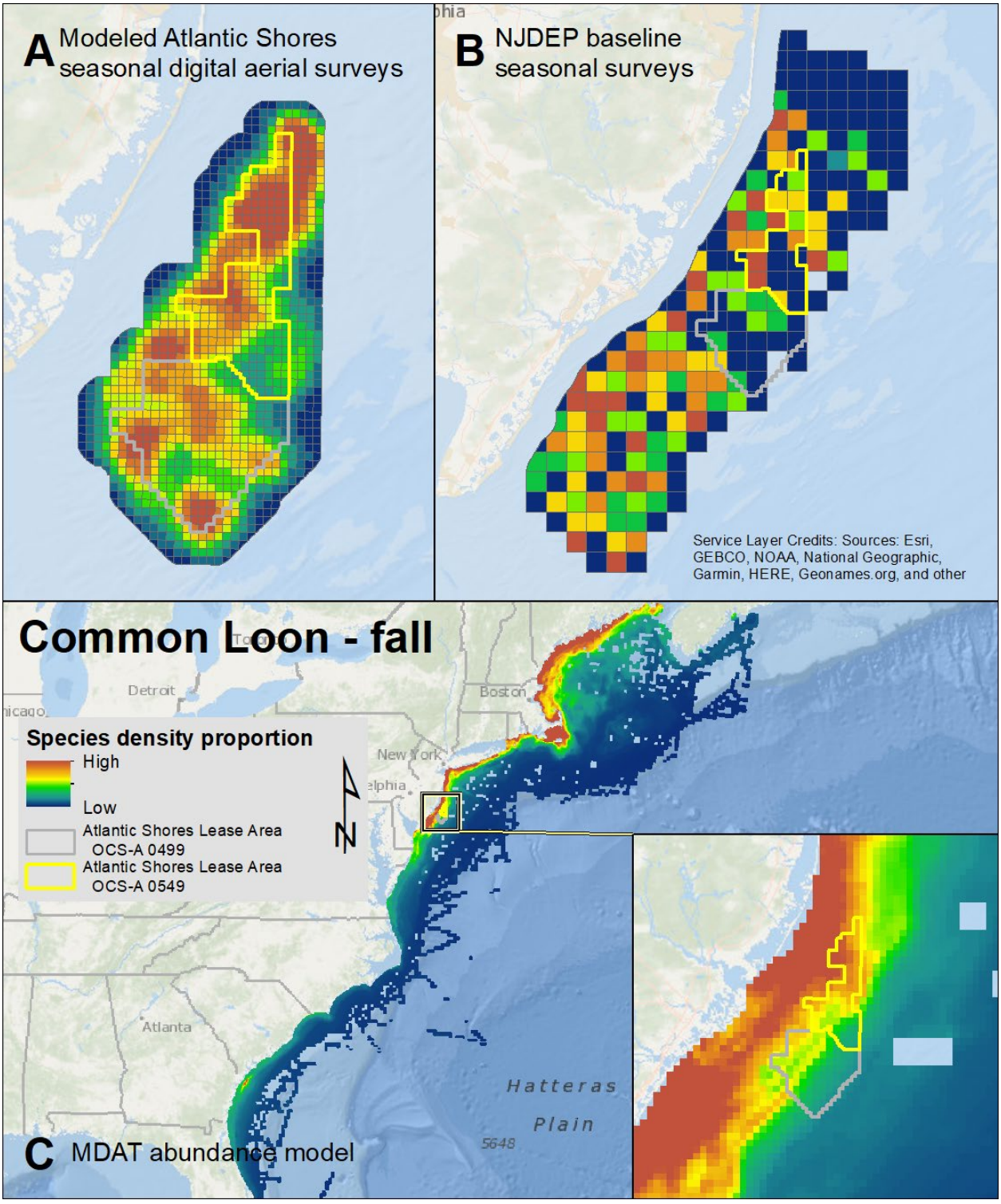

Map 27. Fall Common Loon modeled density proportions in the Atlantic Shores seasonal digital aerial surveys (A), density proportions in the NJDEP baseline survey data (B), and the MDAT model outputs at local and regional scales (C). The scale for all maps is representative of relative spatial variation in the sites within the season for each information source.

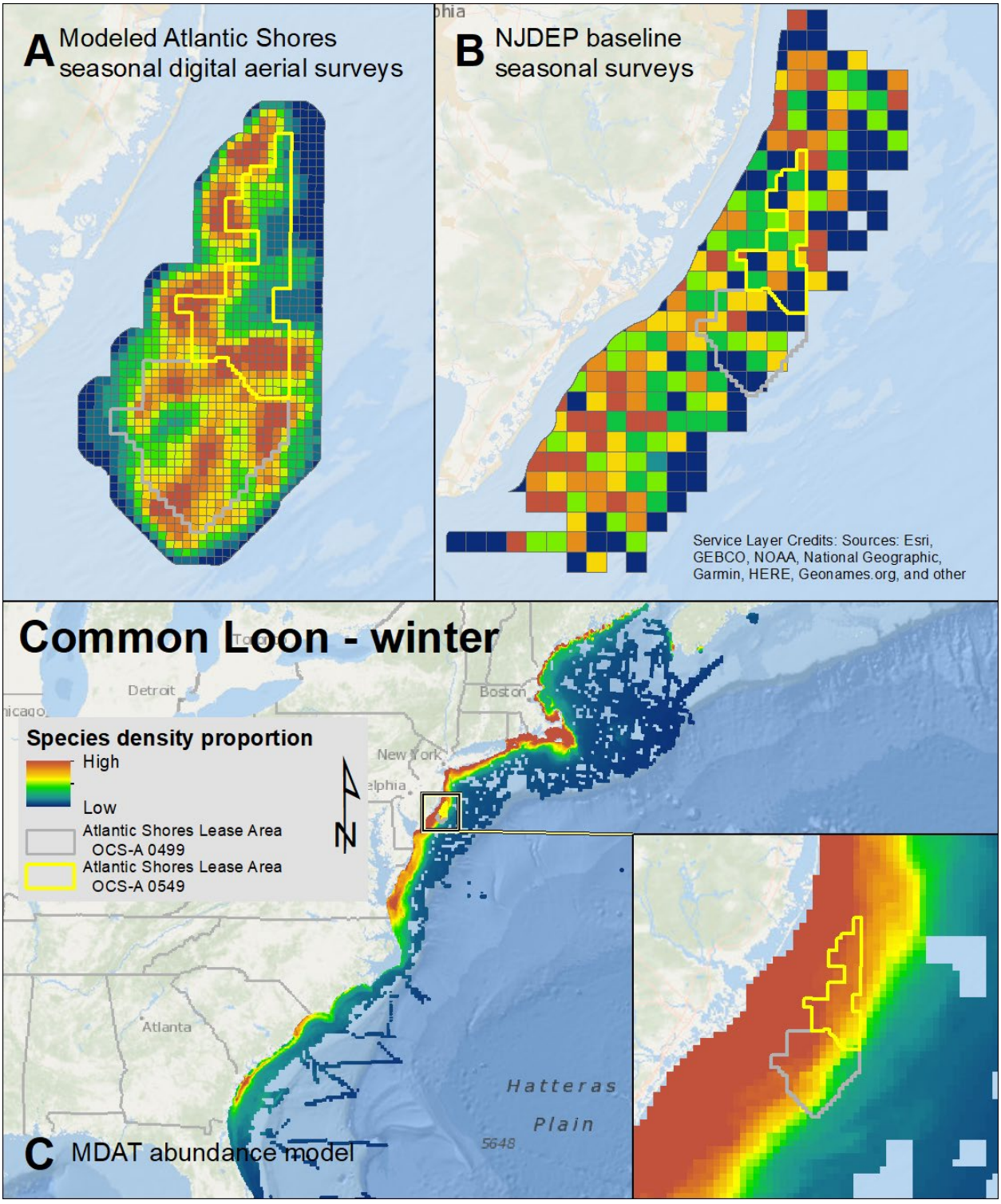

Map 28. Winter Common Loon modeled density proportions in the Atlantic Shores seasonal digital aerial surveys (A), density proportions in the NJDEP baseline survey data (B), and the MDAT model outputs at local and regional scales (C). The scale for all maps is representative of relative spatial variation in the sites within the season for each information source.

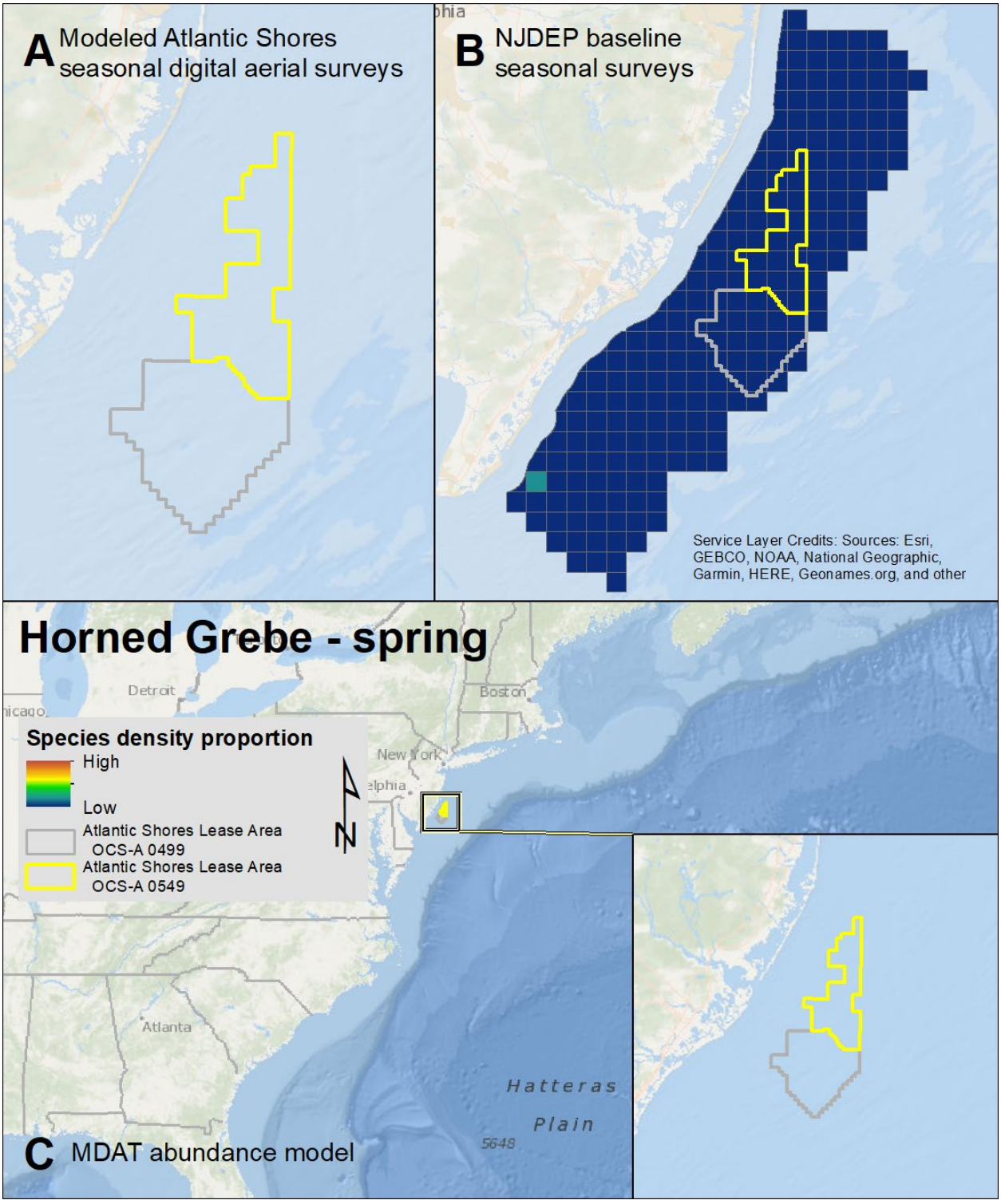

Map 29. Spring Horned Grebe modeled density proportions in the Atlantic Shores seasonal digital aerial surveys (A), density proportions in the NJDEP baseline survey data (B), and the MDAT model outputs at local and regional scales (C). The scale for all maps is representative of relative spatial variation in the sites within the season for each information source.

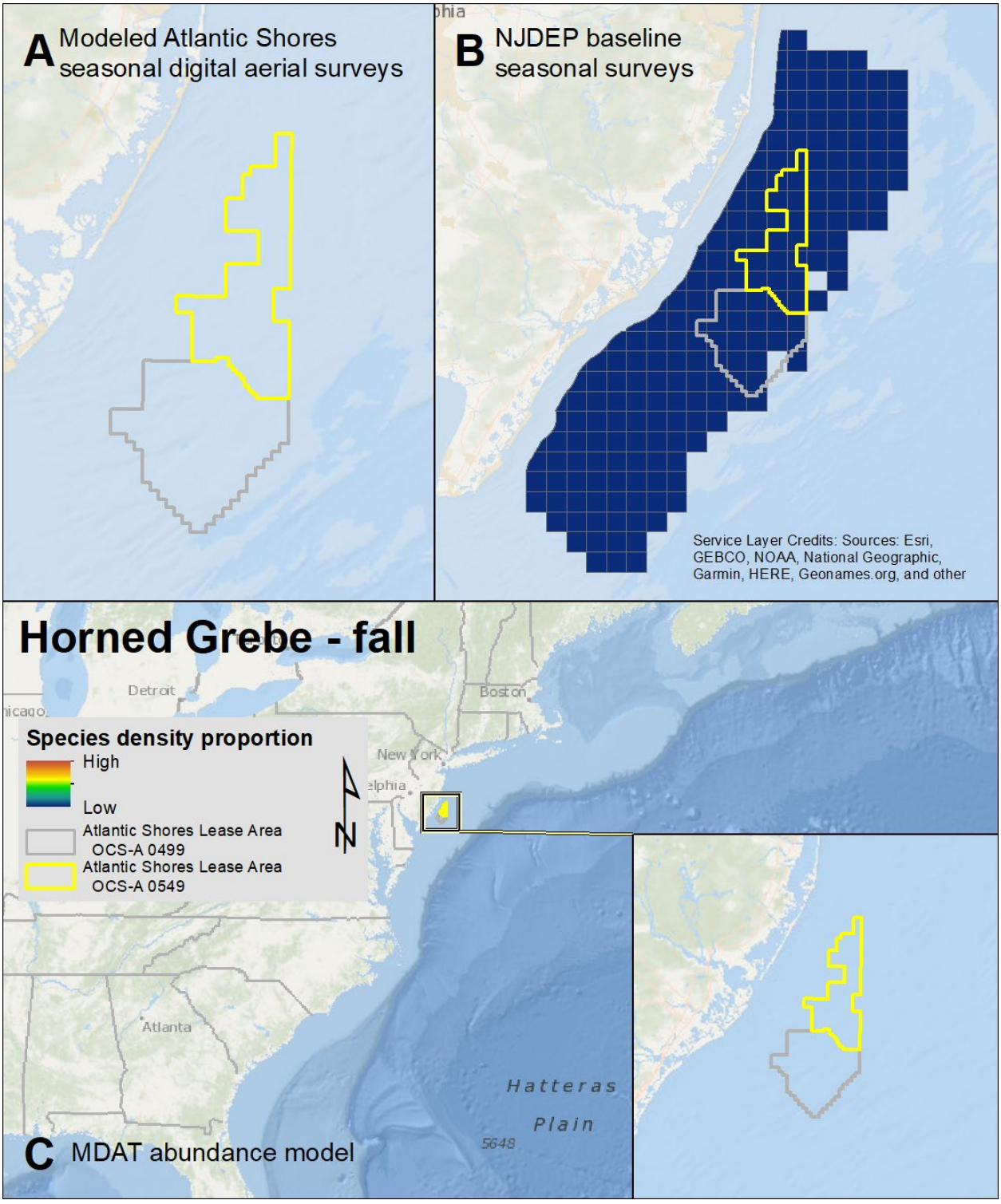

Map 30. Fall Horned Grebe modeled density proportions in the Atlantic Shores seasonal digital aerial surveys (A), density proportions in the NJDEP baseline survey data (B), and the MDAT model outputs at local and regional scales (C). The scale for all maps is representative of relative spatial variation in the sites within the season for each information source.

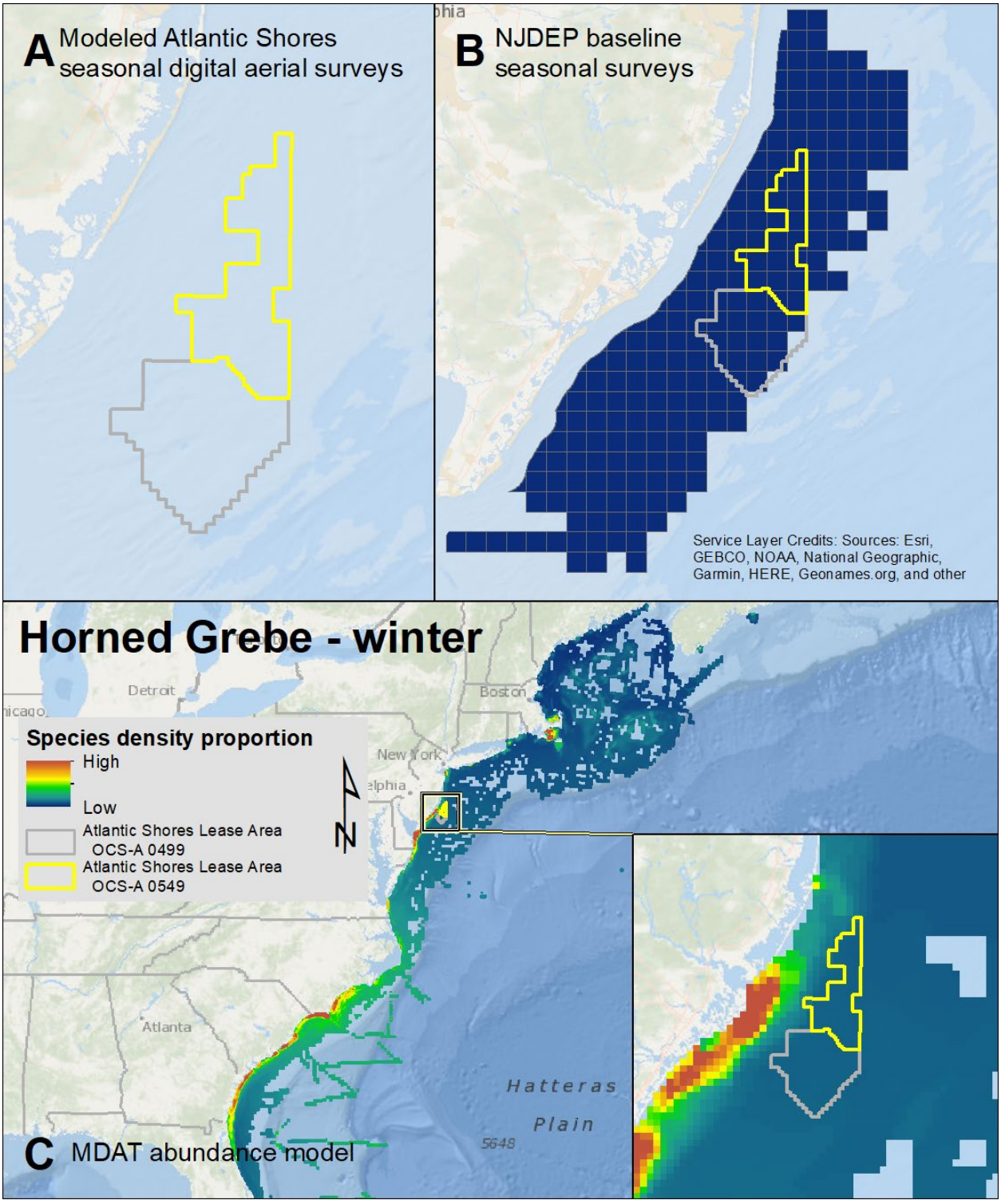

Map 31. Winter Horned Grebe modeled density proportions in the Atlantic Shores seasonal digital aerial surveys (A), density proportions in the NJDEP baseline survey data (B), and the MDAT model outputs at local and regional scales (C). The scale for all maps is representative of relative spatial variation in the sites within the season for each information source.

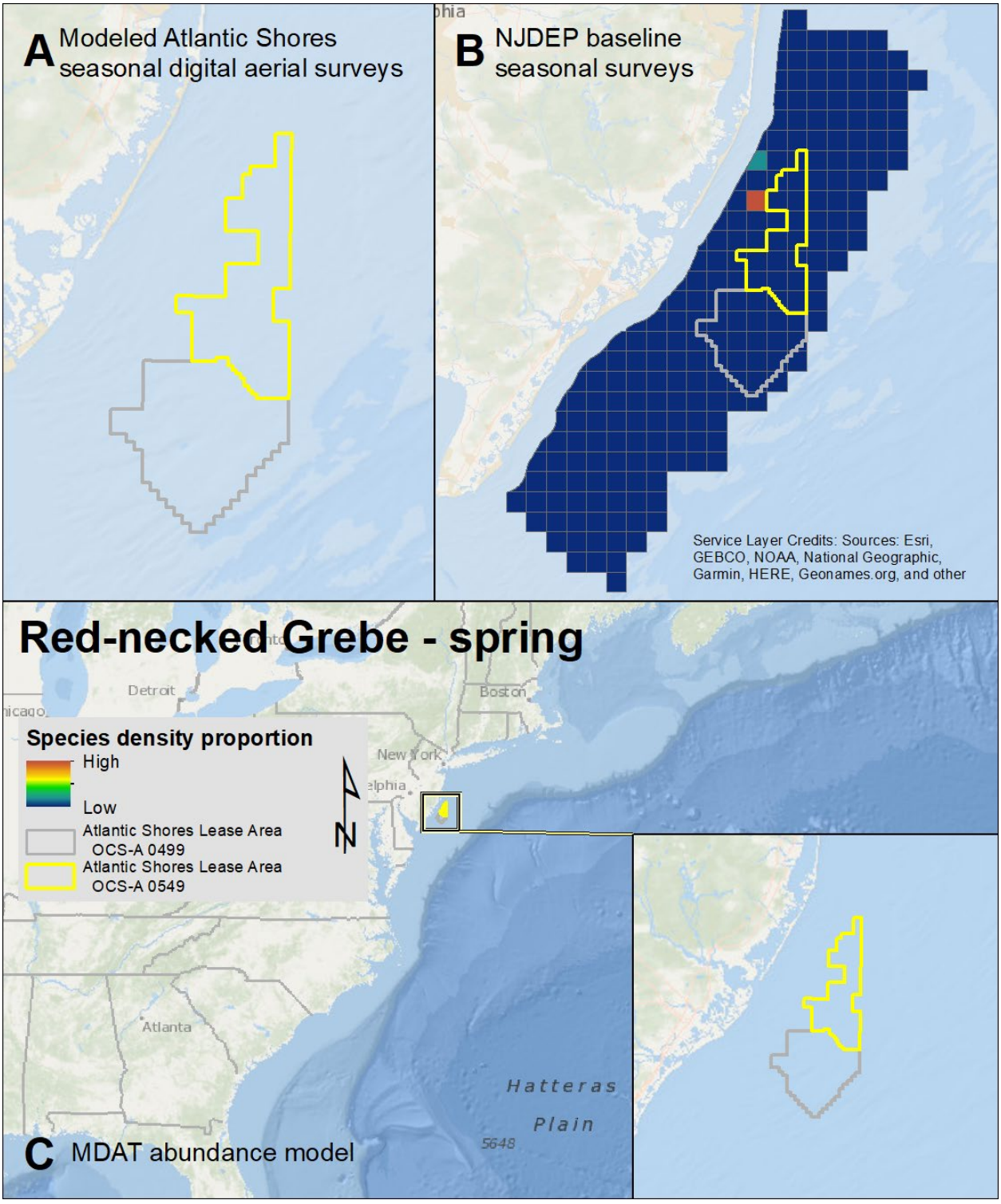

Map 32. Spring Red-necked Grebe modeled density proportions in the Atlantic Shores seasonal digital aerial surveys (A), density proportions in the NJDEP baseline survey data (B), and the MDAT model outputs at local and regional scales (C). The scale for all maps is representative of relative spatial variation in the sites within the season for each information source.

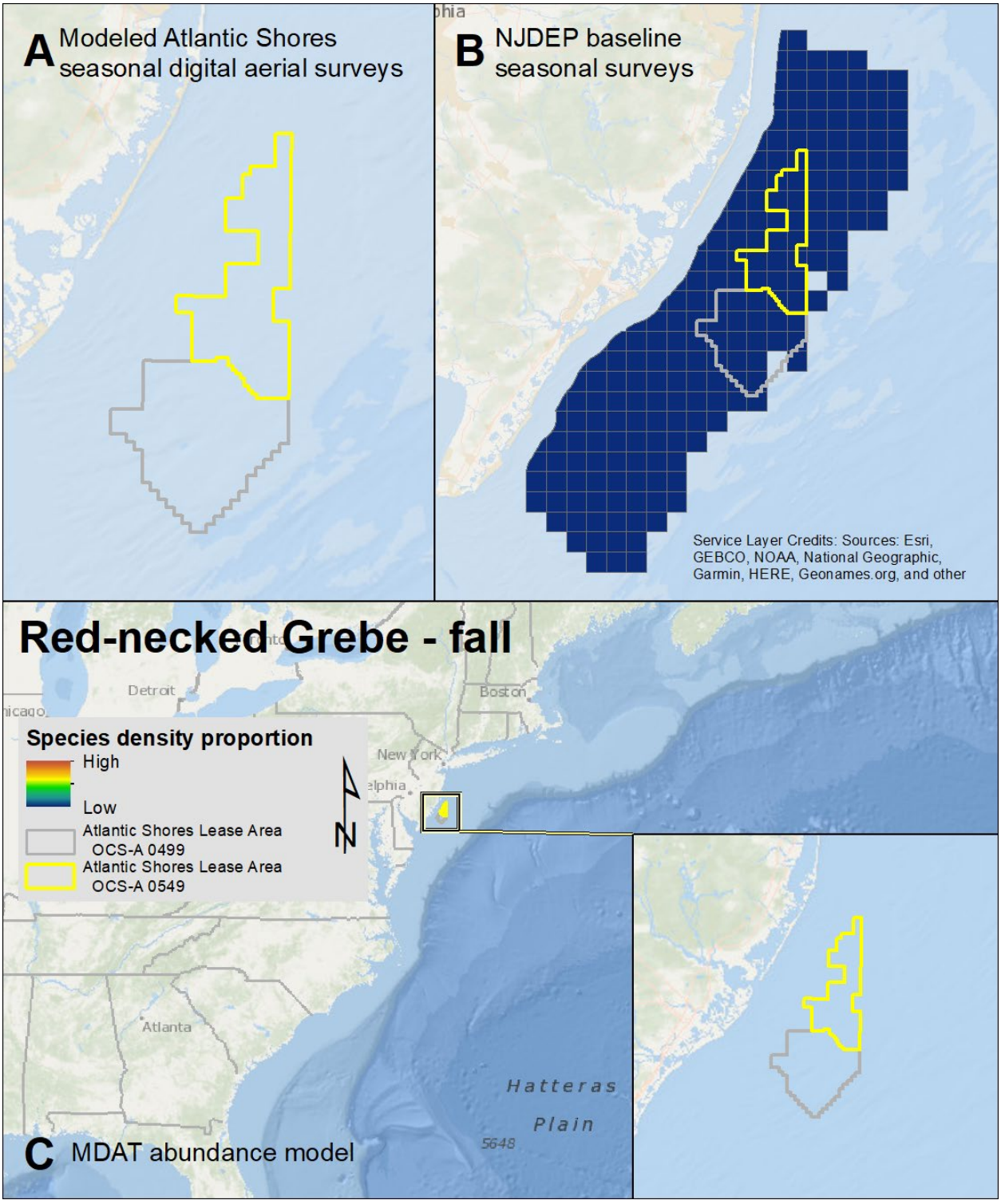

Map 33. Fall Red-necked Grebe modeled density proportions in the Atlantic Shores seasonal digital aerial surveys (A), density proportions in the NJDEP baseline survey data (B), and the MDAT model outputs at local and regional scales (C). The scale for all maps is representative of relative spatial variation in the sites within the season for each information source.

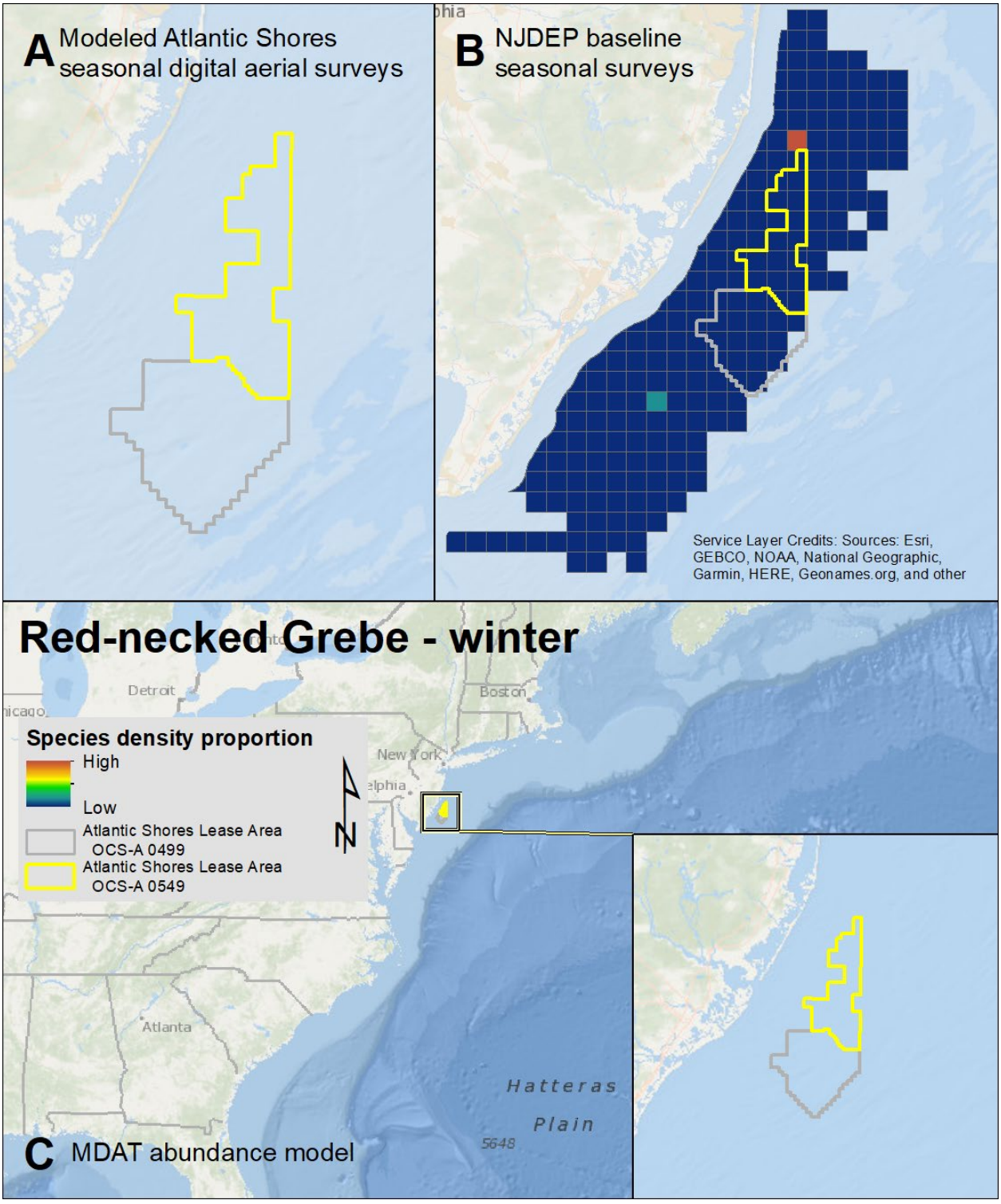

Map 34. Winter Red-necked Grebe modeled density proportions in the Atlantic Shores seasonal digital aerial surveys (A), density proportions in the NJDEP baseline survey data (B), and the MDAT model outputs at local and regional scales (C). The scale for all maps is representative of relative spatial variation in the sites within the season for each information source.

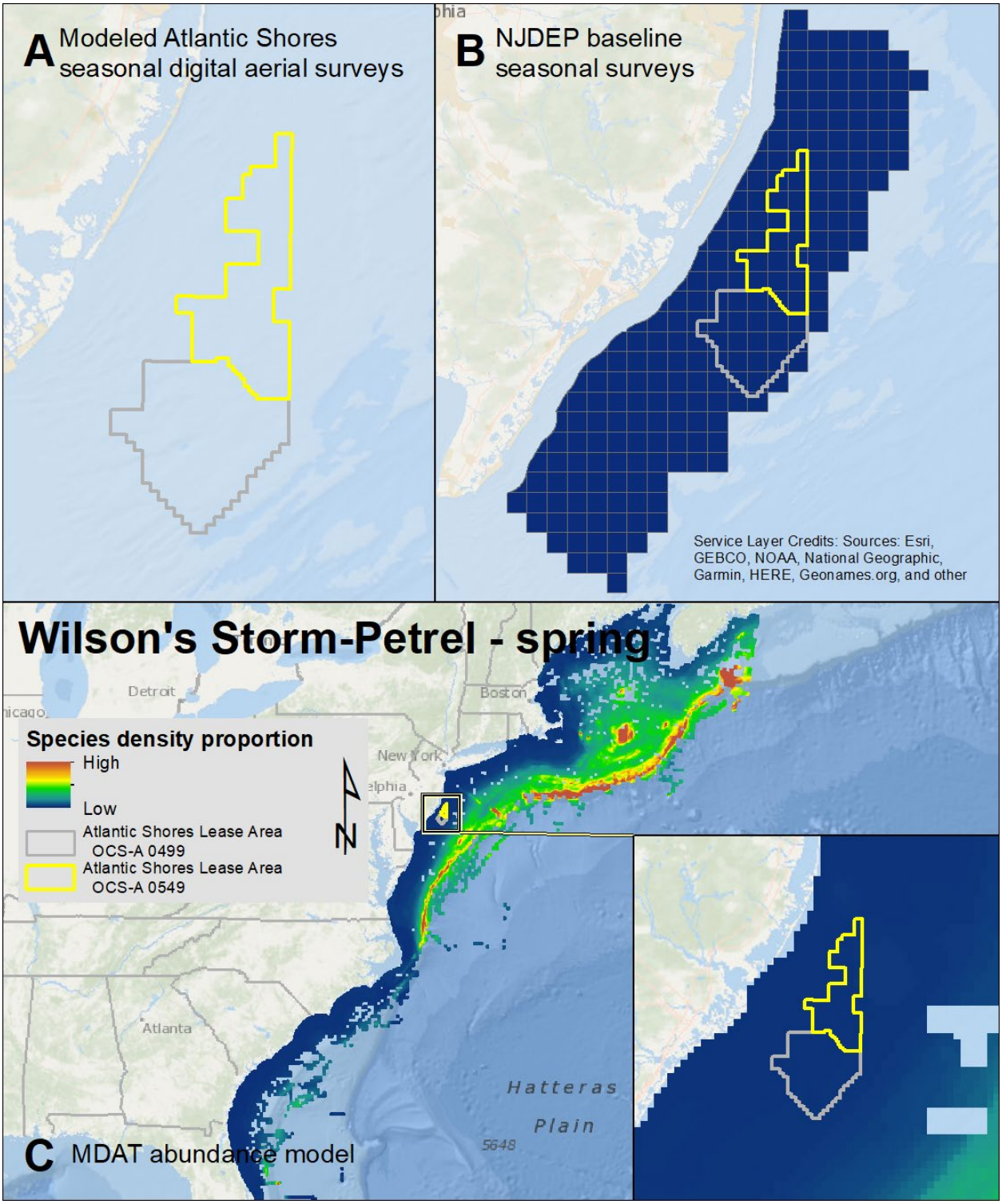

Map 35. Spring Wilson's Storm-Petrel modeled density proportions in the Atlantic Shores seasonal digital aerial surveys (A), density proportions in the NJDEP baseline survey data (B), and the MDAT model outputs at local and regional scales (C). The scale for all maps is representative of relative spatial variation in the sites within the season for each information source.

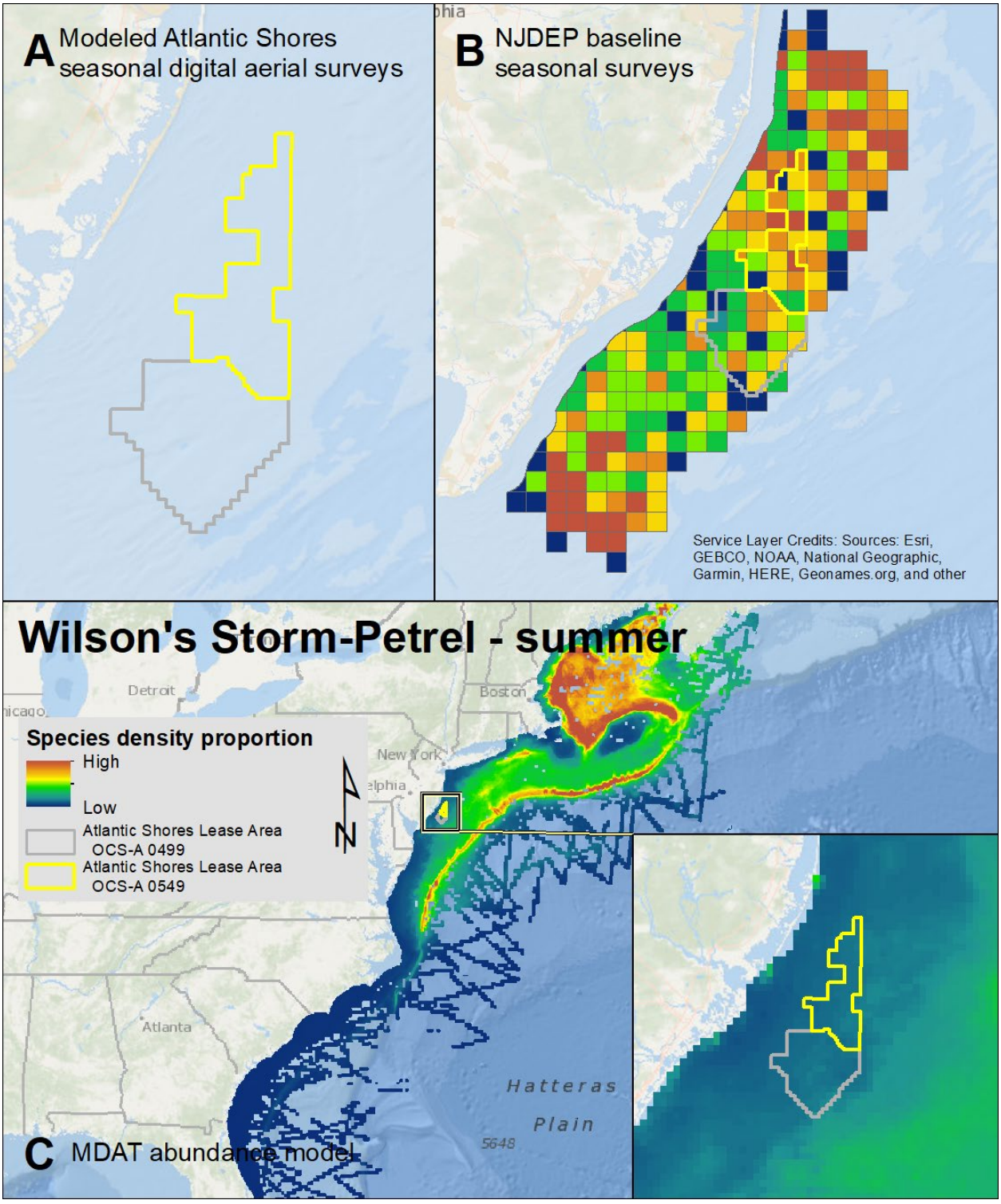

Map 36. Summer Wilson's Storm-Petrel modeled density proportions in the Atlantic Shores seasonal digital aerial surveys (A), density proportions in the NJDEP baseline survey data (B), and the MDAT model outputs at local and regional scales (C). The scale for all maps is representative of relative spatial variation in the sites within the season for each information source.

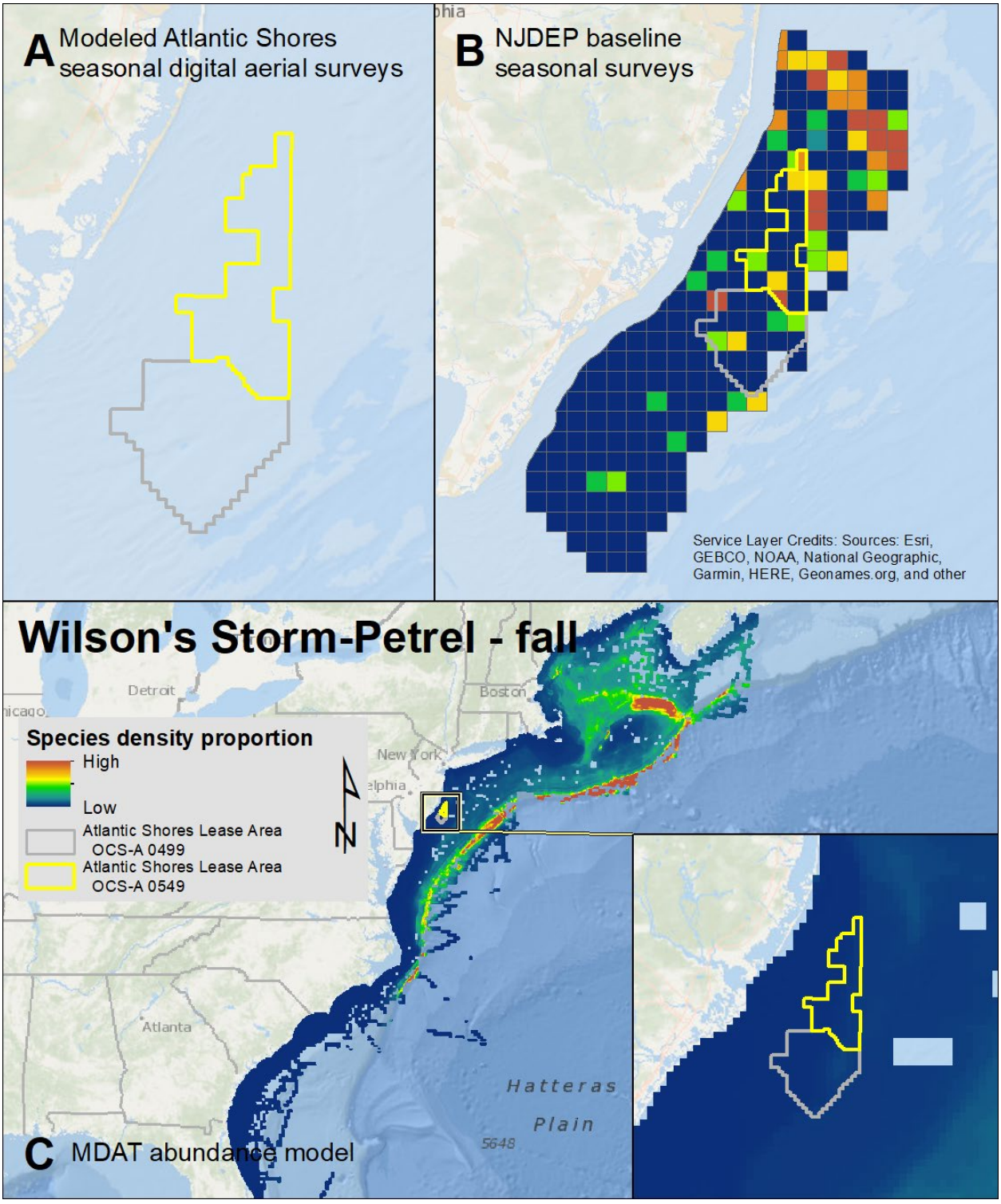

Map 37. Fall Wilson's Storm-Petrel modeled density proportions in the Atlantic Shores seasonal digital aerial surveys (A), density proportions in the NJDEP baseline survey data (B), and the MDAT model outputs at local and regional scales (C). The scale for all maps is representative of relative spatial variation in the sites within the season for each information source.

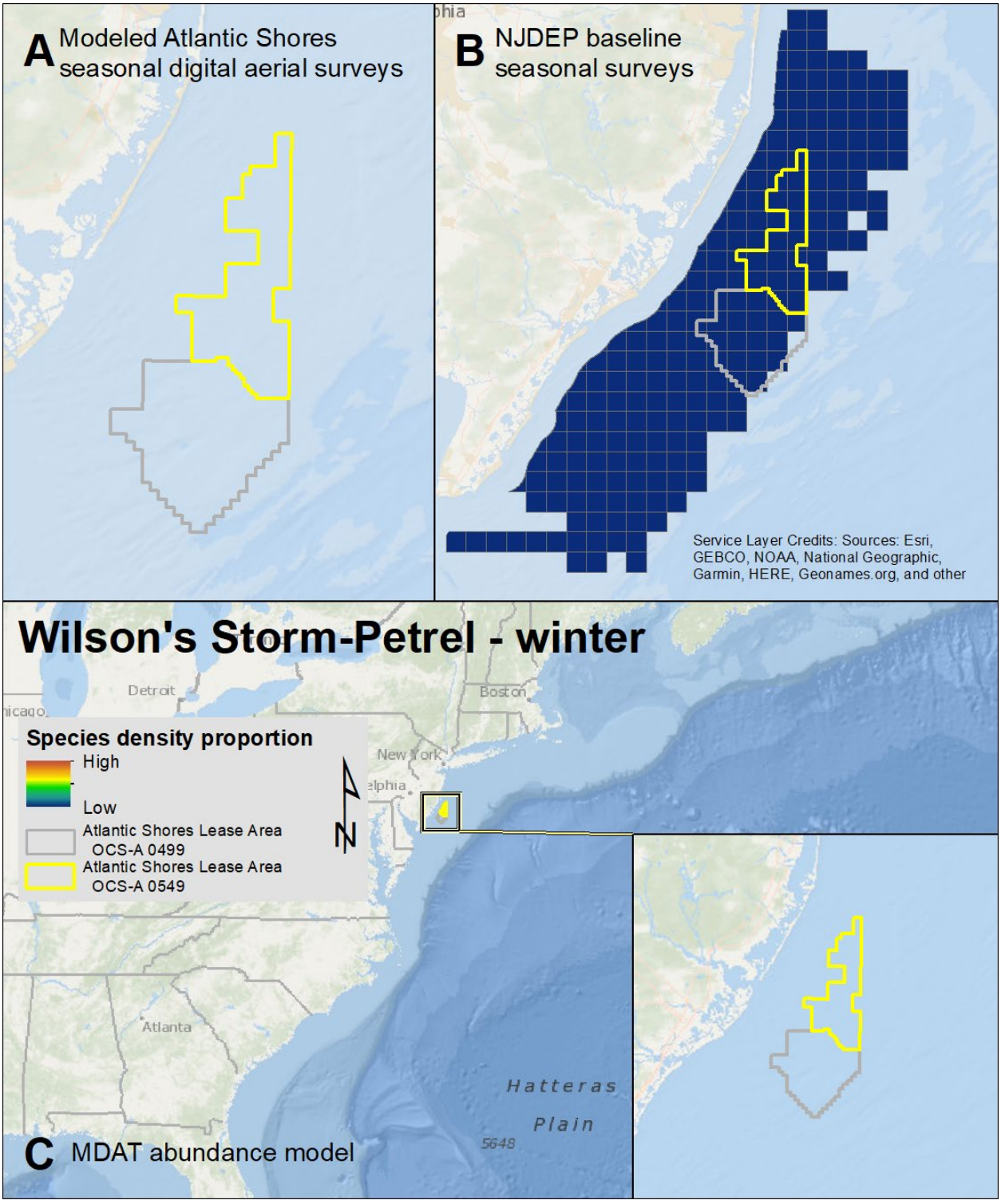

Map 38. Winter Wilson's Storm-Petrel modeled density proportions in the Atlantic Shores seasonal digital aerial surveys (A), density proportions in the NJDEP baseline survey data (B), and the MDAT model outputs at local and regional scales (C). The scale for all maps is representative of relative spatial variation in the sites within the season for each information source.

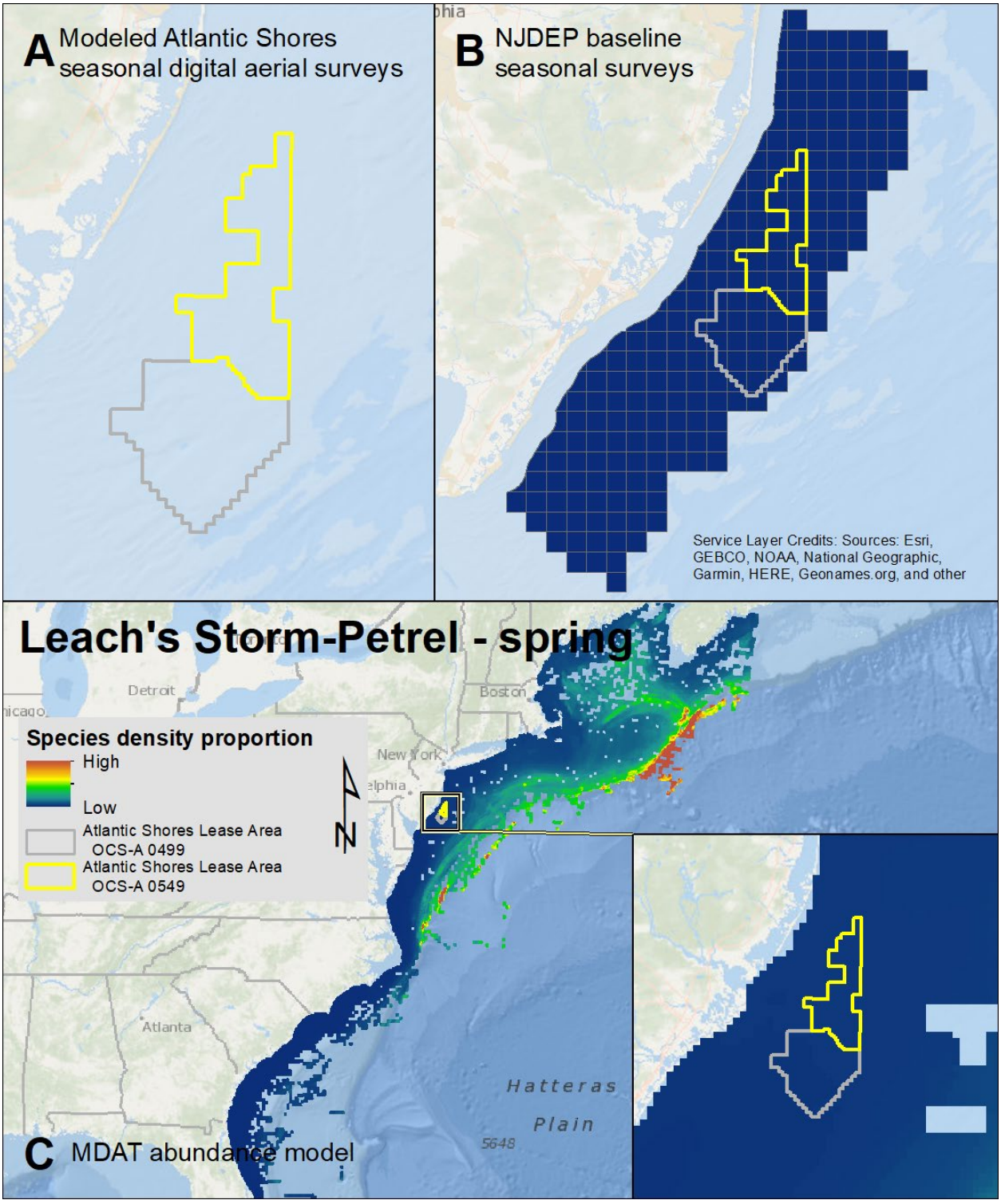

Map 39. Spring Leach's Storm-Petrel modeled density proportions in the Atlantic Shores seasonal digital aerial surveys (A), density proportions in the NJDEP baseline survey data (B), and the MDAT model outputs at local and regional scales (C). The scale for all maps is representative of relative spatial variation in the sites within the season for each information source.

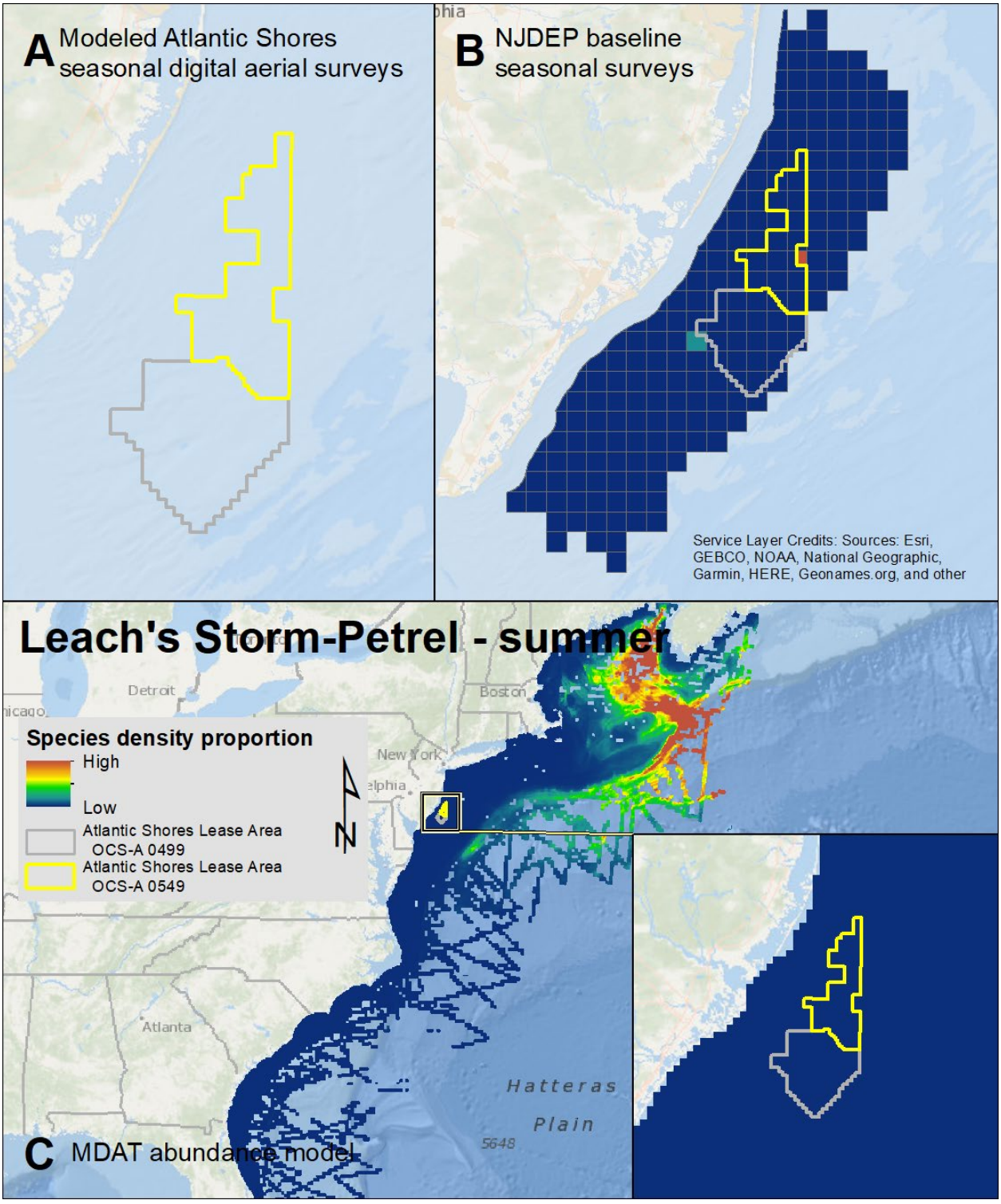

Map 40. Summer Leach's Storm-Petrel modeled density proportions in the Atlantic Shores seasonal digital aerial surveys (A), density proportions in the NJDEP baseline survey data (B), and the MDAT model outputs at local and regional scales (C). The scale for all maps is representative of relative spatial variation in the sites within the season for each information source.

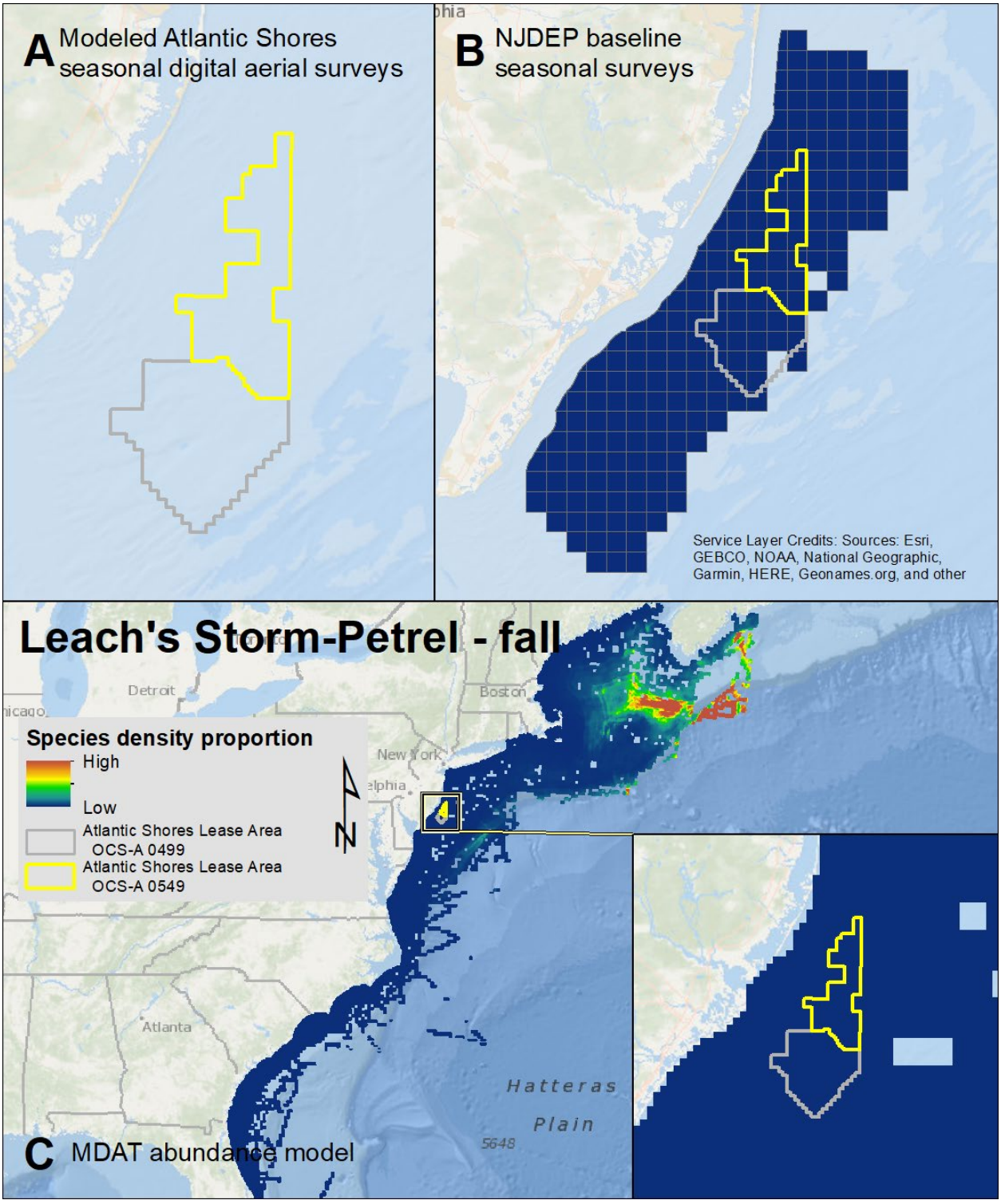

Map 41. Fall Leach's Storm-Petrel modeled density proportions in the Atlantic Shores seasonal digital aerial surveys (A), density proportions in the NJDEP baseline survey data (B), and the MDAT model outputs at local and regional scales (C). The scale for all maps is representative of relative spatial variation in the sites within the season for each information source.

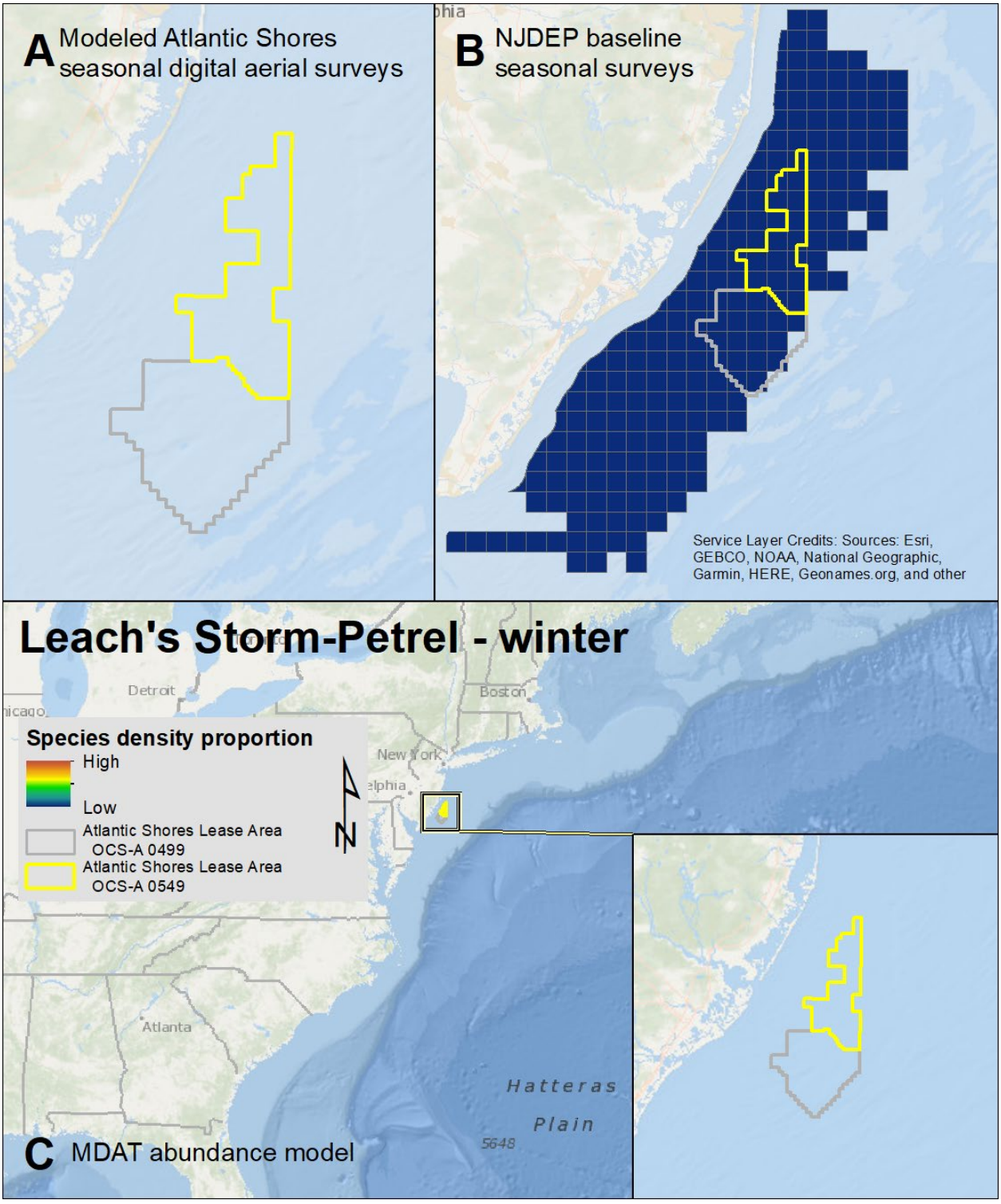

Map 42. Winter Leach's Storm-Petrel modeled density proportions in the Atlantic Shores seasonal digital aerial surveys (A), density proportions in the NJDEP baseline survey data (B), and the MDAT model outputs at local and regional scales (C). The scale for all maps is representative of relative spatial variation in the sites within the season for each information source.

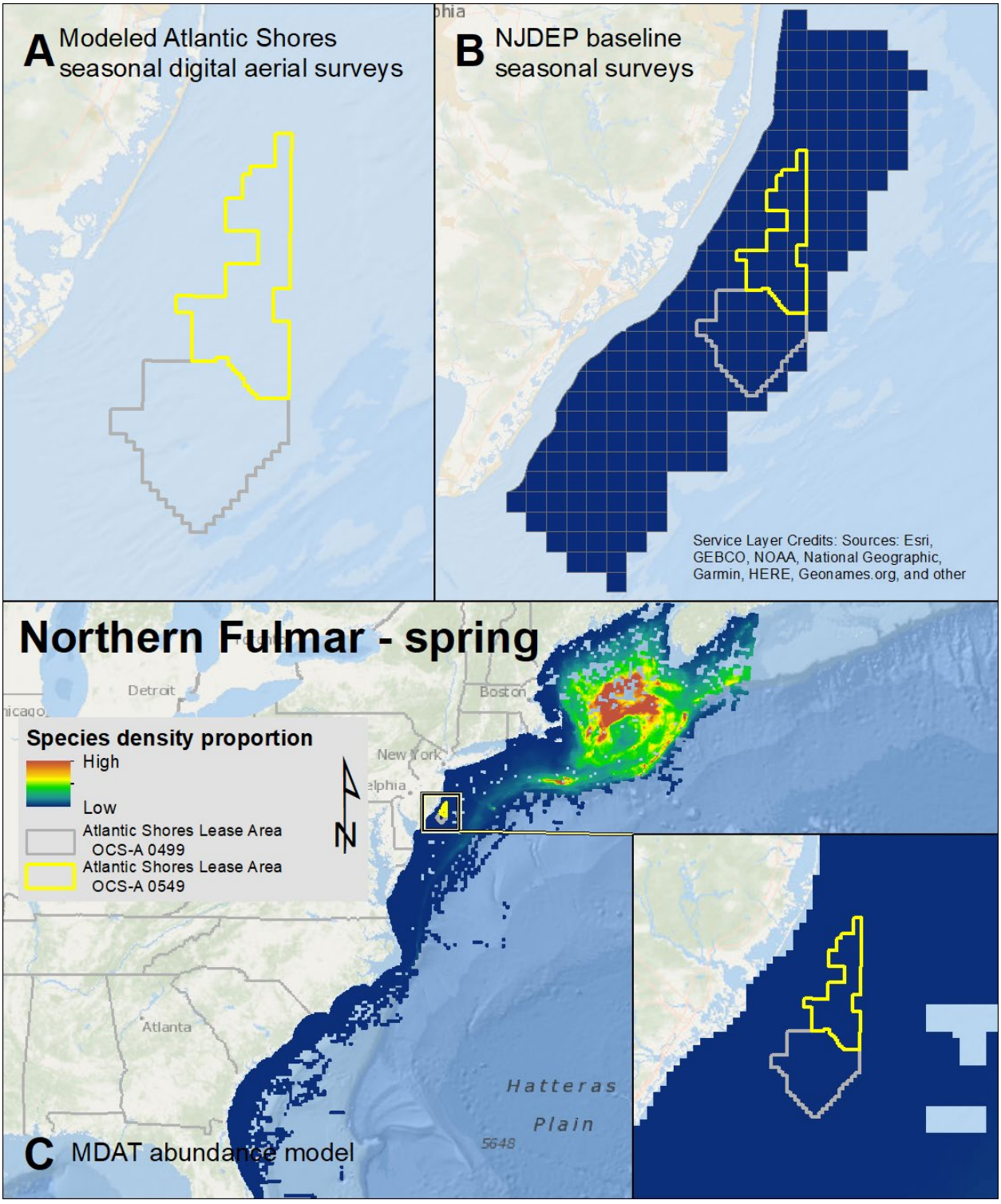

Map 43. Spring Northern Fulmar modeled density proportions in the Atlantic Shores seasonal digital aerial surveys (A), density proportions in the NJDEP baseline survey data (B), and the MDAT model outputs at local and regional scales (C). The scale for all maps is representative of relative spatial variation in the sites within the season for each information source.

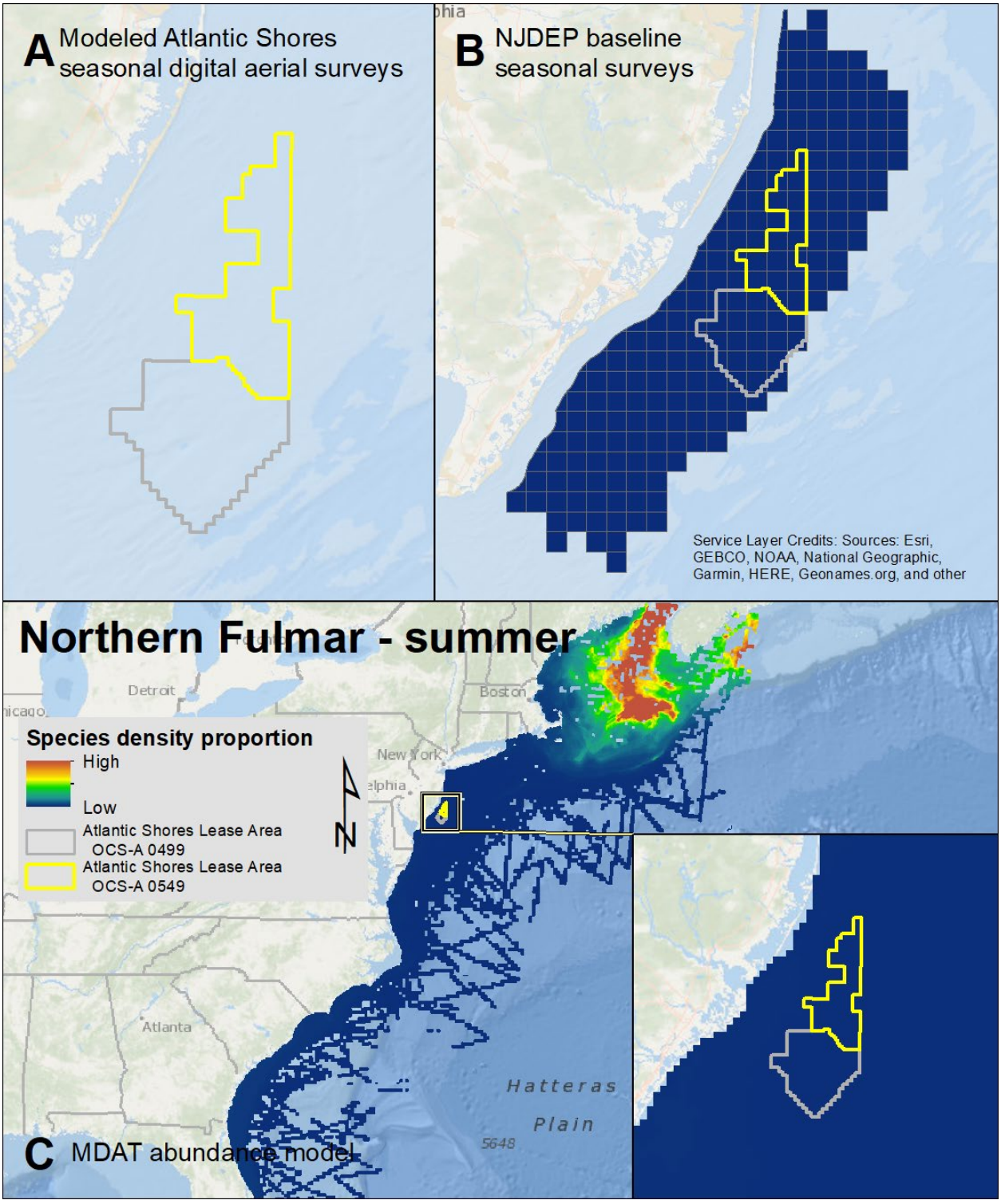

Map 44. Summer Northern Fulmar modeled density proportions in the Atlantic Shores seasonal digital aerial surveys (A), density proportions in the NJDEP baseline survey data (B), and the MDAT model outputs at local and regional scales (C). The scale for all maps is representative of relative spatial variation in the sites within the season for each information source.

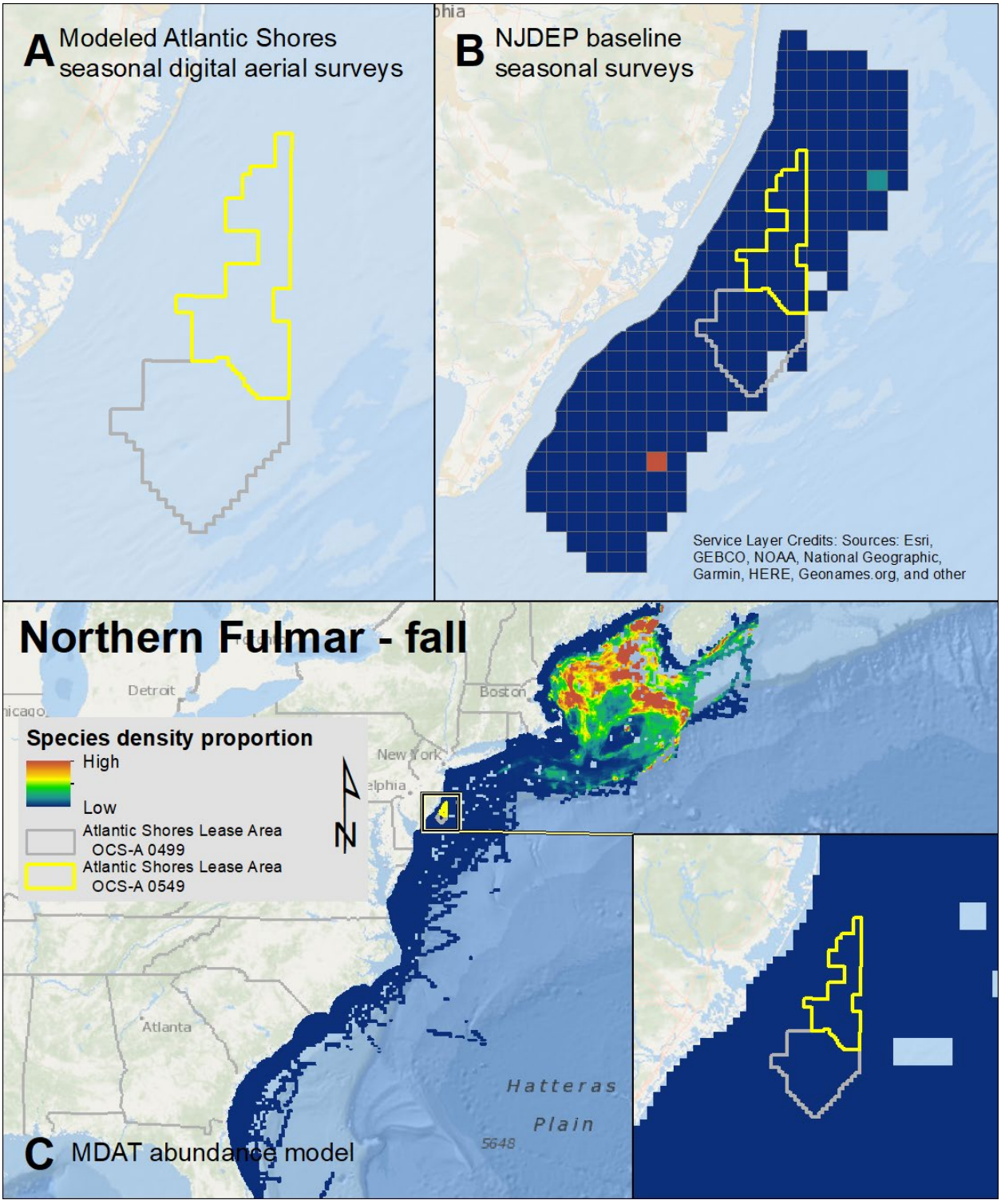

Map 45. Fall Northern Fulmar modeled density proportions in the Atlantic Shores seasonal digital aerial surveys (A), density proportions in the NJDEP baseline survey data (B), and the MDAT model outputs at local and regional scales (C). The scale for all maps is representative of relative spatial variation in the sites within the season for each information source.

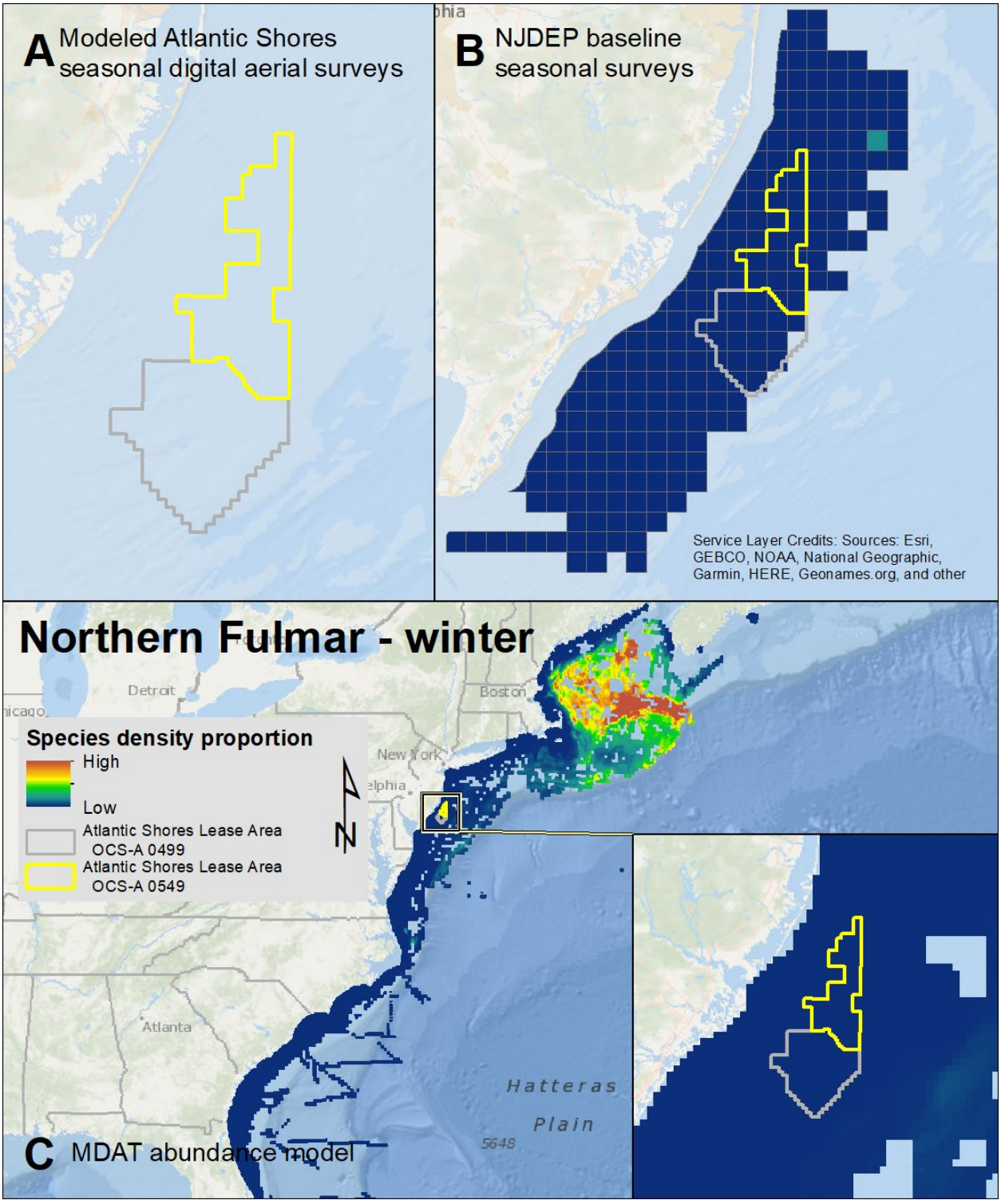

Map 46. Winter Northern Fulmar modeled density proportions in the Atlantic Shores seasonal digital aerial surveys (A), density proportions in the NJDEP baseline survey data (B), and the MDAT model outputs at local and regional scales (C). The scale for all maps is representative of relative spatial variation in the sites within the season for each information source.

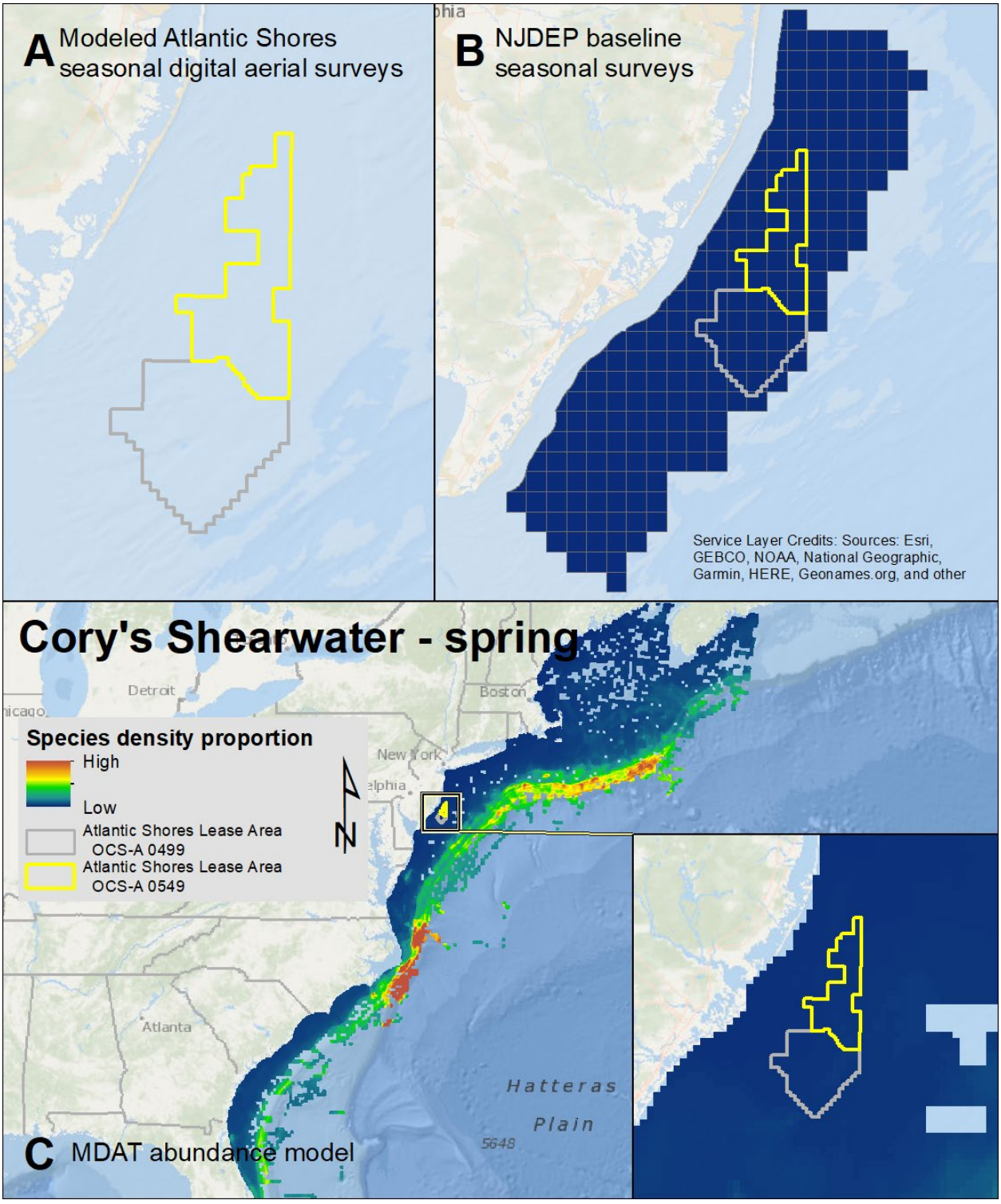

Map 47. Spring Cory's Shearwater modeled density proportions in the Atlantic Shores seasonal digital aerial surveys (A), density proportions in the NJDEP baseline survey data (B), and the MDAT model outputs at local and regional scales (C). The scale for all maps is representative of relative spatial variation in the sites within the season for each information source.

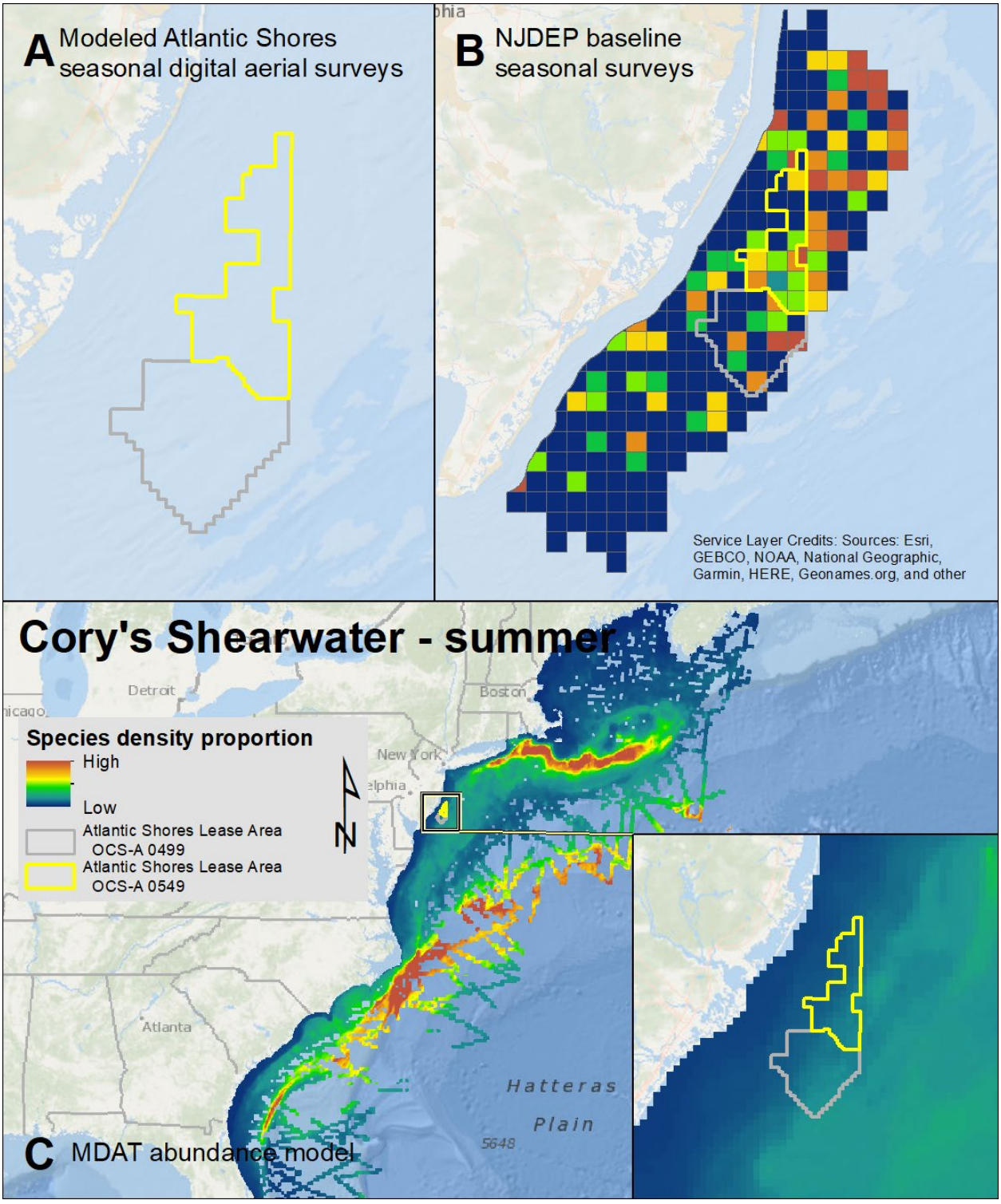

Map 48. Summer Cory's Shearwater modeled density proportions in the Atlantic Shores seasonal digital aerial surveys (A), density proportions in the NJDEP baseline survey data (B), and the MDAT model outputs at local and regional scales (C). The scale for all maps is representative of relative spatial variation in the sites within the season for each information source.

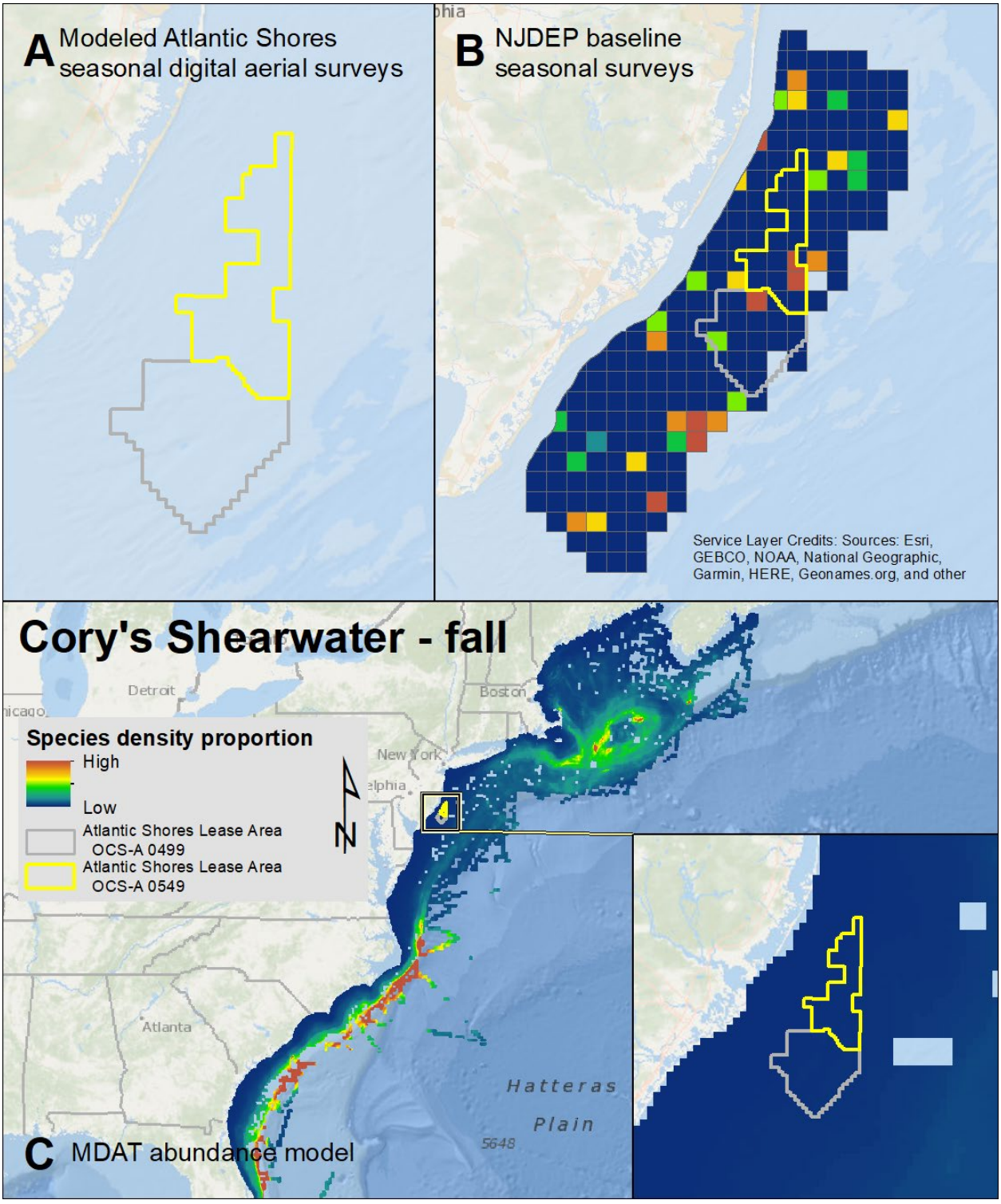

Map 49. Fall Cory's Shearwater modeled density proportions in the Atlantic Shores seasonal digital aerial surveys (A), density proportions in the NJDEP baseline survey data (B), and the MDAT model outputs at local and regional scales (C). The scale for all maps is representative of relative spatial variation in the sites within the season for each information source.

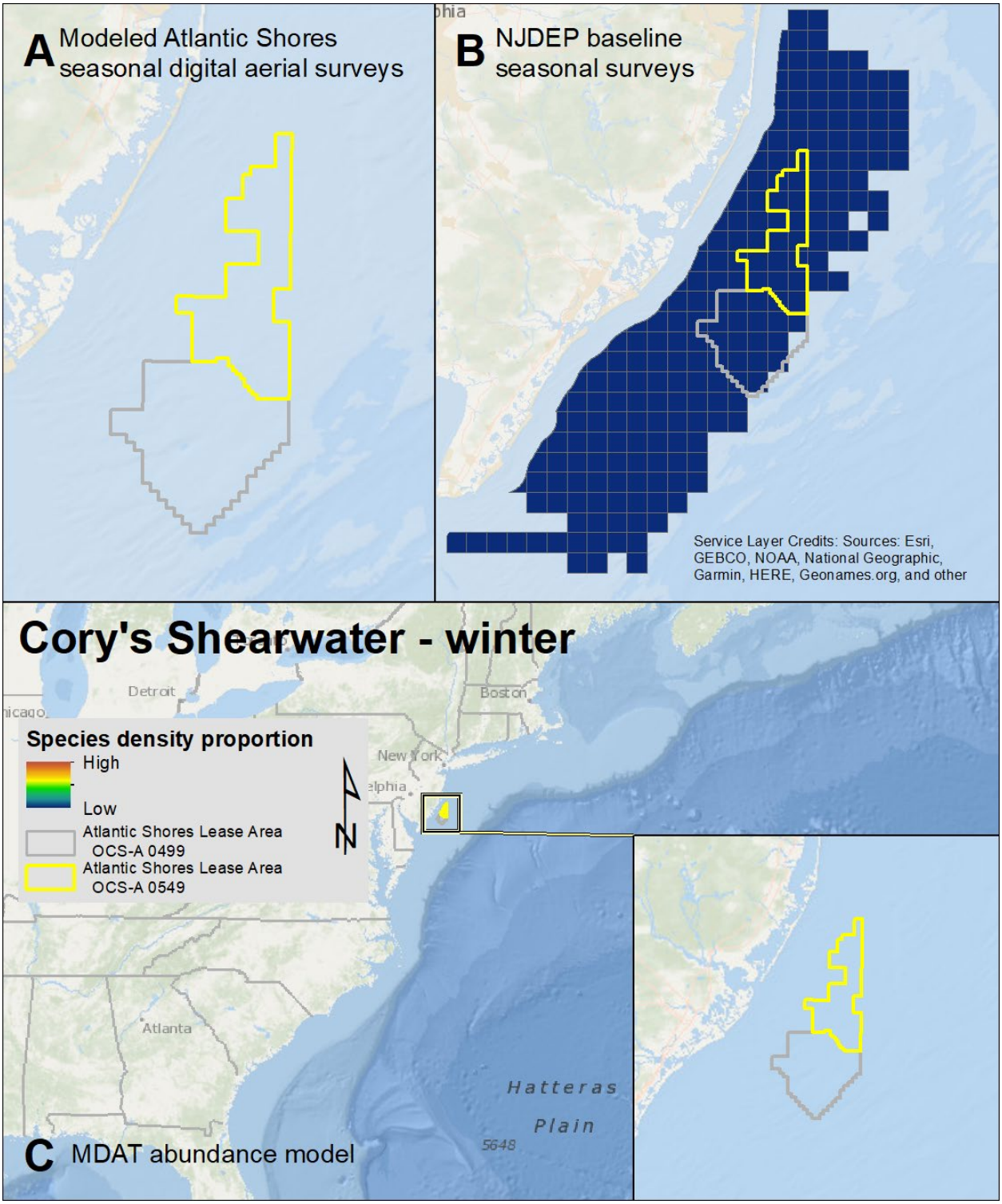

Map 50. Winter Cory's Shearwater modeled density proportions in the Atlantic Shores seasonal digital aerial surveys (A), density proportions in the NJDEP baseline survey data (B), and the MDAT model outputs at local and regional scales (C). The scale for all maps is representative of relative spatial variation in the sites within the season for each information source.

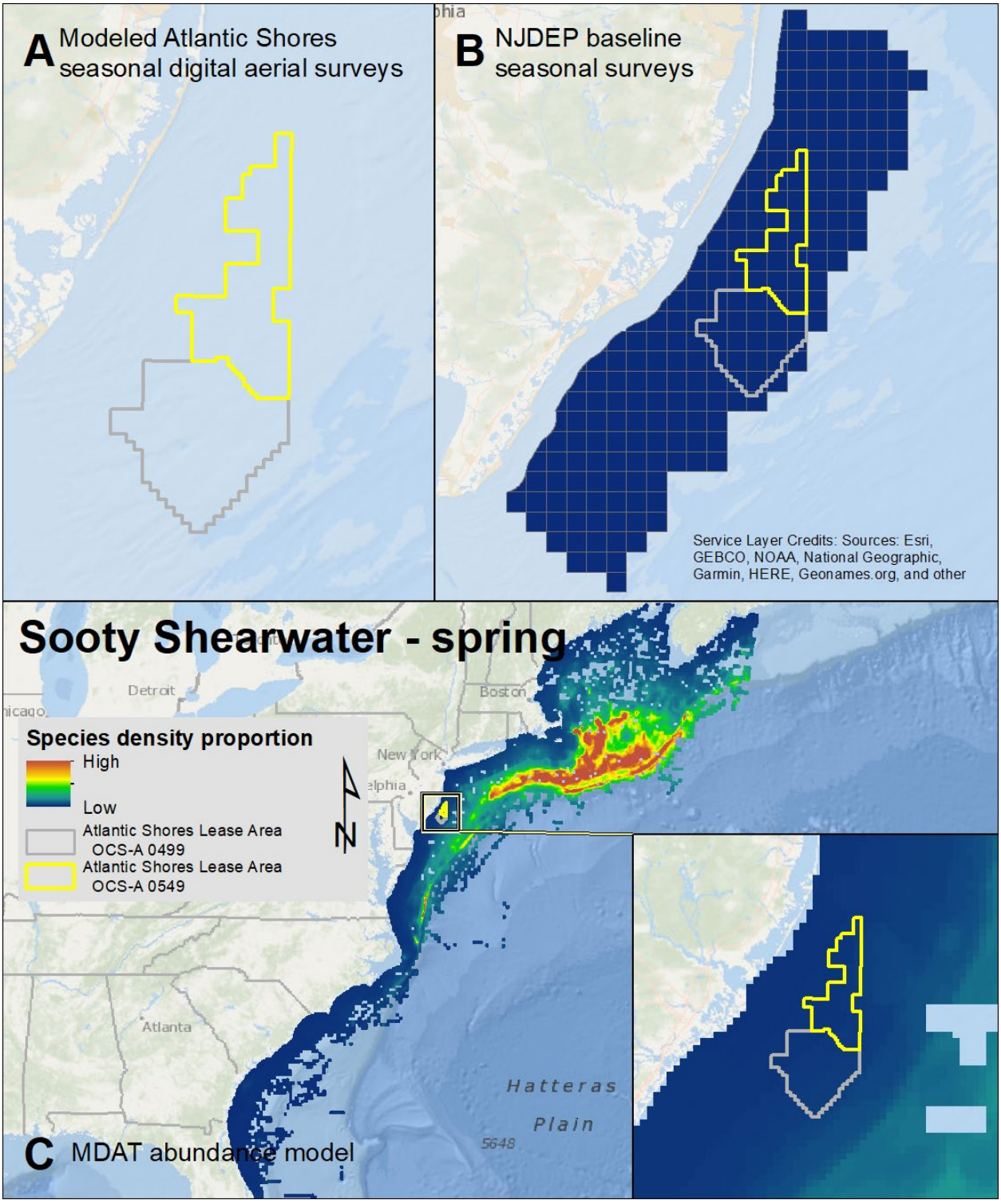

Map 51. Spring Sooty Shearwater modeled density proportions in the Atlantic Shores seasonal digital aerial surveys (A), density proportions in the NJDEP baseline survey data (B), and the MDAT model outputs at local and regional scales (C). The scale for all maps is representative of relative spatial variation in the sites within the season for each information source.

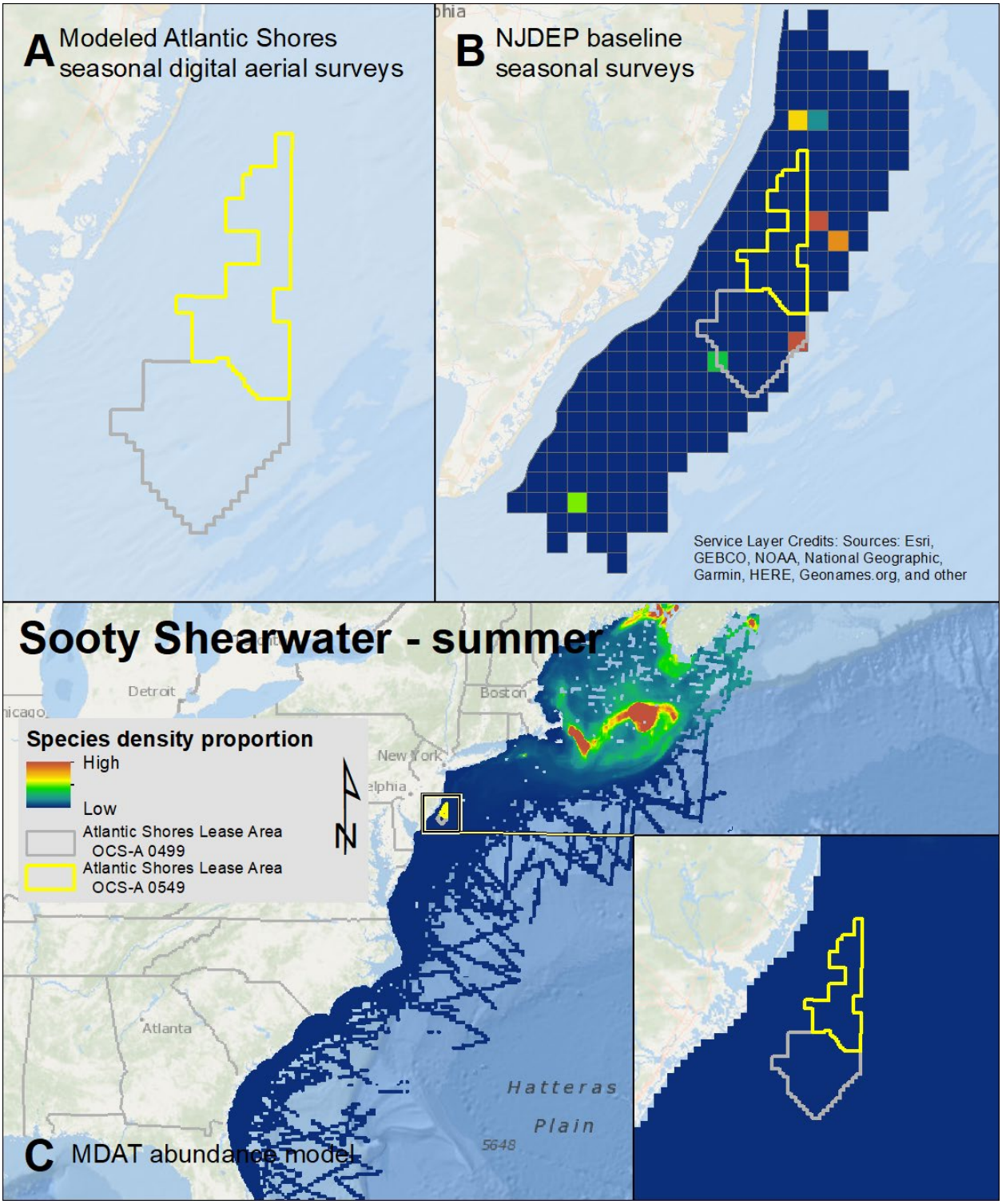

Map 52. Summer Sooty Shearwater modeled density proportions in the Atlantic Shores seasonal digital aerial surveys (A), density proportions in the NJDEP baseline survey data (B), and the MDAT model outputs at local and regional scales (C). The scale for all maps is representative of relative spatial variation in the sites within the season for each information source.

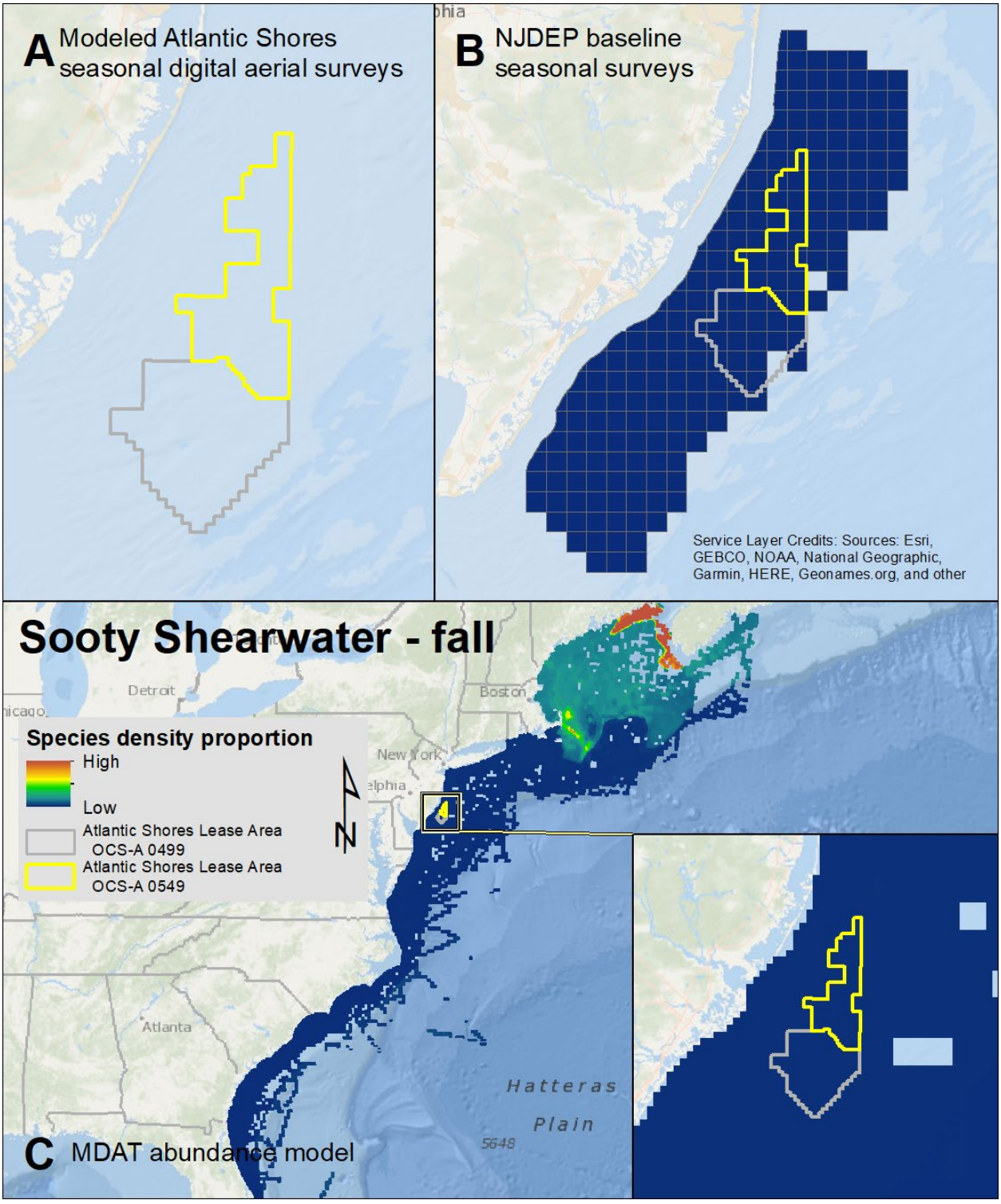

Map 53. Fall Sooty Shearwater modeled density proportions in the Atlantic Shores seasonal digital aerial surveys (A), density proportions in the NJDEP baseline survey data (B), and the MDAT model outputs at local and regional scales (C). The scale for all maps is representative of relative spatial variation in the sites within the season for each information source.

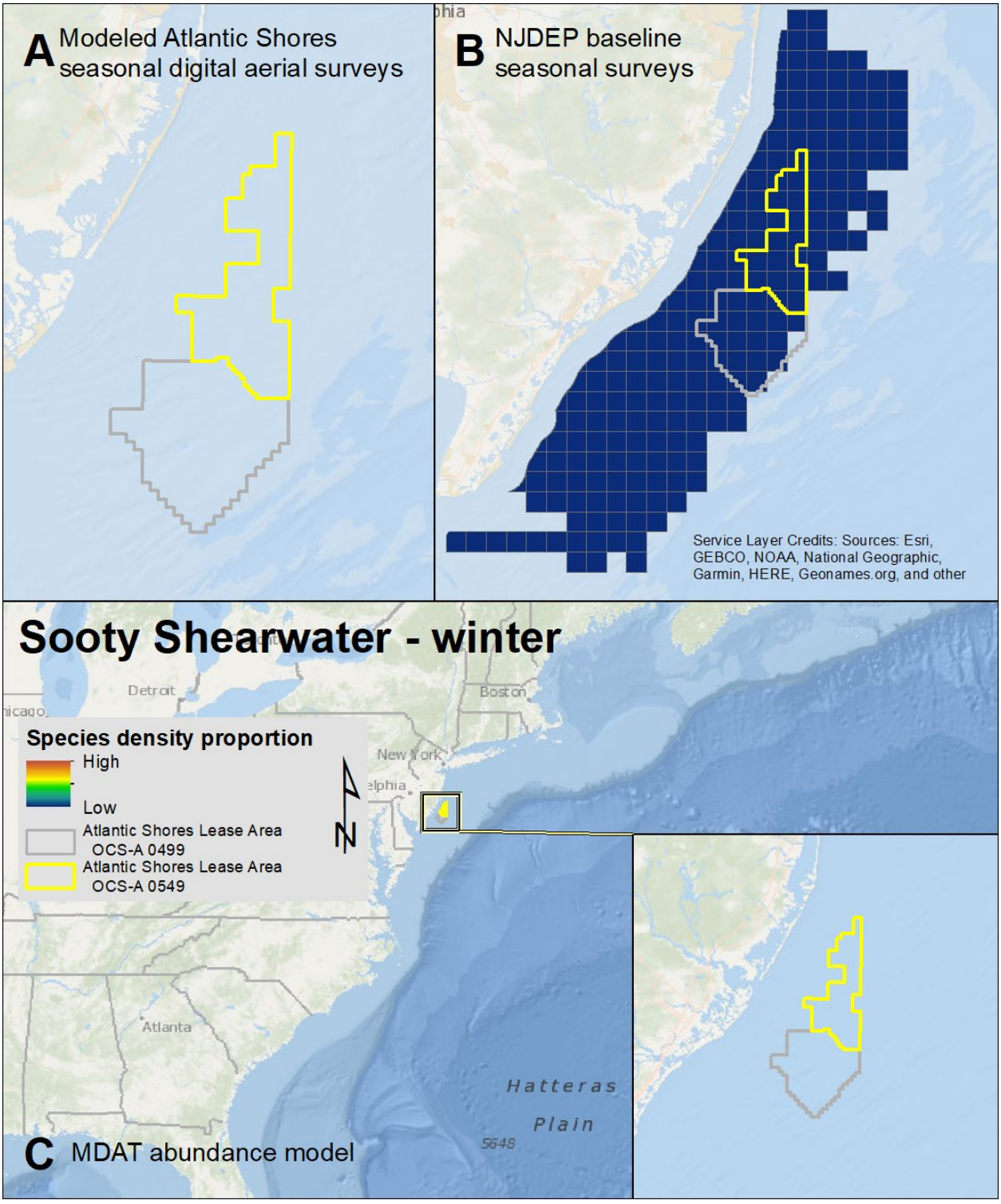

Map 54. Winter Sooty Shearwater modeled density proportions in the Atlantic Shores seasonal digital aerial surveys (A), density proportions in the NJDEP baseline survey data (B), and the MDAT model outputs at local and regional scales (C). The scale for all maps is representative of relative spatial variation in the sites within the season for each information source.

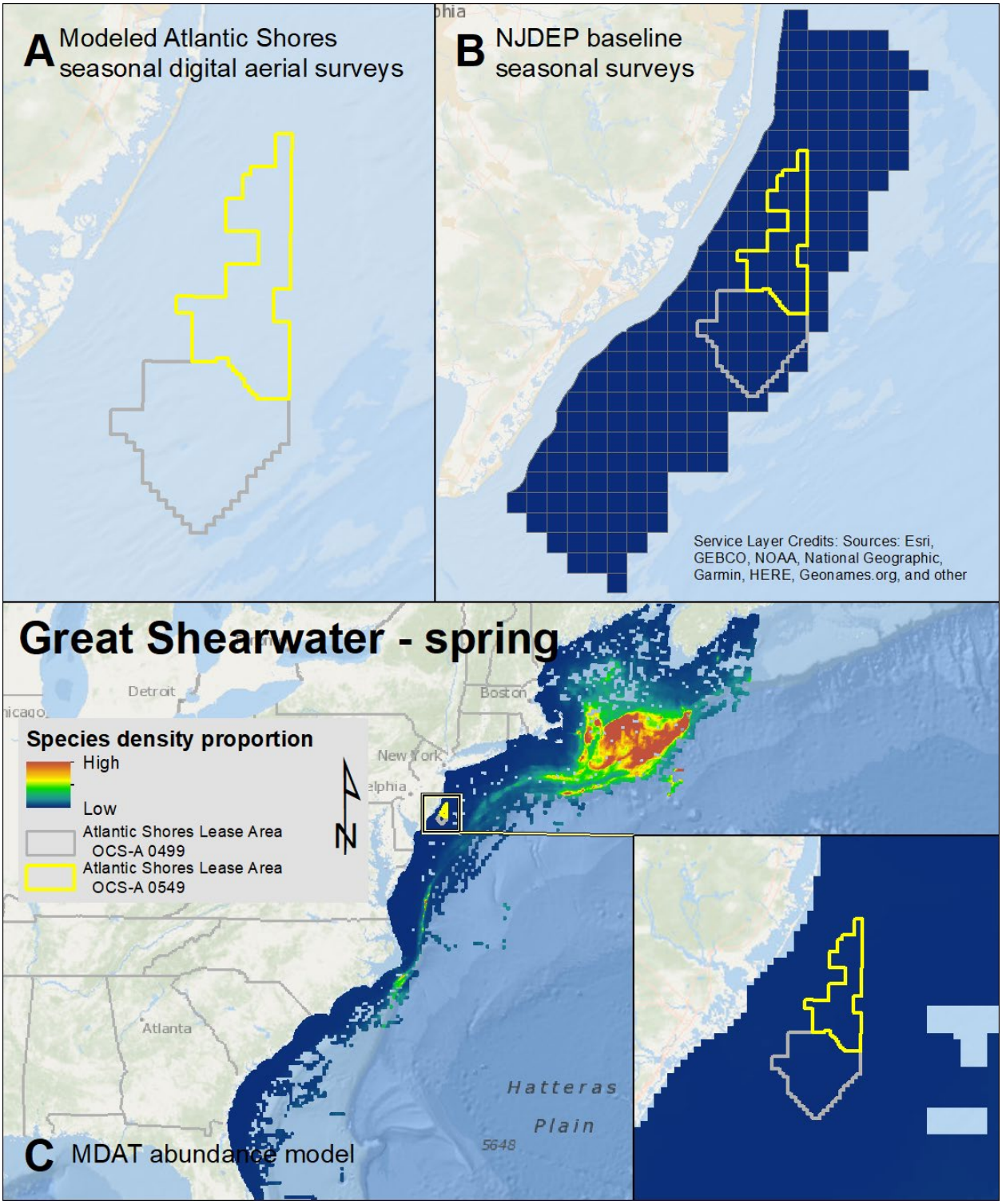

Map 55. Spring Great Shearwater modeled density proportions in the Atlantic Shores seasonal digital aerial surveys (A), density proportions in the NJDEP baseline survey data (B), and the MDAT model outputs at local and regional scales (C). The scale for all maps is representative of relative spatial variation in the sites within the season for each information source.

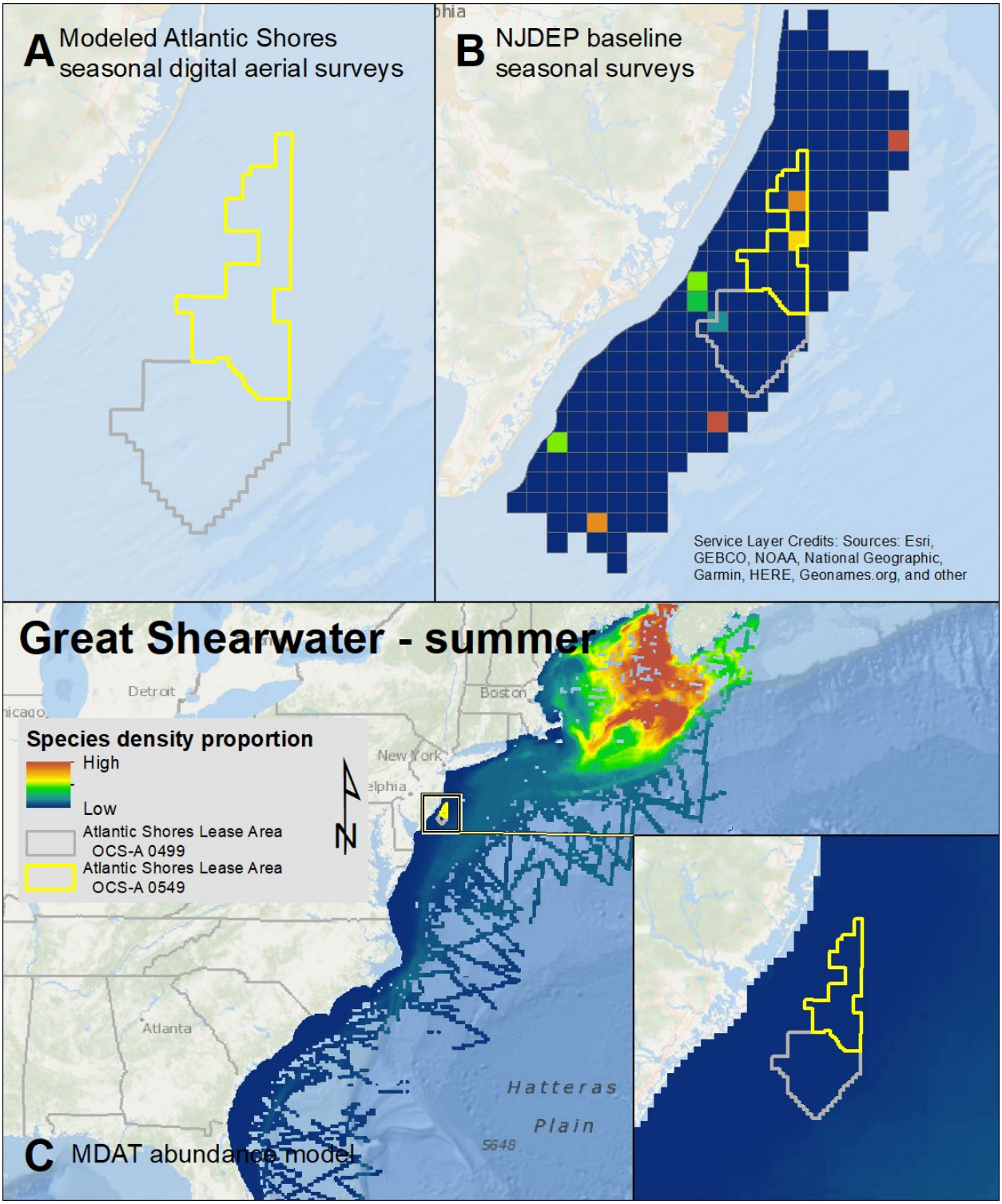

Map 56. Summer Great Shearwater modeled density proportions in the Atlantic Shores seasonal digital aerial surveys (A), density proportions in the NJDEP baseline survey data (B), and the MDAT model outputs at local and regional scales (C). The scale for all maps is representative of relative spatial variation in the sites within the season for each information source.

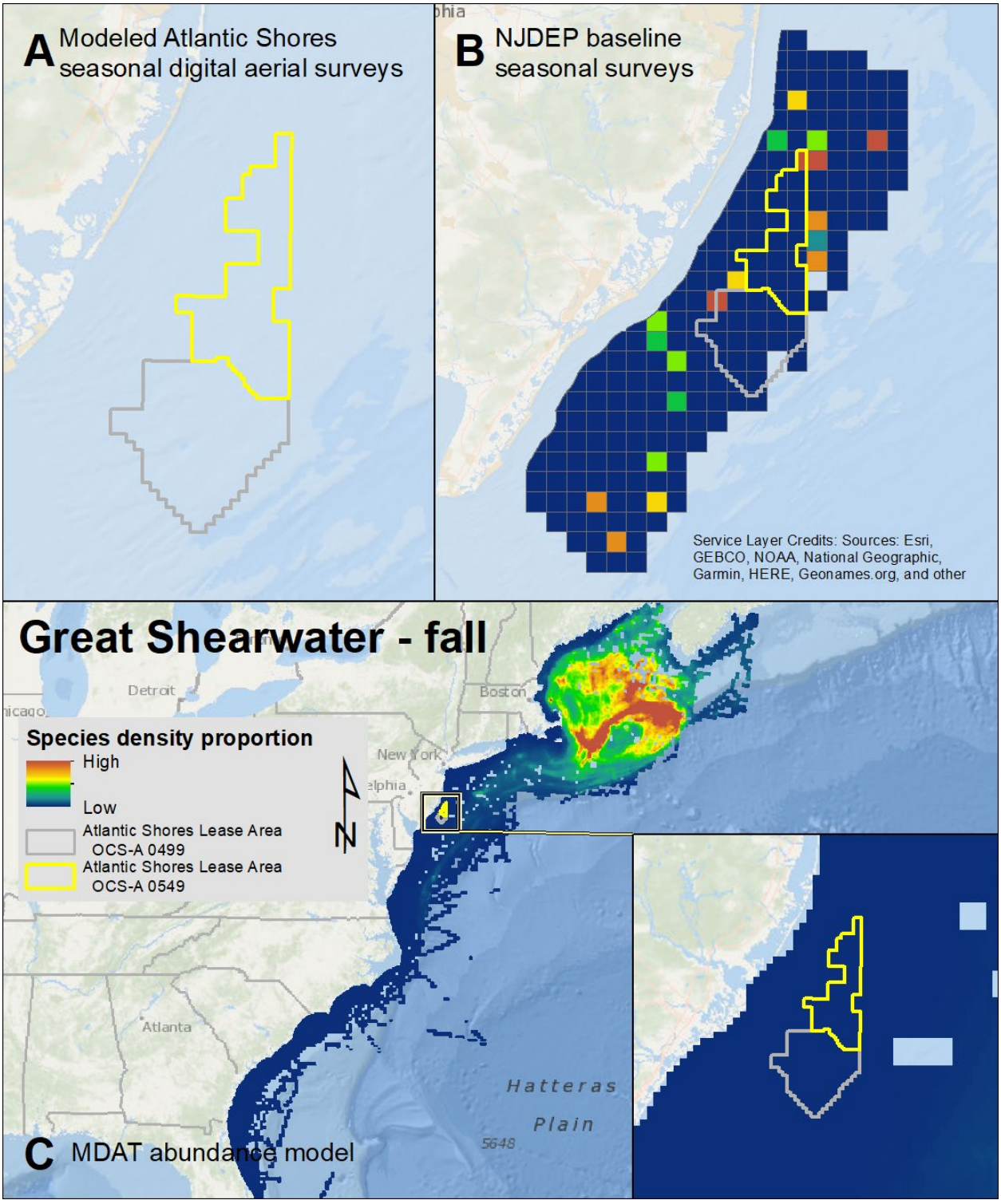

Map 57. Fall Great Shearwater modeled density proportions in the Atlantic Shores seasonal digital aerial surveys (A), density proportions in the NJDEP baseline survey data (B), and the MDAT model outputs at local and regional scales (C). The scale for all maps is representative of relative spatial variation in the sites within the season for each information source.

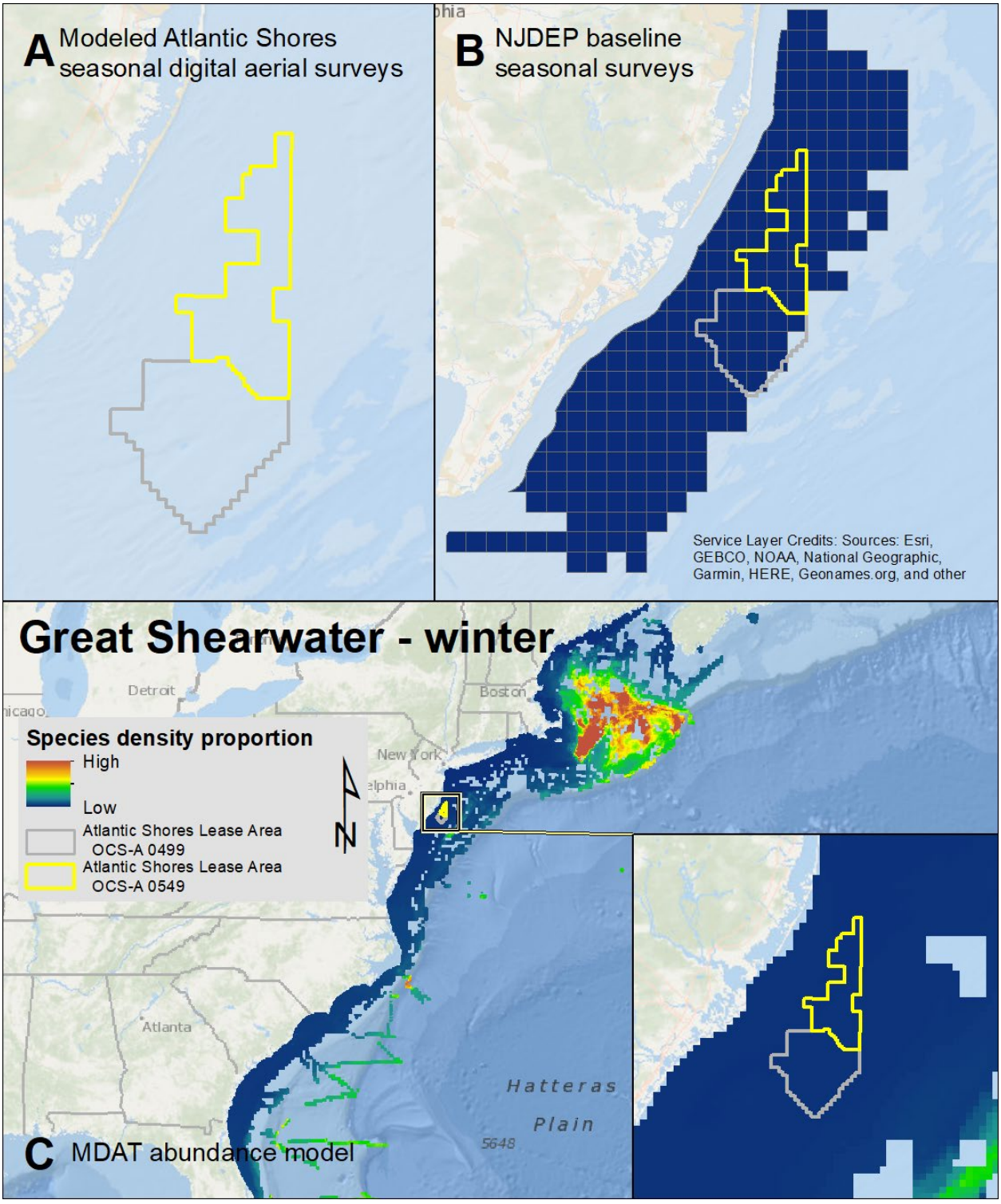

Map 58. Winter Great Shearwater modeled density proportions in the Atlantic Shores seasonal digital aerial surveys (A), density proportions in the NJDEP baseline survey data (B), and the MDAT model outputs at local and regional scales (C). The scale for all maps is representative of relative spatial variation in the sites within the season for each information source.

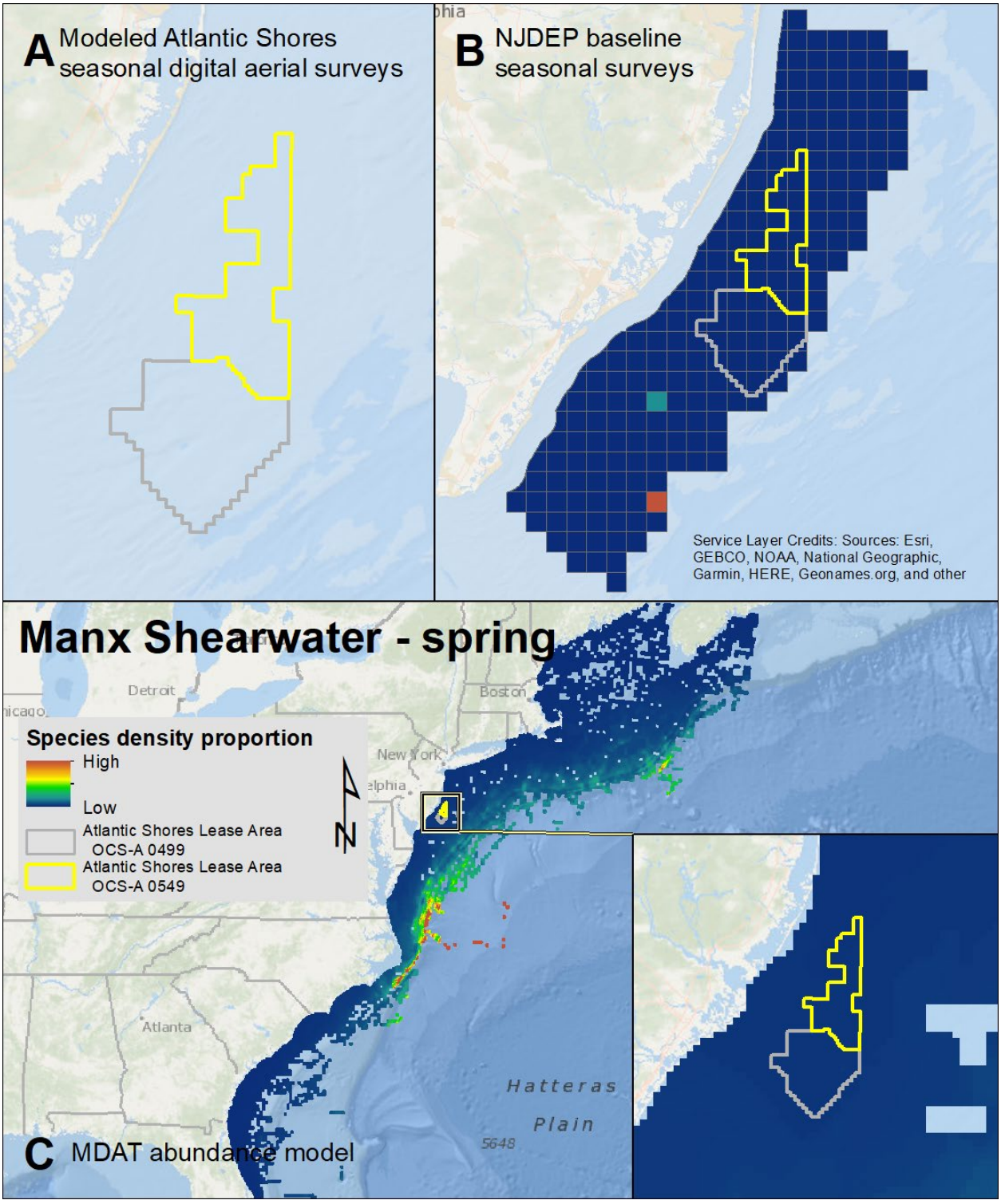

Map 59. Spring Manx Shearwater modeled density proportions in the Atlantic Shores seasonal digital aerial surveys (A), density proportions in the NJDEP baseline survey data (B), and the MDAT model outputs at local and regional scales (C). The scale for all maps is representative of relative spatial variation in the sites within the season for each information source.

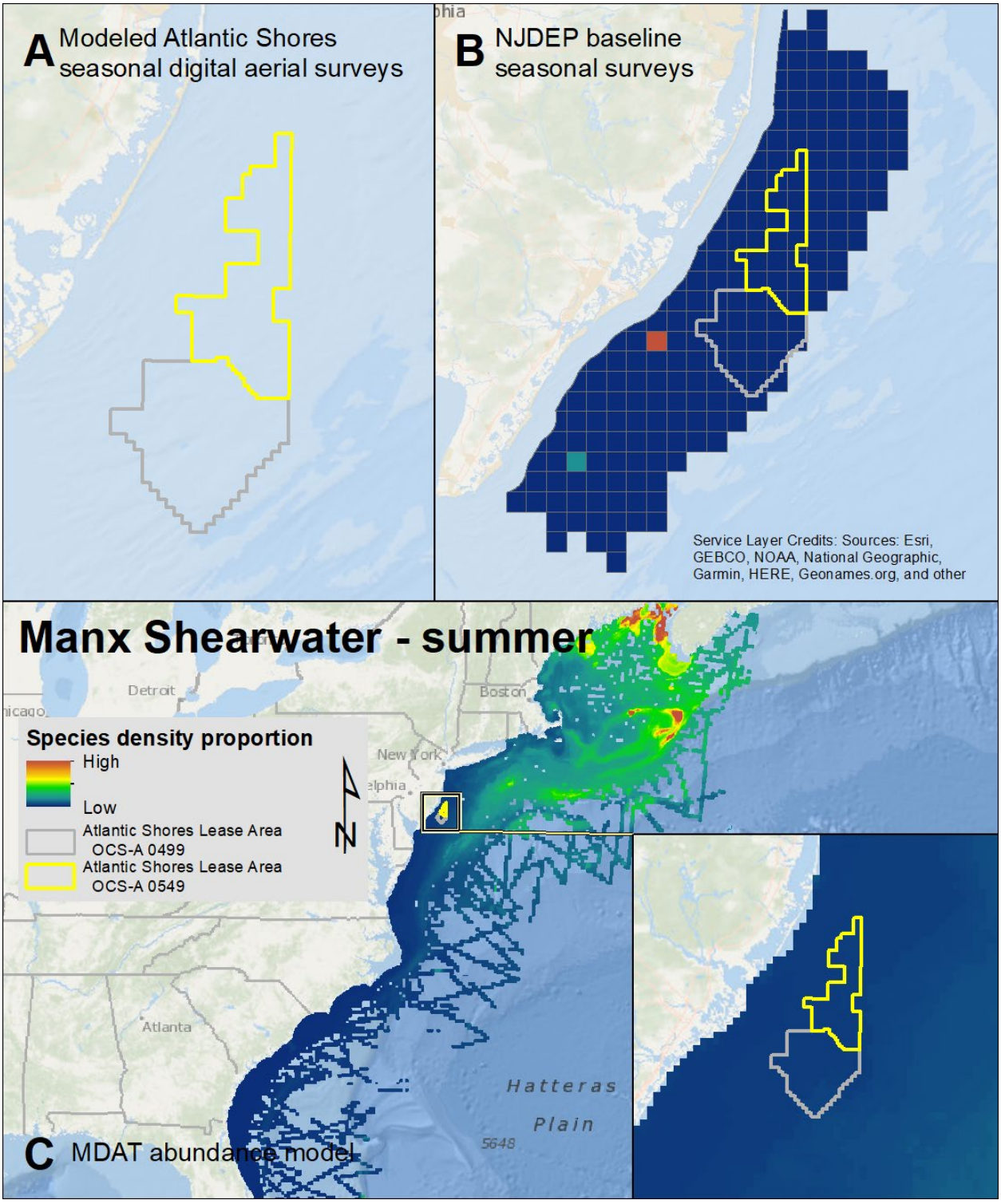

Map 60. Summer Manx Shearwater modeled density proportions in the Atlantic Shores seasonal digital aerial surveys (A), density proportions in the NJDEP baseline survey data (B), and the MDAT model outputs at local and regional scales (C). The scale for all maps is representative of relative spatial variation in the sites within the season for each information source.

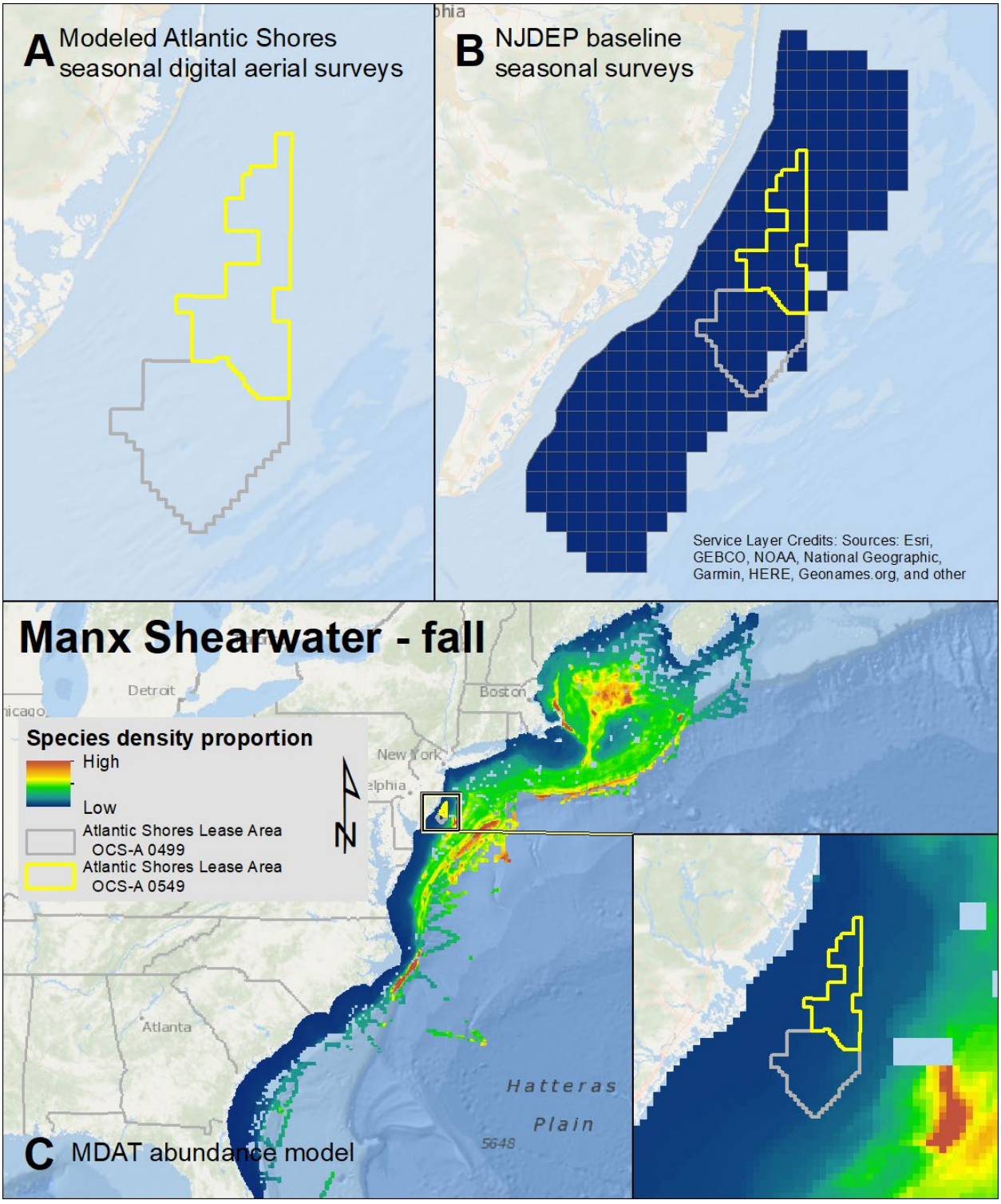

Map 61. Fall Manx Shearwater modeled density proportions in the Atlantic Shores seasonal digital aerial surveys (A), density proportions in the NJDEP baseline survey data (B), and the MDAT model outputs at local and regional scales (C). The scale for all maps is representative of relative spatial variation in the sites within the season for each information source.

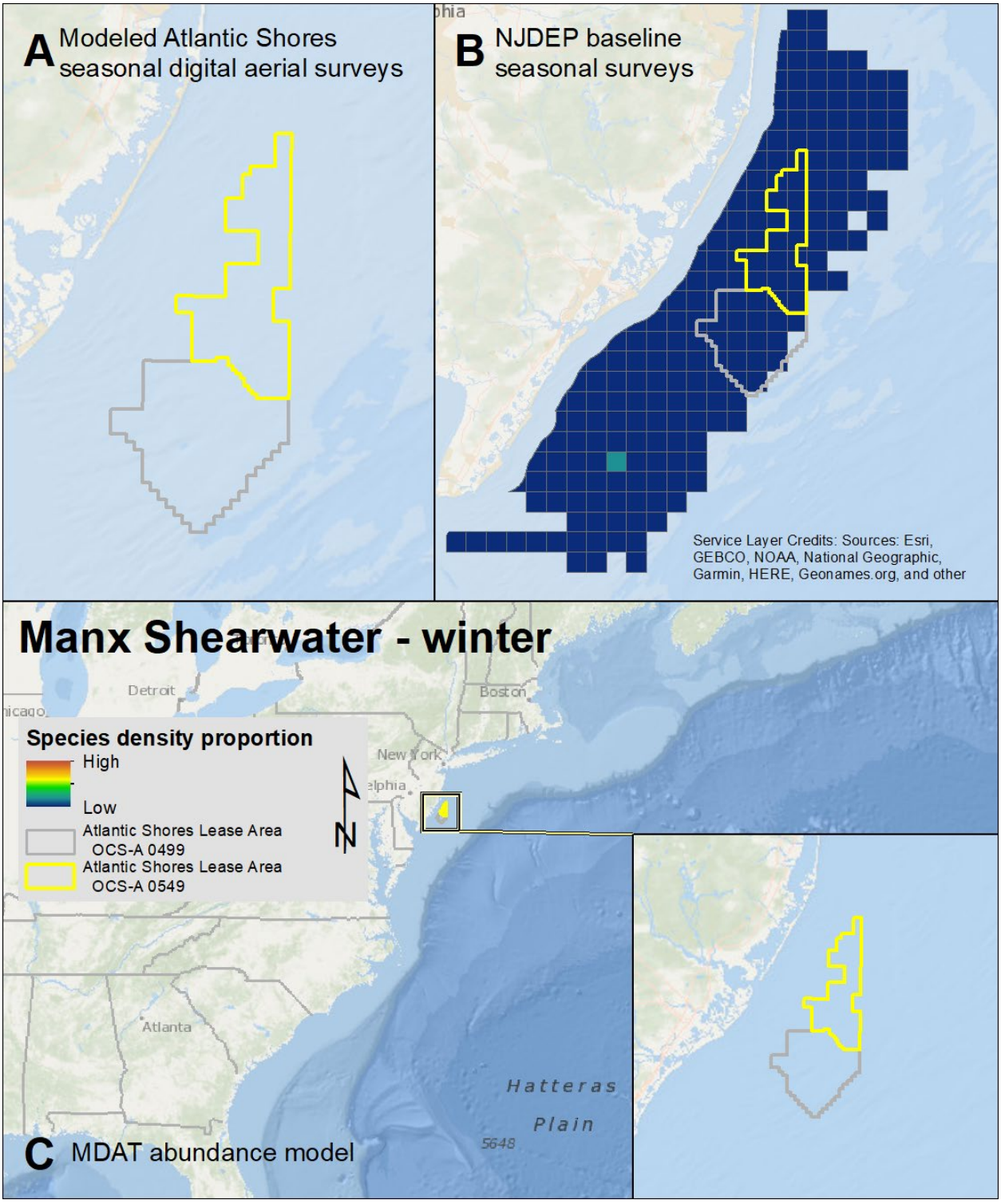

Map 62. Winter Manx Shearwater modeled density proportions in the Atlantic Shores seasonal digital aerial surveys (A), density proportions in the NJDEP baseline survey data (B), and the MDAT model outputs at local and regional scales (C). The scale for all maps is representative of relative spatial variation in the sites within the season for each information source.

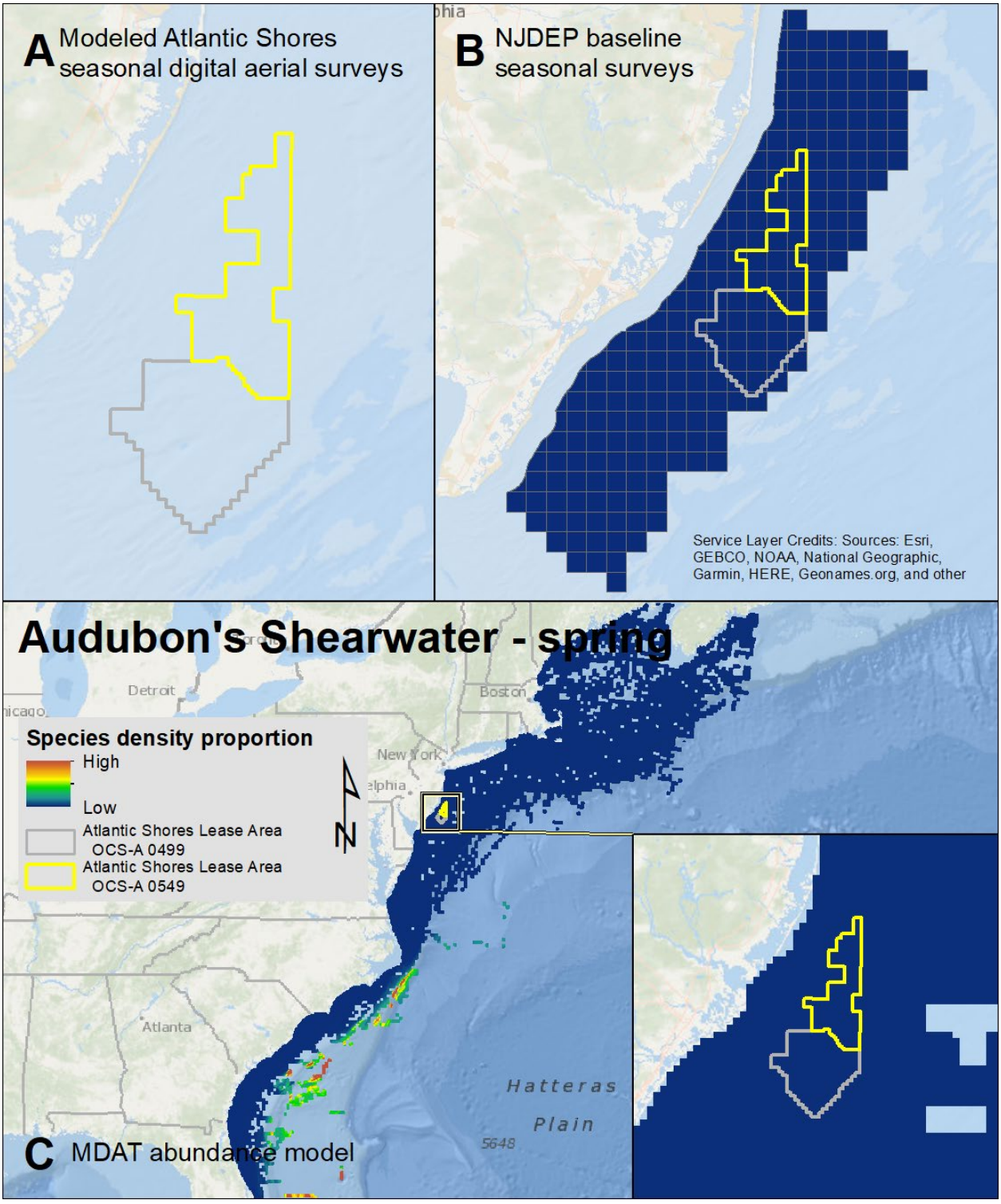

Map 63. Spring Audubon's Shearwater modeled density proportions in the Atlantic Shores seasonal digital aerial surveys (A), density proportions in the NJDEP baseline survey data (B), and the MDAT model outputs at local and regional scales (C). The scale for all maps is representative of relative spatial variation in the sites within the season for each information source.

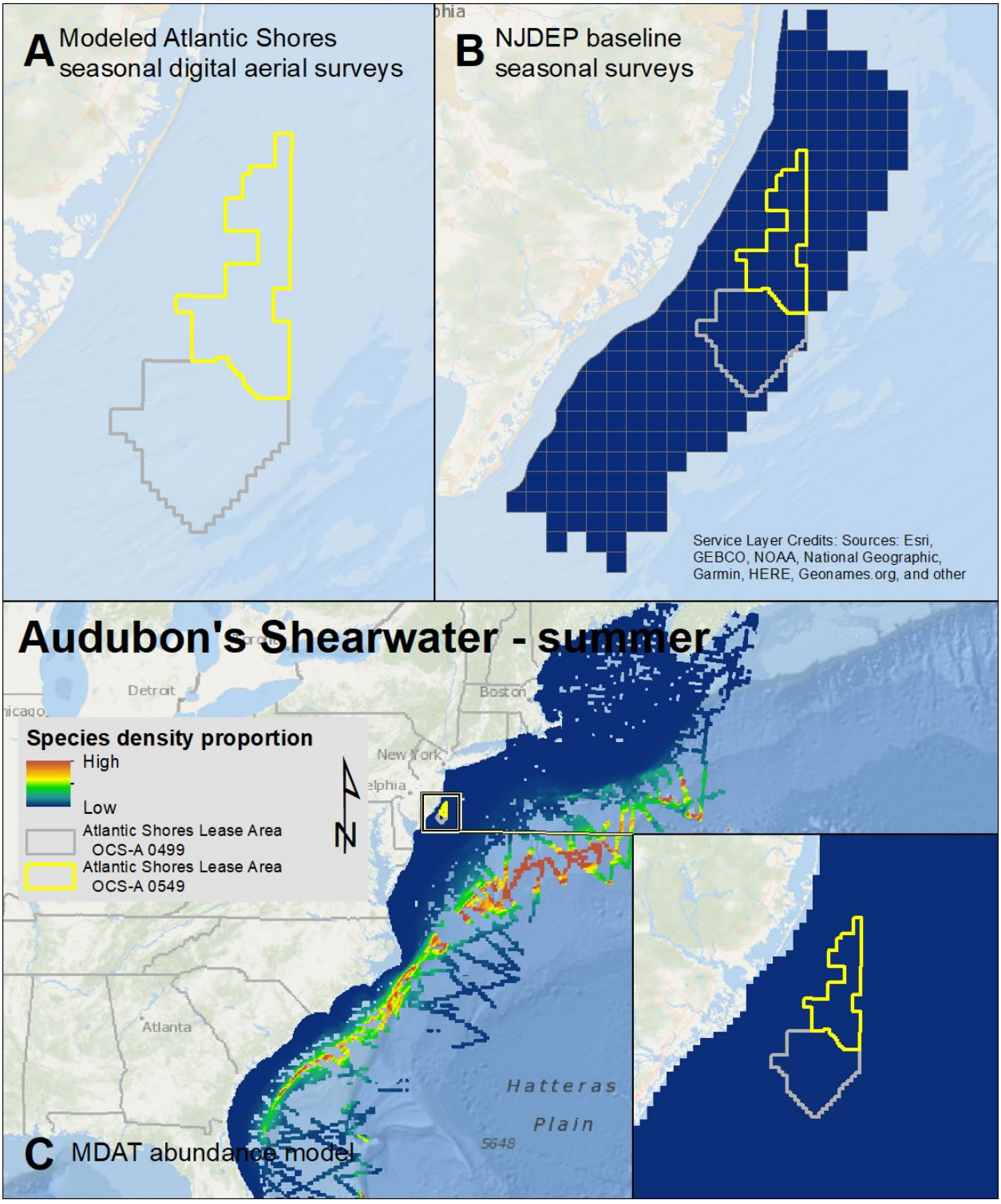

Map 64. Summer Audubon's Shearwater modeled density proportions in the Atlantic Shores seasonal digital aerial surveys (A), density proportions in the NJDEP baseline survey data (B), and the MDAT model outputs at local and regional scales (C). The scale for all maps is representative of relative spatial variation in the sites within the season for each information source.

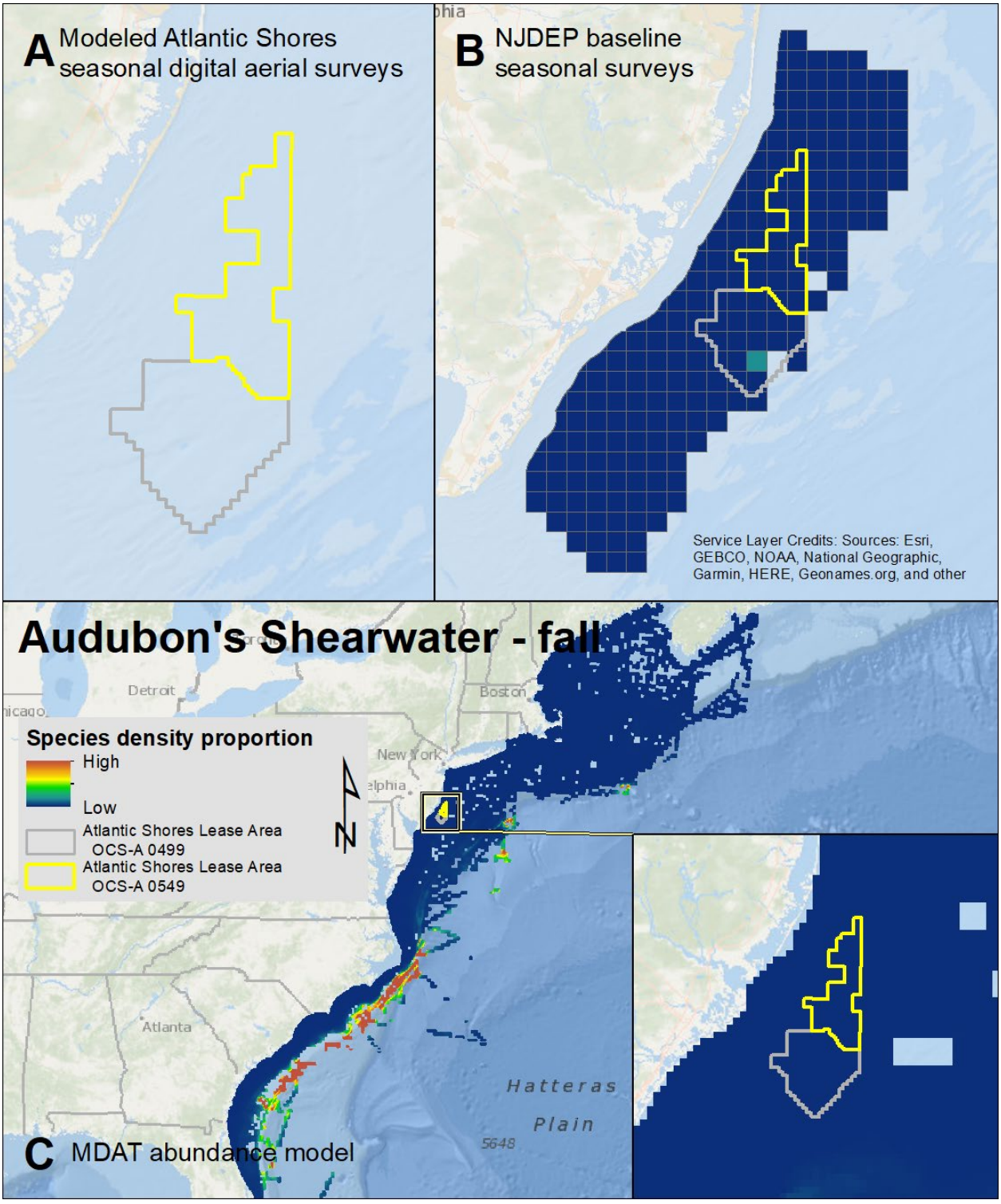

Map 65. Fall Audubon's Shearwater modeled density proportions in the Atlantic Shores seasonal digital aerial surveys (A), density proportions in the NJDEP baseline survey data (B), and the MDAT model outputs at local and regional scales (C). The scale for all maps is representative of relative spatial variation in the sites within the season for each information source.

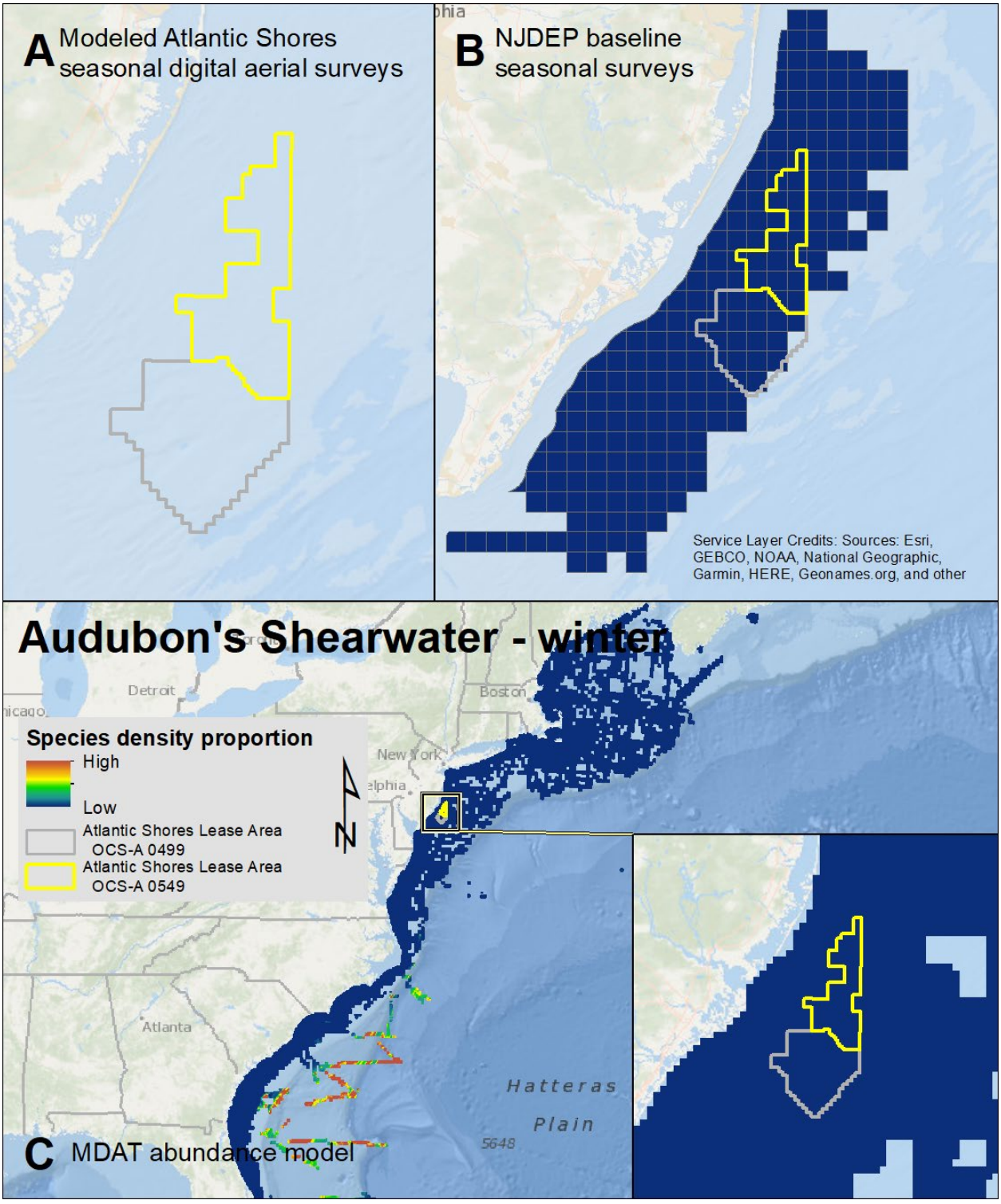

Map 66. Winter Audubon's Shearwater modeled density proportions in the Atlantic Shores seasonal digital aerial surveys (A), density proportions in the NJDEP baseline survey data (B), and the MDAT model outputs at local and regional scales (C). The scale for all maps is representative of relative spatial variation in the sites within the season for each information source.

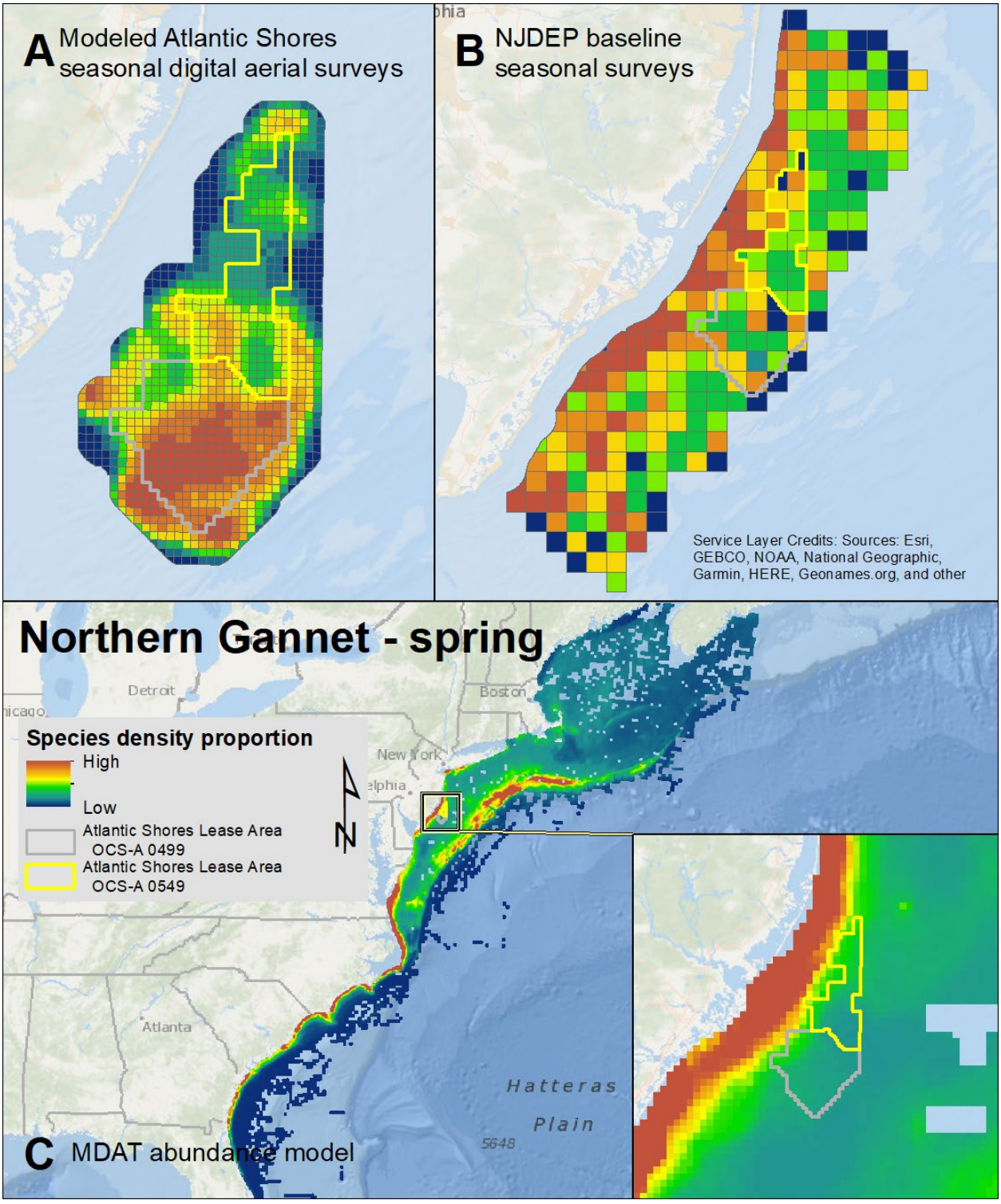

Map 67. Spring Northern Gannet modeled density proportions in the Atlantic Shores seasonal digital aerial surveys (A), density proportions in the NJDEP baseline survey data (B), and the MDAT model outputs at local and regional scales (C). The scale for all maps is representative of relative spatial variation in the sites within the season for each information source.

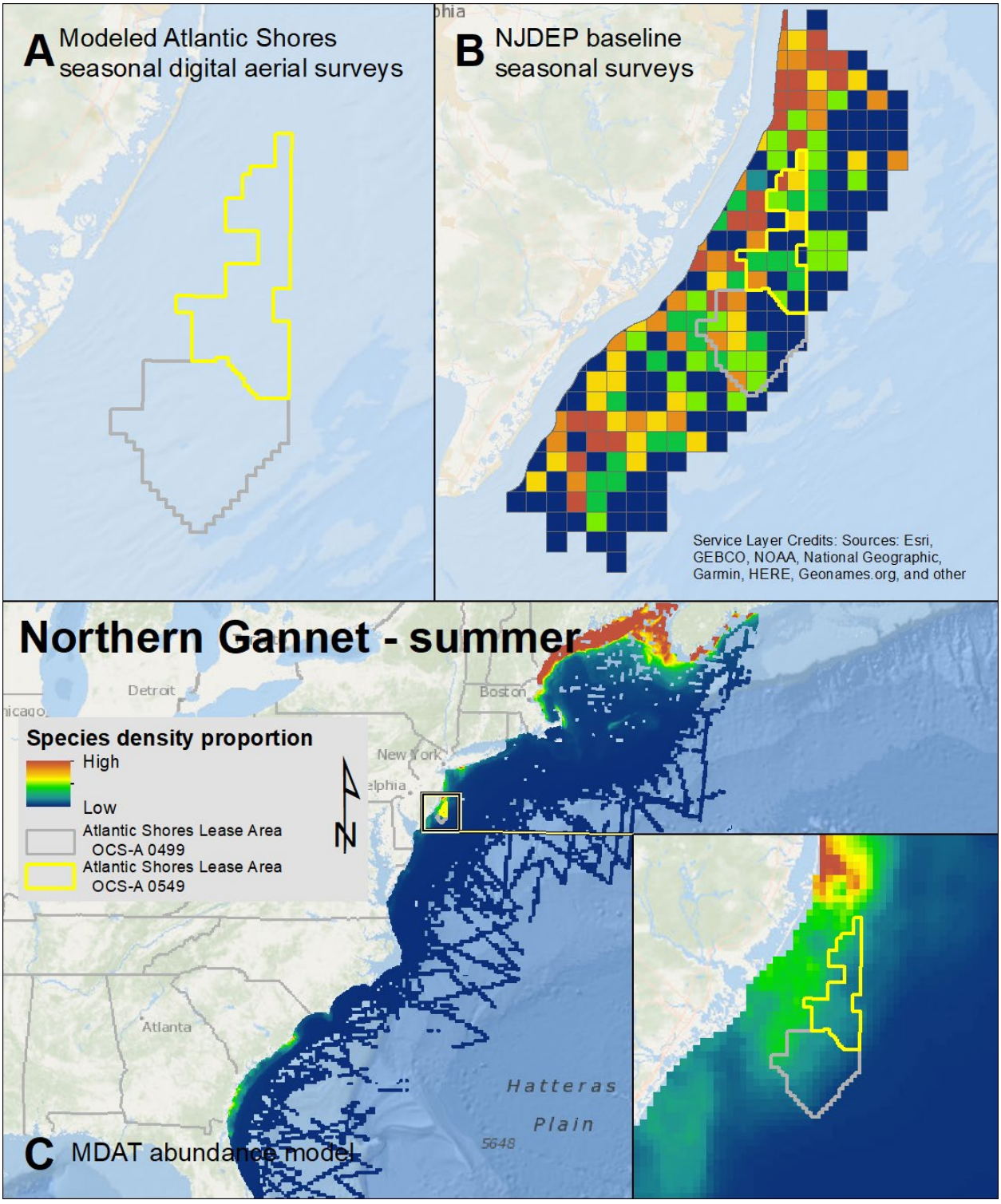

Map 68. Summer Northern Gannet modeled density proportions in the Atlantic Shores seasonal digital aerial surveys (A), density proportions in the NJDEP baseline survey data (B), and the MDAT model outputs at local and regional scales (C). The scale for all maps is representative of relative spatial variation in the sites within the season for each information source.

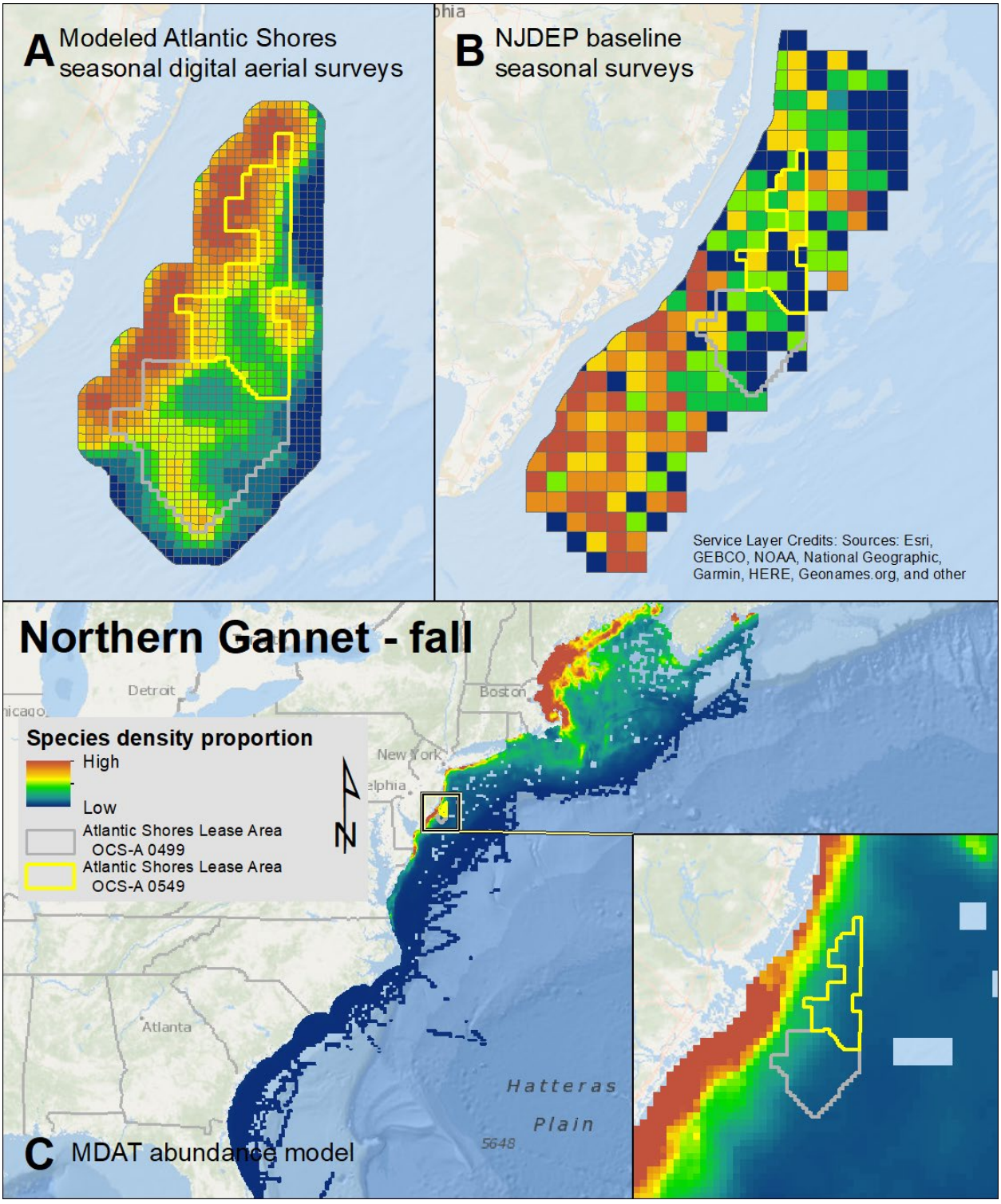

Map 69. Fall Northern Gannet modeled density proportions in the Atlantic Shores seasonal digital aerial surveys (A), density proportions in the NJDEP baseline survey data (B), and the MDAT model outputs at local and regional scales (C). The scale for all maps is representative of relative spatial variation in the sites within the season for each information source.

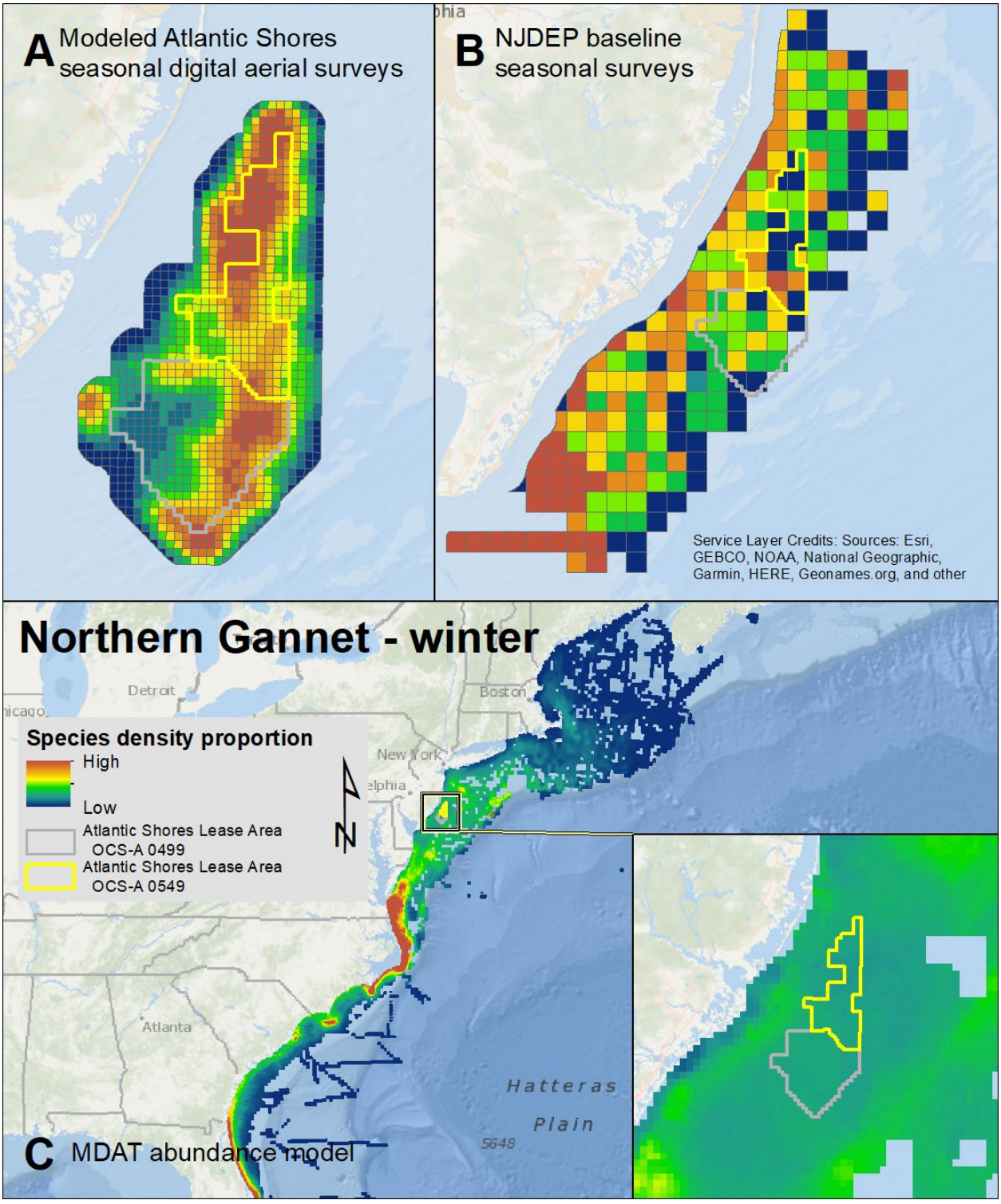

Map 70. Winter Northern Gannet modeled density proportions in the Atlantic Shores seasonal digital aerial surveys (A), density proportions in the NJDEP baseline survey data (B), and the MDAT model outputs at local and regional scales (C). The scale for all maps is representative of relative spatial variation in the sites within the season for each information source.

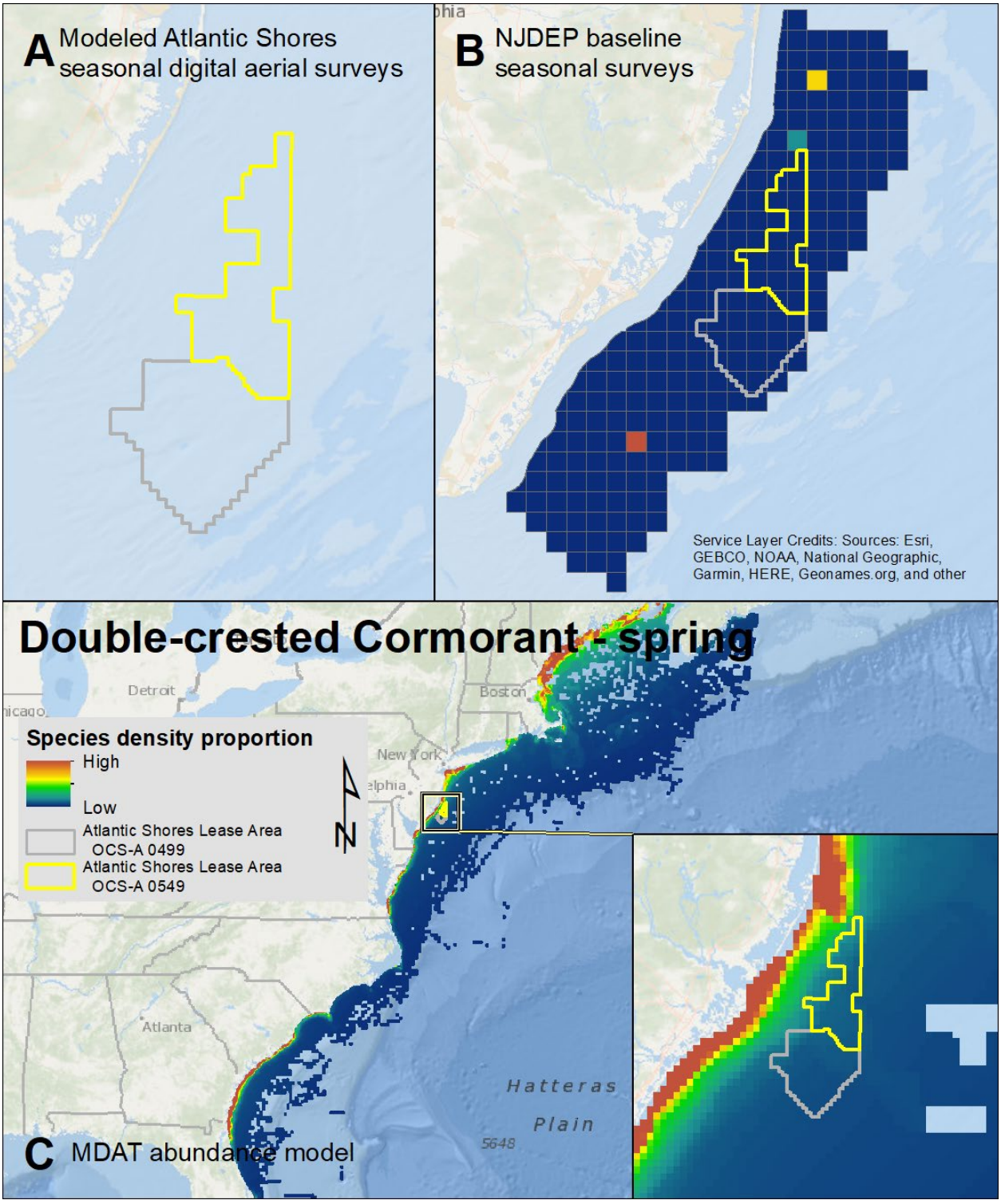

Map 71. Spring Double-crested Cormorant modeled density proportions in the Atlantic Shores seasonal digital aerial surveys (A), density proportions in the NJDEP baseline survey data (B), and the MDAT model outputs at local and regional scales (C). The scale for all maps is representative of relative spatial variation in the sites within the season for each information source.

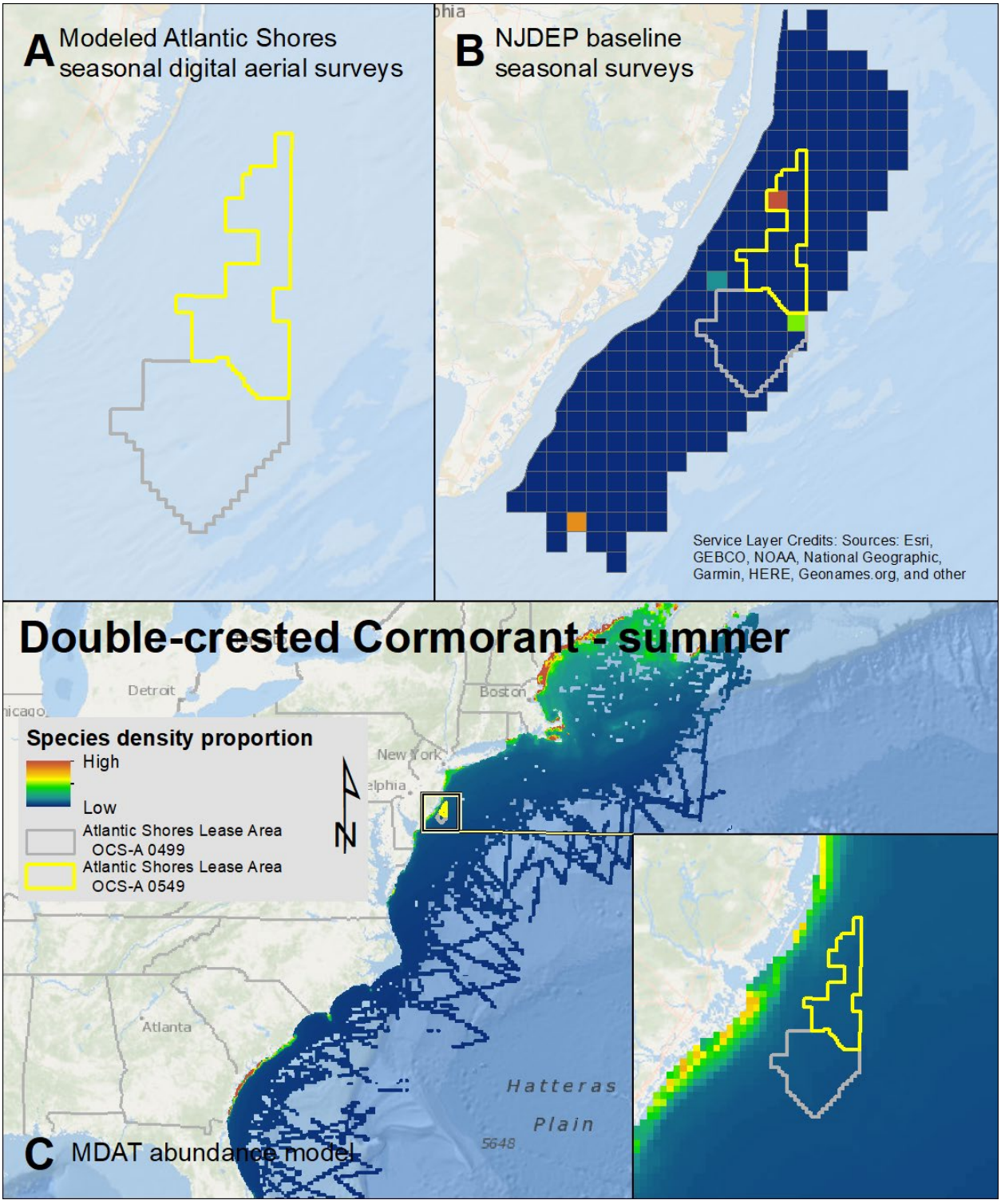

Map 72. Summer Double-crested Cormorant modeled density proportions in the Atlantic Shores seasonal digital aerial surveys (A), density proportions in the NJDEP baseline survey data (B), and the MDAT model outputs at local and regional scales (C). The scale for all maps is representative of relative spatial variation in the sites within the season for each information source.

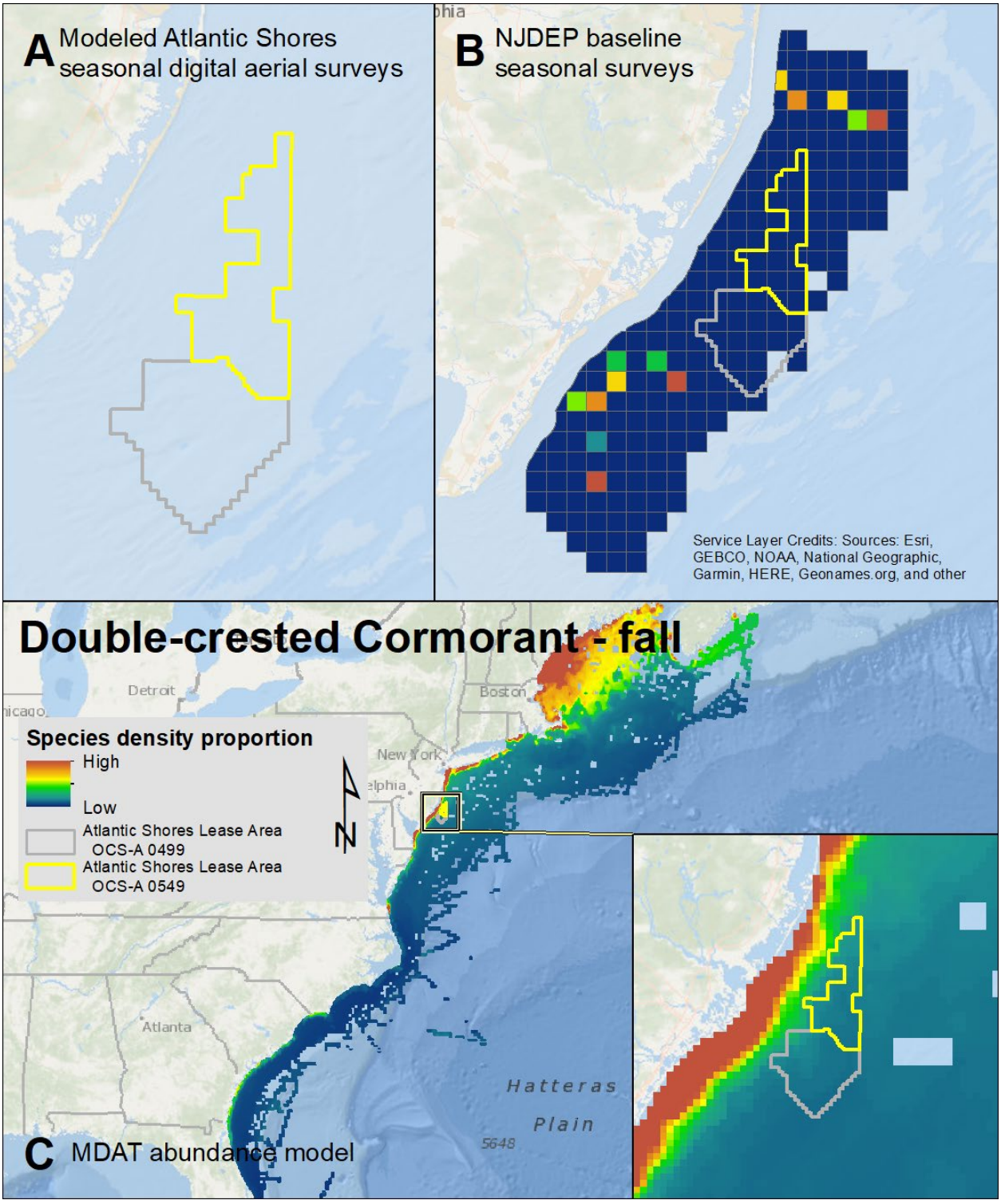

Map 73. Fall Double-crested Cormorant modeled density proportions in the Atlantic Shores seasonal digital aerial surveys (A), density proportions in the NJDEP baseline survey data (B), and the MDAT model outputs at local and regional scales (C). The scale for all maps is representative of relative spatial variation in the sites within the season for each information source.

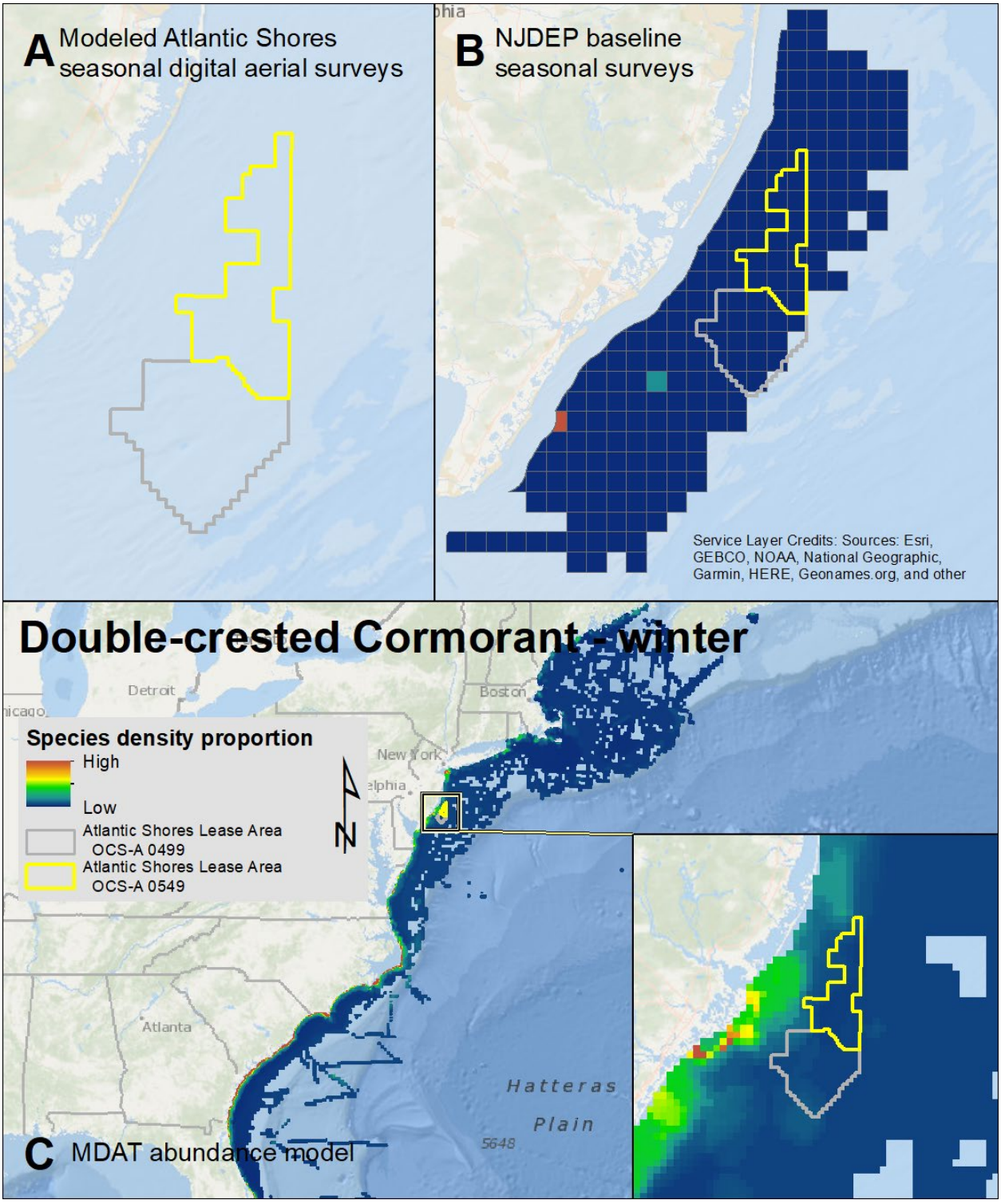

Map 74. Winter Double-crested Cormorant modeled density proportions in the Atlantic Shores seasonal digital aerial surveys (A), density proportions in the NJDEP baseline survey data (B), and the MDAT model outputs at local and regional scales (C). The scale for all maps is representative of relative spatial variation in the sites within the season for each information source.

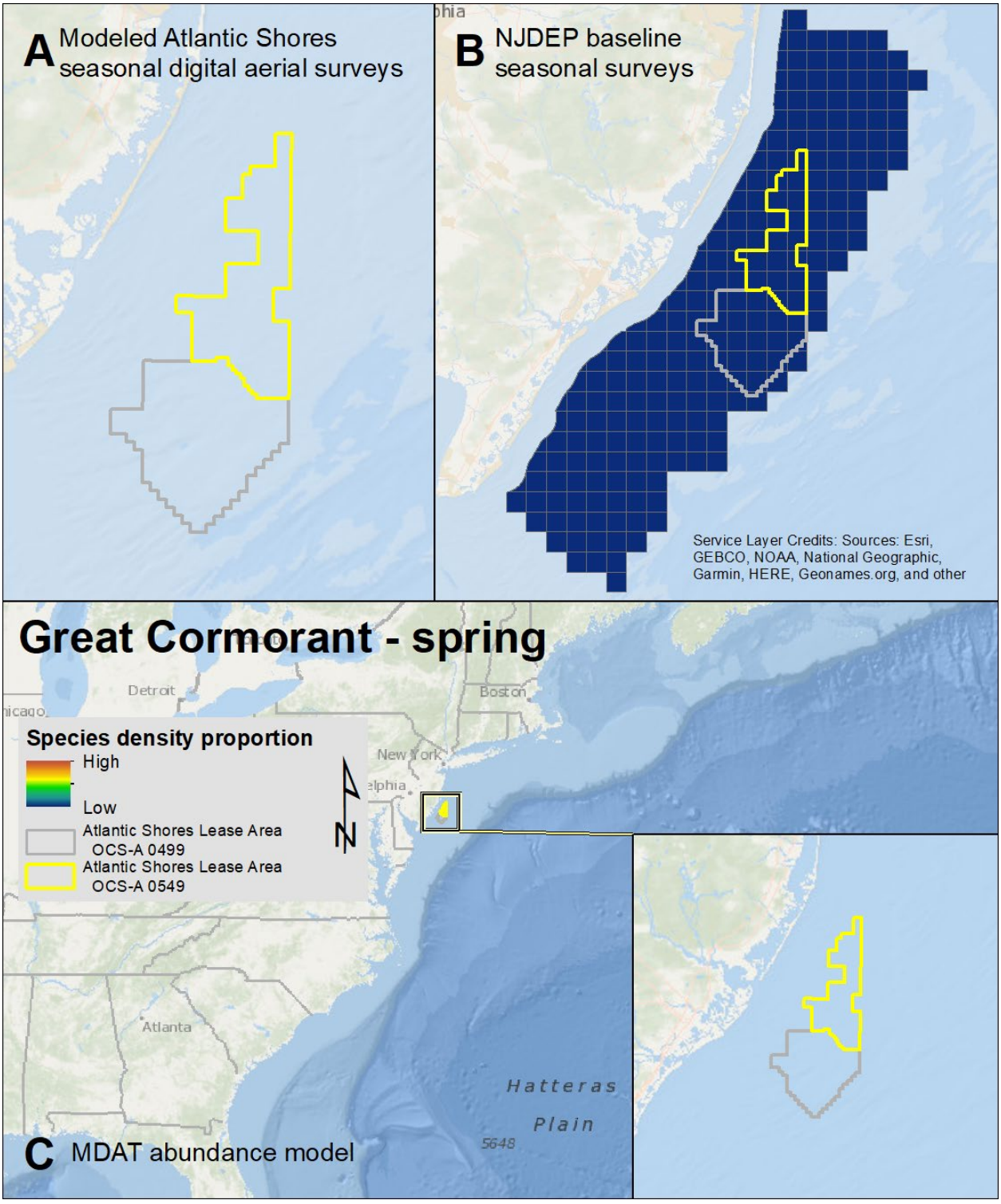

Map 75. Spring Great Cormorant modeled density proportions in the Atlantic Shores seasonal digital aerial surveys (A), density proportions in the NJDEP baseline survey data (B), and the MDAT model outputs at local and regional scales (C). The scale for all maps is representative of relative spatial variation in the sites within the season for each information source.

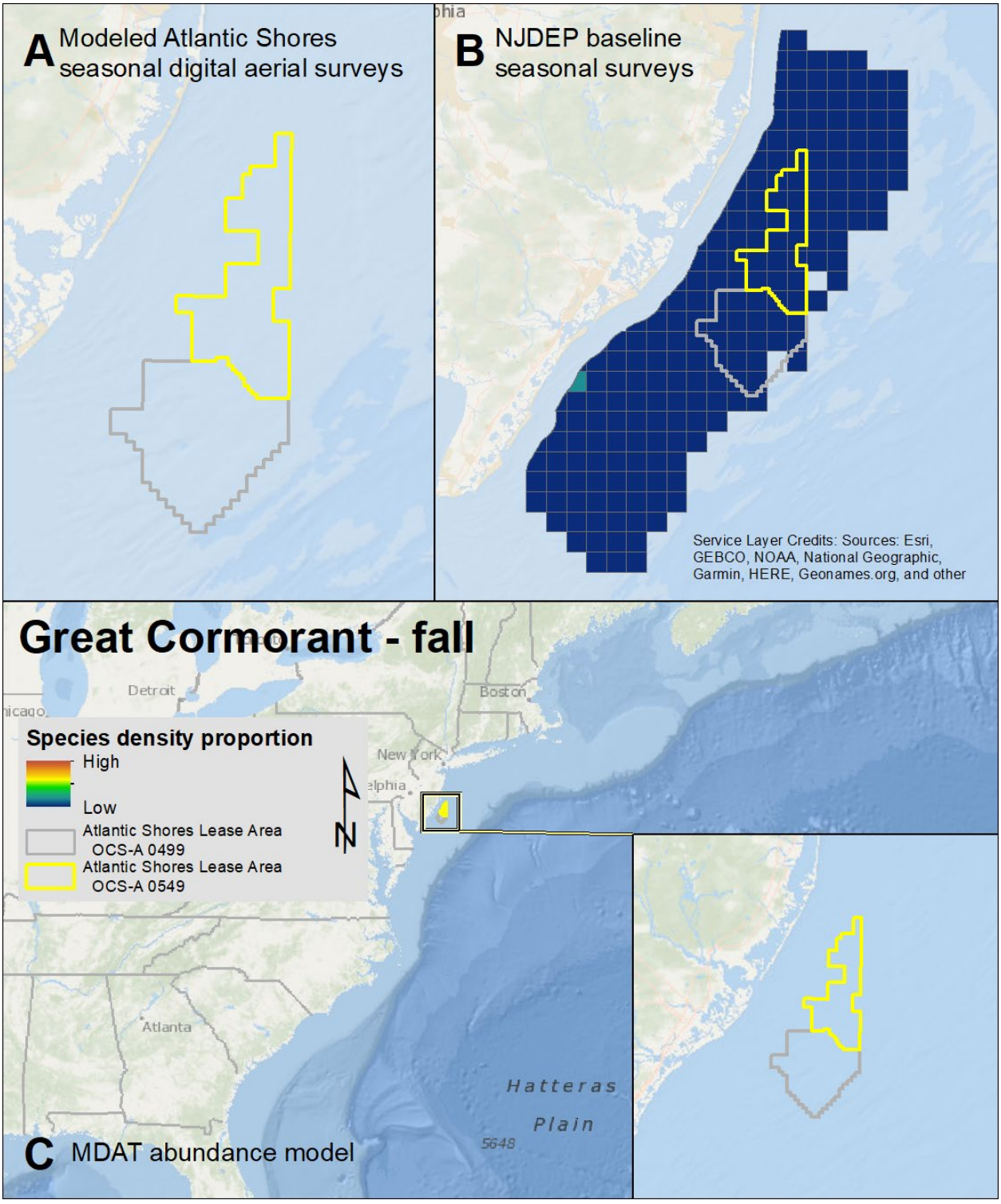

Map 76. Fall Great Cormorant modeled density proportions in the Atlantic Shores seasonal digital aerial surveys (A), density proportions in the NJDEP baseline survey data (B), and the MDAT model outputs at local and regional scales (C). The scale for all maps is representative of relative spatial variation in the sites within the season for each information source.

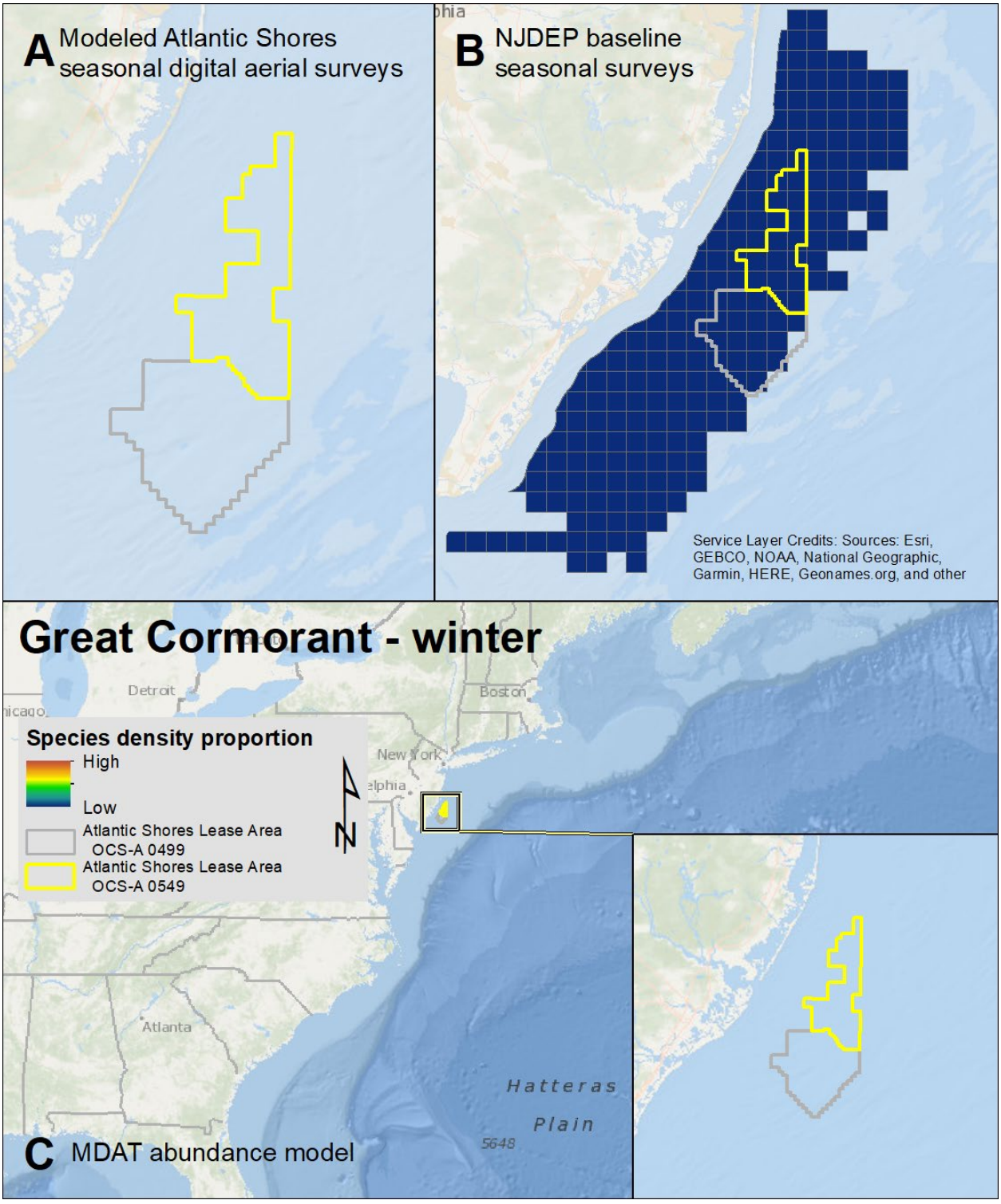

Map 77. Winter Great Cormorant modeled density proportions in the Atlantic Shores seasonal digital aerial surveys (A), density proportions in the NJDEP baseline survey data (B), and the MDAT model outputs at local and regional scales (C). The scale for all maps is representative of relative spatial variation in the sites within the season for each information source.

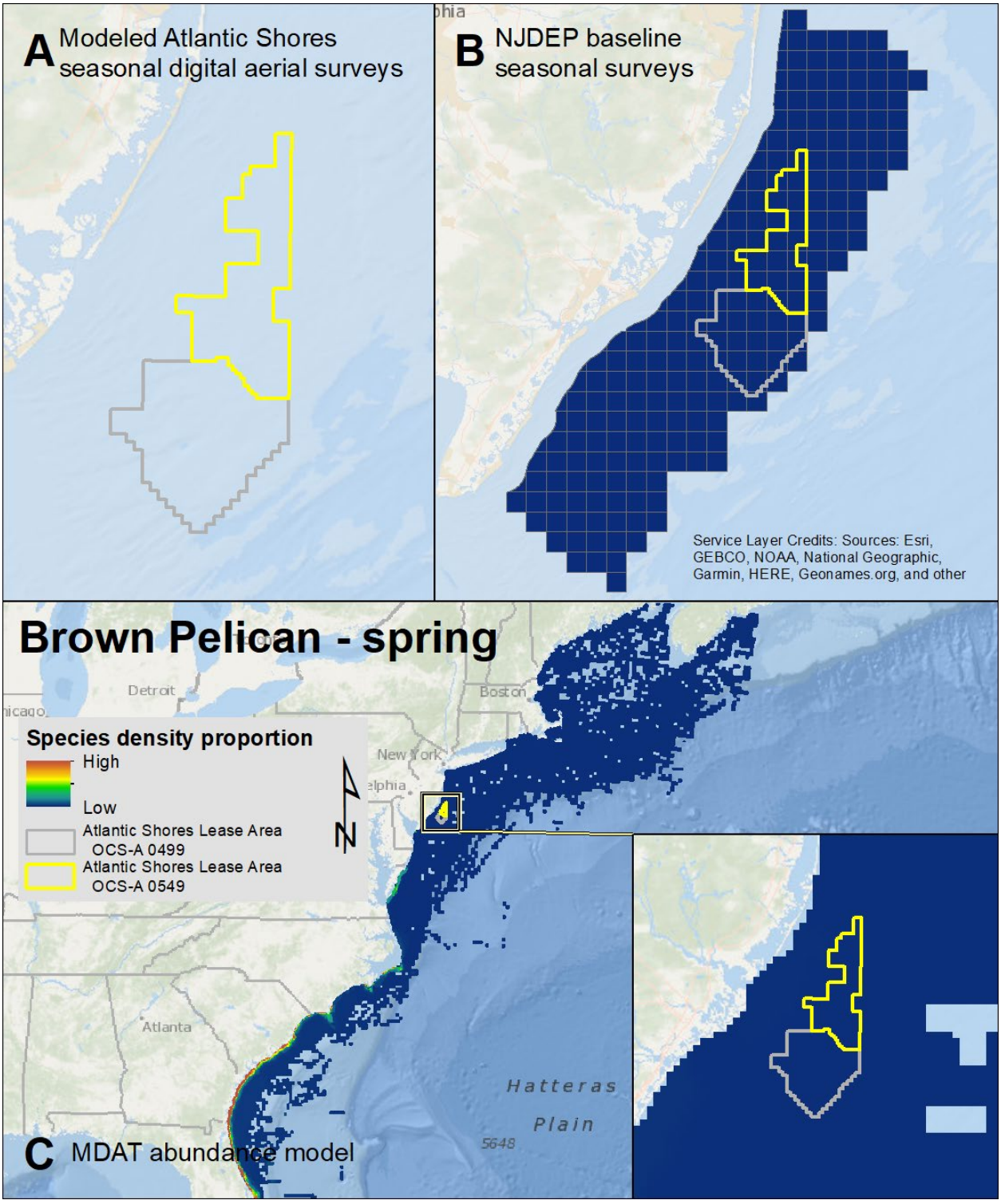

Map 78. Spring Brown Pelican modeled density proportions in the Atlantic Shores seasonal digital aerial surveys (A), density proportions in the NJDEP baseline survey data (B), and the MDAT model outputs at local and regional scales (C). The scale for all maps is representative of relative spatial variation in the sites within the season for each information source.

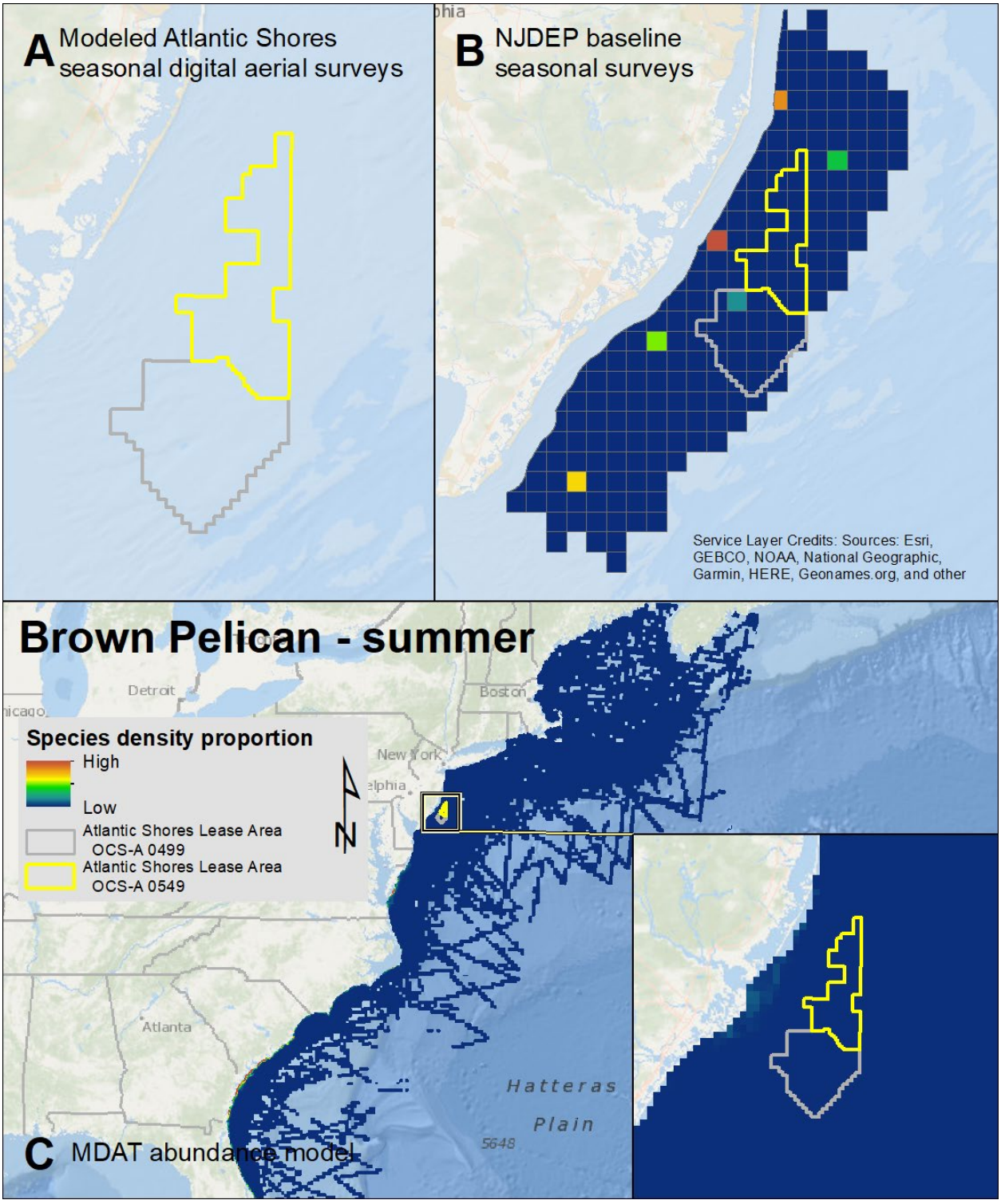

Map 79. Summer Brown Pelican modeled density proportions in the Atlantic Shores seasonal digital aerial surveys (A), density proportions in the NJDEP baseline survey data (B), and the MDAT model outputs at local and regional scales (C). The scale for all maps is representative of relative spatial variation in the sites within the season for each information source.

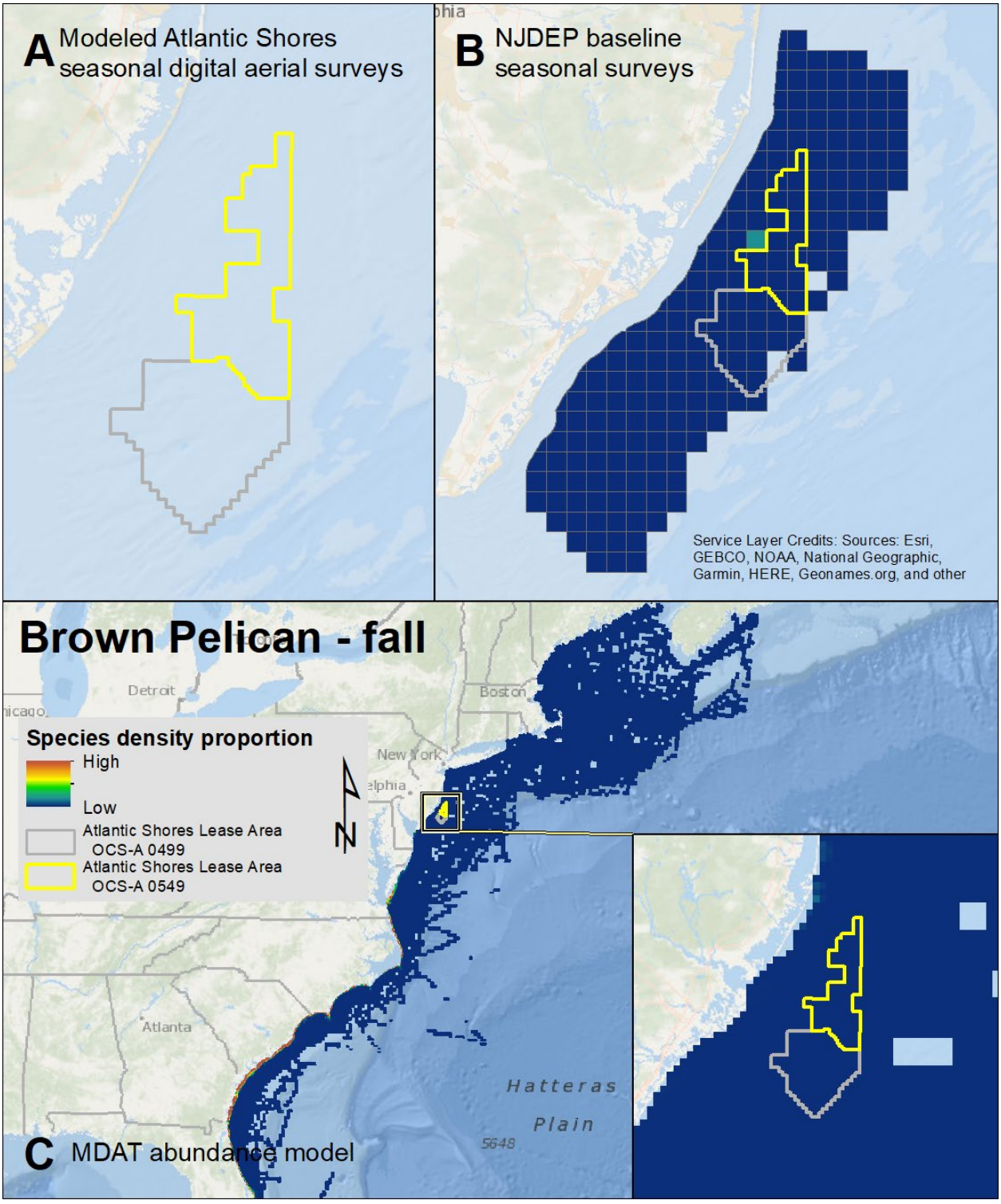

Map 80. Fall Brown Pelican modeled density proportions in the Atlantic Shores seasonal digital aerial surveys (A), density proportions in the NJDEP baseline survey data (B), and the MDAT model outputs at local and regional scales (C). The scale for all maps is representative of relative spatial variation in the sites within the season for each information source.

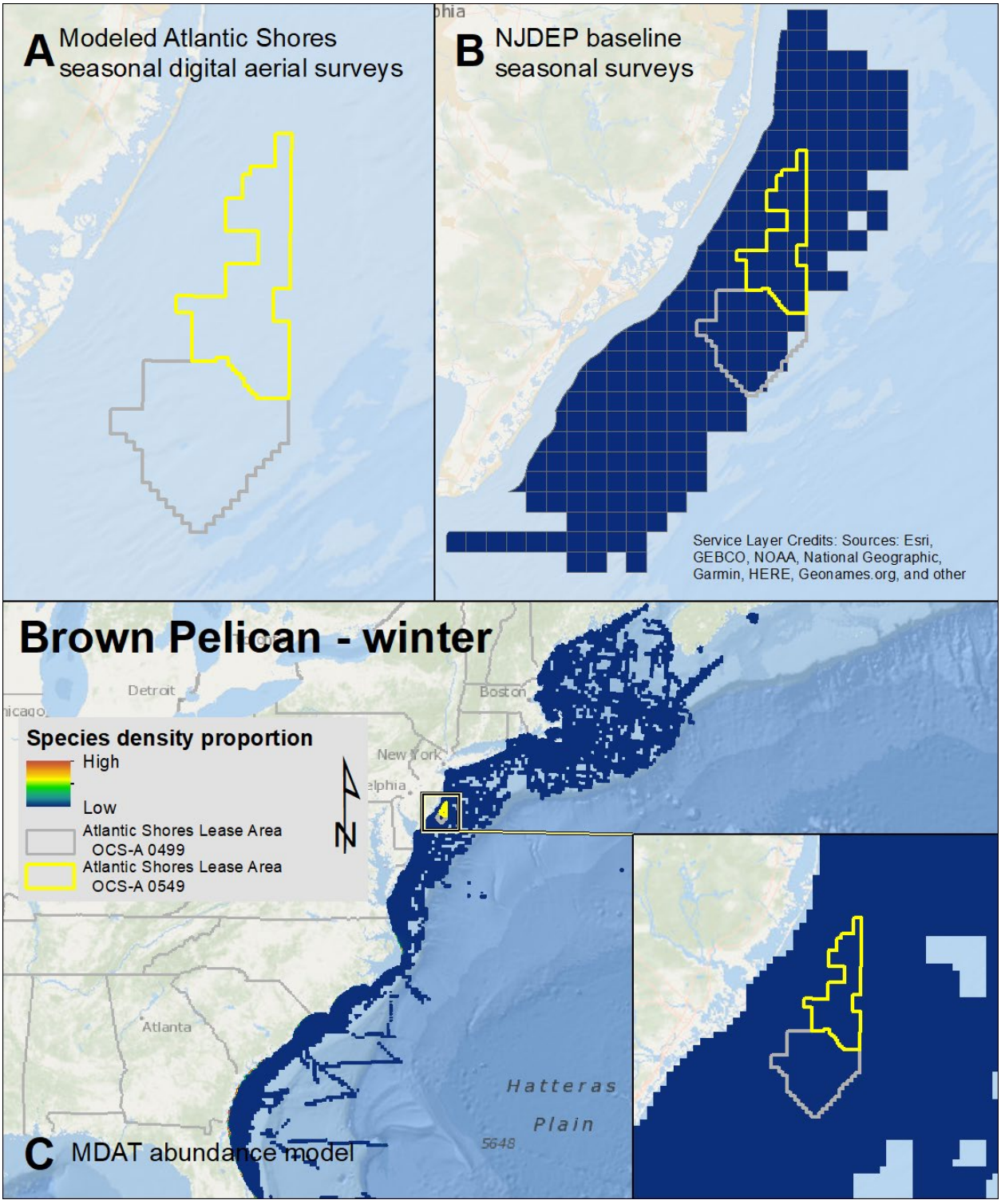

Map 81. Winter Brown Pelican modeled density proportions in the Atlantic Shores seasonal digital aerial surveys (A), density proportions in the NJDEP baseline survey data (B), and the MDAT model outputs at local and regional scales (C). The scale for all maps is representative of relative spatial variation in the sites within the season for each information source.

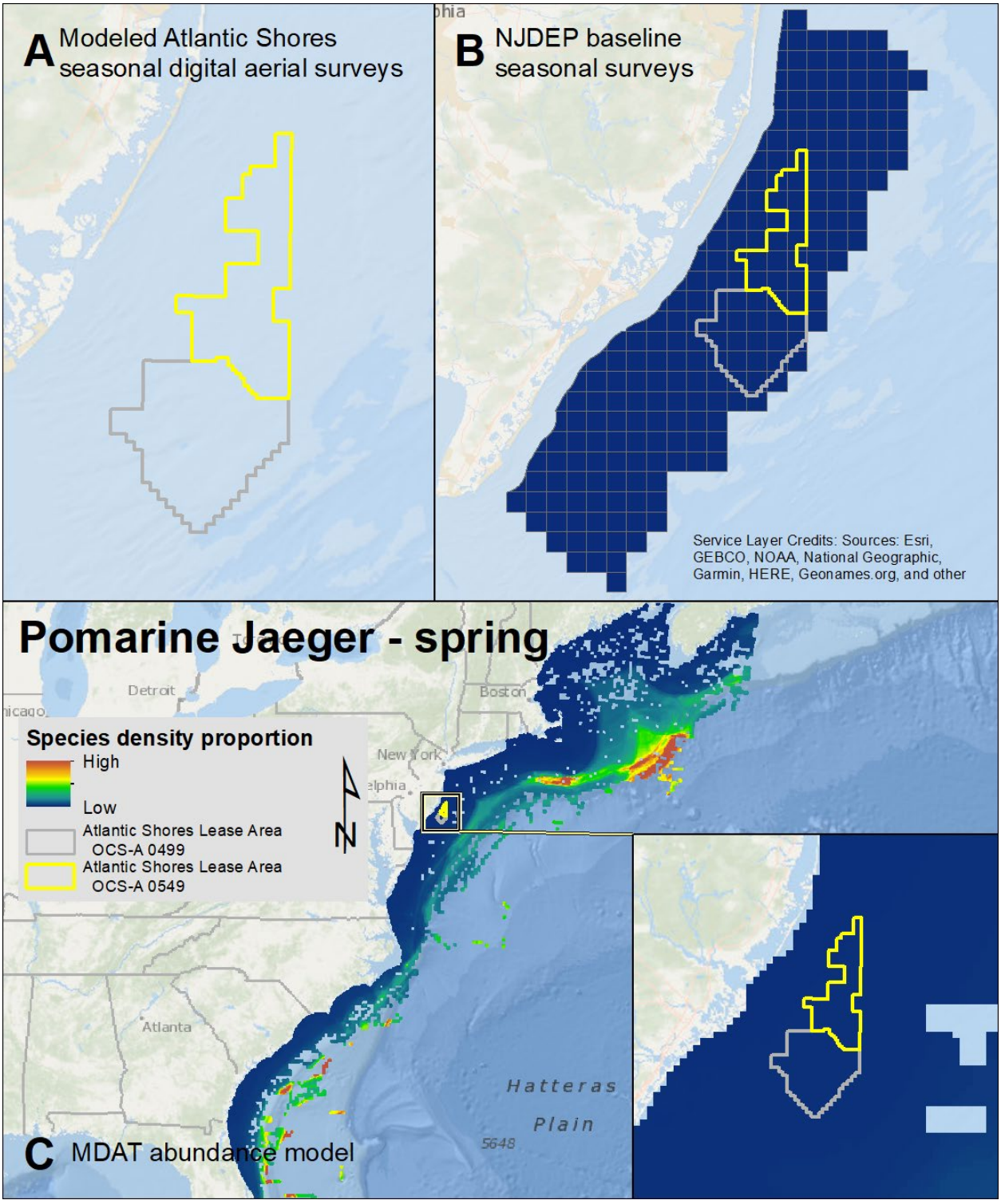

Map 82. Spring Pomarine Jaeger modeled density proportions in the Atlantic Shores seasonal digital aerial surveys (A), density proportions in the NJDEP baseline survey data (B), and the MDAT model outputs at local and regional scales (C). The scale for all maps is representative of relative spatial variation in the sites within the season for each information source.

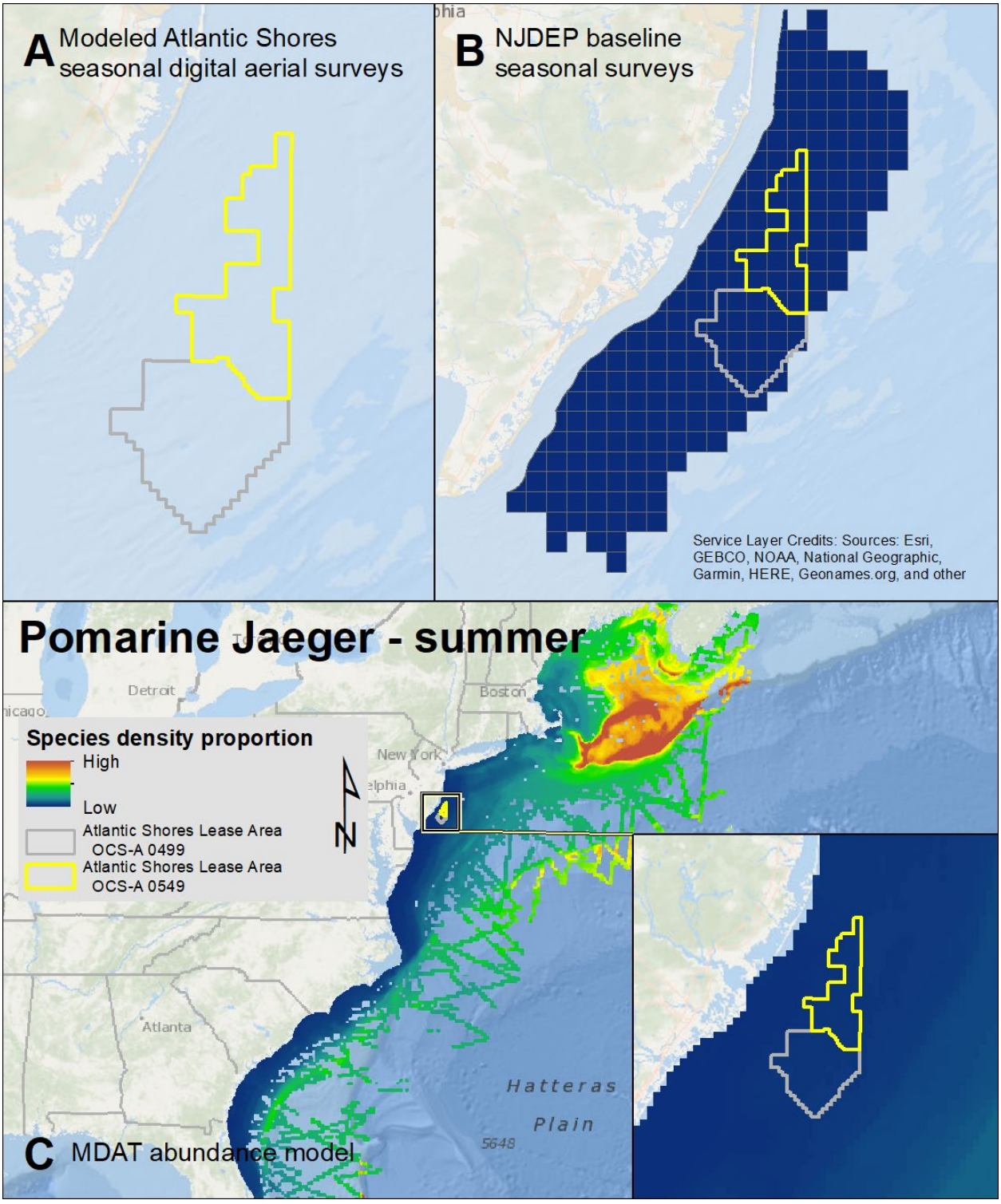

Map 83. Summer Pomarine Jaeger modeled density proportions in the Atlantic Shores seasonal digital aerial surveys (A), density proportions in the NJDEP baseline survey data (B), and the MDAT model outputs at local and regional scales (C). The scale for all maps is representative of relative spatial variation in the sites within the season for each information source.

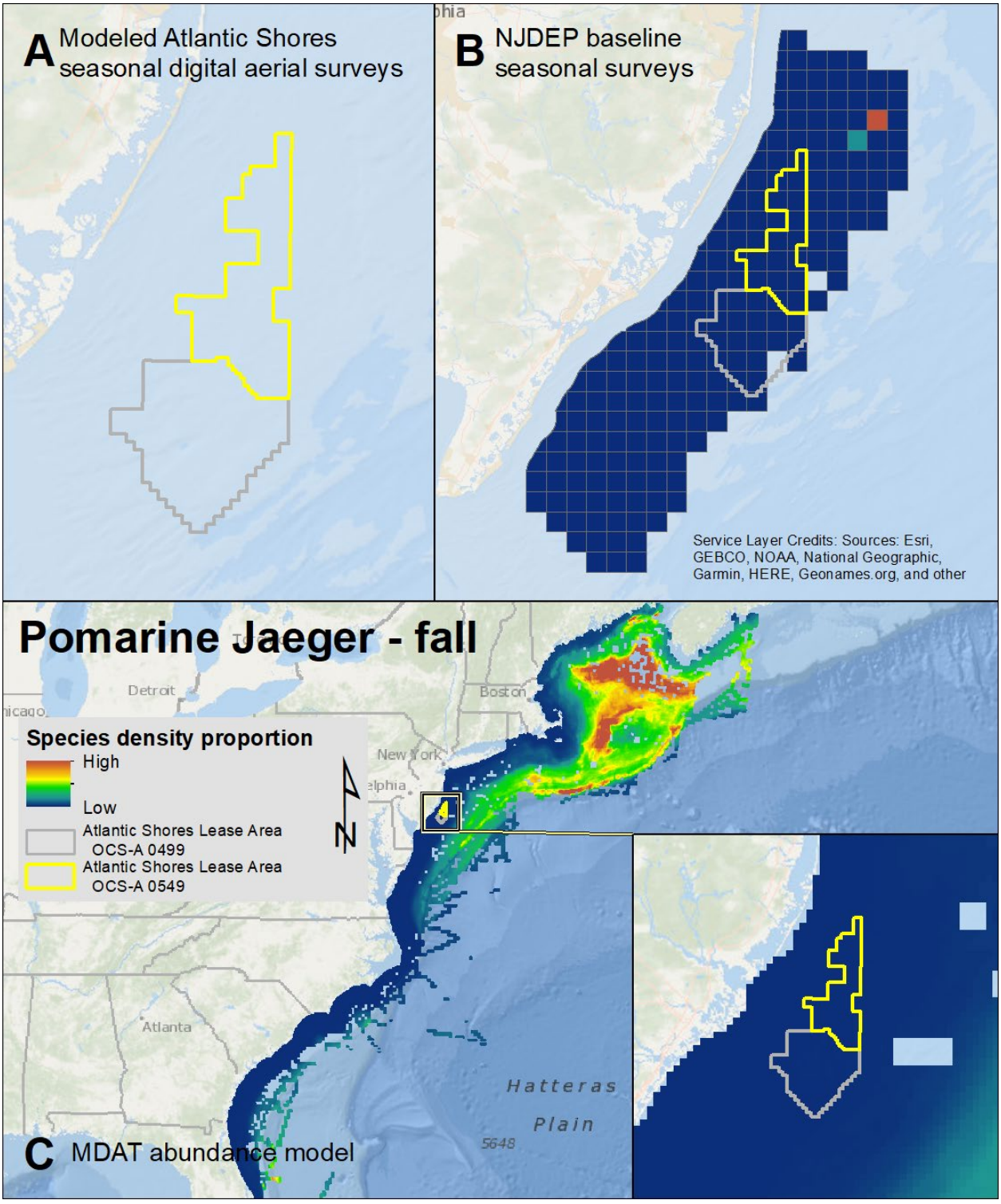

Map 84. Fall Pomarine Jaeger modeled density proportions in the Atlantic Shores seasonal digital aerial surveys (A), density proportions in the NJDEP baseline survey data (B), and the MDAT model outputs at local and regional scales (C). The scale for all maps is representative of relative spatial variation in the sites within the season for each information source.

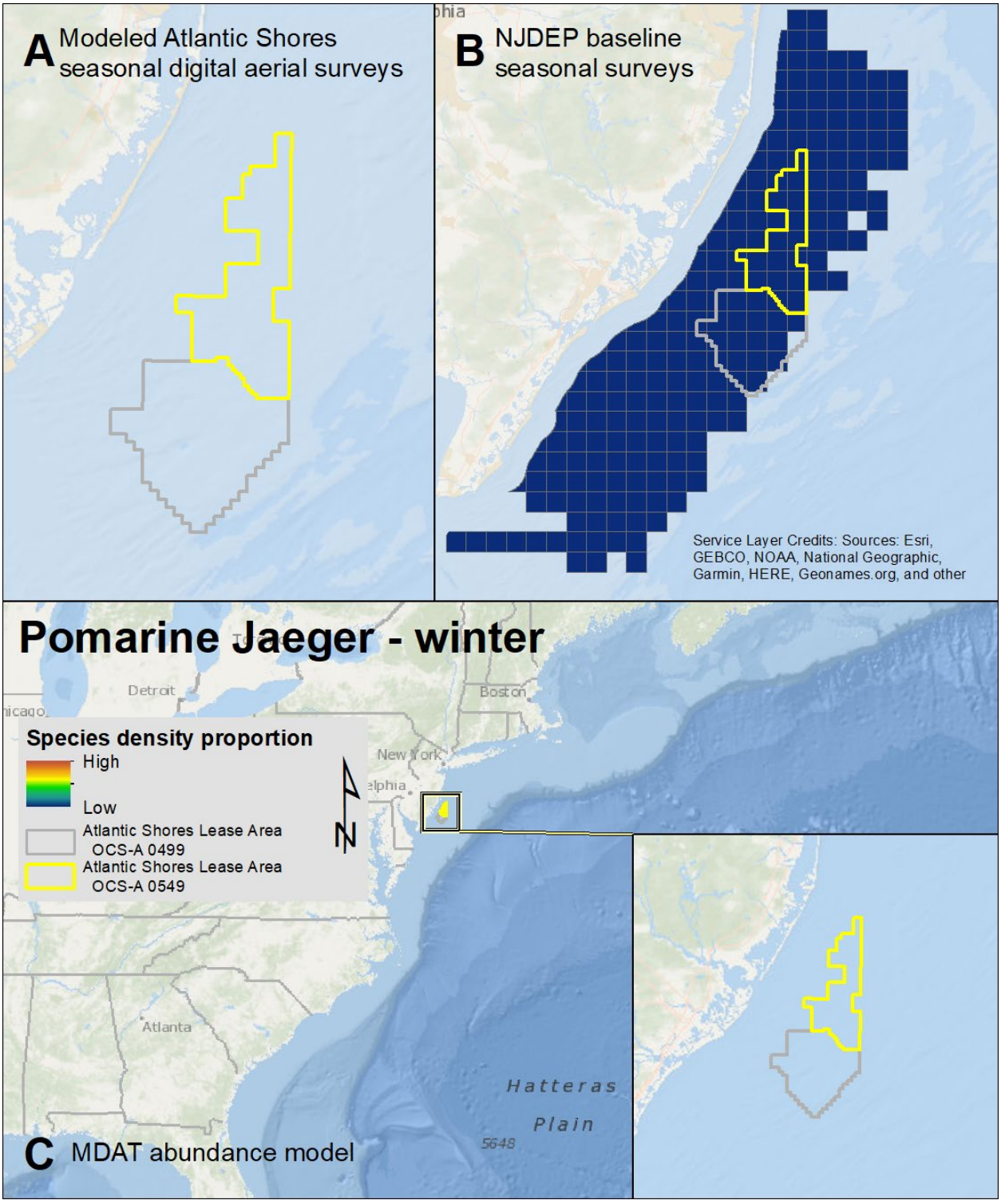

Map 85. Winter Pomarine Jaeger modeled density proportions in the Atlantic Shores seasonal digital aerial surveys (A), density proportions in the NJDEP baseline survey data (B), and the MDAT model outputs at local and regional scales (C). The scale for all maps is representative of relative spatial variation in the sites within the season for each information source.

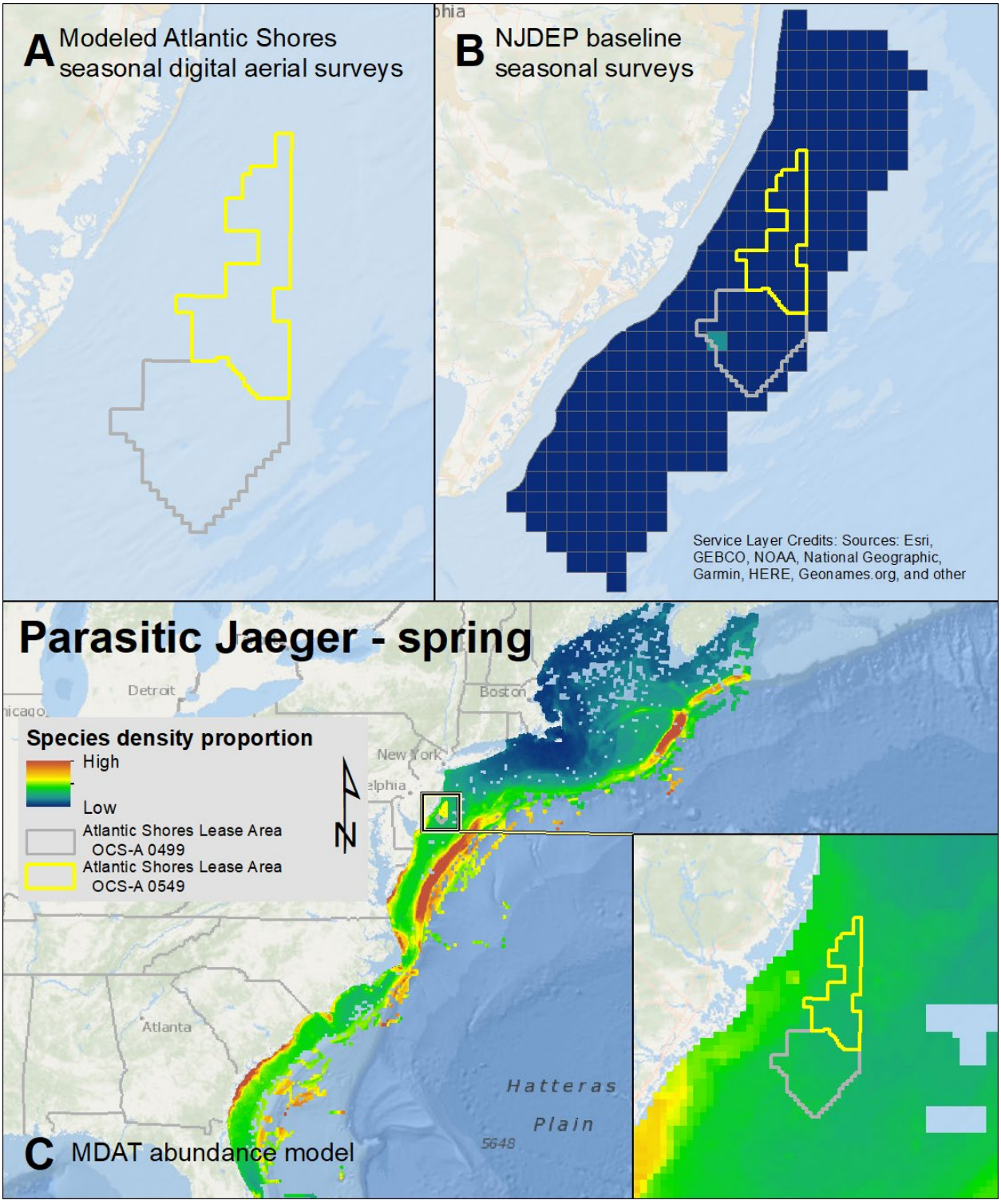

Map 86. Spring Parasitic Jaeger modeled density proportions in the Atlantic Shores seasonal digital aerial surveys (A), density proportions in the NJDEP baseline survey data (B), and the MDAT model outputs at local and regional scales (C). The scale for all maps is representative of relative spatial variation in the sites within the season for each information source.

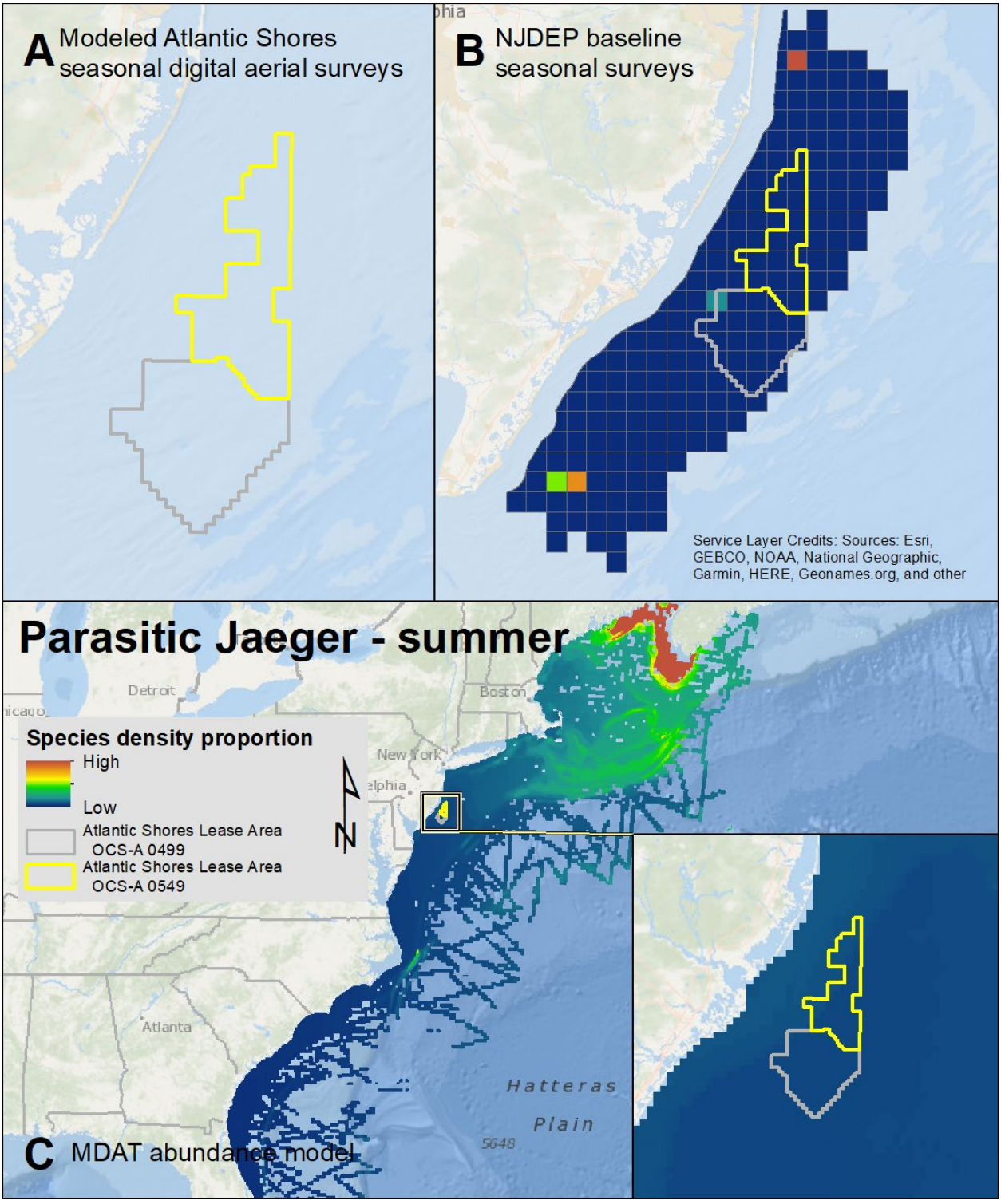

Map 87. Summer Parasitic Jaeger modeled density proportions in the Atlantic Shores seasonal digital aerial surveys (A), density proportions in the NJDEP baseline survey data (B), and the MDAT model outputs at local and regional scales (C). The scale for all maps is representative of relative spatial variation in the sites within the season for each information source.

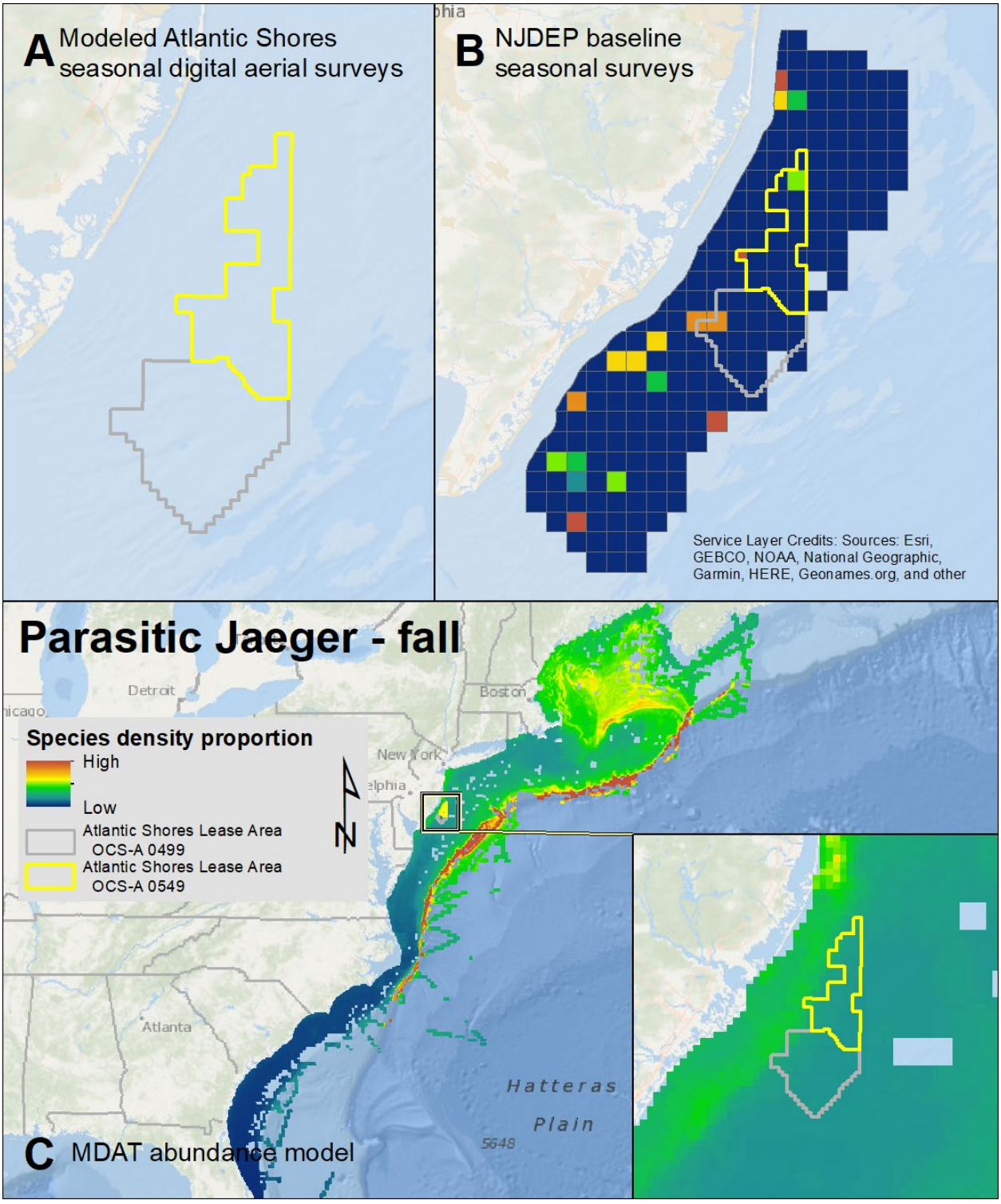

Map 88. Fall Parasitic Jaeger modeled density proportions in the Atlantic Shores seasonal digital aerial surveys (A), density proportions in the NJDEP baseline survey data (B), and the MDAT model outputs at local and regional scales (C). The scale for all maps is representative of relative spatial variation in the sites within the season for each information source.

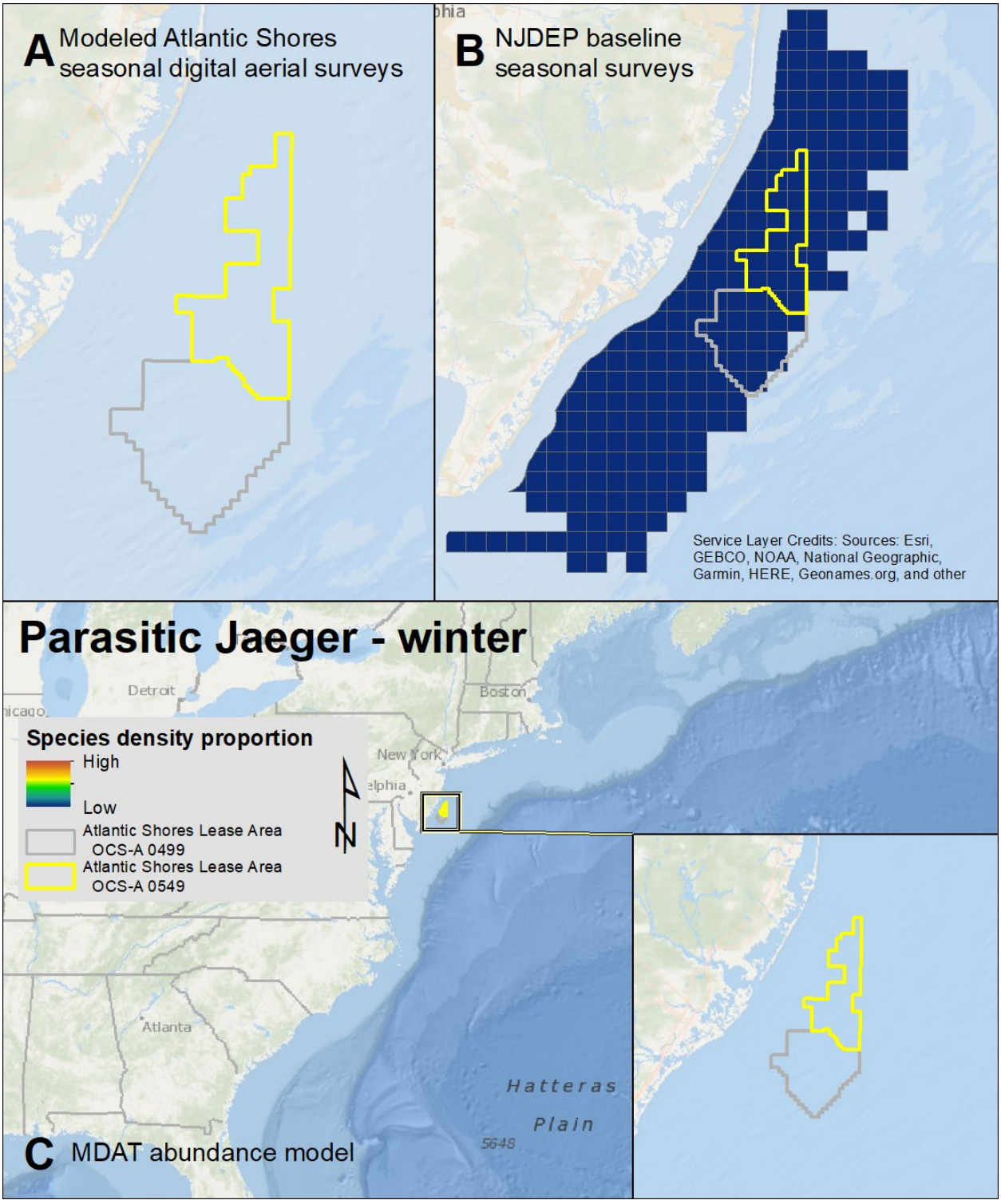

Map 89. Winter Parasitic Jaeger modeled density proportions in the Atlantic Shores seasonal digital aerial surveys (A), density proportions in the NJDEP baseline survey data (B), and the MDAT model outputs at local and regional scales (C). The scale for all maps is representative of relative spatial variation in the sites within the season for each information source.

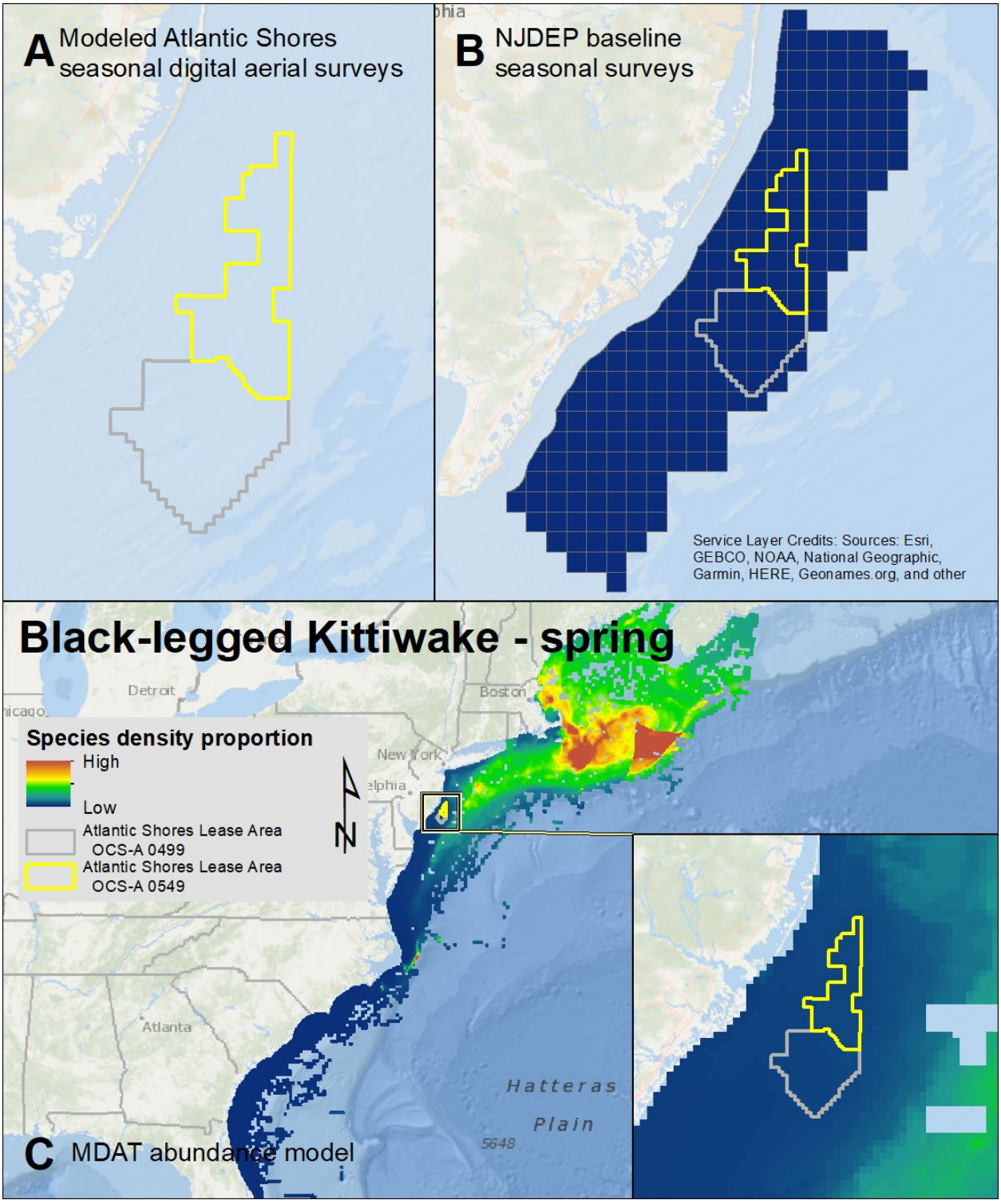

Map 90. Spring Black-legged Kittiwake modeled density proportions in the Atlantic Shores seasonal digital aerial surveys (A), density proportions in the NJDEP baseline survey data (B), and the MDAT model outputs at local and regional scales (C). The scale for all maps is representative of relative spatial variation in the sites within the season for each information source.

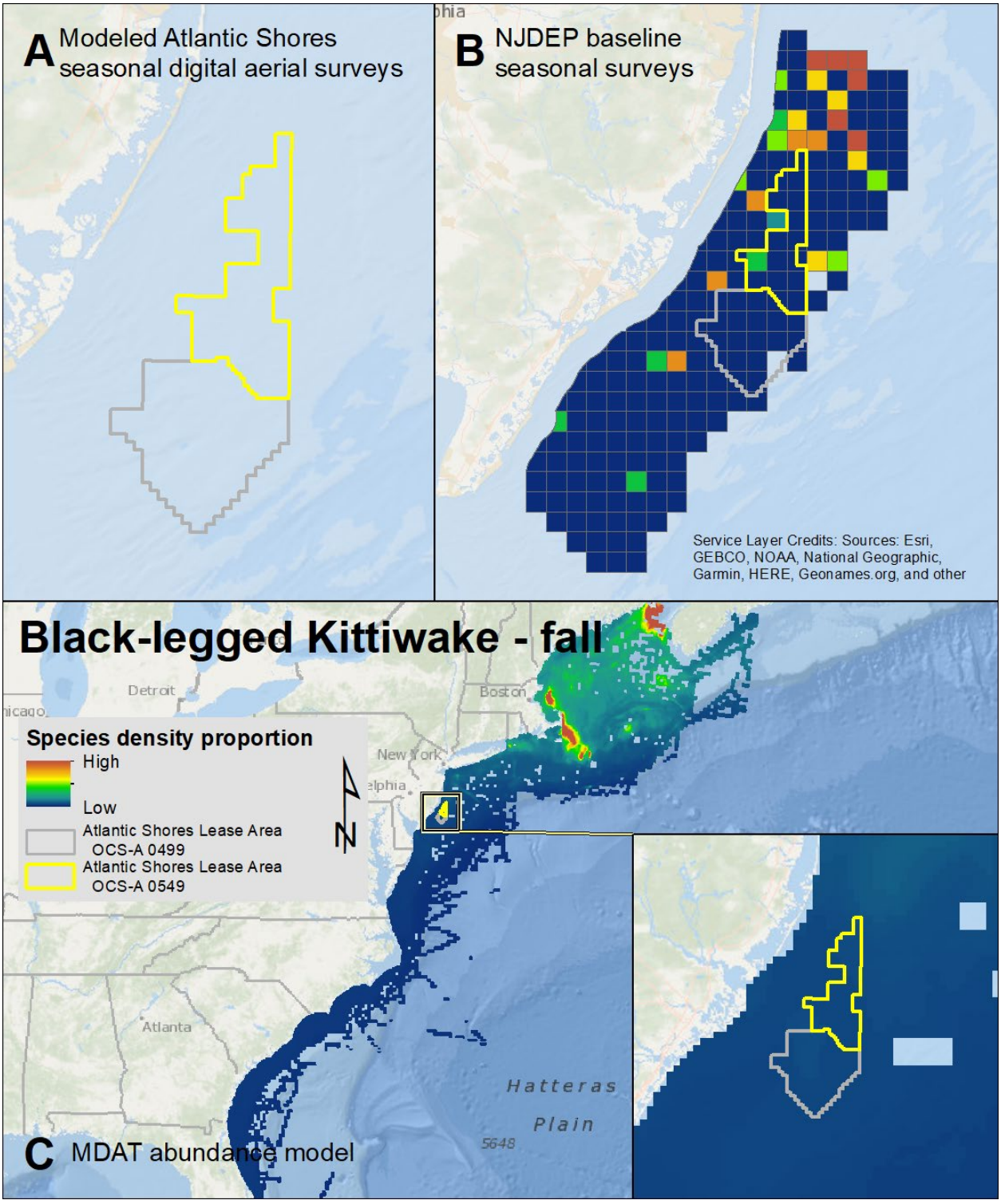

Map 91. Fall Black-legged Kittiwake modeled density proportions in the Atlantic Shores seasonal digital aerial surveys (A), density proportions in the NJDEP baseline survey data (B), and the MDAT model outputs at local and regional scales (C). The scale for all maps is representative of relative spatial variation in the sites within the season for each information source.

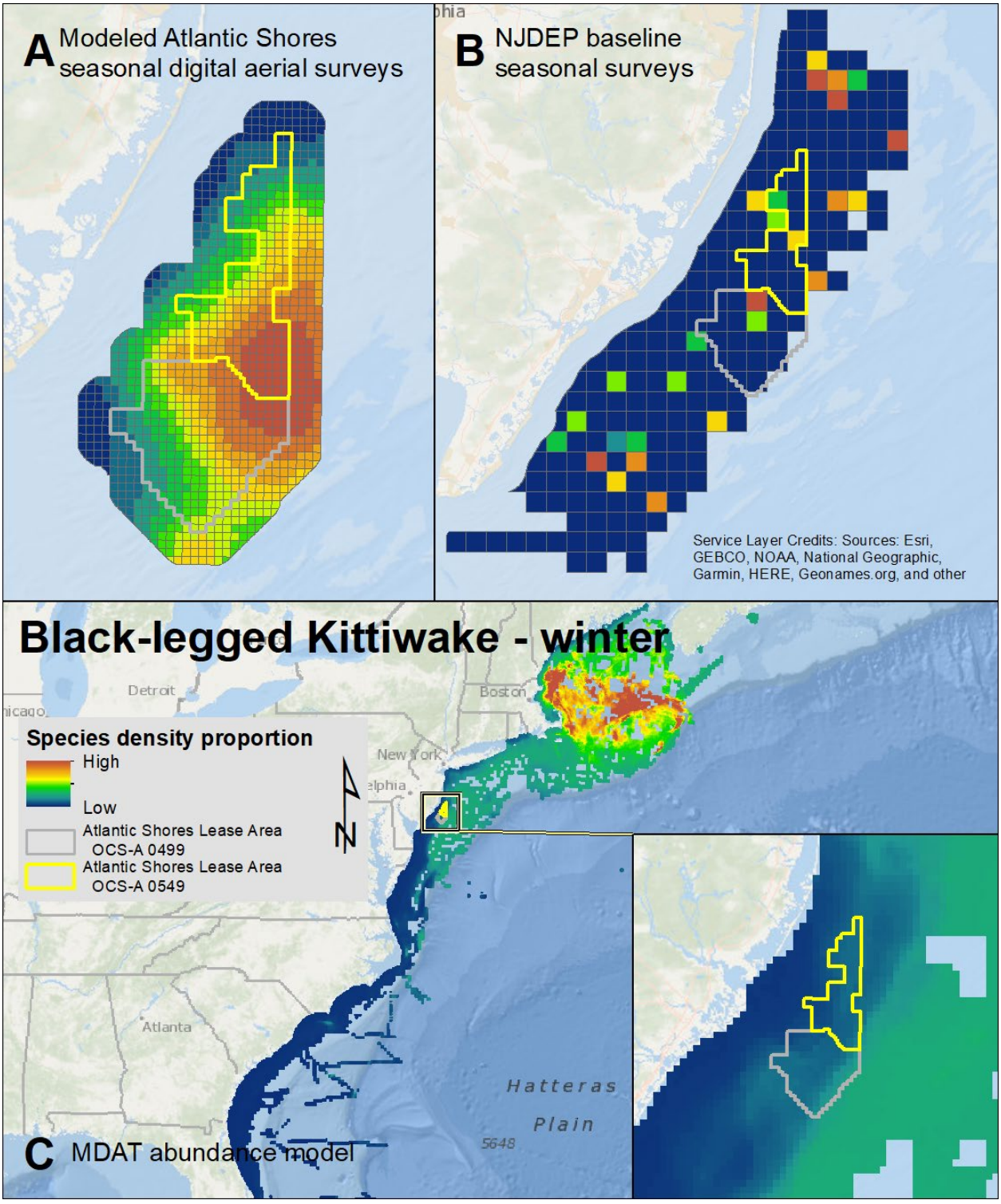

Map 92. Winter Black-legged Kittiwake modeled density proportions in the Atlantic Shores seasonal digital aerial surveys (A), density proportions in the NJDEP baseline survey data (B), and the MDAT model outputs at local and regional scales (C). The scale for all maps is representative of relative spatial variation in the sites within the season for each information source.

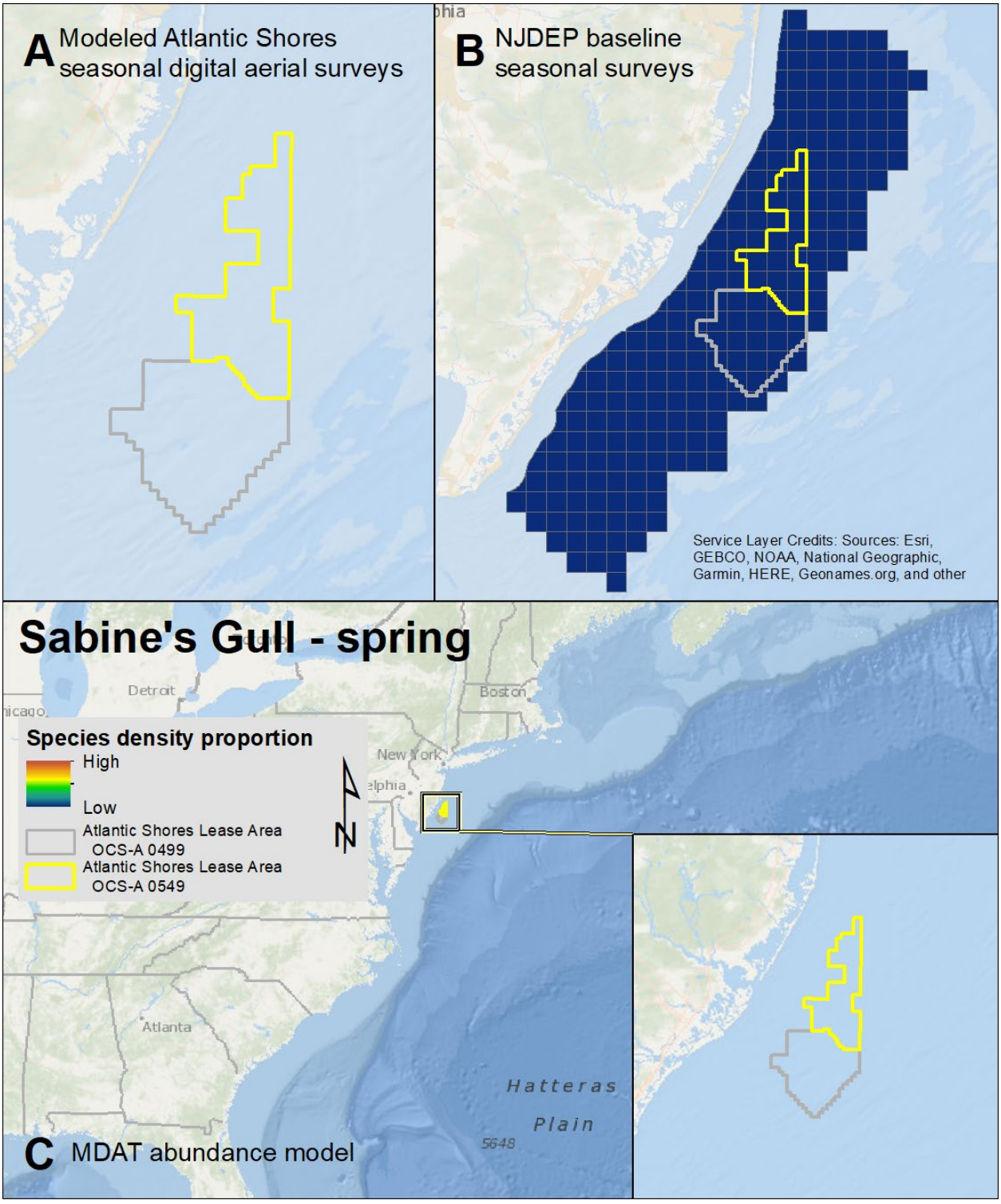

Map 93. Spring Sabine's Gull modeled density proportions in the Atlantic Shores seasonal digital aerial surveys (A), density proportions in the NJDEP baseline survey data (B), and the MDAT model outputs at local and regional scales (C). The scale for all maps is representative of relative spatial variation in the sites within the season for each information source.

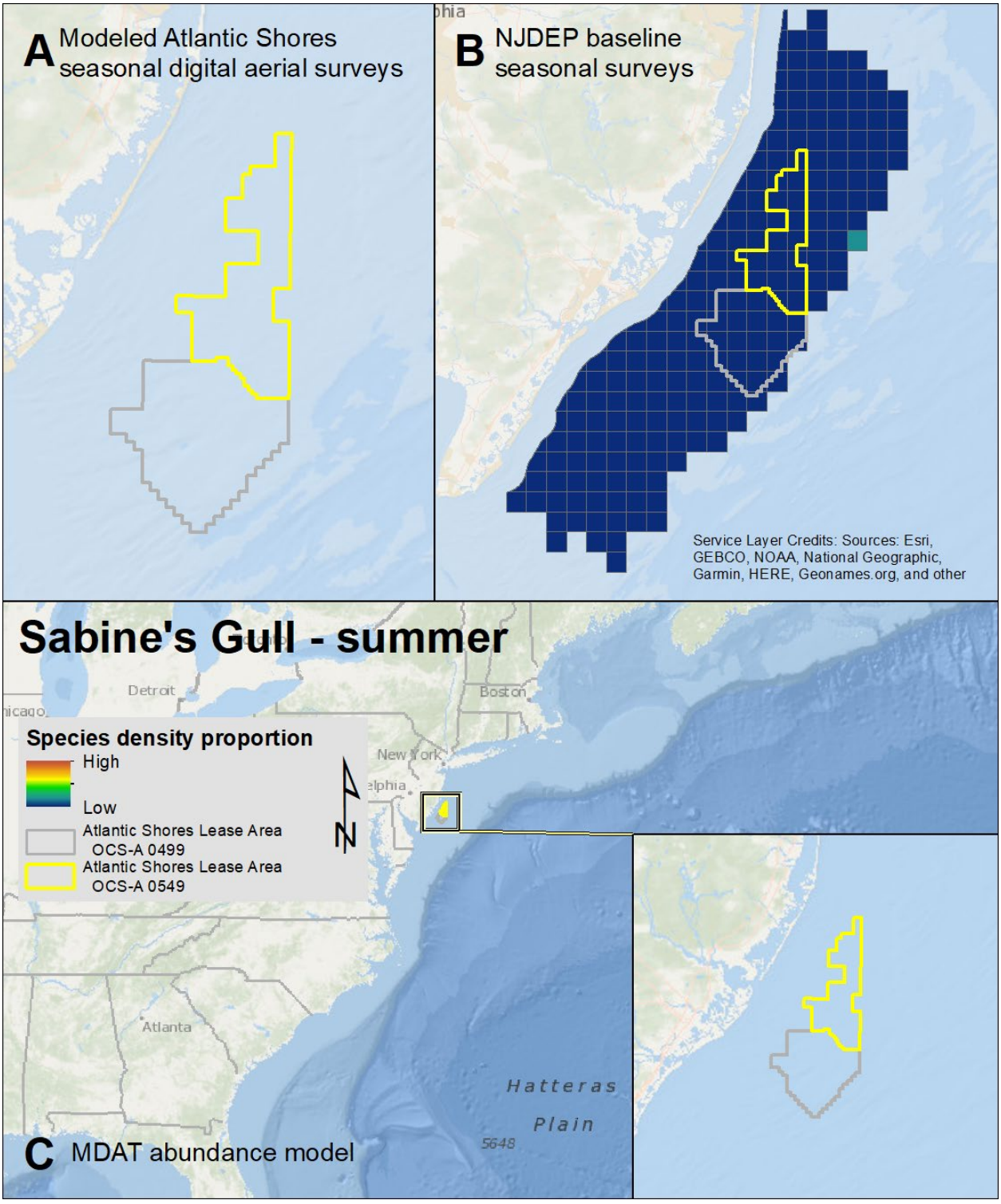

Map 94. Summer Sabine's Gull modeled density proportions in the Atlantic Shores seasonal digital aerial surveys (A), density proportions in the NJDEP baseline survey data (B), and the MDAT model outputs at local and regional scales (C). The scale for all maps is representative of relative spatial variation in the sites within the season for each information source.

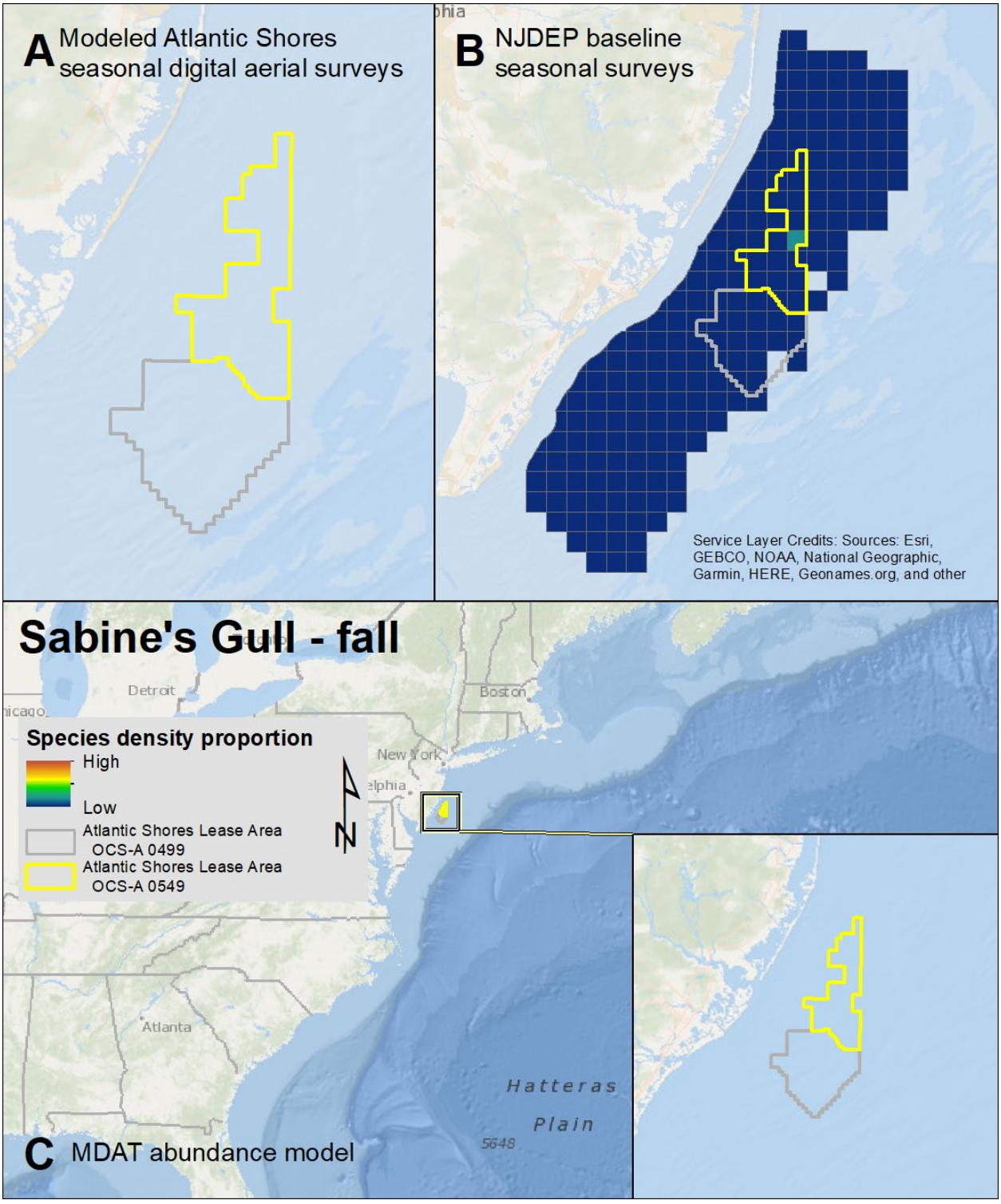

Map 95. Fall Sabine's Gull modeled density proportions in the Atlantic Shores seasonal digital aerial surveys (A), density proportions in the NJDEP baseline survey data (B), and the MDAT model outputs at local and regional scales (C). The scale for all maps is representative of relative spatial variation in the sites within the season for each information source.

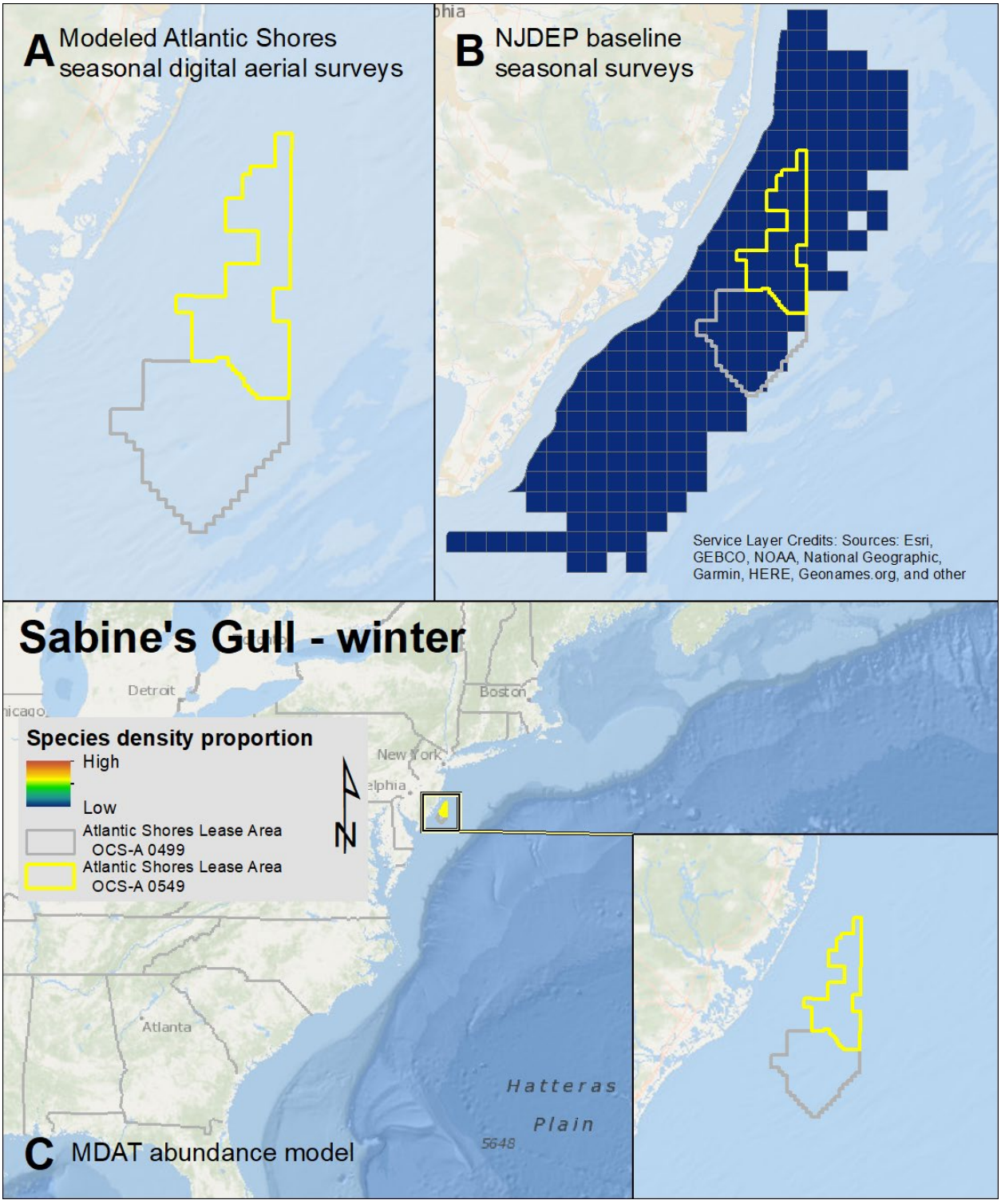

Map 96. Winter Sabine's Gull modeled density proportions in the Atlantic Shores seasonal digital aerial surveys (A), density proportions in the NJDEP baseline survey data (B), and the MDAT model outputs at local and regional scales (C). The scale for all maps is representative of relative spatial variation in the sites within the season for each information source.

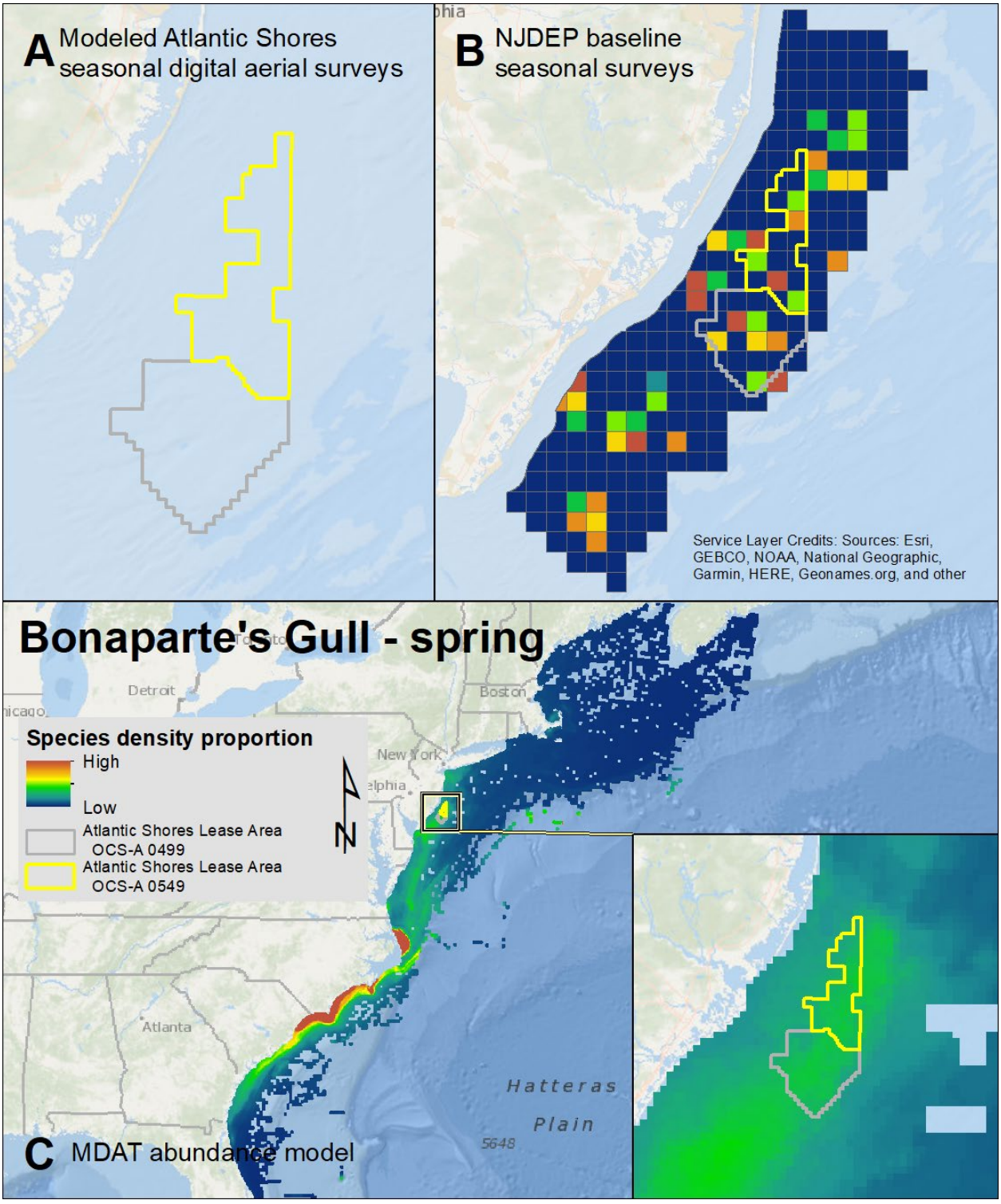

Map 97. Spring Bonaparte's Gull modeled density proportions in the Atlantic Shores seasonal digital aerial surveys (A), density proportions in the NJDEP baseline survey data (B), and the MDAT model outputs at local and regional scales (C). The scale for all maps is representative of relative spatial variation in the sites within the season for each information source.

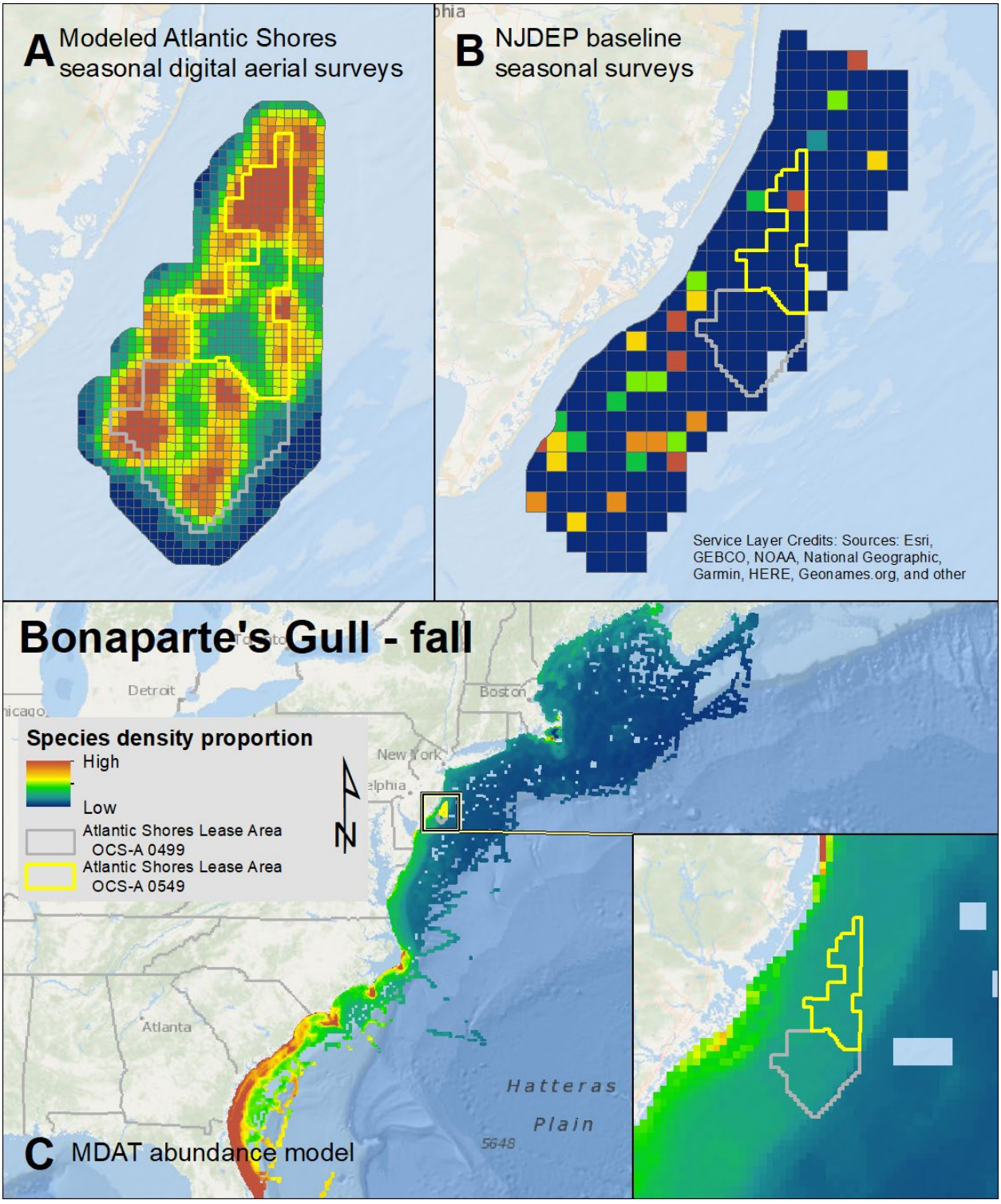

Map 98. Fall Bonaparte's Gull modeled density proportions in the Atlantic Shores seasonal digital aerial surveys (A), density proportions in the NJDEP baseline survey data (B), and the MDAT model outputs at local and regional scales (C). The scale for all maps is representative of relative spatial variation in the sites within the season for each information source.

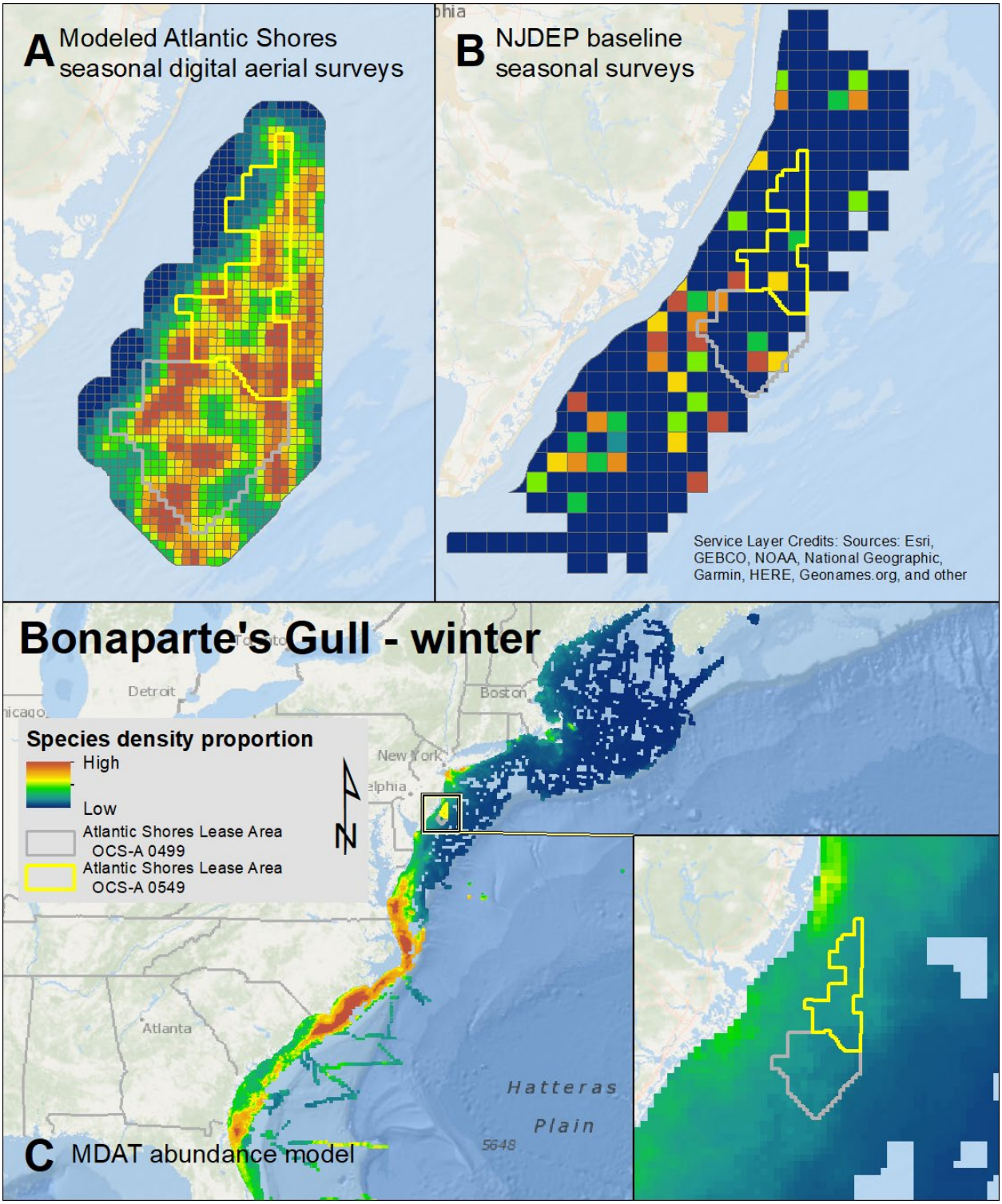

Map 99. Winter Bonaparte's Gull modeled density proportions in the Atlantic Shores seasonal digital aerial surveys (A), density proportions in the NJDEP baseline survey data (B), and the MDAT model outputs at local and regional scales (C). The scale for all maps is representative of relative spatial variation in the sites within the season for each information source.

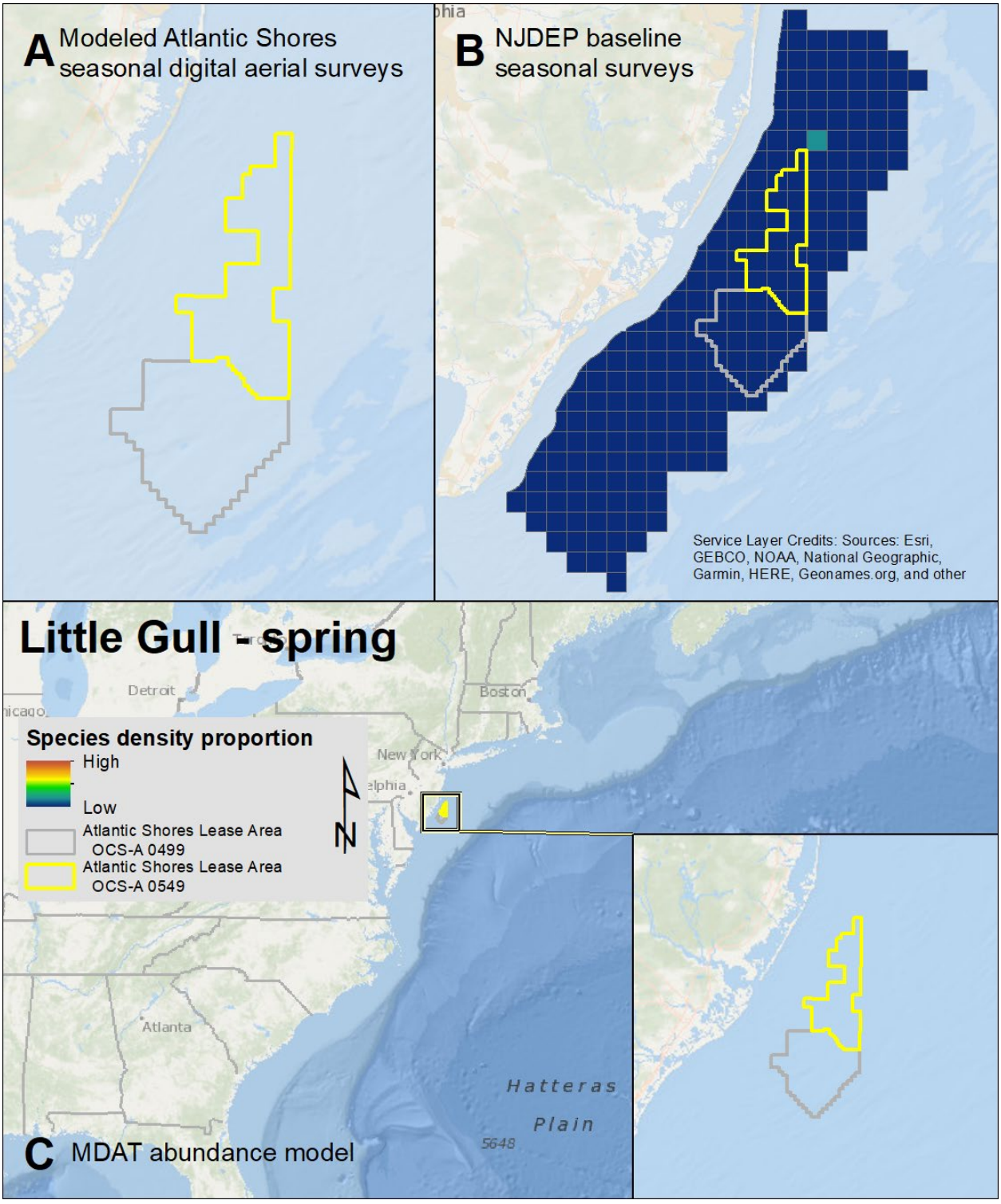

Map 100. Spring Little Gull modeled density proportions in the Atlantic Shores seasonal digital aerial surveys (A), density proportions in the NJDEP baseline survey data (B), and the MDAT model outputs at local and regional scales (C). The scale for all maps is representative of relative spatial variation in the sites within the season for each information source.

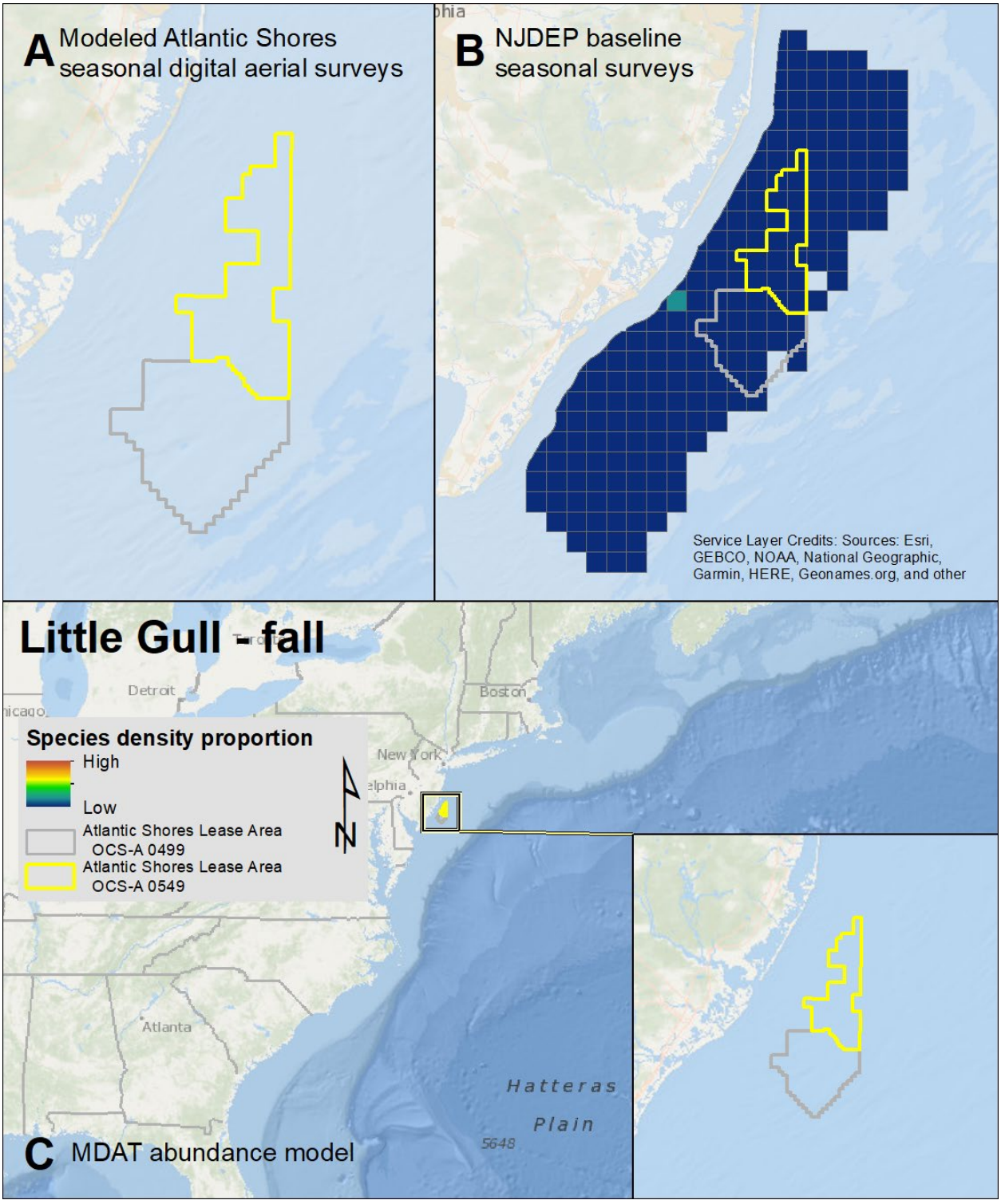

Map 101. Fall Little Gull modeled density proportions in the Atlantic Shores seasonal digital aerial surveys (A), density proportions in the NJDEP baseline survey data (B), and the MDAT model outputs at local and regional scales (C). The scale for all maps is representative of relative spatial variation in the sites within the season for each information source.

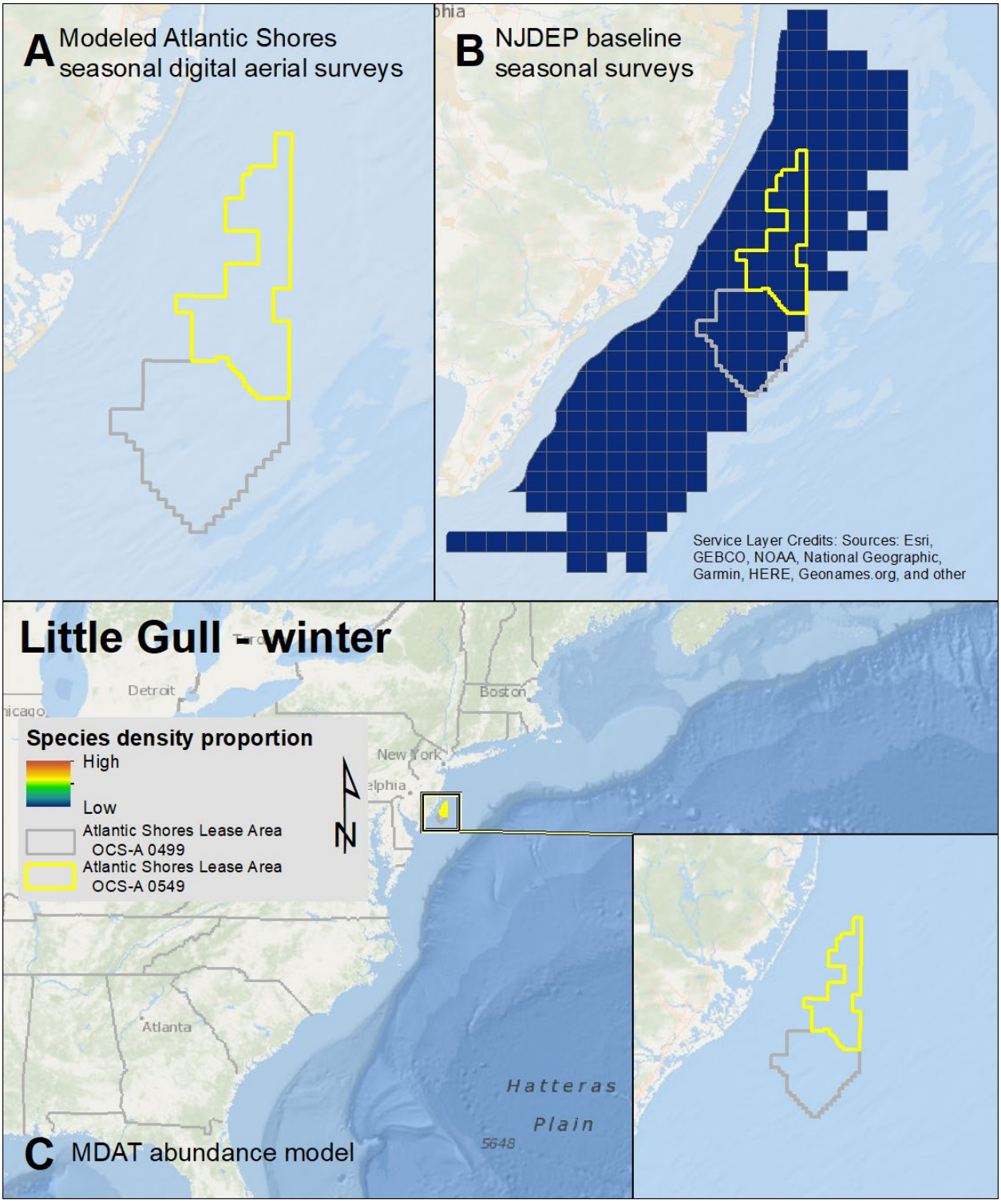

Map 102. Winter Little Gull modeled density proportions in the Atlantic Shores seasonal digital aerial surveys (A), density proportions in the NJDEP baseline survey data (B), and the MDAT model outputs at local and regional scales (C). The scale for all maps is representative of relative spatial variation in the sites within the season for each information source.

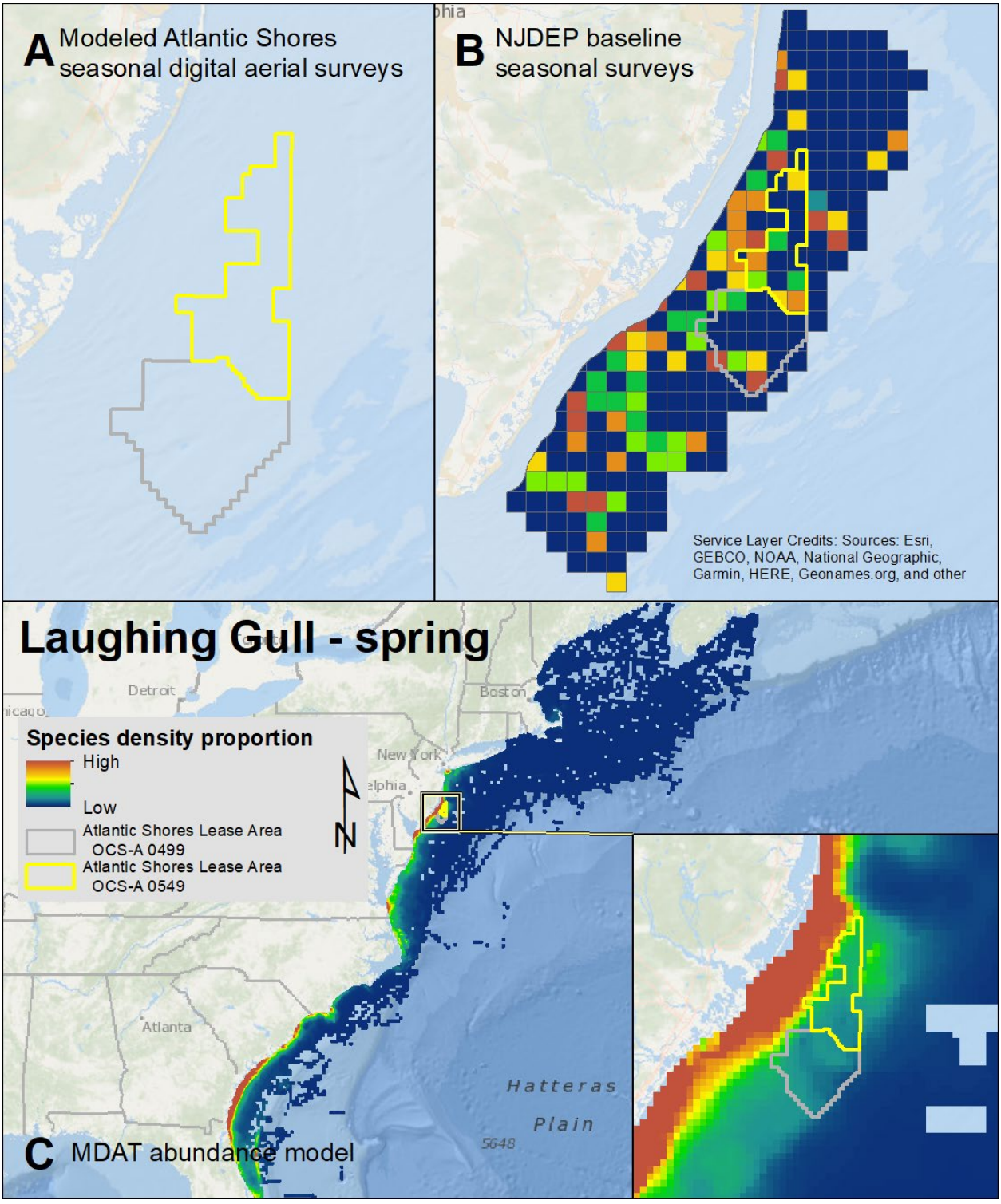

Map 103. Spring Laughing Gull modeled density proportions in the Atlantic Shores seasonal digital aerial surveys (A), density proportions in the NJDEP baseline survey data (B), and the MDAT model outputs at local and regional scales (C). The scale for all maps is representative of relative spatial variation in the sites within the season for each information source.

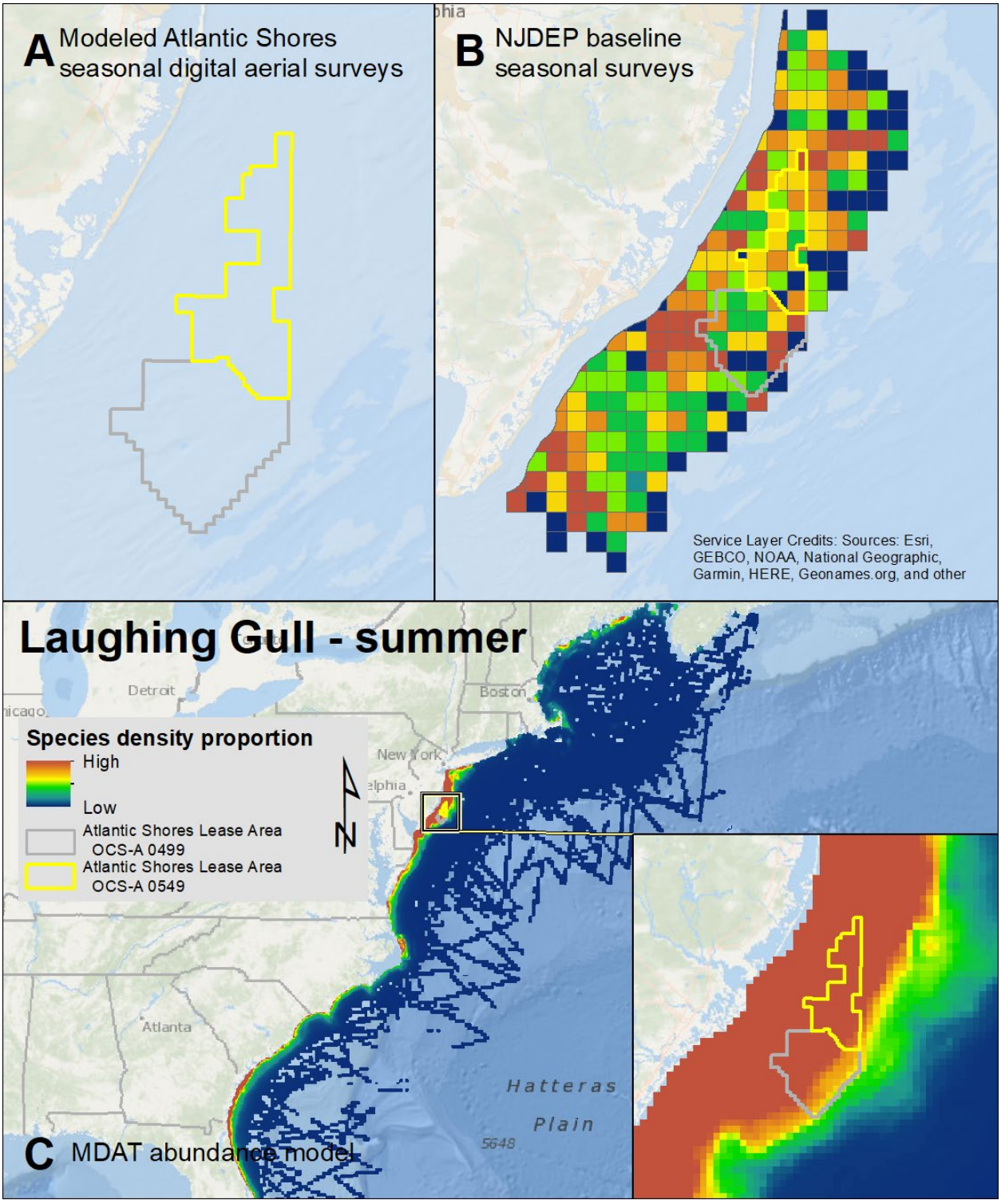

Map 104. Summer Laughing Gull modeled density proportions in the Atlantic Shores seasonal digital aerial surveys (A), density proportions in the NJDEP baseline survey data (B), and the MDAT model outputs at local and regional scales (C). The scale for all maps is representative of relative spatial variation in the sites within the season for each information source.

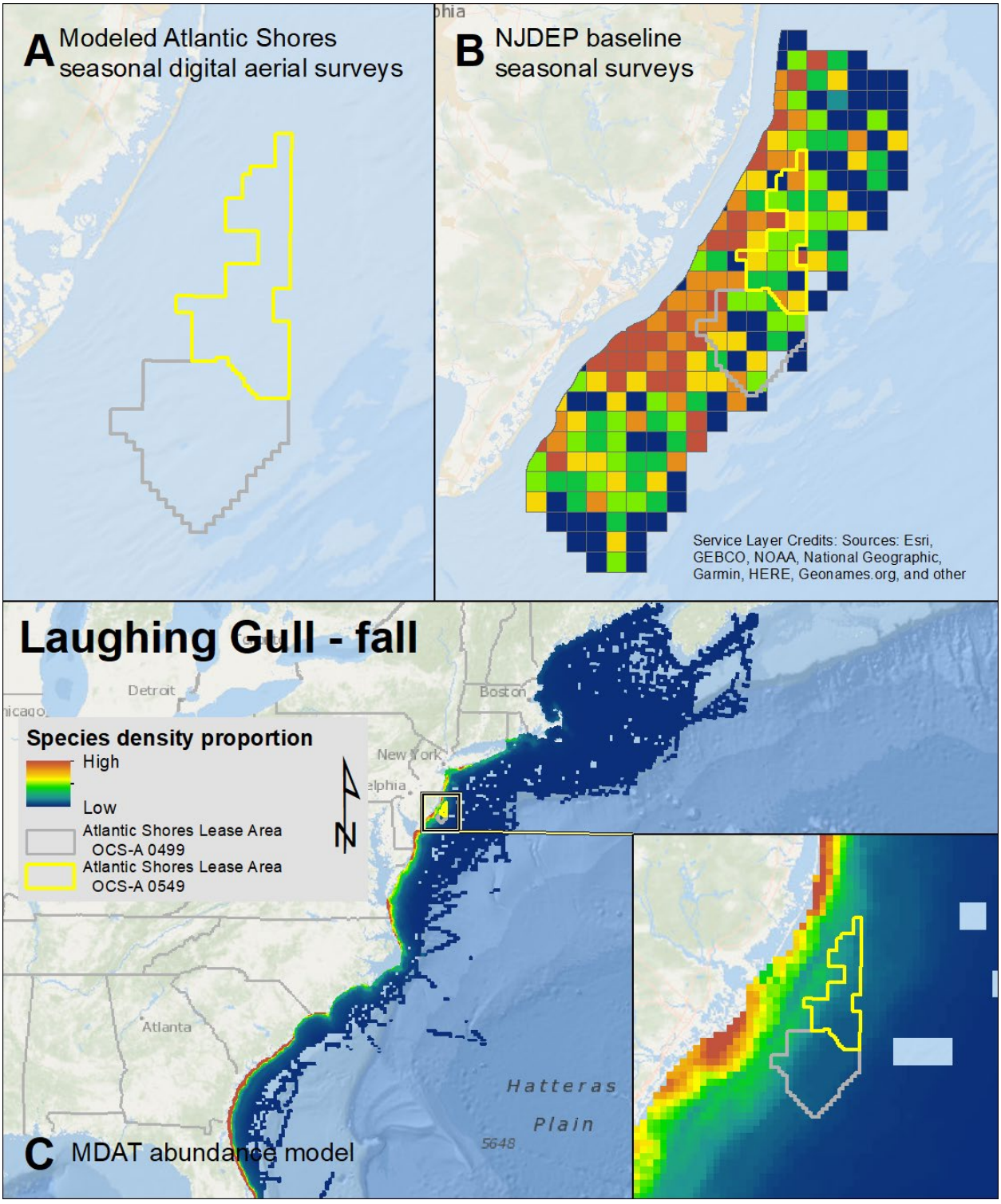

Map 105. Fall Laughing Gull modeled density proportions in the Atlantic Shores seasonal digital aerial surveys (A), density proportions in the NJDEP baseline survey data (B), and the MDAT model outputs at local and regional scales (C). The scale for all maps is representative of relative spatial variation in the sites within the season for each information source.

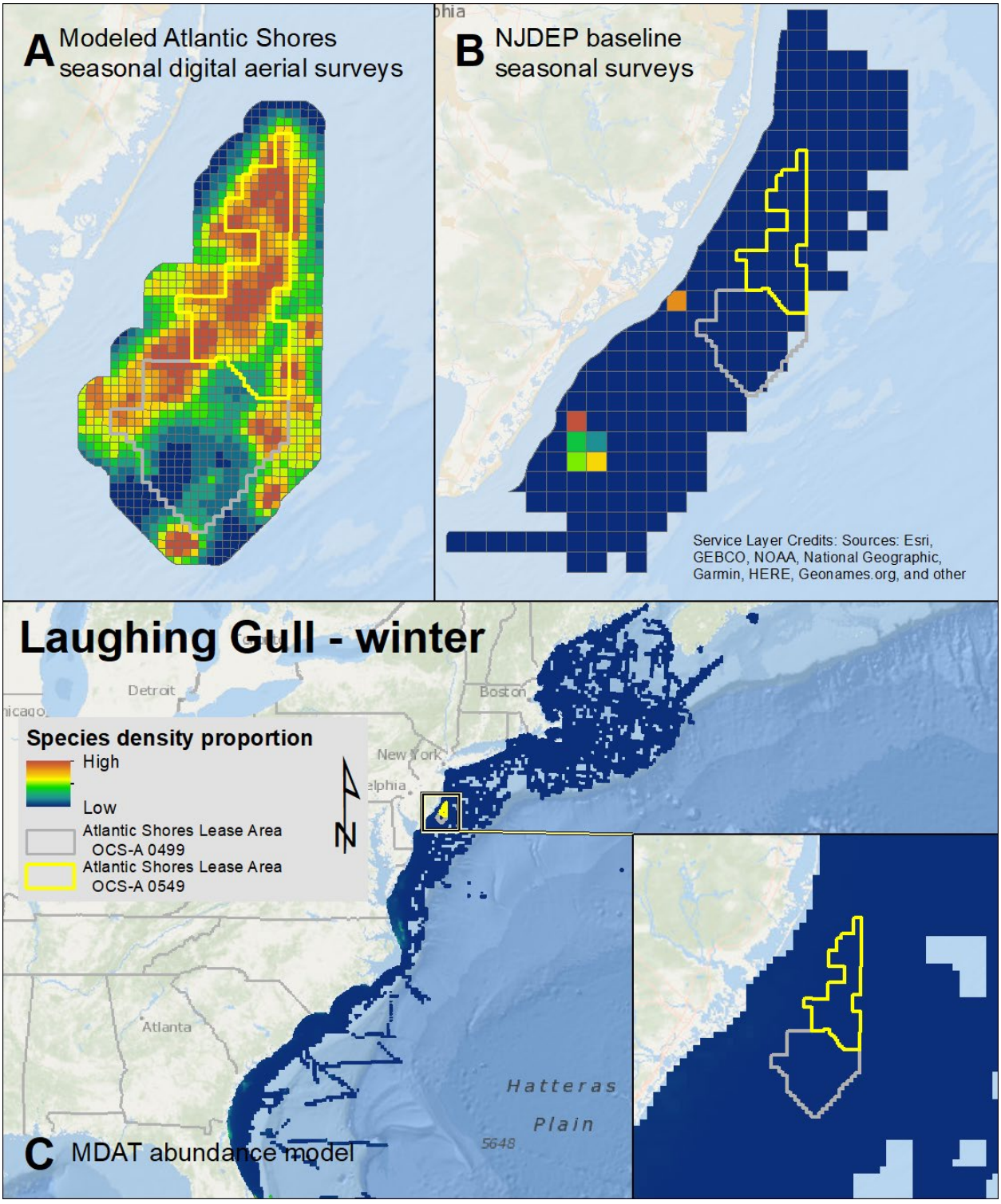

Map 106. Winter Laughing Gull modeled density proportions in the Atlantic Shores seasonal digital aerial surveys (A), density proportions in the NJDEP baseline survey data (B), and the MDAT model outputs at local and regional scales (C). The scale for all maps is representative of relative spatial variation in the sites within the season for each information source.

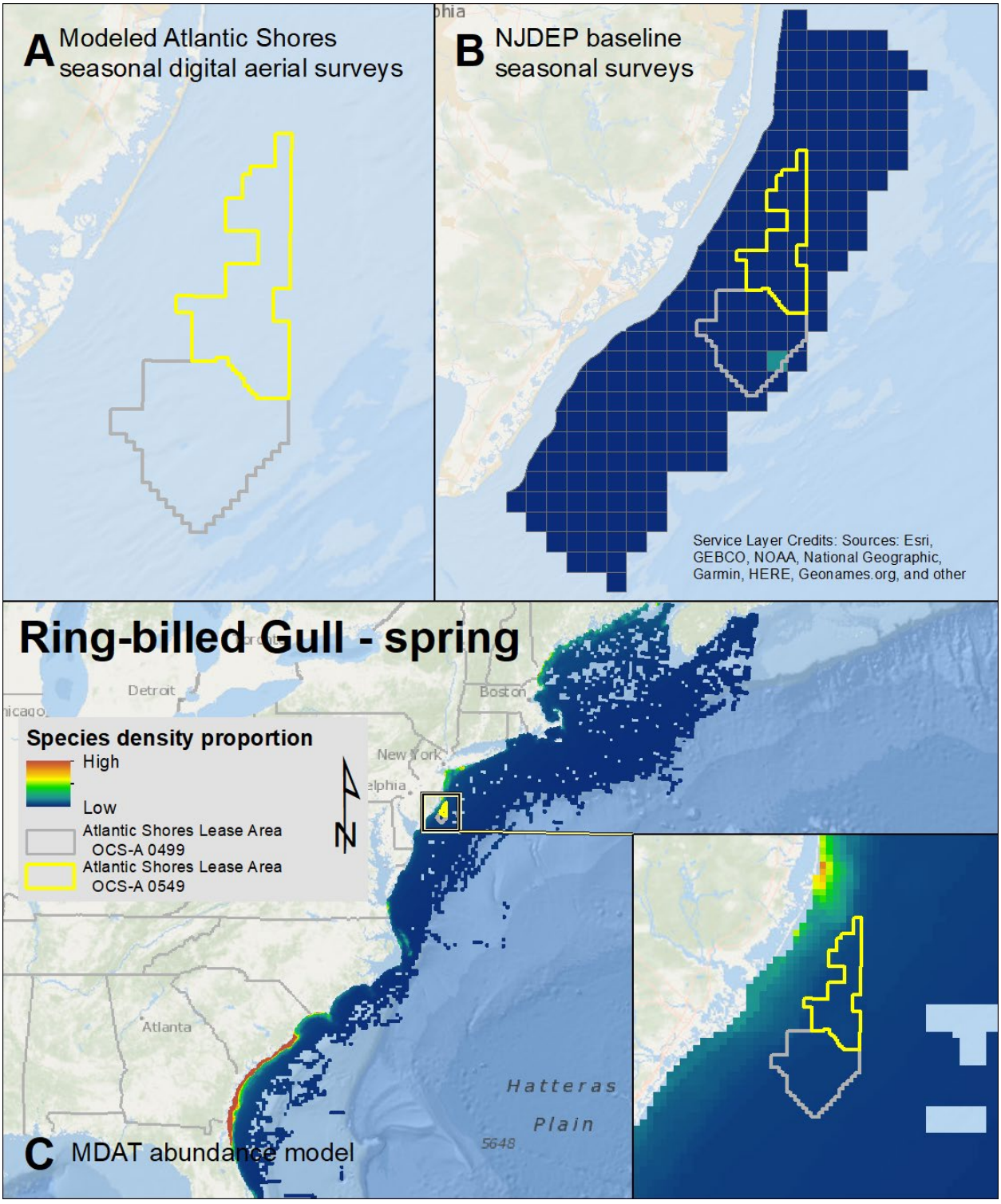

Map 107. Spring Ring-billed Gull modeled density proportions in the Atlantic Shores seasonal digital aerial surveys (A), density proportions in the NJDEP baseline survey data (B), and the MDAT model outputs at local and regional scales (C). The scale for all maps is representative of relative spatial variation in the sites within the season for each information source.

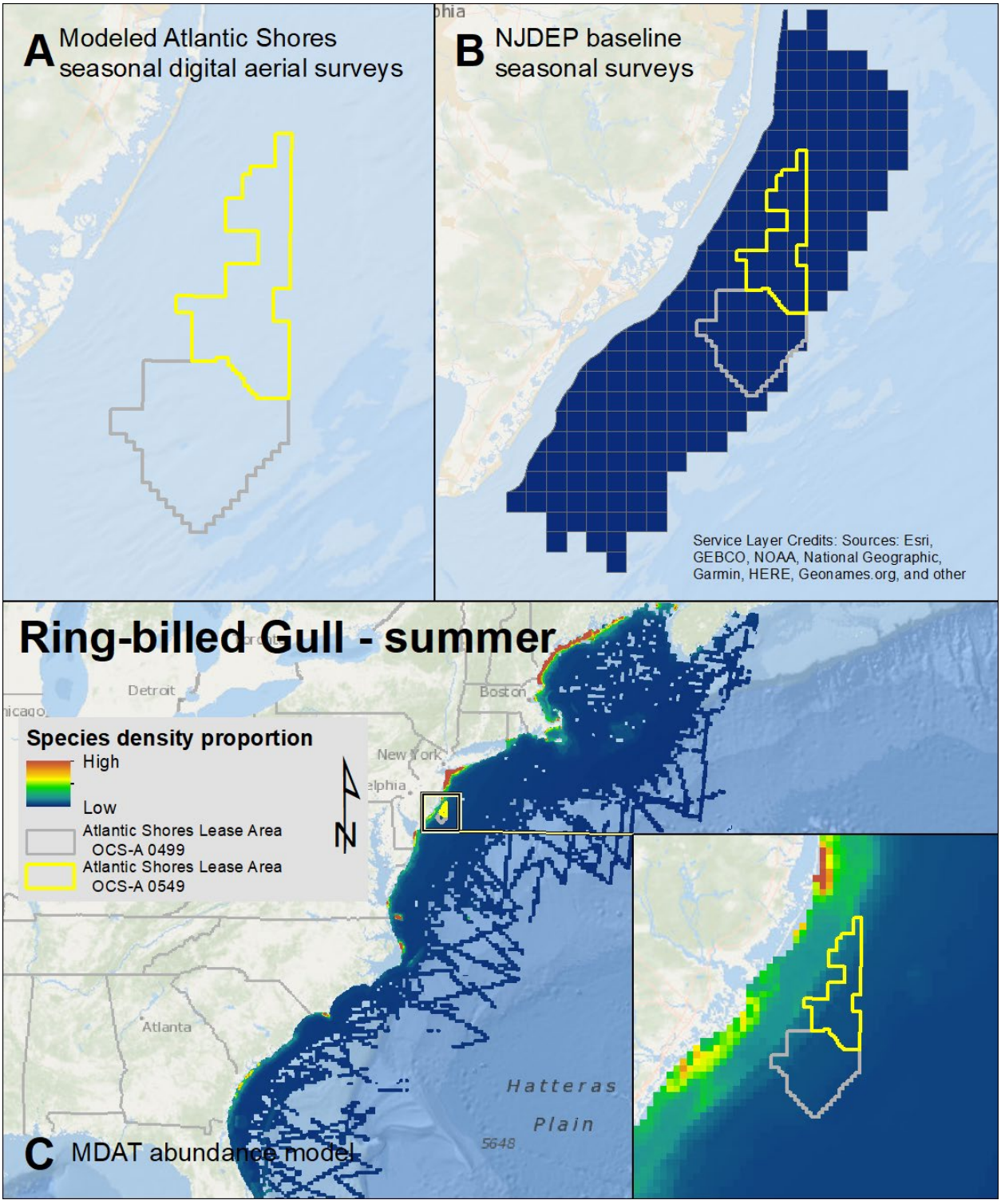

Map 108. Summer Ring-billed Gull modeled density proportions in the Atlantic Shores seasonal digital aerial surveys (A), density proportions in the NJDEP baseline survey data (B), and the MDAT model outputs at local and regional scales (C). The scale for all maps is representative of relative spatial variation in the sites within the season for each information source.

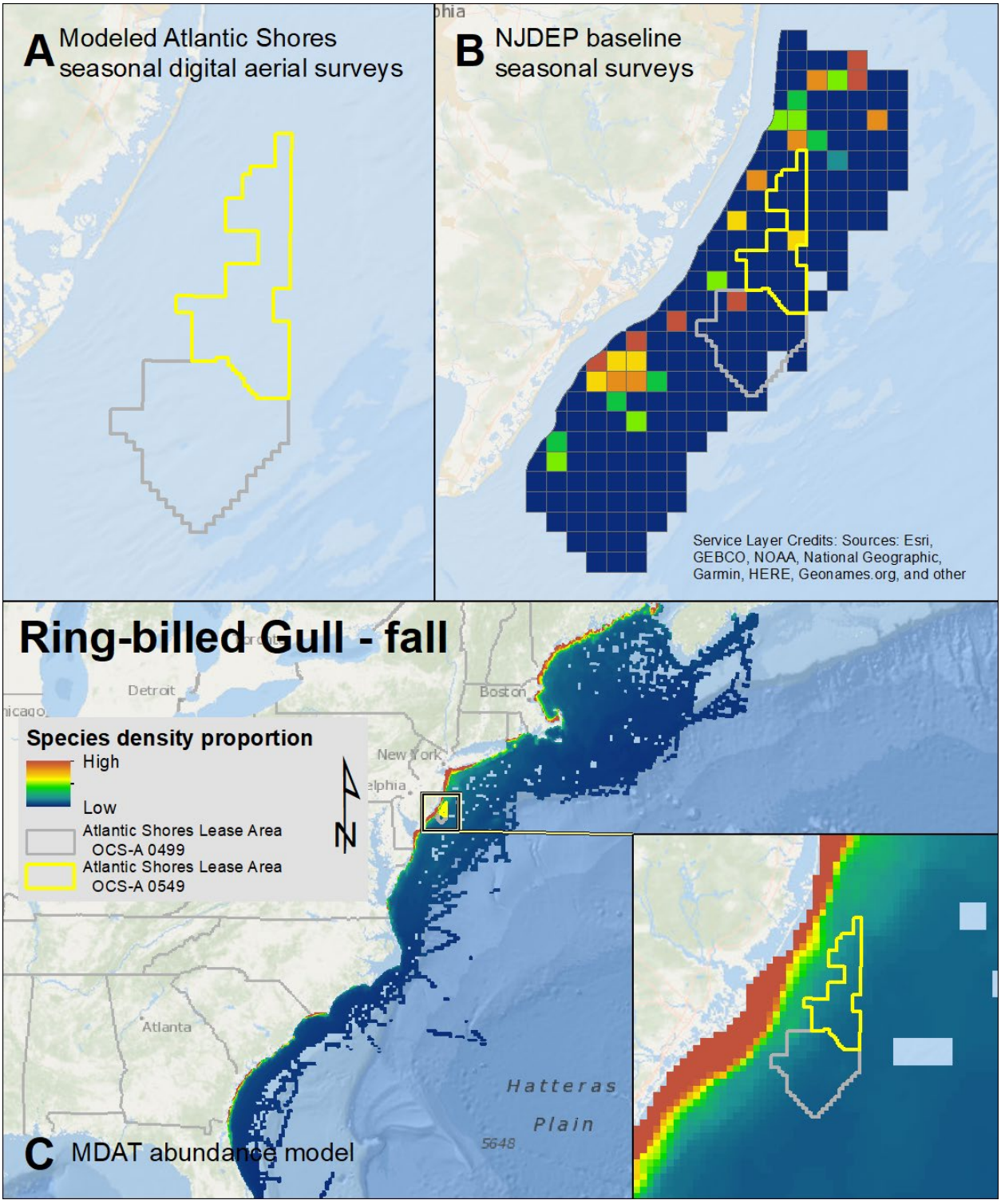

Map 109. Fall Ring-billed Gull modeled density proportions in the Atlantic Shores seasonal digital aerial surveys (A), density proportions in the NJDEP baseline survey data (B), and the MDAT model outputs at local and regional scales (C). The scale for all maps is representative of relative spatial variation in the sites within the season for each information source.

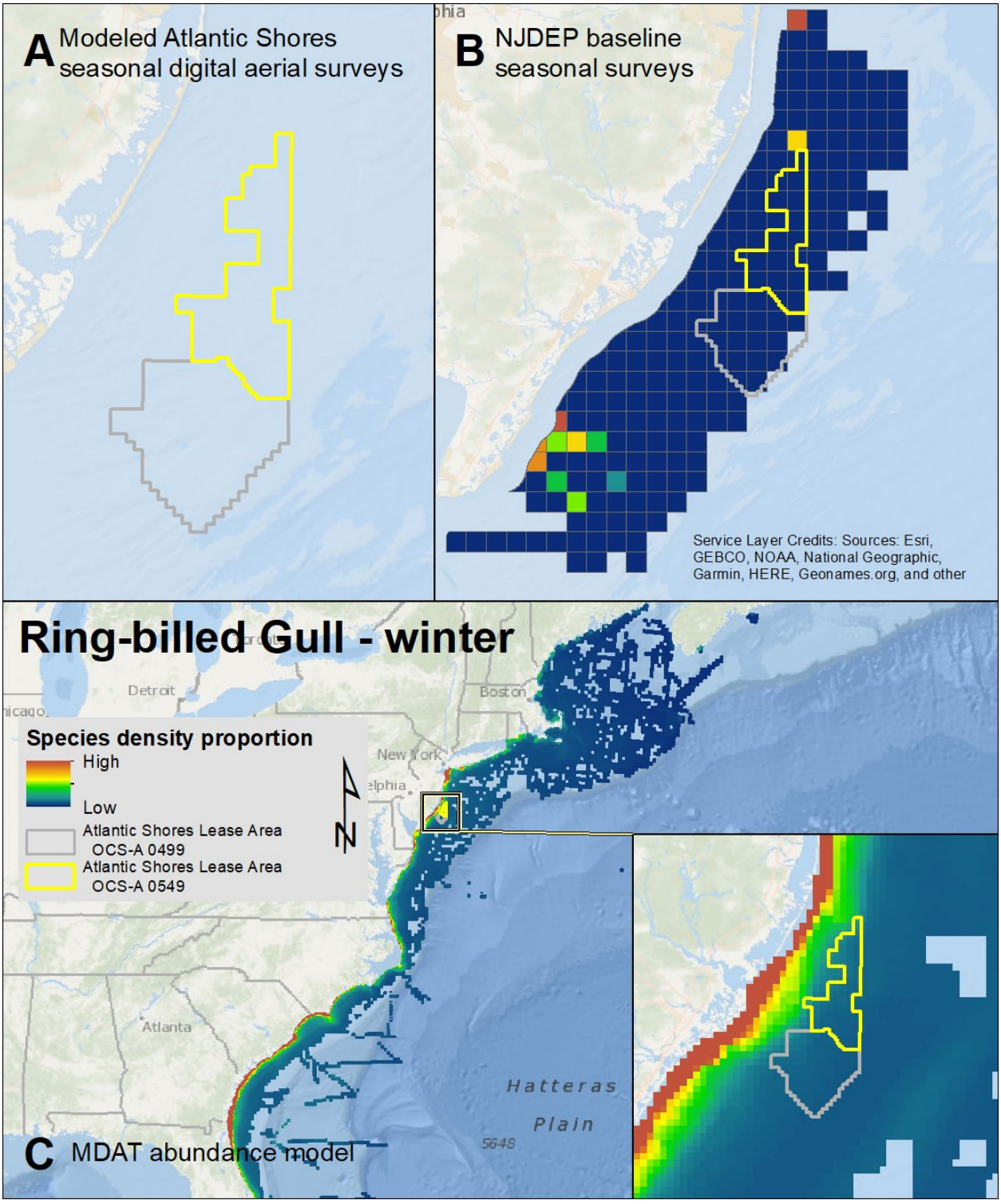

Map 110. Winter Ring-billed Gull modeled density proportions in the Atlantic Shores seasonal digital aerial surveys (A), density proportions in the NJDEP baseline survey data (B), and the MDAT model outputs at local and regional scales (C). The scale for all maps is representative of relative spatial variation in the sites within the season for each information source.

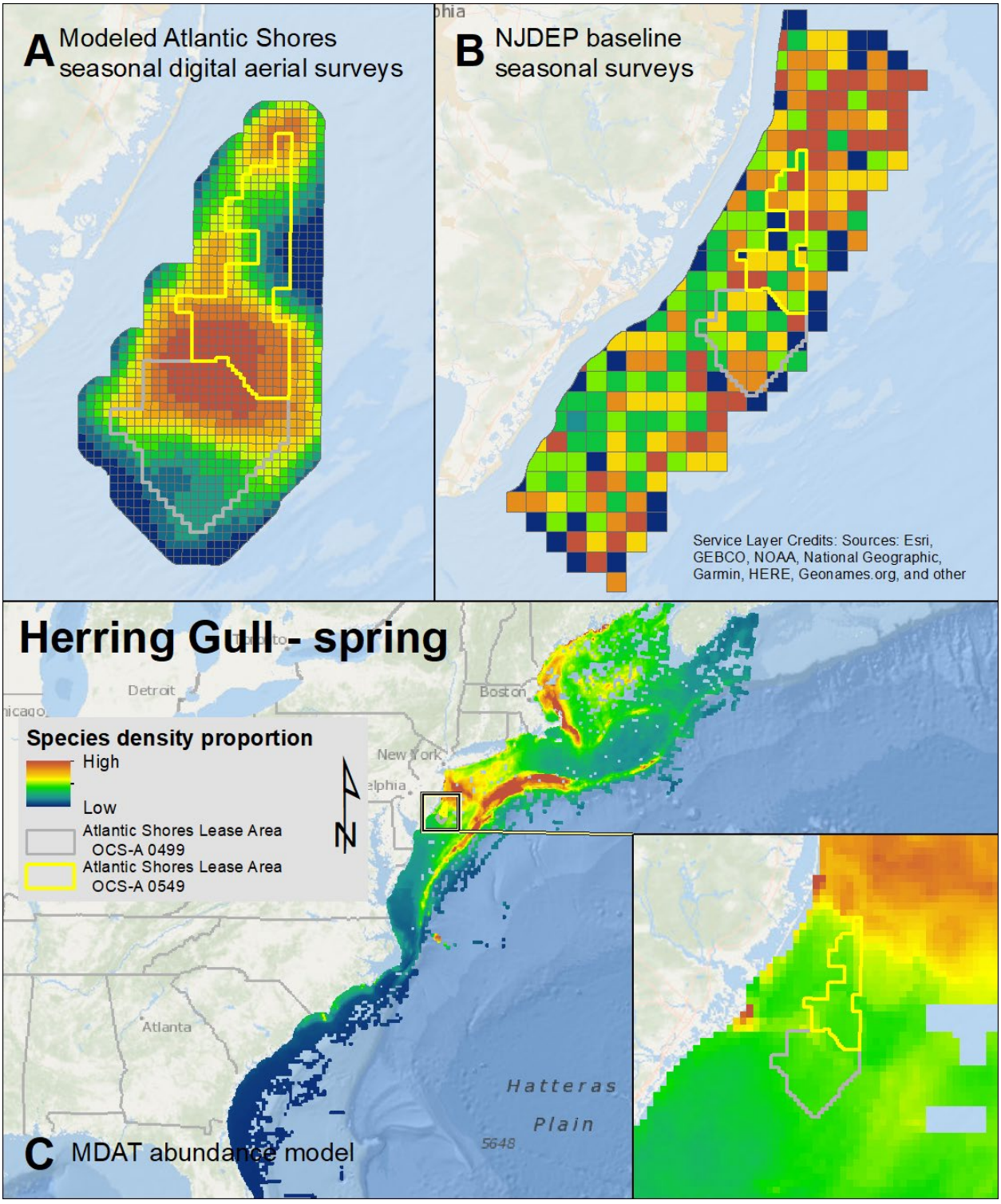

Map 111. Spring Herring Gull modeled density proportions in the Atlantic Shores seasonal digital aerial surveys (A), density proportions in the NJDEP baseline survey data (B), and the MDAT model outputs at local and regional scales (C). The scale for all maps is representative of relative spatial variation in the sites within the season for each information source.

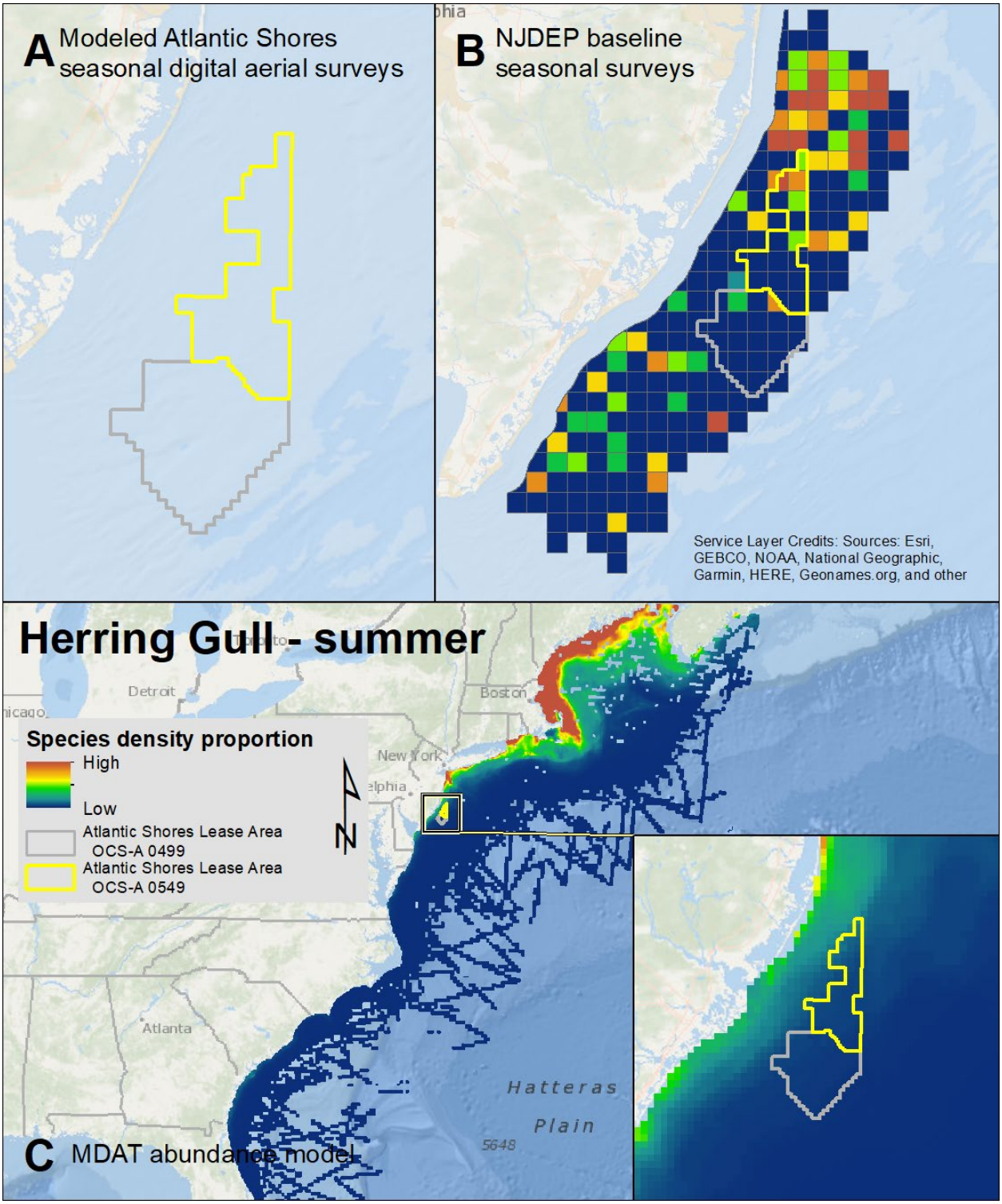

Map 112. Summer Herring Gull modeled density proportions in the Atlantic Shores seasonal digital aerial surveys (A), density proportions in the NJDEP baseline survey data (B), and the MDAT model outputs at local and regional scales (C). The scale for all maps is representative of relative spatial variation in the sites within the season for each information source.

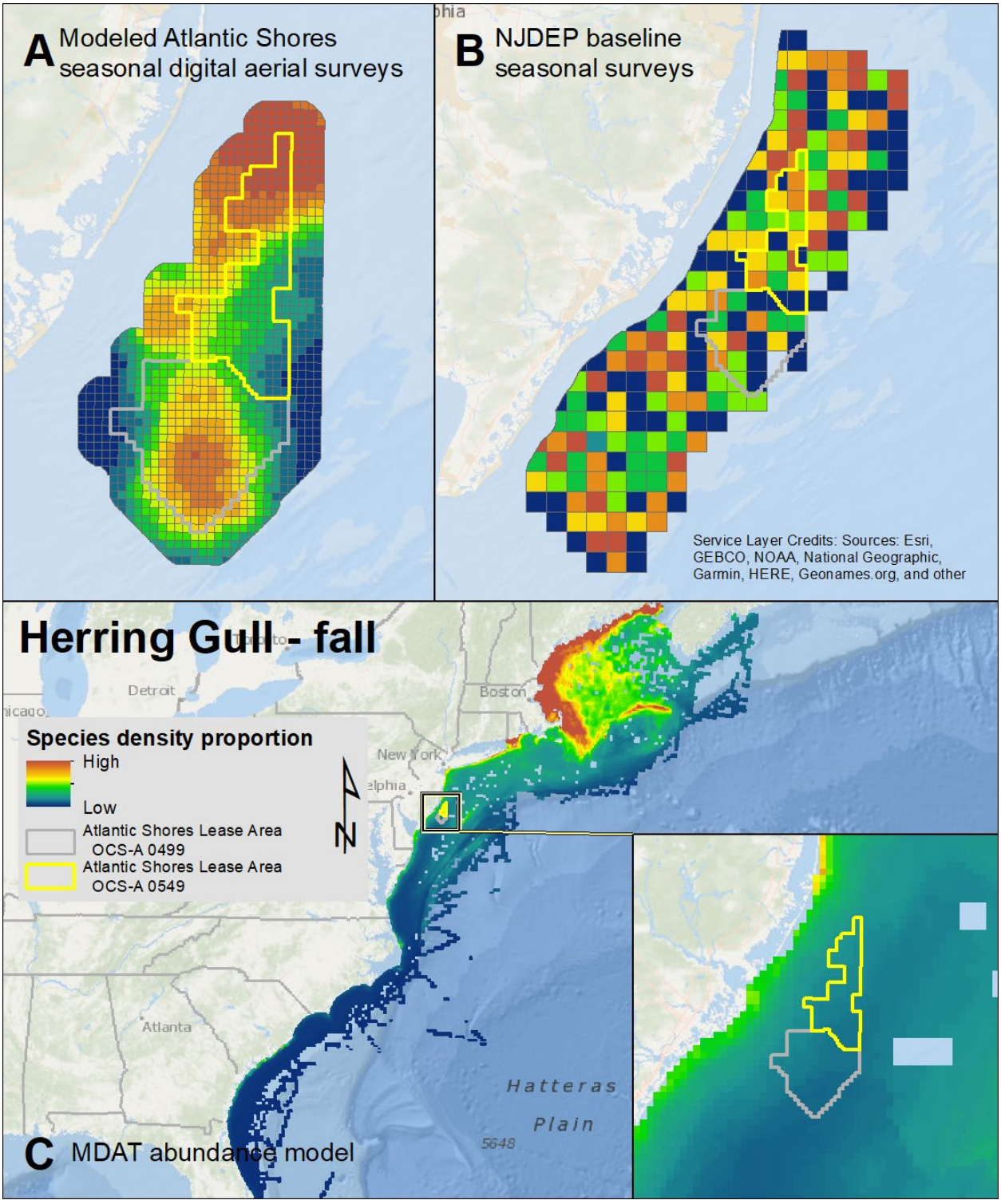

Map 113. Fall Herring Gull modeled density proportions in the Atlantic Shores seasonal digital aerial surveys (A), density proportions in the NJDEP baseline survey data (B), and the MDAT model outputs at local and regional scales (C). The scale for all maps is representative of relative spatial variation in the sites within the season for each information source.

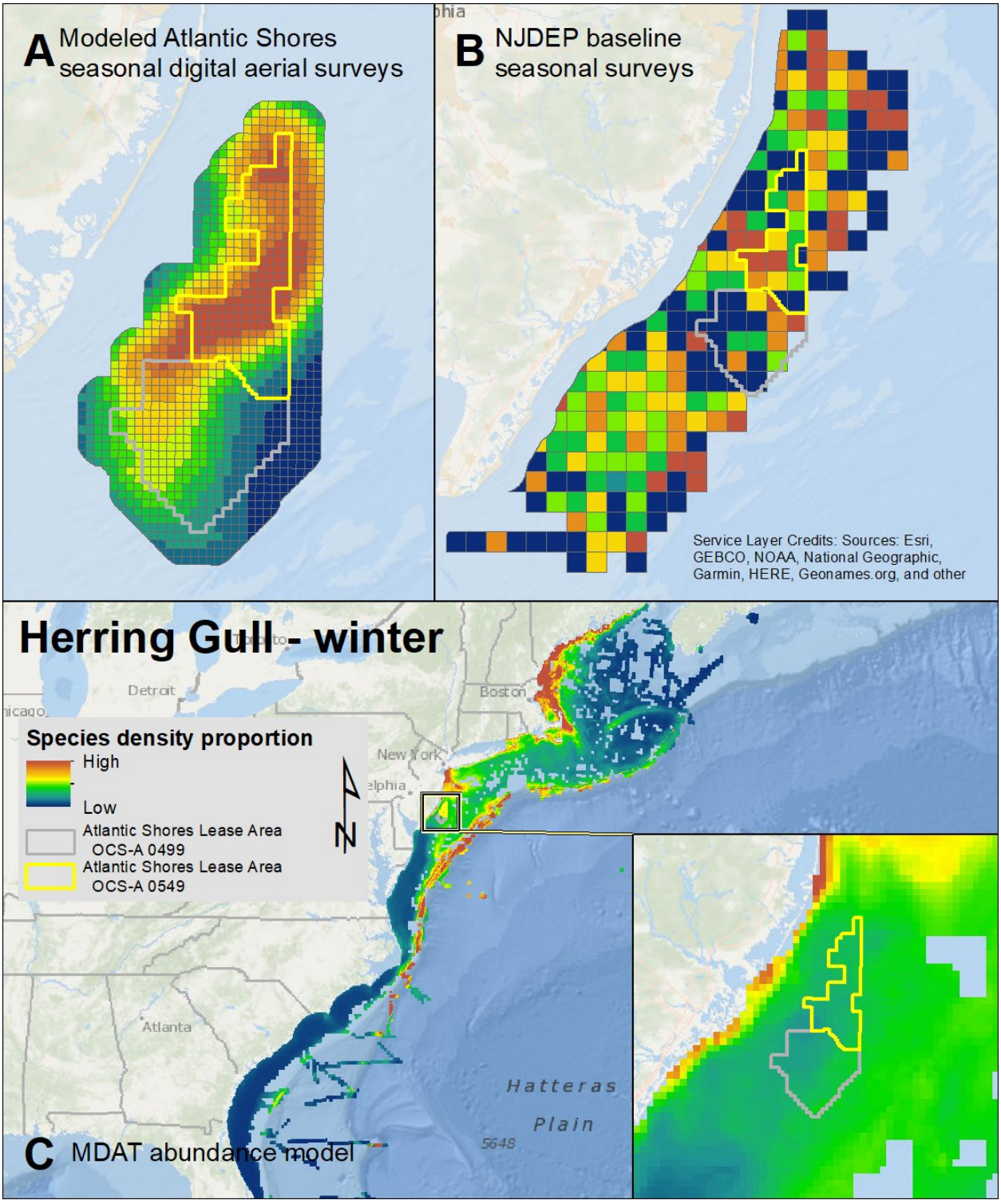

Map 114. Winter Herring Gull modeled density proportions in the Atlantic Shores seasonal digital aerial surveys (A), density proportions in the NJDEP baseline survey data (B), and the MDAT model outputs at local and regional scales (C). The scale for all maps is representative of relative spatial variation in the sites within the season for each information source.

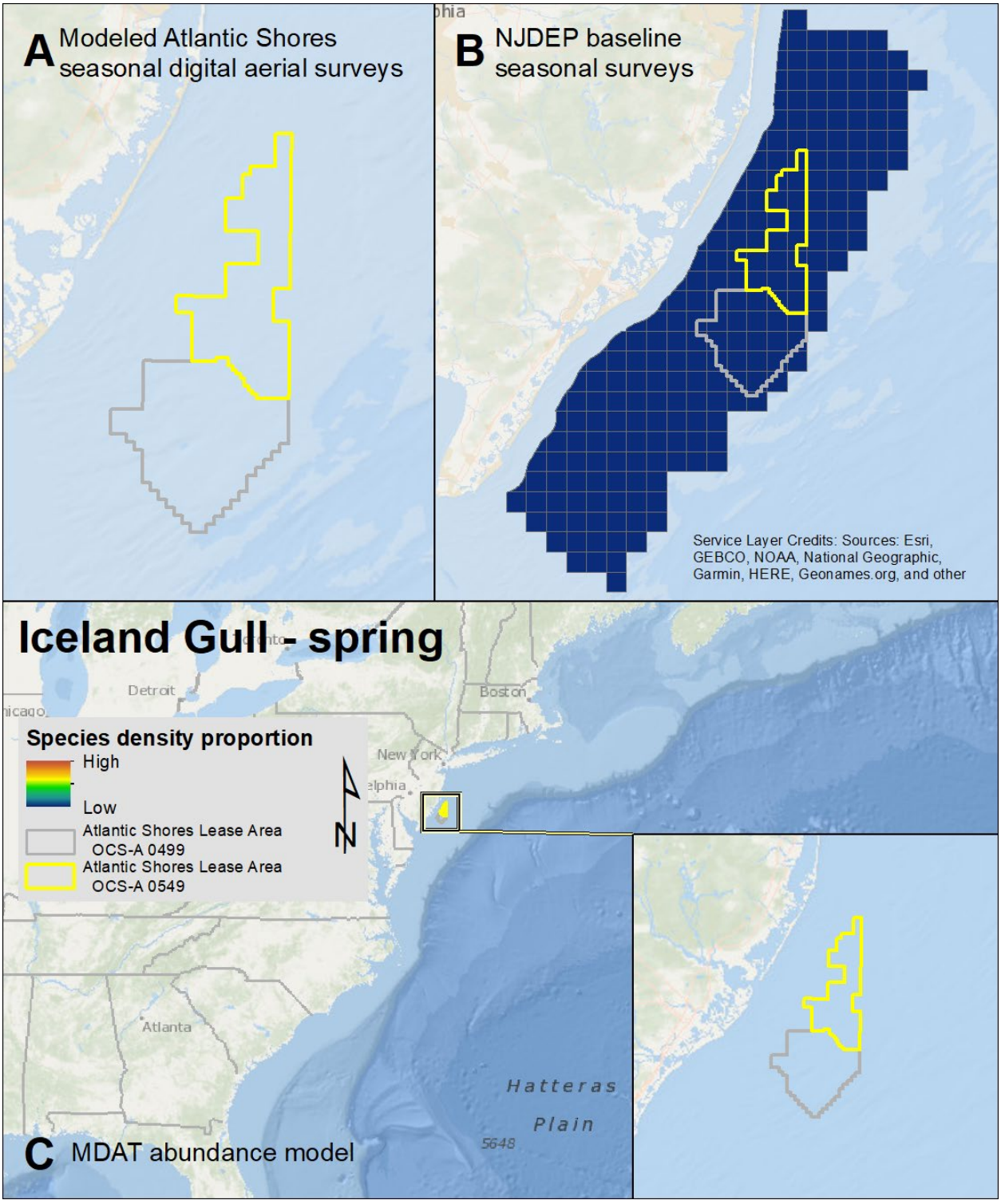

Map 115. Spring Iceland Gull modeled density proportions in the Atlantic Shores seasonal digital aerial surveys (A), density proportions in the NJDEP baseline survey data (B), and the MDAT model outputs at local and regional scales (C). The scale for all maps is representative of relative spatial variation in the sites within the season for each information source.

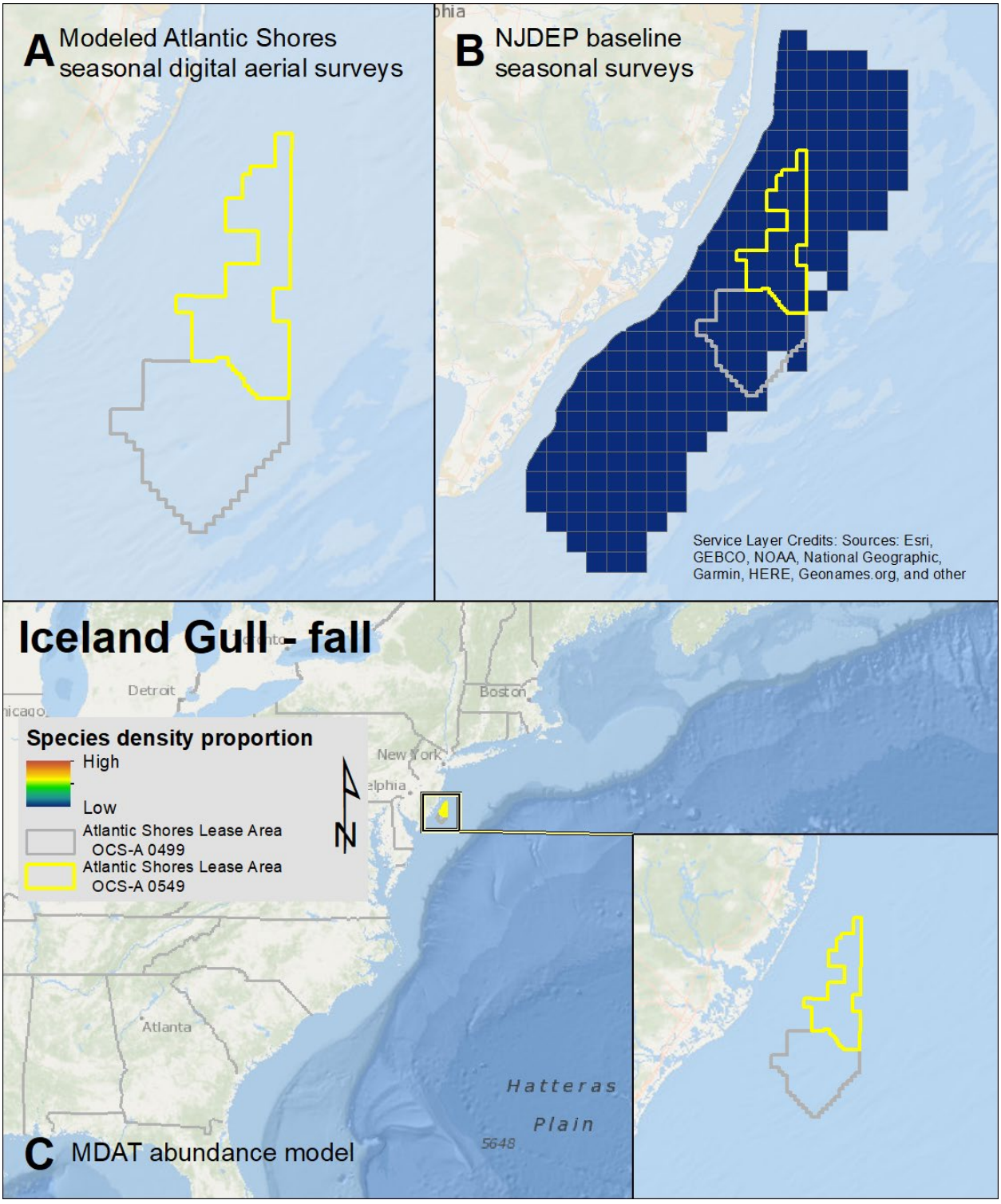

Map 116. Fall Iceland Gull modeled density proportions in the Atlantic Shores seasonal digital aerial surveys (A), density proportions in the NJDEP baseline survey data (B), and the MDAT model outputs at local and regional scales (C). The scale for all maps is representative of relative spatial variation in the sites within the season for each information source.

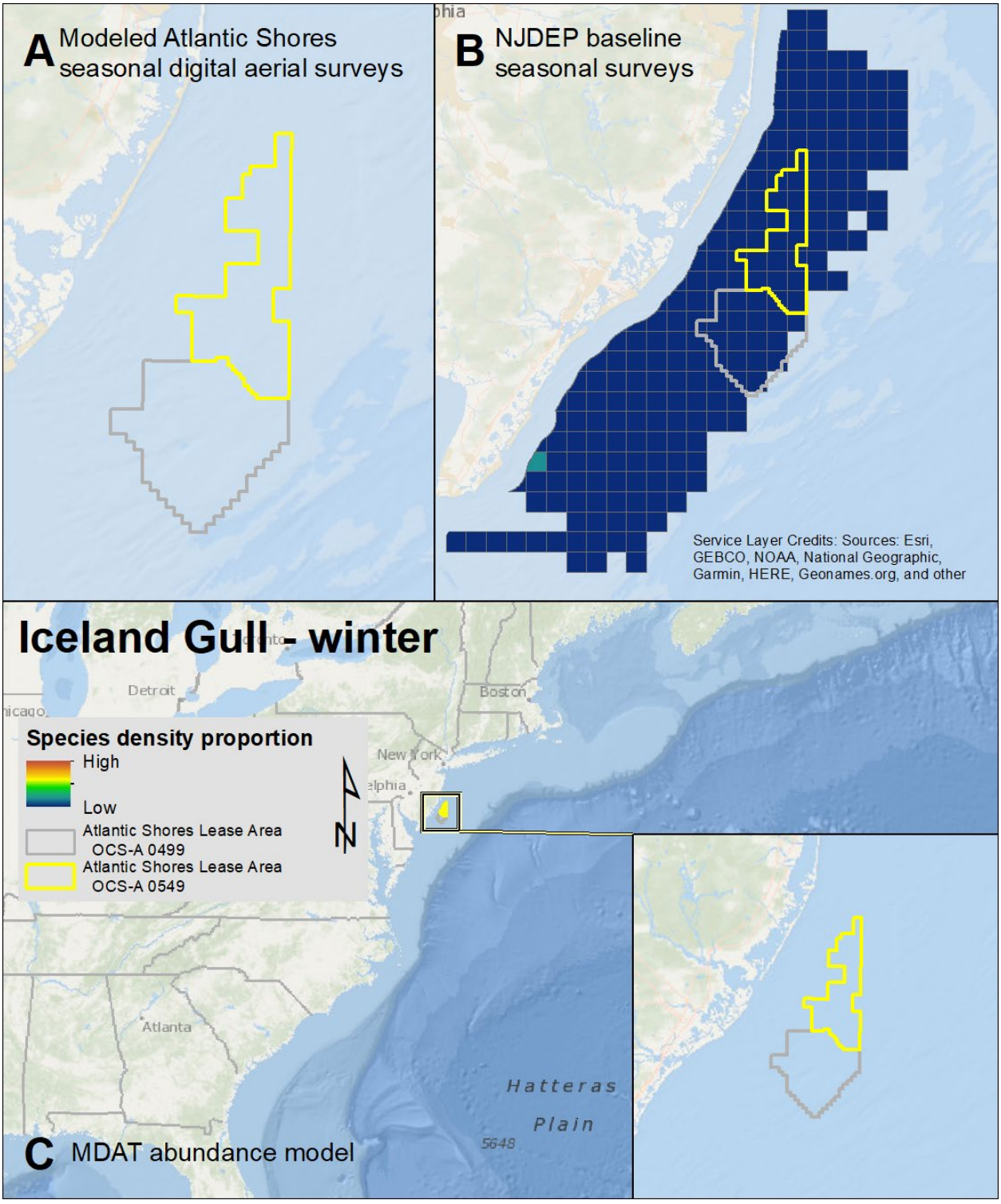

Map 117. Winter Iceland Gull modeled density proportions in the Atlantic Shores seasonal digital aerial surveys (A), density proportions in the NJDEP baseline survey data (B), and the MDAT model outputs at local and regional scales (C). The scale for all maps is representative of relative spatial variation in the sites within the season for each information source.

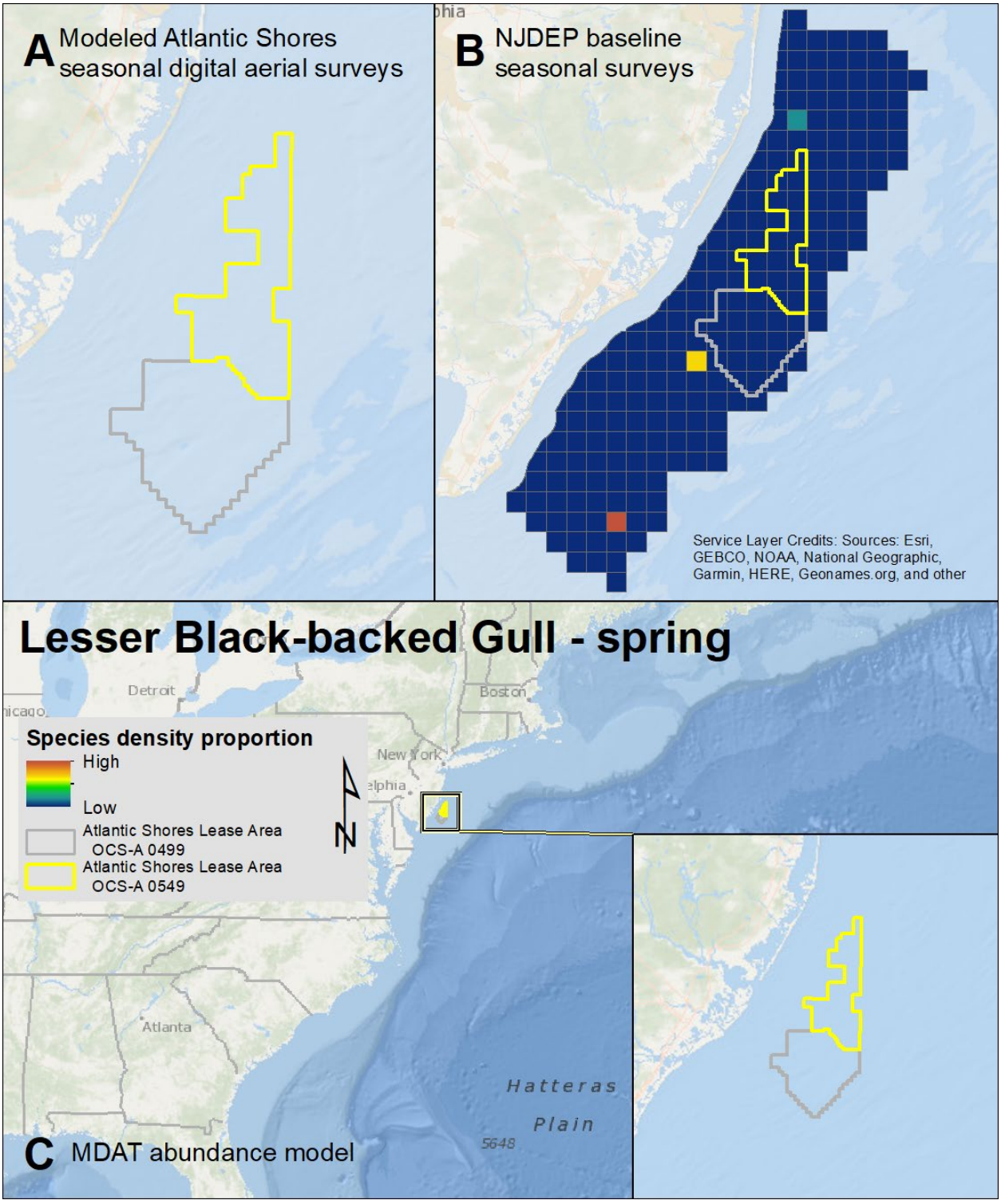

Map 118. Spring Lesser Black-backed Gull modeled density proportions in the Atlantic Shores seasonal digital aerial surveys (A), density proportions in the NJDEP baseline survey data (B), and the MDAT model outputs at local and regional scales (C). The scale for all maps is representative of relative spatial variation in the sites within the season for each information source.

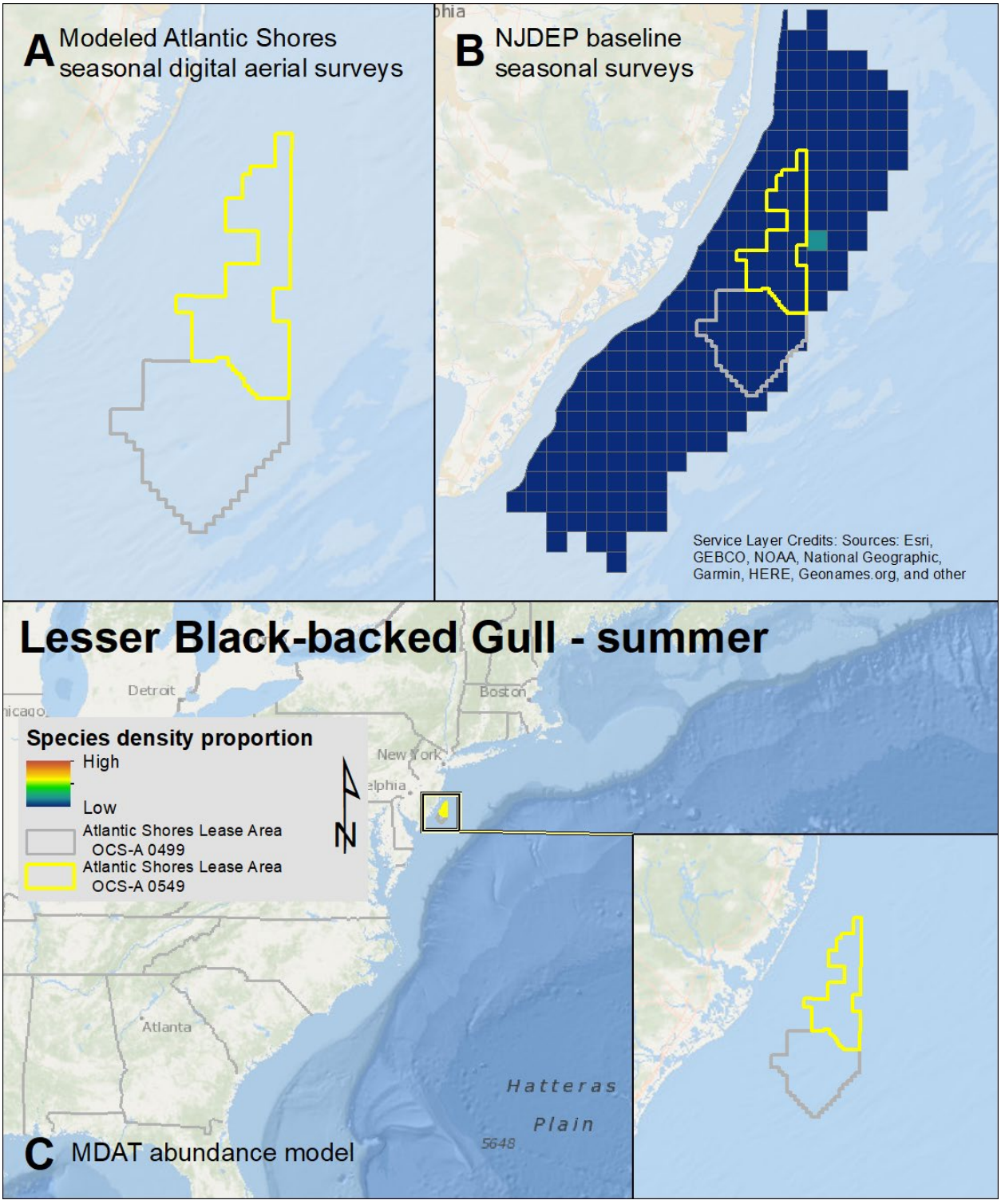

Map 119. Summer Lesser Black-backed Gull modeled density proportions in the Atlantic Shores seasonal digital aerial surveys (A), density proportions in the NJDEP baseline survey data (B), and the MDAT model outputs at local and regional scales (C). The scale for all maps is representative of relative spatial variation in the sites within the season for each information source.

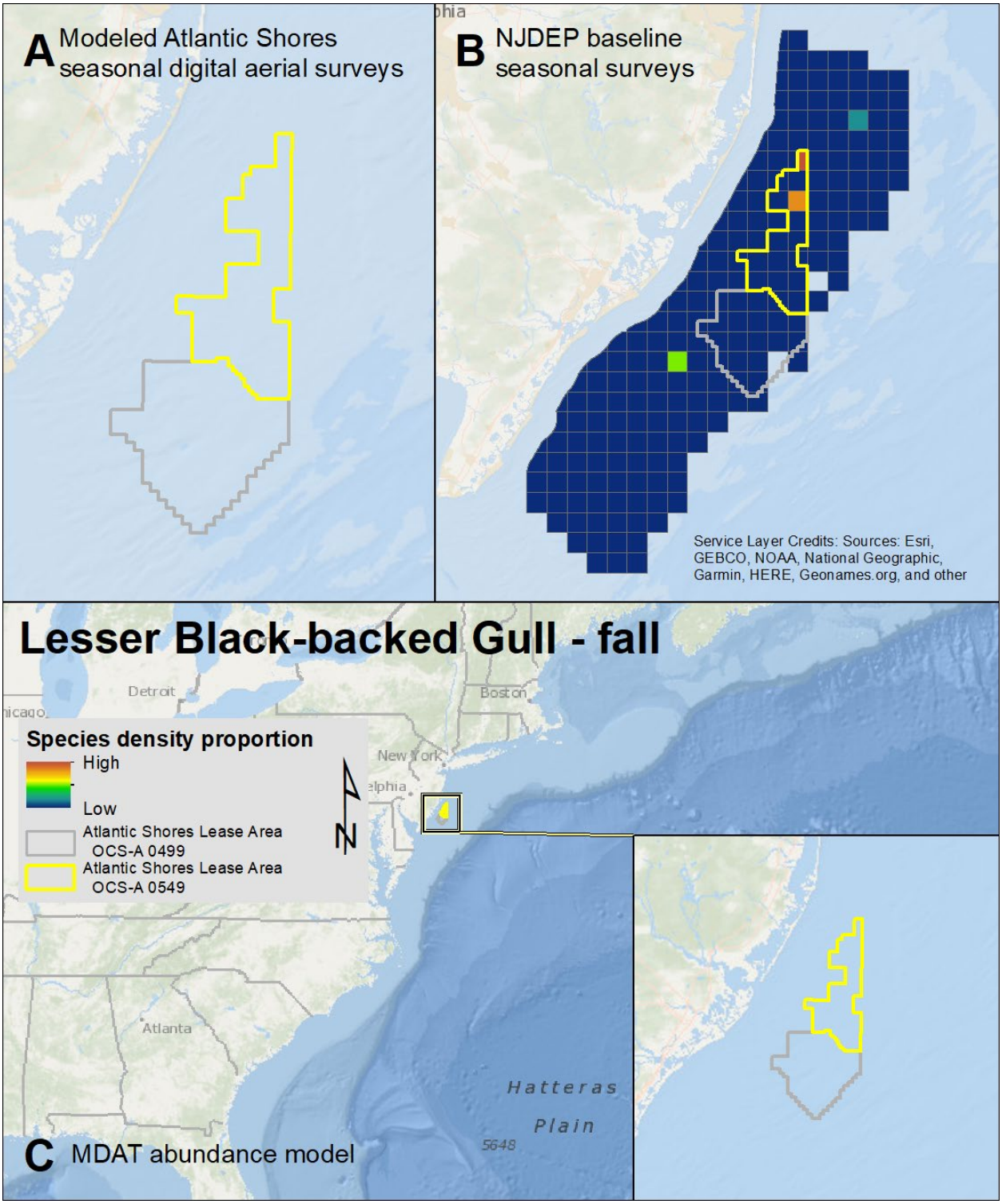

Map 120. Fall Lesser Black-backed Gull modeled density proportions in the Atlantic Shores seasonal digital aerial surveys (A), density proportions in the NJDEP baseline survey data (B), and the MDAT model outputs at local and regional scales (C). The scale for all maps is representative of relative spatial variation in the sites within the season for each information source.

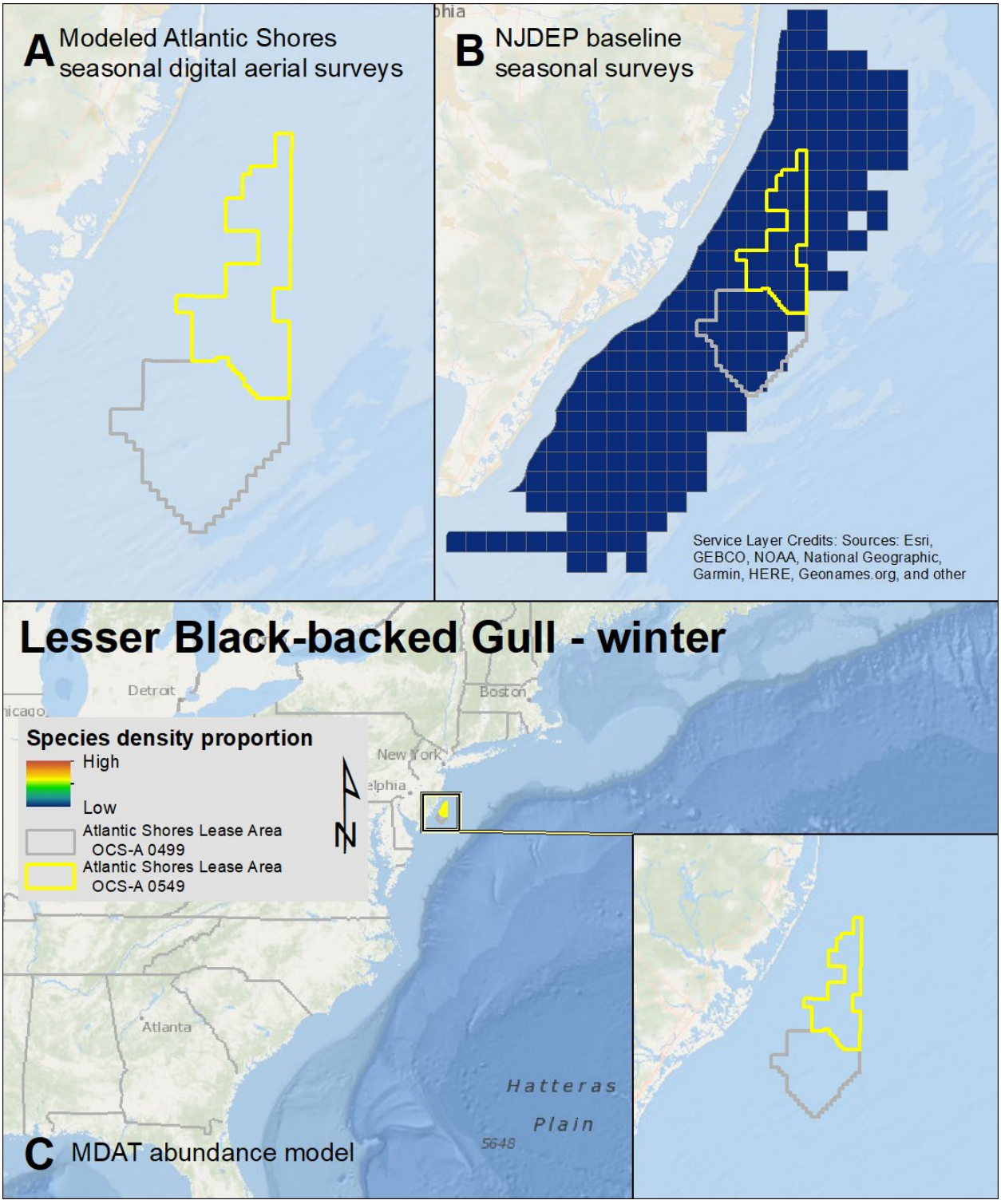

Map 121. Winter Lesser Black-backed Gull modeled density proportions in the Atlantic Shores seasonal digital aerial surveys (A), density proportions in the NJDEP baseline survey data (B), and the MDAT model outputs at local and regional scales (C). The scale for all maps is representative of relative spatial variation in the sites within the season for each information source.

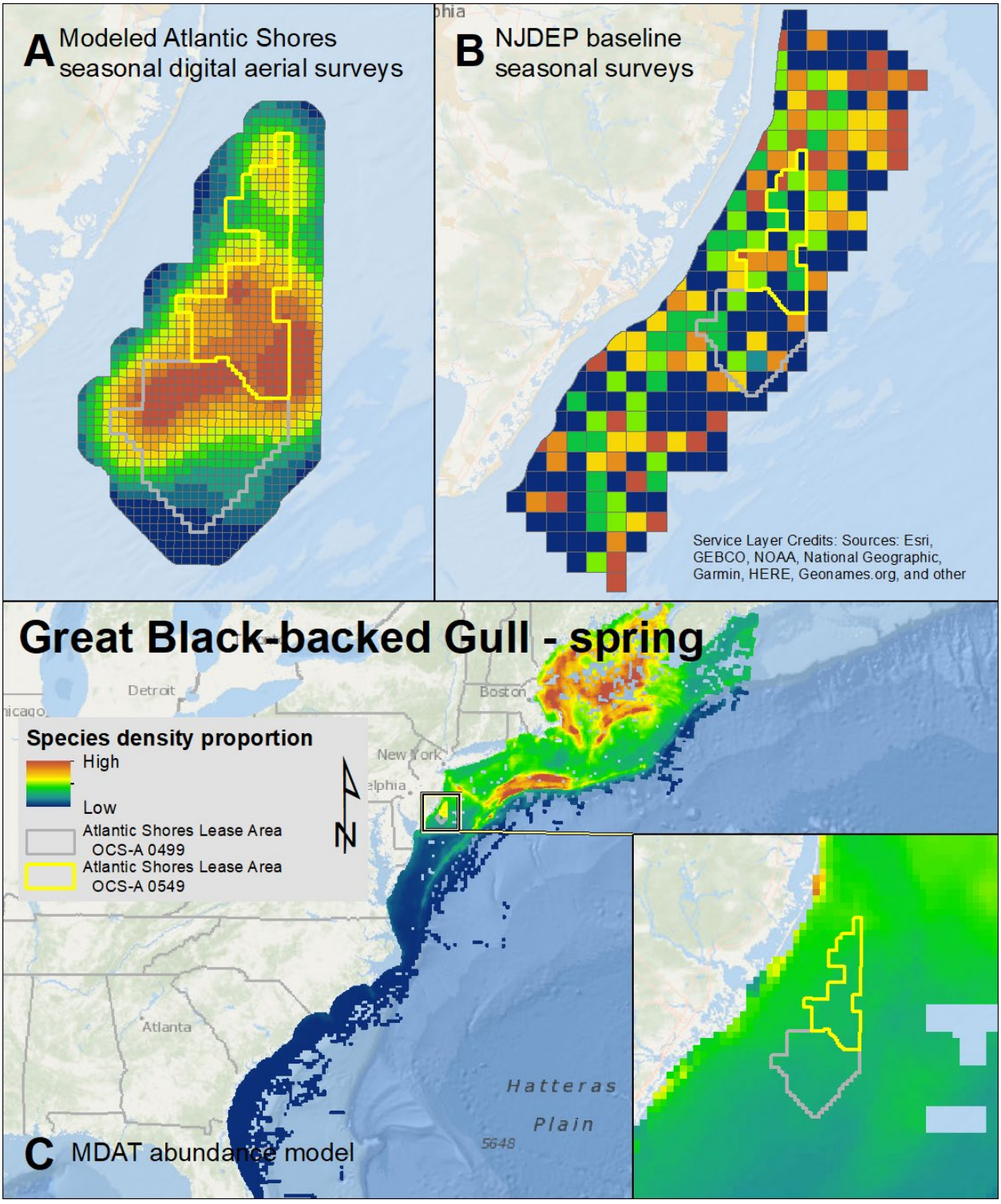

Map 122. Spring Great Black-backed Gull modeled density proportions in the Atlantic Shores seasonal digital aerial surveys (A), density proportions in the NJDEP baseline survey data (B), and the MDAT model outputs at local and regional scales (C). The scale for all maps is representative of relative spatial variation in the sites within the season for each information source.

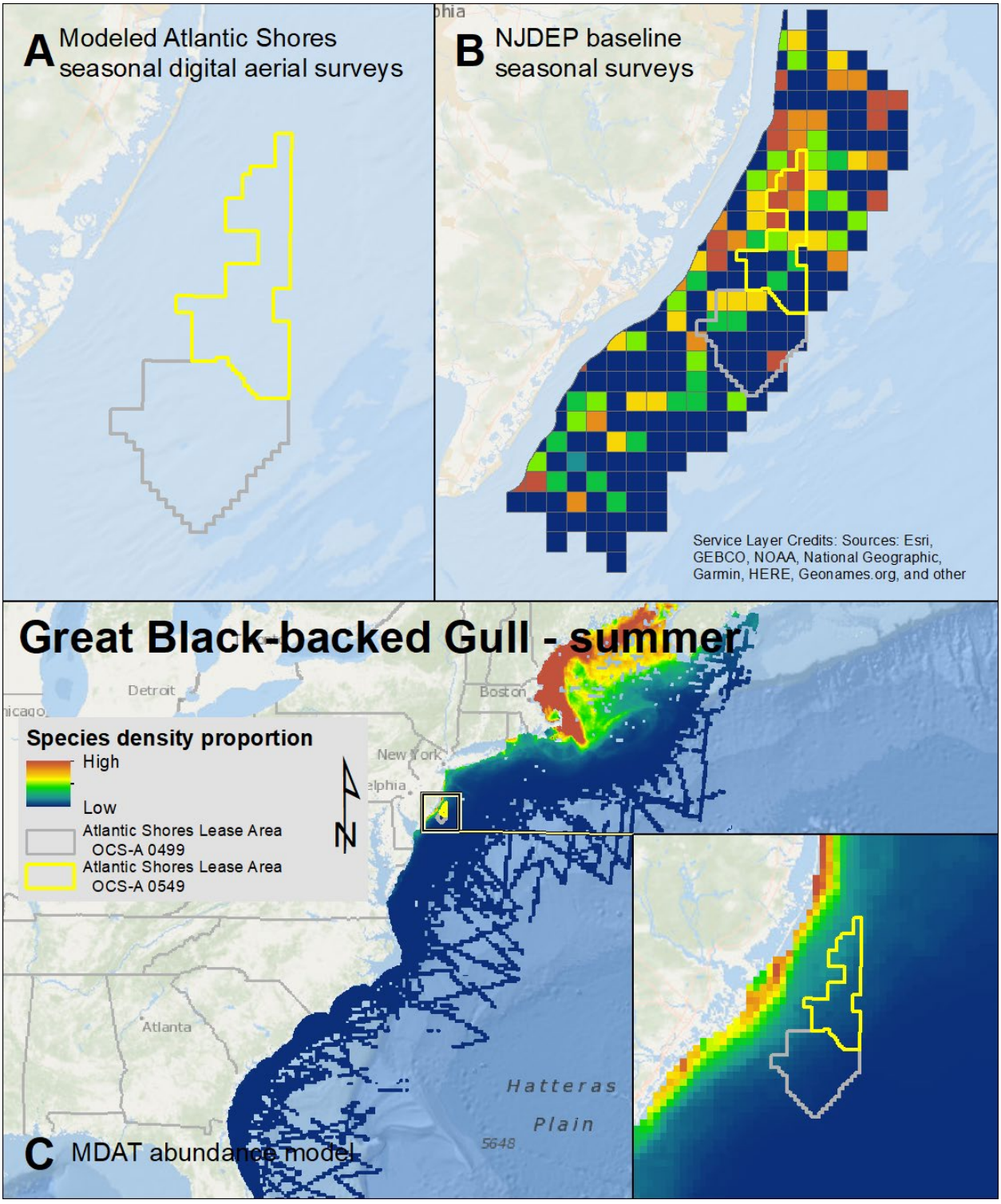

Map 123. Summer Great Black-backed Gull modeled density proportions in the Atlantic Shores seasonal digital aerial surveys (A), density proportions in the NJDEP baseline survey data (B), and the MDAT model outputs at local and regional scales (C). The scale for all maps is representative of relative spatial variation in the sites within the season for each information source.

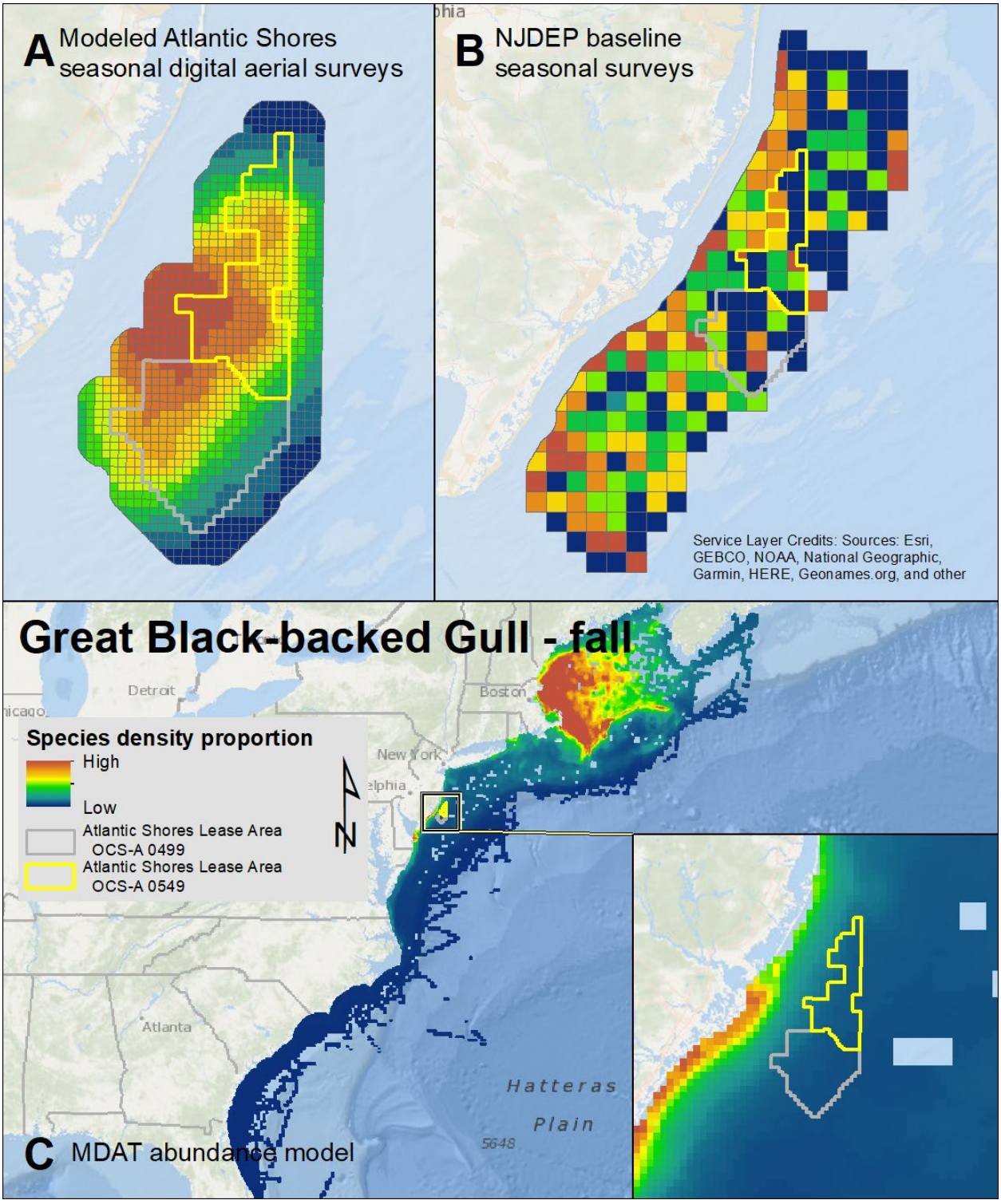

Map 124. Fall Great Black-backed Gull modeled density proportions in the Atlantic Shores seasonal digital aerial surveys (A), density proportions in the NJDEP baseline survey data (B), and the MDAT model outputs at local and regional scales (C). The scale for all maps is representative of relative spatial variation in the sites within the season for each information source.

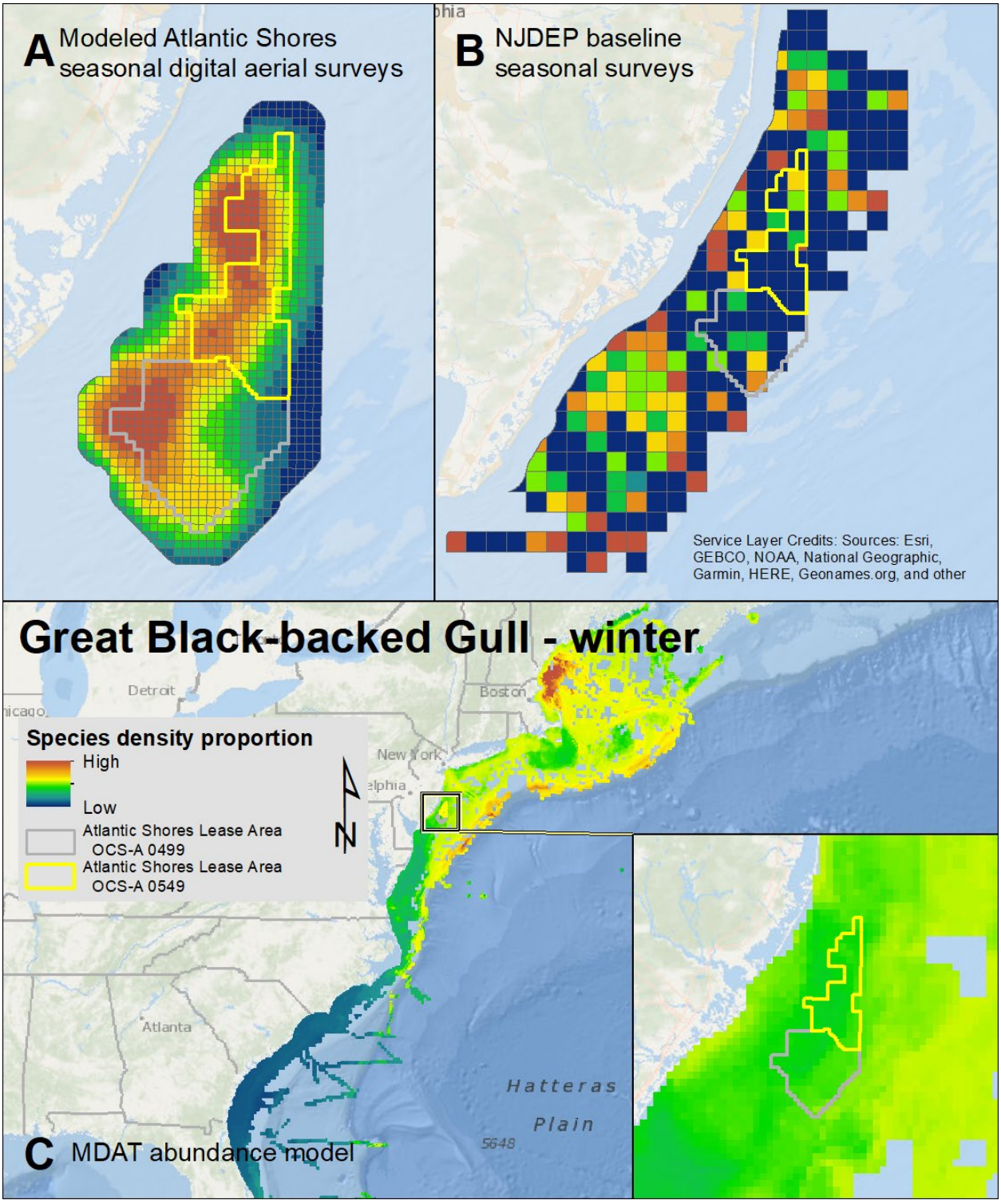

Map 125. Winter Great Black-backed Gull modeled density proportions in the Atlantic Shores seasonal digital aerial surveys (A), density proportions in the NJDEP baseline survey data (B), and the MDAT model outputs at local and regional scales (C). The scale for all maps is representative of relative spatial variation in the sites within the season for each information source.

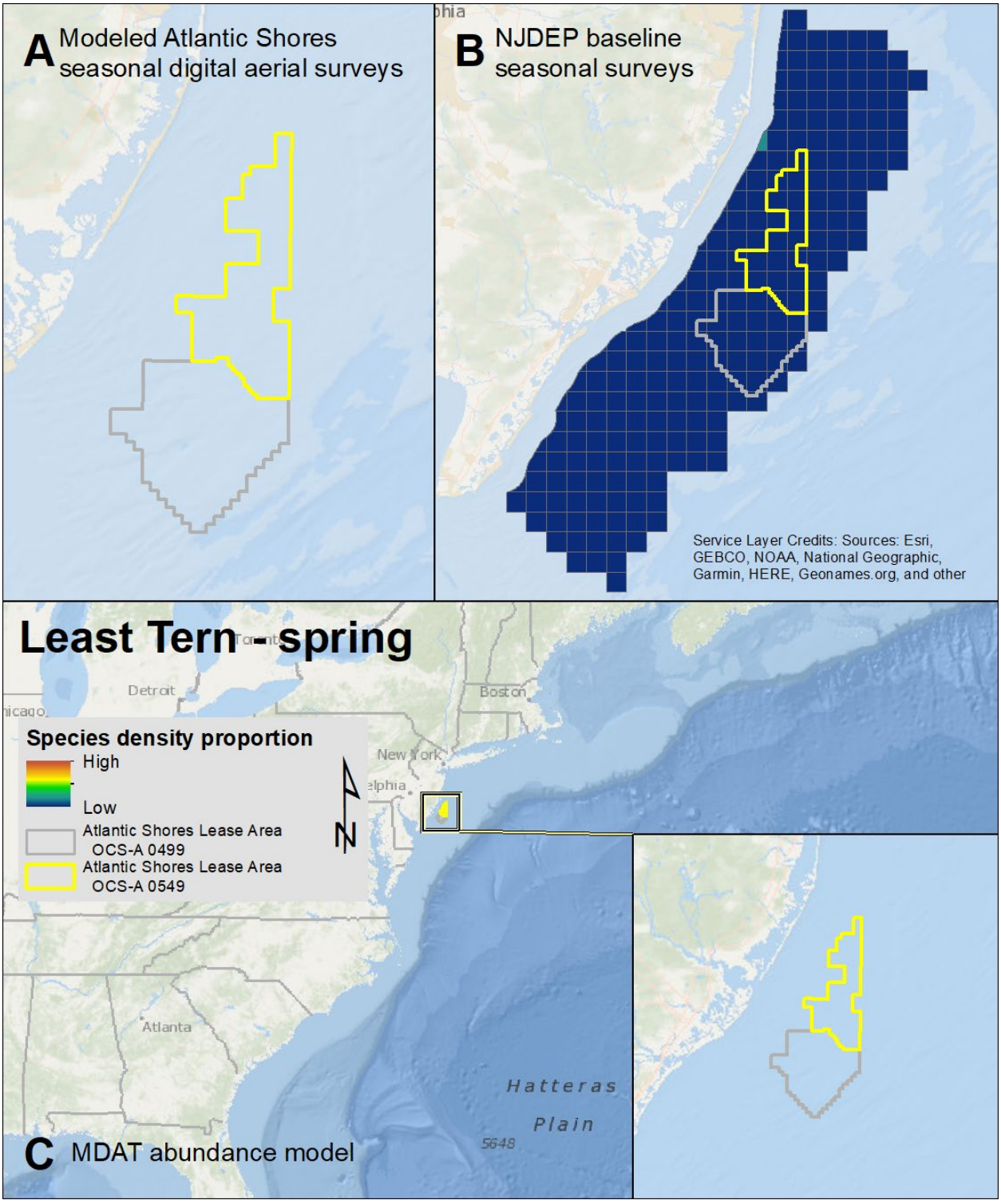

Map 126. Spring Least Tern modeled density proportions in the Atlantic Shores seasonal digital aerial surveys (A), density proportions in the NJDEP baseline survey data (B), and the MDAT model outputs at local and regional scales (C). The scale for all maps is representative of relative spatial variation in the sites within the season for each information source.

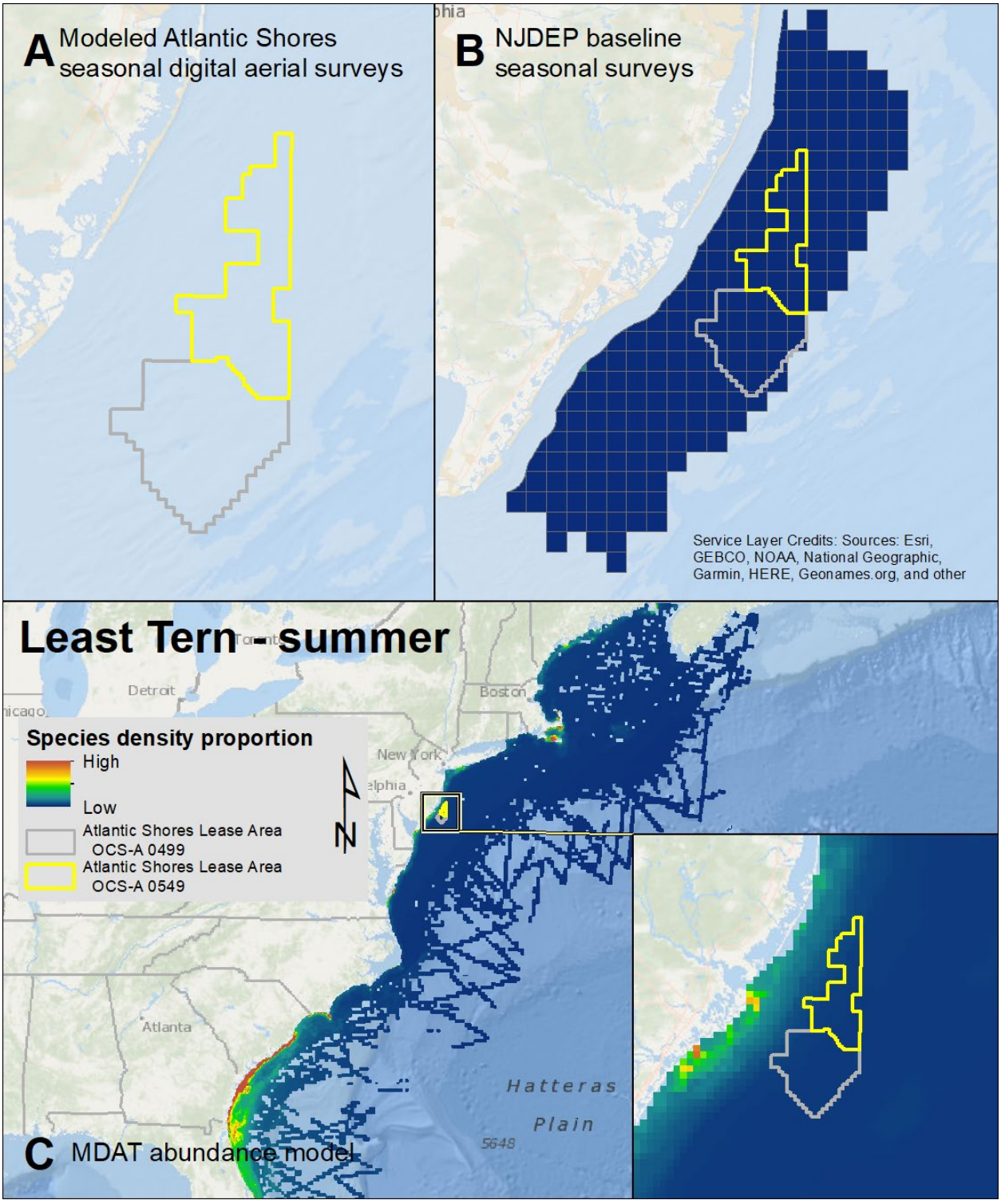

Map 127. Summer Least Tern modeled density proportions in the Atlantic Shores seasonal digital aerial surveys (A), density proportions in the NJDEP baseline survey data (B), and the MDAT model outputs at local and regional scales (C). The scale for all maps is representative of relative spatial variation in the sites within the season for each information source.

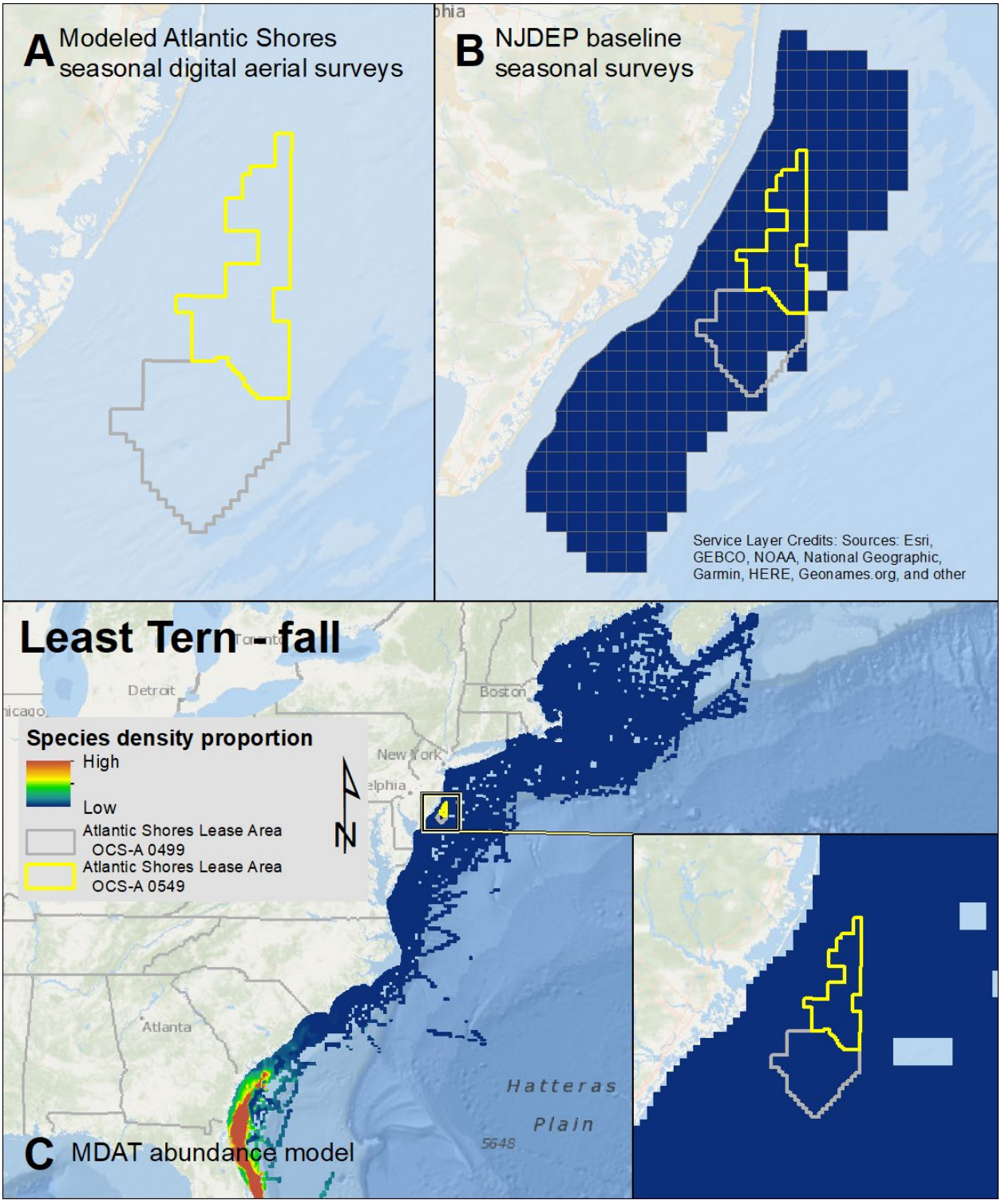

Map 128. Fall Least Tern modeled density proportions in the Atlantic Shores seasonal digital aerial surveys (A), density proportions in the NJDEP baseline survey data (B), and the MDAT model outputs at local and regional scales (C). The scale for all maps is representative of relative spatial variation in the sites within the season for each information source.

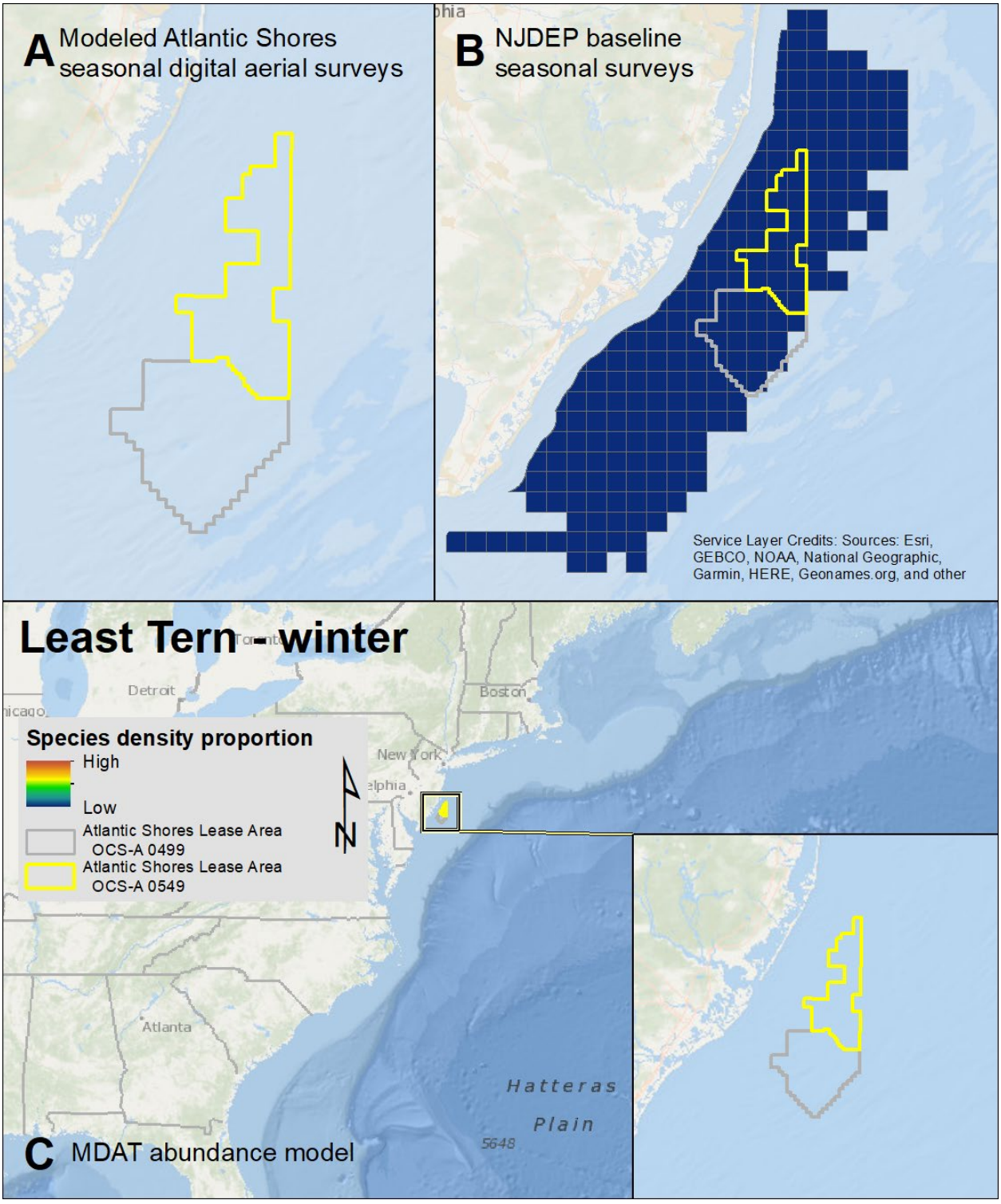

Map 129. Winter Least Tern modeled density proportions in the Atlantic Shores seasonal digital aerial surveys (A), density proportions in the NJDEP baseline survey data (B), and the MDAT model outputs at local and regional scales (C). The scale for all maps is representative of relative spatial variation in the sites within the season for each information source.

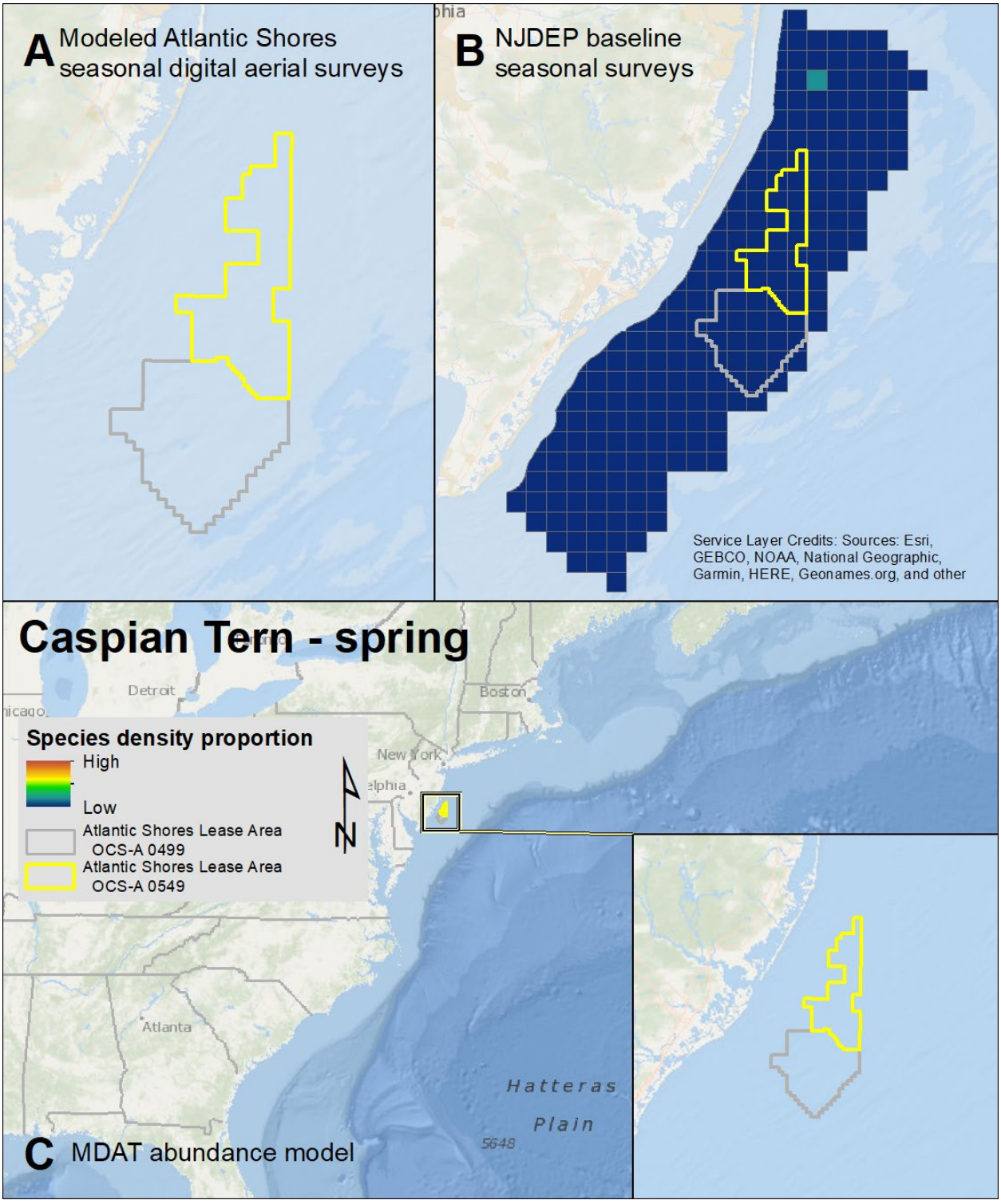

Map 130. Spring Caspian Tern modeled density proportions in the Atlantic Shores seasonal digital aerial surveys (A), density proportions in the NJDEP baseline survey data (B), and the MDAT model outputs at local and regional scales (C). The scale for all maps is representative of relative spatial variation in the sites within the season for each information source.

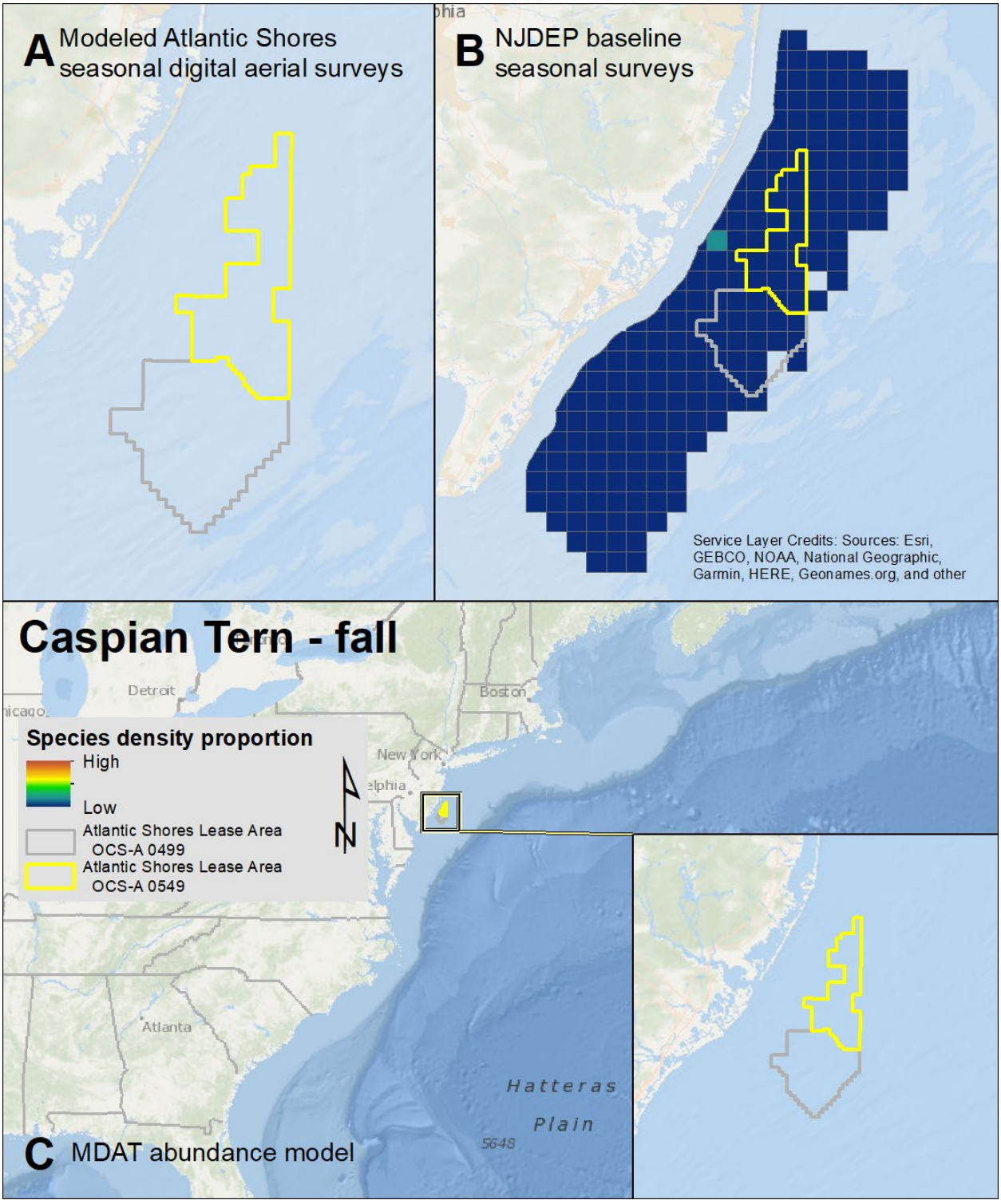

Map 131. Fall Caspian Tern modeled density proportions in the Atlantic Shores seasonal digital aerial surveys (A), density proportions in the NJDEP baseline survey data (B), and the MDAT model outputs at local and regional scales (C). The scale for all maps is representative of relative spatial variation in the sites within the season for each information source.

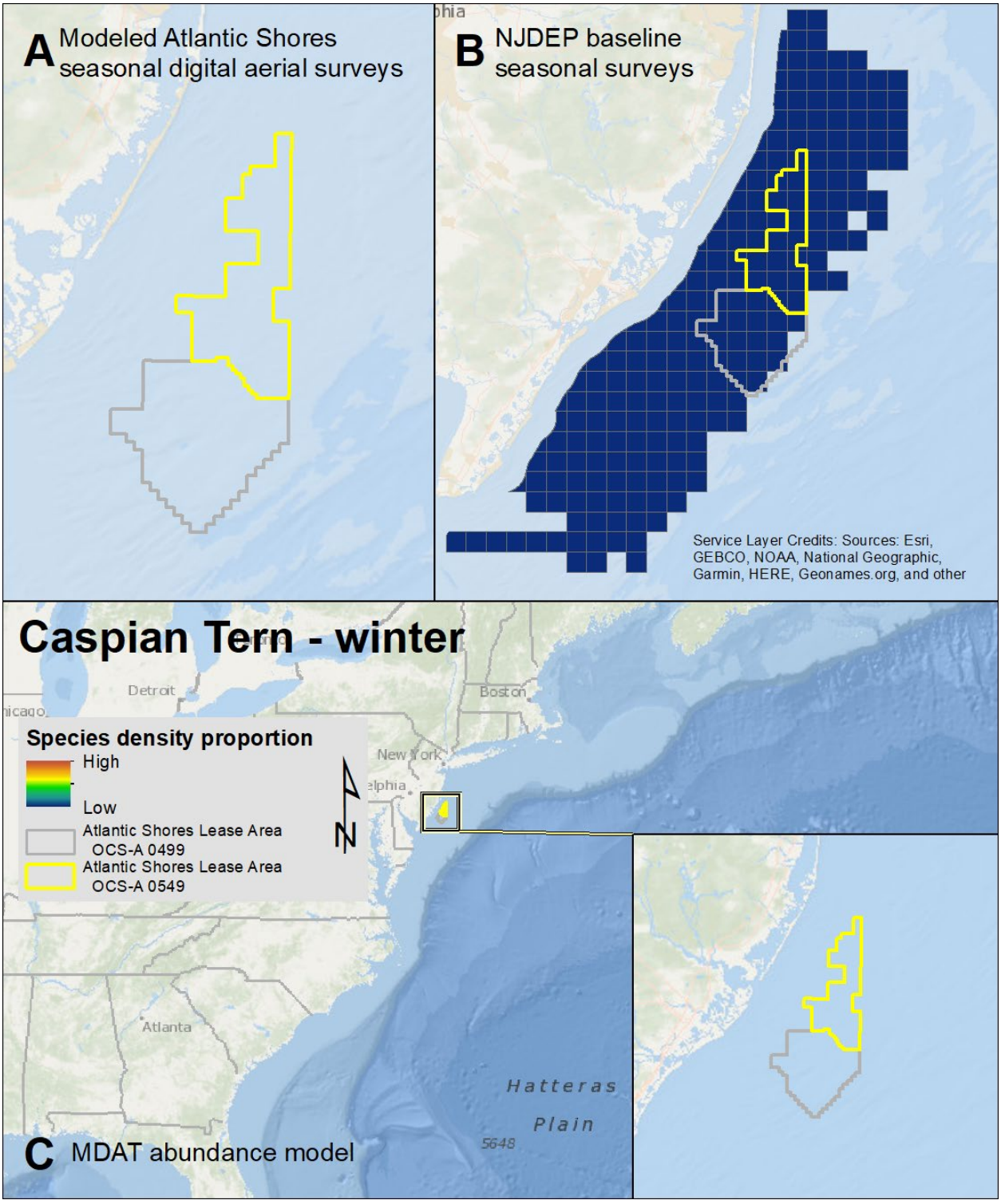

Map 132. Winter Caspian Tern modeled density proportions in the Atlantic Shores seasonal digital aerial surveys (A), density proportions in the NJDEP baseline survey data (B), and the MDAT model outputs at local and regional scales (C). The scale for all maps is representative of relative spatial variation in the sites within the season for each information source.

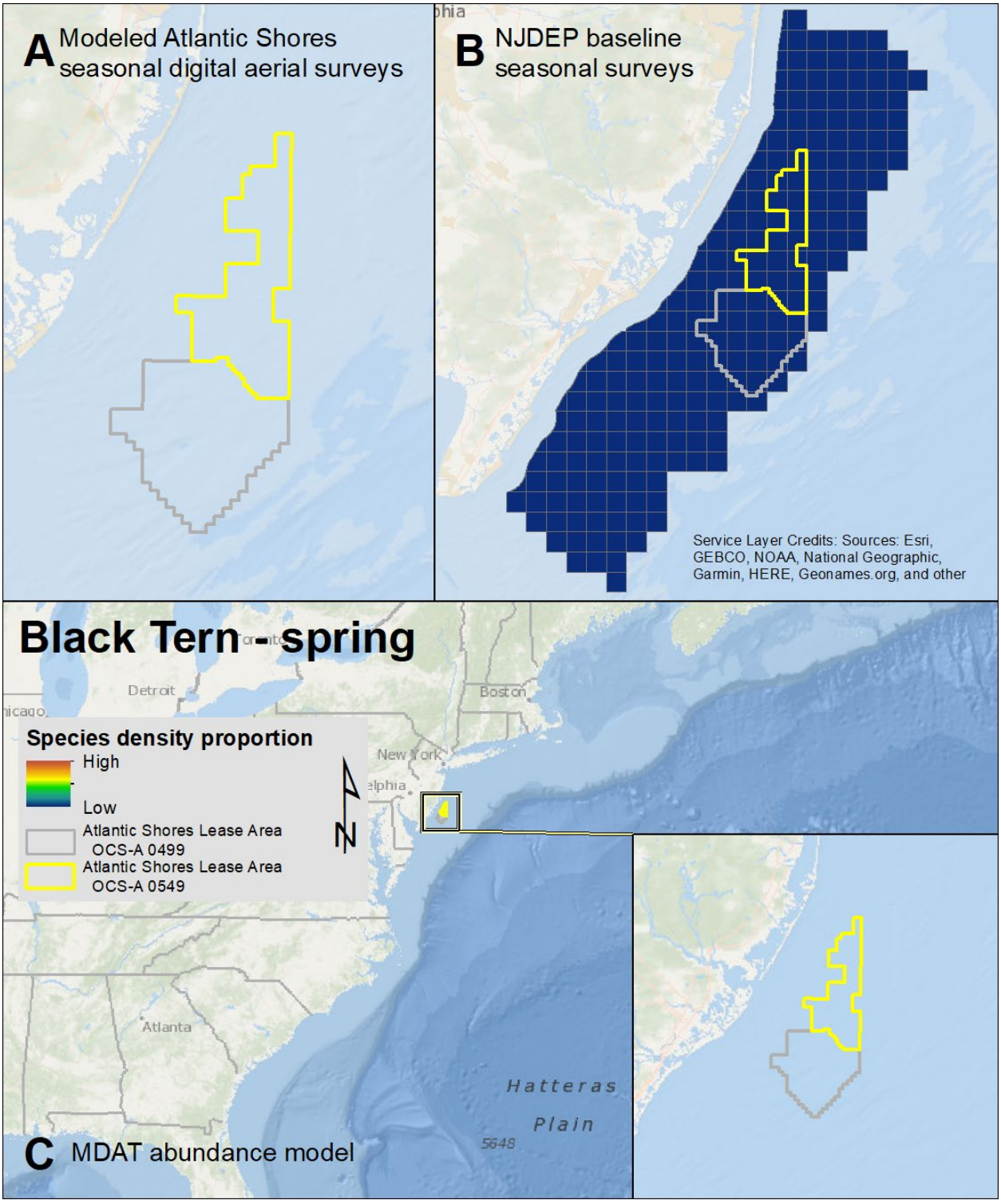

Map 133. Spring Black Tern modeled density proportions in the Atlantic Shores seasonal digital aerial surveys (A), density proportions in the NJDEP baseline survey data (B), and the MDAT model outputs at local and regional scales (C). The scale for all maps is representative of relative spatial variation in the sites within the season for each information source.

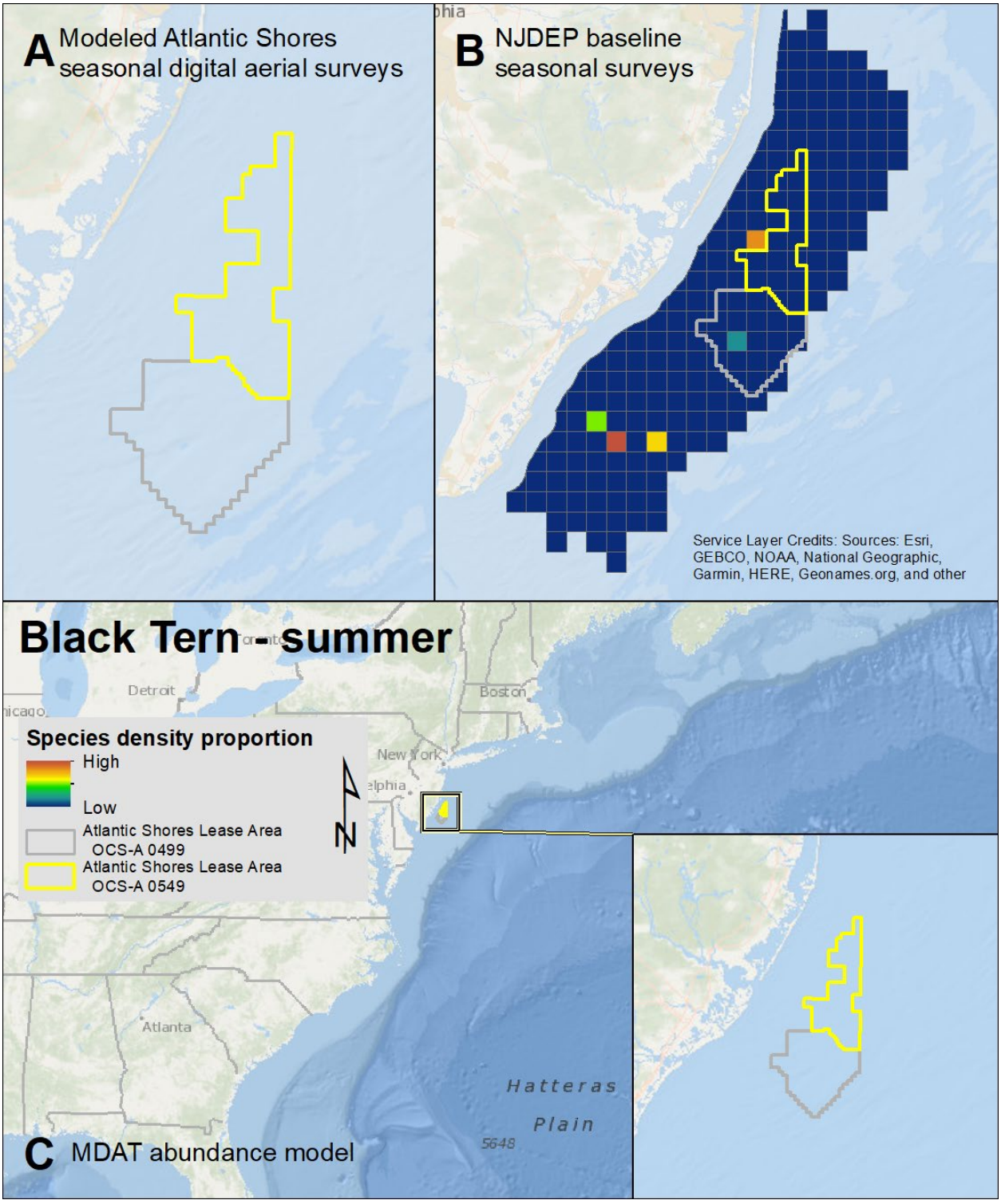

Map 134. Summer Black Tern modeled density proportions in the Atlantic Shores seasonal digital aerial surveys (A), density proportions in the NJDEP baseline survey data (B), and the MDAT model outputs at local and regional scales (C). The scale for all maps is representative of relative spatial variation in the sites within the season for each information source.

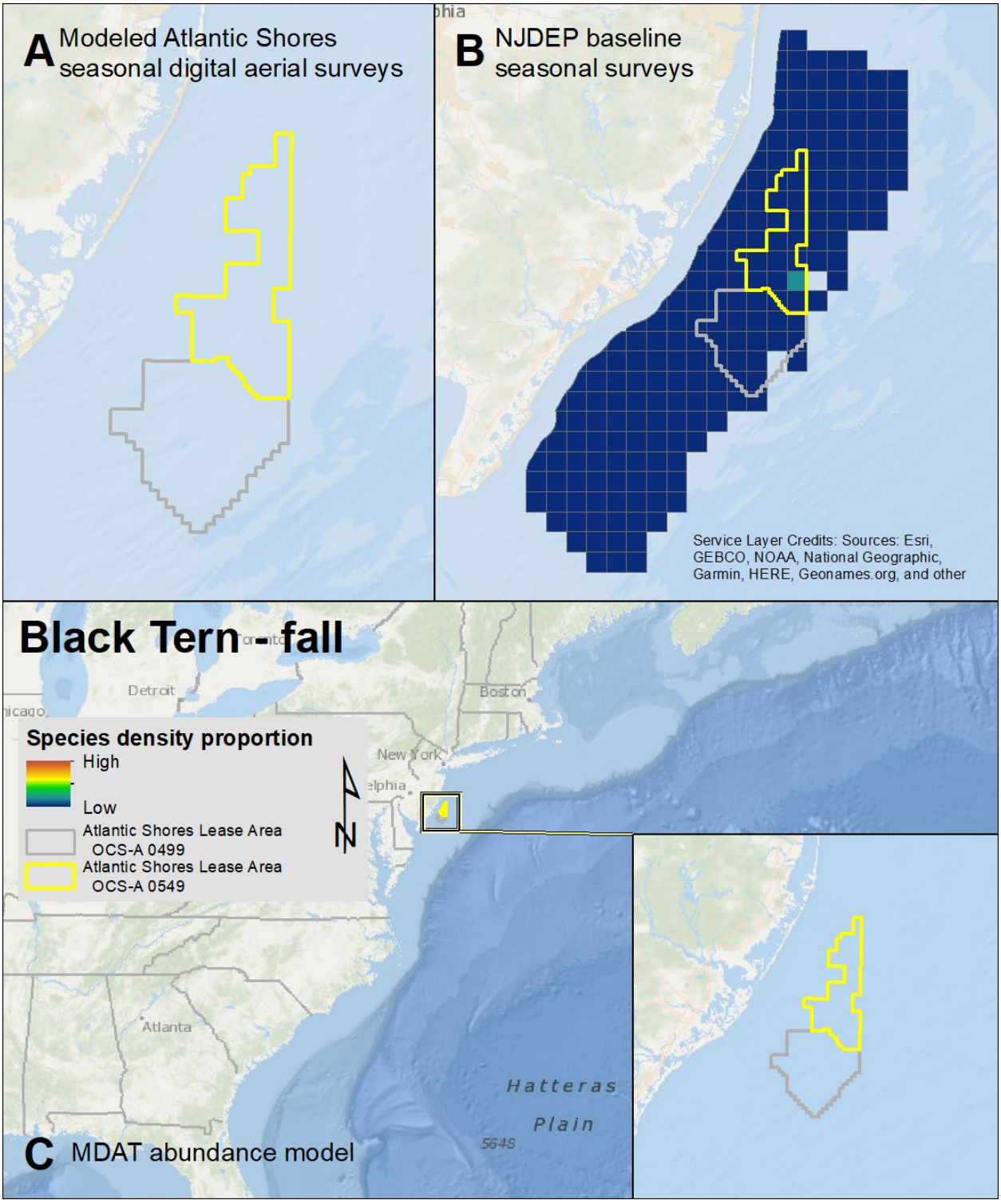

Map 135. Fall Black Tern modeled density proportions in the Atlantic Shores seasonal digital aerial surveys (A), density proportions in the NJDEP baseline survey data (B), and the MDAT model outputs at local and regional scales (C). The scale for all maps is representative of relative spatial variation in the sites within the season for each information source.

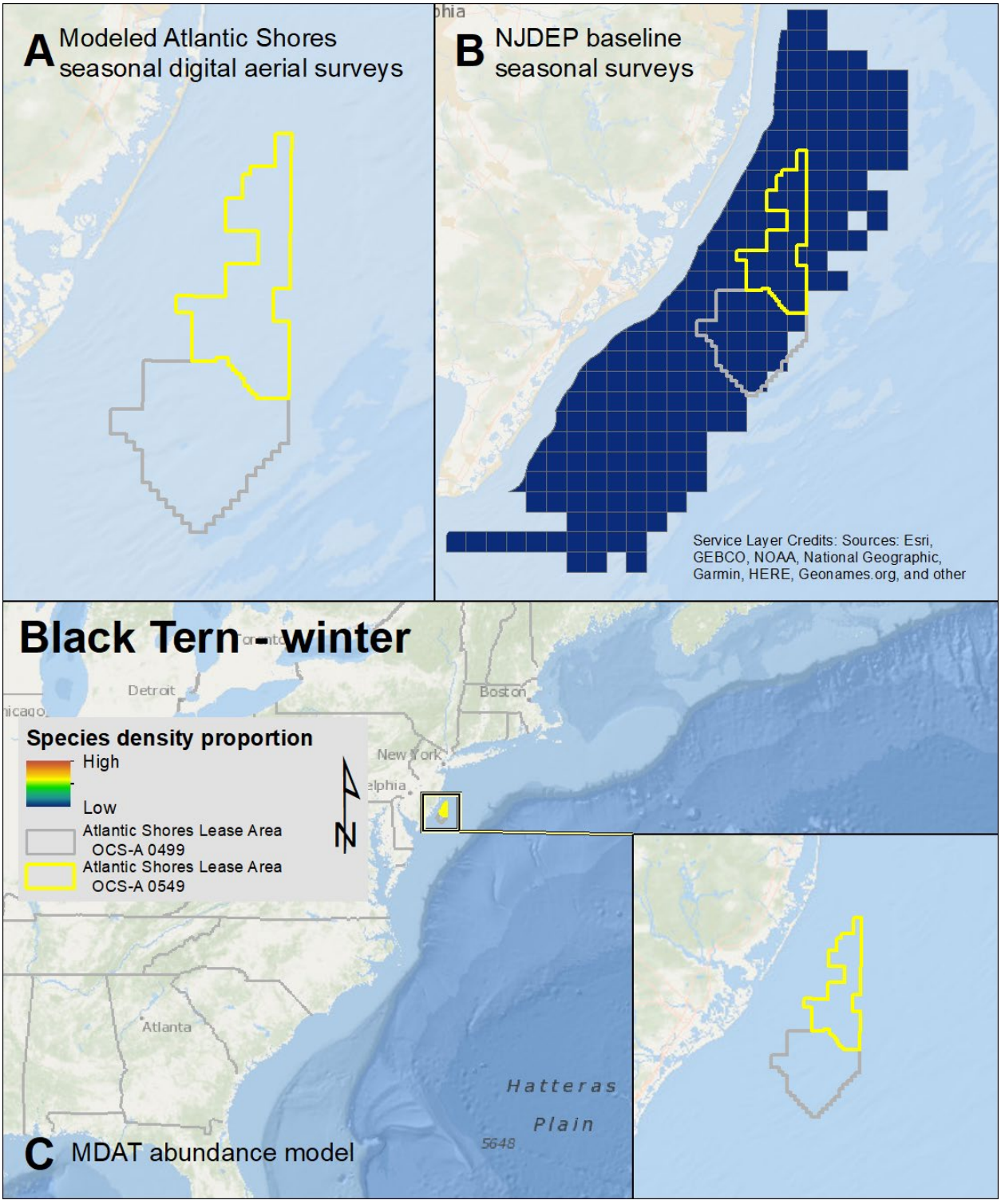

Map 136. Winter Black Tern modeled density proportions in the Atlantic Shores seasonal digital aerial surveys (A), density proportions in the NJDEP baseline survey data (B), and the MDAT model outputs at local and regional scales (C). The scale for all maps is representative of relative spatial variation in the sites within the season for each information source.

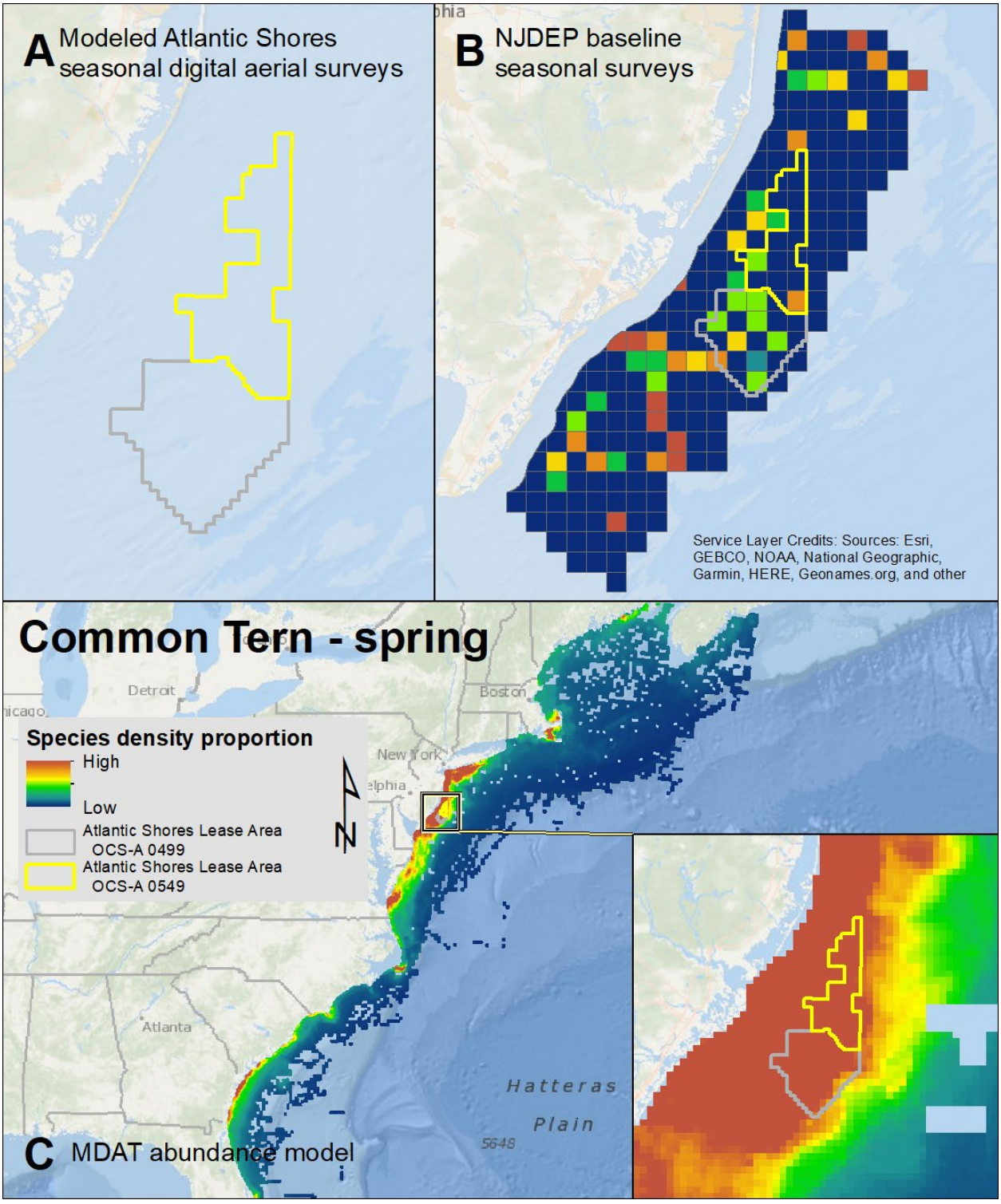

Map 137. Spring Common Tern modeled density proportions in the Atlantic Shores seasonal digital aerial surveys (A), density proportions in the NJDEP baseline survey data (B), and the MDAT model outputs at local and regional scales (C). The scale for all maps is representative of relative spatial variation in the sites within the season for each information source.

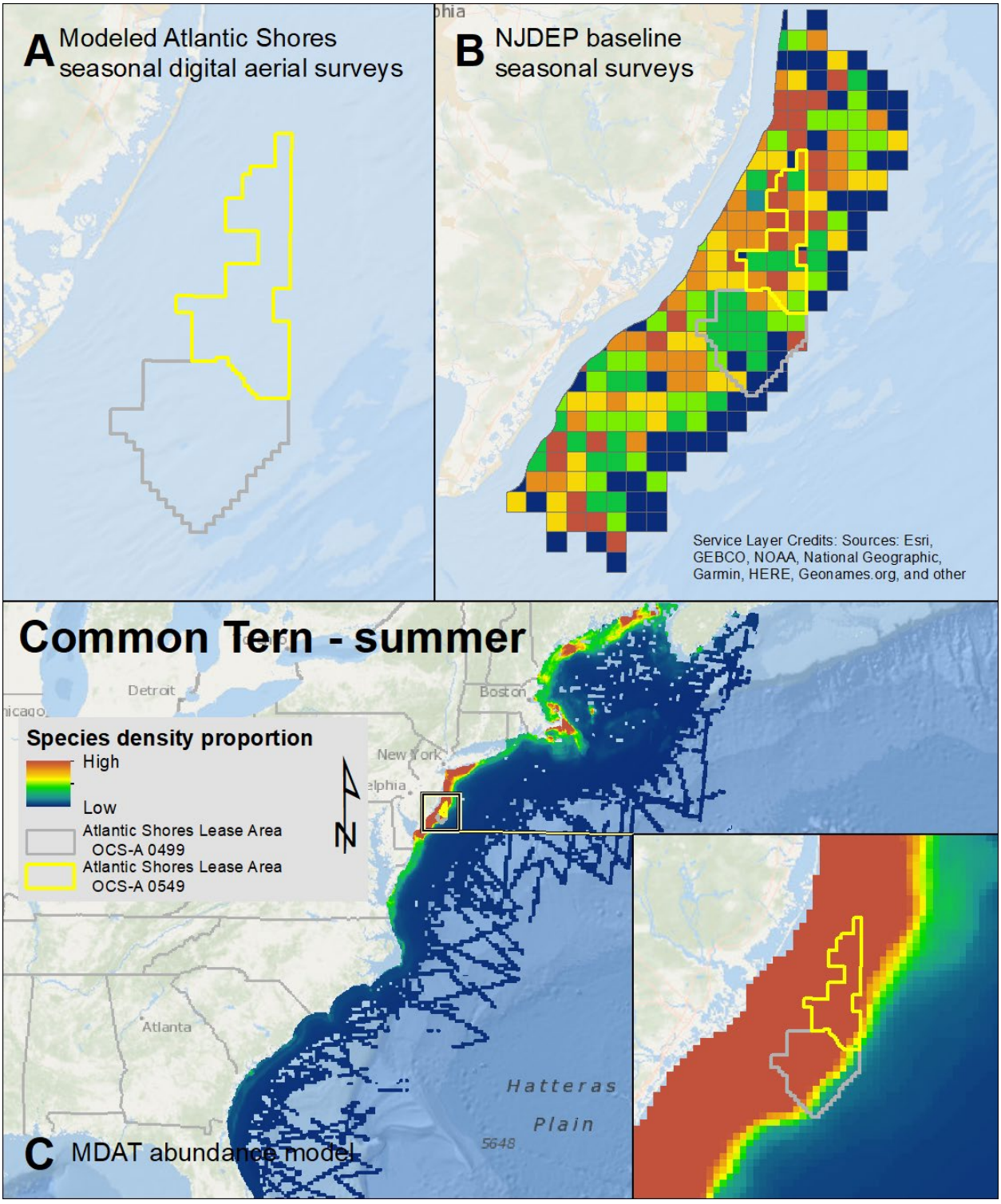

Map 138. Summer Common Tern modeled density proportions in the Atlantic Shores seasonal digital aerial surveys (A), density proportions in the NJDEP baseline survey data (B), and the MDAT model outputs at local and regional scales (C). The scale for all maps is representative of relative spatial variation in the sites within the season for each information source.

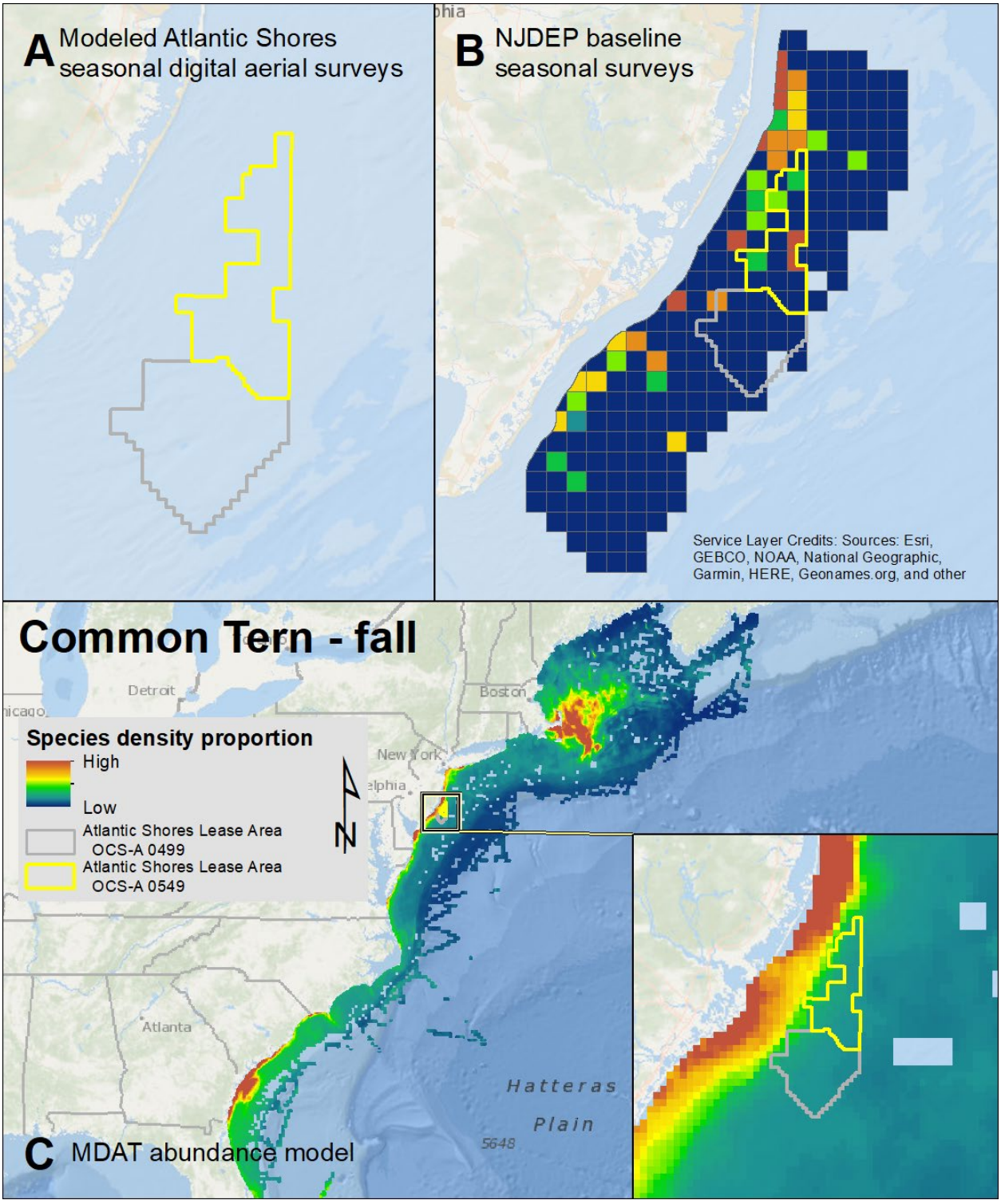

Map 139. Fall Common Tern modeled density proportions in the Atlantic Shores seasonal digital aerial surveys (A), density proportions in the NJDEP baseline survey data (B), and the MDAT model outputs at local and regional scales (C). The scale for all maps is representative of relative spatial variation in the sites within the season for each information source.

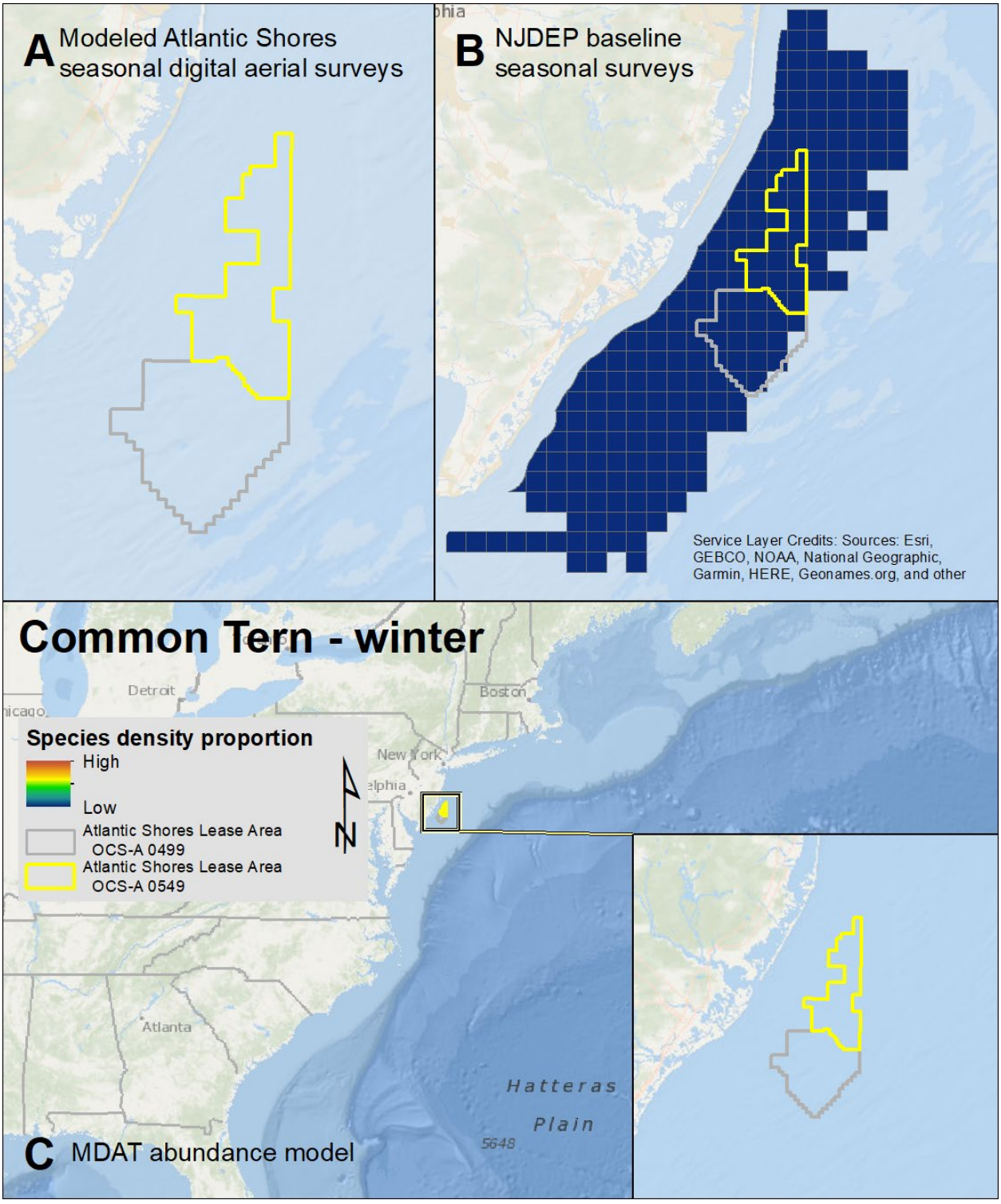

Map 140. Winter Common Tern modeled density proportions in the Atlantic Shores seasonal digital aerial surveys (A), density proportions in the NJDEP baseline survey data (B), and the MDAT model outputs at local and regional scales (C). The scale for all maps is representative of relative spatial variation in the sites within the season for each information source.

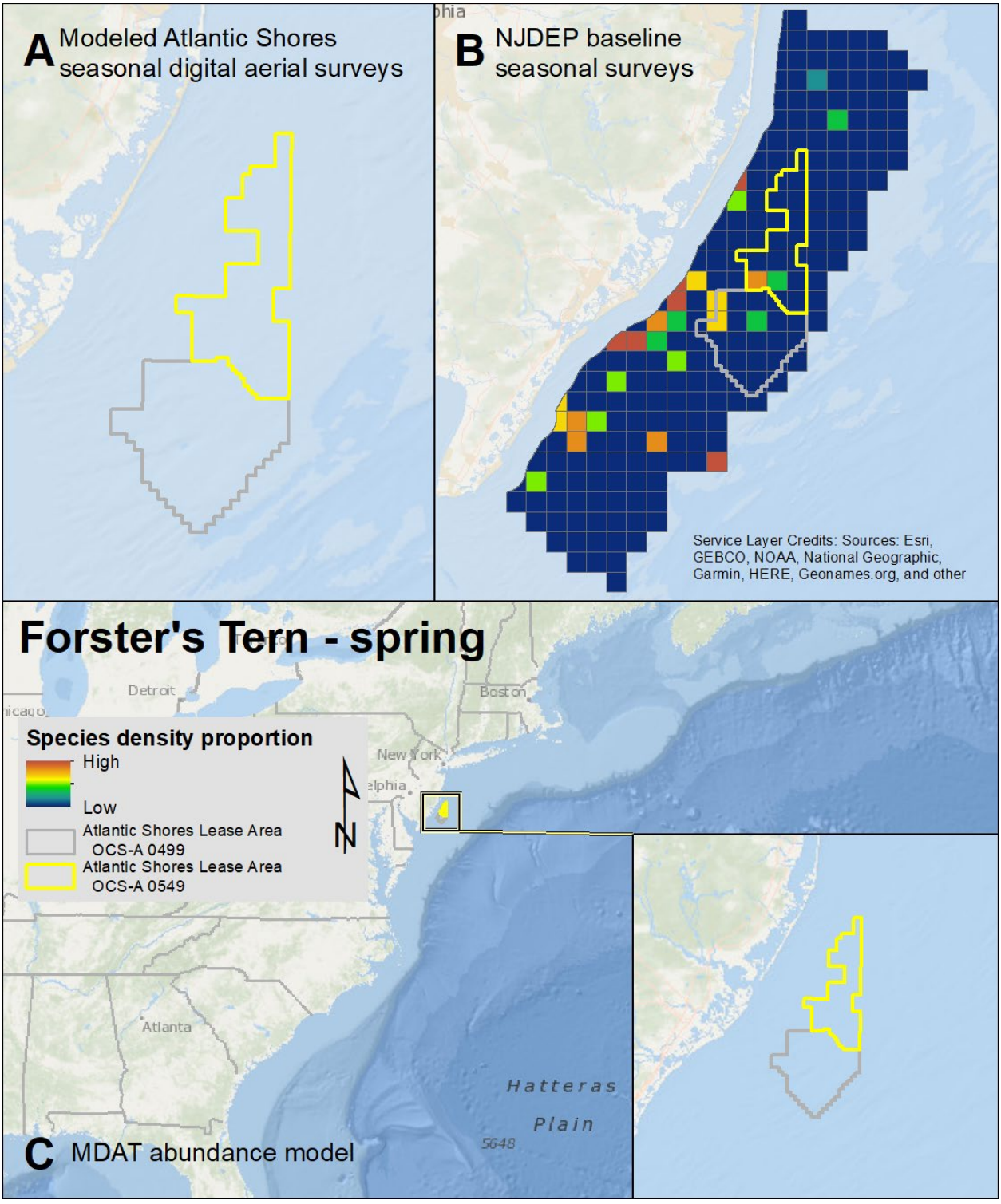

Map 141. Spring Forster's Tern modeled density proportions in the Atlantic Shores seasonal digital aerial surveys (A), density proportions in the NJDEP baseline survey data (B), and the MDAT model outputs at local and regional scales (C). The scale for all maps is representative of relative spatial variation in the sites within the season for each information source.

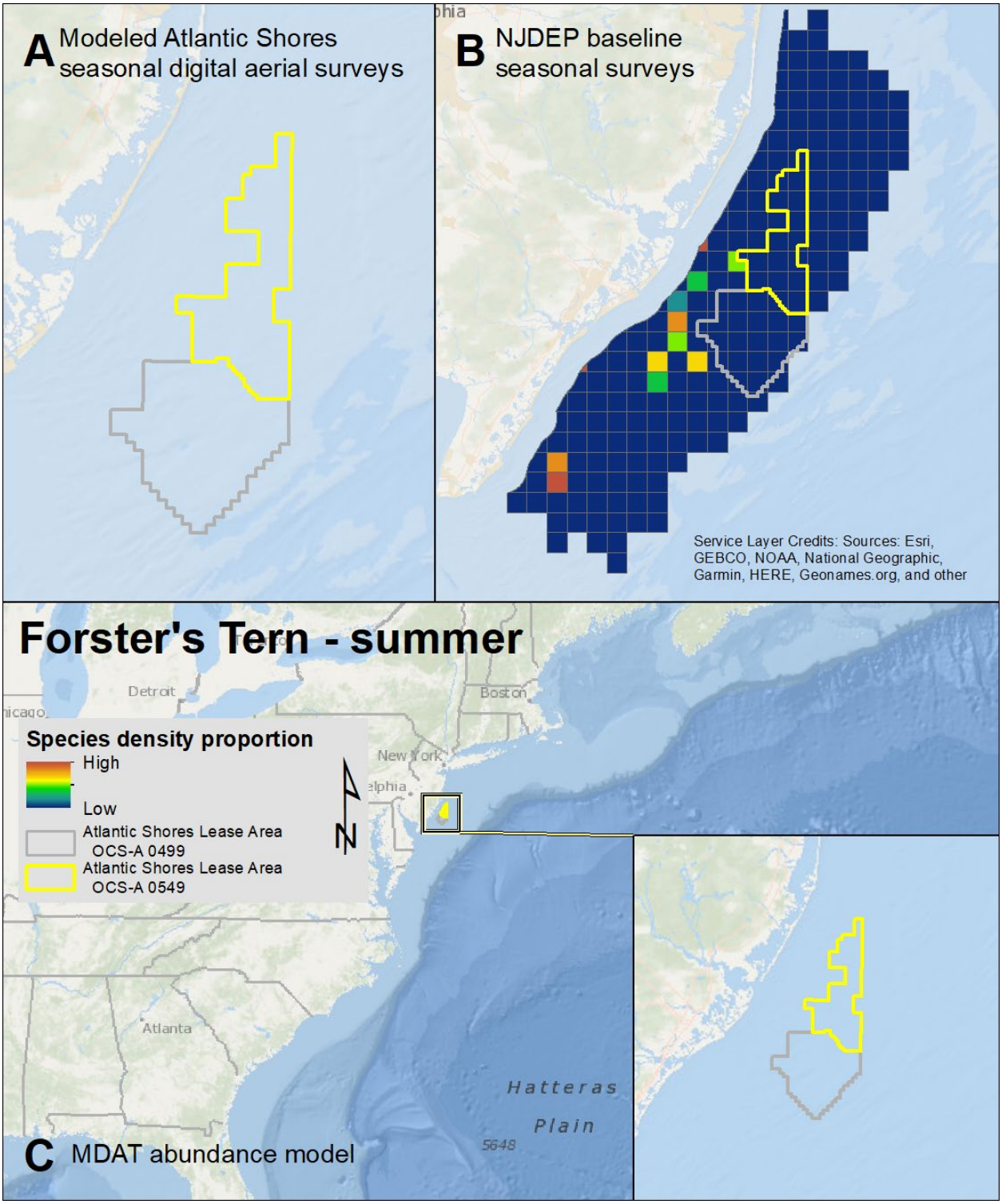

Map 142. Summer Forster's Tern modeled density proportions in the Atlantic Shores seasonal digital aerial surveys (A), density proportions in the NJDEP baseline survey data (B), and the MDAT model outputs at local and regional scales (C). The scale for all maps is representative of relative spatial variation in the sites within the season for each information source.

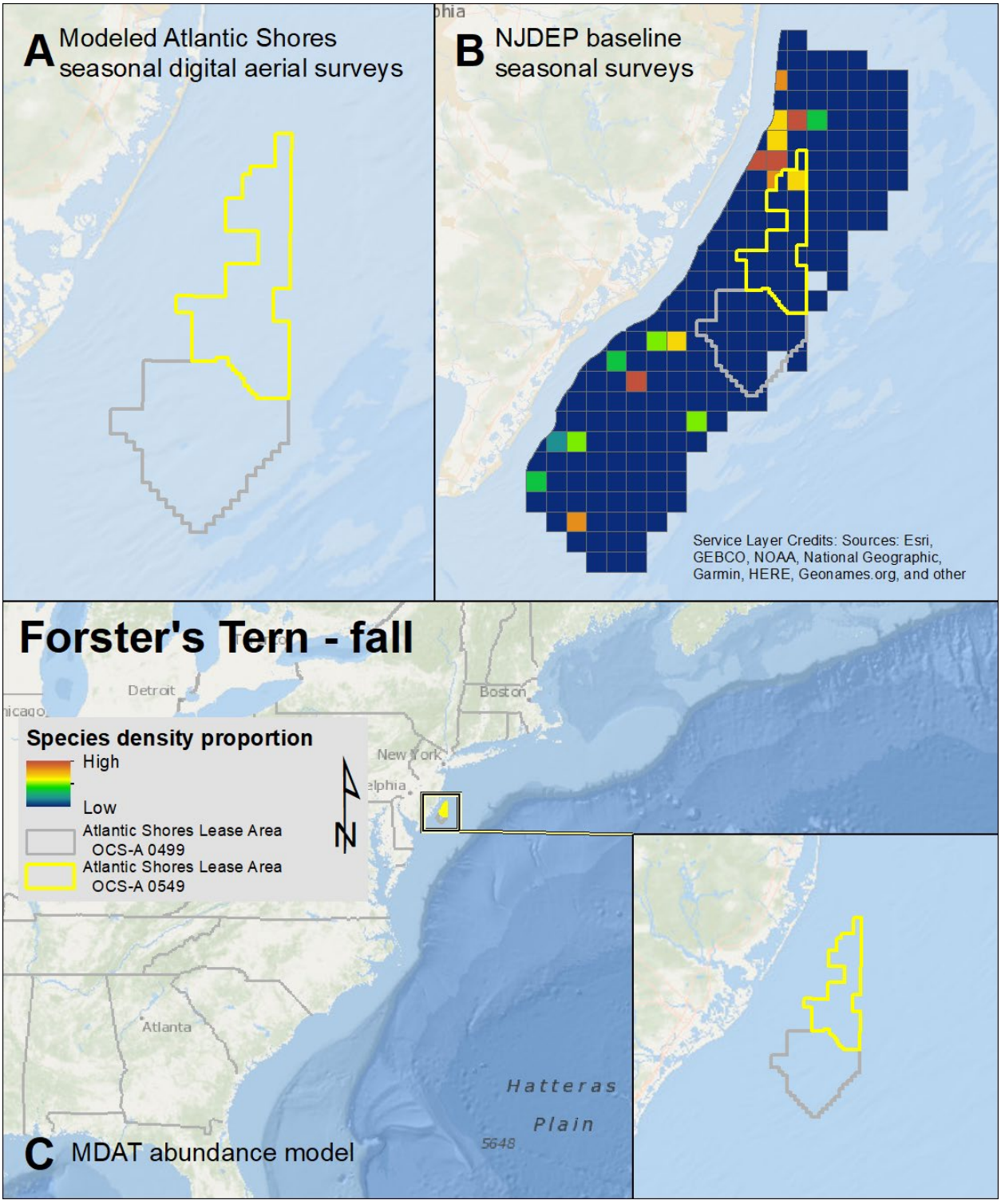

Map 143. Fall Forster's Tern modeled density proportions in the Atlantic Shores seasonal digital aerial surveys (A), density proportions in the NJDEP baseline survey data (B), and the MDAT model outputs at local and regional scales (C). The scale for all maps is representative of relative spatial variation in the sites within the season for each information source.

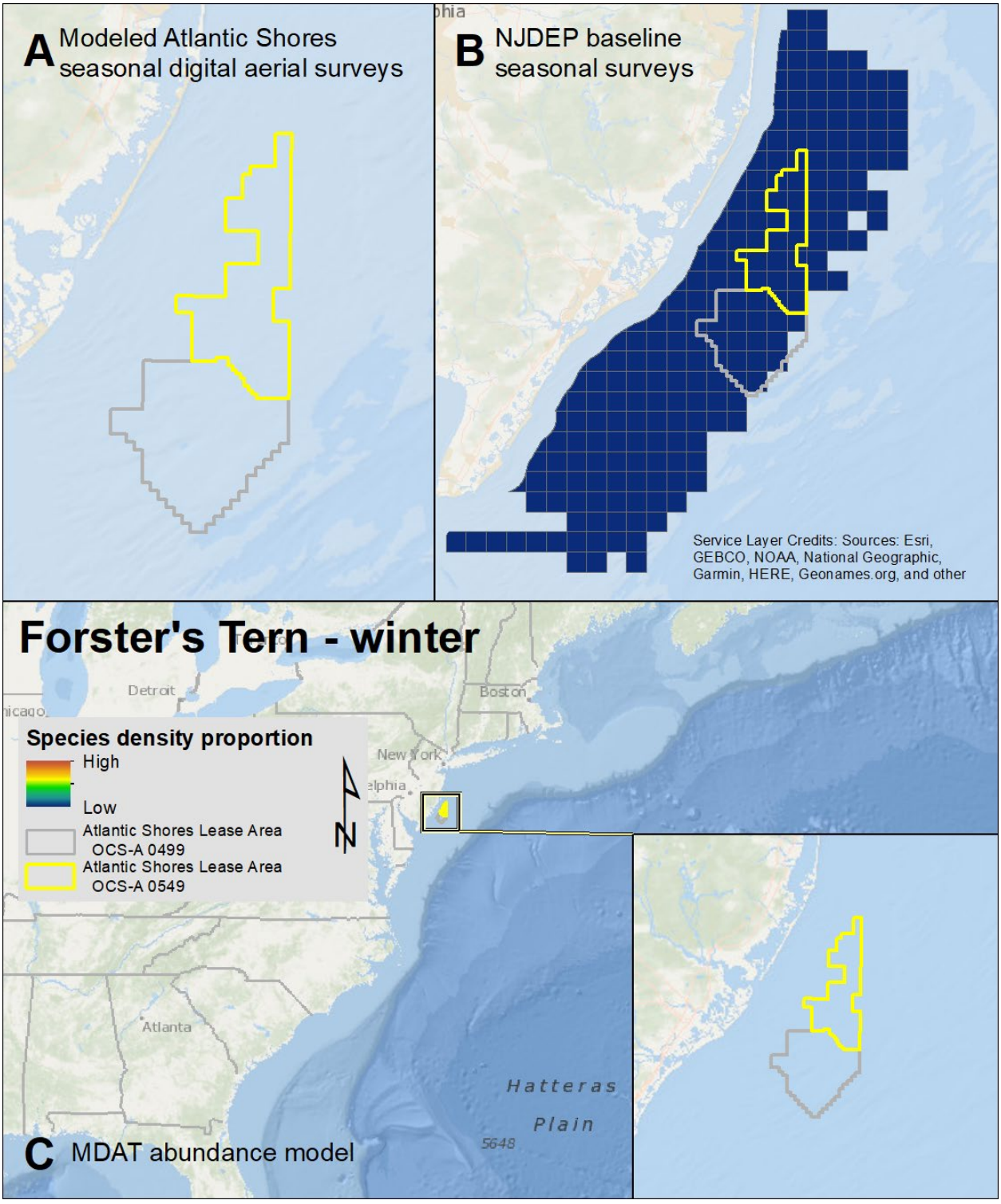

Map 144. Winter Forster's Tern modeled density proportions in the Atlantic Shores seasonal digital aerial surveys (A), density proportions in the NJDEP baseline survey data (B), and the MDAT model outputs at local and regional scales (C). The scale for all maps is representative of relative spatial variation in the sites within the season for each information source.

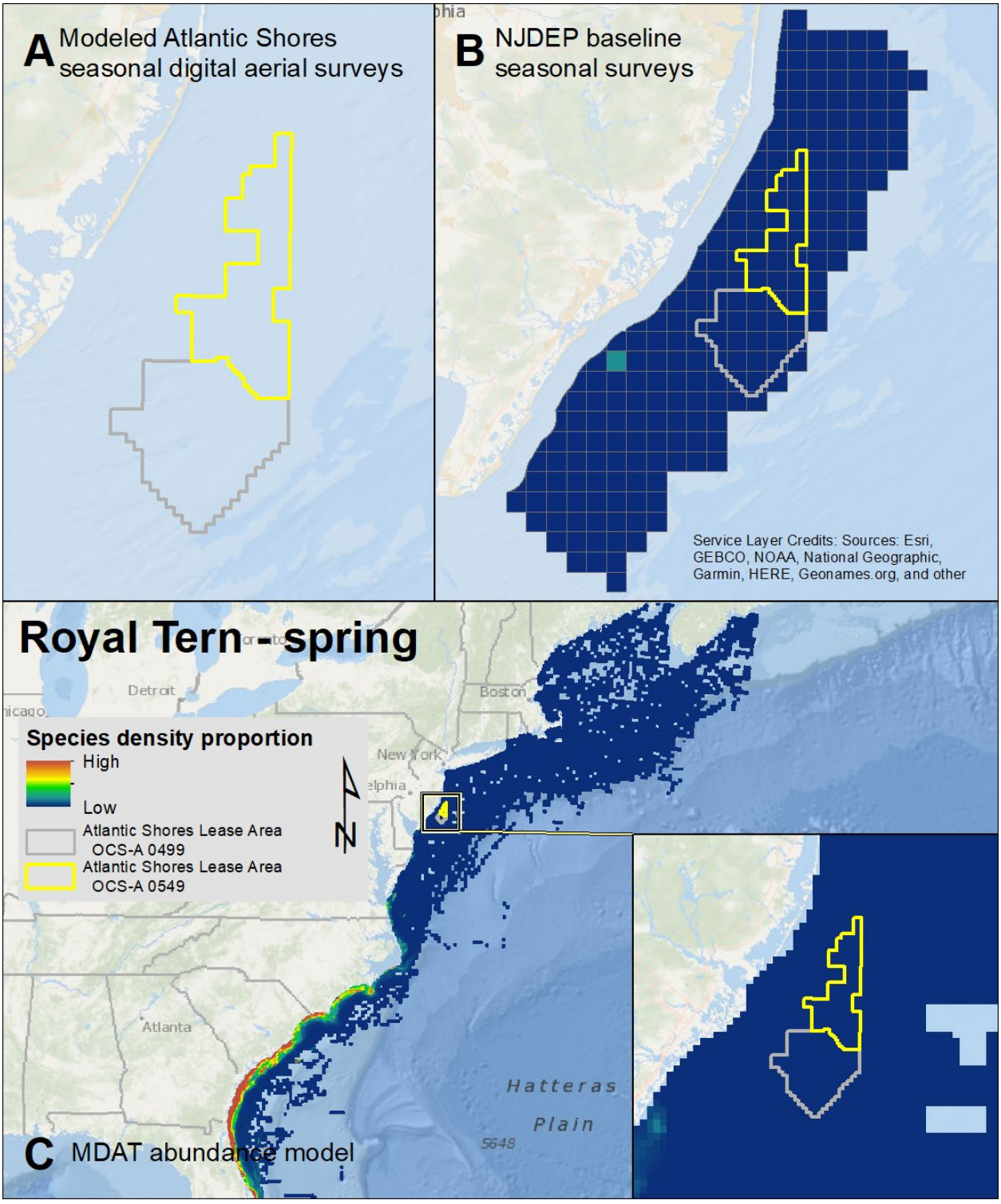

Map 145. Spring Royal Tern modeled density proportions in the Atlantic Shores seasonal digital aerial surveys (A), density proportions in the NJDEP baseline survey data (B), and the MDAT model outputs at local and regional scales (C). The scale for all maps is representative of relative spatial variation in the sites within the season for each information source.

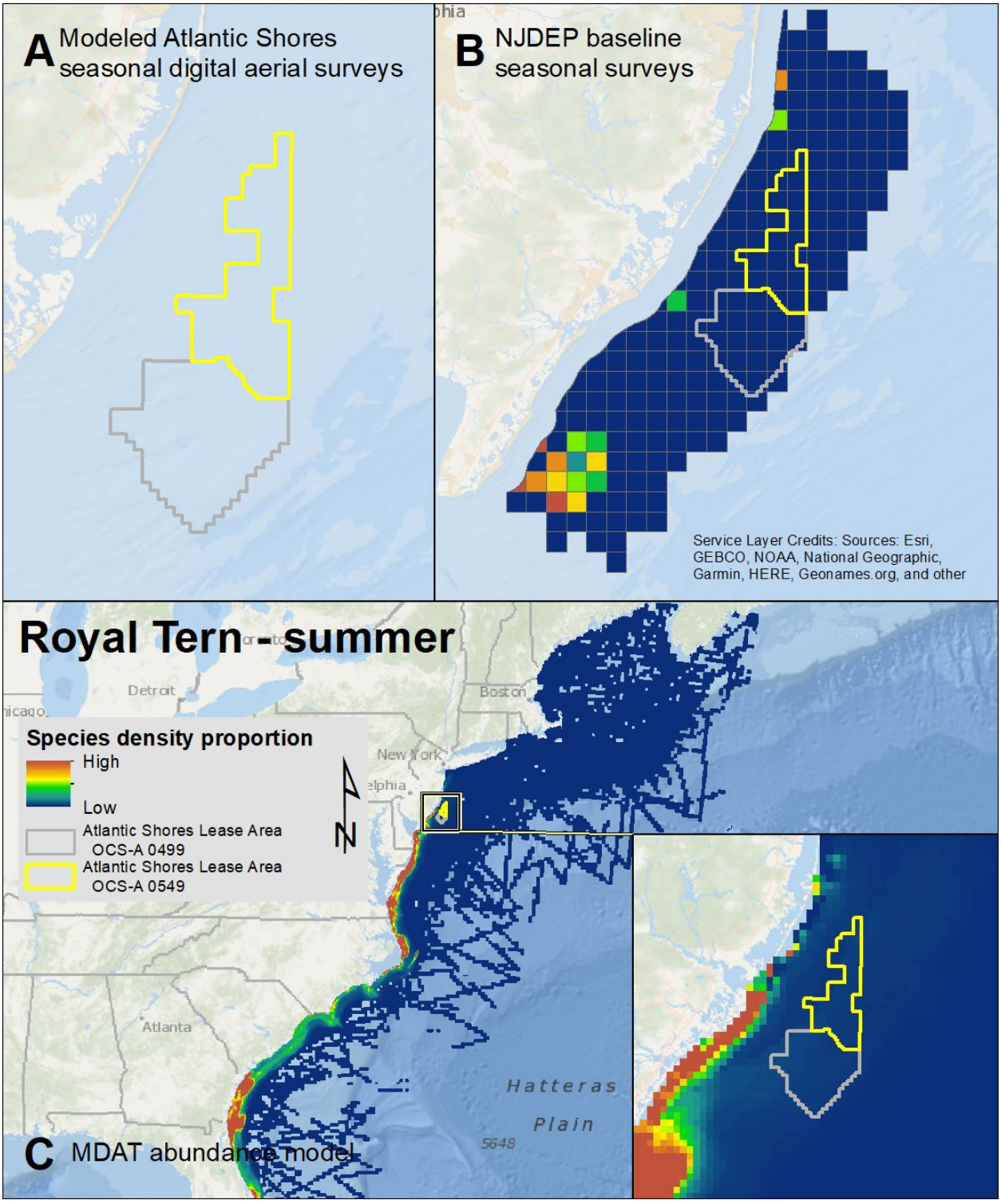

Map 146. Summer Royal Tern modeled density proportions in the Atlantic Shores seasonal digital aerial surveys (A), density proportions in the NJDEP baseline survey data (B), and the MDAT model outputs at local and regional scales (C). The scale for all maps is representative of relative spatial variation in the sites within the season for each information source.

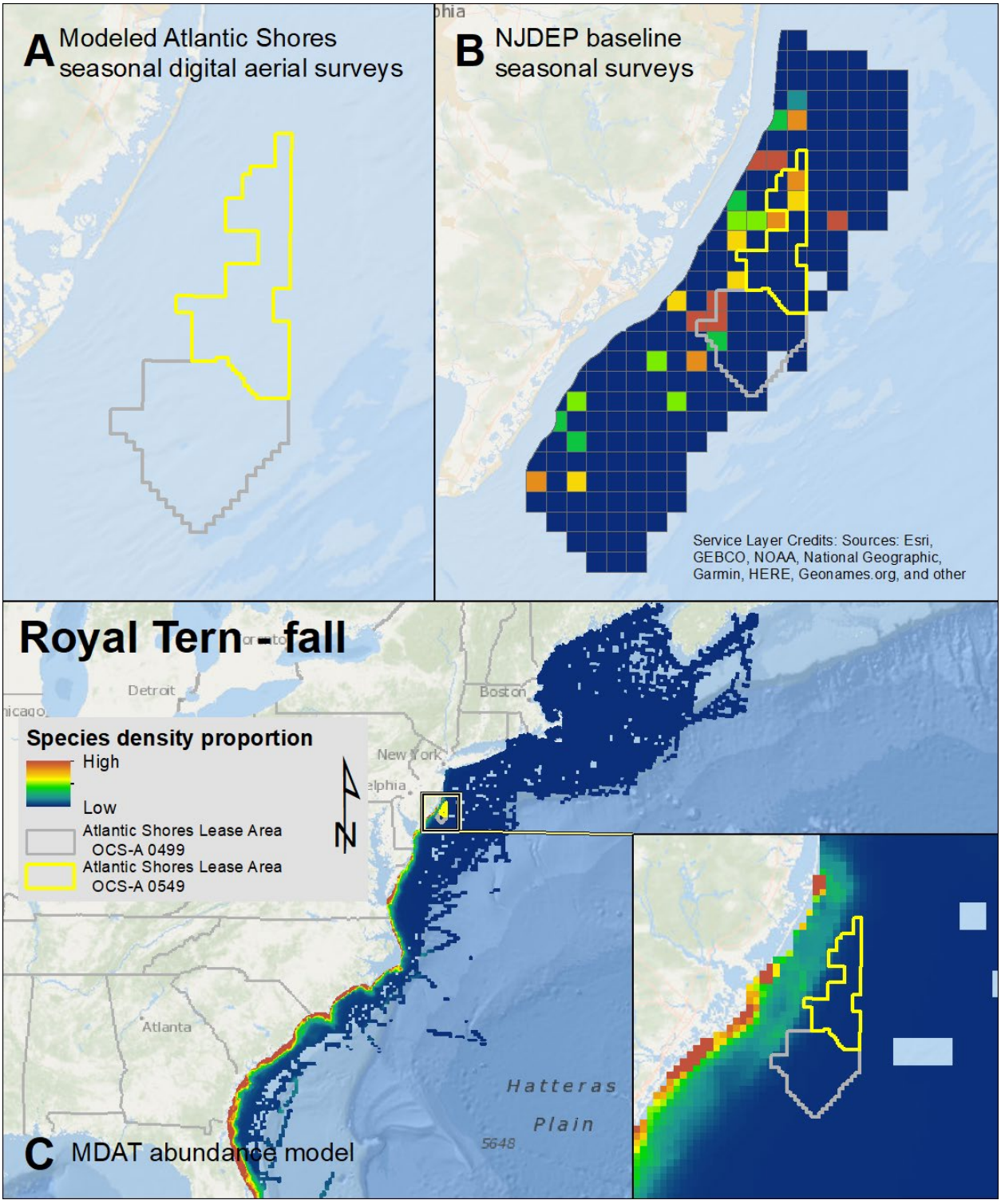

Map 147. Fall Royal Tern modeled density proportions in the Atlantic Shores seasonal digital aerial surveys (A), density proportions in the NJDEP baseline survey data (B), and the MDAT model outputs at local and regional scales (C). The scale for all maps is representative of relative spatial variation in the sites within the season for each information source.

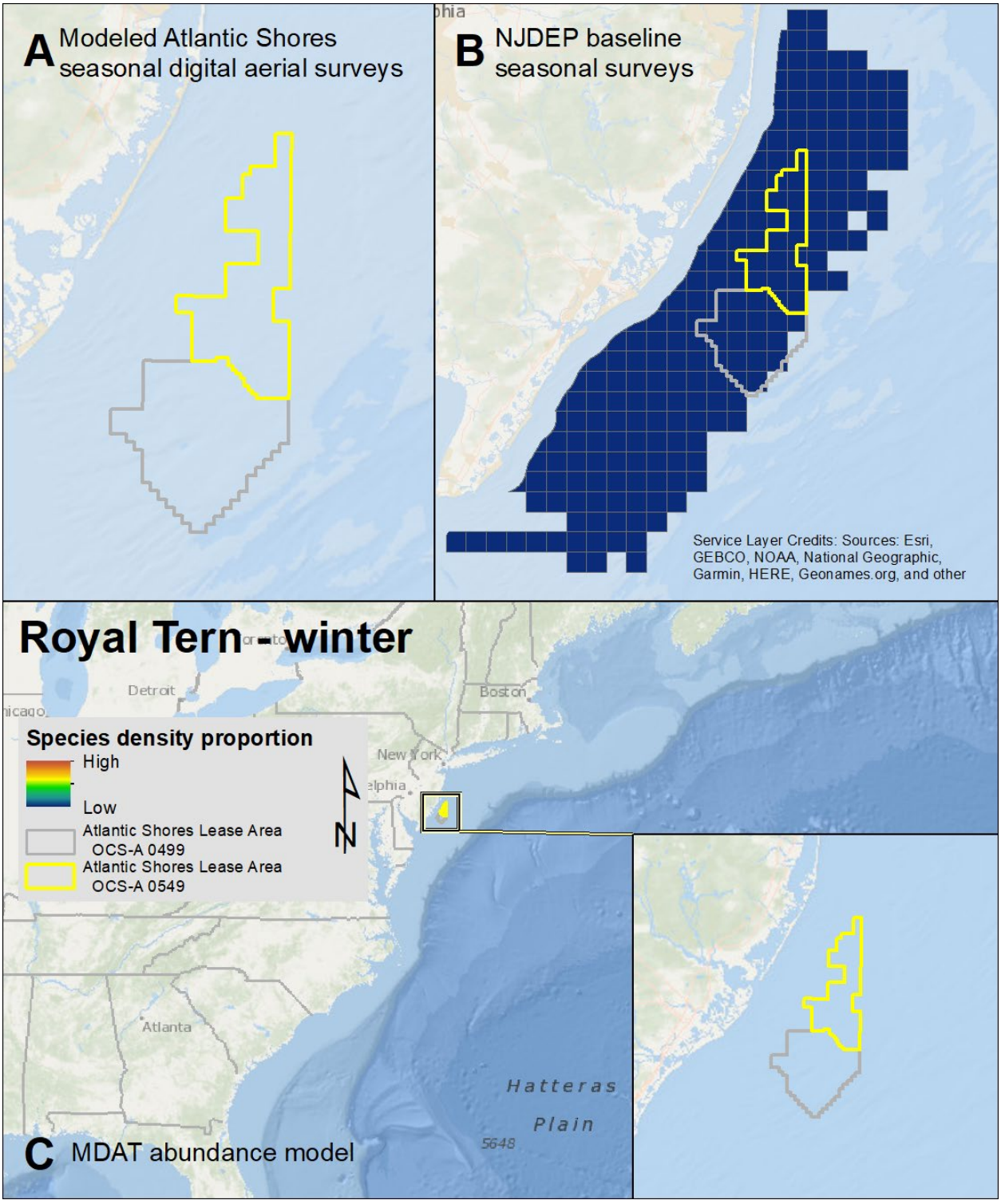

Map 148. Winter Royal Tern modeled density proportions in the Atlantic Shores seasonal digital aerial surveys (A), density proportions in the NJDEP baseline survey data (B), and the MDAT model outputs at local and regional scales (C). The scale for all maps is representative of relative spatial variation in the sites within the season for each information source.

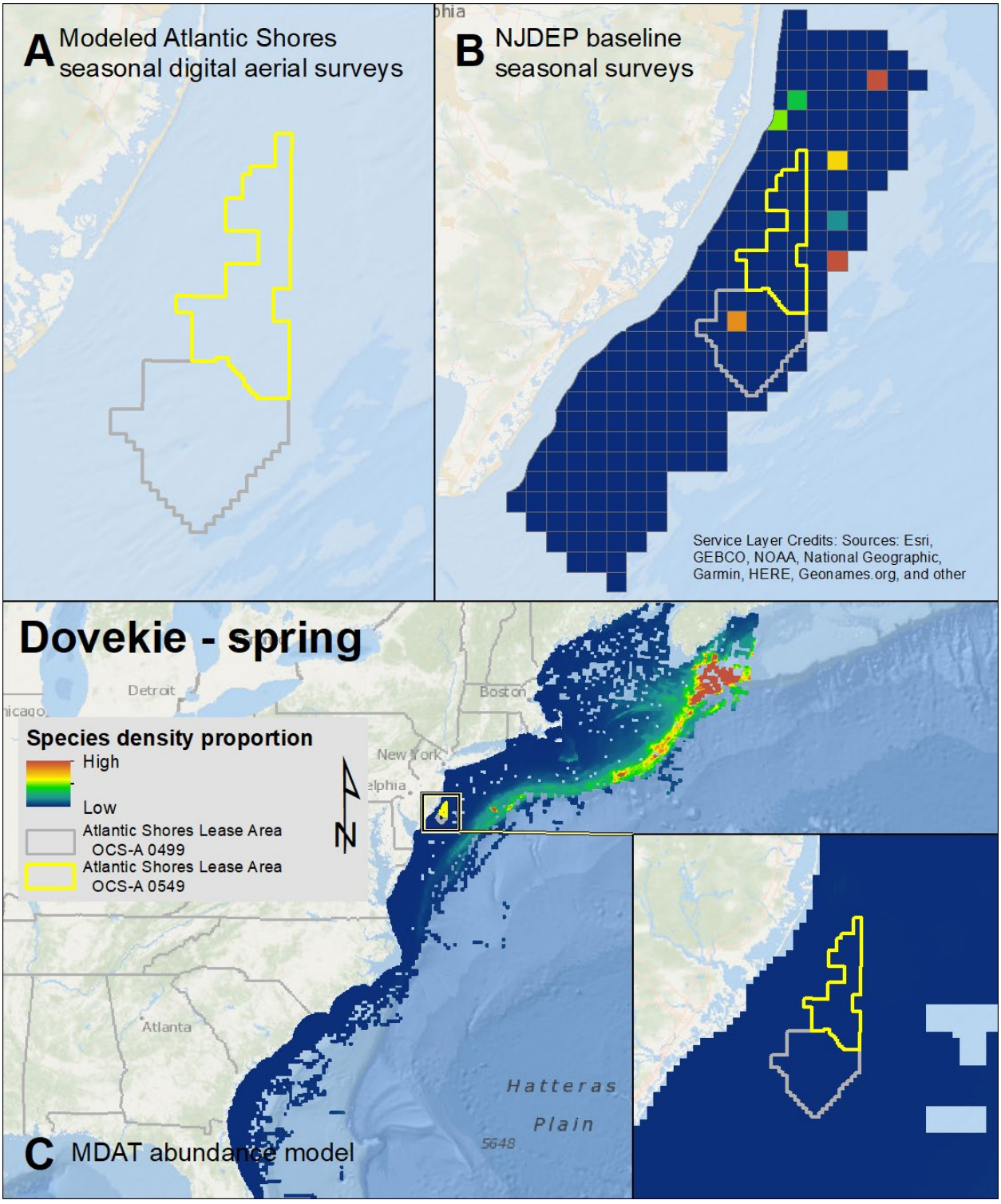

Map 149. Spring Dovekie modeled density proportions in the Atlantic Shores seasonal digital aerial surveys (A), density proportions in the NJDEP baseline survey data (B), and the MDAT model outputs at local and regional scales (C). The scale for all maps is representative of relative spatial variation in the sites within the season for each information source.

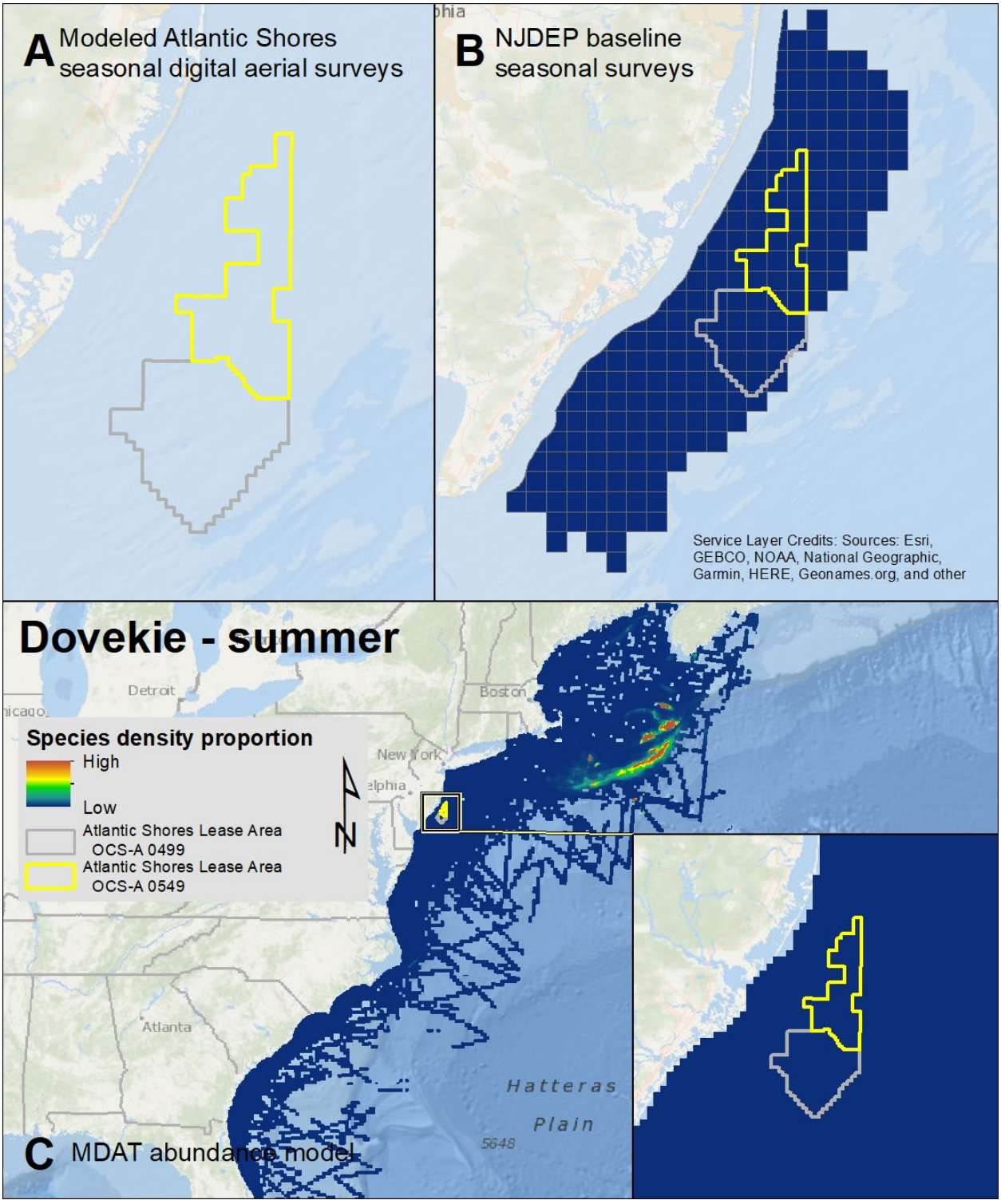

Map 150. Summer Dovekie modeled density proportions in the Atlantic Shores seasonal digital aerial surveys (A), density proportions in the NJDEP baseline survey data (B), and the MDAT model outputs at local and regional scales (C). The scale for all maps is representative of relative spatial variation in the sites within the season for each information source.

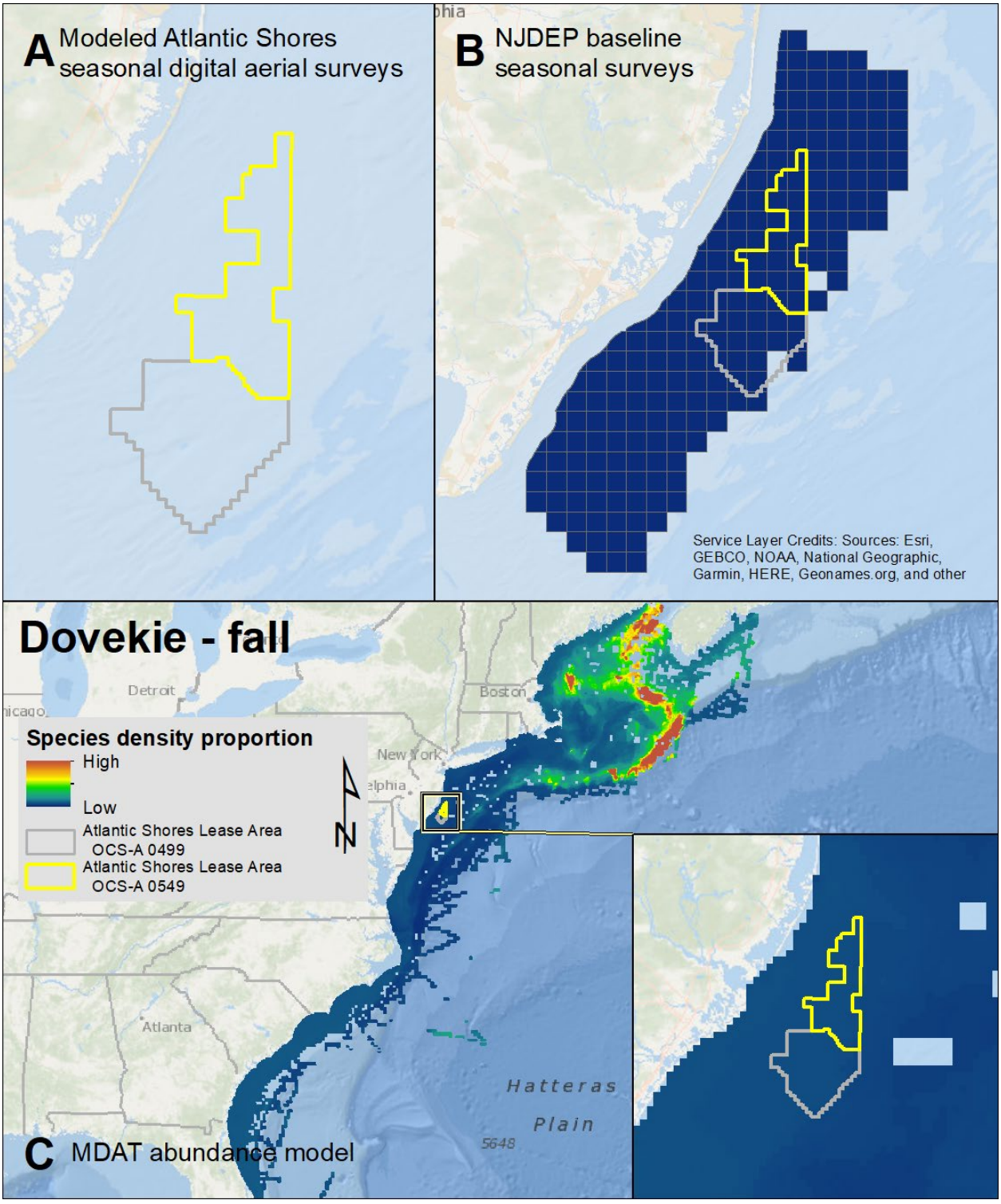

Map 151. Fall Dovekie modeled density proportions in the Atlantic Shores seasonal digital aerial surveys (A), density proportions in the NJDEP baseline survey data (B), and the MDAT model outputs at local and regional scales (C). The scale for all maps is representative of relative spatial variation in the sites within the season for each information source.

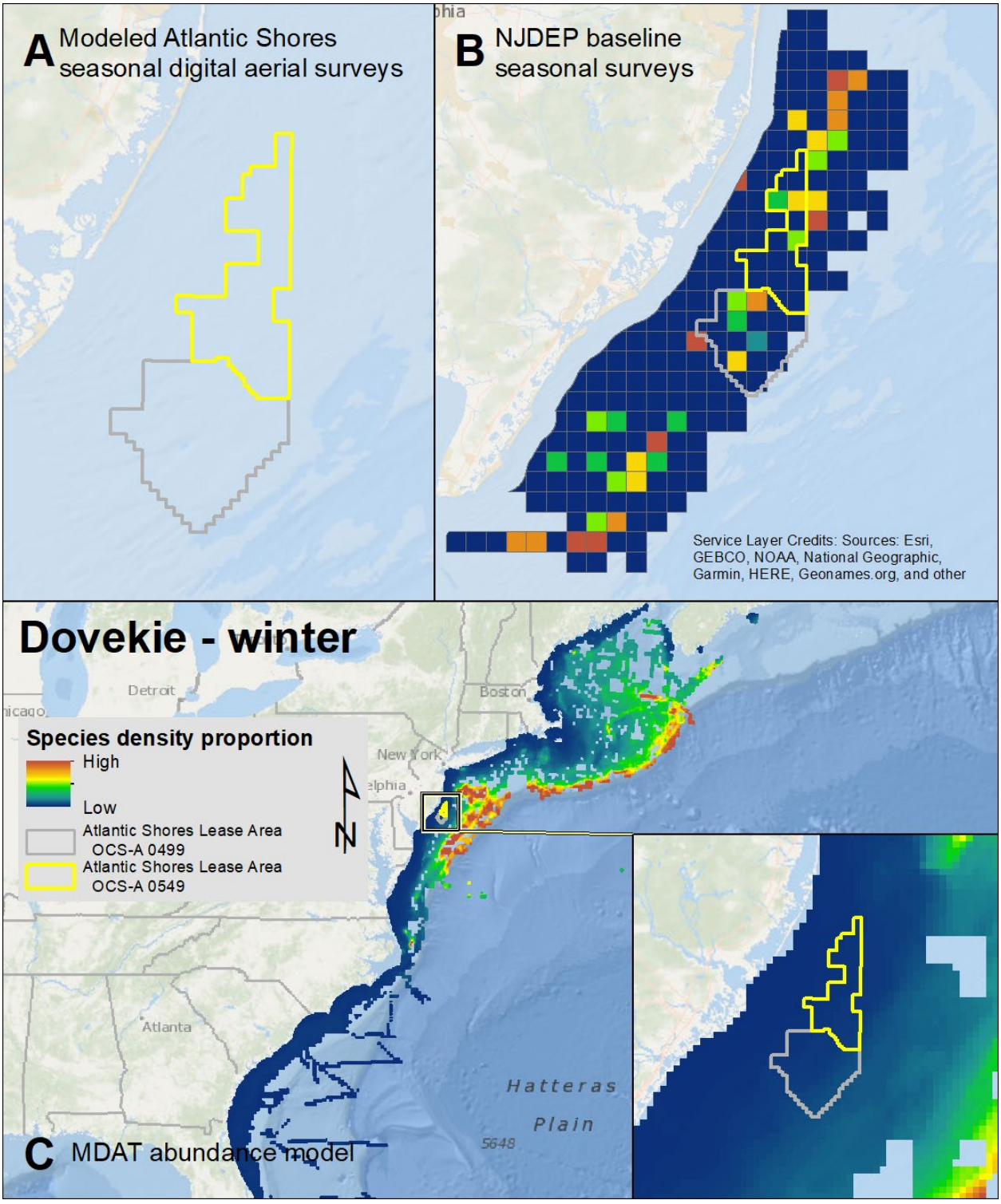

Map 152. Winter Dovekie modeled density proportions in the Atlantic Shores seasonal digital aerial surveys (A), density proportions in the NJDEP baseline survey data (B), and the MDAT model outputs at local and regional scales (C). The scale for all maps is representative of relative spatial variation in the sites within the season for each information source.

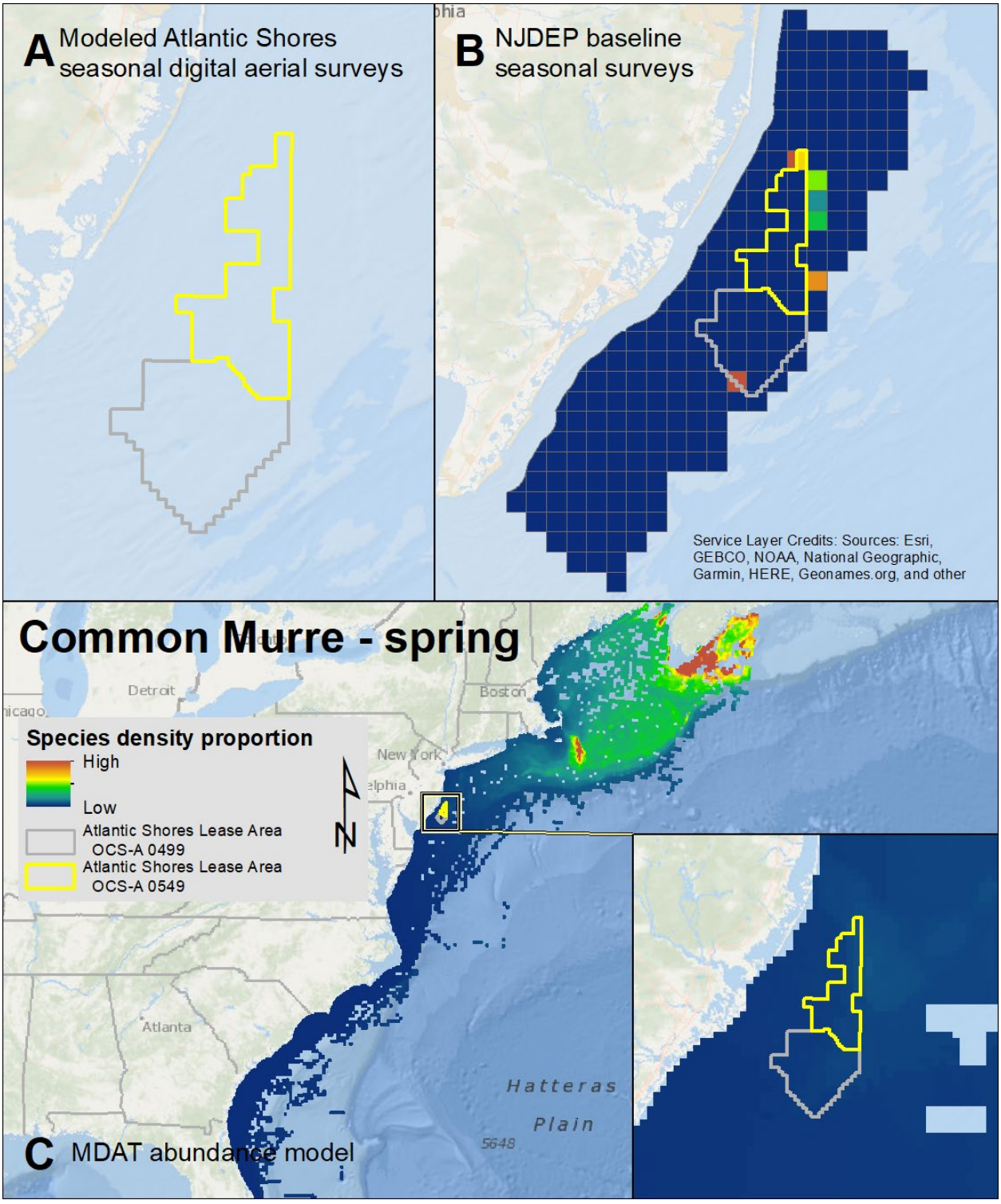

Map 153. Spring Common Murre modeled density proportions in the Atlantic Shores seasonal digital aerial surveys (A), density proportions in the NJDEP baseline survey data (B), and the MDAT model outputs at local and regional scales (C). The scale for all maps is representative of relative spatial variation in the sites within the season for each information source.

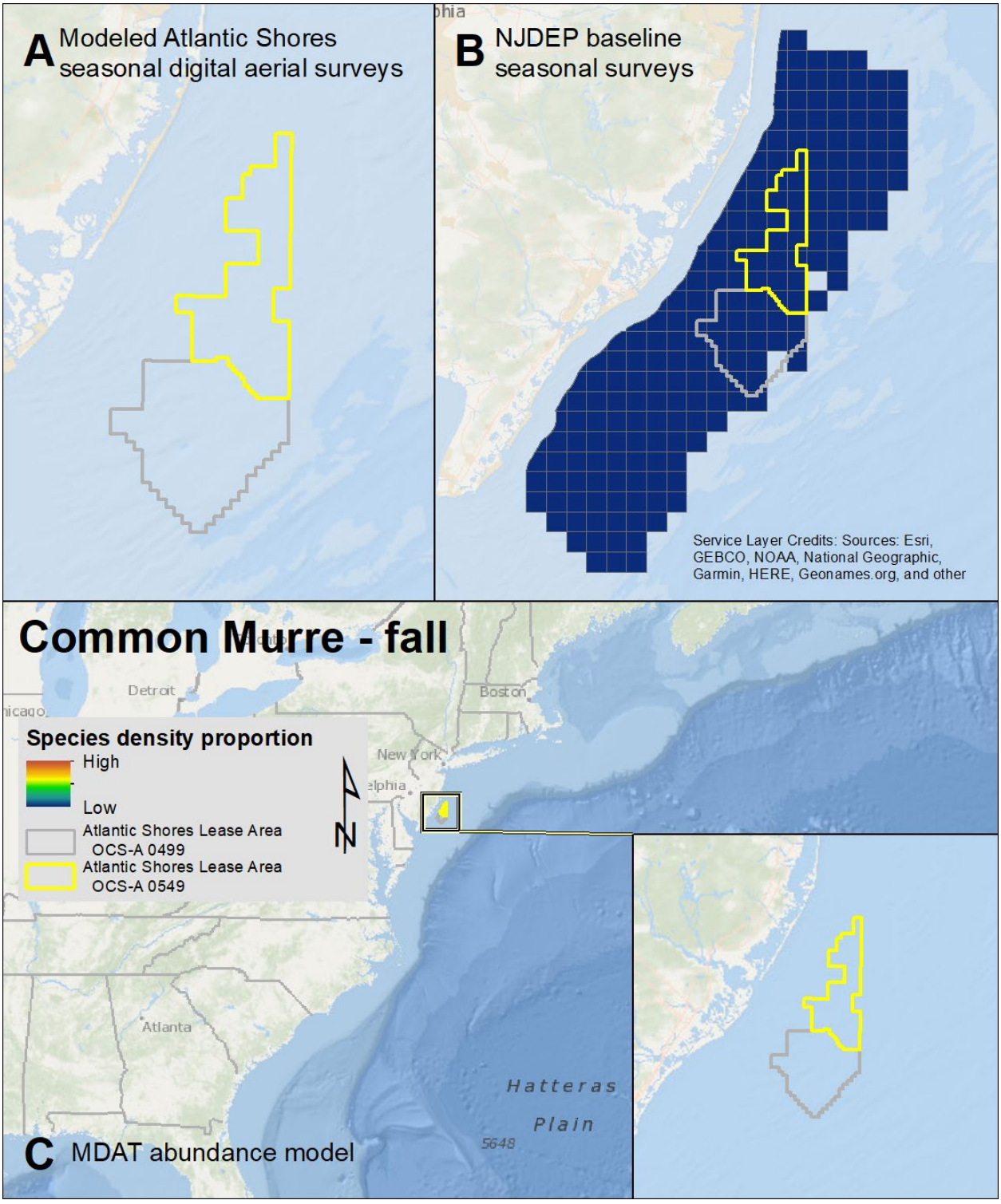

Map 154. Fall Common Murre modeled density proportions in the Atlantic Shores seasonal digital aerial surveys (A), density proportions in the NJDEP baseline survey data (B), and the MDAT model outputs at local and regional scales (C). The scale for all maps is representative of relative spatial variation in the sites within the season for each information source.

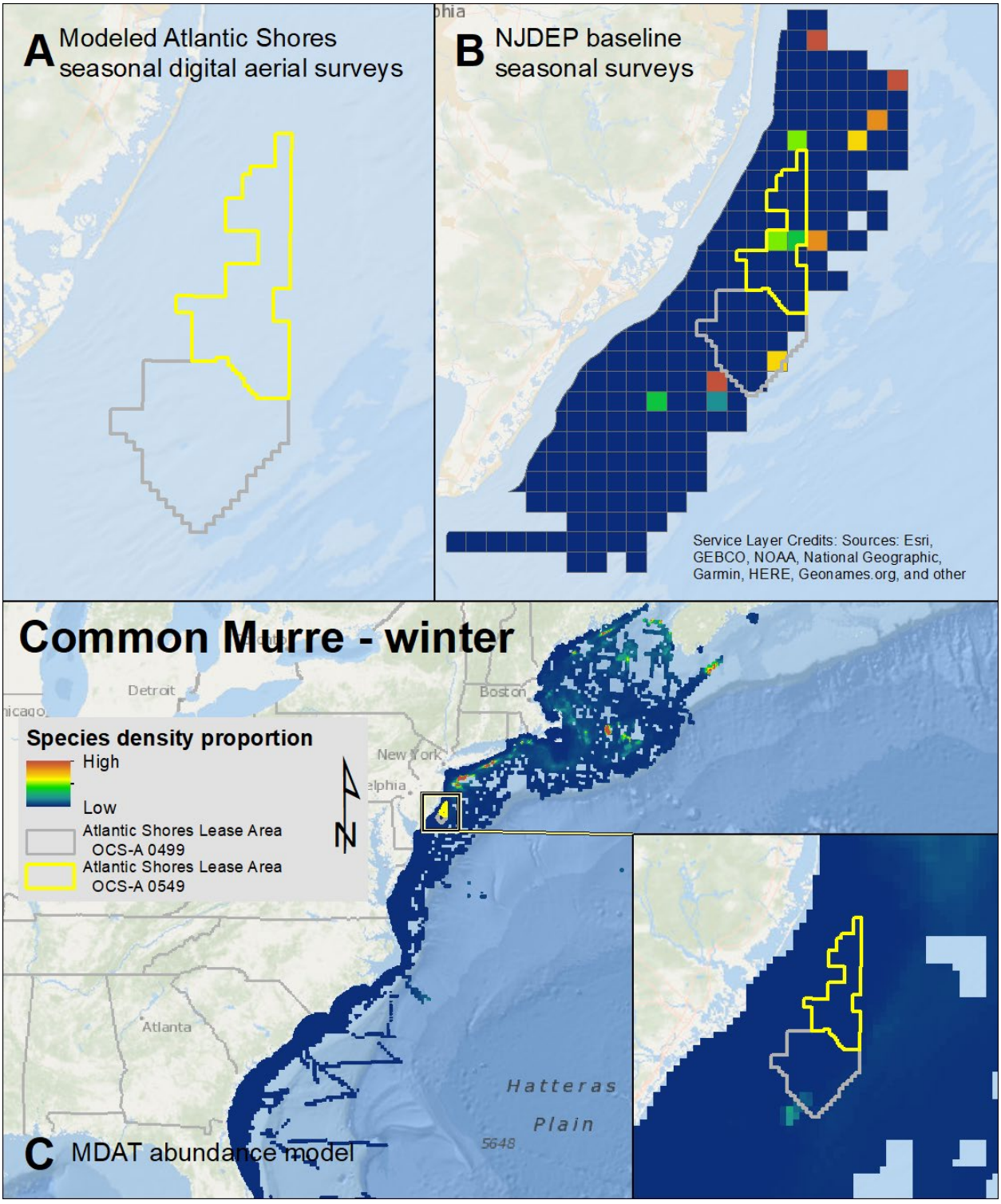

Map 155. Winter Common Murre modeled density proportions in the Atlantic Shores seasonal digital aerial surveys (A), density proportions in the NJDEP baseline survey data (B), and the MDAT model outputs at local and regional scales (C). The scale for all maps is representative of relative spatial variation in the sites within the season for each information source.

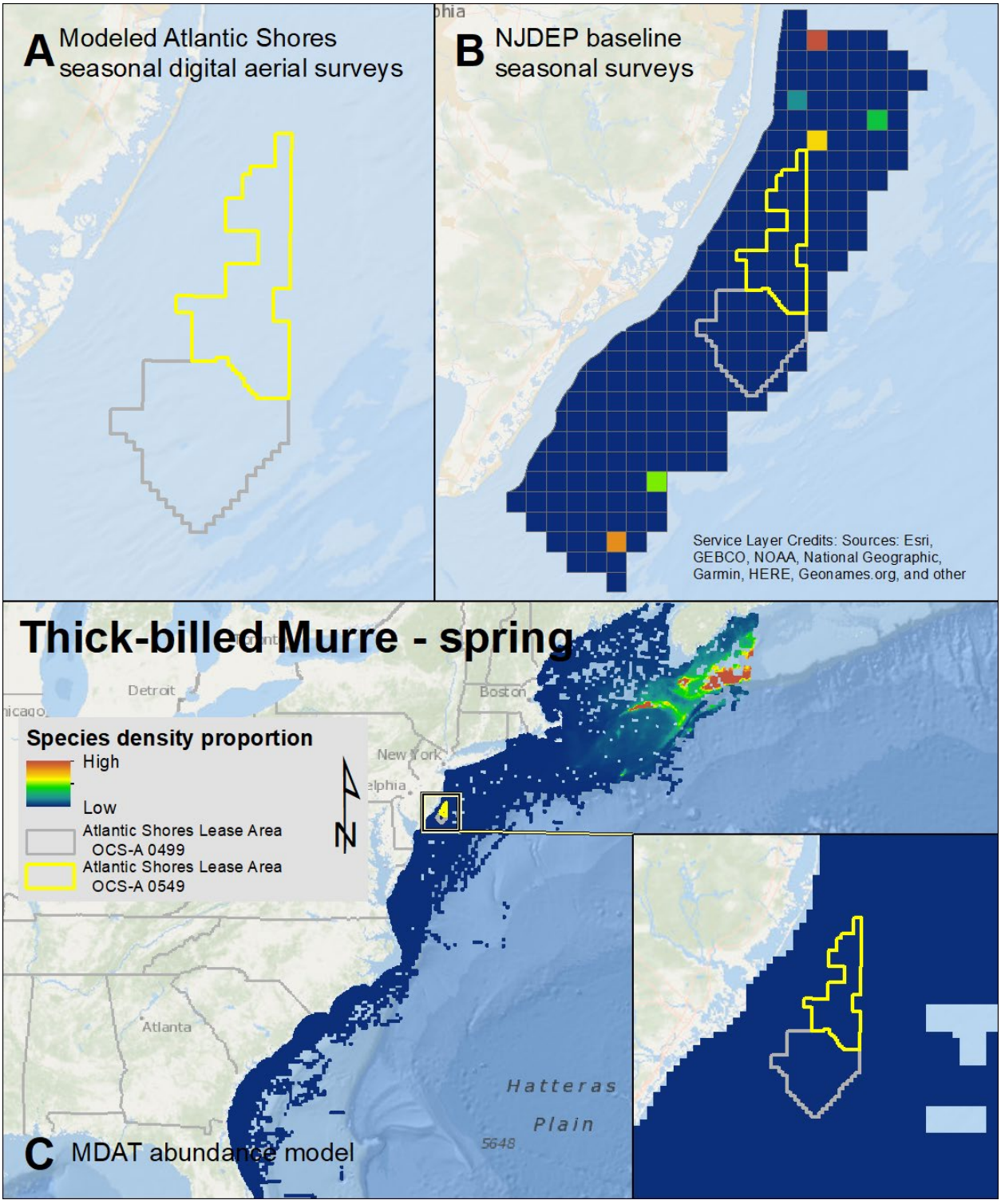

Map 156. Spring Thick-billed Murre modeled density proportions in the Atlantic Shores seasonal digital aerial surveys (A), density proportions in the NJDEP baseline survey data (B), and the MDAT model outputs at local and regional scales (C). The scale for all maps is representative of relative spatial variation in the sites within the season for each information source.

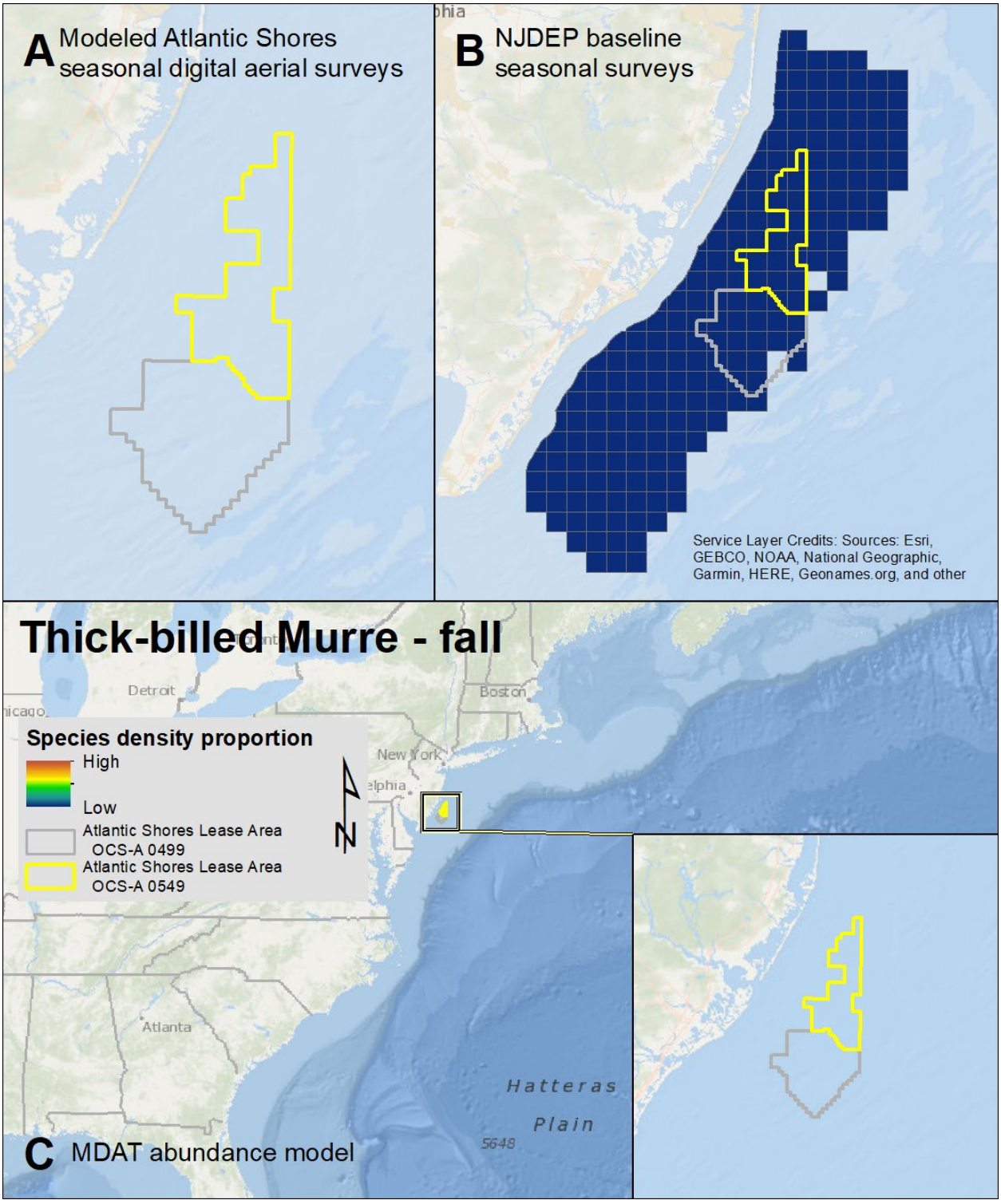

Map 157. Fall Thick-billed Murre modeled density proportions in the Atlantic Shores seasonal digital aerial surveys (A), density proportions in the NJDEP baseline survey data (B), and the MDAT model outputs at local and regional scales (C). The scale for all maps is representative of relative spatial variation in the sites within the season for each information source.

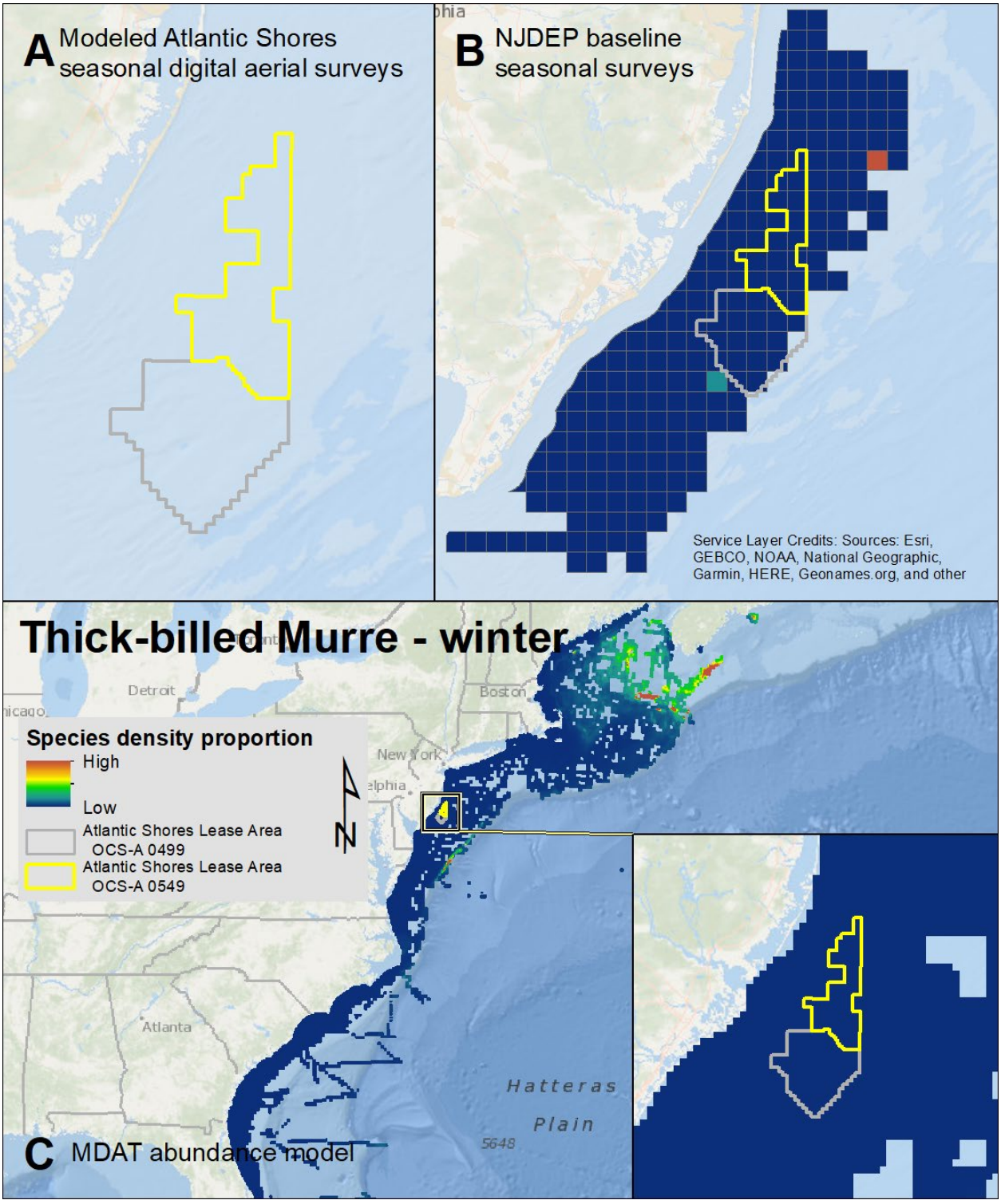

Map 158. Winter Thick-billed Murre modeled density proportions in the Atlantic Shores seasonal digital aerial surveys (A), density proportions in the NJDEP baseline survey data (B), and the MDAT model outputs at local and regional scales (C). The scale for all maps is representative of relative spatial variation in the sites within the season for each information source.

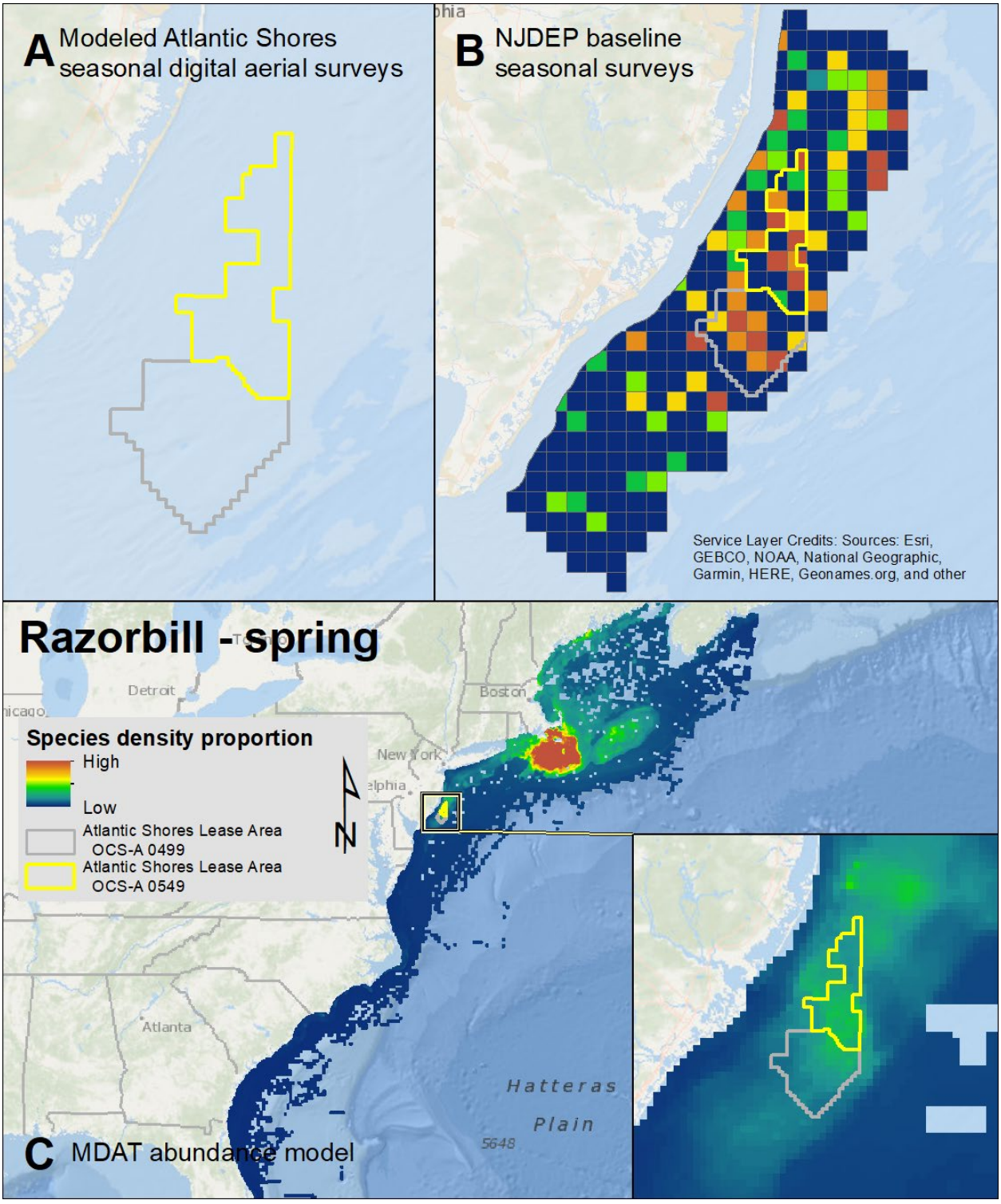

Map 159. Spring Razorbill modeled density proportions in the Atlantic Shores seasonal digital aerial surveys (A), density proportions in the NJDEP baseline survey data (B), and the MDAT model outputs at local and regional scales (C). The scale for all maps is representative of relative spatial variation in the sites within the season for each information source.

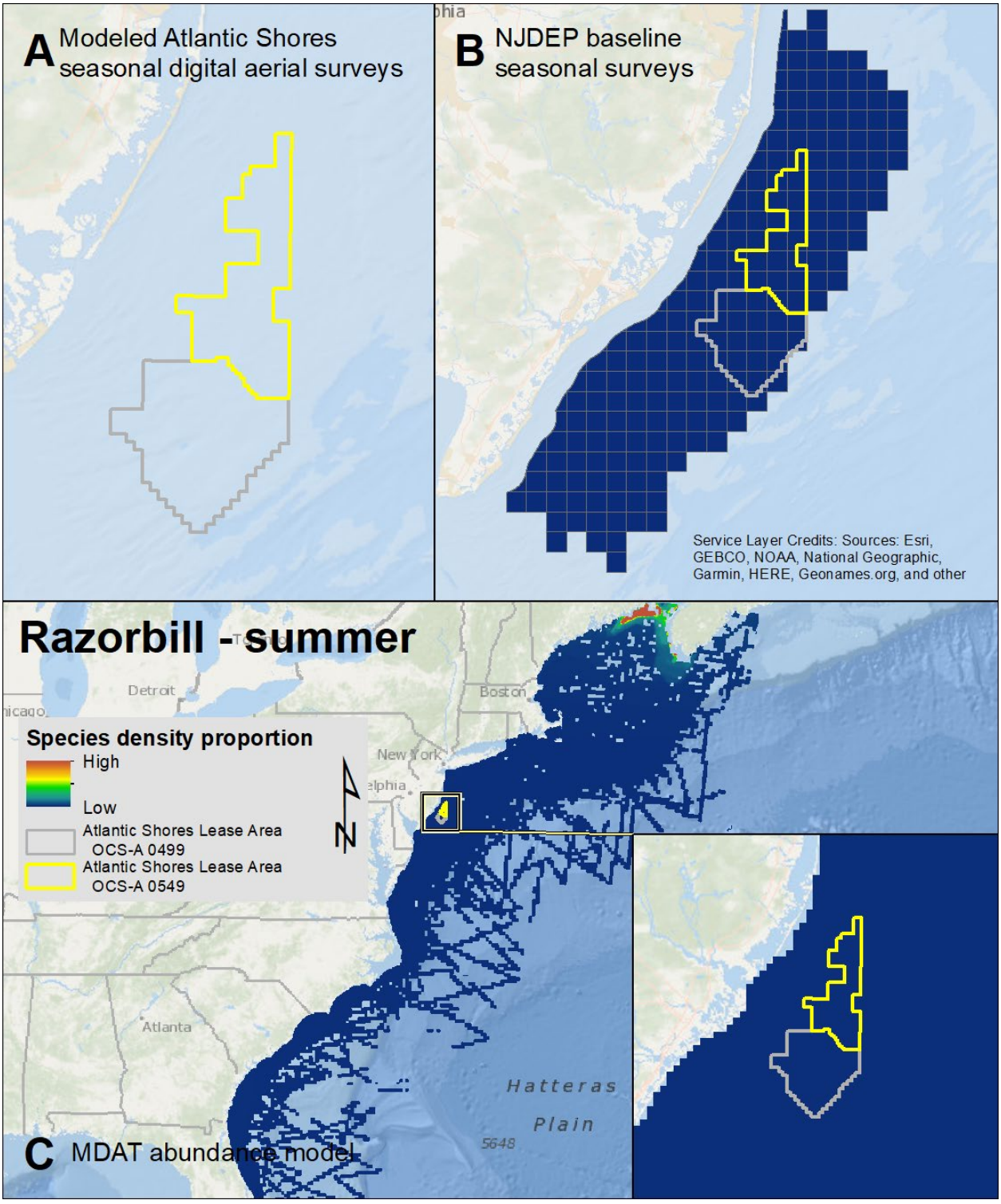

Map 160. Summer Razorbill modeled density proportions in the Atlantic Shores seasonal digital aerial surveys (A), density proportions in the NJDEP baseline survey data (B), and the MDAT model outputs at local and regional scales (C). The scale for all maps is representative of relative spatial variation in the sites within the season for each information source.

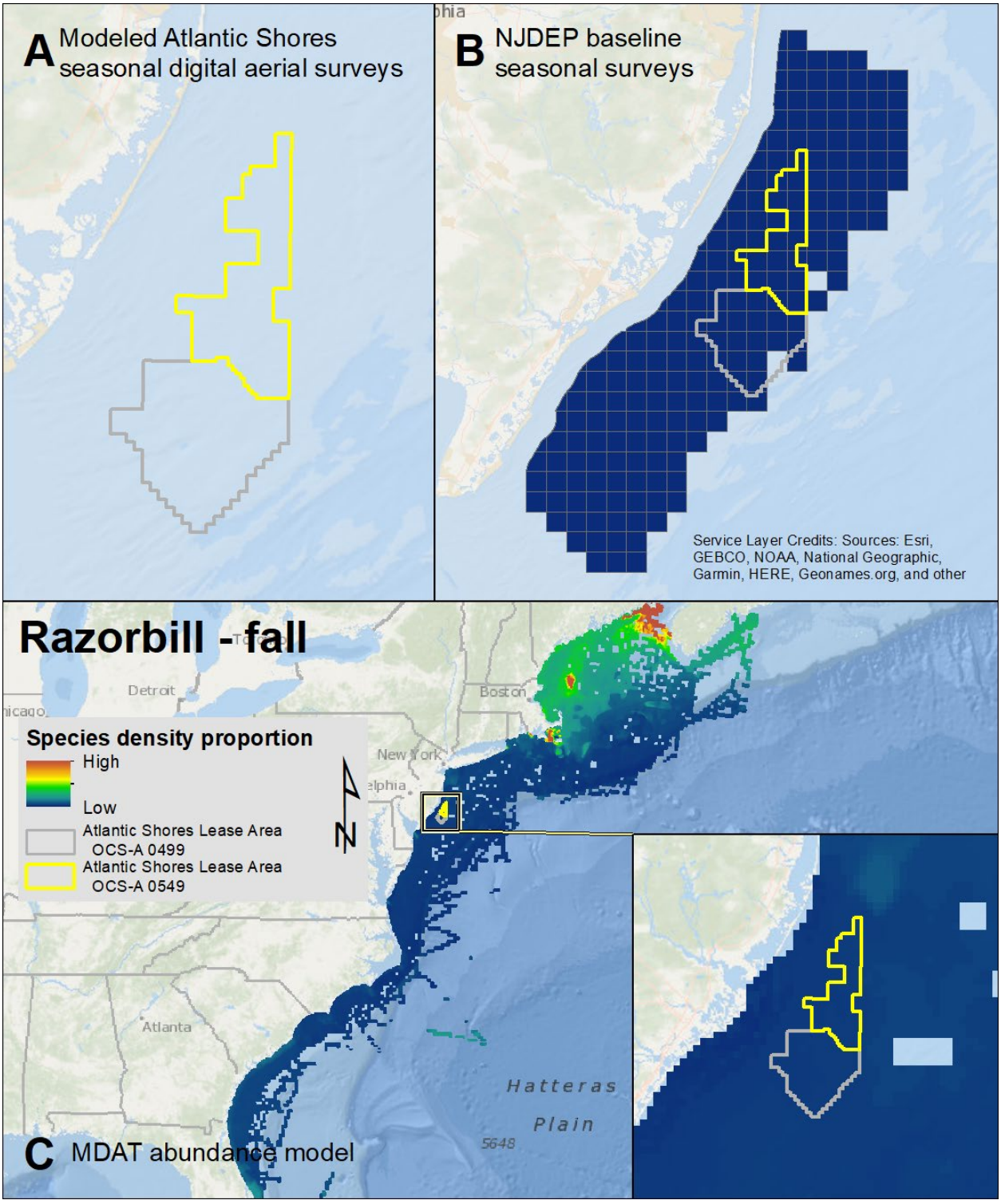

Map 161. Fall Razorbill modeled density proportions in the Atlantic Shores seasonal digital aerial surveys (A), density proportions in the NJDEP baseline survey data (B), and the MDAT model outputs at local and regional scales (C). The scale for all maps is representative of relative spatial variation in the sites within the season for each information source.

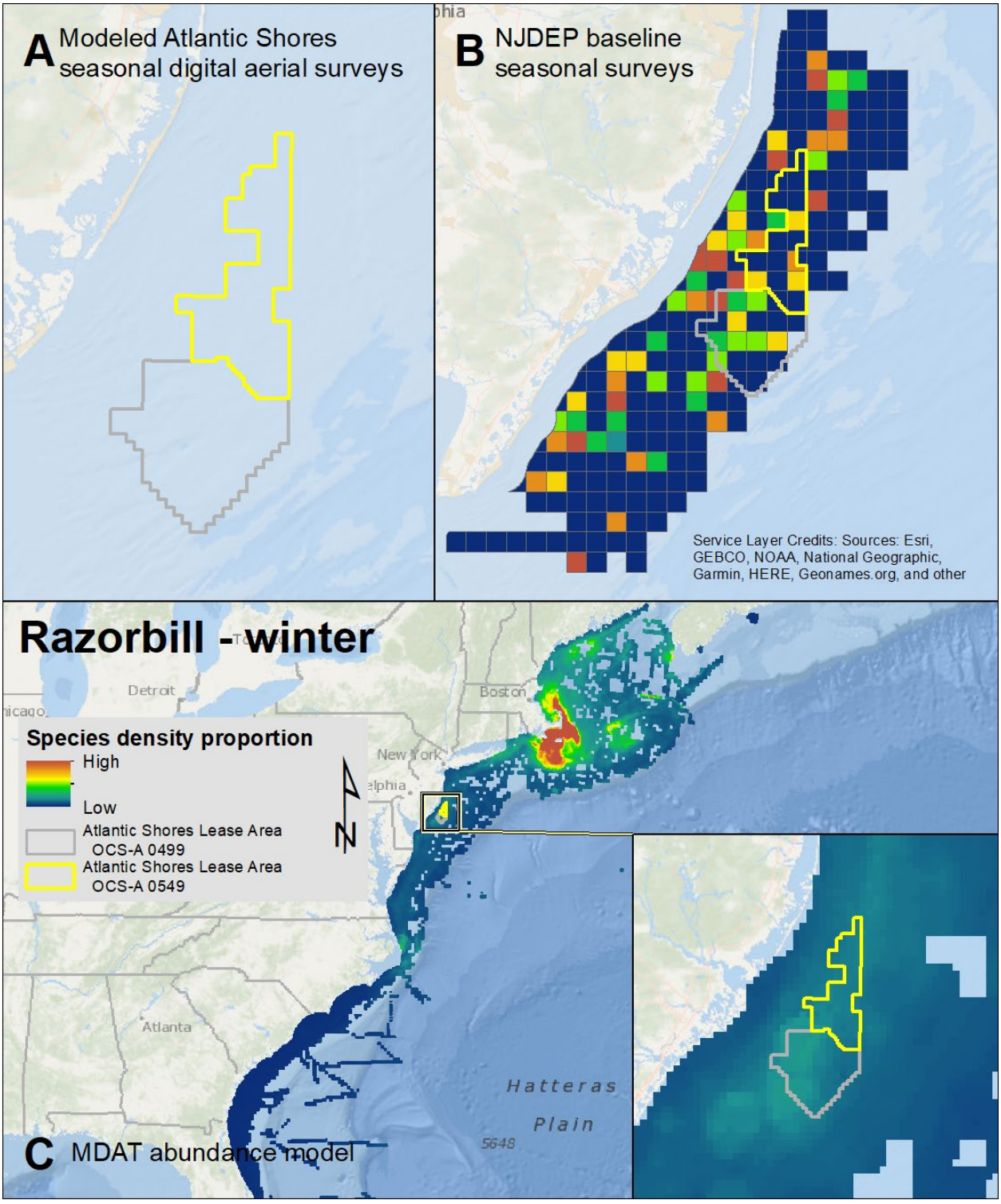

Map 162. Winter Razorbill modeled density proportions in the Atlantic Shores seasonal digital aerial surveys (A), density proportions in the NJDEP baseline survey data (B), and the MDAT model outputs at local and regional scales (C). The scale for all maps is representative of relative spatial variation in the sites within the season for each information source.

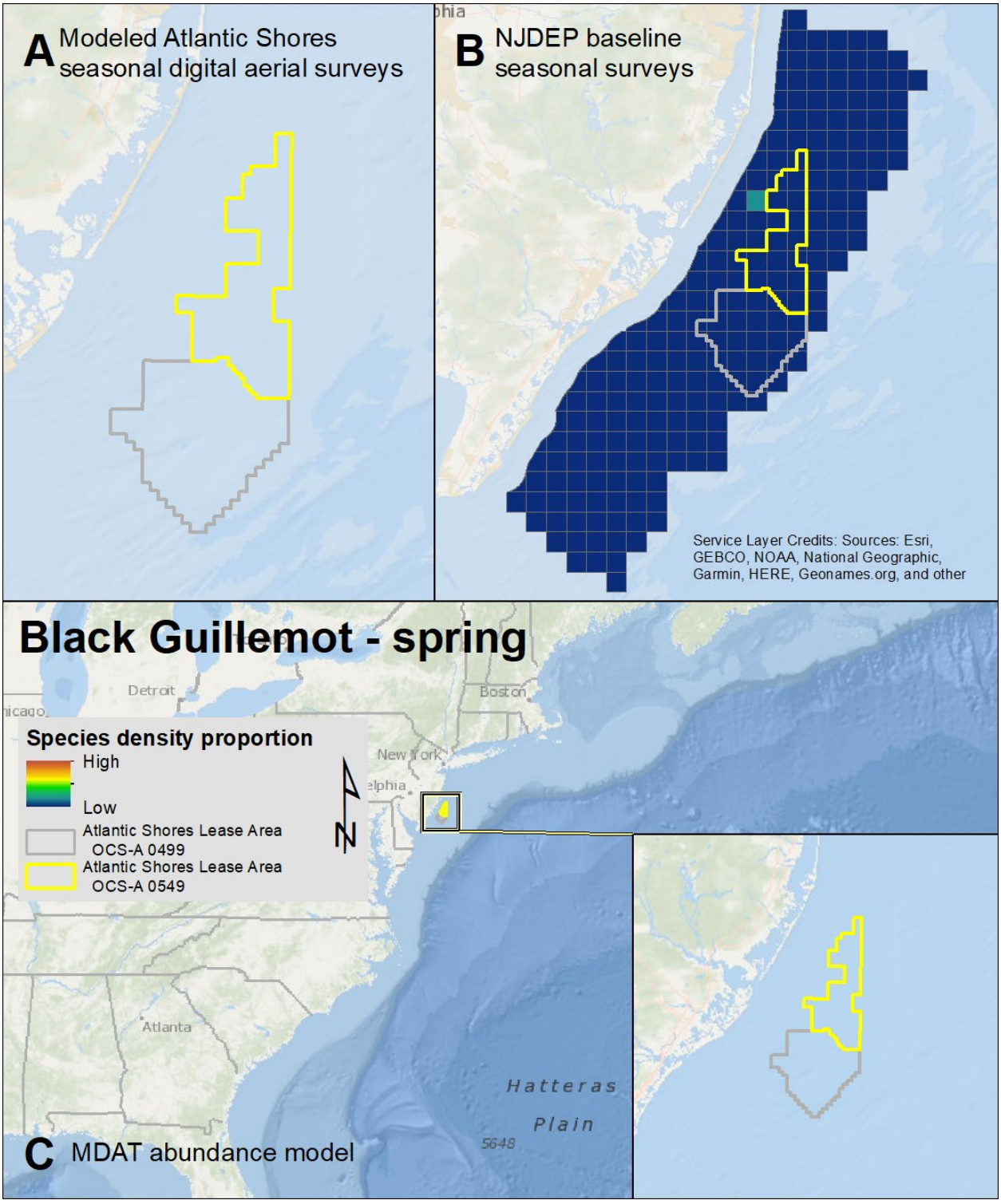

Map 163. Spring Black Guillemot modeled density proportions in the Atlantic Shores seasonal digital aerial surveys (A), density proportions in the NJDEP baseline survey data (B), and the MDAT model outputs at local and regional scales (C). The scale for all maps is representative of relative spatial variation in the sites within the season for each information source.

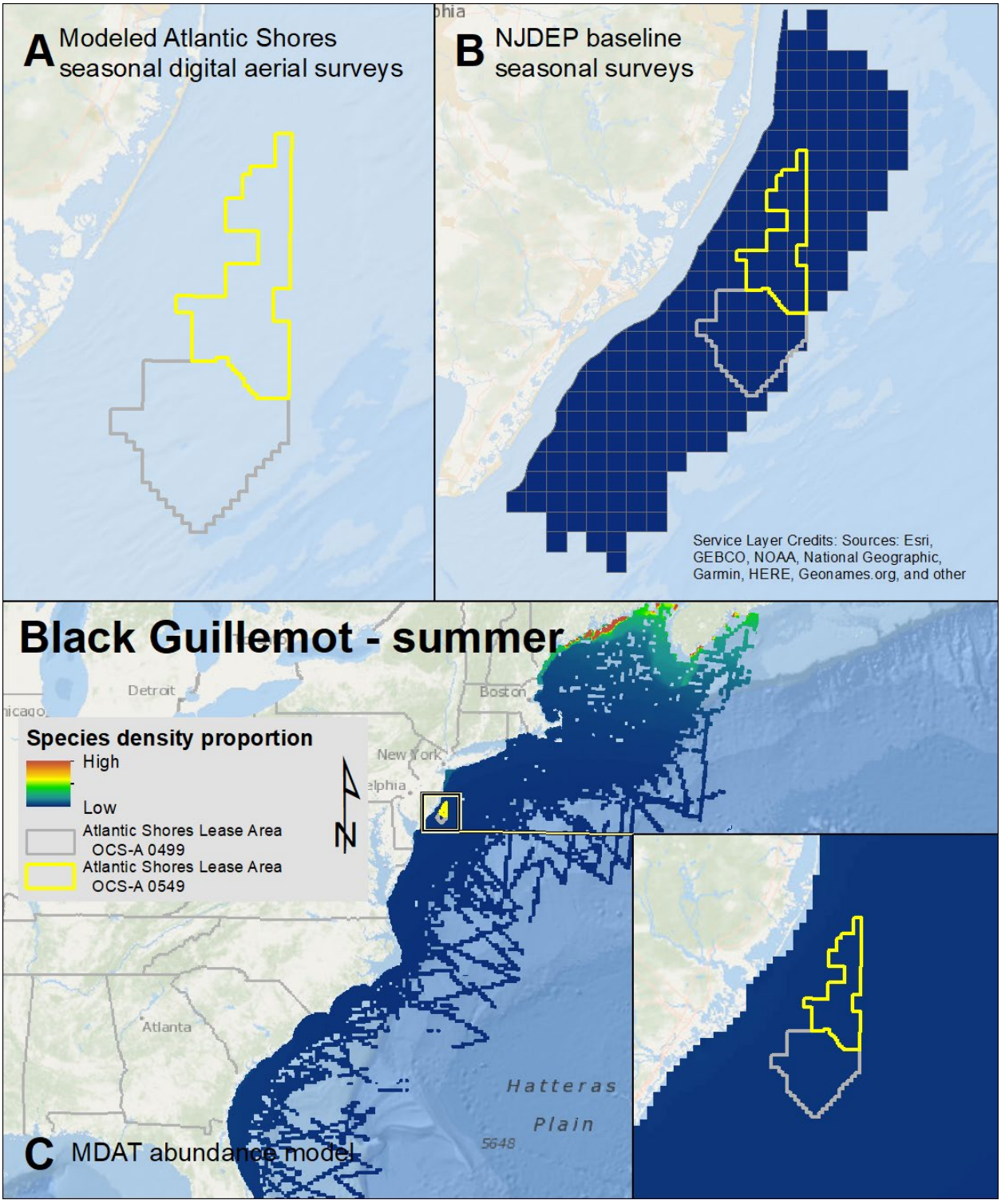

Map 164. Summer Black Guillemot modeled density proportions in the Atlantic Shores seasonal digital aerial surveys (A), density proportions in the NJDEP baseline survey data (B), and the MDAT model outputs at local and regional scales (C). The scale for all maps is representative of relative spatial variation in the sites within the season for each information source.

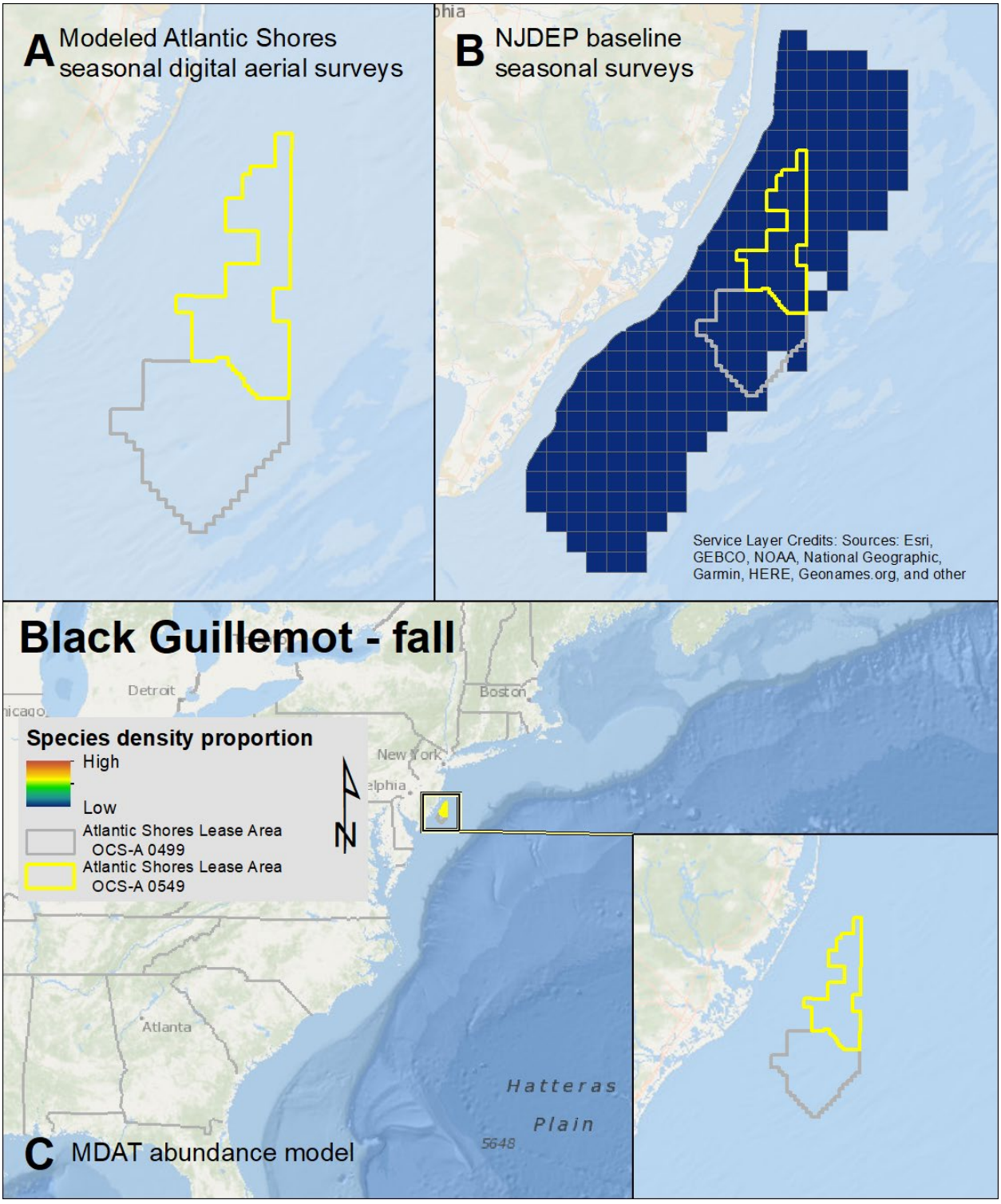

Map 165. Fall Black Guillemot modeled density proportions in the Atlantic Shores seasonal digital aerial surveys (A), density proportions in the NJDEP baseline survey data (B), and the MDAT model outputs at local and regional scales (C). The scale for all maps is representative of relative spatial variation in the sites within the season for each information source.

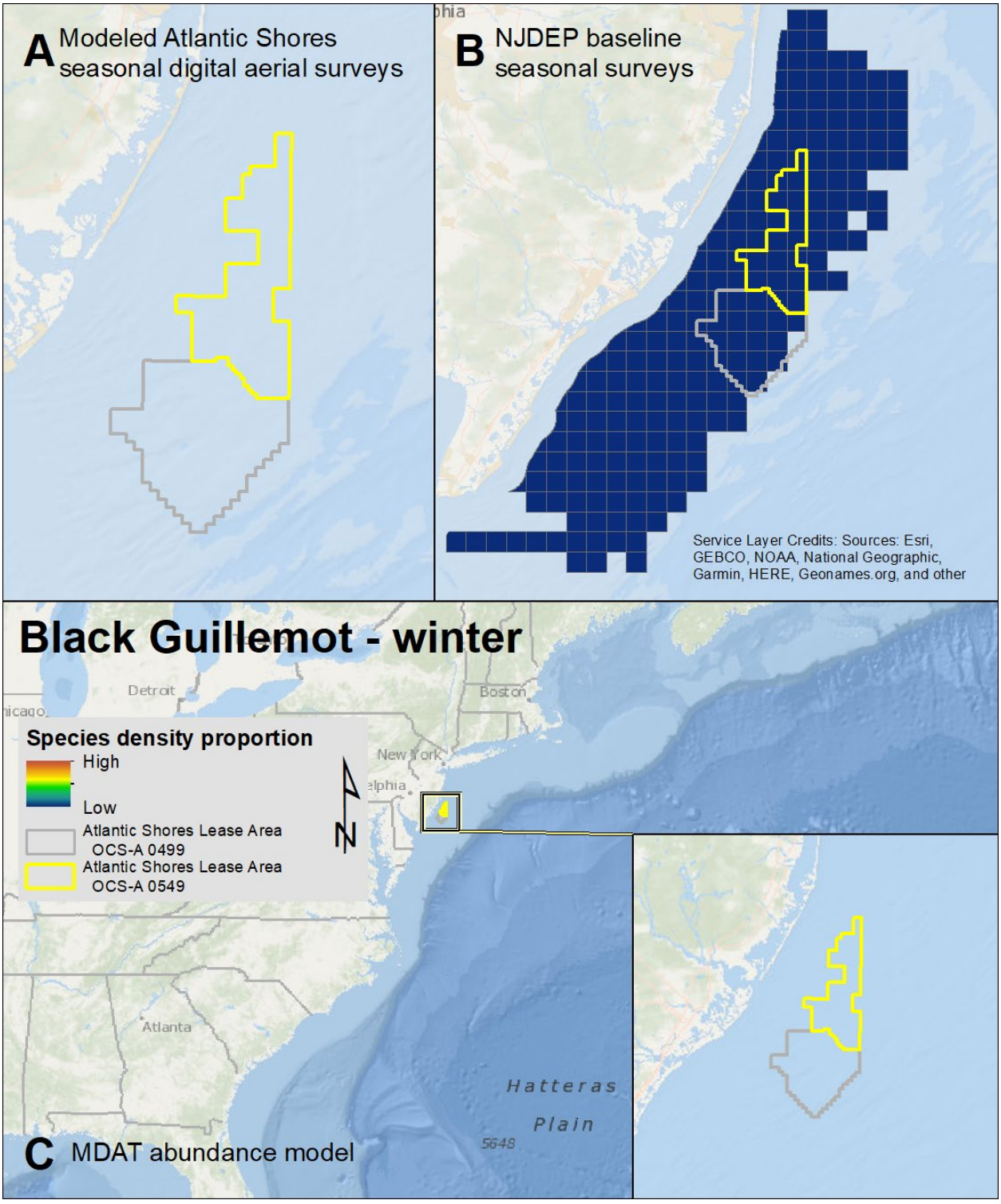

Map 166. Winter Black Guillemot modeled density proportions in the Atlantic Shores seasonal digital aerial surveys (A), density proportions in the NJDEP baseline survey data (B), and the MDAT model outputs at local and regional scales (C). The scale for all maps is representative of relative spatial variation in the sites within the season for each information source.

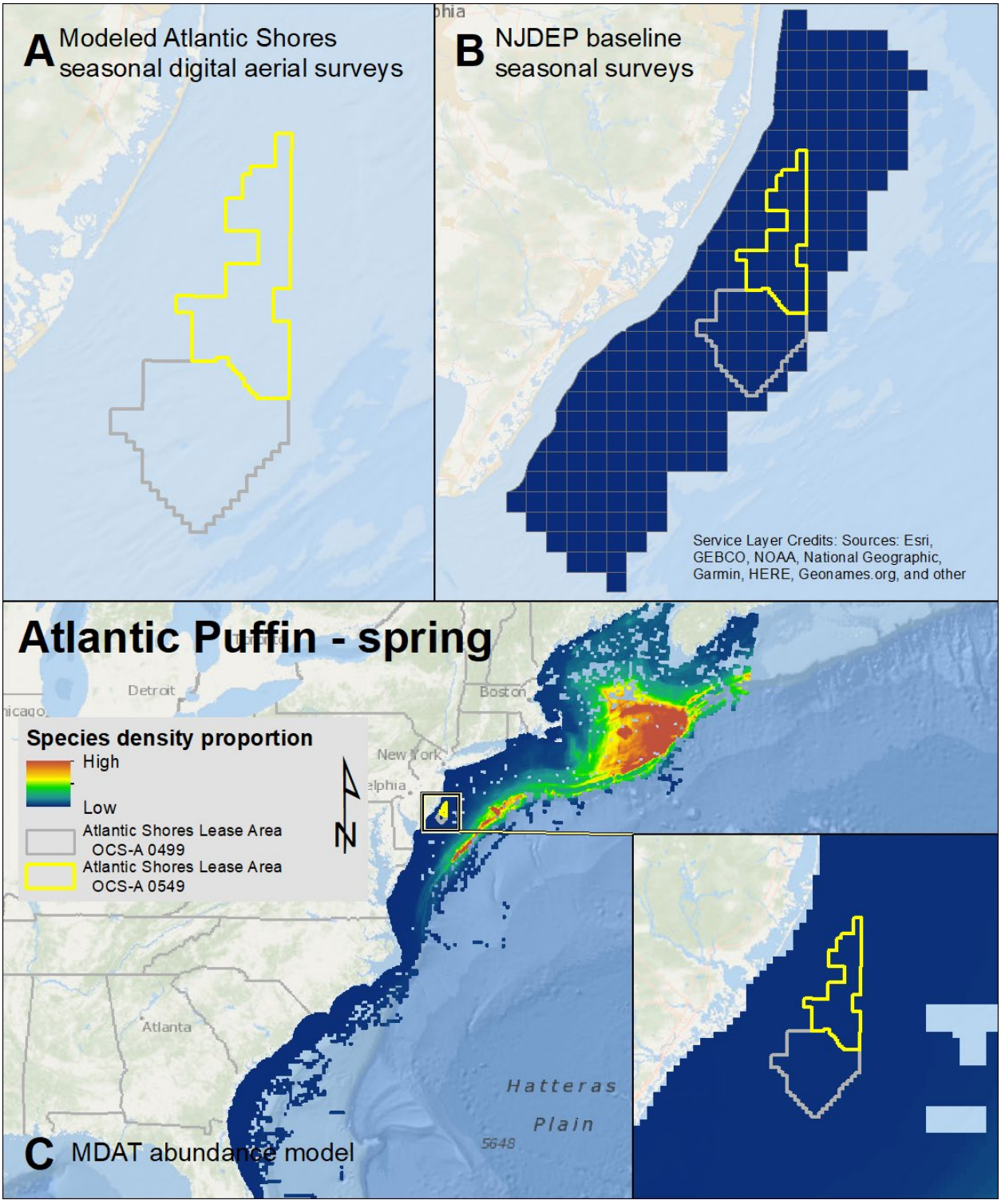

Map 167. Spring Atlantic Puffin modeled density proportions in the Atlantic Shores seasonal digital aerial surveys (A), density proportions in the NJDEP baseline survey data (B), and the MDAT model outputs at local and regional scales (C). The scale for all maps is representative of relative spatial variation in the sites within the season for each information source.

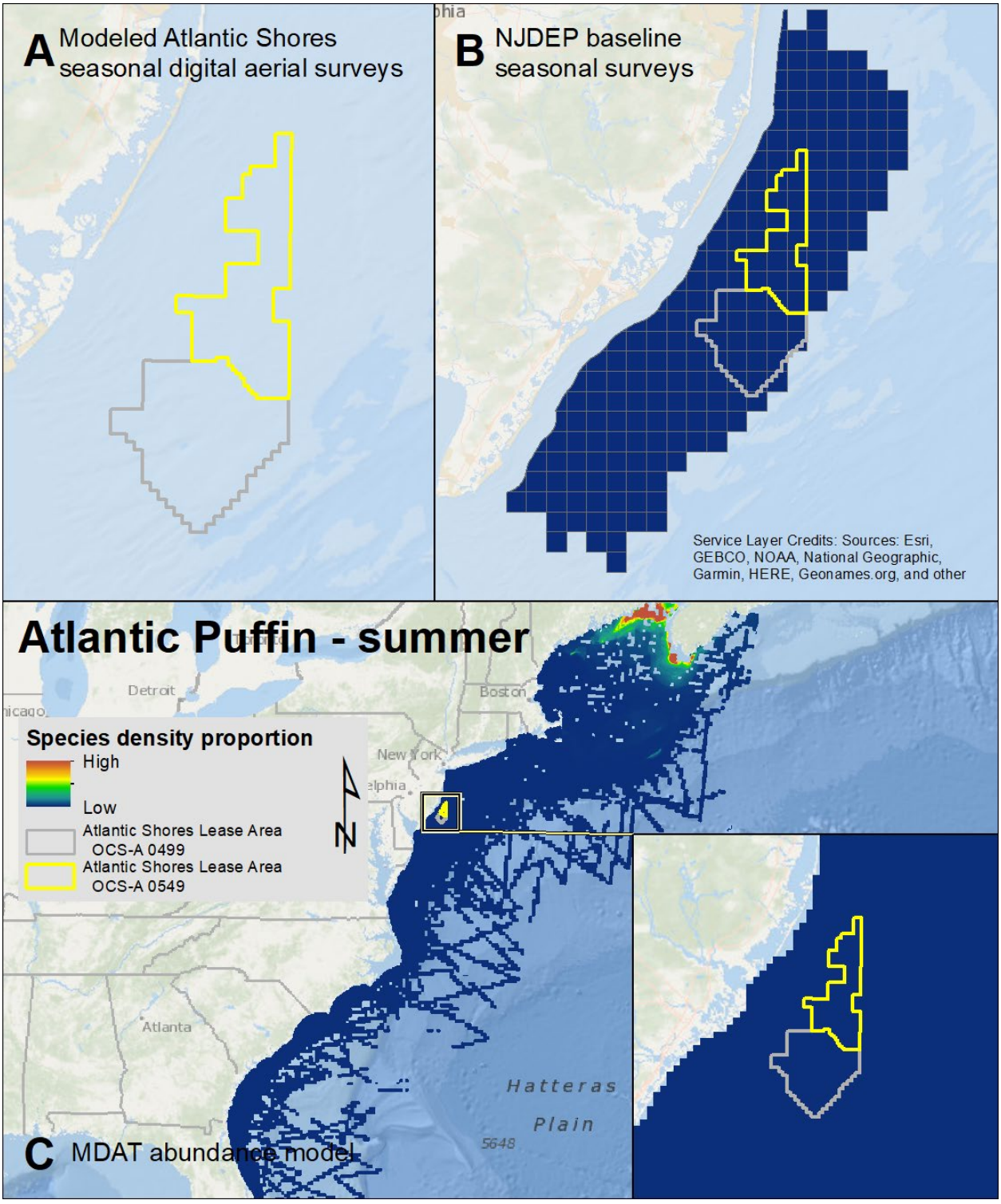

Map 168. Summer Atlantic Puffin modeled density proportions in the Atlantic Shores seasonal digital aerial surveys (A), density proportions in the NJDEP baseline survey data (B), and the MDAT model outputs at local and regional scales (C). The scale for all maps is representative of relative spatial variation in the sites within the season for each information source.

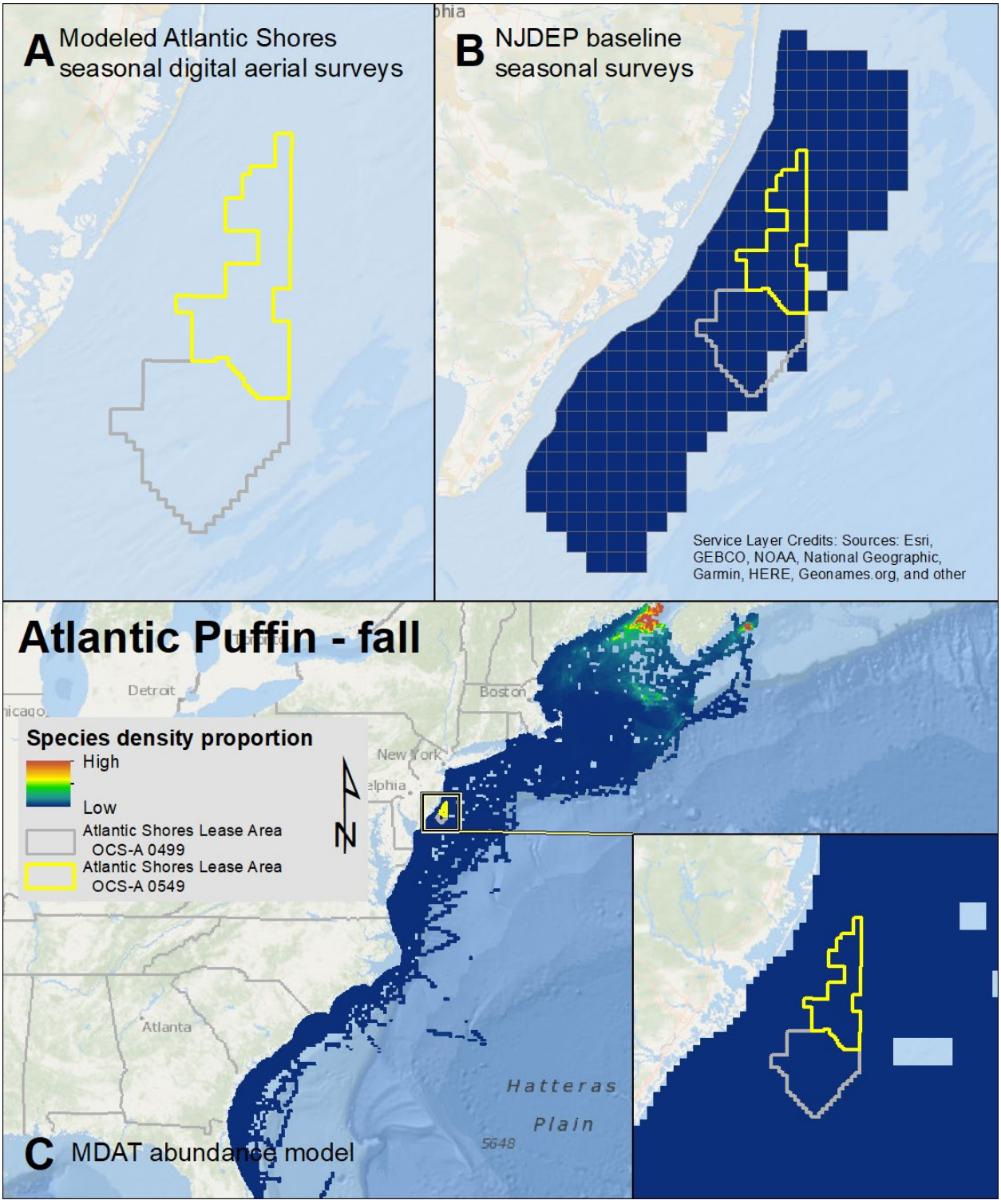

Map 169. Fall Atlantic Puffin modeled density proportions in the Atlantic Shores seasonal digital aerial surveys (A), density proportions in the NJDEP baseline survey data (B), and the MDAT model outputs at local and regional scales (C). The scale for all maps is representative of relative spatial variation in the sites within the season for each information source.

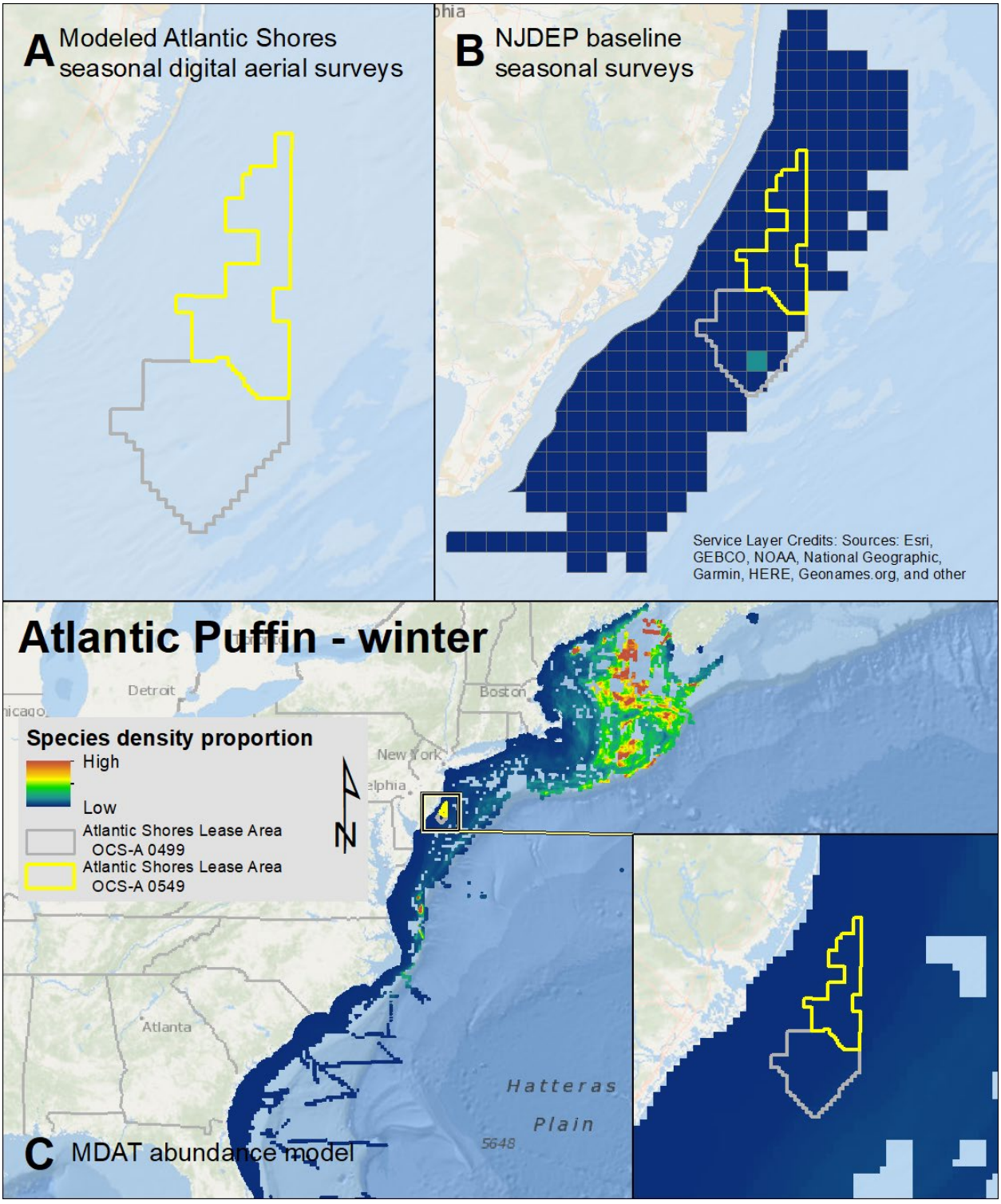

Map 170. Winter Atlantic Puffin modeled density proportions in the Atlantic Shores seasonal digital aerial surveys (A), density proportions in the NJDEP baseline survey data (B), and the MDAT model outputs at local and regional scales (C). The scale for all maps is representative of relative spatial variation in the sites within the season for each information source.

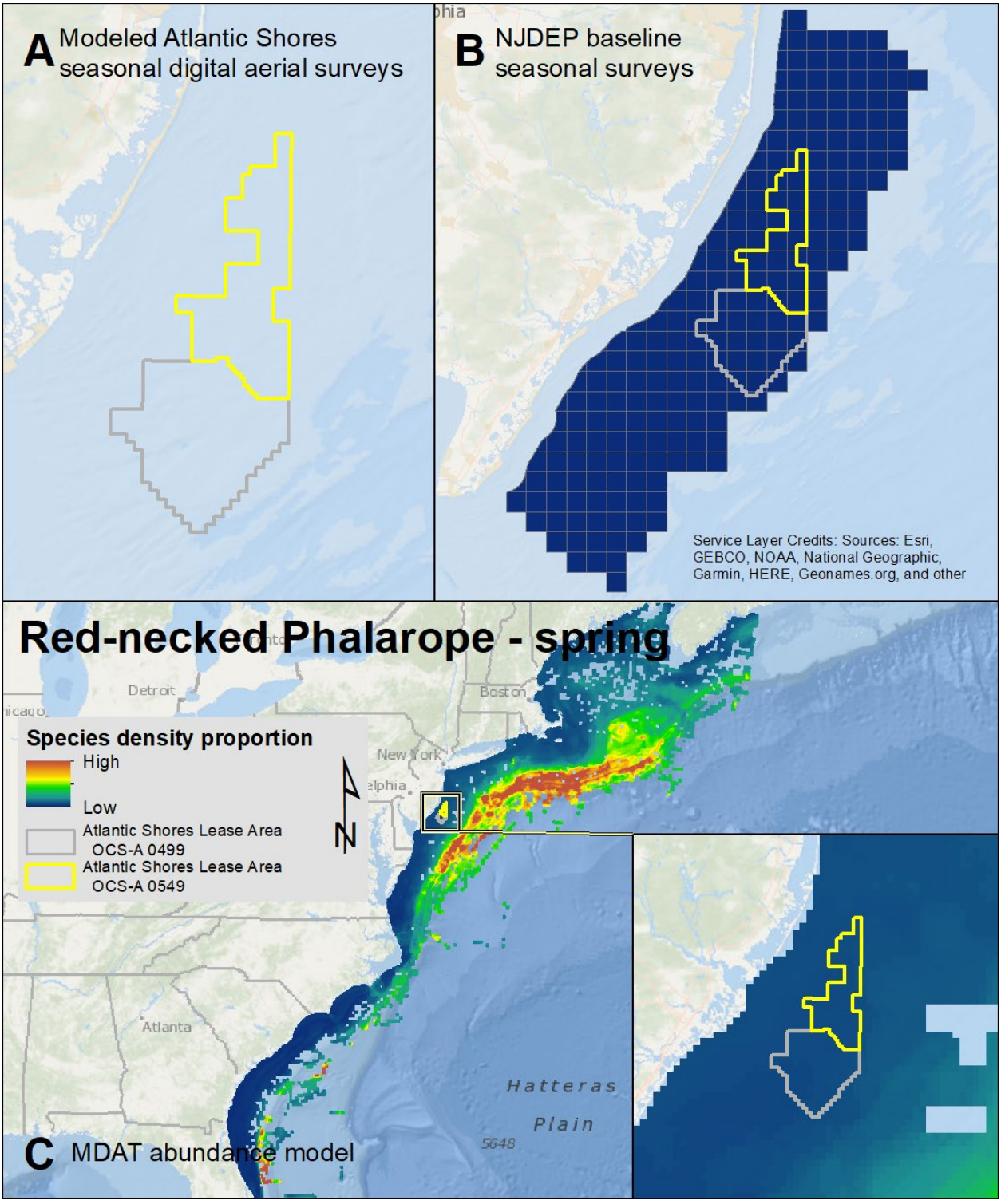

Map 171. Spring Red-necked Phalarope modeled density proportions in the Atlantic Shores seasonal digital aerial surveys (A), density proportions in the NJDEP baseline survey data (B), and the MDAT model outputs at local and regional scales (C). The scale for all maps is representative of relative spatial variation in the sites within the season for each information source.

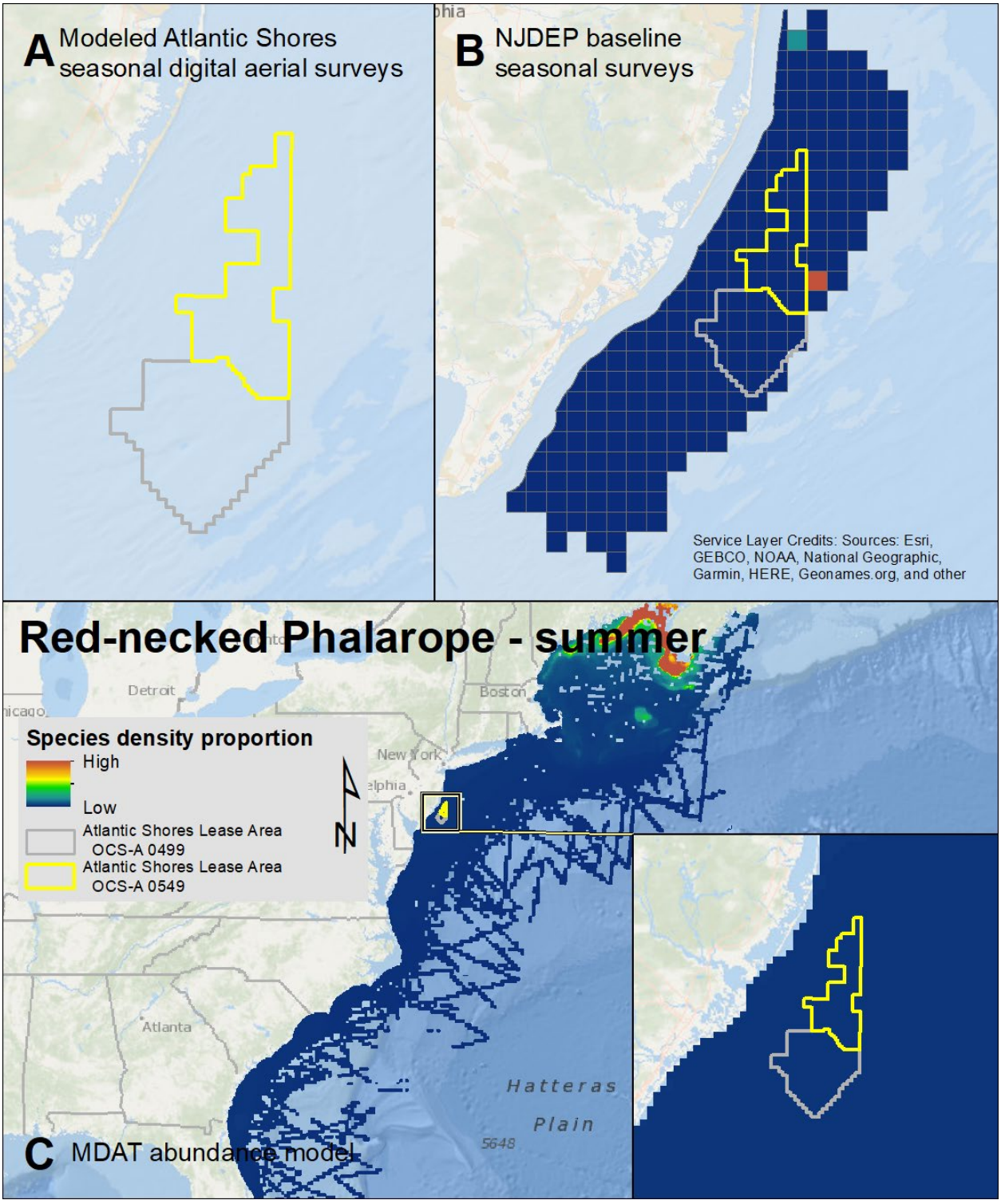

Map 172. Summer Red-necked Phalarope modeled density proportions in the Atlantic Shores seasonal digital aerial surveys (A), density proportions in the NJDEP baseline survey data (B), and the MDAT model outputs at local and regional scales (C). The scale for all maps is representative of relative spatial variation in the sites within the season for each information source.

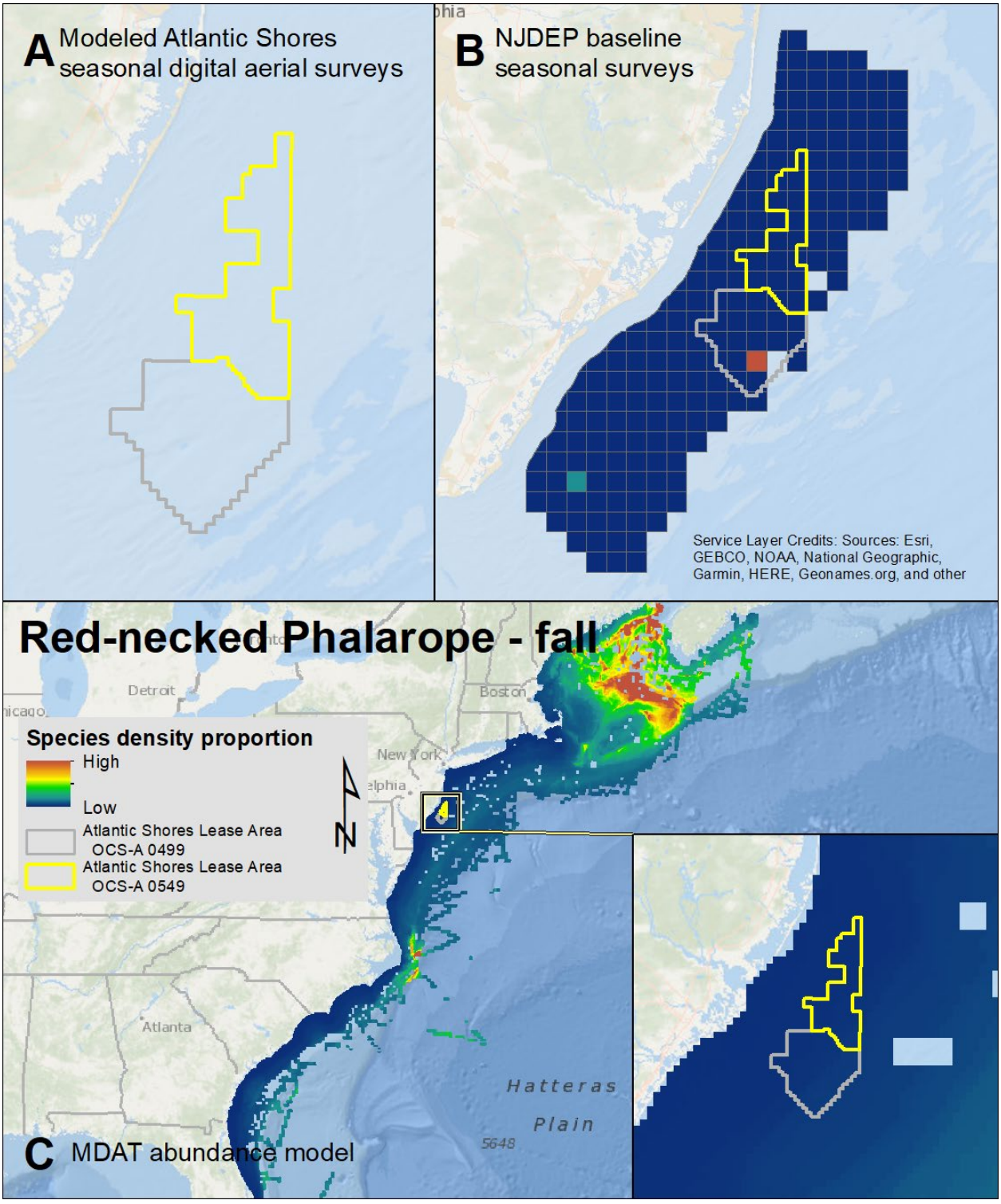

Map 173. Fall Red-necked Phalarope modeled density proportions in the Atlantic Shores seasonal digital aerial surveys (A), density proportions in the NJDEP baseline survey data (B), and the MDAT model outputs at local and regional scales (C). The scale for all maps is representative of relative spatial variation in the sites within the season for each information source.

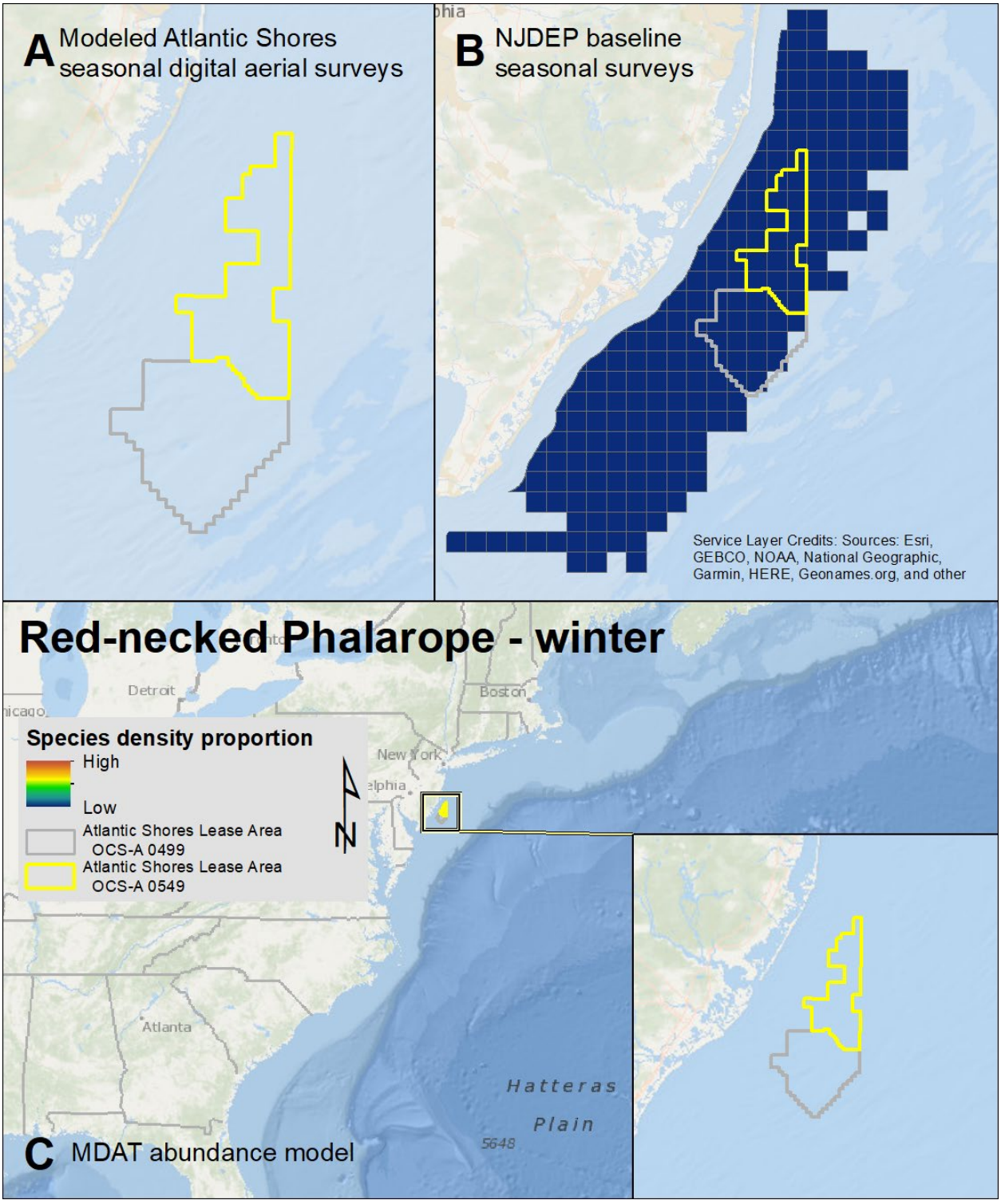

Map 174. Winter Red-necked Phalarope modeled density proportions in the Atlantic Shores seasonal digital aerial surveys (A), density proportions in the NJDEP baseline survey data (B), and the MDAT model outputs at local and regional scales (C). The scale for all maps is representative of relative spatial variation in the sites within the season for each information source.

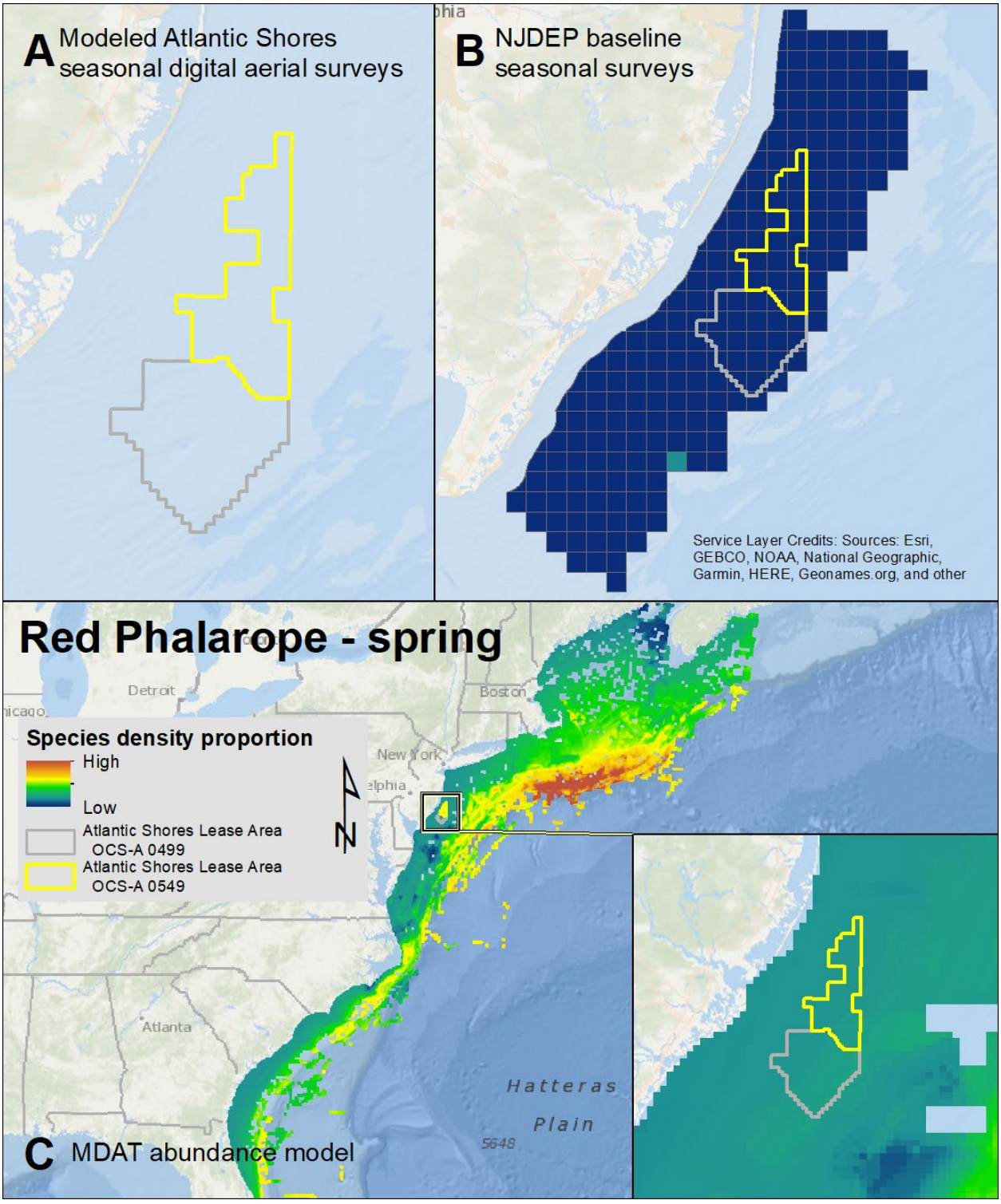

Map 175. Spring Red Phalarope modeled density proportions in the Atlantic Shores seasonal digital aerial surveys (A), density proportions in the NJDEP baseline survey data (B), and the MDAT model outputs at local and regional scales (C). The scale for all maps is representative of relative spatial variation in the sites within the season for each information source.

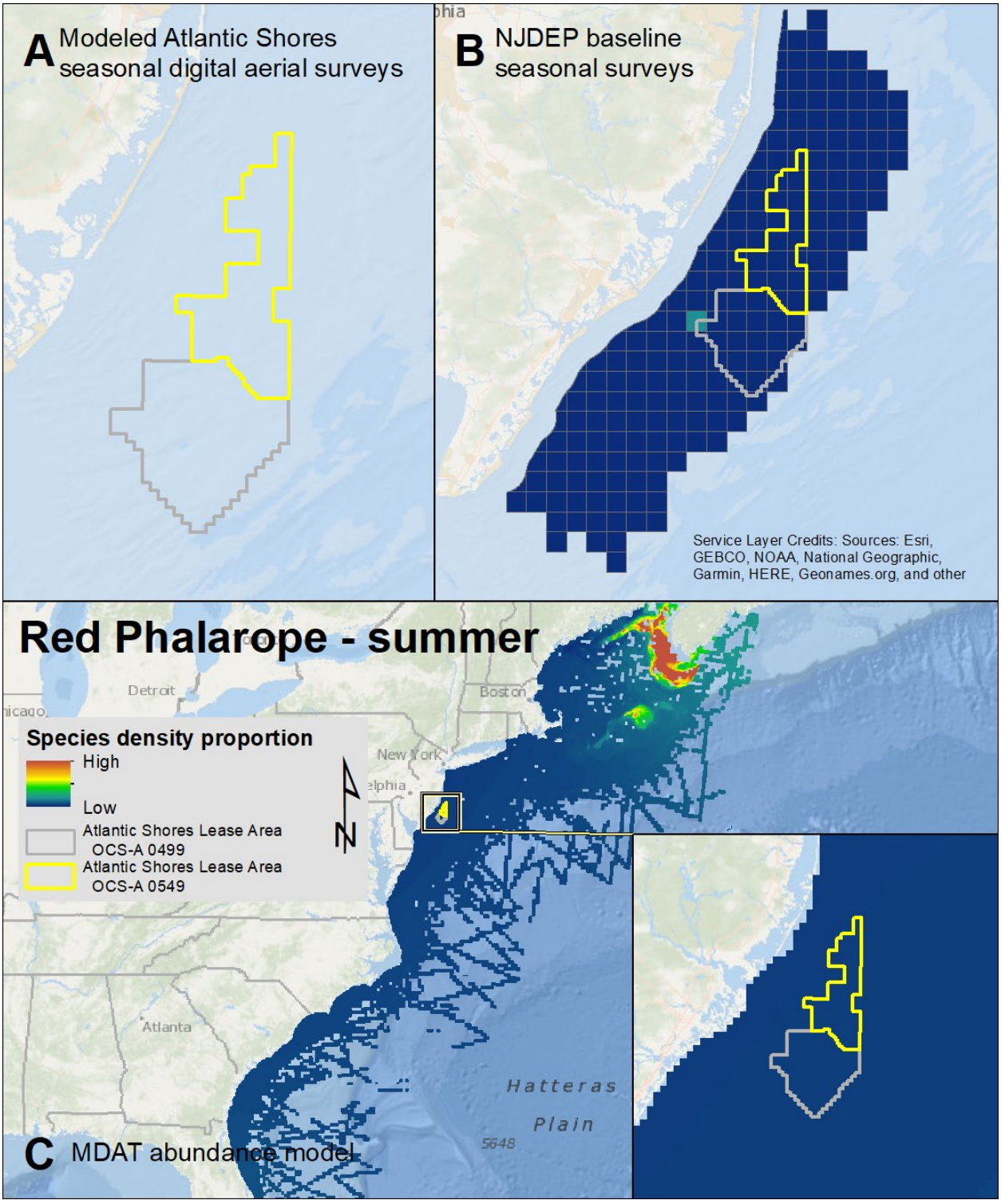

Map 176. Summer Red Phalarope modeled density proportions in the Atlantic Shores seasonal digital aerial surveys (A), density proportions in the NJDEP baseline survey data (B), and the MDAT model outputs at local and regional scales (C). The scale for all maps is representative of relative spatial variation in the sites within the season for each information source.

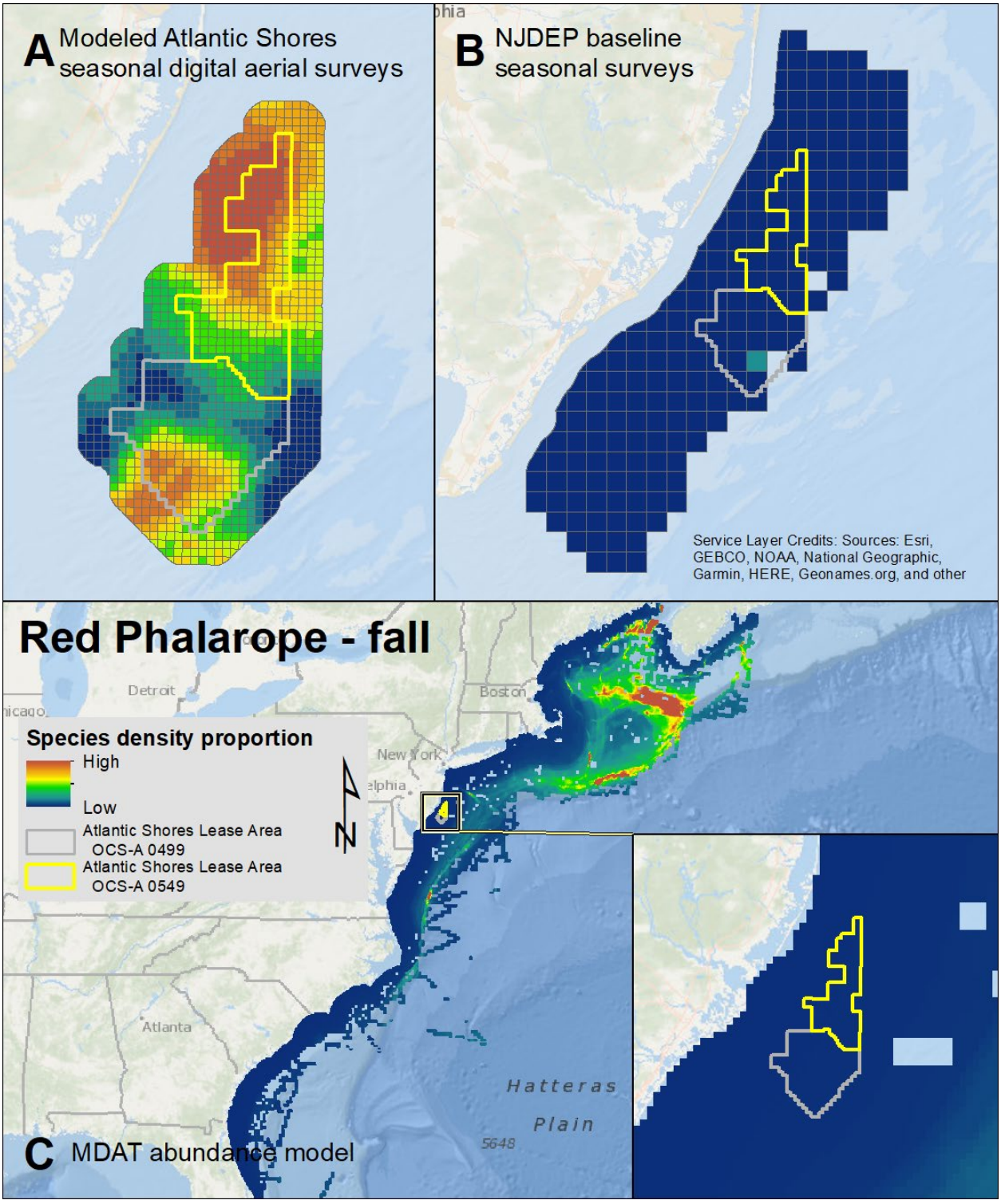

Map 177. Fall Red Phalarope modeled density proportions in the Atlantic Shores seasonal digital aerial surveys (A), density proportions in the NJDEP baseline survey data (B), and the MDAT model outputs at local and regional scales (C). The scale for all maps is representative of relative spatial variation in the sites within the season for each information source.

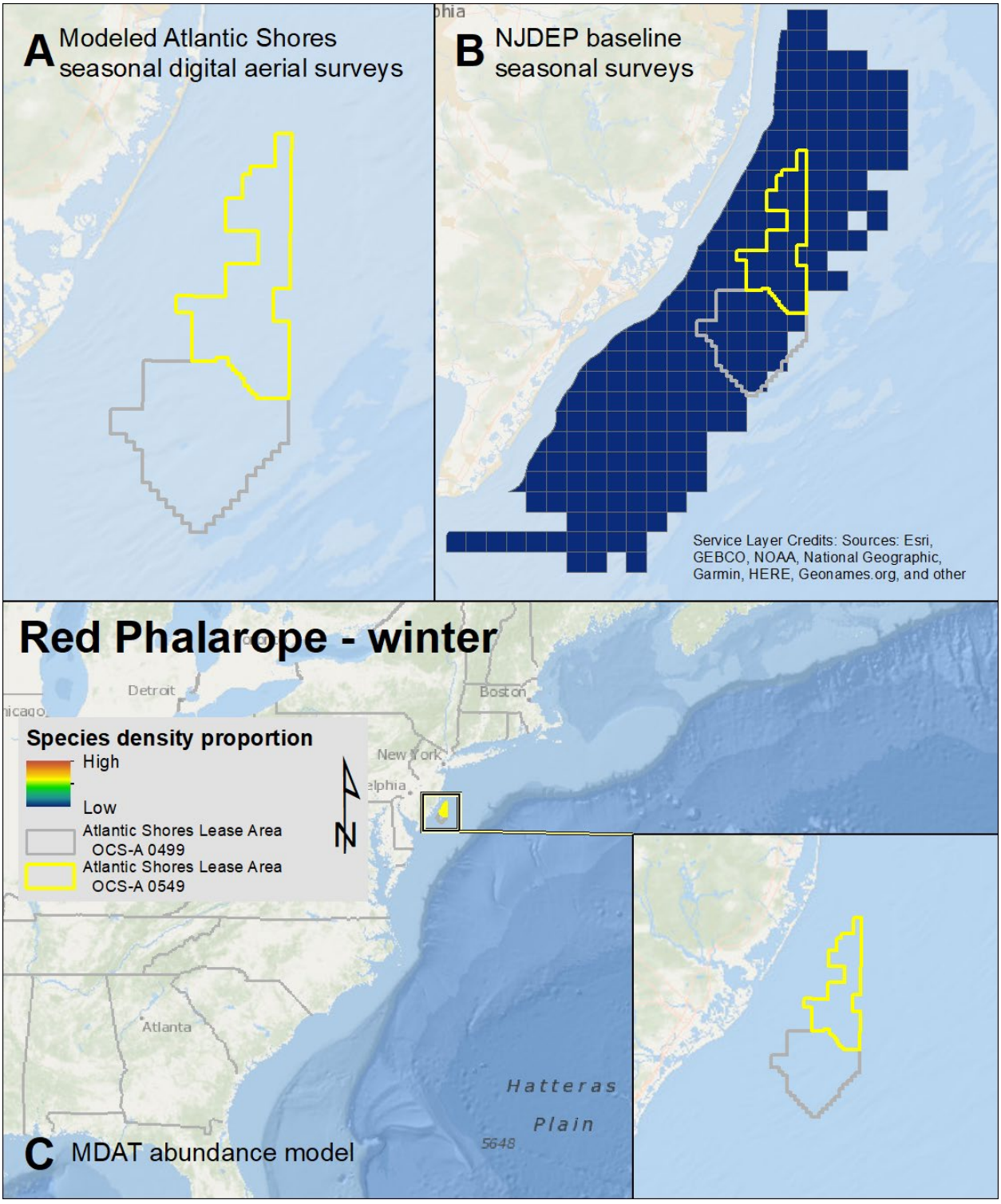

Map 178. Winter Red Phalarope modeled density proportions in the Atlantic Shores seasonal digital aerial surveys (A), density proportions in the NJDEP baseline survey data (B), and the MDAT model outputs at local and regional scales (C). The scale for all maps is representative of relative spatial variation in the sites within the season for each information source.